LABORATORY TECHNIQUES IN BIOCHEMISTRY AND MOLECULAR BIOLOGY

Volume 20

Edited by

R.H. BURDON — *Department of Bioscience and Biotechnology, University of Strathclyde, Glasgow*
P.H. van KNIPPENBERG — *Department of Biochemistry, University of Leiden, Leiden*

ELSEVIER
AMSTERDAM · NEW YORK · OXFORD

IMMOBILIZED pH GRADIENTS: THEORY AND METHODOLOGY

Pier Giorgio Righetti

Department of Biomedical Sciences and Technologies,
University of Milano, Via Celoria 2,
Milano 20133, Italy

1990
ELSEVIER
AMSTERDAM · NEW YORK · OXFORD

Printed on acid-free paper.

ISBN 0-444-81315-2 (pocket edition)
ISBN 0-444-81301-2 (library edition)
ISBN 0-7204-4200-1 (series)

Published by:
ELSEVIER SCIENCE PUBLISHERS B.V. (BIOMEDICAL DIVISION)
P.O. BOX 211
1000 AE AMSTERDAM
THE NETHERLANDS

Sole distributors for the USA and Canada:
ELSEVIER SCIENCE PUBLISHING COMPANY, INC.
655 AVENUE OF THE AMERICAS
NEW YORK, NY 10010
U.S.A.

Printed in The Netherlands

List of abbreviations

1-D	one dimensional
2-D	two dimensional
α_1-AT	α_1-antitrypsin
AcP	acid phosphatase
AEC	3-amino-9-ethyl carbazole
AlP	alkaline phosphatase
AMA	human amnion cells
AMPS	2-acrylamido-2-methyl propyl sulphate
ANS	anilino naphthalene sulphonate
APAAP	alkaline phosphatase anti-alkaline phosphatase complexes
β	buffering power
BAC	bisacrylyl cistamine
Bis	N,N'-methylene bisacrylamide
$C\%$	grams of cross-linker/$\%T$
C3	component 3 in human serum
C18	carbon tail 18 C atoms long
CA	carrier ampholytes
CCD	charge-coupled-device
CHAPS	3-(3-cholamidopropyl)dimethyl ammonio-1-propane sulfonate
CM	carboxy methyl
CN	4-chloro-1-naphthol
CSF	cerebrospinal fluid
CZE	capillary zone electrophoresis
d(pH)/dx	slope of the pH gradient over the separation axis
D	diffusion coefficient
DAB	3,3'-diamino benzidine
DATD	N,N'-diallyltartardiamide
DBM	diazobenzyl oxymethyl
DEAE	diethylamino ethyl
DHEBA	N,N'-1,2-dihydroxyethylene bisacrylamide
DMAPMA	N,N-dimethylamino propyl methacrylamide
DNA	desoxyribonucleic acid
ΔpI	resolving power
DPP	dipeptidyl peptidase
DTE	dithioerythritol
DTT	dithiothreitol
EDTA	ethylendiamino tetracetic acid
ELISA	enzyme-linked immunosorbent assay
Eq.	equation
Eta	(η) viscosity
FXIIIB	coagulation factor XIIIB
GC	group specific component on human serum

GFF	glass fiber filter
GGT	gamma-glutamyl transferase
H-H	Henderson-Hasselbalch equation
HA	hydroxyapatite
Hb	hemoglobin
HDL	high-density lipoprotein
HRP	horseradish peroxidase
I	ionic strength
IEF	isoelectric focusing
IgG	immunoglobulin G
IPG-DALT	isoelectric focusing in immobilized pH gradients followed by SDS-electrophoresis
IPG	immobilized pH gradients
IR	infrared
ISO-DALT	ISOelectric focusing followed by SDS-electrophoresis (DALTons)
ITP	isotachophoresis
K_d	dissociation constant
Lb	leg hemoglobin
LCAT	lecithin : cholesterol acyltransferase
MAD	mixed ionic detergent
MAPTAC	methacrylamidopropyl trimethyl ammonium chloride
MDPF	2-methoxy-2,4-diphenyl-3(2H)furanone
mequiv.	milli equivalents
M_r	relative molecular mass
mS	milli siemens (conductivity)
N	number of theoretical plates
NAB	non-amphoteric buffers
NANA	*N*-acetyl neuraminic acid
NC	nitrocellulose
NMR	nuclear magnetic resonance
NP-40	nonidet P-40
Omega	(Ω) electric resistance
PAGE	polyacrylamide gel electrophoresis
PAP	peroxidase anti-peroxidase complexes
PBMC	peripheral blood mononuclear cells
PBS	phosphate buffered saline
PC	protein C
PEHA	pentaethylene hexa-amine
PGM	phosphoglucomutase
pH_m	pH value at midpoint in an IPG interval
pH_{max}	highest pH extreme of an IPG interval
pH_{min}	lowest pH extreme of an IPG interval
PI	protease inhibitor
pI	isoelectric point
pixel	picture element
pK_{prox}	pK of an ionizable group nearest to the pI of a carrier ampholyte
ppm	parts per million
PVC	polyvinyl chloride
PVDF	polyvinilidene difluoride
QA-GFF	quaternary amino glass fiber filter

QAE	quaternary amino ethyl
rDNA	recombinant DNA
Rho	(ρ) density
RNA	ribonucleic acid
SB	sulphobetaine
SDS	sodium dodecyl sulphate
SP	sulpho-propyl
$T\%$	(grams acrylamide + grams cross-linker)/100 ml solution
TCA	trichloroacetic acid
TEMED	N,N,N',N'-tetramethyl etylene diamine
TEPA	tetraethylene penta-amine
TETA	tetraethylene tetra-amine
Tf	transferrin
tPA	tissue plasminogen activator
Tris	Tris(hydroxymethyl)amino methane
TTR	transthyretrin
UK	urokinase
V/cm	field strength (volts/cm)
V	volts
VLDL	very low density
Z	charge of an ion

Acknowledgments

The striking developments in the field of IPGs reported here would have been impossible without the heroic efforts of a group of 'desperados'. Over the years I have enjoyed the close collaboration of my own group in Milan, Dr. E. Gianazza, Dr. C. Gelfi, and Dr. M. Chiari. In addition, I would like to mention my collaboration with a host of foreign associates: Dr. P.K. Sinha (Berlin), Dr. T. Rabilloud (Paris), Dr. M. Faupel (Basle), Dr. E. Wenisch (Vienna), Dr. J.P. Wahrmann (Paris), Dr. P. Sorroche (Buenos Aires), Dr. M. Rimpilainen (Oulu), and Dr. H. Kilias (Bayreuth). Furthermore, Dr. B. Bjellqvist (Bromma) and Dr. A. Goerg (Munich), with whom I have had a long-term collaboration, and who have worked their own independent way through the IPG riddle. The research from my own group reported here has been supported by two five-year grants from Consiglio Nazionale delle Ricerche (CNR, Progetti Finalizzati Chimica Fine I and Salute dell'Uomo) and is now supported by two new five-year grants (CNR, Progetti Finalizzati Biotecnologie e Biosensori and Chimica Fine II). Finally I would like to thank the colleagues who have supplied me with the original photographs of their work which have been reproduced in this volume.

Introduction

It is my pleasure to sandwich the present manual between two 'electrodes': 'Galvani' and (in the *Post Scriptum*) 'Volta'. They are the two Italians who most contributed to the development and understanding of electric phenomena, the first from a physiological point of view, the second from a physical approach. This is not, by all means, to diminish the contributions from all other scientists, but, being an Italian too, I felt particularly obliged to pay a tribute to them.

Luigi Galvani (Bologna, 1737–1798) (Fig. 0.1) became a professor of Anatomy and Surgery at the University of Bologna in 1763. In 1780, he started his famous experiments on electricity in frogs. He noticed that, when skinned frogs, hanging out from his balcony, with a metal wire connected to the central spinal nerve, were wired to the metal railings of the balcony, contractions were produced during lightning in a thunderstorm. He thought he had discovered 'animal electricity' and his studies led him to formulate a theory on the electric nature of nerve fluid, theory which initiated modern electrophysiology. The conclusive experiment was produced on September 20, 1786, when Galvani observed that, when a bridge was made between the spinal nerve and an extremity of a skinned frog leg, an electric reaction was produced in frog muscle (see Fig. 0.2). However, the bridge consisted of two segments of two different metals, zinc and copper. At that time, a physicist from the University of Pavia, Alessandro Volta, was on leave to follow a course with Galvani (*clerici vagantes*, i.e., itinerant students, were quite popular in universities since the Middle Ages; thus the Erasmus Program, now promoted by the European Community to move students around european universities, is a rediscovery of an old principle) and was quite thrilled by this experiment. He felt intuitively that contact between two metals would create electricity; that if insulated zinc were touched against insulated copper, the

Fig. 0.1. Woodcut of Luigi Galvani, ca. 1780; unknown author.

zinc would collect the positive electricity and the copper would gather the negative electricity. He maintained that this was because of the particular nature of each metal, and that metals can be arranged in order according to the electric charge they can hold (zinc, lead, copper, silver, gold platinum), so that copper, which is negative with tin or zinc, becomes positive with silver or platinum. A particularly interesting experiment Volta devised was the taste produced when a piece of one metal was placed below the tongue and a piece of another metal was positioned above the tongue and

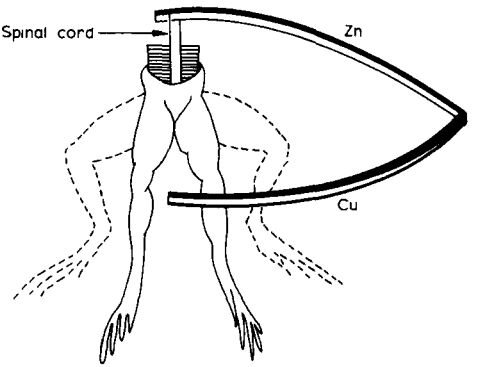

Fig. 0.2. The classical 'frog-leg' experiment of Luigi Galvani. When an arc was made between the spinal nerve and a pair of skinned frog legs, the legs would contract (dotted profile) each time the circuit (made by two pieces of Cu and Zn, joined in the middle) was closed. Galvani's interpretation: 'animal electricity'. Volta's interpretation: potential difference (voltage, to be sure) generated at the contact between two unlike metals.

when the two were connected by a wire (this observation was later on to lead him to the invention of the 'pile'). Volta's explanation of Galvani's experiments led to a quarrel between the two that lasted to the very end of Galvani's days, and greatly embittered the 'maestro'. Yet, by one of the peculiarly tortuous ways of science, they were both right: Galvani had discovered electrical currents in nerve systems and Volta had found that contact between two unlike metals could produce a potential difference!

Galvani's experiments were so famous that the verb 'galvanize' has become a permanent expression in all idioms: we 'galvanize' metals (i.e., plate them electrolytically with another metal) and we 'galvanize' people (i.e. excite them). I do hope to be able to galvanize the readers for the present manual.

The chemicals

1.1. Isoelectric focusing: an evolving concept

This section will summarize the series of steps and discoveries which led to present-day isoelectric focusing (IEF) in immobilized pH gradients (IPG). Four major evolutionary events have been identified and will be described below.

1.1.1. The first generation

The first approach to IEF was a two-step technique, by which the pH gradient along the separation path would be established by diffusion between two limiting solutions titrated to the starting and ending pH values, followed by a quick electrophoretic step. It seems that Kolin (1977) conceived this idea during a train ride from Chicago to Fort Collins, upon reading Abramson's book on 'Electrokinetic Phenomena' (1934). This idea of 'focusing ions in a continuous pH gradient', stabilized by a sucrose density gradient, was brought forward by Kolin in a series of articles in 1954 and 1955 (Kolin 1954, 1955a and b). Kolin used the term 'isoelectric spectrum' to denote a distribution pattern established by a sorting process. The pH gradient was generated by placing the substance to be separated at the interface between an acidic and a basic buffer, in a Tiselius like apparatus, and, after a proper diffusion time, by applying an electric field. In these 'artificial' pH gradients, Kolin was able to obtain 'isoelectric line spectra' of dyes, proteins, cells, microorganisms and viruses on a time scale ranging from 40 s up to a few minutes, a rapidity still unmatched in the field of electrophoresis. Concomitant with the pH gradient, a density gradient, an electrical conductivity gradient and a vertical temperature gradient were acting upon the separation cell.

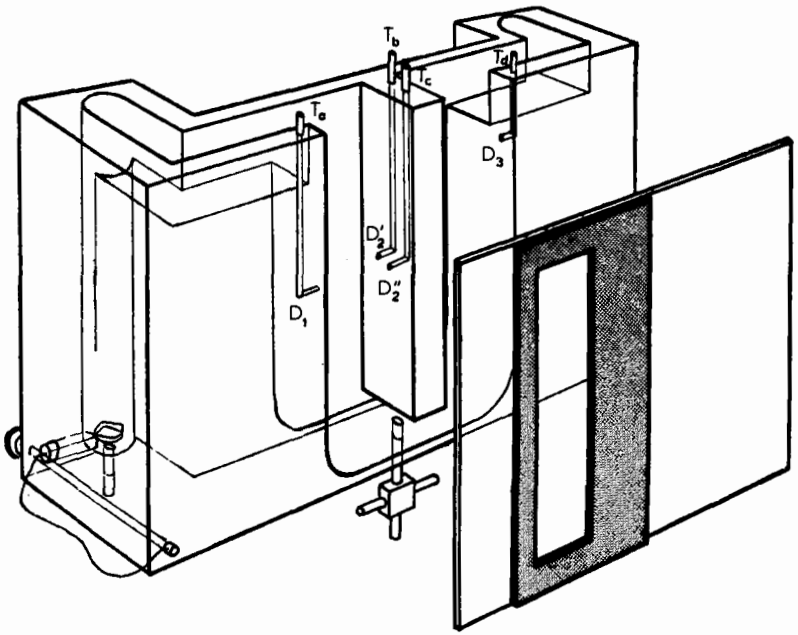

Fig. 1.1. The first IEF generation: pH gradients generated by diffusion followed by electrophoretic protein transport. Perspective view of the Kolin electrophoretic fractionation cell. T_a, T_b, T_c and T_d: hypodermic syringe tubings. D_1, D_2', D_2'' and D_3: corresponding horizontal ducts (by courtesy of Dr. A. Kolin).

The design of the cell, shown in Fig. 1.1, indicates that Kolin's method was quite an advanced technique. A U-cell was machined out of a Lucite block, with the electrode compartments quite removed from the separation cell (one electrode can be seen in the left side). The front and back Lucite plates could be lifted from the cell body and were provided with a glass or quartz window covering the left leg of the cell. Separation would usually take place on this left limb of the U-cell, which was also provided with tubes D_1, D_2' and D_2'' for sample loading and harvesting at the end of the separation.

Interestingly, a similar principle, called electrophoretic focusing of ions (EFI) (focusing ion exchange) was reported by Friedli and Schumacher (1961) for separation of rare earth mixtures in com-

bined proton (pH) and ligand (pL) gradients. EFI-spectra of La-Tb and Eu-Lu groups were obtained in the course of 5 min. Not exactly focusing, but electrophoresis perpendicular to a pre-established pH gradient was practiced already in 1952 by Michl: it was an embrionic form of 'titration (pH/mobility) curves', as later developed by utilizing IEF in the first dimension (Righetti and Gianazza, 1981). pH gradients generated by diffusion were also used by Stahl (1964; Stahl and Miller, 1981) for obtaining 'titration curves' in thin-layer chromatography (pH/R_f curves) and later by Tate (1981) in paper electrophoresis (determination of ionization constants of nucleotides) and by Jokl et al. (1979) in hydro-organic solvents.

1.1.2. The second generation

In 1976, when the first manual on isoelectric focusing was written, it was dedicated to 'Prof. H. Svensson-Rilbe, father of the fine art of isoelectric focusing' (Righetti and Drysdale, 1976). In 1983, when the sequel was printed, it was dedicated to 'Prof. H. Svensson-Rilbe, Prof. A. Kolin and Dr. O. Vesterberg, the Trimurti of isoelectric focusing' (Righetti, 1983a). By the late fifties, it was understood that Kolin's pH gradients, obtained by diffusion of non-amphoteric buffers, could not stand the ordeal of an electrophoretic step, since they would be quickly destroyed by electric migration of buffer and titrant ions. Svensson's (later Rilbe) (1961, 1962a and b) brilliant theoretical work synthesized the minimum basic requirement for stable pH gradients in an electric field in the term 'carrier ampholyte' (CA). The buffers used in this system had to have two fundamental properties: (a) to be amphoteric (so that they would reach a steady-state position along the separation column) and (b) to be 'carrier'. This last concept is more subtle but just as fundamental. Not any ampholyte could be used for IEF, only a carrier ampholyte, i.e., a compound capable of 'carrying' the current (a good conductor) and capable of 'carrying' the pH (a good buffer). Thus the concept of carrier ampholyte as one with two dissociation steps not far from the isoelectric point (or, if you prefer, a species satisfying the inequality $|\mathrm{pI} - \mathrm{p}K_{\mathrm{prox}}| \leqslant 0.5$) was

understood. It took then the elegant synthesis of Vesterberg (1969) of such ampholytes to make such a dream possible.

This was not the only approach to the 2nd generation IEF. As early as 1957, Kauman discussed a paper at the Belgian Royal Academy 'on the electrophoretic separation of ampholytes in a medium of non-uniform pH'. The paper was presented by Nobel laureate I. Prigogine, who had in fact suggested such an investigation. In this article, the behavior of amphoteric electrolytes under the combined action of a gradient of pH and an electrostatic potential was investigated. It was shown that ampholytes could be separated and concentrated if the positive electrode was placed on the acidic side of the pH gradient. To quote verbatim: 'under these conditions, the distribution of the ampholyte at the stationary state will vary approximately as a Gaussian error function of distance with the maximum at the isoelectric point. The band width of the maximum is found to depend inversely on the magnitude of the gradient'.

The problem, in Kauman's and Svensson's approaches, was how to find CA chemicals suitable for an IEF fractionation. Carrier ampholytes more acidic than pI = 4 were abundant in commercial catalogues of organic compounds, but only a few ones more basic than pI = 7 could be found, and carrier ampholytes isoelectric between pH 4 and 7 seemed to be completely non-existent. To fill the pH 4–7 gap, Svensson started synthesizing, but with limited success, ampholytes based on imidazole as starting material. Finally, he resorted to the only remaining possibility: production of oligopeptides by partial hydrolysis of hemoglobin or whole blood (Rilbe, 1976a,b). The final solution came in the spring of 1964, when Vesterberg finally solved the problem of obtaining good carrier ampholytes over the pH 3–10 scale by reacting the double bond of unsaturated carboxylic acids to oligoamines. The concept of this second IEF generation is shown in Fig. 1.2.

1.1.3. The third generation

We started an extensive investigation on the synthesis and properties of Vesterberg-type carrier ampholytes (Righetti et al., 1975, 1977; Galante et al., 1975). In 1978 we started also 'immobilizing'

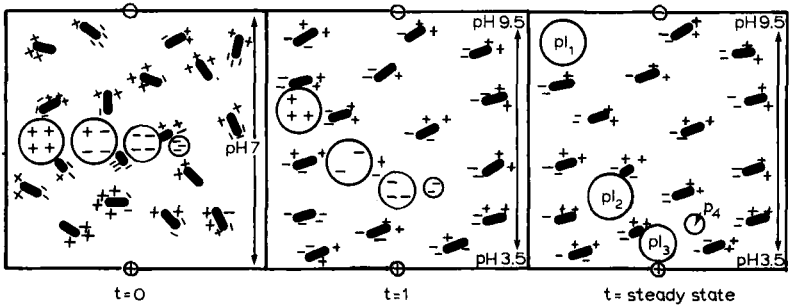

Fig. 1.2. The second IEF generation: pH gradients generated by amphoteric buffers transported by the current in an electric field. At $t = 0$, there is no pH gradient existing in the cell (left panel) and both proteins and CAs carry net negative or positive charges. At $t = 1$, the carrier ampholytes have already reached a steady-state, and thus created a pH gradient over the separation axis, while the proteins are still migrating. At t = steady-state, also the macroions have reached their isoelectric point (pI) (modified from the LKB catalogue, 1987).

buffers, and precisely the carrier ampholytes for conventional isoelectric focusing. The idea was to utilize these immobilized pH gradients for preparative protein purification, since, in preparative IEF, it has always been difficult to completely eliminate the CA buffers contaminating the protein. The experimental protocol was as follows: activated Sephadex was used as a granulated bed support. On it, activated CA buffers were focused and then, at steady-state, grafted with catalysts to the Sephadex beads. After electrophoretic depletion of catalysts, the protein would be applied and focused on the preformed and insolubilized pH gradient. Several approaches were tried:

(a) allyl-carrier ampholytes (obtained by reaction with allyl bromide) were focused on a bed of allyl-Sephadex (prepared by reacting Sephadex at alkaline pH, in 0.5% $NaBH_4$, with allyl bromide) and then insolubilized in situ;
(b) carrier ampholytes were reacted with 2,4,6-triallyloxy-triazine and focused and grafted onto activated Sephadex;
(c) carrier ampholytes were reacted with methacrylic acid 2,3-epoxypropylester and then focused and grafted onto activated Sephadex;

(d) carrier ampholytes were activated with triacryloyl hexahydro-1,3,5-triazine and then focused and grafted onto activated Sephadex.

The research progressed and we were indeed able to graft the desired pH gradient, but the results in preparative protein purification did not live up to our expectations (E. Gianazza, O. Brenna and P.G. Righetti, unpublished). The problem was analogous to the one of Svensson: lack of suitable chemicals to be grafted to the polyacrylamide matrix. In 1975, Gasparic et al., had been grafting allyl and vinyl compounds (e.g., vinyl His) to acrylic double bonds. Allylic and vinylic double bonds had reactivities 1,000 to 10,000 times lower than acrylic double bonds, thus acting in practice as inhibitors of polymerization (radical sinks) (Bianchi-Bosisio et al., 1980). It was thus decided to synthesize a series of acrylamido buffers and titrants, in fact the present generation of Immobiline. Due to her role in developing ultrathin IEF gel matrices (Görg et al., 1978) and in pouring gradient gels in ultrathin chambers (Görg et al., 1980), Görg's group was asked to join in the project. Thus, with the combined efforts of these groups, the third generation of IEF was launched (Bjellqvist et al., 1982). Fig. 1.3 gives a pictorial representation of an Immobiline gel and of proteins focusing in these matrices.

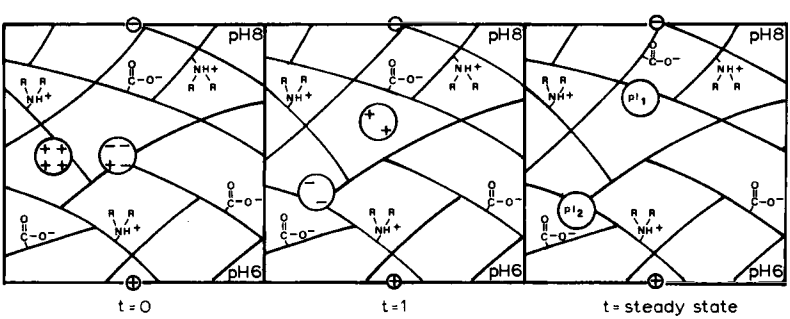

Fig. 1.3. The third IEF generation: immobilized pH gradients. Note that at all stages of electrophoresis ($t = 0$ to t = steady-state, the pH gradient is already fully established and immobile in the electric field. Thus, only the proteins keep migrating under the applied voltage till reaching a steady-state (modified from an erroneous drawing in the LKB catalog, 1987).

1.1.4. The fourth generation

There were some inherent problems with CA-IEF, e.g., the uneven conductivity and buffering capacity along the separation track (due to the steady-state stacking of the amphoteric buffers), the extremely low ionic strength (favoring near-isoelectric precipitation), the pH gradient instability (cathodic drift) and the inability of performing pH gradient engineering (i.e., tailoring the width and shape of the pH gradient to any possible different separation problem). As the IPG technique expanded and different applications were tried, it was comforting to see that all above problems had been effectively wiped out (Righetti, 1984). However, often new techniques invented to solve the problems of existing methodologies generate new, unexpected problems on their own. IPG are no exception to this rule. We had often experienced problems of sample streaking and even precipitation at the application site, particularly evident with membranaceous proteins. So, in 1985, we proposed what I here call the fourth generation: mixed-bed CA/IPG gels, in which a primary, insolubilized pH gradient coexists with a secondary, soluble, carrier ampholyte driven, gradient (Rimpilainen and Righetti, 1985). In this mixed-bed technique we achieved remarkable IPG patterns of membrane proteins, suggesting that CAs, when added to solubilized membrane components (in this case in presence of 2% Nonidet P-40 but in the absence of urea) had a marked solubilization property, perhaps via formation of mixed, zwitterionic CA-detergent micelles. The same CA/IPG mixed bed technique (whose principle is depicted in Fig. 1.4) was also proposed by Fawcett and Chrambach (1986) and by Altland and Rossman (1985), although for different purposes and with different mechanisms (mostly conductivity problems of IPG gels were their main concern). Later on (Righetti et al., 1987c,d; Rabilloud et al., 1987a,b) we reported another, unexpected problem of IPGs: spontaneous homopolymer formation of the four alkaline species (p*K*s 6.2, 7.0, 8.5 and 9.3), simply upon storage of their water solutions (even frozen), with generation of oligomers to *n*-mers. These homopolymers have the peculiar property of precipitating large proteins (e.g, ferritin, human serum components) out of solution by cross-linking them via mixed ionic-hydrophobic

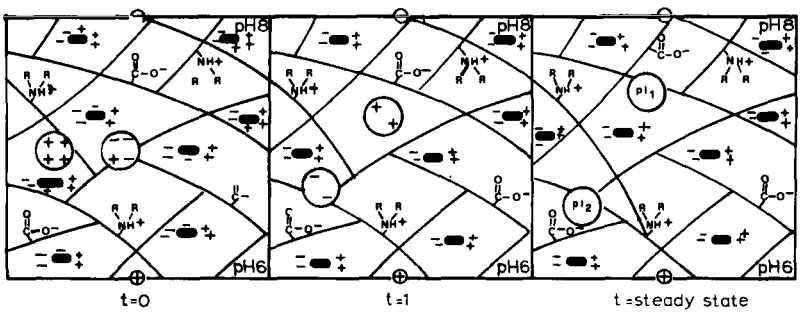

Fig. 1.4. The fourth IEF generation: mixed-bed carrier ampholyte-Immobiline. In the preformed immobilized pH gradient carrier ampholytes and proteins reach the steady-state. CA chemicals seem to be needed to temporarily buffer the protein ions when applied to the IPG gel surface and to quench hydrophobic interactions between proteins and the IPG matrix (especially in alkaline pH regions) (from Righetti, 1988; with permission of Elsevier).

interaction. Moreover, even in the absence of these homopolymers, alkaline IPG ranges tend to adsorb proteins by hydrophobic interaction, as the four alkaline Immobilines, when deprotonated, enhance their hydrophobic properties. Here too addition of CAs to both gel matrix and sample considerably improved the IPG banding patterns, abolishing any sample precipitation. We thus expanded our earlier model on the solubilizing power of added CAs (Rimpilainen and Righetti, 1985) by proposing that CAs might just act as shielding molecules, coating, on the one side, the polyacrylamide matrix studded with Immobilines (especially the hydrophobic basic species) and, on the other side, patching hydrophobic spots onto the protein surface. Later on, a new, unexpected effect of added CAs was found: in samples containing high levels (> 40 mM) of strong salts (e.g., NaCl, Na_2SO_4, Na_2HPO_4) CAs, added solely to the sample layer, would prevent sample precipitation and modification simply by buffering the moving anion and cation boundaries generated in the electric field (Righetti et al., 1988e). Thus, it appears that the fourth generation is here to stay and to accompany us into the year 2000.

1.2. *Comparison between carrier ampholyte and Immobiline chemicals*

We have briefly described some properties of the carrier ampholyte (CA) chemicals in §1.1.2. What exactly these compounds are is shown in Fig. 1.5. They are aliphatic oligoamino oligocarboxylic acids, each of which containing, according to the original Vesterberg's patent, 'at least four weak protolytic groups, at least one being a carboxylic group and at least one a basic nitrogen atom, but no peptide bond'. In practice, the synthesis is achieved by reacting highly heterogeneous mixtures of oligoamines (e.g., tetraethylenepentamine, pentaethylenehexamine) with an α,β-unsaturated acid (acrylic acid being the preferred compound) at an ideal nitrogen/carboxyl ratio of 2 : 1. The synthesis generates a multitude of amphoteric buffers (> 600 in the pH 4–10 range). There is no other way than the Vesterberg synthetic approach if one has to fill up the big gap in the pH 5–7 region discovered by

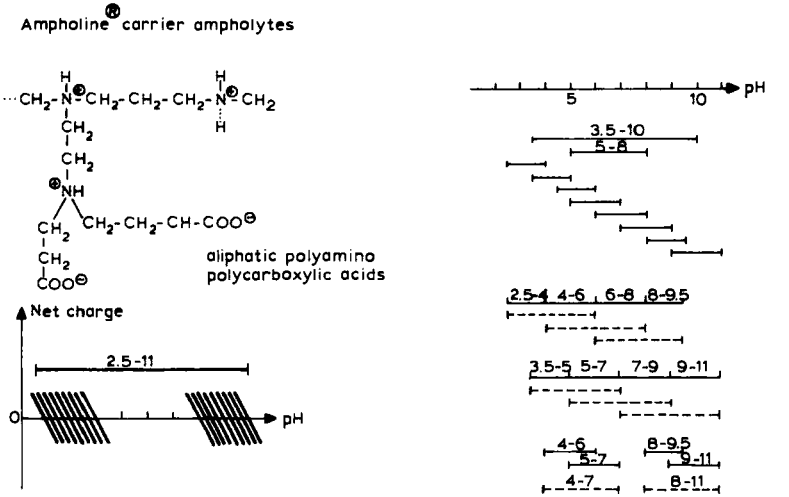

Fig. 1.5. Composition of Ampholine. On the upper left side a representative chemical formula is shown (aliphatic oligo amino oligo carboxylic acids). On the lower left side, portions of hypothetical titration curves of Ampholines are depicted. Right: different pH cuts for wide and narrow range carrier ampholytes (courtesy of LKB Produkter AB).

Svensson-Rilbe (see §1.1.2). Thus, all other chemicals made subsequently (the ones according to the original patent were marketed already in 1966 by LKB Produkter AB under the trade name Ampholine) had to follow the same synthetic route (Servalyte, Buffalyte, Biolyte, you name it). However, in 1978, a new brand was offered in the market: the Pharmalyte chemicals. Pharmalytes were made to contain peptide bonds and could thus be offered in the market without infringing the original patent. A friend of mine (name withheld on request, for ... philosophical reasons), a famous professor of microbiology at the University of Uppsala, at that time was given a few samples of Pharmalytes for trial runs: as he was working with bacterial hexoproteases, he could thus witness the most curious phenomenon of the pH gradient disappearing in front of his own eyes, as the proteases, on their way to the isoelectric point, were furiously chewing up the peptide bonds of Pharmalyte. Nevertheless these chemicals, due to their peculiar synthetic way (Williams and Söderberg, 1979), are believed to contain more than 5000 different chemicals in the pH 2.5–11 interval and are in fact known to produce the smoothest pH gradient (Tollaksen et al., 1981).

Given the remarkable properties of these compounds, and the highly refined state of the art (Righetti, 1983a,b) was there really a need to switch over to a different technique? Well, as methodologies grow old, they start showing the crippling diseases of age: the limits and faults of CA-IEF are listed in Table 1.1. Some of them, like the instability of pH gradient with time, or cathodic drift (Righetti and Drysdale, 1973) had never found a solution and are in fact inherent to the technique per se. Other, like the extremely low ionic strength (believed to be around 1 mequiv. l^{-1} for 2%

TABLE 1.1
Problems with CA-IEF focusing

(a) Medium of very low and unknown ionic strength
(b) Uneven buffering capacity
(c) Uneven conductivity
(d) Unknown chemical environment
(e) Non-amenable to pH gradient engineering
(f) Cathodic drift (pH gradient instability)
(g) Low sample load ability

focused Ampholine) (Righetti, 1980), often cause near isoelectric smears of the most abundant proteins in a mixture. The summation of all these drawbacks had become such a nuisance that, in 1982, Bjellqvist et al., had to introduce the revolutionary concept of immobilized pH gradients.

IPGs are based on the principle that the pH gradient, which exists prior to the IEF run itself, is co-polymerized, and thus insolubilized, within the fibres of the polyacrylamide matrix. This is achieved by using, as buffers, a set of chemicals (called Immobiline, in analogy with Ampholine) having pK values well distributed in the pH 3–10 interval. These compounds are acrylamido derivatives with the general structure: CH_2=CH–CO–NH–R, where R contains either a carboxyl or a tertiary amino group (for present-day commercial Immobiline; we have introduced also strong titrants, containing a sulphate group for the acidic and a quaternary ammonium for the basic species; see Tables 1.2 and 1.3). During gel polymerization, buffers and titrants are efficiently incorporated into the gel, thus ensuring locally a given pH value of unlimited stability. The distance between the double bond and the group taking part in the protolytic equilibrium has in all instances been chosen to be long enough for the influence of the double bond on the dissociation constant to be neglected. As a result, the pK difference between the free and bound Immobiline is mainly due to the presence of the polyacrylamide matrix and to temperature variations during the IPG run. Immobiline-based pH gradients can be cast in the same way as conventional polyacrylamide gradient gels, by using a density gradient to stabilize the Immobiline concentration gradient, with the aid of a standard, two-vessel gradient mixer (see Chapter 3). As shown in the formula, these buffers are no longer amphoteric, as in conventional IEF, but bifunctional: at one extreme of the molecule is located the buffering group, and at the other extreme is the acrylic double bond, which will be consumed during the grafting process.

1.3. Structure and synthesis of acidic Immobiline

The synthetic procedure for the Immobiline chemicals could be devised quite simply upon determination of the structure of these

compounds (Chiari et al., 1989a,b). The structural work was facilitated by some basic information given in the literature (Bjellqvist et al., 1982) that: (a) all compounds contain an acrylamido residue at one end of the molecule and (b) the acidic Immobilines contain a weak carboxyl, while the basic Immobilines contain a tertiary amino group. IR spectra confirmed the presence of a carbonyl engaged in an amido bond in all compounds. It should be stressed that, while the formulas we give for the 11 acrylamido buffers listed in Tables 1.2 and 1.3 are correct, the synthetic route we have devised is not necessarily identical to the approach used by LKB in producing their own commercial Immobiline, although the synthetic approach we propose here seems to be the most natural and direct one.

Synthesis of pK 3.6 Immobiline (N-acryloyl glycine)
To a stirred, cooled (0°C) solution of glycine (5.25 g, 0.07 mol) in 25 ml of 2N NaOH, acryloyl chloride (2.8 ml, 0.035 mol) was added dropwise. After stirring for 1 h, the solution was poured into cold acetone (125 ml), producing two phases. After separation of the oily phase, evaporation yielded 2.2 g of product as white crystals (40% yield). ^{1}H-NMR (D_2O) δ: 4.05 ppm (2H, $-CH_2-$, s), 5.8 ppm (1H, =CH–, m), 6.2 ppm (2H, CH=, m).

Synthesis of pK 4.6 Immobiline (4-acrylamido butyric acid)
To a stirred, chilled solution (0°C) of 4-amino butyric acid (20.6 g, 0.199 mol) in 100 ml of 2N NaOH, acryloyl chloride (9 ml, 0.11 mol) was added dropwise. After stirring for 1 h, the solution was acidified to pH 3 with 10% hydrochloric acid. Acetone was added, and the product was extracted from the oily phase with ethyl acetate (3×70 ml). Evaporation of the solvent gave 7.12 g of 4-acrylamido butyric acid (40% yield). ^{1}H NMR (D_2O) δ: 1.8 ppm (2H, $-CH_2-$, m), 2.35 ppm (2H, $NH-CH_2-$, m), 3.35 ppm (2H, CH_2-COOH, m), 5.75 ppm (1H, =CH–, m), 6.2 ppm (2H, $CH_2=$, m).

Table 1.2 lists the 5 acrylamido acids today available for isoelectric focusing in immobilized pH gradients. In addition to the three commercial Immobilines (p*K*s 3.6, 4.4 and 4.6) we have described two additional compounds, a strong acid (AMPS), needed for

TABLE 1.2
Acidic acrylamido buffers

pK [4]	Formula	Name	M_r	Source
1.2	$CH_2=CH-CO-NH-C(CH_3)(CH_3)-CH_2-SO_3H$	2-acrylamido-2-methylpropane sulfonic acid	207	[1]
3.1	$CH_2=CH-CO-NH-CH(OH)-COOH$	2-acrylamido glycolic acid	145	[2]
3.6	$CH_2-CH-CO-NH-CH_2-COOH$	*N*-acryloyl glycine	129	[3]
4.4	$CH_2=CH-CO-NH-(CH_2)_2-COOH$	3-acrylamido propanoic acid	143	[3]
4.6	$CH_2=CH-CO-NH-(CH_2)_3-COOH$	4-acrylamido butyric acid	157	[3]

[1] Polysciences Inc., Warrington, PA. 18976, USA.
[2] Righetti, P.G., et al. (1988b).
[3] Pharmacia-LKB Biotechnology, Uppsala, Sweden.
[4] The pK values for the three Immobilines are given at 10°C; for 2-acrylamido glycolic acid at 25°C; for AMPS; the temperature of pK measurement is not reported.

generating wide pH intervals (Gianazza et al., 1984a) and a fairly acidic species (pK 3.1), recently utilized for separation of very low pI proteins (Righetti et al., 1988b). We have not reported data on the pK 4.4 compound, as it appears that this chemical will be discontinued, after the report of Gianazza et al. (1984a) that the pKs 4.4 and 4.6 should never be mixed together in wide-pH range formulations, because they will always produce non-linear pH gradients, due to the close proximity of the two pK values.

In any event, the synthetic route for these three chemicals (pKs 3.6, 4.4 and 4.6) is essentially the same: the starting reagents will be acryloyl chloride, on the one side, and either glycine (pK 3.6) or 3-amino propanoic acid (pK 4.4) or 4-amino butyric acid (pK 4.6) on the other side. Condensation of the two precursors to form the amido bond will be obtained in strongly alkaline solutions, able to neutralize the HCl produced by the reaction. It should be borne in mind that this is the classical Schotten-Bauman reaction: already in

1978 Brown et al., used it to produce polyacrylamide beads containing reproducible amounts of carboxylic groups, by preparing reactive monomers such as 6-acrylamido hexanoic acid and *N*-methacryloyl glycylglycine. Quite different is the strategy for the synthesis of 2-acrylamido glycolic acid: here the starting reagents are acrylamide and glycolic acid and condensation on the nitrogen is obtained in highly concentrated sulphuric acid (Schouteeten et al., 1978).

The AMPS chemical, a most useful compound to have when generating wide pH intervals (e.g., IPG pH 3–10), is the species that, in a number of publications, we have labelled as $pK = 0.8$. We now report it here with a $pK = 1.0$ after a publication by Boschetti (1985) attributing a $pK = 1.0$ to an analogous compound, sulphopropyl (SP)-trisacryl. SP-trisacryl could in fact be used as a substitute for AMPS since, due to its similar structure, it should be incorporated at just about the same efficiency (however, we have no experience with this chemical).

Other chemicals could be used as alternative buffers. Thus, in the early days of IPGs, LKB scientists used to incorporate acrylic acid (pK 4.6) as a weakly acidic counterion (B. Bjellqvist, personal communication). The use of acrylic acid was also reported independently by Righetti and Macelloni (1982) and later by Charlionet et al. (1984). There might also be a need for additional chemicals. Thus, according to our computer simulations, due to the big pK gap between the last of the acidic (pK 4.6) and the first of the basic (pK 6.2) Immobilines it would be quite desirable to have a species with a pK around 5.5. Curiously, this compound exists, although it is a dicarboxylic acid: itaconic acid ($pK_1 = 3.85$; $pK_2 = 5.45$). We had advocated its use long ago, in the synthesis of conventional carrier ampholytes, as itaconic acid-reinforced CAs were found to have a much more even conductivity and buffering capacity (β) in the proximity of the much dreaded pH 6.2 β minimum and conductivity gap (Righetti et al., 1977). Charlionet et al. (1984) have in fact recently proposed again the use of itaconic acid in IPGs, although oligoprotic species should be used with parsimony in this technique (Celentano et al., 1988).

1.4. Structure and synthesis of basic Immobiline

Synthesis of pK 6.2 Immobiline (2-morpholinoethyl acrylamide)
To a mechanically stirred, cooled (5°C) solution of 2-morpholino ethylamine (0.07 mol, 9.1 ml) and triethylamine (6.9 ml, 0.05 mol) in dry toluene (90 ml), acryloyl chloride (0.05 mol, 4 ml) was added dropwise. After stirring for 2 h, the reaction mixture was washed with 15% Na_2CO_3. The aqueous solution was extracted three times with chloroform. The combined organic phases were dried with Na_2SO_4 and evaporated in vacuum. The white solid obtained was crystallized from a hot mixture of hexane, ethyl acetate, chloroform (10 : 3 : 1) to give 2.8 g of 2-morpholinoethyl acrylamide (30% yield).

^{1}H-NMR ($CDCl_3$), δ: 2.55 ppm (6H, $(CH_2)_2O$, CH_2–N=, m), 3.5 ppm (2H, NH–$\underline{CH_2}$–, q), 3.8 ppm (4H, –$N(CH_2)_2$, m), 5.8 ppm (1H, =CH–, m), 6.25 ppm (2H, CH_2=, m). IR ($CHCl_3$): 1680 and 1632 cm^{-1}.

Synthesis of pK 7.0 Immobiline (3-morpholinopropyl acrylamide)
To a mechanically stirred, cooled (5°C) solution of 3-morpholino propylamine (0.07 mol, 10.2 ml) and triethylamine (6.9 ml, 0.05 mol) in dry toluene (90 ml), acryloyl chloride (0.05 mol, 4 ml) was added dropwise. After stirring for 2 h, the reaction mixture was washed with 15% Na_2CO_3. The aqueous solution was extracted three times with chloroform. The combined organic phases were dried with Na_2SO_4 and evaporated in vacuum. The crude product was purified by silica gel column chromatography using as eluent a 9 : 1 mixture of CH_2Cl_2/methanol to give 3.6 g of morpholino propyl acrylamide (35% yield).

^{1}H-NMR ($CDCl_3$) δ: 1.75 ppm (2H, –CH_2–, q), 2.45 ppm (6H, CH_2–$N(CH_3)_2$, m), 3.45 ppm (2H, NH–$\underline{CH_2}$–, q), 3.75 ppm (4H, $(CH_2)_2O$–, m), 5.8 ppm (1H, =CH–, m), 6.35 ppm (2H, CH_2=, m). IR ($CHCl_3$): 1680 and 1632 cm^{-1}.

Synthesis of pK 8.5 Immobiline (N,N-dimethylaminoethyl acrylamide)
To a mechanically stirred, cooled (5°C) solution of 2-dimethylaminoethyl amine (0.07 mol, 7.6 ml) and triethylamine (6.9 ml, 0.05

mol) in dry toluene (90 ml), acryloyl chloride (0.05 mol, 4 ml) was added dropwise. After stirring for 2 h, the reaction mixture was washed with 15% Na_2CO_3. The aqueous solution was extracted three times with chloroform. The combined organic phases were dried with Na_2SO_4 and evaporated in vacuum. The crude product, a pale yellow liquid, was distilled under vacuum (155°C, 0.05 mmHg, in presence of polymerization inhibitors) to give 4.26 g of *N,N*-dimethyl aminoethyl acrylamide (60% yield).

^{1}H-NMR ($CDCl_3$) δ: 2.32 ppm (8H, $(CH_3)_2N-CH_2$, m), 3.5 ppm (2H, $NH-\underline{CH_2}-$, q), 5.8 ppm (1H, =CH–, m), 6.35 ppm (2H, $CH_2=$, m). IR ($\overline{CHCl_3}$): 1680 and 1632 cm^{-1}.

Synthesis of pK 9.3 Immobiline (N,N-dimethyl aminopropyl acrylamide

To a mechanically stirred, cooled (5°C) solution of 3-dimethyl-amino-1-propyl amine (0.07 mol, 8.75 ml) and triethylamine (6.9 ml, 0.05 mol) in dry toluene (90 ml), acryloyl chloride (0.05 mol, 4 ml) was added dropwise. After stirring for 2 h, the reaction mixture was washed with 20% Na_2CO_3. The aqueous solution was extracted three times with chloroform. The combined organic phases were dried with Na_2SO_4 and evaporated in vacuum. The crude product, a pale yellow liquid, was distilled under vacuum (175°C, 0.5 mmHg, in presence of polymerization inhibitors) to give 4.6 g of *N,N*-dimethyl aminopropyl acrylamide ^{1}H-NMR ($CDCl_3$) δ: 1.75 ppm (2H, $-CH_2-$, q), 2.4 ppm (8H, $-CH_2-N(CH_3)_2$, m), 3.4 ppm (2H, $-NH-\underline{CH_2}-$, q), 5.65 ppm (1H, =CH–, m), 6.25 ppm (2H, $-CH_2=$, m). IR ($CHCl_3$): 1680 and 1632 cm^{-1}.

Synthesis of the pK 10.3 buffer (N,N-diethyl aminopropyl acrylamide)

To a stirred, cooled (5°C) solution of 3-diethylamino-1-propyl amine (0.07 mol, 11.03 ml) in dry toluene (90 ml), acryloyl chloride (0.05 mol, 4 ml) was added dropwise. After stirring for 2 h, the reaction mixture was acidified with 12 N HCl. The oily precipitate was dissolved in 20% Na_2CO_3 and extracted with CH_2Cl_2. After drying with Na_2SO_4, the excess solvent was evaporated in vacuum. The crude product obtained was distilled under vacuum (200°C,

TABLE 1.3
Basic acrylamido buffers

pK [4]	Formula	Name	M_r	Source
6.2	$CH_2=CH-CO-NH-(CH_2)_2-N$ 	2-morpholino ethylacrylamide	184	[1]
7.0	$CH_2=CH-CO-NH-(CH_2)_3-N$ 	3-morpholino propylacrylamide	199	[1]
8.5	$CH_2=CH-CO-NH-(CH_2)_2-N(CH_3)_2$	*N,N*-dimethyl aminoethyl acrylamide	142	[1]
9.3	$CH_2=CH-CO-NH-(CH_2)_3-N(CH_3)_2$	*N,N*-dimethyl aminopropyl acrylamide	156	[1]
10.3	$CH_2=CH-CO-NH-(CH_2)_3-N(C_2H_5)_2$	*N,N*-diethyl aminopropyl acrylamide	184	[1]
>12 [3]	$CH_2=CH-CO-NH-(CH_2)_2-N(C_2H_5)_3$	QAE-acrylamide	198	[2]

[1] Pharmacia-LKB Biotechnology, Uppsala, Sweden.
[2] IBF, Villeneuve La Garenne, France.
[3] *N,N,N*-triethylamino ethyl acrylamide.
[4] All pK values (except for QAE-acrylamide) measured at 10°C.

0.05 mmHg, in presence of polymerization inhibitors) to give 6.54 g of *N,N*-diethylamino propyl acrylamide (70% yield).

^{1}H-NMR ($CDCl_3$) δ: 1 ppm [6H, $N(CH_2\text{-}\underline{CH_3})_2$, m], 1.7 ppm (2H, $-CH_2-$, q), 2.55 ppm (2H, $=N-CH_2$, m), 3.5 ppm (2H, $NH-\underline{CH_2}$, q), 5.65 ppm (1H, =CH–, m), 6.3 ppm (2H, CH=, m). IR ($\underline{CHCl_3}$): 1680 and 1632 cm^{-1}.

Table 1.3 lists the six additional basic acrylamido derivatives we propose for IEF in IPGs. With the combined data of this and of the previous section (1.3), we have listed a set of eleven (10 in reality, as the pK 4.4 Immobiline is seldom used today) acrylamido buffers, nine of which are weak acids and bases and two strong titrants, able to cover the entire pH 2.5–11 interval. With this, we feel that the IPG technique has come of age and will long remain the unrivalled electrokinetic method for charge-fractionation of amphoteric molecules.

Generally speaking, the synthetic route of the basic chemicals is a classical reaction, by which an acrylic double bond is introduced in a diamine of general formula $R_2N-(CH_2)_n-NH_2$. This is obtained by condensing the primary amino group of the latter with acryloyl chloride in a basic milieu able to neutralize the HCl produced in the formation of the amido bond. The tertiary amino group at the opposite extreme (i.e., in distal position to the double bond) will provide a protolytic moiety with pK values varying according to the type of substituents. Just as an example, the synthetic route for the pK 6.2 Immobiline (2-morpholino ethyl acrylamide) was fully detailed already in 1966 by Danusso et al., who synthesized (and patented) exactly the same compound and prepared morpholino-polyacrylamides atactic and partially stereoregular. Curiously, these slightly basic co-polymers were synthesized to neutralize the cytotoxic properties of silica powder, in the hope of preventing silicosis in miners.

Although a lot of other slightly different chemicals could be synthesized, I feel that the set of compounds presented here represents possibly the best set available. When LKB scientists choose their seven Immobiline products, they selected them under the stringent requirement that their reactivity would be very similar to that of the neutral monomers (acrylamide and Bis). This is certainly so: in presence of oxygen, the co-polymerization efficiency is 85%, and 95% under anaerobic conditions (Righetti et al., 1984). In the early days of IPGs, the only chemical available, vinyl-histidine, had to be incorporated under a flux of gamma rays produced by a Co bomb, (Righetti, 1988). *N,N*-dimethylamino propyl methacrylamide (DMAPMA), proposed in 1982 by Righetti and Macelloni and later exploited by Charlionet et al. (1984), is an example of a substitute for the pK 9.3 Immobiline: however, due to the presence of an extra methyl group, it is bound to be somewhat more hydrophobic than the latter and its reactivity might be different, due to its being a methacrylic compound. However, there could be some valid alternatives for the strong basic titrant (pK > 12): one could be methacrylamido propyl trimethyl ammonium chloride (MAPTAC) (Righetti and Macelloni, 1982), the other could be QAE-Trisacryl. MAPTAC is bound to be considerably less hydrophobic than QAE-acrylamide, as it

contains a trimethyl ammonium, as opposed to a triethyl ammonium moiety. However, it is commercially supplied as a chloride salt, while it is highly desirable to have it as a free base. The latter, however, is extremely unstable and spontaneously autopolymerizes. Nevertheless, with the recently proposed solvent, *n*-propanol (Gåveby et al., 1988), it should be possible to store it properly as a free base. QAE-Trisacryl is also attractive as a quaternary acrylamido titrant, due to the strong hydrophilicity of this molecule. This compound too tends to autopolymerize quite easily, but again storage in *n*-propanol should stabilize it.

1.5. Physico-chemical properties of Immobiline

In terms of their physical state at room temperature, only the pK 8.5, 9.3 and 10.3 species are liquid, all the other compounds being solid, white powders.

The most important parameter when discussing IPG technology is the correct assessment of the pK value of all the chemicals used to produce the pH gradient, since only the proper knowledge of this value and of its variation under different conditions (e.g., temperature, ionic strength, dielectric constant of the solvent) will ensure reproducible results under fully controlled experimental parameters.

One of the most critical factors for reproducible results is control of the temperature during an IPG run. Usually, up to now, physical chemists have always given pK values at 25°C, and this is the value which is most of the times tabulated in all text books. However, for protein stability during an electrophoretic run, it is not advisable to use such relatively high temperatures. In conventional IEF, the suggested temperature for an IEF run is between 2 to 4°C. However, due to difficulties in properly assessing a pK value at such a low temperature, we have measured the Immobiline pK values at 10°C and thus we suggest to always run an IPG gel at such a temperature.

Fig. 1.6 gives the temperature coefficients (dpK/dT) for the seven LKB Immobiline species in the range 10–25°C. In agreement with their known chemical composition, it can be seen that the

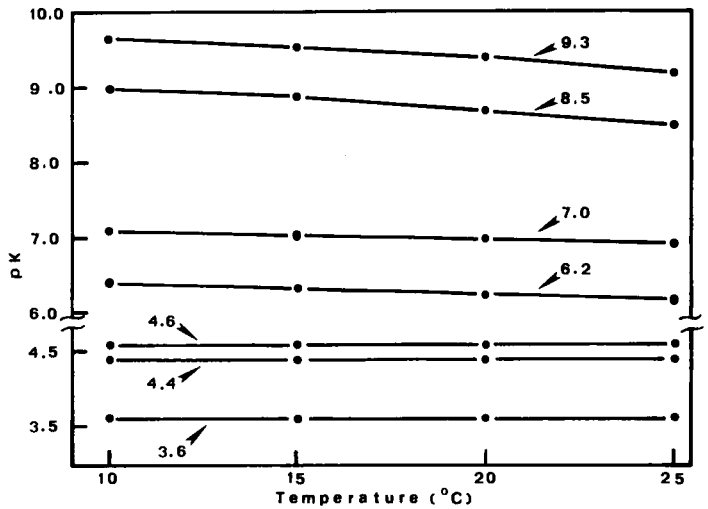

Fig. 1.6. Temperature coefficients (dpK/dT) for the seven Immobiline chemicals in the temperature range 10–25°C (from Righetti et al., 1983a; with permission of Elsevier).

three carboxyl compounds, which are known to have in general very small standard heats of ionization (ca. 1 kcal/mol), exhibit negligible pK variations in this temperature range. On the other hand, the four tertiary amino derivatives, known to have larger standard heats of ionization (6–14 kcal/mol) (Fredriksson, 1977), display progressively increasing ΔpK values in this temperature range (the largest one, $\Delta pK = 0.44$, corresponding to Immobiline of pK 8.5) (in connection with this, it should be stated that conventional carrier ampholytes, being composed of carboxyl and amino groups, exhibit similar temperature dependencies of their pKs). Therefore, for reproducible runs and calculations, all the experimental parameters have been fixed at 10°C (Bjellqvist et al., 1982).

Temperature is not the only variable that will affect Immobiline pKs (and therefore the actual pH gradient generated): additives in the gel that will change the water structure (chaotropic agents, such as urea) or will lower its dielectric constant will alter their pK values. As one of the most common additives, especially when

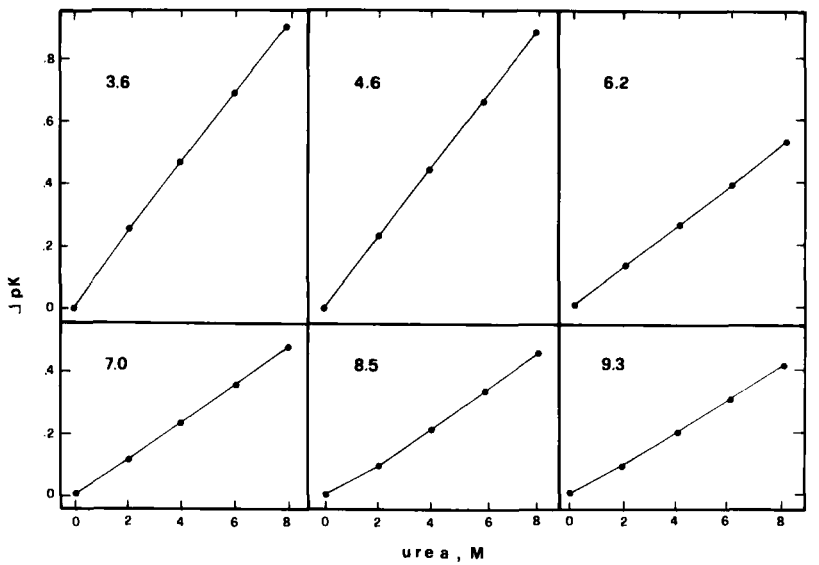

Fig. 1.7. Dependence of Immobiline pKs on urea concentration. A 20 mM solution of each Immobiline was titrated to its pK (with Immobiline of pK 3.6 or 9.3 as counter-ion). Aliquots of this stock solution were diluted to a 10 mM concentration in the presence of various amounts of urea. pH readings were made at 20°C. ΔpK refers to $pK_{urea} - pK_{water}$ (from Gianazza et al., 1983c; with permission of Verlag Chemie).

working with two-dimensional (2-D) maps, is 8 M urea, we have measured the ΔpK of each Immobiline in such solutions. As shown in Fig. 1.7, the effect of 8 M urea on Immobiline pK values is quite pronounced. Interestingly, the ΔpK (pK_{urea}-pK_{H_2O}) is higher for acidic Immobilines (0.9 pH unit for the pK 3.6) and progressively lower for the alkaline species, down to only 0.42 pH unit for the pK 9.3 compound. The new pK values, measured at 20°C, in 8 M urea are as follows: pK 3.6 = 4.46; pK 4.4 = 5.21; pK 4.6 = 5.48; pK 6.2 = 6.81; pK 7.0 = 7.48; pK 8.5 = 9.13 and pK 9.3 = 9.84. One of the best ways to incorporate urea in IPG gels (see also Chapter 3) is to polymerize an empty gel, wash it, dry it onto the Gel Bond PAG foil and reswell it in a solution of appropriate urea molarity (Gelfi and Righetti, 1984).

Another additive universally used, again particularly in 2-D maps of sparingly soluble samples, is a detergent moiety, especially the neutral (e.g., Nonidet P-40, NP-40) or the zwitterionic class, such as sulphobetaines or CHAPS. As shown in Fig. 1.8, the effect

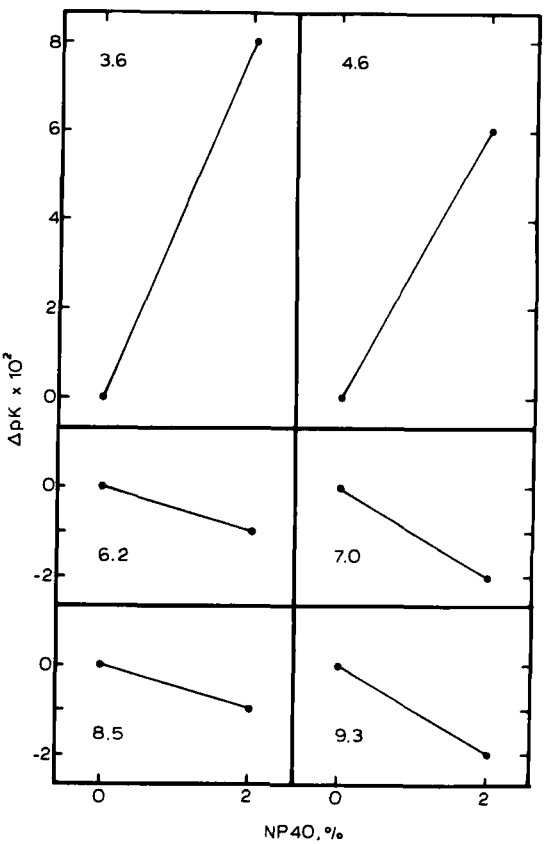

Fig. 1.8. Dependence of Immobiline pKs upon the presence of neutral detergent. A 20 mM solution of each Immobiline titrated at its pK was diluted to a 10 mM concentration in presence of 2% Nonidet P-40 (NP-40), and the new pH of the buffer was read at 20°C. The $\Delta pKs_{(NP\text{-}40\text{-}water)}$ are plotted. The new measured pKs (20°C, 2% NP-40) were: pK 3.6 = 3.65; pK 4.4 = 4.44; pK 4.6 = 4.65; pK 6.2 = 6.27; pK 8.5 = 8.58 and pK 9.3 = 9.40). Note the positive slope for the acidic and the negative increments for the four basic Immobilines (from Gianazza et al., 1983c; with permission of Verlag Chemie).

of 2% NP-40 on Immobiline pKs is quite small: it is virtually negligible for tertiary amine species (of the order of 0.01 pH unit) and slightly larger for the acidic compounds (up to 0.08 pH unit for the pK 3.6 Immobiline). This is comforting, and suggests that acidic and basic Immobilines have little tendency to conglomerate into detergent micelles, unlike conventional carrier ampholytes, which form mixed micelles with neutral detergents (Gianazza et al., 1979). Moreover, unlike in urea solutions, the behavior of acidic and basic Immobilines in detergents is monotonic; both species become weaker acids and weaker bases, respectively, which means a pK increase for the acids and a pK decrease for the bases.

Finally, we have enquired if the Immobiline chemicals could potentially interfere with protein amino acid analysis, as the IPG technique appears to be particularly attractive for preparative protein purification. We have thus taken the commercial chemicals

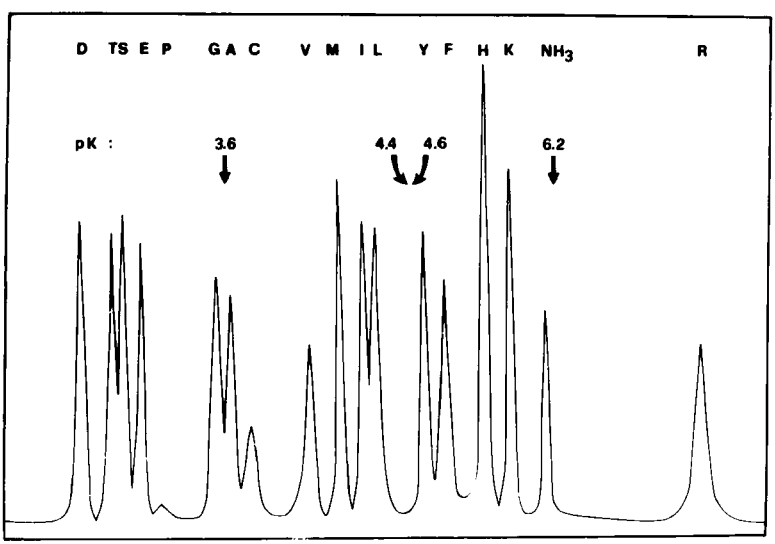

Fig. 1.9. Interference from Immobilines in amino acid analysis. A sample of each Immobiline was hydrolized and run on an ion-exchange automatic chromatograph for amino acid analysis. The elution profiles of their split products are shown by arrows on a typical chromatogram of natural amino acids, which are identified by their one-letter symbols in the top row (from Gianazza et al., 1983b; with permission of Elsevier).

and subjected them to standard hydrolysis for proteins (azeotropic HCl, 24 h, 110°C, nitrogen atmosphere) and run them through the amino acid auto analyzer. As shown in Fig. 1.9, four peaks appear in the eluate, obscuring the following peaks: alanine (pK 3.6), tyrosine (pK 4.4 and 4.6) and ammonia (pK 6.2). Thus, it is not desirable to have a peptide or protein peak, recovered from an IPG matrix, contaminated by the Immobiline chemicals. Luckily, this should be a very rare event: polymerization conditions have been described ensuring 85% conversion of monomers into the polymeric matrix (Righetti et al., 1984). In addition, free monomeric Immobilines, being charged, should be electrophoretically transported either at the anode or at the cathode. Moreover, Immobiline gels are in general extensively washed (3 times for analytical gels, up to 1 day for preparative gels) so that the possibility of coeluting, together with the protein zone of interest, short gel segments non-covalently bound to the bulk of the matrix, should be quite remote.

1.6. Problems with the Immobiline chemicals

Given such a sophisticated and highly reproducible methodology, the first true example of 'pH gradient engineering', it is important to know how to handle the Immobiline chemicals for optimum performance run after run. Curiously, in the first few years after the introduction of the IPG methodology, not much work was devoted to study the shelf life of the Immobiline species. As problems began to be reported by users, we started a long overdue study on the stability of Immobiline buffers (Pietta et al., 1985). Given their structure, it was apparent that these chemicals could degrade through two major pathways: (1) autopolymerization (a simple check for it is that the solution becomes slightly opalescent) or (2) hydrolysis along the amide bond, thus splitting the acrylamide moiety from the buffering group at the other extremity of the molecule (producing free acrylic acid and an amino acid in the case of the acidic Immobilines and free acrylic acid and a diamine in the case of the basic Immobilines). In both cases the results of an IPG experiment would fail. We thus studied the stability with time of

Immobiline solutions and of precast Immobiline gels as a function of pH and temperature. The results are summarized in Fig. 1.10A and B. Temperature seems to affect these chemicals most: whatever degradation occurs at 20°C within a few weeks time, it is operative

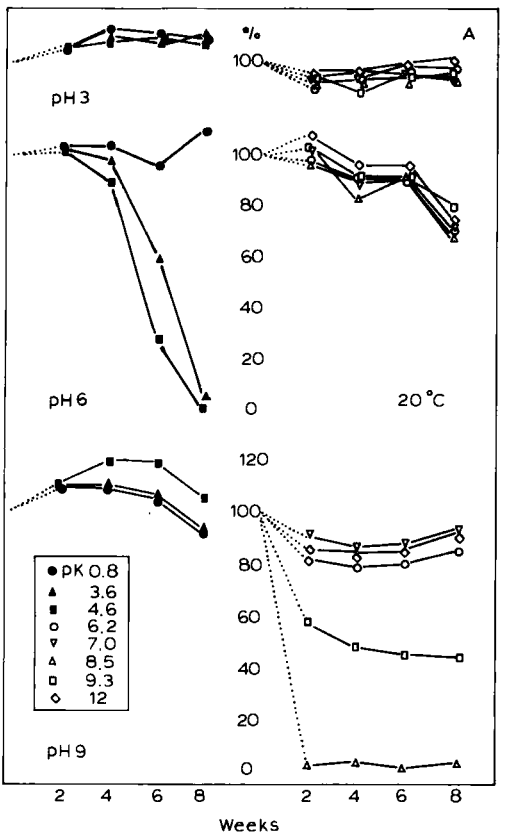

Fig. 1.10. Kinetics of Immobiline degradation upon storage at 20°C (A) or at 60°C (B). 200 μl of a solution 2.5 mM in each Immobiline at pH 3 (top), 6 (middle) or 9 (bottom panel) were sealed in vials and kept at 20°C or at 60°C for various lengths of time; quantitation of the remaining Immobiline was then performed by HPLC, by reversed phase on a micro-Bondapak C_{18} column and isocratic elution for the acidic monomers (data plotted on the left) or by cation exchange on a Zorbax SCX300 column under isocratic elution for the basic monomers (on the right). Symbols are listed in the inset (from Pietta et al., 1985; by permission of Verlag Chemie).

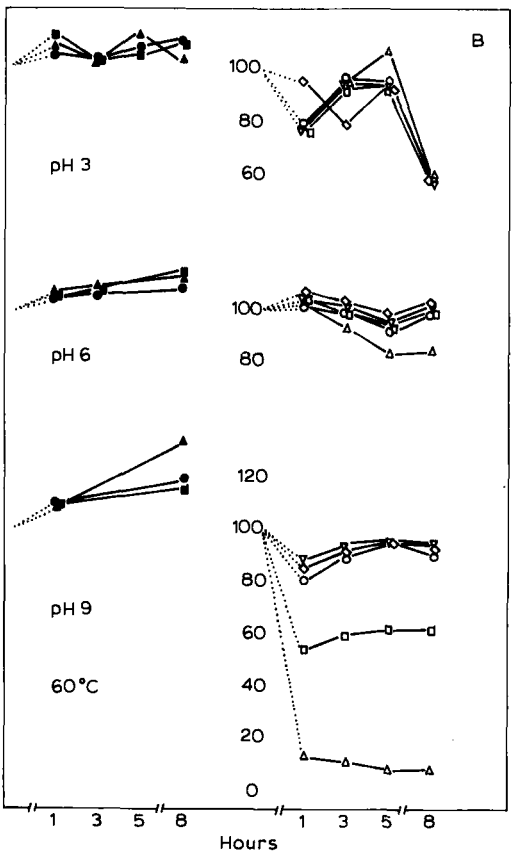

Fig. 10 (continued).

at 60°C within a few days or few hours. pH alters these buffers in different ways: acidic Immobilines (pKs 3.6, 4.4 and 4.6) are more degraded around neutrality (pH 6 to 7), whereas basic species (especially pKs 8.5 and 9.3) are extensively destroyed in alkaline solutions (pH 9), acidic pH values (pH 3 to 4) ensuring maximum stability for all Immobiline chemicals (it would thus appear that all these chemicals are most stable in their protonated form). For medium-term storage of precast gels, wet matrices exhibit least degradation if titrated to ca. pH 4, formic acid being the best

titrant because it can be efficiently removed during the focusing step with formation of the narrowest salt front at the anode (in addition, in its protonated form it is quite volatile). Dry matrices have much longer stability (> 2 months) but should be stored in presence of ca. 2% glycerol, to prevent the gel from cracking and peeling off the plastic support, which would occur in the absence of humidity. On the basis of these observations, it would appear that the best way to store the Immobiline chemicals would be to titrate their solutions (all stock Immobiline solutions, after being reconstituted in water, or other appropriate solvent, are 0.2 M) to ca. pH 4 (this ensuring absence of hydrolysis, autopolymeriation and inhibiting also CO_2 absorption in the case of the basic buffers). Although recommended by us (Pietta et al., 1985), this procedure has never been adopted in practice, as it would render extremely difficult any attempt at checking the pH of the limiting solutions when preparing any desired pH range. Thus, we proposed the most simple alternative: dispensing the stock Immobiline solutions (delivered as 25 ml bottles) into 5 ml aliquots, which would be kept frozen at −20°C. Even this solution, though, would turn out not to be optimal for very long term storage conditions (see below).

1.6.1. Hydrolysis of Immobiline

By an accident, we later discovered that even in the frozen state some of the alkaline Immobilines (notably the pK 9.3 species) would degrade, notwithstanding the low temperature value (−20 to 25°C) (Astrua-Testori et al., 1986). It just happened that, over a time period of 2 years, on a collaboration on the analysis of myosin chains by 2-D maps, I had to re-use the same chemicals kept frozen in the laboratory of Dr. J. P. Wahrmann in Paris. On an IPG range of barely 1 pH unit, we noticed a marked cathodic shift of the train of spots of myosin light chains. With the aid of the Henderson Hasselbalch equation we could recalculate the new apparent pH interval and determine the extent of loss of the pK 9.3 titrant (the IPG pH 4.1–5.1 interval used contained just two Immobilines, the pK 4.6 as buffering and the pK 9.3 as titrant ion; see Chapter 2). As shown in Fig. 1.11, the apparent degradation of the pK 9.3 chemical was as high as 20% per year, indeed much too high for

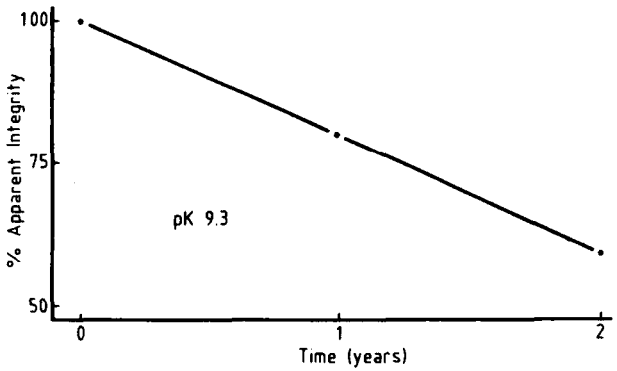

Fig. 1.11. Decay kinetics of the pK 9.3 Immobiline. A 0.2 M water solution of this buffer was kept frozen at −20°C over a 2-year period and analyzed at 1-year intervals. For calculating the percentage of hydrolysis, the pI shifts of a train of myosin light chains were used to obtain the modified pH intervals with the aid of the adapted H-H Eqn. 3 (from Astrua-Testori et al., 1986; with permission of Verlag Chemie).

reproducible results, as expected from the Immobiline technology. It appears strange that an hydrolysis reaction should occur in the frozen state, yet reactions in frozen solutions are not uncommon: e.g., Kiowsky and Pincock (1966) have reported the spontaneous mutarotation of glucose. In our case, since the Immobiline pK 9.3 is a liquid, it could be hypothesized that, during freezing, the pure water solvent and the pure Immobiline would separate into two distinct phases. Traces of humidity in the pure Immobiline phase (which would have a rather high pH, since a 0.2 M solution already exhibits an apparent pH value of 11.5) would thus favor a spontaneous hydrolytic process.

1.6.2. Autopolymerization

This discovery of the instability of the Immobilines chemicals caused considerable dismay, but it was not the end of our troubles. Soon a new, more devastating phenomenon could be appreciated in all of its disrupting power: autopolymerization. This is also quite deleterious for the IPG technique. Just like hydrolysis, autopolymerization occurs particularly to the four alkaline Immobilines and

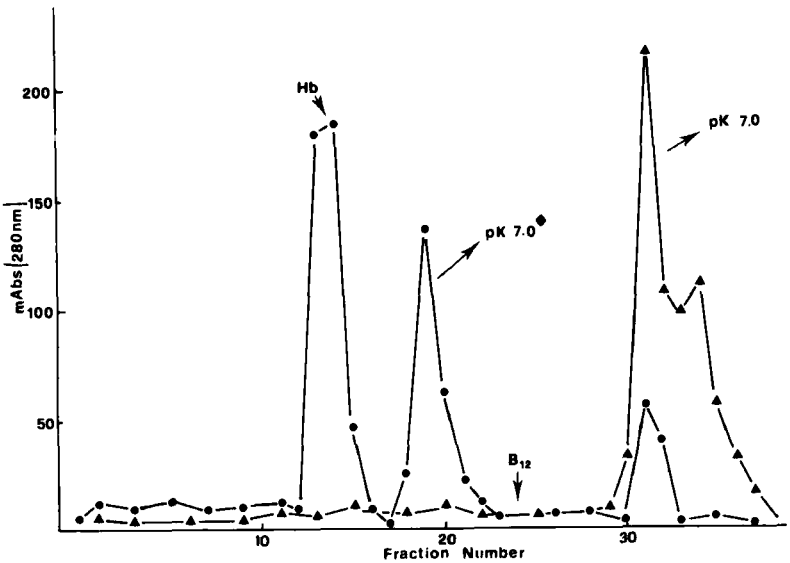

Fig. 1.12. Measurement of the polydispersity of Immobiline chemicals. A Bio-Gel P-2 column (0.8×45 cm) equilibrated with 50 mM phosphate buffer, pH 7.0, was loaded with 50 µl solutions of p*K* 6.2 Immobiline. The column was eluted at a rate of 3 ml/h and 0.8 ml aliquots collected. The absorbance (mAbs) was read at 280 nm. Hb: elution position of hemoglobin (void volume); B_{12}: elution position of vitamin B_{12}; triangles: control p*K* 6.2 (unable to precipitate ferritin); solid circles: mildly polymerized p*K* 6.2 Immobiline (able to precipitate ferritin) (from Rabilloud et al., 1987b; with permission of Verlag Chemie).

is purely autocatalytical, as it is greatly accellerated by deprotonated amino groups (Rabilloud et al., 1987b). By this process, oligomers and *n*-mers are formed, which stay in solution and can even be incorporated into the IPG gel, as in principle they still contain a double bond at one extremity (unless they anneal to form a ring). As shown in Fig. 1.12, upon analysis on a Bio Gel P-2 column, these autopolymerization products are seen to range in size from simple dimers and trimers to molecules having the same elution volume of a 64,000 dalton protein, like hemoglobin. Analysis of the p*K* 8.5 Immobiline stored frozen revealed, after more than 6 months of storage, the presence of ca. 3% polymer (Fig. 1.13). These products of autopolymerization, when added to pro-

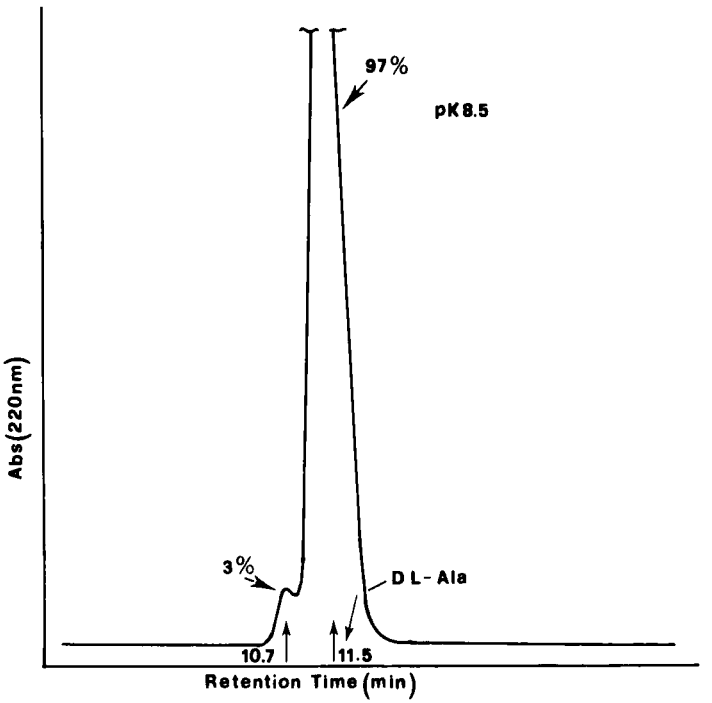

Fig. 1.13. Control of the degree of polymerization of the Immobiline chemicals. Analysis performed by HPLC in a Bio-Gel TSK 30 column. Samples and column were buffered at pH 6.8 with 20 mM phosphate. 10 μl of 50 mM pK 8.5 Immobiline were injected and eluted at 1 ml/min flow rate. The eluate was monitored at 220 nm and automatically integrated. Note the large amount of polymeric material (3%) present in the sample (a 0.2 M water solution of pK 8.5 stored frozen for up to 1 year). D,L-Ala: elution position of alanine, marker of the column total volume (from Rabilloud et al., 1987b; with permission of Verlag Chemie).

teins in solution, are able to bridge them via two unlike binding surfaces (ionic on one side, hydrophobic in the opposite surface; see the model of bridging of two ferritin molecules depicted in Fig. 1.14); a lattice is formed and the proteins (especially larger ones, like ferritin, α_2-macroglobulin, thyroglobulin) are precipitated out of solution. This precipitation power is quite strong and begins already at the level of short oligomers (> decamer). There is an

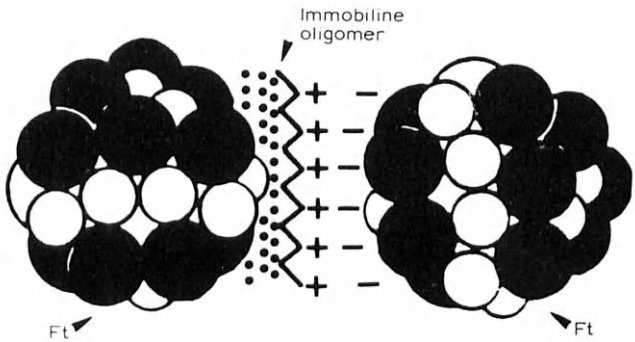

Fig. 1.14. Model of the interaction among ferritin and precipitating Immobilines. This model is a modification of a previous one (Righetti et al., 1987c) in which a stack of 5–6 basic Immobilines was supposed to bridge ferritin (Ft) shells by two unlike types of interaction: ionic at one extremity, hydrophobic at the opposite end. In the present model, it is shown that the 'zipper' between two ferritin macroions is indeed a short oligomeric chain, possibly 10–12 residues in length. The oligomer is seen to have two unlike surfaces, ionic and hydrophobic (the latter represented as a π-electron cloud on the left side (from Rabilloud et al., 1987b; with permission of Verlag Chemie).

easy test to check for the presence of polymers, called 'ferritin precipitation test' (Righetti et al., 1987c and d). As a short term remedy, we have described an easy method for oligomer removal, based on adsorption onto hydrophobic polymer phases (e.g., the XAD-2 polymer or a C_{18}-bonded phase (Righetti et al., 1987d; Rabilloud et al., 1987a). This is quite easily achieved since, at alkaline pH values, where the alkaline Immobiline species are extensively deprotonated, oligomers and *n*-mers would exhibit a marked hydrophobic character. It turned out that this problem of autopolymerization, long neglected or simply ignored by all of us, had in fact plagued most of the users of the IPG technique up to the year 1987. For scientists trying to apply the IPG method as a first dimension in 2-D maps, the results had been quite disastrous. As an example, Hochstrasser et al. (1986a) had lamented substantial losses of all polypeptide chains, in 2-D maps of human sera, larger that 100,000 daltons, no doubt due to their precipitation out of solution by oligomers and *n*-mers present in alkaline Immobilines.

1.6.3. pH-dependent formation of N-oxides

The two degradation pathways mentioned above are not all the problems associated with the Immobiline chemicals. We have now discovered a third accident, which can cause severe problems when focusing cysteine-rich proteins in alkaline pH ranges: oxidation of the tertiary amino group of the alkaline buffers. We are reporting it here separately, since the two former phenomena are common to all Immobiline chemicals (acidic and basic, even though only the basic species produce serious problems), whereas this last degradation pathway occurs only with the alkaline species.

Table 1.4 summarizes all the possible decomposition routes of Immobilines (again, with particular emphasis on the alkaline species), while Fig. 1.15 gives an example of the products generated upon degration of a specific Immobiline, the pK 9.3 compound. Formation of N-oxides could possibly occur even during storage of the pure chemicals (the kinetics of this phenomenon have not been investigated, but it is surely a slow reaction and can be avoided by storing the alkaline chemicals under an inert atmosphere); what we have observed, though, is the instantaneous, quite extensive oxidation produced in all alkaline Immobiline species by the persulphate used as catalyst during the gel polymerization process (Righetti et al., 1989). At appropriate pH values, all alkaline Immobiline chemicals are modified by persulphate under the standard, commonly adopted polymerization conditions. The oxidized Immobiline species form products which show similar types of chromophores in the 320 to 350 nm wavelength range. By measuring the absorbance of these peaks, we were able to understand the mechanism of formation of these N-oxides: it appears that this oxidation phenomenon is strongly pH-dependent. As shown in Fig. 1.16, when plotting the extent of oxidation for 4 alkaline Immobilines

TABLE 1.4
Degradation pathways of alkaline Immobilines

(1) Hydrolysis to acrylic acid and a diamine
(2) Autopolymerization to oligomers and n-mers
(3) pH-dependent formation of N-oxides

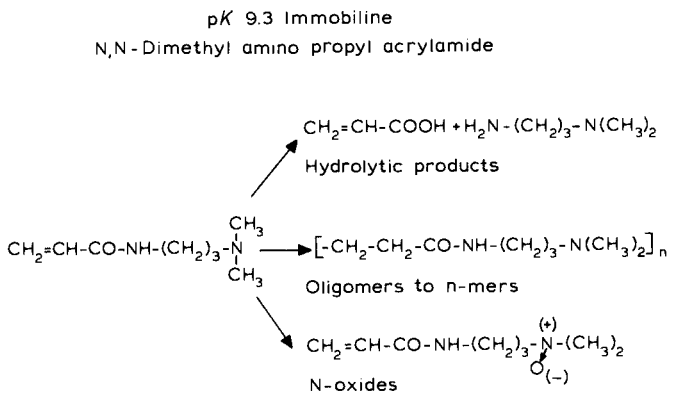

Fig. 1.15. Demonstration of the three degradation pathways of alkaline Immobilines, exemplified by the example of the pK 9.3 species. Note that the first two degradation processes are in common with the acidic Immobilines, while the oxidation phenomenon only occurs with the alkaline compounds.

(pKs 6.2, 7.0, 8.5 and 9.3) as a function of pH of polymerization, a family of quasi-linear, quasi parallel curves is obtained, whose intercept on the x-axis gives the pH value at which the persulphate effect is abolished. A general rule can thus be derived: for all alkaline Immobilines, persulphate oxidation is essentially abolished 1.5 pH unit below the pK of each species. Protonation of the tertiary amino group seems thus to be the golden rule for preventing oxidation. It is clear that, if gels (containing wide pH gradients utilizing all alkaline Immobilines) were polymerized at pH 5, essentially no oxidation of Immobilines would occur. However, at this pH value, poor incorporation of Immobilines and poor gelling conditions are obtained (Righetti et al., 1984). Thus, we propose an alternate route: polymerization is still carried around pH 7 as recommended (Righetti, 1984) and the two oxidized morpholino derivatives (see Fig. 1.16) reduced by a short washing step in 100 mM ascorbic acid at pH 4.5 (Righetti et al., 1989a).

The presence of these $R_3N^+O^-$ species would affect an IPG run in at least two ways: (a) by altering the slope of the theoretically predicted pH gradient (N-oxides cannot be protonated any longer) and (b) by oxidizing –SH groups in Cys residues. Since the red-ox potential in reactions involving nitrogens is of the order of +0.5 V,

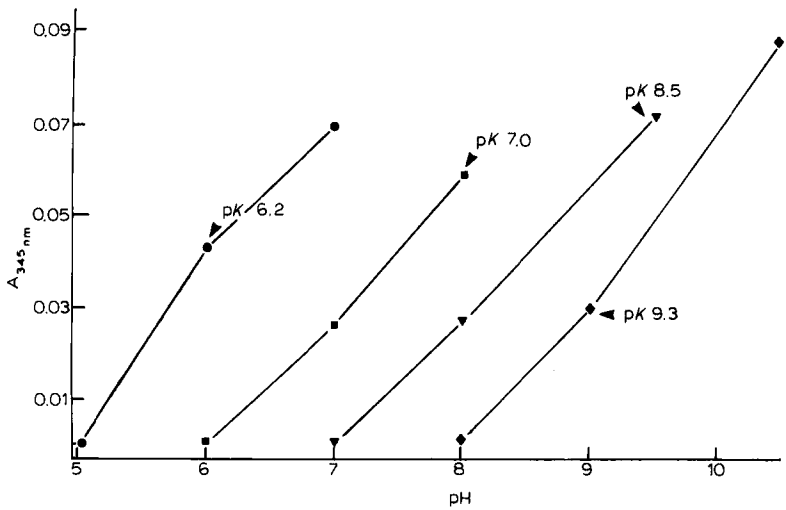

Fig. 1.16. Oxidation vs. pH for the four alkaline Immobilines. Four curves are costructed by taking the $A_{345\ nm}$ of the four different Immobilines polymerized at three different pH values and plotting them vs. the respective pH values. A set of quasi-parallel, quasi-linear curves is obtained, whose intercept on the x-axis defines the pH values at which each Immobiline species is not oxidized by incubation with persulphate during polymerization. Note that total extinction of the AP oxidation power is obtained only by polymerizing a gel at pH 5 (from Righetti et al., 1989a; with permission from MacMillan Press).

while the red-ox potential of similar reactions involving sulphur is of the order of -0.5 V, it is clear that the N-oxides formed during gel polymerization and covalently bound to the matrix will act as oxidizing agents, at alkaline pH values, on free –SH groups (possibly even on –S–S– bridges) producing species of higher oxidation level. An example of this is shown in Fig. 1.17a: the α-chains of human hemoglobin show a strong band with higher isoelectric point, which we attribute to the formation of an inter-chain –S–S– bridge, with loss of negative charges due to the ionization of free –SH groups. Conversely, when the same gel, prior to the run, is reduced by a washing step in 100 mM ascorbic acid, at pH 4.5, the oxidation band of α-globin chain completely disappears (Fig. 1.17b).

We had recently become aware (Righetti et al., 1989a) that, when focusing in strongly alkaline pH gradients, strange phenomena occurred to cysteine-rich protein molecules. For example, in the case of pro-urokinase (a 46 kDa protein containing 24 Cys out of a total of 411 amino acids and exhibiting a pI of ca. 9.8) a size-homogeneous preparation would be resolved, in IPGs, in an

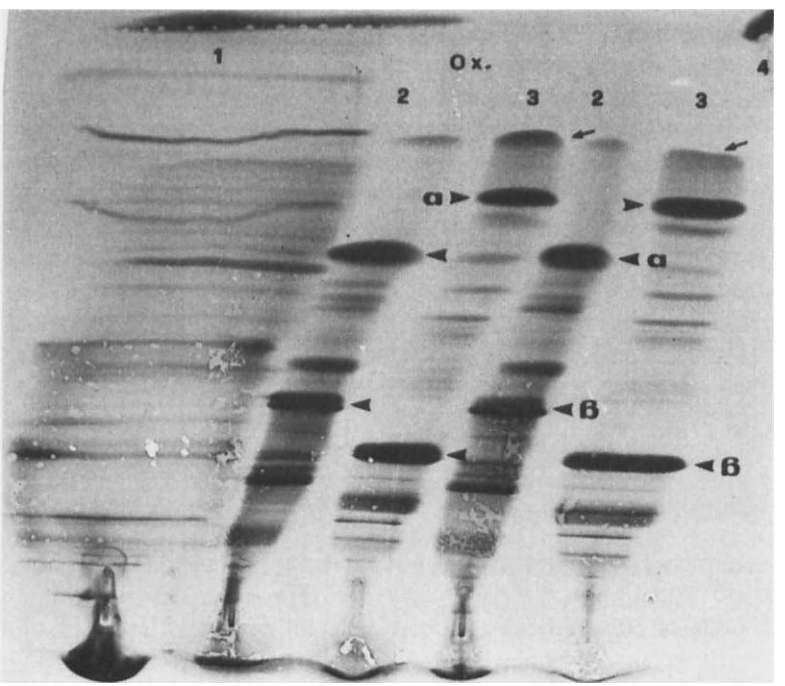

Fig. 1.17a. Oxidation power of an alkaline IPG gel. A 4% *T*, 4% *C* gel containing all the four alkaline Immobilines in the pH 6.3–10.5 range was polymerized under standard conditions. After opening the cassette, the gel is cut into two halves: one half is reduced in 200 ml of 100 mM ascorbic acid, pH 4.5, for 45 min and then washed in distilled water for 3 times, while the reduction step is eliminated into the other one. They are both re-swollen in 0.5% Ampholine pH 6.5–10.5 and 8 M urea and subjected to 5 h of IEF at 10°C (500 V for the first 2 h followed by 3 h at 2000 V). Staining in Coomassie Blue R-250 in presence of Cu^{2+}. Samples: 1 and 4: cytochrome *c*; 2: globin chains from bovine hemoglobin; 3: human globin chains. Red.: reduced gel; Ox: untreated gel. Note, in the reduced gel, the total disappearance of the α-chain having cysteine oxidized to cystine (marked by an arrow (from Righetti et al., 1989a; with permission from MacMillan Press).

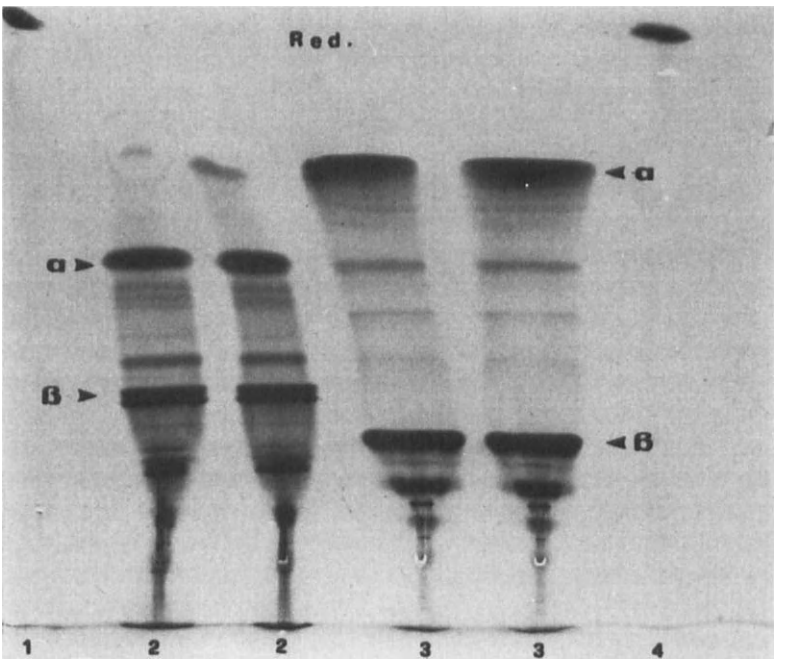

Fig. 17b.

extremely large number of bands (at least 10 major and 10 minor bands focusing in the pH 7–10 range). Having ruled out common sources of polydispersity, such as different degrees of glycosylation or IEF artefacts, such as binding to carrier ampholytes or carbamylation by urea, we could attribute this phenomenon to the coexistence among species in the –SH, –S–S– and SO_3^- states. This equilibrium could remain undetected in the majority of cases, since two thirds of the known proteins have isoelectric points falling in the acidic portion of the pH scale (Righetti et al., 1981). Given the mildly alkaline pK of the –SH group of Cys (pK = 8.3), the presence of an –SH rather than an –S–S– group would go undetected in acidic proteins, since neither would contribute to the surface charge. However, in urokinase-like molecules, due to the high isoelectric point of the 'native' forms and to the presence of

an unusually high number of Cys, an equilibrium between –SH and –S–S– states would be immediately visible by producing a series of charge-altered species. For example, the disappearance of two –SH groups, with the formation of a single –S–S– bridge, would produce species with a net loss of two negative charges, since, at the high pI of the 'native' protein molecules (pI 9.8), such groups would be fully ionized. It is a fact that the high pI pro-urokinase form was found to have almost no titratable –SH groups (less than 1 mol/mol of protein), in agreement with literature data, whereas the lower-pI components had a somewhat higher number of available –SH groups. However, this number was much lower than the theoretically expected amount of 24 –SH groups/mol of protein. As an answer we had proposed that oxidation of Cys could proceed to an irreversible state, i.e., cysteic acid. From a point of view of charge, high pI molecules carrying a free –SH group or its fully oxidized cysteic acid derivative should be quite indistinguishable, since both would carry a net negative charge. However, titration with Ellman reagent would reveal only the former and ignore Cys residues transformed to cysteic acid and in fact lower pI pro-urokinases had very few extra –SH groups which could be titrated (Righetti et al., 1989b).

Indeed, this phenomenon of Cys oxidation was described so long ago that it has probably been forgotten. Thus, as early as 1971, Jacobs (1971, 1973) first reported the partial modification of Cys and Met to cysteic acid and methionine sulfoxide, upon prolonged IEF, in bovine ribonuclease (also an alkaline protein). These oxidation phenomena could be largely suppressed by removal of O_2 from the IEF column (at that time most IEF experiments were run in a vertical column in a sucrose density gradient) and by addition of antioxidants, such as thiodiglycol and ascorbic acid. With the advent of open-face IEF gels, both of these remedies were abandoned as impractical (thiol groups are inhibitors of gel polymerization). However, with the IPG technology, such remedies can easily be exploited again, as IPG gels are routinely washed and dried and can be reswollen in the solvent of choice (including any desired reducing agent).

The present findings finally shed light on these phenomena: it is clear that these red-ox reactions occur during the IPG run itself

and that it is the IPG matrix which is directly responsible for oxidation of Cys residues in proteins. The alkaline Immobilines themselves (oxidized during the polymerization process by persulphate) act as electron acceptors in this red-ox process. We suggest that, during the IPG run (see Fig. 1.17a), two reactive Cys residues in a protein release two protons and two electrons which are captured by an oxygen atom bound to the tertiary amine, thus reducing the latter and forming a molecule of water. If this is the mechanism, it is clear that protection against oxidation should be obtained by direct reduction of the matrix. In fact, according to Fig. 1.17b, washing the matrix in 100 mM ascorbic acid, at pH 4.5, affords full protection against oxidation of the α-globin chains.

What happens to the four alkaline Immobilines when they are exposed to ammonium persulphate could simply be the addition of oxygen to the tertiary amino group giving amine oxides ($R_3N^+O^-$). It is known that this reaction is facile and usually occurs readily at room temperature in water, alcohol or benzene solvents in presence of even dilute solutions of organic peracids (as low as 3%, but here we demonstrate that it occurs even down to 0.04% AP) (Challis and Butler, 1975). The mechanism of tertiary amine oxide formation has not been studied in detail, but by analogy with primary amines, the reaction must involve attack by the electrophilic peroxidic oxygen on the amine lone pair, followed by anion elimination and proton loss, according to the following scheme:

$$R_3NO\text{–}O\text{–}C\text{–}R \rightarrow R_3N^+OH + CH_3COO^-$$

$$R_3N^+OH \rightarrow R_3N^+O^- + H^+$$

In accord with this conclusion, the reactions are first order with respect to each reactant, and the protonated amine is unreactive (see in fact Fig. 1.16).

1.7. Storage of Immobiline: a new generation

Given the above findings, by the end of 1986 our moral was at the lowest level and it was clear to all IPG users that the technique

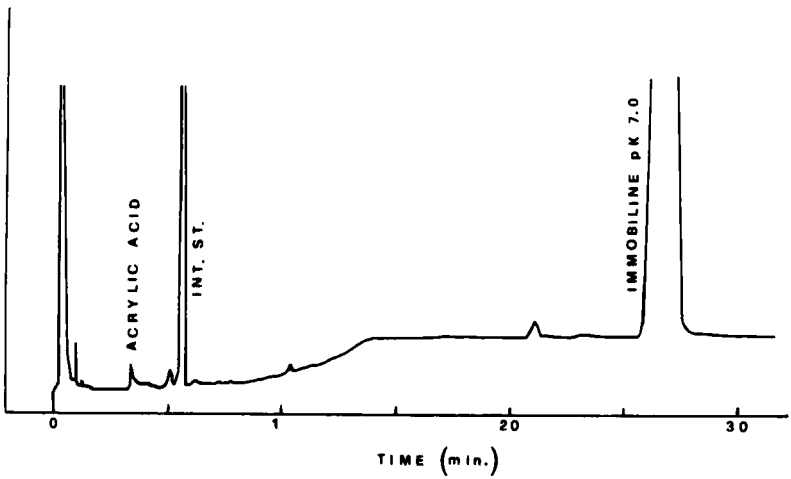

Fig. 1.18. GC analysis of Immobiline pK 7.0 as 0.2 M solution in n-propanol containing 191 μg/ml n-octadecane, on a fused silica capillary column coated with Carbowax 20 M. Program: hold 2 min at 115°C, then a temperature gradient from 115°C to 220°C at 6°C/min. Injector, 200°C. Flame ionization detector, 250°C. 2 μl sample injected. Attenuator, 0. The acrylic acid concentration in the sample was 0.10 mole-% (from Gåveby et al., 1988; with permission of Elsevier).

needed a new foundation if it had to survive and gain widespread acceptance. Thus, we joined forces again trying to solve this noxious problem of Immobiline degradation. B.M. Gåveby, from Bromma, visited us and proposed a radical solution: the Immobiline chemicals should be dispensed in a solvent able to completely inhibit both degradation pathways; n-propanol seemed to possess these special requirements. With the summer of 1988 a new generation, called Immobiline II, has been launched: the chemicals are supplied directly as 0.2 M solutions, in water (laced with inhibitor) for the acidic species, and in n-propanol for the basic compounds. Before, all Immobilines were supplied as free powders or liquids, in brown bottles to be added with 25 g of water in order to produce a 0.2 M solution.

The validity of this approach is shown in Fig. 1.18: here gas chromatographic analysis of pK 7.0 Immobiline, subjected to forced ageing in n-propanol for 5 days at 60°C, failed to reveal any trace of acrylic acid (the detection limit being 0.03 mol%). These data

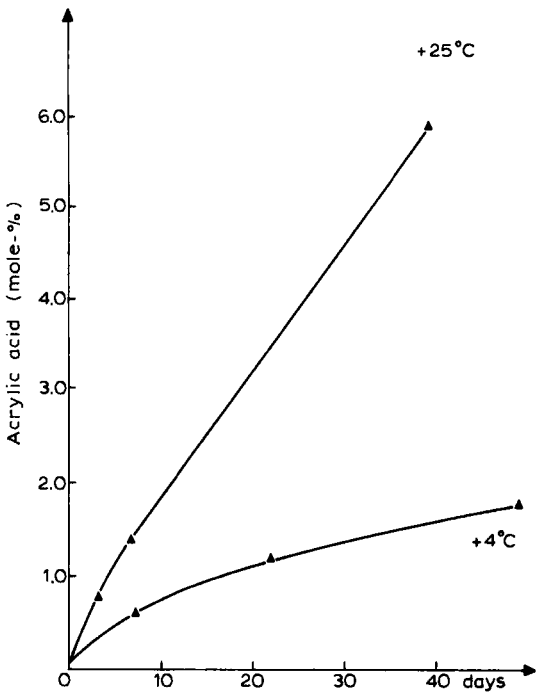

Fig. 1.19. Mole-% of acrylic acid formed in Immobiline pK 8.5 as 0.2 M solution in water at +4°C and at room temperature as a function of time. The acrylic acid concentration was determined by isotachophoresis (from Gåveby et al., 1988; by permission of Elsevier).

should be compared with Fig. 1.19: here the pK 8.5 Immobiline, dissolved in water, was stored at 25 or at 4°C: after 40 days, the former sample had already hydrolized to an extent of 6%, and the latter to a level of 2%. Also gel analysis confirmed the stability of *n*-propanol-dissolved Immobilines: separation of ovalbumin in a very narrow IPG range (pH 4.28–4.90) in which the pK 8.5 titrant had been subjected to forced ageing, showed identical banding patterns (Fig. 1.20; note that, if the same Immobiline had been dissolved in water, the tremendous acidification of the IPG range, due to incorporation of acrylic acid generated by the hydrolysis of pK 8.5, would have meant total loss of the ovalbumin bands at the

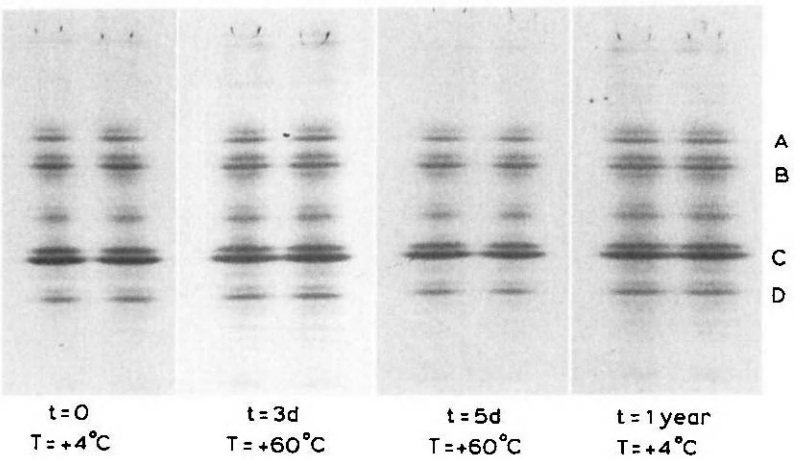

Fig. 1.20. IEF of ovalbumin in a pH 4.28–4–90 IPG range. The gel was made with Immobiline p*K* 4.6 as buffer and Immobiline p*K* 8.5 as titrant. The latter was dissolved in *n*-propanol (containing < 500 ppm H_2O) and incubated 3 or 5 days at 60°C or 1 year at 4°C. Note the identical banding patterns under all storage conditions (from Gåveby et al., 1988; with permission of Elsevier).

cathode). If we assume that 1% acrylic acid is the maximum tolerated level of degradation in the Immobiline II generation, we can ask how long a storage time would be required to reach this cut-off limit. The Arrhenius plot of Fig. 1.21 gives the answer for the two acidic Immobilines: by extrapolation, it appears that, to reach this guard level (1% acrylic acid) the p*K* 3.6 should be stored 1200 days and the p*K* 4.6 as much as 4800 days (both at a temperature of 8°C).

At the beginning, it was thought that, in order to guarantee this much extended stability, the alkaline Immobilines should be stored in totally anhydrous *n*-propanol. We then realized that, upon prolonged use, simply by opening and closing the bottles, these solutions would quickly absorb substantial humidity from the air (see the semi-log plot in Fig. 1.22); thus, it was decided that the solvent should already contain 1% water. In fact, all the data here presented refer to *n*-propanol containing 1% water as the Immobiline solvent. If there is any residual doubt on the validity of this approach, the data in Fig. 1.23 would easily dispell it. In these 2-D

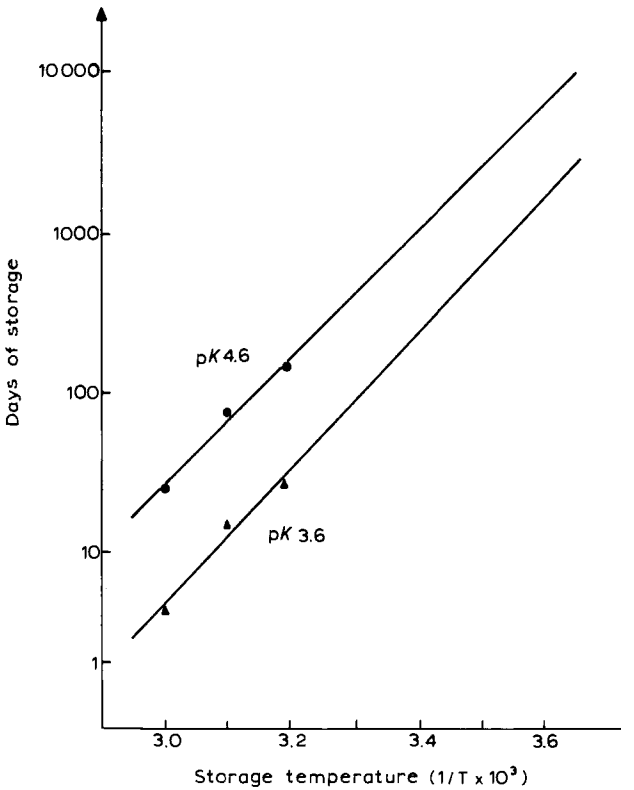

Fig. 1.21. Arrhenius plot showing how many days Immobilines pK 3.6 (▲▲▲) and pK 4.6 (●●●) can be stored at different temperatures as 0.2 M solutions in water (containing 5 ppm inhibitor) before the acrylic acid concentration reaches 1 mole-% of the Immobiline level. From extrapolated data, it appears that the pK 3.6 can be stored 1200 days and the pK 4.6 species 4800 days at +8°C (from Gåveby et al., 1988; with permission of Elsevier).

maps of seed proteins, the multitude of spots remains remarkably constant when using propanol-dissolved alkaline Immobilines, whereas, when the same species are dissolved in water, as done in the past, and subjected to forced ageing, all the train of alkaline spots is quickly lost at the cathodic end (take as reference spots Nos. 3 to 5).

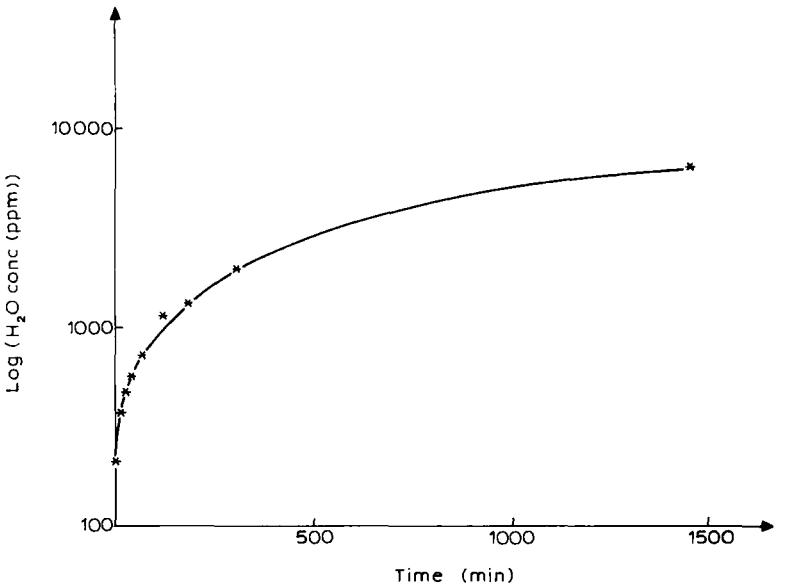

Fig. 1.22. Absorption of water in *n*-propanol from air, at 40% relative humidity at room temperature. Water content assessed by the Karl-Fischer method (from Gåveby et al., 1988; by permission of Elsevier).

The strategy now adopted seems to abolish efficiently both degradation pathways. The protocols proposed below vary according to the type and chemical properties of the Immobiline species.

Acidic Immobiline

Here the situation is quite simple. As these chemicals are most stable at the natural, acidic pH of their 0.2 M water solutions (Pietta et al., 1985), they are still dissolved in water and they are simply added with 5 ppm of an inhibitor (hydroquinone monomethylether), just to prevent any potential polymer formation. Under these conditions, acidic Immobilines appear to be quite stable and essentially free of acrylic acid and polymers (see also Fig. 1.21).

Basic Immobiline

Due to the much stronger reactivity of these four chemicals, the

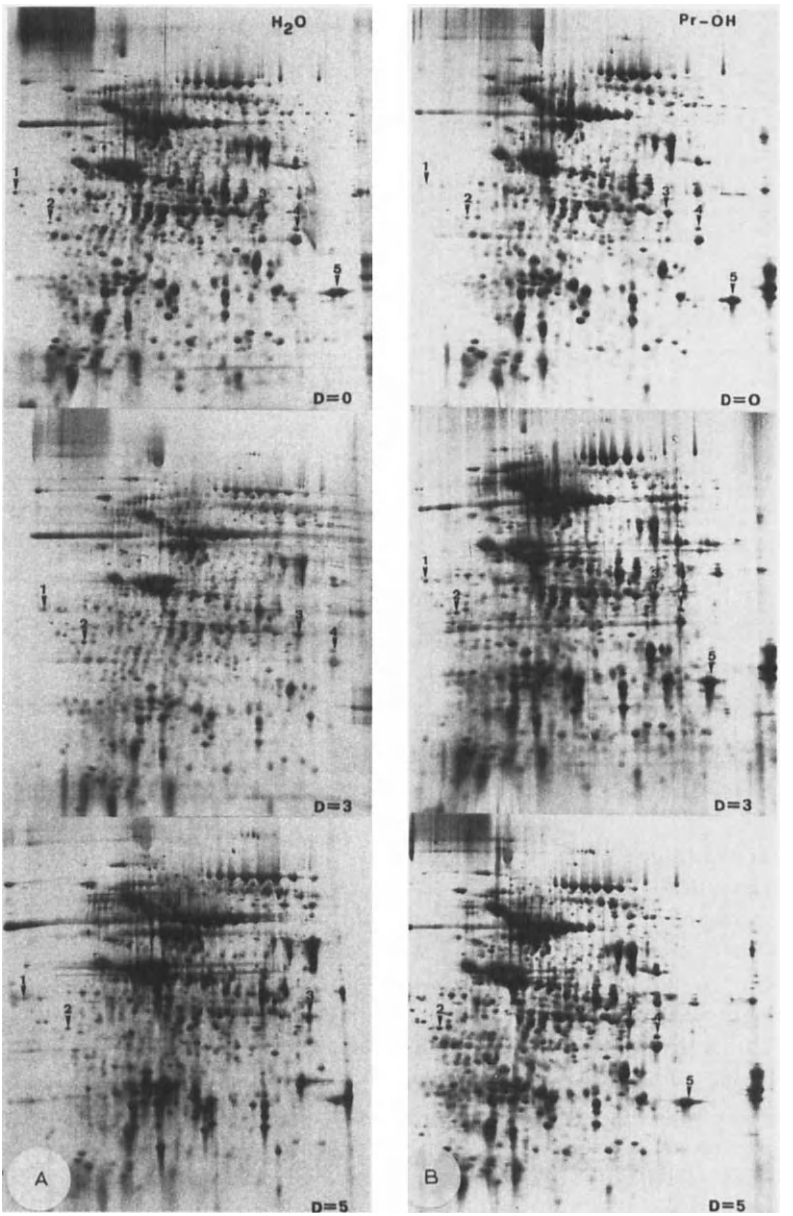
H_2O
Pr-OH
D=0
D=0
D=3
D=3
D=5
D=5
A
B

solvent has been substituted with *n*-propanol. Originally, we had aimed towards an almost anhydrous solvent (< 60 ppm water, obtained by storing *n*-propanol over molecular sieves). However, it was found that even in presence of 1% water, *n*-propanol solubilized alkaline Immobiline appear to be completely stable (devoid of acrylic acid and polymers) for at least 1 year of storage at +4°C.

There were several reasons for adopting *n*-propanol as solvent for alkaline Immobiline. First of all, the vapor pressure and boiling point of *n*-propanol are about the same as water. In addition, *n*-propanol is fully miscible with water in any ratio. However, there are some minor drawbacks with the use of *n*-propanol, which the users of IPGs should be aware of. At the maximum concentration of *n*-propanol (ca. 10%, in formulations utilizing all 4 alkaline Immobilines) dilute gels (e.g., in recipes utilizing only 3% *T* or lower) or gels polymerized with unproperly purified monomers, might not polymerize satisfactorily and have a gluey aspect (it is known that alcohols have in general an inhibitory power on polymerization). In such cases, we suggest increasing the amount of catalysts till proper polymerization is achieved (in general, at least 20% more of both catalysts, TEMED and persulphate, should be adopted). The second effect is simply due to the decrease of dielectric constant in presence of *n*-propanol. At the maximum added level (10%) there is a non-negligible effect on the p*K*s of the Immobiline, a positive shift (+0.07 pH units) for the acidic, a negative shift (−0.12 pH units) for the alkaline species (see Fig. 1.24). On the other hand the acidic and basic groups in proteins will show p*K* shifts of the same magnitude and only a minor shift

Fig. 1.23. Comparison of 2-D maps with the four alkaline Immobilines aged in water (A) or in *n*-propanol (B). First dimension: IPG pH 4–8 interval, gel 4% *T*, 4% *C* in presence of 8 M urea and 0.5 M NP-40. Second dimension: horizontal SDS-PAGE; stacking gel: 6% *T*, in 125 mM Tris–HCl, pH 6.8 and 0.1% SDS; running gel: 12–15% *T* gradient in 375 mM Tris–HCl, pH 8.8 and 0.1% SDS. Sample: *Vicia faba*, cv. Kristall. Ground bean seeds extracted in a lysis buffer containing 9 M urea, 2% NP-40, 2% 2-mercaptoethanol and 0.8% Ampholine pH 3.5–10. Two acidic (1 & 2) and 3 basic (3–5) spots are numbered in the maps. In A (labelled H_2O) the basic Immobiline have been dissolved in water and incubated at 60°C for zero time (D = 0), 3 days (D = 3) or 5 days (D = 5). The same applies to B (labelled Pr-OH) except that the basic Immobiline were dissolved in *n*-propanol (from Gåveby et al., 1988; with permission of Elsevier).

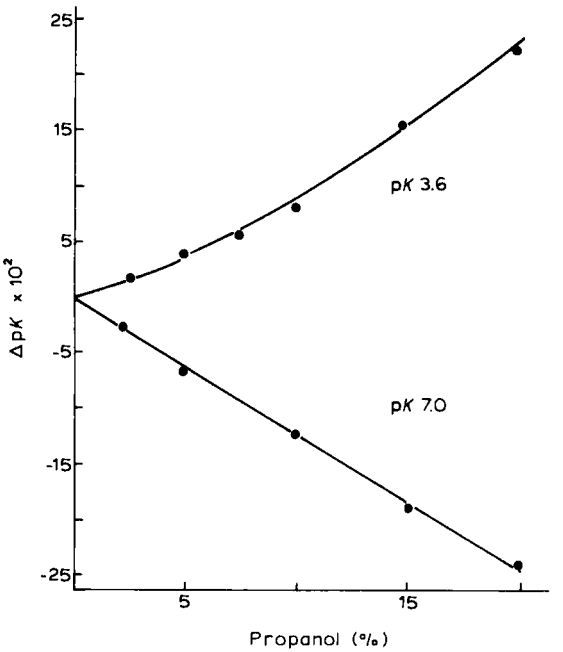

Fig. 1.24. pK shifts of one acidic (pK 3.6) and one alkaline (pK 7.0) Immobiline as a function of % n-propanol in water. The pK shifts have been determined by measuring the pH of solutions titrated to the pK value (2:1 molar ratio buffer:titrant) in presence of different amounts of n-propanol in water at 25°C. The concentrations used were 10 mM for the buffering group and 5 mM for the titrant (from Gåveby et al., 1988; with permission of Elsevier).

in the focusing position will thus be found. In addition, as the Immobiline gels are routinely washed, the n-propanol will only be present during polymerization, but not during the IPG run, so that there will be no detrimental effects.

I am confident that with the solutions adopted here for the second Immobiline generation, IPG technology should now be really trouble-free and I hope scientists will gain confidence in this methodology, by far the most advanced of all electrokinetic separations.

1.8. Conclusions

Although I had been asked to write a manual on IPGs in 1984, I felt so unsecure with regard to the technique that I had to turn down the offer. I kept turning down this proposal for all subsequent years and in fact, at the end of 1986, I thought that the situation was so bleak that, rather than writing a manual, I felt I should sink the technique altogether. The recent breakthroughs reinstate this methodology and I feel that now we can offer it quite safely to the scientific community. It was clear that the Achilles' heel of the technique was the instability of the Immobiline chemicals, especially the alkaline species. With the recent decoding of the structure of the Immobiline chemicals, as manufactured by LKB, we have also been able to propose quite a few additional ones, extending the fractionation range at both pH extremes, acidic and alkaline. We now have available recipes for pH gradients covering a pH range as wide as 8.5 pH units (pH 2.5 to 11.0). Thus, even though not theoretically predictable, immobilized pH gradients have a more extended fractionation capability than conventional isoelectric focusing in amphoteric buffers.

As we will see in the next chapter, there are still a few gaps in which it would be desirable to produce additional acrylamido buffers: one is the gap starting with Immobiline pK 4.6 and ending with the pK 6.2, the other is the gap between the pK 7.0 and 8.5 species. Ideally, two additional Immobilines with pKs centred midway in these two gaps would facilite pH gradient formulations, even though, with our proposed computer simulations (see Chapter 2) we could quite efficiently cover these two gaps with the presently available chemicals. Yet, the search continues and it might very well be that, in the near future, we could have, in addition to the 11 acrylamido buffers here proposed, some new ones coming.

Theory

2.1. *Per aspera ad astra*

In this chapter I will outline the basic theory allowing a correct use of the IPG technique. This will range from very simple equations, like the Henderson-Hasselbalch (H-H) taught in every freshman course, linking the pH prevailing in solution to the pK of a weak protolytic group and to its molar dissociate fraction, to quite complex formulas allowing the prediction of the pH course, buffering power and ionic strength generated upon mixing several buffering species titrated in a given pH interval. I know that in life sciences a lot of us general practitioners do not want to be bothered by complex theories and would rather have ready-made concoctions for immediate use. In those days and ages of speed, angel-dust, coca leaves, immediate results are sought with no suffering in between, getting there in a whiff, like in a trip provoked by hallucinogens. Yet, there is no easy trip in Science. As the title of this section says, the road to heaven (or to glory, or to success) is only through a hard path and dedicated labor. Thus, those of you who want to follow me in this strenuous path, perhaps will find this chapter most rewarding at the end. The others who just desire a quick recipe can browse through the Tables in this section and just pick up the needed concoction.

For the generation of reproducible pH gradients suitable for IEF in IPGs, the following criteria should be met: (a) the pH gradient should be linear (except in some cases, as discussed in §2.3.4); (b) the buffering capacity (β) should be sufficiently high to render the pH gradient insensitive to impurities and to some inaccuracy in the preparation of the starting solutions (e.g., acrylic acid in the acrylamide stock solution); (c) the β power should be as constant as possible in order to minimize deviations from linearity of the desired pH gradient and to reduce the effect of small

disturbances in the gel mixing and casting on the generated pH gradient.

2.2. *Narrow and ultra-narrow pH gradients*

2.2.1. *The principle of an Immobiline pH gradient*

When casting a narrow Immobiline pH gradient, only a single buffering species is needed and is titrated around its pK value with another, fully dissociated Immobiline. Why then, is a linear pH gradient obtained as shown in Fig. 2.1? Any weak acid or base, when titrated around its pK, will automatically generate a linear pH gradient, which corresponds to a portion of its titration curve, centred on pH = pK. Fig. 2.1 shows the titration of Immobiline of pK 7.0, at constant concentration in solution, with 0.1 N HCl (when casting an IPG gel, though, the titrant should be another

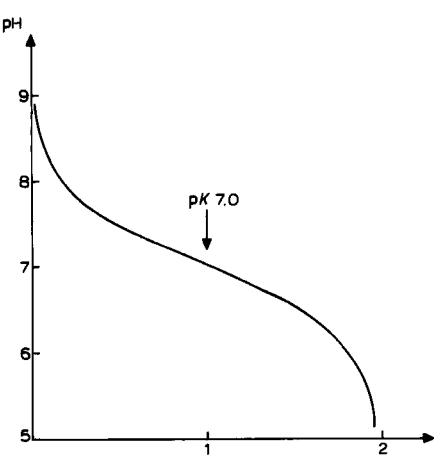

Fig. 2.1. Titration of pK 7.0 Immobiline with 0.1 M hydrochloric acid. If the buffering Immobiline concentration is kept constant, the titration curve produces a linear gradient within pK + 0.5 pH unit and pK − 0.5 pH unit (i.e., 1 pH unit interval having the pK value as inflection point) (by courtesy of LKB Produkter AB).

Immobiline, e.g., the pK 3.6 or the strongly acidic titrant, the pK 1.0). The free base, in solution, will give an alkaline pH; on addition of the first few drops of HCl, the pH decays exponentially and then linearly in the pH interval (pK + 0.5 pH unit) to (pK − 0.5 pH unit). Below the lower limit, the pH drops dramatically to the pH produced by the excess of free HCl, at a given concentration, in solution. So, by titrating any Immobiline chemical in a pH interval no greater than 1 pH unit, centred on its pK value, we can automatically generate any linear pH gradient in the pH range 2.5–11.0.

2.2.2. The Henderson-Hasselbalch (H-H) equation

The random distribution of Immobilines within the gel fibers means that the protolytic equilibria existing in an IPG matrix can be described by the classical H-H equation:

$$\mathrm{pH} = \mathrm{p}K_i + \log[\mathrm{B}_i]/[\mathrm{A}_i] \tag{1}$$

where $\mathrm{p}K_i$, as for any monofunctional weak acid and base, is a constant for each type of Immobiline, $[\mathrm{A}_i]$ is the molar concentration of the Immobiline in its acidic (protonated) form and $[\mathrm{B}_i]$ the corresponding molarity of the Immobiline in its basic (non-protonated) form.

The H-H equation and the electroneutrality conditions give the relation between the pH and the total concentration of Immobilines. If only two Immobilines are used, of which one can be regarded as fully ionized (titrant), the pH can be calculated directly from the Immobiline concentrations, with the aid of slightly modified H-H equations, depending on which species (an acid or a base) is used as a buffering group for an Immobiline gradient. If the buffer is an acidic Immobiline, it will be:

$$\mathrm{pH} = \mathrm{p}K_\mathrm{A} + \log[C_\mathrm{B}/(C_\mathrm{A} - C_\mathrm{B})] \tag{2}$$

whereas, for a basic Immobiline, the corresponding expression is:

$$\mathrm{pH} = \mathrm{p}K_\mathrm{B} + \log[(C_\mathrm{B} - C_\mathrm{A})/C_\mathrm{A}] \tag{3}$$

where C_A is the molarity of the acidic Immobiline with $pK = pK_A$ and C_B is the molarity of the basic Immobiline with $pK = pK_B$. If the concentration of the buffering Immobiline is kept constant along the generated pH interval, the pH gradient resulting from linear gradient mixing will correspond to an ordinary titration curve. The best gradients with respect to linearity and buffering capacity, in such a case, will be those having the midpoint centred on the pK value of the buffering species.

2.2.3. *Narrow and ultra-narrow pH gradients with mid-point centred or removed from the buffering pK*

We have just seen (Fig. 2.1) that when a buffer is titrated in a pH interval from $pK + 0.5$ pH unit to $pK - 0.5$ pH unit a linear pH gradient will be generated by this titration process. This is plotted in Fig. 2.2 (left side): this is a graphic representation of the simple case in which $|pH_m - pK| = 0$ (where $pH_m = pH$ at the mid-point of the desired pH interval). In Fig. 2.2 we have also drawn the

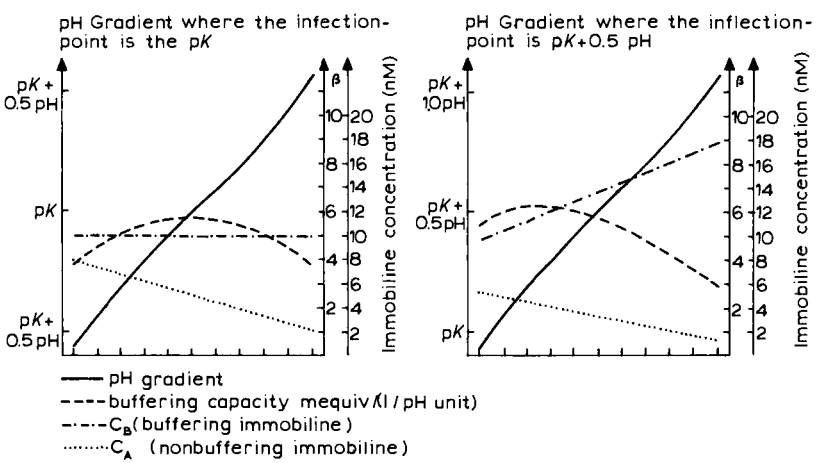

Fig. 2.2. pH gradients with midpoint (pH_m) centred or removed from the buffer pK. Left: the simple case in which $pH_m = pK$; right: extreme case in which $pH_m = (pK + 0.5$ pH unit). Solid lines: pH gradients; broken curves: β power courses; broken and dotted lines: concentration courses of buffering Immobilines; dotted lines: concentration profiles of titrant Immobilines (courtesy of LKB Produkter AB).

molarity of the buffering Immobiline (constant, zero slope), the molarity variation of the titrating (non-buffering) Immobiline (a line of negative slope, as we go from the acidic to the basic interval in titrating a basic buffer) and the profile of the accompanying buffering power (β): a dome-shaped, almost symmetrical curve with $\beta_{max} = pK$, just as expected. However, if we could only work under the condition $|pH_m - pK| = 0$, it would be a disaster, as only 9 different pH gradients could be generated, centred on the pK of each of the nine Immobilines. Luckily, we can also work under the condition $|pH_m - pK| \neq 0$, by having the pH_m removed from the pK of the buffer by as much as ± 0.5 pH unit (Bjellqvist et al., 1982): this gives us a practically unlimited number of pH intervals to work with. The results are shown in Fig. 2.2 (right). This time $pH_m = (pK + 0.5)$ pH unit, and yet we can still arrange for an almost linear pH gradient (solid curve) by generating also a gradient of buffering species. As there would be much more buffering power at the acidic extreme (pH_{min}) of the pH interval (which, in this case, would be $pH_{min} = pK$), the concentration of the buffering Immobiline is progressively increased towards the basic extreme of our pH interval (line $-\cdot-\cdot-\cdot$ of positive slope) so as to increase the β value in this region. The resulting β profile is now skewed, but it gives an acceptably linear pH gradient. The rationale for arriving at Fig. 2.2 (right) is as follows: from the H-H equation it is clear that a certain difference between a pH value and the pK defines a molar ratio between buffering and non-buffering Immobiline. If pH_m is the mid-point of the desired pH range, and if the concentrations of the acidic and basic Immobilines at pH_m are C_{A_m} and C_{B_m}, respectively, the pH, in distance relative to the mid-point, will be given by the expression:

$$\Delta pH = pK - pH_m + \log\left[\frac{C_{B_m} + bx}{C_{A_m} - C_{B_m} + (a-b)x}\right] \qquad (4)$$

if the buffering Immobiline is an acid, whereas if the buffering Immobiline is a base, the corresponding relation derived from Eq. (3) will hold. In this expression, x is the distance from the mid-point and a and b are dC_A/dx and dC_B/dx, respectively.

From the criterion that $d^2pH/dx^2 = 0$, it is found that, in order to convert pH_m into the inflection point of the function $pH = f(x)$, the following relation should be satisfied:

$$a/b = \pm(2 - C_{A_m}/C_{B_m}) \tag{5}$$

where the negative sign results when the buffering Immobiline is a base. With the aid of this relation it is possible to generate any linear narrow pH range in the interval 2.5–11 with the aid of available Immobilines. As a general rule, in order to obtain a good buffering capacity with a minimum of incorporated Immobiline, the buffering species should have a pK value as close as possible to the pH of the mid-point of the pH gradient, while the non-buffering counter-ion should have a pK so far away from the desired pH range (> 2 pH units) that it can be regarded as fully ionized. Note that the requirement $|pH_m - pK| = 0$ is, in principle, similar to the Rilbe's requirement for carrier ampholytes that $|pI - pK_{prox}| \leqslant 0.5$, where pI is the isoelectric point of the amphoteric buffer and pK_{prox} is the nearest protolytic group (be it a base or an acid) to the pI value (Rilbe, 1973).

2.2.4. *Selection criteria for 1 pH unit wide IPGs: the tandem principle*

Table 2.1 gives a selection guide of some 1 pH unit intervals which can be generated with the aid of presently available Immobilines. We work on a 'tandem' principle, i.e., knowing the desired pH interval, we select one Immobiline with the criterion that $pH_{min} < pK < pH_{max}$ (in other words, having the pK inside the limits of our pH interval; this is the general case, except in the pH intervals 4.9–5.9 and 7.3–8.3, where we have to work with 'outside' pKs): this will be called the 'buffering' Immobiline. We will then need a titrant Immobiline, which will be called 'non-buffering', selected with the criterion that its pK will be as far away as possible from the desired pH interval (ideally pH_{min} or pH_{max} should be at least 3 pH units removed from the pK of the titrant). Under these conditions, the titrant Immobiline will be an 'ideal titrant', i.e., it will only provide equivalents of acid or base to titrate the buffering

TABLE 2.1
Selection of Immobilines for 1 pH unit wide gradients

pH gradient desired (10 °C, in gel)	Immobiline		Buffering Immobiline		For ultra-narrow pH gradients within stated pH range, use nomogram No.
	Buffering	Non-buffering	An acid	A base	
3.8– 4.8	pK 4.4	pK 9.3	+		I
4.0– 5.0	pK 4.6	pK 9.3	+		I
4.9– 5.9	pK 4.6	pK 6.2	+	+	III
5.7– 6.7	pK 6.2	pK 3.6		+	II
6.6– 7.6	pK 7.0	pK 3.6		+	II
7.3– 8.3	pK 7.0, 8.5	pK 3.6		+	–
8.0– 9.0	pK 8.5	pK 3.6		+	II
9.0–10.0	pK 9.3	pK 3.6		+	II

From LKB Application Note No. 321.

group but will not itself buffer in the desired pH interval. The guidelines on how to generate these pH gradients and on the calculations required are given in the nomograms below.

2.2.5. The use of nomograms. Tabulated 1-pH-unit recipes

In practice, if we had to use each time Eqs. (4) and (5) for deriving any desired narrow pH gradient, the calculations required would be laborious and might discourage the reader from ever entering the field. For your peace of mind, Dr. B. Bjellqvist has compiled three nomograms (whose use is suggested in Table 2.1), which can be found in LKB Application Note No. 321 (August 1982), and which exemplify well the calculations needed. I report here nomogram I (to be used when the buffering Immobiline is an acid) in Fig. 2.3 and nomogram II (to be used when the buffering Immobiline is a base) in Fig. 2.4. Let me give a practical example: suppose one wants to focus human hemoglobins (Hb); Hb A, the adult species, has a pI (at 10°C) in IPGs of 7.3. We shall therefore prepare a 1 pH unit wide gradient, pH 6.8–7.8, so that HbA will focus just in the middle of the pH gradient; the chances are that most HbA mutants will be found within this pH interval. The Immobiline with pK nearest to the mid-point ($pH_m = 7.3$) is the pK 7.0 species

Symbols used in the nomograms and calculations

C = concentration of Immobiline in mol/litre
A, B = subscripts referring to acidic and basic Immobilines, resp.

$K_A = \frac{dC_A \text{ mol/litre}}{dpH \text{ pH unit}}$ $K_B = \frac{dC_B \text{ mol/litre}}{dpH \text{ pH unit}}$

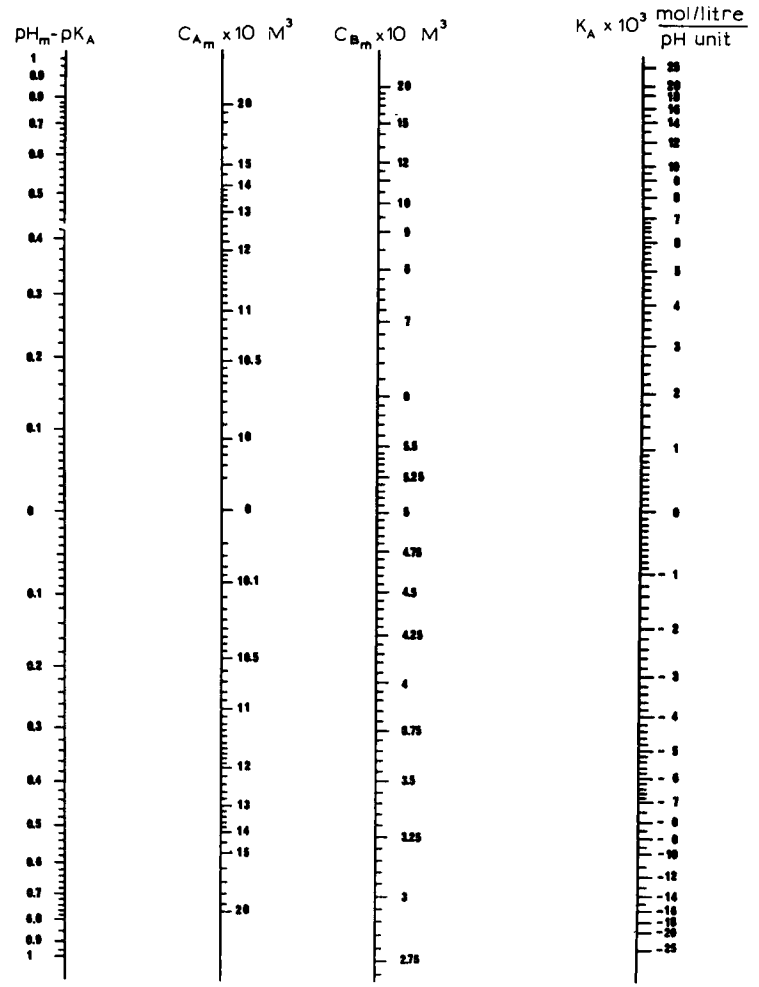

Fig. 2.3. Nomogram No. 1, to be used to calculate the amounts of buffering and titrating Immobilines in the dense and light solutions in the case in which the buffering species is an acid. For its use, see the practical example in the text (from LKB Application Note No. 321, 1982; by courtesy of LKB Produkter AB).

m = midpoint, subscript referring to the concentration, C, or pH at the midpoint of the pH gradient
a = subscript referring to the concentration, C, or pH of the acidic, dense solution used in gradient formation
b = subscript referring to the concentration, C, or pH of the basic, light solution used in gradient formation.

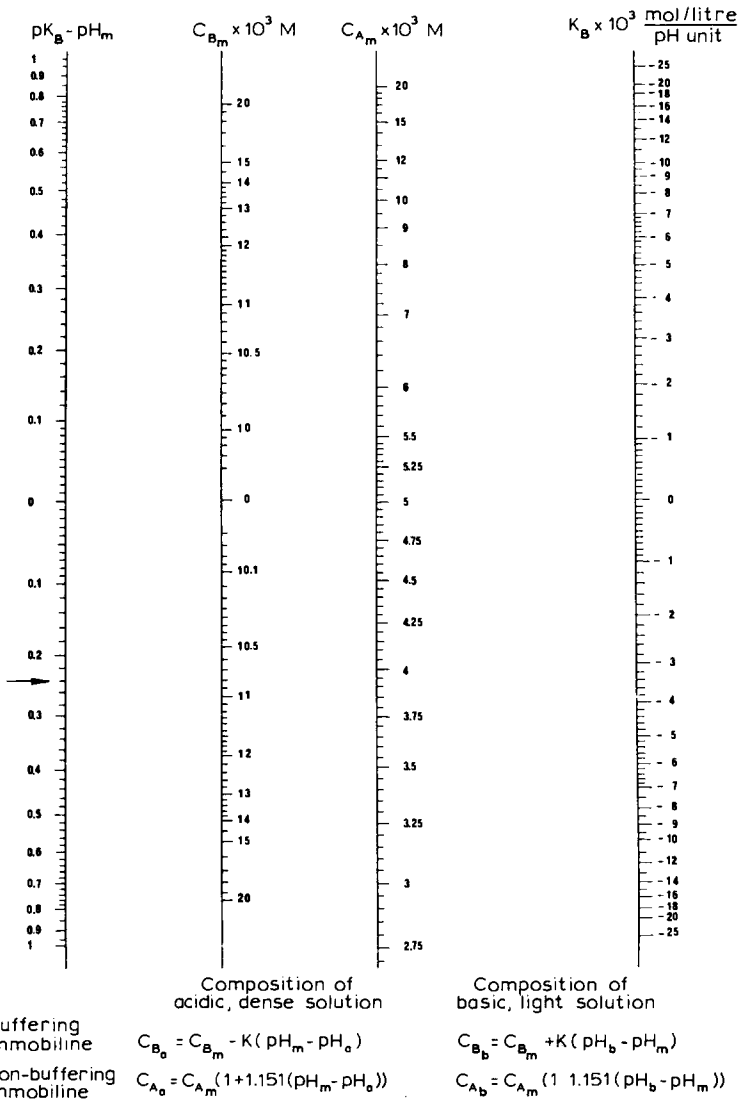

Fig. 2.4. Nomogram No. 2, to be used to calculate the amounts of buffering and titrant Immobilines in the dense and light solutions in the case in which the buffering species is a base. For its use, see the example in the text and follow the general instructions in LKB Application Note No. 321 (1982) (by courtesy of LKB Produkter AB).

(for calculations, though, use the pK value at 10°C, which is 7.06). The nomogram to be used is thus No. II: it is entered on the far left column with the value of the difference $pK_B - pH_m = -0.24$ (see the arrow in Fig. 2.4). With the aid of a ruler set perpendicular to the vertical line of the far left column, and aligned on the -0.24 value, we draw a line that will intersect at right-angles columns 2, 3 and 4. At the intersection points, we read the following values: $C_{B_m} = 10.9$ mM, $C_{A_m} = 3.95$ mM and $K_B = 3.4$ mM. These values will be used to solve numerically the set of four equations at the bottom of Fig. 2.4, with the understanding that $pH_a = 6.8$ (this is the acidic extreme of our desired pH interval) and $pH_b = 7.8$ (this is the corresponding alkaline extreme). Thus:

$$C_{B_a} = 10.9 - 3.4(7.3 - 6.8) = 9.2 \text{ mM}$$
$$C_{A_a} = 3.95[1 + 1.151(7.3 - 6.8)] = 6.2 \text{ mM}$$

Hence, if at the acidic extreme of our pH gradient we prepare a mixture of 9.2 mM Immobiline of pK 7.0 and 6.2 mM Immobiline of pK 3.6 (titrant) and we read its value at 10°C, it will give a pH = 6.8. The second set of equations is needed for calculation of the composition of the basic, light solution. Accordingly:

$$C_{B_b} = 10.9 + 3.4(7.8 - 7.3) = 12.6 \text{ mM};$$
$$C_{A_b} = 3.95[1 - 1.151(7.8 - 7.3)] = 1.68 \text{ mM}.$$

This means that, if the basic end of our pH gradient contains a mixture of 12.6 mM Immobiline of pK 7.0 and 1.68 mM of Immobiline of pK 3.6, the pH (at 10°C) will be 7.8. In practice, these nomograms are a combined, graphical representation of Eqs. (4) and (5). By entering in nomogram II the value of the difference $pK - pH_m$ (see Eq. 4) we obtain directly the molarities of the buffering ion (C_{Bm}) and of the titrant (C_{Am}) as calculated at the mid-point of the desired pH interval. However, as discussed above (§2.2.3), C_{Bm} cannot be kept constant as we would have too much buffering power at the acidic extreme (barely 0.2 pH unit removed from the pK of the buffer) and too little at the alkaline end (0.8 pH

unit away from the pK 7.0 Immobiline). If $C_{pK7.0}$ were kept constant, we would have a shallow pH gradient at the acidic end and a steep slope at the alkaline end. Thus, a correction factor is introduced which subtracts a given amount from the concentration of C_{Bm} to obtain C_{Ba} and adds back this same amount to C_{Bm} to generate the value of C_{Bb}; the rationale for this is to try to smooth the β power as much as possible over the desired pH interval. One last note: you will have noticed that the nomograms span a 2 pH unit interval, 1 above and 1 below the pK, and this is in contrast with what I have stated above (p$K \pm 0.5$ pH unit, see §2.2.3). In fact, this has been done for the sake of calculations: I suggest you stay within the recommended interval (p$K \pm 0.5$ pH unit), as outside these limits the scales are too compressed and the resulting errors very large; moreover, it will be very hard to compensate for the huge loss of buffering power at the 'wrong' end of the pH interval.

Even with these nomograms I am afraid a lot of users would rather have pre-calculated recipes and not bother with all the cumbersome calculations required. LKB scientists must have had the same feelings, since in 1984 they prepared a new Application Note (No. 324) listing no less than 58, 1 pH unit wide gradients, starting with the pH 3.8–4.8 interval and ending with the pH 9.5–10.5 range, separated by 0.1 pH unit increments. In Table 2.2 are the relative recipes giving the Immobiline volumes (for 15 ml of mixture) needed in the acidic (mixing) chamber to obtain pH_{min} and the corresponding volumes for the basic (reservoir) chamber of the gradient mixer needed to generate pH_{max} of the desired pH interval. We work on the 'troika' principle only between pH 4.6–5.1 (pH_{min}) and 7.2–7.4 (pH_{min}) for in these regions there are wide gaps in the pKs of neighboring Immobilines. As an example, take the pH 4.6–5.6 interval: there are no available Immobilines with pKs within this pH region, so the nearest species, pKs 4.6 and 6.2, will act as both partial buffers and partial titrants; then there is a need for a third Immobiline in each vessel, a true titrant that will bring the pH to the desired value (as titrant we will use for pH_{min} pK 3.6 and for pH_{max} pK 9.3). Note that the Table gives, in addition to the pH range (bold central two lanes) also the pH of mid-point (pH_m, as always required in nomograms). The pH range

TABLE 2.2
1-pH unit gradients: volumes of Immobiline for 15 ml each of starting solution (2 gels)

Control pH at 20 °C	Volume (μl) 0.2 M Immobiline p*K* Acidic dense solution							pH range
	3.6	4.4	4.6	6.2	7.0	8.5	9.3	
3.81 ± 0.03	–	750	–	–	–	–	139	3.8–4.8
3.94 ± 0.03	–	710	–	–	–	–	180	3.9–4.9
4.03 ± 0.03	–	–	753	–	–	–	137	4.0–5.0
4.13 ± 0.03	–	–	713	–	–	–	177	4.1–5.1
4.22 ± 0.03	–	–	689	–	–	–	203	4.2–5.2
4.32 ± 0.03	–	–	682	–	–	–	235	4.3–5.3
4.42 ± 0.03	–	–	691	–	–	–	273	4.4–5.4
4.51 ± 0.04	–	–	716	–	–	–	325	4.5–5.5
4.61 ± 0.05	582	–	600	863	–	–	–	4.6–5.6
4.75 ± 0.03	458	–	675	863	–	–	–	4.7–5.7
4.86 ± 0.04	352	–	750	863	–	–	–	4.8–5.8
4.96 ± 0.03	218	–	863	863	–	–	–	4.9–5.9
5.07 ± 0.03	158	–	863	863	–	–	–	5.0–6.0
5.17 ± 0.04	113	–	863	863	–	–	–	5.1–6.1
5.24 ± 0.18	1251	–	–	1355	–	–	–	5.2–6.2
5.33 ± 0.12	1055	–	–	1165	–	–	–	5.3–6.3
5.43 ± 0.12	899	–	–	1017	–	–	–	5.4–6.4
5.52 ± 0.09	775	–	–	903	–	–	–	5.5–6.5
5.62 ± 0.07	676	–	–	817	–	–	–	5.6–6.6
5.71 ± 0.06	598	–	–	755	–	–	–	5.7–6.7
5.81 ± 0.06	536	–	–	713	–	–	–	5.8–6.8
5.91 ± 0.05	486	–	–	689	–	–	–	5.9–6.9
6.01 ± 0.05	447	–	–	682	–	–	–	6.0–7.0
6.10 ± 0.04	416	–	–	691	–	–	–	6.1–7.1
6.11 ± 0.11	972	–	–	–	1086	–	–	6.2–7.2
6.21 ± 0.09	833	–	–	–	956	–	–	6.3–7.3
6.30 ± 0.08	722	–	–	–	857	–	–	6.4–7.4
6.40 ± 0.07	635	–	–	–	783	–	–	6.5–7.5
6.49 ± 0.06	565	–	–	–	732	–	–	6.6–7.6
6.59 ± 0.05	509	–	–	–	699	–	–	6.7–7.7
6.69 ± 0.05	465	–	–	–	683	–	–	6.8–7.8
6.78 ± 0.04	430	–	–	–	684	–	–	6.9–7.9
6.88 ± 0.04	403	–	–	–	701	–	–	7.0–8.0
6.98 ± 0.04	381	–	–	–	736	–	–	7.1–8.1
7.21 ± 0.06	1028	–	–	–	750	750	–	7.2–8.2
7.31 ± 0.06	983	–	–	–	750	750	–	7.3–8.3
7.41 ± 0.05	938	–	–	–	750	750	–	7.4–8.4
7.66 ± 0.15	1230	–	–	–	–	1334	–	7.5–8.5
7.75 ± 0.12	1037	–	–	–	–	1149	–	7.6–8.6
7.85 ± 0.10	885	–	–	–	–	1004	–	7.7–8.7
7.94 ± 0.08	764	–	–	–	–	893	–	7.8–8.8
8.04 ± 0.07	667	–	–	–	–	810	–	7.9–8.9

mid point	Control pH at 20 °C	Volume (μl) 0.2 M Immobiline p*K* Basic light solution						
		3.6	4.4	4.6	6.2	7.0	8.5	9.3
4.3	4.95 ± 0.06	–	750	–	–	–	–	391
4.4	5.04 ± 0.07	–	810	–	–	–	–	667
4.5	5.14 ± 0.06	–	–	745	–	–	–	384
4.6	5.23 ± 0.07	–	–	803	–	–	–	659
4.7	5.33 ± 0.08	–	–	884	–	–	–	753
4.8	5.42 ± 0.10	–	–	992	–	–	–	871
4.9	5.32 ± 0.12	–	–	1133	–	–	–	1021
5.0	5.61 ± 0.14	–	–	1314	–	–	–	1208
5.1	5.69 ± 0.04	–	–	863	863	–	–	103
5.2	5.79 ± 0.04	–	–	863	863	–	–	150
5.3	5.90 ± 0.04	–	–	863	863	–	–	202
5.4	5.99 ± 0.03	–	–	863	863	–	–	248
5.5	6.09 ± 0.04	–	–	863	803	–	–	338
5.6	6.20 ± 0.04	–	–	863	713	–	–	443
5.7	6.34 ± 0.04	337	–	–	724	–	–	–
5.8	6.43 ± 0.03	284	–	–	694	–	–	–
5.9	6.53 ± 0.03	242	–	–	682	–	–	–
6.0	6.63 ± 0.03	209	–	–	686	–	–	–
6.1	6.73 ± 0.03	182	–	–	707	–	–	–
6.2	6.82 ± 0.03	161	–	–	745	–	–	–
6.3	6.92 ± 0.03	144	–	–	803	–	–	–
6.4	7.02 ± 0.03	131	–	–	884	–	–	–
6.5	7.12 ± 0.03	120	–	–	992	–	–	–
6.6	7.22 ± 0.03	112	–	–	1133	–	–	–
6.7	7.21 ± 0.03	262	–	–	–	686	–	–
6.8	7.31 ± 0.03	224	–	–	–	682	–	–
6.9	7.41 ± 0.03	195	–	–	–	694	–	–
7.0	7.50 ± 0.03	171	–	–	–	724	–	–
7.1	7.60 ± 0.03	152	–	–	–	771	–	–
7.2	7.70 ± 0.03	137	–	–	–	840	–	–
7.3	7.80 ± 0.03	125	–	–	–	934	–	–
7.4	7.90 ± 0.03	116	–	–	–	1058	–	–
7.5	8.00 ± 0.03	108	–	–	–	1217	–	–
7.6	8.09 ± 0.03	103	–	–	–	1422	–	–
7.7	8.36 ± 0.03	548	–	–	–	750	750	–
7.8	8.46 ± 0.05	503	–	–	–	750	750	–
7.9	8.56 ± 0.03	458	–	–	–	750	750	–
8.0	8.76 ± 0.04	331	–	–	–	–	720	–
8.1	8.85 ± 0.03	279	–	–	–	–	692	–
8.2	8.95 ± 0.03	238	–	–	–	–	682	–
8.3	9.05 ± 0.06	206	–	–	–	–	687	–
8.4	9.14 ± 0.06	180	–	–	–	–	710	–

TABLE 2.2 (CONTINUED)

Control pH at 20 °C	Volume (μl) 0.2 M Immobiline p*K* Acidic dense solution							pH range
	3.6	4.4	4.6	6.2	7.0	8.5	9.3	
8.13 ± 0.06	591	–	–	–	–	750	–	8.0– 9.0
8.23 ± 0.06	530	–	–	–	–	710	–	8.1– 9.1
8.33 ± 0.05	482	–	–	–	–	687	–	8.2– 9.2
8.43 ± 0.04	443	–	–	–	–	682	–	8.3– 9.3
8.52 ± 0.04	413	–	–	–	–	692	–	8.4– 9.4
8.62 ± 0.04	389	–	–	–	–	720	–	8.5– 9.5
8.40 ± 0.14	1208	–	–	–	–	–	1314	8.6– 9.6
8.49 ± 0.12	1021	–	–	–	–	–	1133	8.7– 9.7
8.59 ± 0.10	871	–	–	–	–	–	992	8.8– 9.8
8.68 ± 0.08	753	–	–	–	–	–	884	8.9– 9.9
8.78 ± 0.07	659	–	–	–	–	–	803	9.0–10.0
8.87 ± 0.06	584	–	–	–	–	–	743	9.1–10.1
8.97 ± 0.05	525	–	–	–	–	–	707	9.2–10.2
9.07 ± 0.04	478	–	–	–	–	–	686	9.3–10.3
9.16 ± 0.07	440	–	–	–	–	–	682	9.4–10.4
9.26 ± 0.07	410	–	–	–	–	–	694	9.5–10.5

From LKB Application Note No. 324 (1984). The pH range (given in the middle two columns) is the one existing in the gel during the run at 20 °C. For controlling the pH of the starting solutions, the values (control pH) are given at 20 °C.

TABLE 2.3
Broad pH gradients: volumes of Immobiline for 15 ml of each starting solution

Control pH at 20 °C	Volume (μl) 0.2 M Immobiline p*K* Acidic dense solution							pH range
	3.6	4.4	4.6	6.2	7.0	8.5	9.3	
3.53 ± 0.06	299	–	223	157	–	–	–	3.5– 5.0
4.00 ± 0.06	569	–	99	439	–	–	–	4.0– 6.0
4.54 ± 0.06	415	–	240	499	–	–	–	4.5– 6.5
5.08 ± 0.03	69	–	428	414	–	–	–	5.0– 7.0
5.56 ± 0.03	–	–	450	354	113	–	–	5.5– 7.5
6.06 ± 0.08	435	–	–	323	208	44	–	6.0– 8.0
6.56 ± 0.13	771	–	–	276	185	538	–	6.5– 8.5
7.03 ± 0.24	1349	–	–	–	272	372	845	7.0– 9.0
7.50 ± 0.11	668	–	–	–	445	226	348	7.5– 9.5
8.10 ± 0.07	399	–	–	–	364	355	94	8.0–10.0
4.01 ± 0.05	578	–	110	450	–	–	–	4.0– 7.0
5.03 ± 0.12	702	–	254	416	133	346	–	5.0– 8.0
6.04 ± 0.14	779	–	–	402	93	364	80	6.0– 9.0
6.98 ± 0.07	542	–	–	–	378	351	–	7.0–10.0

From LKB Application Note No. 324 (1984).

mid point	Control pH at 20 °C	Volume (μl) 0.2 M Immobiline p*K* Basic light solution						
		3.6	4.4	4.6	6.2	7.0	8.5	9.3
8.5	9.24 ± 0.06	139	–	–	–	–	750	–
8.6	9.34 ± 0.06	143	–	–	–	–	810	–
8.7	9.44 ± 0.06	130	–	–	–	–	893	–
8.8	9.54 ± 0.06	119	–	–	–	–	1004	–
8.9	9.64 ± 0.06	111	–	–	–	–	1119	–
9.0	9.74 ± 0.06	105	–	–	–	–	1334	–
9.1	0.50 ± 0.06	323	–	–	–	–	–	716
9.2	9.59 ± 0.06	275	–	–	–	–	–	691
9.3	9.69 ± 0.06	233	–	–	–	–	–	682
9.4	9.79 ± 0.06	203	–	–	–	–	–	689
9.5	9.88 ± 0.06	177	–	–	–	–	–	713
9.6	9.98 ± 0.06	157	–	–	–	–	–	755
9.7	10.08 ± 0.06	141	–	–	–	–	–	817
9.8	10.18 ± 0.06	129	–	–	–	–	–	903
9.9	10.28 ± 0.06	119	–	–	–	–	–	1017
10.0	10.38 ± 0.06	111	–	–	–	–	–	1165

Mid point	Control pH at 20 °C	Volume (μl) 0.2 M Immobiline p*K* Basic light solution						
		3.6	4.4	4.6	6.2	7.0	8.5	9.3
4.25	5.06 ± 0.07	212	–	310	465	–	–	–
5.0	6.09 ± 0.14	390	–	521	276	–	–	722
5.5	6.53 ± 0.05	–	–	570	244	235	–	297
6.0	7.01 ± 0.06	–	–	474	270	219	–	320
6.5	7.51 ± 0.09	347	–	–	236	287	284	–
7.0	8.11 ± 0.09	286	–	–	174	325	329	–
7.5	8.66 ± 0.06	192	–	–	153	278	362	–
8.0	8.94 ± 0.07	484	–	–	–	232	189	546
8.5	9.37 ± 0.06	207	–	–	–	925	139	346
9.0	9.89 ± 0.05	91	–	–	–	329	366	289
5.5	7.02 ± 0.14	302	–	738	151	269	–	876
6.5	8.12 ± 0.07	175	–	123	131	345	346	–
7.5	9.01 ± 0.06	241	–	–	161	449	237	225
8.5	9.88 ± 0.05	90	–	–	–	324	350	280

given is the one existing in the gel (4 or 5%T, 10°C) upon incorporation of the chemicals in the polyacrylamide matrix. However, during preparation of the two limiting solutions (pH_{min} and pH_{max}) it is often desirable to check the pH values of these two solutions, in order to ensure that no experimental errors have been made (e.g., pipetting the wrong Immobiline or a wrong volume of buffering or titrant ion). As pH determinations at 10°C would require special setting of a pH-meter (routinely set at room temperature), Table 2.2 gives also the control pH value of each limit solution at 20°C.

Note an important convention: since an IPG gel is cast with the aid of a two-vessel gradient mixer (see Chapter 3) the two limiting solutions, during pouring in the cassette, have to be stabilized by a co-linear density gradient. Thus, a density-forming agent (in general 20% glycerol) has to be added to one of the two solutions. In order to avoid confusion, it has been decided that the 'dense' solution will always be the most acidic (or least basic) of the two prepared solutions. Thence the denominations 'acidic dense solution' and 'basic light solution' that you will find all throughout this treatise and in general in all papers dealing with the IPG methodology.

2.2.6. *Interpolation of ultra-narrow pH gradients based on the tandem principle*

Let us go back to the above example, the separation of Hbs in a pH 6.8–7.8 gradient. We have just derived the molarities of the buffering and titrant Immobilines for the two extremes of our pH interval. In practice, for two gels of $125 \times 110 \times 0.5$ mm dimensions, we shall mix in the acidic dense solution (the pH 6.8 extreme) 364 μl of 0.2 M Immobiline of pK 7.0 and 236 μl of 0.2 M Immobiline of pK 3.6 (for a total final volume of 8 ml) and for the basic chamber (the pH 7.8 extreme) the corresponding amounts will be 536 and 64 μl, respectively. Once the extremes of this pH interval have been calculated, any narrower pH range within the pH limits 6.8 and 7.8 can be derived by a simple linear interpolation of intermediate Immobiline molarities. Fig. 2.5 gives a graphic representation of the method employed: for instance, for resolving

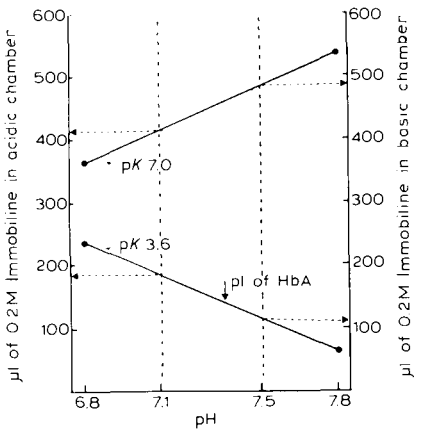

Fig. 2.5. Graphic representation of the preparation of narrow (up to 1 pH unit) IPG gradients based on the 'tandem' principle. The limiting molarities of pK 7.0 (buffering species) and pK 3.6 (titrant) Immobilines needed to generate a pH 6.8–7.8 interval are calculated with the aid of nomogram II in LKB Application Note No. 321 (or simply read out from Table 2.2). These points are joined by straight lines and the new molarities needed to generate any narrower pH gradient within the stated pH intervals are obtained by simple linear interpolation (broken vertical and horizontal lines). In this example, a narrow pH 7.1–7.5 gradient is graphically derived (from Rochette et al., 1984; with permission of Elsevier).

Hb San Diego from Hb A it was found necessary to operate over a narrow interval of 0.4 pH unit (pH 7.1–7.5). The limiting molarities of the two Immobilines in the 1 pH unit interval are joined by a straight line (because the pouring of the gradient from the two-chamber mixers is done linearly) and then the new pH interval is defined according to experimental needs (in our case, pH 7.1–7.5). Two lines are drawn from the two new limits of the pH interval, parallel to the ordinates (broken vertical lines). Where they intersect the two sloping lines defining the two Immobiline molarities, four new molarities of the two Immobilines defining the new pH interval are read directly on the ordinates (broken horizontal lines with arrows). This process can be repeated for any desired pH interval, down to ranges as narrow as 0.1 pH unit. Within these limits (up to 1 pH unit) it is preferable to work on a 'tandem' principle, i.e., with only one buffering and one non-buffering Immobiline.

2.3. *Extended pH gradients*

We have seen, so far, the generation of narrow and ultra-narrow IPGs; there are cases, however, when it might be advantageous to mix two or more buffering Immobilines, in order to cover wider pH intervals, to be used as the first dimension of two-dimensional (2-D) techniques. 2-D maps are most sensitive to disturbances in the first dimension (e.g., cathodic drift, near isoelectric precipitation) which lead to altered or blurred spots in the final 2-D plane. The insensitivity of grafted pH gradients to such disturbances, and the ease of control of the form and width of these gradients make them the natural choice for this application. There appear to be three ways of producing wide pH gradients (> 2 pH units) with Immobilines: (a) multi chamber mixers; (b) two-chamber mixers with identical molarities of buffering species and varying concentrations of titrants; (c) two-chamber mixers containing different amounts of the same Immobiline species. I shall review here these three approaches (two, in reality, since multi-chamber mixers have been totally abandoned and are given here more for historical reasons on the development of IPG concepts).

2.3.1. Multi-chamber mixers

It was in the summer of 1982 that, in collaboration with Drs. Dossi, Gianazza and Prof. Celentano, we started out to solve the problem of generating wide IPG gradients. As odd as it sounds, when IPGs were launched it was believed that their main use would be in narrow and ultra-narrow pH gradients, a sort of a super-tool which would confound any scientist claiming he had a pure protein preparation (even today protein chemists are dumbfound by the enormous resolving power of the IPG technique and are trying to convince the Food and Drug Administration to ban the use of IPGs as a proof of protein homogeneity: the fact being that, by the IPG criterion, nothing is homogeneous any more). At the beginning, nobody had the faintest idea on how to tackle the problem. Finally, after a long literature search, we started out with a pestiferous but most admirable gadget, a nine-chambered mixing device designed by Peterson and Sober in 1959 and adapted to the

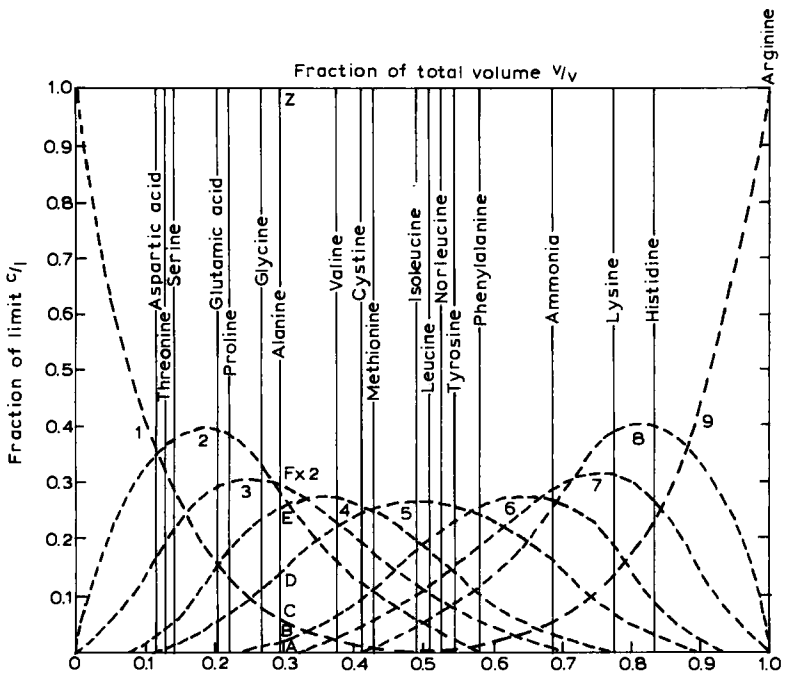

Fig. 2.6. Composition of the eluate from a nine-chambered gradient in terms of the contribution of each buffer in a single chamber (numbered 1–9). The vertical lines represent the elution position of each amino acid from the Autoanalyzer when using a Varigrad for mixing the eluent buffers (modified from Peterson and Sober, 1959).

Technicon Analyzer for amino acid elution. If the nine chambers are filled equally with nine different solutions, it can be demonstrated that the elution profile will be as depicted in Fig. 2.6: only the solutions in the first and last chambers will exhibit an exponential decay, reaching zero concentration in the middle (chamber 5) and only the solution in vessel 5 will show a symmetrical distribution (a dumbbell-shaped function). In all other chambers the elution profile will be skewed, with the distribution curves of chambers 6, 7 and 8 being the specular image of vessels 4, 3 and 2, respectively. An important lessson was learned from this graph: if we were to place in each chamber a different Immobiline, in order

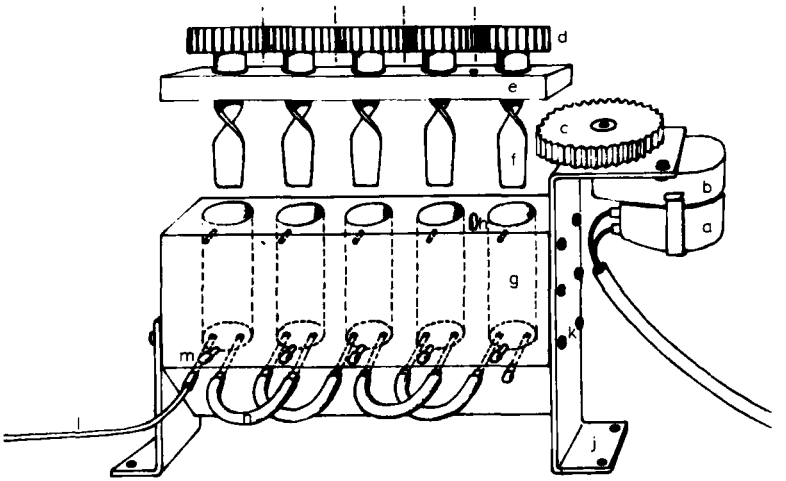

Fig. 2.7. View of the five-chamber gradient mixer of Dossi et al. (1983) (the stirring pad block is lifted). Letterings: (a): motor (power = 3 W, 24 V a.c.); (b): reduction unit (60 rpm); (c): driving gear (nylon, 80 mm diameter, 80 teeth); (d): transmitting gears (30 mm diameter, 30 teeth); (e): ball-bearings housing (rigid double crown; O.D. = 22 mm, I.D. = 15 mm; h = 7 mm); (f): stirring paddles (Plexiglass spiral, 70 mm long, 20 mm top and 12 mm bottom width, fitted in the hub of a cylindrical block); (g): Plexiglass block with five cylindral chambers; (h): pins for fastening the stirring paddle unit to the multi-chamber block; (i): air vents; (j): supporting feet; (k): screws for assembling the feet to the block (l): outlet pump; (m): drain tubes and (n): connection tubes (from Dossi et al., 1983; with permission of Elsevier).

of increasing pK, titrated to increasing pH values (in fact, close to their pK values), by elution under appropriate conditions we could not only generate a linear pH gradient, but could also confine each Immobiline species to the pH interval in which it would exhibit maximum buffering power. On a hot and humid day in July, 1982, the late Dr. G. Dossi appeared in my laboratory with the gadget shown in Fig. 2.7: a five-chambered mixer in which five of the seven Immobilines were used as buffers (a single species in each chamber) and the remaining two as titrants (the pK 3.6 acid for the three bases and the pK 9.3 base for the two acids) (Dossi et al., 1983). We made at least one basic mistake though: we used two acids (pKs 4.4 and 4.6), with adjacent pKs, in the same mixture, so that we could never straighten up the acidic end of our pH gradient (too much buffering power – remember what is stated in §2.2.3).

For that matter, we could never maintain a linear course also at the alkaline extreme, and that was the second mistake, to try to titrate the upper end to a pH outside the last available pK.

In connection with this, a computer program was developed which, given the molarity and type of Immobiline in each chamber, would predict the course of the pH gradient generated, together with the buffering capacity (β) and ionic strength (I) profiles associated with that particular pH range. For that, we had to derive some basic equations describing the system. By writing the equilibrium constants of the dissociation of acidic and basic Immobilines, and considering the electroneutrality law, we can derive the first one:

$$\sum_{j=1}^{l} [B_j^+] \frac{[H^+]}{[H^+] + K_j} - \sum_{i=1}^{m} [A_i^-] \frac{K_i}{[H^+] + K_i} = 0 \qquad (6)$$

where $[A_j^-]$ and $[B_j^-]$ are the molar dissociated fractions of acidic and basic Immobilines, respectively, and K_i and K_j are the numerical values of their respective pKs. Eq. 6 is a polynomial of degree $(m + 1)$ in $[H^+]$. This equation can be solved numerically by Newton's approximation when the actual concentration of all the Immobilines in the output flow are known. These can be calculated with the generalized Peterson-Sober (1959) equation:

$$C_i = \sum_{j=1}^{N} L_{ij} \frac{(N-1)!}{(N-j)!(j-1)!} \left(1 - \frac{v}{V}\right)^{N-j} \left(\frac{v}{V}\right)^{j-1} \qquad (7)$$

where C_i is the output concentration of species i, L_{ij} is the initial concentration of species i in the jth chamber, N is the number of chambers used, V is the total volume in the system and v is the dispensed volume.

This approach was clever in a way, but required laborious manipulations and too much care in handling so many different solutions, so we realized it was bound to end up in a dusty corner in a Science museum (we hope it will, one day). The reason being that users are already upset in having two use a two-chamber mixer, imagine a five- (or even worse, a nine-) chambered appara-

tus! We were thus forced to resort to a second approach, as outlined below.

2.3.2. Two chamber mixers with identical buffer concentration

The problem of generating extended pH gradients with a two-chamber mixer could have two different solutions. In one approach, a two-chamber device of non-identical cross section is used. The mixture of buffering components, titrated with a non-buffering species to one extreme of the pH interval, is placed in the mixing chamber, while the titrant, needed to bring the mixture to the other extreme of the chosen range, is filled into a reservoir of highly reduced cross section. In this system, however, because the volume in the reservoirs is small in comparison with the volume of the titrated solution, and assuming that the pK of the titrant ion is well outside the generated pH interval, so that it is fully dissociated throughout, an exponential pH gradient is generated whose slope depends on the ratio of the two volumes.

In another approach (the one finally adopted), a mixer having two chambers of identical cross-section is used. In this case, the eluate contains linearly increasing amounts (from 0 to 100%) of the species present in the reservoir and linearly decreasing amounts (from 100 to 0%) of the compunds initially present in the mixing chamber. This behavior, fully predicted by Eq. 7, suggests the use of the same buffering species, in identical concentration, in both chambers of the gradient mixer, titrated with the aid of non-buffering Immobilines (fully dissociated in the entire interval of the generated pH gradient) to the two extremes of the desired pH interval. During elution, the concentration of the buffering species is strictly constant while the concentration of the non-buffering compounds in the eluate varies linearly, thus giving a true titration of the buffering groups. The buffering power (β) is defined as:

$$\beta = \mathrm{d}B/\mathrm{d}(\mathrm{pH}) \tag{8}$$

where $\mathrm{d}B$ and d(pH) are infinitesimal variations of the titrant species and of pH, respectively. Eq. 7 shows that the titrant

concentration changes linearly as a function of the eluted volume (v), therefore:

$$dB/dv = \text{constant} \tag{9}$$

Therefore, as under our experimental conditions we aim at generating linear pH gradients, which is to say:

$$d(pH)/dv = \text{constant} \tag{10}$$

it follows that, by substituting Eqs. 9 and 10 into Eq. 8:

$$\beta = \text{constant} \tag{11}$$

In other words, *the fundamental requirement for generating a linear pH gradient is that the buffering power is constant throughout.* Note that, while Eq. 11 seems matter of fact, a sort of a trivial truth, in reality it has never been spelled out before in any treatise dealing with the concept of pH values and titration; thus, only now, with the advent of the Immobiline technology, its full value and impact has been realized. For optimization of pH gradient linearity, the most convenient solution is to keep varying the relative concentrations of the buffering species, until the β power reaches a constant value in the desired pH interval. For this purpose, in the computer program described above, we have introduced a procedure for optimizing the composition of the solutions used in the mixing chambers. This algorithm minimizes the coefficient of variation of the buffering capacity (β), in the interval of the generated pH gradient, by progressively varying the relative concentrations of the buffering species until peaks and valleys of β power are flattened out (Gianazza et al., 1983a; 1984a). A comparison between the multi-chamber and two-chamber mixer approaches is shown in Fig. 2.8. In both instances a fairly linear pH 4–9 gradient is generated, with a reasonably smooth β power and acceptable ionic strength profiles (the two-chamber approach, though, appears better because the Immobiline mixture could be optimized with the aid of the newly developed computer program). The solution adopted for generating wide pH gradient intervals

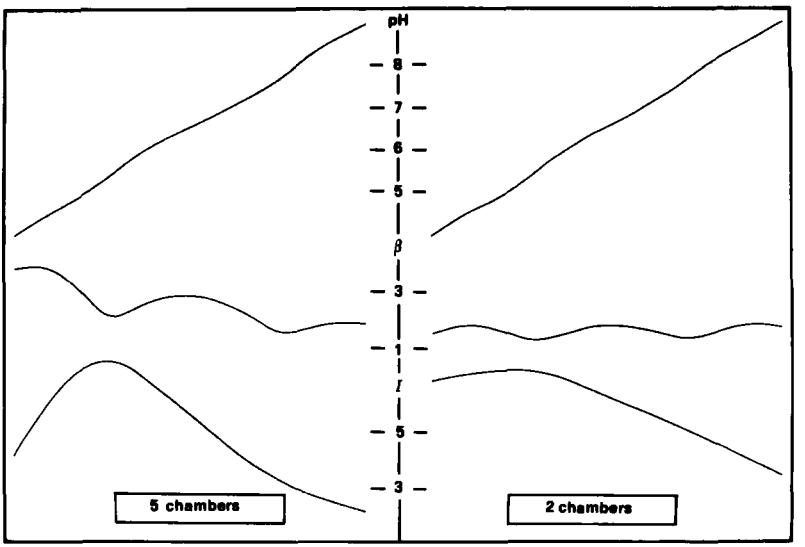

Fig. 2.8. Generation of extended IPG intervals. A 5-pH-unit gradient (pH 4–9) was generated with either a five or a two-chamber mixing unit. In both instances the accompanying buffering power (β) and ionic strength (I) values are plotted. Both graphs have been generated with the aid of the computer program of Celentano et al. (1987) except that the pH gradient profile has also been checked by eluting 1 ml aliquots from the two devices and measuring the pH in each solution (from Righetti et al., 1983a; with permission of Elsevier).

with a two-chamber device under the constant concentration concept is by far the simplest: a single mixture of the desired buffering species is made, with relative molarities optimized in terms of constant β power and pH gradient linearity. This solution is then divided into two equal portions: to one enough equivalents of the pK 1 acidic titrant are added to lower the pH to the desired acidic extreme; the other is titrated, with the aid of the quaternary acrylamido-base, to the other extreme of the pH interval. The two solutions are then poured, with the aid of a two-vessel gradient mixer, in the gel cassette, thus automatically creating a linear pH gradient between these two extremes. However, the multi-chamber approach, as devised at the beginning of our IPG saga, was valuable to us for at least one practical reason: in the absence of commercially available strong titrants (we started introducing them

during 1983, but LKB has officially ignored them for all these years), only this device allowed the generation of fairly extended pH intervals (at that time, the widest one we could generate was an IPG pH 4–9) with the use of the buffering species alone, thus disposing of non-buffering titrants.

2.3.3. Two-chamber mixers with different buffer concentrations

By computer modelling, it was shown that linear pH gradients could be obtained only by arranging for an even buffering power throughout the titration interval (see Eq. 11). The latter could be ensured only by ideal buffers spaced apart by $\Delta pK = 1$. In practice, since there are only 6 Immobiline species rather than 7 (the pKs 4.4 and 4.6 should never be mixed together!) there are two ways to smooth the β power along the pH scale. In the approach seen above (§2.3.2), the concentration of each buffer is kept constant throughout the span of the pH gradient and 'holes' of buffering power are filled by increasing the amounts of the buffering species bordering the largest ΔpKs (Fig. 2.9A). In the other approach (varying buffer concentration, Fig. 2.9B) the variation in concentration of different buffers along the width of the desired pH gradient results in a shift in each buffer's apparent pK, along with the ΔpK values evening out (Gianazza et al., 1984a).

It might be asked what is the use of all the calculations and computer simulations given above. Well, they have been the base for generating all the recipes for extended IPG gradients. For example, Table 2.3 gives the formulations for 2- and 3-pH unit wide gradients whose intervals can be generated without the aid of strongly acidic and basic titrants. In Table 2.4 are computed the remaining pH intervals, 4-, 5- and 6-pH unit wide gradients. In this Table, for each pH interval we give two formulations: on the left side, we show the recipe with identical molarities of the buffering Immobilines in the two vessels of the gradient mixer (according to §2.2.3 and to Fig. 2.9A), which are then titrated with strong acid and bases to the two extremes and, on the right side, we list the corresponding recipes formulated according to the principle of 'unequal concentration' of the buffering ions in the two vessels (e.g., Fig. 2.9B). All these formulations have a 'pedigree', namely:

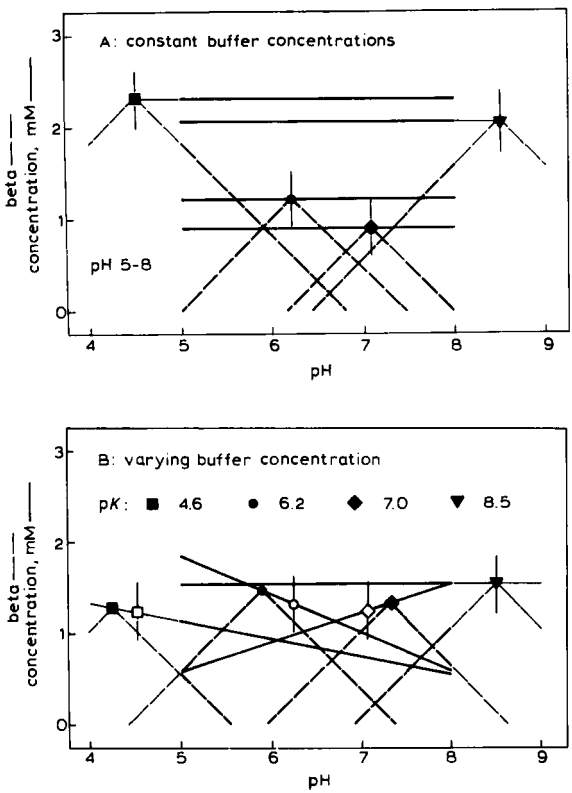

Fig. 2.9. Illustration of two alternative methods for the preparation of IPGs. (A): same concentration of each buffer in both chambers; (B): varying buffer concentration between the chambers. The same pH 5–8 gradient is taken as an example in both cases. The concentrations of the various Immobilines are represented with continuous thick lines (horizontal in panel A, slanted in panel B) within the span of the gradient, and with thin lines when extrapolated outside it. The buffering power (β) courses are approximated by wedges (broken lines) with apexes centred at the pKs of the different Immobilines (the scale of β is in arbitrary units). The solid symbols refer to the position of the apparent pKs under the actual gradient conditions, and the barred open symbols to conditions of ideal titration (when distinct from above). The identification between the various symbols and the different Immobilines is given in panel b (from Gianazza et al., 1984b; with permission of Verlag Chemie).

(a) they are guaranteed to generate pH gradients with deviation from linearity not exceeding 1% of the stated pH interval (e.g., a maximum of 0.01 pH unit deviation on a 1 pH unit interval and so on); (b) they have been calculated to give a minimum comsumption of Immobiline species, by providing an average β value of 3 mequiv.$l^{-1}pH^{-1}$ (amply satisfactory for most analytical separations; in fact, acceptable separations can still be obtained with a β power as low as 1 mequiv.$l^{-1}pH^{-1}$).

These are not the only formulations we have tabulated. Since for years the two strong titrants we have now listed in Tables 1.2 and 1.3 of Chapter 1 (AMPS and QAE-acrylamide) have not been available to the scientific community (and still now are not on the list of the offical LKB Immobilines), we have been besieged by requests to re-formulate our recipes for wide IPG gradients without the aid of strong titrants. This could still be possible if a multichamber apparatus (see Fig. 2.7) were used; yet such a device would not be practical for laboratories that routinely use two-chamber mixers. To solve this dilemma, we have recalculated and listed in Table 2.5 (A to F) all gradients between 4 and 6 pH units in the absence of the strong titrants (i.e., solely with the six LKB Immobilines). How can the recipes in Tables 2.4 and 2.5 be compared? In terms of linearity of the pH course, the quality of the gradients is comparable for the pH 5–9, 6–10 and 5–10 intervals. Worse results are observed, however, with the pH 4–8, 4–9 and 4–10 gradients (standard deviation 2–3 times larger in Table 2.5 than in Table 2.4). In general, the largest deviations (sometimes as high as 5%) are to be found in the acidic portion of the gradient, between pH 4 and 6. Even with these shortcomings, the recipes of Table 2.5 are still acceptable and can be used with full confidence in those laboratories unable to obtain the two strong titrants.

In Table 2.5 (entries G and H) formulations are given for the widest possible pH span, a pH 3–10 interval, prepared with a two-chamber mixer either according to the 'same concentration' (G) or to the 'different concentration' (H) approaches (Gianazza et al., 1985b). Both formulations (G and H) perform well and with practically identical results in the analysis of complex protein mixtures. It is clear, however, that in neither case could such a wide pH range be created without resorting to strong titrants.

TABLE 2.4
4, 5 and 6 pH unit-wide immobilized pH gradients

4–8
Initial pH: 4.000
Final pH : 8.000
Notes : 4.068–8.153(7.813) : 4.084–8.004(7.689)
Buffer concentrations

				mM		mM
n. 1	pK	0.80	Cham 1	11.085	Cham 2	0.000
n. 2	pK	3.57	Cham 1	0.564	Cham 2	0.864
n. 3	pK	4.51	Cham 1	5.259	Cham 2	5.259
n. 4	pK	6.21	Cham 1	4.167	Cham 2	4.167
n. 5	pK	7.06	Cham 1	2.379	Cham 2	2.379
n. 6	pK	8.50	Cham 1	6.432	Cham 2	6.432
n. 8	pK	12.00	Cham 1	0.000	Cham 2	0.924

4–9
Initial pH: 4.000
Final pH : 9.000
Notes : 4.071–9.086(8.007) : 4.088–3.925(7.876)
Buffer concentrations

				mM		mM
n. 1	pK	0.80	Cham 1	11.649	Cham 2	0.000
n. 2	pK	3.57	Cham 1	0.657	Cham 2	0.657
n. 3	pK	4.51	Cham 1	5.394	Cham 2	5.394
n. 4	pK	6.21	Cham 1	3.888	Cham 2	3.888
n. 5	pK	7.06	Cham 1	2.943	Cham 2	2.943
n. 6	pK	8.50	Cham 1	4.734	Cham 2	4.734
n. 7	pK	9.59	Cham 1	1.857	Cham 2	1.857
n. 8	pK	12.00	Cham 1	0.000	Cham 2	3.399

Initial pH: 4.015
Final pH : 8.008
Notes : 4.076–8.112 : 4.091 – 7.986
Buffer concentrations

				mM		mM
n. 1	pK	0.80	Cham 1	8.643	Cham 2	0.000
n. 2	pK	3.57	Cham 1	1.420	Cham 2	0.000
n. 3	pK	4.51	Cham 1	4.560	Cham 2	6.519
n. 4	pK	6.21	Cham 1	5.222	Cham 2	1.975
n. 5	pK	7.06	Cham 1	2.326	Cham 2	4.586
n. 6	pK	8.50	Cham 1	3.276	Cham 2	3.822
n. 8	pK	12.00	Cham 1	0.000	Cham 2	3.130

Initial pH: 4.019
Final pH : 8.996
Notes : 4.067–8.900 : 4.081–8.825
Buffer concentrations

				mM		mM
n. 1	pK	0.80	Cham 1	11.793	Cham 2	0.000
n. 2	pK	3.57	Cham 1	2.832	Cham 2	4.130
n. 3	pK	4.51	Cham 2	7.780		
n. 4	pK	6.21	Cham 1	5.353	Cham 2	2.635
n. 5	pK	7.06	Cham 1	0.585	Cham 2	4.252
n. 6	pK	8.50	Cham 1	4.814	Cham 2	3.056
n. 7	pK	9.59	Cham 1	4.196	Cham 2	4.654
n. 8	pK	12.00	Cham 1	0.000	Cham 2	7.415

5–9
Initial pH: 5.000
Final pH : 9.000
Notes : 5.076–9.086(7.544) : 5.085–8.926(7.457)
Buffer concentrations

				mM		mM
n. 1	pK	0.80	Cham 1	7.527	Cham 2	0.000
n. 3	pK	4.51	Cham 1	7.089	Cham 2	7.089
n. 4	pK	6.21	Cham 1	3.408	Cham 2	3.406
n. 5	pK	7.06	Cham 1	3.180	Cham 2	3.180
n. 6	pK	8.50	Cham 1	4.683	Cham 2	4.683
n. 7	pK	9.59	Cham 1	1.839	Cham 2	1.839
n. 8	pK	12.00	Cham 1	0.000	Cham 2	4.464

5–0
Initial pH: 5.000
Final pH : 10.000
Notes : 5.076–9.892(8.171) : 5.086–9.745(8.034)
Buffer concentrations

				mM		mM
n. 1	pK	0.80	Cham 1	9.102	Cham 2	0.000
n. 3	pK	4.51	Cham 1	7.179	Cham 2	7.179
n. 4	pK	6.21	Cham 1	3.210	Cham 2	3.210
n. 5	pK	7.06	Cham 1	3.531	Cham 2	3.531
n. 6	pK	8.50	Cham 1	3.729	Cham 2	3.729
n. 7	pK	9.59	Cham 1	4.275	Cham 2	4.275
n. 8	pK	12.00	Cham 1	0.000	Cham 2	5.922

Initial pH: 5.022
Final pH : 9.037
Notes : 5.100–9.080 : 5.110–8.921
Buffer concentrations

				mM		mM
n. 1	pK	0.80	Cham 1	11.404	Cham 2	0.000
n. 3	pK	4.51	Cham 1	7.989	Cham 2	3.498
n. 4	pK	6.21	Cham 1	3.102	Cham 2	3.493
n. 5	pK	7.06	Cham 1	1.908	Cham 2	2.933
n. 6	pK	8.50	Cham 1	11.020	Cham 2	4.091
n. 7	pK	9.59	Cham 1	1.694	Cham 2	2.692
n. 8	pK	12.00	Cham 1	0.000	Cham 2	0.438

Initial pH: 4.993
Final pH : 10.034
Notes : 5.068–9.933 : 5.075–9.779
Buffer concentrations

				mM		mM
n. 1	pK	0.80	Cham 1	7.605	Cham 2	0.295
n. 3	pK	4.51	Cham 1	6.260	Cham 2	0.805
n. 4	pK	6.21	Cham 1	4.044	Cham 2	0.454
n. 5	pK	7.06	Cham 1	3.717	Cham 2	5.677
n. 6	pK	8.50	Cham 1	3.088	Cham 2	4.197
n. 7	pK	9.59	Cham 1	1.730	Cham 2	3.687

TABLE 2.4 (CONTINUED)

6–10

Initial pH: 6.000
Final pH : 10.000
Notes : 6.039–9.886 : 5.088–9.733
Buffer concentrations

				mM		mM
n. 1	pK	0.80	Cham 1	12.060	Cham 2	0.000
n. 1	pK	0.80	Cham 1	1.323	Cham 2	1.323
n. 4	pK	6.21	Cham 1	3.351	Cham 2	3.351
n. 5	pK	7.06	Cham 1	3.603	Cham 2	3.603
n. 6	pK	8.50	Cham 1	3.711	Cham 2	3.711
n. 7	pK	9.59	Cham 1	4.299	Cham 2	4.299
n. 8	pK	12.00	Cham 1	0.000	Cham 2	0.000

Initial pH: 5.994
Final pH : 9.996
Notes : 6.035–9.376 : 5.986–9.723
Buffer concentrations

				mM		mM
n. 2	pK	3.57	Cham 1	12.919	Cham 2	1.370
n. 4	pK	6.21	Cham 1	3.748	Cham 2	4.583
n. 5	pK	7.06	Cham 1	3.339	Cham 2	4.962
n. 6	pK	8.50	Cham 1	3.585	Cham 2	3.283
n. 7	pK	9.59	Cham 1	3.891	Cham 2	4.475

4–10

Initial pH: 4.000
Final pH : 10.000
Notes : 4.079–9.891(8.658) : 4.097–9.742(8.502)
Buffer concentrations

				mM		mM
n. 1	pK	0.80	Cham 1	13.656	Cham 2	0.000
n. 3	pK	4.51	Cham 1	5.712	Cham 2	5.712
n. 4	pK	6.21	Cham 1	3.609	Cham 2	3.609
n. 5	pK	7.06	Cham 1	3.342	Cham 2	3.342
n. 6	pK	8.50	Cham 1	3.765	Cham 2	3.765
n. 7	pK	9.59	Cham 1	4.305	Cham 2	4.305
n. 8	pK	12.00	Cham 1	0.000	Cham 2	4.431

Initial pH: 4.026
Final pH : 9.968
Notes : 4.105–9.826 : 4.121–9.675
Buffer concentrations

				mM		mM
n. 1	pK	0.80	Cham 1	15.849	Cham 2	0.000
n. 3	pK	4.51	Cham 1	4.740	Cham 2	2.446
n. 4	pK	6.21	Cham 1	6.645	Cham 2	0.000
n. 5	pK	7.06	Cham 1	0.000	Cham 2	6.799
n. 6	pK	8.50	Cham 1	6.633	Cham 2	1.977
n. 7	pK	9.59	Cham 1	3.776	Cham 2	5.641
n. 8	pK	12.00	Cham 1	0.000	Cham 2	0.715

From Gianazza et al. (1984b). The "same concentration" formulations are listed in the left column, the ones with "different concentrations" on the right. In each mixture record: initial and final pHs in the gel phase, at 10 °C. Notes: pH of the limiting solutions (and of the buffer mixture, prior to the addition of titrants) at 20 °C (figures before) and at 25 °C (figures after the colon). Buffer concentrations: expressed as mM/l (to convert into μl/ml, for 0.2 M Immobiline concentration, multiply by 5).

TABLE 2.5
4, 5 and 6 pH unit-wide gradients prepared with only six available Immobiline

A 4-8, No titrants

Initial pH: 4.090
Final pH : 8.010
Notes : pH in solution at 25 °C: 4.12–7.97
Buffer concentrations

			mM		mM
pK	3.57	Cham 1	7.850	Cham 2	0.000
pK	4.51	Cham 1	3.380	Cham 2	7.384
pK	6.21	Cham 1	3.136	Cham 2	4.792
pK	7.06	Cham 1	1.564	Cham 2	1.894
pK	8.50	Cham 1	2.261	Cham 2	4.454
pK	9.59	Cham 1	0.000	Cham 2	3.838

B 5-9, No titrants

Initial pH: 5.060
Final pH : 9.040
Notes : pH in solution at 25 °C: 5.13–8.91
Buffer concentrations

			mM		mM
pK	3.57	Cham 1	11.059	Cham 2	0.000
pK	4.51	Cham 1	7.759	Cham 2	3.317
pK	6.21	Cham 1	2.903	Cham 2	3.510
pK	7.06	Cham 1	1.835	Cham 2	2.833
pK	8.50	Cham 1	10.601	Cham 2	3.892
pK	9.59	Cham 1	1.630	Cham 2	3.071

C 6-10, No titrants

Initial pH: 5.980
Final pH : 10.000
Notes : pH in solution at 25 °C: 5.97–9.72
Buffer concentrations

			mM		mM
pK	3.57	Cham 1	12.546	Cham 2	1.329
pK	6.21	Cham 1	3.634	Cham 2	4.446
pK	7.06	Cham 1	3.237	Cham 2	4.813
pK	8.50	Cham 1	3.471	Cham 2	3.185
pK	9.59	Cham 1	3.761	Cham 2	4.341

D 4-9, No titrants

Initial pH: 4.140
Final pH : 8.920
Notes : pH in solution at 25 °C: 4.18–8.65
Buffer concentrations

			mM		mM
pK	3.57	Cham 1	11.048	Cham 2	1.964
pK	4.51	Cham 1	3.138	Cham 2	5.656
pK	6.21	Cham 1	3.092	Cham 2	4.801
pK	7.06	Cham 1	0.298	Cham 2	3.952
pK	8.50	Cham 1	3.336	Cham 2	0.942
pK	9.59	Cham 1	2.951	Cham 2	8.834

TABLE 2.5 (CONTINUED)

E 5-10, No titrants

Initial pH: 5.040
Final pH : 10.040
Notes : pH in solution at 25 °C: 5.11–9.79
Buffer concentrations

			mM		mM
pK	3.57	Cham 1	7.505	Cham 2	0.286
pK	4.51	Cham 1	6.178	Cham 2	0.788
pK	6.21	Cham 1	3.970	Cham 2	0.447
pK	7.06	Cham 1	3.646	Cham 2	5.593
pK	8.50	Cham 1	3.027	Cham 2	4.138
pK	9.59	Cham 1	1.689	Cham 2	3.637

F 4-10, No titrants

Initial pH: 4.150
Final pH : 9.950
Notes : pH in solution at 25 °C: 4.16–9.66
Buffer concentrations

			mM		mM
pK	3.57	Cham 1	14.699	Cham 2	0.000
pK	4.51	Cham 1	0.000	Cham 2	1.523
pK	6.21	Cham 1	6.073	Cham 2	0.667
pK	7.06	Cham 1	1.187	Cham 2	6.503
pK	8.50	Cham 1	4.452	Cham 2	2.089
pK	9.59	Cham 1	0.000	Cham 2	4.763

G 3-10, Same concentration

Initial pH: 3.000
Final pH : 10.000
Notes : pH in solution at 25 °C: 3.02–9.75 (mixture: 7.76)
Buffer concentrations

			mM		mM
pK	0.80	Cham 1	14.211	Cham 2	0.000
pK	3.57	Cham 1	4.137	Cham 2	4.137
pK	4.51	Cham 1	3.764	Cham 2	3.764
pK	6.21	Cham 1	4.017	Cham 2	4.017
pK	7.06	Cham 1	3.041	Cham 2	3.041
pK	8.50	Cham 1	3.780	Cham 2	3.780
pK	9.59	Cham 1	4.278	Cham 2	4.278
pK	12.00	Cham 1	0.000	Cham 2	6.647

H 3-10, Different concentrations

Initial pH: 2.970
Final pH : 9.960
Notes : pH in solution at 25 °C: 3.00–9.66
Buffer concentrations

			mM		mM
pK	0.80	Cham 1	17.083	Cham 2	0.000
pK	3.57	Cham 1	2.252	Cham 2	0.000
pK	4.51	Cham 1	5.013	Cham 2	2.596
pK	6.21	Cham 1	6.688	Cham 2	0.000
pK	7.06	Cham 1	0.000	Cham 2	7.115
pK	8.50	Cham 1	6.931	Cham 2	2.072
pK	9.59	Cham 1	3.946	Cham 2	5.899

From Gianazza et al. (1985b). See also footnote to Table 2.4

2.3.4. Non-linear, extended pH gradients

Up to now IPG formulations have been given only in terms of rigorously linear pH gradients. Although this has been the only solution adopted so far, it might not be the optimal one in some cases. The pH slope might need to be altered in pH regions that are overcrowded with proteins. In conventional IEF, flattening of the gradient slope in some regions was obtained in three different ways: (1) by adding amphoteric spacers (separator IEF of Brown et al., 1977), (2) by changing the gel thickness ('thickness-modified' slope of Altland and Kaempfer, 1980) and (3) by changing the concentration of carrier ampholytes ('concentration-modified' slope of Låås and Olsson, 1981).

Table 2.6 gives two examples of a non-linear, pH 4–10 interval, obtained without titrants (upper) or with only a strongly acidic

TABLE 2.6
Nonlinear 4–10 Immobilized pH gradient

"IDEAL" 4–10					
Initial pH		: 4.190			
Final pH		: 9.980			
Notes		: pH in solution at 25 °C: 4.24–9.70			
buffer concentrations		(no titrants)			
			mM		mM
p*K*	3.57	Cham 1	9.321	Cham 2	0.577
p*K*	4.51	Cham 1	4.327	Cham 2	0.000
p*K*	6.21	Cham 1	8.943	Cham 2	2.596
p*K*	7.06	Cham 1	0.000	Cham 2	3.173
p*K*	8.50	Cham 1	0.000	Cham 2	1.154
p*K*	9.59	Cham 1	0.000	Cham 2	1.846
"IDEAL" 4–10					
Initial pH		: 4.04			
Final pH		: 9.880			
Notes		: pH in solution at 25 °C: 4.13–9.61			
Buffer concentrations		(with acidic titrant)			
			mM		mM
p*K*	0.80	Cham 1	7.028	Cham 2	0.910
p*K*	4.51	Cham 1	7.659	Cham 2	0.000
p*K*	6.21	Cham 1	9.010	Cham 2	2.703
p*K*	7.06	Cham 1	0.000	Cham 2	3.604
p*K*	8.50	Cham 1	0.000	Cham 2	1.352
p*K*	9.59	Cham 1	0.000	Cham 2	2.523

From Gianazza et al. (1985a)

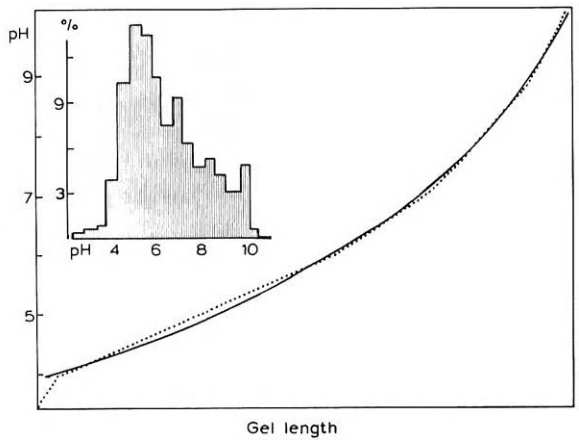

Fig. 2.10. Non-linear pH 4–10 gradient. Dotted line: ideal; solid line: actual (lower formulation, including acidic titrant from Table 2.6) pH courses. The shape for the ideal profile was computed from data on the statistical distribution of protein pIs (Gianazza and Righetti, 1980). The relevant histogram is redrawn in the figure inset (from Gianazza et al., 1985b; with permission from Verlag Chemie).

titrant (lower panel). This has been calculated for a general case involving the separation of proteins in a complex mixture, such as a cell lysate. Gianazza and Righetti (1980) have computed the statistical distribution of the pIs of the water soluble proteins given in the histogram shown in Fig. 2.10. With the relative abundance of different species, it is clear that an optimally resolving pH gradient should have a gentler slope in the acidic portion and a steeper course in the alkaline region. Such a general course has been calculated by assigning to each 0.5 pH unit interval in the pH 3.5–10 region a slope inversely proportional to the relative abundance of proteins in that interval: by such a procedure the ideal curve (dotted line) in Fig. 2.10 was obtained. Of the two formulations given in Table 2.6, the one including the strongly acidic titrant followed most closely the theoretically predicted course (solid line). In a separation of a crude lysate of *Klebsiella pneumoniae*, a great improvement in resolution for the acidic cluster of bands, without loss of the basic portion of the pattern, was obtained (Gianazza et al., 1985a). What is also important here is the establishment of a new principle in IPG technology, namely

that the pH gradient and the density gradient stabilizing it need not be colinear, because the pH can be adjusted by localized flattening for increased resolution while leaving the density gradient unaltered. Though we have considered only the example of an extended pH gradient, narrower pH intervals can be treated in the same fashion.

2.3.5. Computer simulations

The computer program we have developed (Celentano et al., 1987) has helped us to understand to a greater depth the basic behavior of IPGs; in fact, such a sophisticated technique would be misused if one could not control the experimental parameters and the possible sources of errors connected with the dispensing of the Immobiline chemicals. I should also like to add that this knowledge is not strictly related to IPGs: the basic principles will also apply to separations in ion-exchange chromatography and chromatofocusing, thus greatly broadening our horizons. Here are some examples of the applications: greater details are to be found in Celentano et al. (1987).

2.3.6. How to smooth the β power

As a constant β power appears to be fundamental for generating linear pH gradients with the above approaches, we have simulated the behavior of the β course as a function of the ΔpKs of the buffers. As shown in Fig. 2.11, the smoothest β power course is obtained when buffers have evenly spaced pKs at 1 pH unit intervals. As the ΔpKs are increased, peaks and walleys of β power become more pronounced, with concomitant increments of pH deviation from linearity. Conversely, nothing is gained if the ΔpKs are progressively decreased below 1 pH unit, as already at $\Delta pK = 1$ a very linear pH gradient (deviation ± 0.003 pH unit) and a fairly smooth β power are obtained. What is detrimental to pH gradient linearity, therefore, is an uneven distribution of the pKs of the buffers. One practical consequence is immediately apparent: when generating extended pH gradients, Immobilines of pK 4.4 and 4.6 should never be mixed together (after realizing that, LKB has

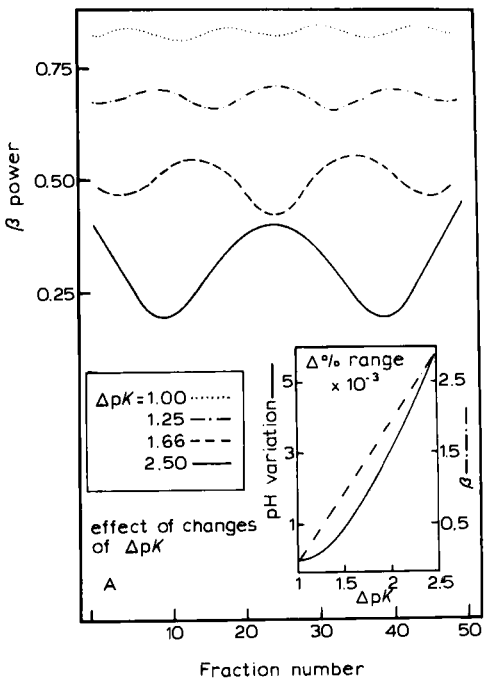

Fig. 2.11. Effect of changes in the number of (evenly spaced) buffering components. The optimal concentrations of fictitious buffers (bases), with pKs differing by 1, 1.25, 1.66 and 2.5 pH units, were calculated so as to cover the pH range 4.5–8.5. The resulting courses of β power are shown as a function of ΔpK. The insert is a plot of the percentage variation, in comparison with the case $\Delta pK = 1$, of the ranges of deviation of pH (left-handed scale) and of β (right-handed scale). Simulation obtained with the computer program developed by Celentano et al. (1987) (from Gianazza et al., 1983a; with permission of Elsevier).

discontinued the production of the pK 4.4 species). Thus, basically, with a set of barely 8 buffers (+2 strong titrants) it is possible to cover the entire pH 2.5–11 scale. This is a far cry from conventional pH gradients with carrier ampholytes, where it had been calculated that a minimum of 20 species, evenly spaced at $\Delta pI = 0.05$, were required per pH unit for generating a stepless pH course (Almgren, 1971) (in reality, there might be a few hundred species per pH unit). We have learned another interesting lesson from our computer simulation: when presently available Immobilines are

titrated over 4 pH units (pH 4.5–8.5) a fairly even β power throughout can be arranged, which is still fairly well maintained when this range is extended to 5 pH units (pH 4–9). However, as soon as the pH interval is extended to pHs outside pK_{min} and pK_{max} of the components of the mixture (e.g., pH 3.5–9.5 with commercially available Immobilines, pH 3–10.5 with the set given

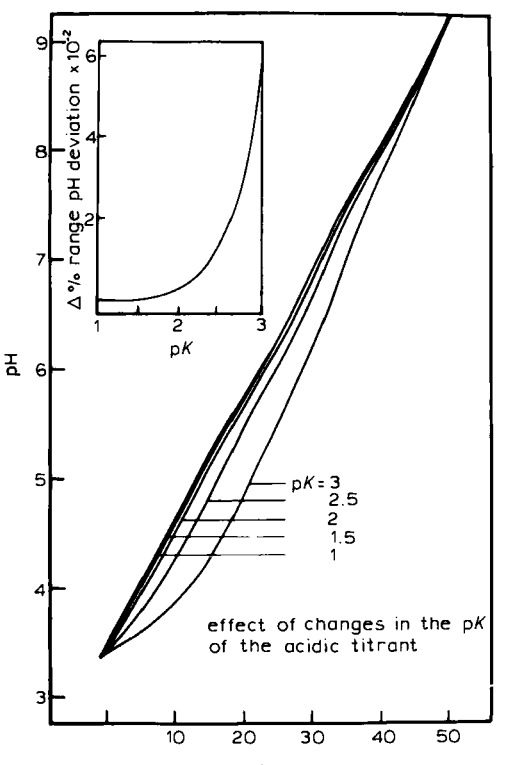

Fig. 2.12. Effect of changes in the pK of the acidic titrant. A reference Immobiline mixture was titrated to the same pH value with fictitious acids whose pK was 0.5, 1.0, 1.5, 2.0 and 2.5 pH untis lower than the gradient's limit (in this case, pH_{min} = 3.5) and the pH course was calculated for the five cases. The insert is a plot of the percentage variation of deviation from linearity as the titrant's pK increases. Simulation obtained with the computer program developed by Celentano et al. (1987) (from Gianazza et al., 1983a; with permission of Elsevier).

in Tables 1.1 and 1.2 of Chapter 1), two sharp hills of β form at the two extremes, and the pH gradient looses its linear course.

What is an acceptable deviation from linearity in our IPG system? We have taken as a maximum deviation 1% of the stated pH interval (in pH units). Thus, in a 1 pH unit interval, the maximum acceptable deviation will be ± 0.01 pH unit, and so on. In practice, it is possible to do better than that: in the pH ranges tabulated in Tables 2.3 and 2.4, the deviation from linearity is of the order of a few thousandths of a pH unit.

2.3.7. How to choose the titrants

The need to have strongly acidic and strongly basic titrants, for generating wide pH intervals, was immediately apparent from Fig. 2.11. I have previously defined a titrant as a species that is fully dissociated in the desired pH interval: if it becomes progressively undissociated it means that it has a pK within the operative pH range and as such it will behave as a buffer and will automatically influence the pH course. In Fig. 2.12 we have simulated the case of an acidic titrant: as long as the distance between pH_{min} and the titrant pK is above 2 pH units, this compound will behave as an ideal titrant and will not affect the slope of the desired pH gradient. However, as $pK - pH_{min}$ becomes smaller than 1, the acidic portion of the pH curve will be flattened out; when this distance is only 0.5 pH unit, the effect on the pH gradient will be felt even up to alkaline pHs (pH 8 and above; see Fig. 2.12). The same reasoning will apply to the alkaline branch of the pH gradient in the case of a basic titrant.

2.3.8. On the architecture of our computer program

Basically, the computer program we have written for simulating the behavior of IPGs in narrow and wide pH gradients, contains:

(1) The basic stoichiometric equations for dissociation of monoprotic weak acids (A_iH) and weak bases (B_jOH), i.e.:

$$[A_i^-] = k_i[AH]_T/(k_i + [H^+]) \tag{12}$$

$$[B_j^-] = [B_jOH]_T[H^+]/(k_j + [H^+]) \tag{13}$$

where, as usual, the square brackets denote concentrations and $[A_iH]_T$ and $[B_jOH]_T$ are the total concentrations of acid and base actually present in the solution;

(2) The electroneutrality condition, imposing that the sum of the positively charged species equals the sum of the negatively charged ones (Eq. 6). Eq. 6 neglects the $[H^+]$ and $[OH^-]$ contributions to the charge in the solution: such an approximation seems reasonable when $4 < pH > 10$ and, at the same time, the buffer concentration is at least 10 mM (which is the case in most of the IPG recipes given). In any case, at extreme pH values, water itself behaves as a buffer and, since it is in great excess, its mobility and concentration variations can be neglected, allowing it to be treated as an immobilized buffer (Righetti et al., 1986c);

(3) An equation giving the total buffering power of the solution as the sum of all the partial β values of all Immobilines in the system (see ahead);

(4) An equation giving the total ionic strength of the system (see ahead);

(5) the Peterson-Sober equation given before (Eq. 7) allowing the calculation of the actual concentrations dispensed in each liquid element eluted from a multichamber mixer. Eq. 7, in reality, has been modified into Eq. 14, due to the fact that today we only use a two-chamber mixer ($N = 2$):

$$C_h = L_{h1} + (L_{h2} - L_{h1})v/V \tag{14}$$

which indicates that the output concentration either increases or decreases linearly, beginning at the L_{h1} value and ending at L_{h2}. In order to compute the pH, buffering power and ionic strength of the output gradient, the concentrations of the different species have to be calculated, according to Eq. 14, for an adequate number of elution steps (in general 20 steps, but the number can be varied up to 50), and introduced into Eqs. 6, 16 and 20. By comparing the pH of each fraction with the linear regression between the gradient extremes, the deviation of each point from linearity is evaluated.

(6) An optimization algorithm, having as a goal, for maintenance of pH gradient linearity, Eq. 11 (i.e., that β be constant throughout the titration interval). Given this goal, for each elution step we can compute, using Eq. 20, the buffering power of the mixture and minimize the coefficient of variation of the buffering capacity, $CV(\beta)$, in the pH interval of the gradient, defined as the ratio between the standard deviation of the buffering capacity itself, $SD(\beta)$, and its mean value β:

$$CV(\beta) = SD(\beta)/\beta \tag{15}$$

Such a choice for the target function is justified by the fact that the function to be optimized will oscillate around the constant goal function (Fig. 2.13), and a normal distribution of the deviations cannot be expected, so that all the prerequisites of the least square method vanish. In such a situation an optimization method based on the CV(β) minimization seems quite acceptable, on heuristic grounds.

2.3.9. The simulation and optimization program

An overview of the structure of the automatic program for gradient simulation can be seen in Fig. 2.14. This program (about 4000 lines of code), which has been developed on a SAGA FOX CP/M computer with a 64K memory, has been possible only by exploiting the SEGMENT and FORWARD declarations of the UCSD Pascal. These allow division of the program into separately compiled segments, each performing logically distinct functions. The drawback of such a choice is that it is impossible to use double precision calculations and sophisticated mathematical libraries, such as are available in FORTRAN.

As usual in structured Pascal programming, the main program simply calls the initialization segment, which defines the global variables, declares the common procedures and functions collected in a following segment, calls the service units, opens the required files, reads the system configuration parameters in an external ASCII file and offers a menu of the first level options (see Fig.

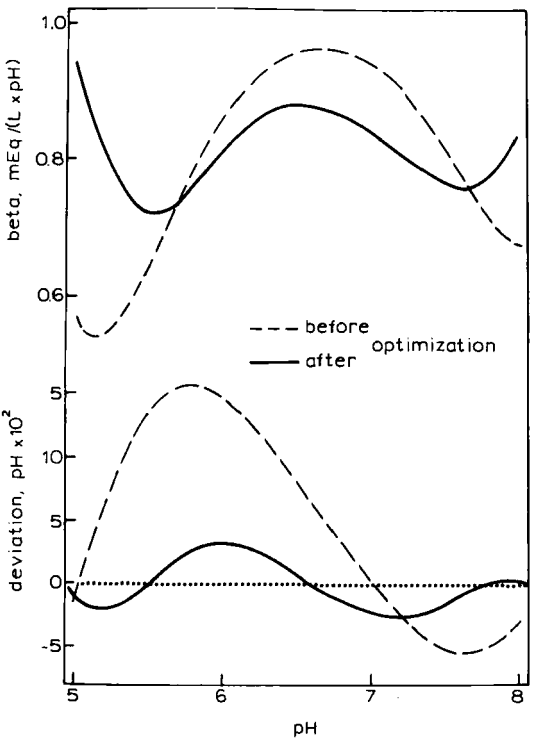

Fig. 2.13. Profiles of the buffering power (β, upper) and of the deviation from linearity of the pH course (lower) for a pH 5–8 range, computed when all buffers (pK 4.6, 6.2, 7.0 and 8.5) are given the same concentration, 1 mM ('before' optimization, broken tracing) and with pK = 2.318 mM, pK 6.2 = 1.217 mM, pK 7.0 = 0.906 mM, pK 8,.5 = 2.053 mM ('after' optimization, continuous tracing). In both cases, the two limiting solutions contain the same concentration of each buffer, and are titrated to the gradient extremes with a strong acid (pK 1.0) and a strong base (pK > 12) Simulation obtained with the computer program developed by Celentano et al. (1987) (with permission of Elsevier).

2.14, level 1), selected by typing a single letter in the usual UCSD Pascal style:

T(erminate, B(uffer, G(radient, bE(ta, where B calls the buffers archive manager, consisting of an editor and other filing utilities, allowing the user to:

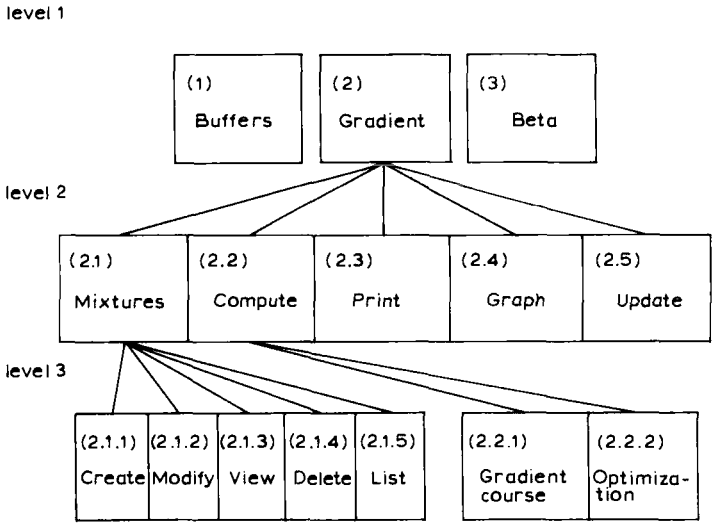

Fig. 2.14. An overview of the structure of the automatic program for pH gradient, β and I simulation in IPGs. Notice the tree-like organization inherent to the Pascal language (from Celentano et al., 1987; with permission of Elsevier).

Q(uit, C(reate, M(odify, V(iew, D(elete, L(ist a buffer (see Fig. 2.14, level 3).

The information contained in each record includes the data required for the calculations as well as the buffer name, producer, catalog number and additional notes by the user.

The G(radient and bE(ta options are similar in scope. Both contain a mixture editor, allowing the user to create, view, list, delete mixtures of the buffers contained in the proper archive. Then they allow the simulation or the optimization of the gradient, displaying the results as a printout or as a graph.

The difference between the two options is mainly in the mixture editor, as the one in bE(ta is intended for creating the mixtures for the two chambers (equal concentration) method. It should be underlined that all the methods for finding a gradient can be simulated and optimized using the same procedure. The one which avoids the use of the Peterson-Sober equation and automatically inserts the equal concentration constraints, results in faster com-

puter response. In practice, both the segments Gradient and Beta, besides the various common service procedures, call the same Calculate and Dotitration segments, and actually perform the required calculations. The segments of the program are as follows:

1	PHGRADIENT	(main)
2	SCREEN CONTROLLER	(screen manager)
3	DBWORKER	(data base manager)
4	INIT	(program initialization)
5	BUFEDIT	(buffer manager)
6	GRADIENT	(simulation and optimization)
7	BETA	(as above for two-chambers equal concentration)
8	MIXEDIT	(mixture manager for GRADIENT)
9	BCEDIT	(mixture manager for BETA)
10	CALCULATIONS	(gradient calculation and optimization)
11	DOTITRATION	(mixture titration to required pH)

All the common procedures for writing, making graphs, etc. are declared FORWARDS and collected in a twelfth segment.

The graphic part of the program is not linked to any particular hardware: it is composed of alphanumeric symbols, can be run on any alphanumeric screen and can be printed by any alphanumeric printer. In theory, this fact allows the program to be run on any computer for which an UCSD compiler and interpreter is available.

In practice, as the SAGA FOX computer we had utilized for this first version of the program turned out to be incompatible with just about any other computer available in the world, we have recently proposed a much advance version with the following main features:

(a) it is under MS-DOS, thus it is fully compatible with IBM hardware;
(b) the modules are written using the FORTRAN 77 subset implemented by the Microsoft FORTRAN 3.2 compiler, with the graphic functions in GW-BASIC;
(c) it allows computation of pH gradient, β and ionic strength not only of monoprotic, but also of polyprotic buffers each with up to 10 protolytic groups;

(d) it can handle a much complex mixture of up to 48 polyprotic buffers plus two titrants (the former program could handle only 10 monoprotic buffers).

As the accompanying equations describing the system are quite complex, I am just quoting this most recent program here and refer the interested readers to the original articles (Celentano et al., 1988; Righetti et al., 1988a). Why have we introduced simulations for polyprotic buffers in IPGs, where all the available buffers are monoprotic? Well, a paper had already appeared suggesting the use of a diprotic component (itaconic acid; Charlionet et al., 1984; see Chapter 1). In addition, we had quite a wild idea: creation of any IPG gradient with only two components: a strong acid and an oligoprotic basic buffer. The idea would be similar to the striking concept of Vesterberg (1969) for creating carrier ampholytes: use of oligoamines (PEHA, TETA, TEPA, see Chapter 1) to be reacted with acrylic acid. In our case, we would have taken PEHA, introduced an acrylic double bond at one extremity, and used this as a polybase with multiple pK values to be grafted to the polyacrylamide gel, titrated within any desired pH range with a strong acid (AMPS). The idea sounded nice, in theory, but in practice it was quite a disaster (due to the hydrophobicity of the unprotonated oligoamine in basic ranges and to the great uncertainty on pK values) thus it was abandoned (Righetti, Chiari and Gelfi, unpublished results). Even so, the new program is much better and more powerful than the previous one, and will soon be made commercially available through the Elsevier software library.

2.4. *How to deal with experimental errors*

If we believe in the properties of Immobilines and in the H-H equation (Eq. 1), there should be no doubt that highly reproducible pH gradients should be obtained run after run. However, as we do not live in an error-free environment, the reproducibility of our system will be only as good as our ability to minimize experimental errors (given for granted the fact that we now have completely solved the other major source of imprecision, the instability of the Immobiline chemicals; see Chapter 1, §1.7). The most dramatic

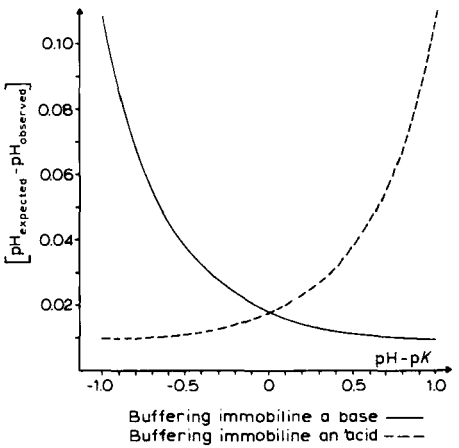

Fig. 2.15. Effect of a 2% error in dispensing the Immobilines on the pH of the solution, in relation to the pK of the buffering base and the buffering acid. Note how, in both cases, a very low experimental error is produced in the proximity of the pK values (pH $-$ pK = 0) (from LKB Application Note No. 321; by courtesy of LKB Produkter AB).

effect will thus be given by inaccuracy in dispensing the Immobiline solutions, as their concentration ratios determine the width and slope of the wanted pH gradient and as, in thin gels, the volumes required are small, usually of the order of a few microliters. Fig. 2.15 shows a plot of the deviation of the expected pH gradient as a function of an inaccuracy of measurement of 2%, for an acidic buffering species (broken line) and for a basic Immobiline (solid line). The ordinate represents the deviation from the desired pH interval ($pH_{expected} - pH_{observed}$), plotted as a function of the distance between the prevailing pH in solution and the pK of the buffering ion (pH $-$ pK) on the abscissa. The two curves are reciprocal, symmetrical exponentials with a cross-over point at (pH $-$ pK) = 0 (the point of maximum buffering power, remember; this point being also very close to an absolute minimum, as expected from the local high β value). With an acidic buffering Immobiline, at negative pH $-$ pK values the error becomes progressively negligible, being only 0.01 pH unit when the pH in solution is 1 unit below the pK (at this pH value the carboxyl

group will be 90% protonated); however, on the opposite side, when the solution pH is 1 unit above the pK (and therefore the acid is 90% dissociated) the effect of a 2% inaccuracy becomes more relevant, giving a deviation 10 times higher than in the former case (0.1 pH unit). The same reasoning, but with a 'mirror immage', applies when the buffering Immobiline is a base: the minimum pH deviation (0.01 pH unit) will be expected at a pH 1 unit above the pK (where the base is 90% deprotonated) while the maximum deviation (0.1 pH unit) will be found at a pH 1 unit below the pK (where the base is 90% protonated).

What should one do, in practice? We recommend three practical, simple rules:

(a) when casting thin gels (which in general require only 15 ml of total solution for the two chambers, i.e., 7.5 ml per each chamber) prepare a double volume of solution, for two gels; in this way, the pipetting error will be minimized;
(b) when dispensing the four alkaline chemicals, wash the tip of the pipette several times in the gelling solution, since the new Immobiline solutions (in n-propanol) tend to wet (and thus to adhere to) the plastic disposable tips of modern micro-pipettes (this was not a problem in water-dissolved Immobilines);
(c) mark with a color code or with any distinctive sign the various Immobiline bottles (all the solutions come in identical brown vials) so as to be sure that you are dispensing the correct Immobiline (dispensing the uncorrect one, even the nearest pK, will surely change your pH gradient!).

2.5. *Ionic strength* (I)

Through its influence on the activity factors, the ionic strength will affect the pK values of proteins. In contrast to the situation existing in a carrier ampholyte-based pH gradient, the ionic strength in a focused Immobiline pH gradient is known, and is given by the following relationship:

$$I = \sum C_{A_i} = \frac{10^{(pH-pK_{A_i})}}{10^{(pH-pK_{A_i})}+1} = \sum C_{B_i} \frac{1}{10^{(pH-pK_{B_i})}+1} \quad (16)$$

where C_{A_i} is the concentration of acidic Immobiline with $pK = pK_{A_i}$ and C_{B_j} is the concentration of the basic Immobiline with $pK = pK_{B_j}$. It should be noted that the pK values of the Immobilines also vary with the ionic strength. From the Debye-Hückel (1924) law, the variation for Immobiline can be given approximately by:

$$pK = pK_0 - 0.5Z^2\sqrt{I} \tag{17}$$

where pK_0 is the pK value at an ionic strength (I) of zero and Z is equal to -1 for acids and $+1$ for bases; thus, the pK increases with I for acids, and decreases for bases. When Immobilines are used according to recommendations, these pK variations, which are less than 0.03 pH unit, can normally be neglected; however, they should be kept in mind when using high Immobiline molarities (e.g., 30 mM), as in these instances the band positions might be influenced.

2.6. *Buffering capacity (β)*

The partial buffering power for each acid or basic species in a mixture can be computed from Eqs. 12 and 13, respectively, remembering that $[H^+] = 2.3 \exp(-pH)$. Thus one obtains, for an acid:

$$d[A_i^-]/dpH = -2.3\, k_i [A_iH]_T [H^+]/(k_i + [H^+])^2 \tag{18}$$

and for a base:

$$d[B_j^+]/dpH = -2.3\, k_j [B_jOH]_T [H^+]/(k_j + [H^+])^2 \tag{19}$$

Now, summing for all the $m + 1$ buffering species present in the mixture, C_i being both the total acid and base concentrations, the total buffering power β assumes the form:

$$\beta = 2.3 \sum_{i=1}^{l+m} C_i \frac{K_i [H^+]}{(K_i + [H^+])^2} \tag{20}$$

Eqs. 16 and 20, together with those listed in §2.3.1 and §2.3.8, form the core of the computer program we have described (Celentano et al., 1987) which, given any mixture of Immobilines in any pH range, will automatically simulate and optimize the eluted pH gradient together with the accompanying I and β values. With the aid of Eqs. 18 and 21, the I and β curses can also be calculated manually, usually with 0.1 pH unit increments.

The buffering capacity must be high enough to make the pH gradient insensitive to impurities (e.g., acrylic acid from the acrylamide and Bis monomers) and should also be even, in order to minimize the effects of small disturbances in forming the gradient and when casting the gel (Gianazza et al., 1983a; 1984a). For analytical purposes most of our recipes are calculated to give an average β value of 3 mequiv.$l^{-1}pH^{-1}$, quite sufficient to produce stable and well-functioning IPG gels. A higher buffering capacity gives more sharply focused bands (Gelfi and Righetti, 1983); however, such gels start swelling considerably during staining and destaining if the total molar concentration of the buffering species exceeds 30 mM.

2.7. *Conductivity*

The initial conductivity in an Immobiline gel is determined by the amount of free, non-covalently bound ions in the matrix. This is also true when the gel has been washed, as a matrix containing Immobiline will function to some extent as an ion exchanger. Thus, ions from the polymerization catalysts, and trace amount of ungrafted Immobiline, cannot be completely washed out from the gel with distilled water. When the unbound ions leave the gel, the conductivity will fall dramatically; this ion transport can be followed visibly by refractive lines moving towards the anode and/or cathode, marking the rear border of compounds transported towards the electrodes. If the gel initially contains large amounts of free ions, the ion transport is connected with a visible electrosmotic transport of water within the gel, resulting in the build-up of a ridge towards one of the electrodes.

With the Immobiline concentrations normally used (ca. 10 mM buffering ion), the conductivity falls to values of the order of 0.2–2.0 10^{-6} Ω^{-1} cm^{-1} for pH gradients in the middle of the pH scale. This is about 100 times lower than the conductivity in a conventional carrier ampholyte pH gradient (Righetti and Hjertèn, 1981). This extremely high resistance means that H^+ and OH^- start to contribute to the conductivity already below pH 5 (on the acidic side) and above pH 9 in the basic region (see also §2.9); below and above these values the conductivity will increase sharply (see Fig. 2.17). In reality, this does not seem to reduce the possibility of focusing in narrow gels covering a width of up to 1 pH unit even in extreme regions of pH (Bianchi-Bosisio et al., 1986; Gelfi et al., 1987b). In addition, the low absolute value of conductivity in the pH 5–9 region means that there will be no 'hot spots' in the gel (i.e., region of abrupt conductivity drops, which would cause a high voltage gradient and thus a high joule effect, as often occurring at plateau regions in CA-IEF), this guaranteeing avoidance of thermal protein denaturation. The stability of the gradient is also such that even proteins with a low mobility near their pI will have time to reach their equilibrium position even in extremely shallow pH gradients.

2.8. *Electroendosmosis*

Electroendosmosis is normally not a problem in Immobiline pH gradients, as the gel will not have any appreciable net charge after traces of catalysts and non-incorporated Immobilines have been electrophoretically transported away. Generally, however, at low and high pH values the presence of H^+ and OH^- means that the matrix adopts a net charge (e.g., 1 mM net negative charge at pH 3, to counteract the excess 1 mM protons in solution and, conversely, 1 mM net positive charge to balance the excess 1 mM OH^- in solution at pH 11) (Bianchi-Bosisio et al., 1986; Mosher et al., 1986) which will result in water transport towards the cathode at low pH and towards the anode at high pH. A trough (a much thinned gel region) thus forms close to the electrodes in these extreme pH ranges and eventually the gel could dry out and burn

(how to prevent these phenomena will be explained in §2.9). This phenomenon in general does not occur in the pH interval 4–10, so the vast majority of users will not experience any trouble; but at extreme pH values, this will be a severe problem.

Carbon dioxide from the air is also expected to provoke electro-endosmosis. Delincée and Radola (1978) were the first to describe the effect of carbon dioxide in conventional IEF. Gaseous CO_2 dissolves in the gel, especially at pH > 6.3 (the solubility of CO_2 increases with pH, pH 6.3 being the first pK value of H_2CO_3), forming HCO_3^- ions as follows:

$$CO_2 + H_2O \rightarrow H^+ + HCO_3^-$$

While this acidification, in conventional IEF, causes the part of the pH gradient above pH 6.3 to drift towards the cathode, by charging and mobilizing electrophoretically the focused carrier ampholytes (possibly by salt formation), it cannot act on IPGs by the same mechanism, but it will certainly alter the slope of the theoretical pH gradient depending on the local ratio $\beta(HCO_3^-)/\beta$(Immobiline) (it is in fact like introducing a new buffer with pK 6.3 in the immobilized pH gradient). The HCO_3^- ion migrates electrophoretically (Fig. 2.16) from the cathodic side towards the anode. At pH 6.3, gaseous CO_2 starts to form, and is liberated from the gel. At the same time OH^- is formed according to the equation:

$$HCO_3^- \rightarrow OH^- + CO_2 \text{ (gas)}$$

The gas released at the anodic gel side can be re-adsorbed at the cathode and thus re-circulate through the system as depicted in Fig. 2.16 (Burdett, 1982). In analogy with this, volatile amines will cause exactly the same disturbances, but in the opposite direction (it is not recommended, therefore, to use ethanolamine, ethylendiamine and the like as catholytes). Even in IPGs a very marked effect on band sharpness is observed if CO_2 is excluded from the system in alkaline pH ranges. For this, the IEF cell should be airtight and flushed with inert gases (denser than air, such as argon; nitrogen is lighter and will float!) and also covered in the

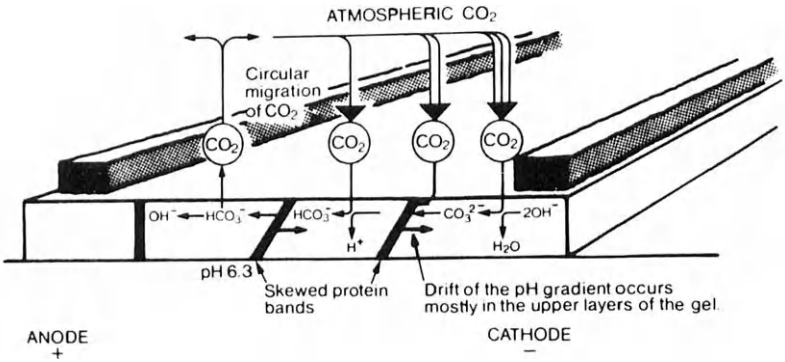

Fig. 2.16. Diagram illustrating the principle of interference by atmospheric carbon dioxide at high pH. Hypothetical cross-section of a gel. Note that, at pH 10 and above the CO_3^{2-} ion predominates, whereas between pH 6.3 and 10.3 the HCO_3^- is the most abundant species. Below pH 6, the adsorbed CO_2 is released back in the atmosphere as gaseous carbon dioxide (from Burdett, 1982; by courtesy of Pharmacia Fine Chemicals).

gel-free space with sponges impregnated with NaOH or better with $Ca(OH)_2$ (the latter will irreversibly trap CO_2 by forming insoluble bicarbonate). In alkaline ranges, we also recommend to cover the open gel surface (after sample entry) with the Gel Bond PAG foil (use the hydrophobic surface in contact with the gel, though, otherwise the foil will not peel off at the end of the run) so as to prevent direct CO_2 absorption by this large surface. Alkaline gels which are not protected in any possible way against CO_2 adsorption will show severe streaking towards the cathodic gel region and, in general, very poor sample focusing into sharp bands.

2.9. The limits of IPGs: how to break barriers

As stated in §2.8, when trying to formulate IPG recipes outside the pH 4–10 range, e.g., a more acidic (pH 3–4) or more alkaline (pH 10–11) IPG interval, one is faced with severe problems, as two new 'Immobilines' become operative, a weak base with a $pK = -1.74$ and a weak acid with a $pK = 15.74$. They are the H^+ and OH^- ions in equilibrium with undissociated water. It might be argued that

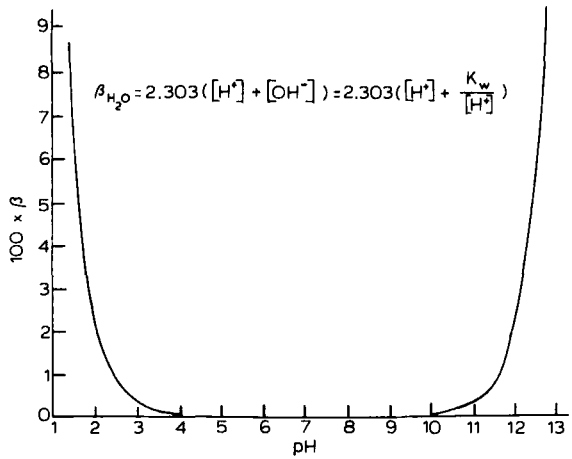

Fig. 2.17. Buffering power (β) of water along the pH axis. For calculations, we have taken as pK of the base H^+ the value of -1.74 and as pK of the conjugated acid OH^- the value of 15.74 (the molarity of water being 55.56). K_w is the ionic product of water. It is seen that water does not have any appreciable buffering power in the pH 4–10 interval. Calculations and simulations according to the new computer program of Celentano et al. (1988).

their pKs are so remote from the extremes of even the most extended IPG intervals (pH 3–11) that they should not alter these pH values. They do, in fact, as there are constantly 55.56 moles of water present throughout the system (hence the provocative concept of water as an Immobiline) vs. ca. 3–10 mM of each buffering Immmobiline, as adopted in most IPG formulations. The effects of water on the sytem can be appreciated in Fig. 2.17: it is seen that already at pH 3 and pH 11 the buffering power of water is non-negligible, while outside these limits it rises so sharply as to nullify any attempt at using IPGs in these regions. In addition to the problems of the buffering power of water, there is another serious drawback at using IPGs at these pH extremes: the matrix acquires a net charge, negative at lower pH, positive at high pH. For example, at pH 3 the Immobiline matrix must contain 1 mM extra carboxyls to neutralize the 1 mM protons defining the pH value in the bulk water; at pH 11 it will bear an extra 1 mM positively charged amino groups for balancing the 1 mM oxydryls

in solution (see also §2.8). These excess bound charges will produce, during the electrophoretic run, a strong electrosmotic flow (proportional to the applied voltage gradient) which will eventually dry out the cathodic and anodic extremes, with consequent burning of the gel matrix. There is an additional problem, moreover: at very low and high pH values, the background conductivity becomes prominent, much higher than the conductivity of the IPG gel. As a result of this, ampholytes will focus at these pH extremes with distribution profiles exhibiting both skewness and curtosis (in other words, they should produce strongly asymmetric and broad peaks, due to the fact that the voltage gradient across the gel will be strongly uneven, i.e., quite low in region of high conductivity, and quite high in regions of low conductivity). Thus, it might even be doubtful that focusing at these pH extremes could be feasible at all. On the contrary, we have obtained excellent separations in the pH 3–4 and pH 10–11 ranges by resorting to viscosity gradients (which act as quenchers of conductivity and electrosmosis) incorporated in the gel matrix. These viscosity gradients (in general sucrose or sorbitol, up to 30%) will be oriented so as to have the denser part in the most conducting region of the gel (Bianchi-Bosisio et al., 1986; Mosher et al., 1986). Fig. 2.18 shows the effect of incorporating these viscosity gradients in the gel (in this particular case, a gradient of linear liquid polyacrilamide, LLPAA, had been polymerized withing the gel fibers): as the viscosity is increased towards the most conducting gel regions (pH 3 at acidic, pH 11 at alkaline values) the voltage gradient over the gel length (which drops exponentially following the increments of conductivity) tends to be smoothed as the viscosity is increased. As a result of a more even voltage profile, good focusing is thus ensured even under the most adverse conditions (Gelfi et al., 1987b, Sinha and Righetti, 1987; Righetti et al., 1988b).

Table 2.7 gives a recipe for an IPG pH 3–4 gradient, in which water is incorporated as an Immobiline having pK 0.00 and a unit molar concentration (when the concentration is expressed as the activity coefficient on the molar fraction scale; this being equivalent to consider water as a basic Immobiline with $pK = -1.74$ and standard concentration of 55.56 M). Failure to add water in this recipe will give completely erroneous pH gradients, as shown

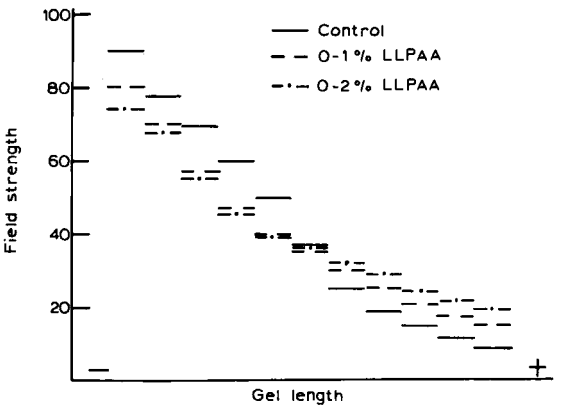

Fig. 2.18. Use of 'conductivity and electroendosmosis quenchers' at extreme pH values in IPGs. Voltage gradients across an Immobiline pH 3–4 gel. Three gels were made, a control and two additional ones containing a 0–1% and a 0–2% gradient of liquid linear polyacrylamide (LLPAA). All gels were prerun overnight at 800 V/cm, then, while under a total voltage drop of 500 V (over a 9.5 cm electrode distance), segmental voltage gradients were measured at 6.5 mm increments from cathode to anode by moving manually the voltage probe across the pH gradient. In the graph, each horizontal bar represents a 6.5-mm gel distance. The gel polarity is marked by − and + signs. The ordinate units are V/cm (from Mosher et al., 1986; with permission from Verlag Chemie).

in Fig. 2.19 (an error of 0.27 pH unit over a 1 pH unit interval!). Tables 2.8 and 2.9 given the respective gel formulation for the most acidic (pH 2.5–3.5) and the most basic (pH 10–11) IPG intervals today obtainable with presently described Immobilines, while Figs.

TABLE 2.7
Recipe for an optimized pH 3–4 gradient. All values in mM.

Immobiline	Chamber 1 (pH 3.0)	Chamber 2 (pH 4.0)
pK 0.00 (water) [a]	1000	1000
pK 1.0	1.01	0.00
pK 3.6	3.85	3.49
pK 4.4	2.49	3.42
pK 7.0	0.90	3.42

[a] Water is considered as a basic Immobiline with pK = 0.00.

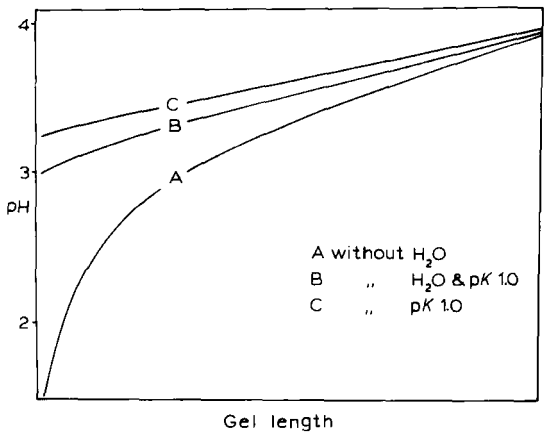

Fig. 2.19. Simulated pH gradients in the absence of some components from the recipe for the pH 3–4 gradient in Table 2.10. A: pH gradient in the absence of the 'Immobiline' water (1 M); B: pH gradient obtained by the simultaneous subtraction of water and Immobiline pK 1.0; C: pH gradient without the Immobiline pK 1.0 in the formulation (from Righetti et al., 1986c; by permission of Elsevier).

2.20 and 2.21 give the respective 'pedigrees', as calculated with our computer simulations (note that, owing to these findings, our newest computer program, Celentano et al., 1988, contains the hydrolytic products of water in all formulations). In Chapter 6, examples will be given of the excellent separations obtained even at these most adverse pH values.

TABLE 2.8
Recipe for a pH 2.5–3.5 IPG gradient [a]

Additive	Acidic chamber	Basic chamber
pK 3.1	800 μl	800 μl
pK 9.3	145 μl	350 μl
$T\%$ = 30, C% = 4	1.3 ml	1.3 ml
Sorbitol	2.4 g	–
Ampholyte 2.5–4.5	200 μl	200 μl
Pharmalyte 2.5–5	200 μl	200 μl
TEMED	5 μl	5 μl
Persulphate (40%)	7 μl	7 μl

[a] All Immobilines, 0.2 M solutions; final volume in each chamber: 7 ml.

TABLE 2.9
Recipe for a pH 10–11 Immobiline gradient

Additives	Chamber 1 (pH 11)	Chamber 2 (pH 10)
pK 3.6	2.5 mM	6.4 mM
pK 10.3	17.8 mM	9.2 mM
pK 14 (H_2O)	1000 mM	1000 mM
Sorbitol	30%	3%
Acrylamide	4%	4%
Pharmalyte (pH 8–10.5)	1%	1%
Ampholine (pH 9–11)	1%	1%

2.10. *Resolving power. Rilbe's equation*

In capillary zone electrophoresis (CZE) the resolving power is given in number of theoretical plates (N), according to the equation:

$$N = \mu V/2D \tag{21}$$

where V is the applied field strength (V/cm) and μ is the analyte's

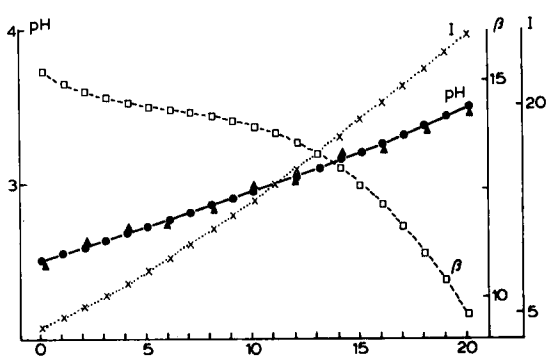

Fig. 2.20. Computer simulation of the physico-chemical parameters of a pH 2.5–3.5 gradient utilizing 2-acrylamido glycolic acid (AGA) as a buffering group (pK 3.1). A 20 mM solution of AGA was titrated in the pH 2.5–3.5 interval with the pK 9.3 as a titrant Immobiline. The computer then automatically calculates the pH (solid circles), buffering power (β, open squares) and ionic strength (I, crosses) of the 20 fractions eluted. Experimentally, a gradient was prepared with a 2-vessel gradient mixer and 11, 1 ml fractions collected. The pH of the experimental gradient is reported with solid triangles (from Righetti et al., 1988b; be permission of Elsevier).

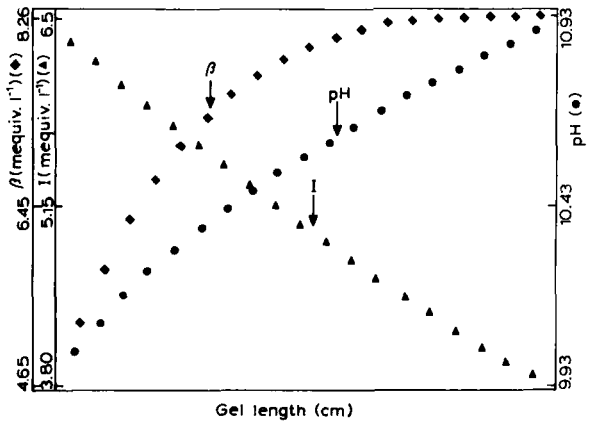

Fig. 2.21. Computer simulation of an Immobilized pH 10–11 gradient. Buffering Immobiline: pK 10.3; titrant Immobiline: pK 3.6 (see recipe in Table 2.9). The values of pH, buffering power (β) and ionic strength (I) are calculated at 0.05 pH increments according to Celentano et al. (1987) (from Gelfi et al., 1987b; with permission of Elsevier).

electrophoretic mobility (Jorgensson, 1987). Recent data suggest that CZE is capable of achieving a resolving power better than 1 million theoretical plates, a remarkable resolution indeed. In IEF (and thus in IPGs) the resolving power, as derived by Rilbe (1973), is given by:

$$\Delta \mathrm{p}I = 3\sqrt{\frac{[D\ \mathrm{d(pH)}/\mathrm{d}x]}{[E(-\mathrm{d}u)/\mathrm{d(pH)}]}} \qquad (22)$$

where D is the diffusion coefficient of a protein having a titration curve (pH/mobility slope) of $\mathrm{d}u/\mathrm{d(pH)}$, E = electric field strength (V/cm), $\mathrm{d(pH)}/\mathrm{d}x$ = slope of the pH gradient in the IEF gel and ΔpI = difference in isoelectric points between a protein and the nearest resolvable contaminant (note the similarity between the two equations).

In order to increase the resolving power, we have to find experimental conditions that minimize the value of ΔpI. There are three ways in which this can be done: (a) decrease the numerator; (b) increase to denominator and (c) simultaneously increase and

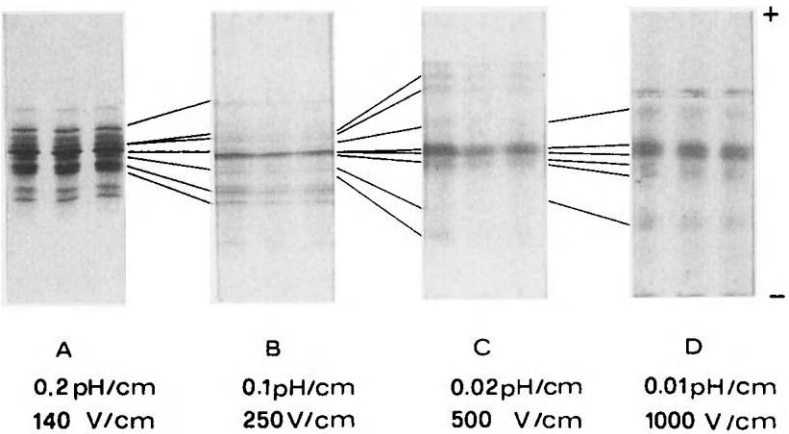

Fig. 2.22. Resolving power in IPGs. Ovalbumin focused on a narrow Ampholine pH 4–6 gradient (A) and on Immobiline gradients with varying pH slopes (B to D). Strips B to D contain 5×10^{-3} M Immobiline of pK 4.6 titrated with Immobiline of pK 9.3 to the respective pH slopes. Ovalbumin loads in the sample tracks (from left to right): 40, 20 and 20 μg. The resolving power in panel D between the two central major components was estimated to be ΔpI = 0.002 pH unit (from Bjellqvist et al., 1982; with permission of Elsevier).

decrease both. However, some parameters in this equation cannot be manipulated: for any given protein, D is constant and proportional to its mass and $du/d(pH)$ is constant and proportional to its charge, and that is the end of it. Here is where the 'magic' of Immobiline pH gradients step in: as the conductivity is extremely low (ca. one hundredth of the value for CA gels) and as the pH gradient width can be mathematically determined, we can simultaneously decrease $d(pH)/dx$ and increase E almost at leisure. The resulting resolving power is almost unbelivable: ΔpI = 0.002 in a 0.01 pH unit/cm gradient (Righetti et al., 1983a). This can be appreciated in Fig. 2.22: when a commercial ovalbumin sample was run in a conventional Ampholine pH 4–6 gradient, with a slope of ca. 0.2 pH/cm, it was resolved into a number of bands, of which the dark, central band (panel A) appeared as a single, homogeneous component. However, when the same sample was run in Immobiline gels of only 0.02 pH/cm (panel C, 0.2 pH interval across the entire gel length), this major band was clearly split into

two components (Bjellqvist et al., 1982). The pI difference between these two bands was estimated to be 0.002 pH unit, which corresponds to a charge difference between the two species of only 2/100 of a unit proton charge (probably these two bands represent a neutral → neutral amino acid replacement). This is a far cry from the resolving limit for conventional IEF given by Vesterberg and Svensson (1966) as a ΔpI = 0.02 pH unit. If we compare IPGs with the leading electrophoretic technique of the 1960s, disc electrophoresis (Ornstein, 1964), the increment of resolution is even more striking: in the latter technique, two species would be resolved only when the difference in surface charge was of the order of 1 proton unit.

2.11. Alternatives for buffer focusing

In a way IPGs can be regarded as a system for performing isoelectric focusing in non-amphoteric buffers (NAB-IEF), and as such they would seem to go back to Kolin's (1977) 'artificial' pH gradients. In reality, Kolin's approach was ineffective because it did not allow control of the pH gradient slope with time: upon prolonged electrolysis, the buffers and titrants would collect at the anode and cathode, forming strongly acidic and basic solutions with a great pH drop in between. By insolubilizing our non-amphoteric buffers, and titrating them near their pKs, unlimited stability with time and the needed buffering capacity coupled to the correct ionic strength is ensured. Over the years other laboratories have tried to develop other systems for NAB-IEF, such as: (1) 'stack' or 'train' of free acids or bases 'arrested' by a protonation or deprotonation mechanism, respectively (Chrambach and Hjelmeland, 1984); (2) 'physically bonded' or 'quasi immobilized' pH gradients (Bier et al., 1984) and (3) 'steady-state rheoelectrolysis' (Rilbe, 1978).

I will analyze in depth some of these approaches, in particular the one developed by Bier's group, which consists of highly sophisticated theories and models that show some striking similarities to the notion of IPGs. Their results are summarized in Fig. 2.23. Bier et al. (1984) were able to generate 'quite stable pH

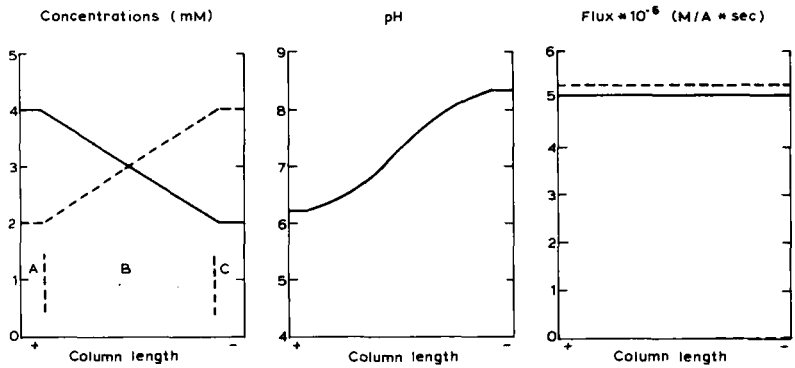

Fig. 2.23. Schematic presentation of the courses and concentration of Tris–cacodylate, of their respective fluxes and of their resulting pH gradients. Micro-computer calculated flux values are also plotted, assuming for Tris (dashed lines) a mobility of 2.42 $cm^2/(V/s)$ and a pK of 8.3, and for cacodylate (solid lines) a mobility of 2.31 $cm^2/(V/s)$ and a pK of 6.21. A and C in the left panel (B) mark the beginning of the anodic and cathodic reservoirs, respectively (from Bier et al., 1984; with permission of Springer Verlag).

gradients formed using a simple system of a weak acid and a weak base (around neutrality), mixed in the proportions required to cover the desired pH range'. In the simple case shown in Fig. 2.23, a gradient of a buffering acid (cacodylate, pK 6.2), varying linearly from 4 to 2 mM (anode to cathode) is titrated with a reciprocal linear gradient of buffering base (Tris, pK 8.3) ranging from 2 to 4 mM (anode to cathode). Although Bier and his coworkers claim that their system defies classification in terms of conventional modes of electrophoresis as it is not isoelectric focusing (i.e., no one of the components of the buffers are isoelectric) and not IPG as their buffers are not immobilized, close scrutiny of their data reveals that the buffers are a bit of both. The similarity with IPGs is striking. An analogous situation occurs in IPGs in the pH region 4.4–6.2, with Immobilines pK 4.4 (a weak acid) and pK 6.2 (a weak base), where the system is under conditions in which the two components act simultaneously as buffers and titrants. As seen in Fig. 2.23A, the concentrations of the two are reciprocal, symmetrical linear gradients, generating a pH gradient from 6.2 (the pK of cacodylate, because the ratio [cacodylate]/[Tris] is 2:1) to pH 8.3

(the pK of Tris, because the ratio [Tris]/[cacodylate] is 2:1). However, the pH gradient is not linear but slightly sigmoidal, because the $\Delta pK = 2$, as predicted by our computer modelling (Gianazza et al., 1984a).

Such a situation was indeed fully predicted by our general theory on IPGs (Dossi et al., 1983; Celentano et al., 1987) and we have simulated their data with our computer algorithm by assuming that the two species are Immobilines (which in a way they are as constant flux is assumed from infinite reservoirs, which means that the concentration of the two species in the electrophoresis cell will be constant with time, just like in IPGs). As shown in Fig. 2.24, we obtain identical results. The expected pH gradient is identical in the two cases, except that the deviation from linearity is quite high (maximum deviation, positive + negative, is 0.3 pH unit, i.e., 15% of the stated pH interval; for typical IPG gradients, the deviation is usually within 1% of the pH span generated). We have also simulated the β and I courses (Fig. 2.24, lower panel). As expected, they appear in the figure as two reciprocating, bell-shaped functions, with a minimum of β power half way between the two peaks, corresponding to a maximum of ionic strength (by titrating the two species 'inside' the two pKs, conditions of maximum ionization of the buffering groups are ensured).

Although with true Immobilines we can arrange for smoother β and I courses, the physico chemical parameters of Bier's system are acceptable and compatible with a well-functioning IEF set-up. Of course it is true that the buffers here are not 'chemically immobilized' but they nevertheless ensure a substantial stability of the system because they are immobilized according to physical laws. The fundamental requirement of Bier's gradients is that the flux of the two species is constant across the whole length of the column. In fact Bier and his coworkers have introduced a parameter, ρ, that is predictive of the stability of the system and is defined as:

$$\rho = \frac{M_{a^-}^{A} M_{b^+}^{C}}{M_{b^+}^{A} M_{a^-}^{C}} \tag{23}$$

where M is the concentration of the acid (a^-) and base (b^+) in reservoirs A and C. Only when $\rho = 1$ would there be perfect

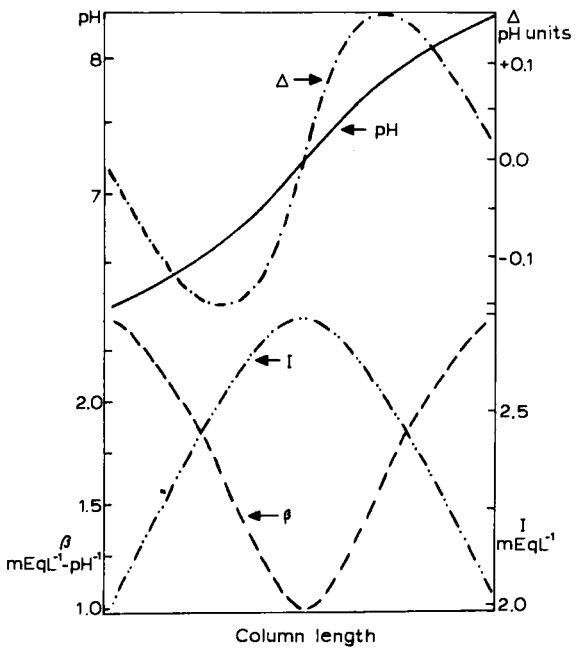

Fig. 2.24. pH gradient, deviation from linearity (Δ, in positive and negative pH values), buffering power (β) and ionic strength (I) of Bier's system of Fig. 2.23. Their data have been recalculated by using the same molarity and pK values and the same pH interval as in Fig. 2.23, except that Tris and cacodylate were assumed to be two Immobilines (i.e., with mobility = 0, flux = 0, diffusion coefficien $t = 0$). Note that the shape of the expected pH gradient is identical in the two different computer models. Our computer simulation (according to Celentano et al., 1987) predicts that Bier's gradient is fully compatible with a well-functioning IEF system (from Righetti and Gianazza, 1985a; by permission of Elsevier).

migrational stability, and this is one of the weaknesses of the system. As shown in Fig. 2.23C, the flux of Tris is slightly higher than the flux of cacodylate, and eventually the system is bound to decay.

The four modes of non-amphoteric buffer IEF summarized here and compared clearly demonstrate that the system no longer depends on amphoteric species. However, a properly performing IEF system still has as an absolute requirement the concept of 'carrier'. The 'carrier' principle requires that the chemicals used to generate and stabilize the pH gradient behave as 'good buffers' and 'good

conductors' (Rilbe, 1973; 1976b). Systems 2 and 3 discussed here (and IPGs, of course) fulfill this fundamental requirement: in these three cases quasi-linear pH gradients are generated by titrating weak acids and bases symmetrically around their respective pKs, where they automatically provide the much needed buffering capacity and conductivity.

In the Chrambach 'arrested stack' the system breaks down because the potential buffers are allowed to be stripped electrophoretically of counter ions and thus to collect in strongly acidic anodic layers and strongly basic cathodic zones, where they are deprived of their buffering and conducting powers. Although in Chrambach's system a 'natural' pH gradient can still form (it is in fact a pH gradient generated by a stack of moving boundaries, as in isotachophoresis), it can hardly be controlled (for lack of β power) and can never assumed to become stationary (for lack of immobilization). Indeed, the so called 'arrested stack' created by protonation of acids and deprotonation of bases is never quite arrested: it could only be so when the current in the system bocomes zero, but at this point it would be quite meaningless still to speak in terms of 'electrophoresis' (which, by definition, requires current flowing through the system). As for the other systems, although all three are based on sound and correct hypotheses, they are markedly different in operational terms.

Bier's system is subjected to two inherent disturbances: migrational instability (the parameter ρ very rarely will be unitary) and diffusional instability (decay of the boundaries). The two instabilities are additive and will ensure ultimate decay of the pH gradient. In Rilbe's system, again what theory predicts and what practice can achieve rapidly come into conflict: the predicted pH courses are only established in the absence of internal liquid flow (i.e., inside the electrophoresis cell). Unfortunately, there is always a net liquid flow within electrolyzers, and this induces exponential and slowly decaying pH gradients.

2.12. Conclusions

What lessons can we draw from this chapter? First of all, that IPG gradients can be extended considerably outside their 'natural'

boundaries of a pH 4–10 interval, as theoretically predicted. With the synthesis of more acidic (pK 3.1) and more alkaline (pK 10.3) buffering-acrylamido derivatives (See Chapter 1), coupled to control of the gel matrix by the use of conductivity and electroendosmosis quenchers, it is possible to have IPG gradients fully operative in the pH 2.5–11 range. This extends our fractionation capability probably to more than 99% of all the possible phenotypes expressed by living systems. As a second lesson, we have learned that IPGs offer a resolving power unrivalled by other techniques. We have shown separations exhibiting a ΔpI of only 0.002 pH unit (see Fig. 2.22) and it is easy to demonstrate that the present, practical limit (i.e., in terms of applicable voltage and shallowness of pH gradient) is of the order of 0.001 pH unit, a truly superb resolving power to have at hand. Thirdly, while it is true that over the years scientists have tried to invent some alternatives to IPGs, some quite disastrous (like the Chrambach approach) others on sound and correct theoretical grounds (the Rilbe's and Bier's systems), nevertheless, today it appears that there is no simple, practical, truly working alternative to the IPG technique, which I have the feeling is going to accompany us well in the year 2000.

Analytical IPGs

3.1. General considerations

The following chapter will deal with all the fundamental methods pertaining to the analytical phases of IPGs. A detailed treatise will be found on all the aspects of gel polymerization, gradient mixing, drying and reswelling of IPG gels, use of the fourth generation of IEF, i.e., the mixed-bed CA-IPG, the effect of salts on protein patterns, and so on. Part of the material which refers to analytical IPGs has been reported elsewhere, in particular all the tables providing any possible recipe for IPG intervals, which have been listed under Chapter 2. The reason for this is that these tables have been obtained with the aid of our computer program, which is extensively described under the theory section (Chapter 2), so that it was felt more appropriate to give this information there rather than in the present chapter. Another important aspect of analytical IPGs is definitely their use in two-dimensional (2-D) maps. However, just because 2-D maps are gaining widespread acceptance, I opted for reserving for them an entire chapter (No. 4). Thus, I believe that this and the following chapter will provide the 'core' information for most users of the IPG technique.

3.1.1. The basic method

IEF in IPGs is an electrophoretic technique by which amphoteric compounds are fractionated according to their pIs along a continuous pH gradient (Bjellqvist et al., 1982). Contrary to zone electrophoresis, where the constant (buffered) pH of the separation medium establishes a constant charge density at the surface of the molecule and causes it to migrate with constant mobility (in the absence of molecular sieving), the surface charge of an amphoteric compound in IEF keeps changing, and decreasing, according to its

titration curve, as it moves along a pH gradient until it reaches its equilibrium position, i.e., the region where the pH matches its pI. There, its mobility equals zero and the molecule comes to a stop.

Contrary to conventional IEF in amphoteric buffers, where the gradient is created, and maintained, by the passage of an electric current through a solution of amphoteric compounds having closely spaced pIs, in IPGs the pH gradient pre-exists to the passage of the current, is created when casting the gel matrix and is copolymerized within the gel fibers (see Chapter 1). This fact overcomes all the problems connected to CA-IEF and represents a major revolution in protein separation techniques.

3.1.2. Applications and limitations

The technique only applies to amphoteric compounds and more precisely to good ampholytes with a steep titration curve around their pI, *conditio sine qua non* for any compound to focus in a narrow band. This is very seldom a problem with proteins but it may be so for short peptides, that need to contain at least one acidic, or basic, amino acid residue, in addition to the $-NH_2$ and $-COOH$ termini. Peptides which have only these terminal charges are isoelectric over the entire range of approximately pH 4 and pH 8 and so do not focus. However, while with CA-IEF another major limitation with short peptides is encountered at the level of detection, since CAs are reactive to most peptide stains, this problem does not exist in IPGs, which do not give background reactivity to nihydrin and other common stains for primary amino groups (e.g., dansyl chloride, fluorescamine) (Gianazza et al., 1983b).

When a restrictive support like polyacrylamide (PAA) is used, a size limit is also imposed for sample proteins. This can be defined as the size of the largest molecules which retain an acceptable mobility through the gel. A conservative evaluation sets an upper molecular mass limit of about 750,000 when using standard techniques. The molecular form in which the proteins are separated strongly depends upon the presence of additives, such as urea and/or detergents. Moreover, supramolecular aggregates or complexes with charged ligands can be focused only if their dissociation constant (K_d) is lower than 1 μM and if the complex is stable

at pH = pI (Krishnamoorthy et al., 1978). An aggregate with a higher K_d is easily split by the pulling force of the current.

3.1.3. Specific advantages

(i) IEF in IPGs is an equilibrium technique; therefore the results do not depend (within reasonable limits) upon the mode of sample application, the total protein load or the time of operation.

(ii) an intrinsic physico-chemical parameter of the protein (its pI) may be measured.

(iii) IEF in IPGs requires only a limited number of chemicals, is completed within a few hours, is less sensitive than most other techniques to the skill (or lack of it) of the operator.

(iv) IEF in IPGs allows excellent resolution of proteins whose pIs differ by only 0.001 pH units (today accepted as a practical limit, although no theoretical limit to the resolving power of IPGs exists); the protein bands are very sharp due to the focusing effect.

3.2. Equipment

This section will describe the minimum basic equipment for performing a successful run in IPG (and in conventional focusing as well). While I report here only commercially available equipment, it is clear that any home-made apparatus fulfilling the basic requirements listed below will be just as adequate.

3.2.1. Electrophoretic equipment

Three major items of apparatus are required; an electrophoretic chamber, a power supply and a thermostating unit.

Electrophoretic chamber

The optimal configuration of the electrophoretic chamber is for the lid to contain movable platinum wires (e.g., in the LKB Ultrophor 2217 and Multiphor 2, in the Pharmacia FBE3000 or in the Bio Rad chambers mod. 1045 and 1415). This allows researchers to use gels of various sizes and to apply high field strengths across just a

portion of the separation path. A typical chamber is shown in Fig. 3.1.

Power supply

The most suitable power supplies for IEF are those with automatic constant power operation and with voltage maxima at 2–2500 V. The minimal requirements for good resolution are a limiting voltage of 1,000 V and a reliable amperometer with a full scale not exceeding 50 mA. Lower field strengths cause the protein bands to spread (resolution is proportional to $\sqrt{E}$; see Eq. 22 in Chapter 2). The amperometer monitors the conductivity and so allows periodic manual adjustment of the electrophoretic conditions to keep the delivered power as close as possible to a constant value (for those power supplies unable to operate at constant wattage).

Thermostatting unit

Efficient cooling is extremely important for IEF because it allows high field strengths to be applied without overheating. Tap water circulation is adequate for 8 M urea gels but not acceptable for gels lacking urea. Setting the electrophoretic apparatus in a cold room may be beneficial to prevent water condensation around the unit in very humid climates, but it is inadequate as a substitute for coolant circulation. Thus a thermostat is in general recommended, even though in IPGs the temperature setting is in general moderately higher than in conventional IEF (10°C as opposed to 2–4°C in the latter technique; the reason for this value being that all Immobiline pK values have been measured at 10°C). Most modern thermostats have digital readings and are accurate to the value of 0.01°C, although an accuracy of 0.1°C is more than adequate. As an example, I am quoting here the LKB Multitemp temperature control unit.

3.2.2. Polymerization cassette

The polymerizing cassette is the chamber that is used to form the gel for IEF. It is assembled from the following elements; a gel supporting plate, a spacer, a cover (molding) plate and some clamps.

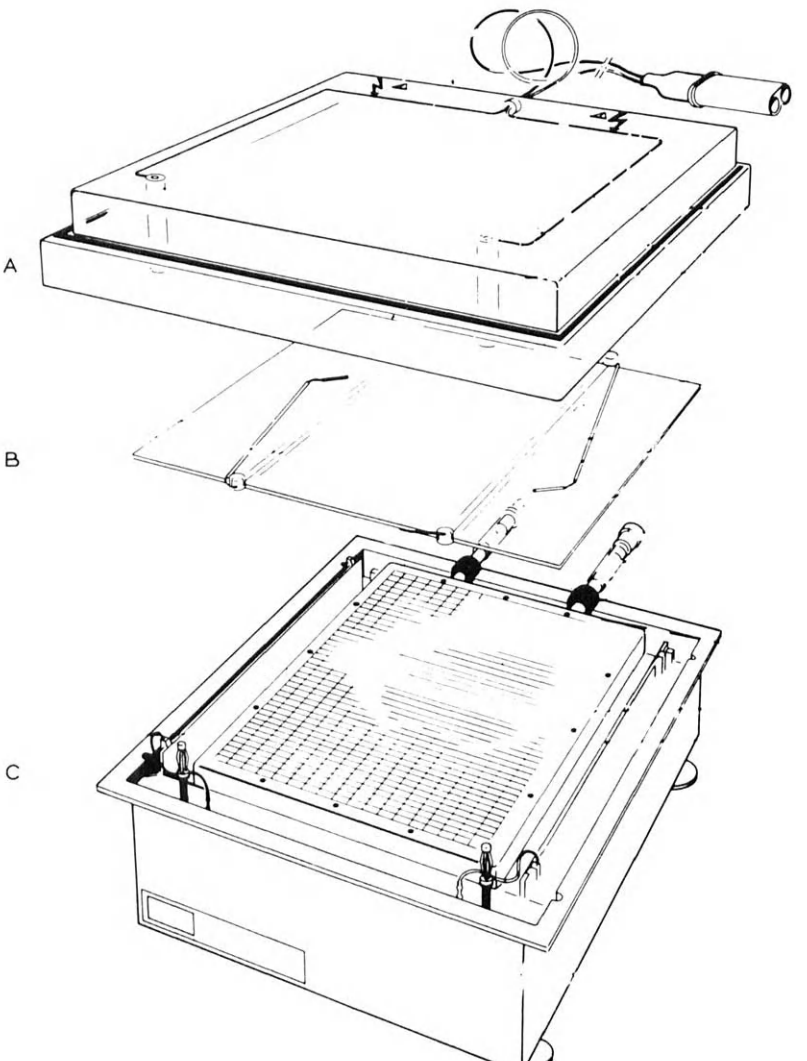

Fig. 3.1. Drawing of the LKB Multiphor II chamber. (A) cover lid; (B) cover plate with movable platinum electrodes; (C) base-chamber with ceramic cooling block for supporting the gel slab (courtesy of LKB Produkter AB).

Gel supporting plate

A plain glass plate is sufficient to support the gel when detection of the separated proteins does not require processing through several solutions (e.g., when the sandwich technique for zymograms or immuno-blotting are to be applied) or when the polyacrylamide matrix is sturdy (gels > 1 mm thick, $> 5\%$ T). However, for thin, soft gels a permanent support is required. Glass coated with γ-methacryl oxypropyl trimethoxy silane (available as Silane A-174 from Pharmacia, as Bind-Silane from LKB or as Polyfix 1000 from Desaga) is the most reliable reactive substratum and is the most suitable for autoradiographic procedures (Bianchi-Bosisio et al., 1980) (see Table 3.1 for the procedure). It is also the cheapest of such supports: dried-out gels can be removed with a blade and then a brush with some scrubbing powder. Unreacted silane may be hydrolyzed by keeping the plates in Clorox for a few days. This step is unnecessary, however, if they have to go trough successive cycles of silanization. The glass plates used as a support should not be thicker than 1 to 1.2 mm. On the other hand, thin plastic sheets designed to bind polyacrylamide gel firmly (e.g., Gel Bond PAG by Marine Colloids, PAG foils by LKB, Gel Fix by Serva) are more practical if the records of a large number of experiments have to be filed, or when different parts of the gel need to be processed independently (e.g., the first step of a two-dimensional separation or a comparison between different stains). The plastic sheet is

TABLE 3.1
Silanizing solutions

Binding silane (γ-methacryloxy-propyl-trimethoxy-silane) [1]

1. Add 4 ml of silane to 1 liter of distilled water adjusted to pH 3.5 with acetic acid; leave the plates in this solution for 30 min, rinse with distilled water and dry in air. OR:
2. Dip the plates for 30 s in a 0.2% solution of silane in anhydrous acetone; thoroughly evaporate the solvent with hair drier. Rinse with ethanol if required.
3. Store away from untreated glass.

Repelsilane (dimethyl-dichloro-silane) [2]

Swab the glass plates with a wad impregnated in a 2% (w/v) solution of silane in 1,1,1-trichloroethane; dry in a stream of air and rinse with distilled water.

[1] By Union Carbide, available through Pharmacia, Serva, LKB.
[2] By e.g. Merck, Serva, etc.

applied to a supporting glass plate and the gel is cast onto this. Although, in general, IPG gels adhere quite firmly to the Gel Bond PAG, the binding of the polyacrylamide matrix to these substrata is not always stable and so care should be taken in using them, especially for detergent-containing gels, in strongly alkaline IPG intervals (e.g., IPG pH 10–11 ranges) and when using aqueous staining solutions.

Spacer

U-gaskets of any thickness, between 0.2 and 5 mm can be cut from rubber sheets (para-, silicone-, nitrile-rubber). For thin gels, a few layers of Parafilm (each about 120 μm thick) can be stacked and cut with a razor blade (Görg et al., 1978). The width of such U-gaskets should be about 4 mm. In addition, cover plates with a permanent frame are commercially available (2117–901 from LKB). A similar device may be home-made using Dymo tape strips, which are 250 μm thick, to form the permanent spacer frame. Mylar foil strips or self-adhesive tape may be used as spacers for 50–100 μm thick gels. Rubber- or tape-gaskets should never be left to soak in soap (which they absorb) but just rinsed and dried promptly.

Cover plate

Clean glass, glass coated with dimethyl dichloro silane (Repel Silane; Table 3.1) or a thick Perspex sheet are all suitable materials for the cover plate. If you wish to mould sample application pockets into the gel slab during preparation, attach Dymo tape pieces to the plate, or glue small Perspex blocks to the plate with drops of chloroform. Perspex should never be exposed unevenly to high temperatures (for example by being rinsed in running hot water) because it bends even if cut in thick slabs.

Clamps

Clamps of adequate size and strength should be chosen for any gel thickness. Insufficient pressure may result in leakage of the polymerizing solution. The pressure of the clamps must be applied on the gasket, never inside it.

3.3. *The polyacrylamide gel matrix*

3.3.1. *Reagents*

Stocks of dry chemicals (acrylamide, Bis, ammonium persulphate) may be kept at room temperature, provided they are protected from moisture by being stored in air-tight containers. Very large stocks are better sealed into plastic bags, together with Drierite (from Mercks), and stored in a freezer. TEMED stocks should also ideally be kept in a freezer, in an air-tight bottle or better, under nitrogen. Avoid contaminating acrylamide solutions with heavy metals, which can initiate its polymerization.

Acrylamide and Bis (*N*,*N*′-methylene bisacrylamide) for IEF must be of the highest purity to avoid poor polymerization and strong electrosmosis resulting from acrylic acid (Righetti and Macelloni, 1982). Monomer solutions can be purified from contaminating acrylic acid by treatment with ion-exchange resins. Bis

TABLE 3.2
Stock solutions

Name	Composition	For 100 ml	Storage
	$T\%$ [1] = 30 $C\%$ [1] = 2.5	29.25 g A [2] 0.75 g B [2]	
	$T\%$ = 30 $C\%$ = 3	29.10 g A 0.90 g B	
Monomer solution	$T\%$ = 30 $C\%$ = 4	28.80 g A 1.20 g B	At 4 °C for about 1 month
	($T\%$ = 30 (A) + $T\%$ = 2 (B)) to be mixed for C% ≥ 10 [3]		
Initiator of the radical reaction:			
ammonium per sulfate (AP)	40% w/v or 400 mg + 800 μl water		At 4°C for 1 week
Catalyst:			
TEMED	Pure liquid		At 4 °C for months

[1] $T\% = g_{monomers}/100$ ml; $C\% = g_{cross\text{-}linker}/100\ g_{monomers}$.
[2] A = acrylamide; B = *N*,*N*′ = methylen-bis-acrylamide (Bis).
[3] See Table 3.3.

TABLE 3.3
Additives

Name	Purpose	Concentration	Limitations
Sucrose glycerol	Improve the mechanical properties of low T% gels reduce water transport and drift	5–20%	The increased viscosity slightly slows the focusing process
Glycine taurine	Evenly increase the dielectric constant of the medium; increase globulin solubility and reduce ionic interactions	0.1–0.5 M	Glycine is zwitterionic between pH 4 and 8, taurine between 3 and 7 their presence somewhat slows the focusing process and shifts the resulting gradient
Urea	Disaggregation of supramolecular complexes; solubilization of water-insoluble proteins; denaturation of hydrophilic proteins	2–4 M 6–8 M	Instable in solution especially at alkaline pH; solubility limits 10 °C; accelerates PAA polymerization, so reduce TEMED
Non-ionic and zwitterionic detergents	Solubilization of amphiphilic proteins	0.1–1%	To be added to the polymerizing solutions just before the catalysts to avoid foaming; interfere with the binding to reactive substrata; are precipitated by TCA and require a specific staining protocol

is more hydrophobic and more difficult to dissolve than acrylamide, so start by stirring it in a little amount of luke-warm distilled water (the solution process is endothermic), then add acrylamide and water as required. Table 3.2 gives the composition and general storage conditions for monomers and catalyst solutions, while Table 3.3 lists the most commonly used additives in CA-IEF and IPGs.

3.3.2. Gel formulations

In order to allow all the sample components to reach their equilibrium position at essentially the same rate, and the experiment to

be terminated before the pH gradient decay process adversely affects the quality of the separation, it is best to choose a non-restrictive anti convective support. There are virtually no theoretical but only practical lower limits for the gel concentration (the minimum being about 2.2% *T*, 2% *C*). Large pore sizes can be obtained both by decreasing % *T* and by either decreasing or increasing % *C* from the critical value of 5%. Although the pore size of polyacrylamide can be enormously enlarged by increasing the percentage of cross-linker, two undesirable effects also occur in parallel, namely increasing gel turbidity and proneness to syneresis (Righetti et al., 1981). Thus, in practice, the upper limit for a useful highly cross-linked gel appears to be ca. 30% *C* (although this is not recommended for IPGs, as apparently the incorporation of Immobiline chemicals is hampered in highly cross-linked gels). In this respect, DHEBA (*N*,*N*'-1,2-dihydroxyethylene-bisacrylamide), with its superior hydrophilic properties, appears better than bisacrylamide. In contrast, DATD (*N*,*N*'-diallyltartardiamide) inhibits the polymerization process and so gives porous gels just by reducing the actual % *T* of the matrix. Because unpolymerized acryloyl monomers may react with $-NH_2$ and –SH groups on proteins and, once absorbed through the skin, act as neurotoxins, the use of DATD should be avoided altogether. Table 3.4 gives the upper size of proteins which will focus easily in different % *T* gels.

3.3.3. Recipes for IPG intervals

These are listed in Table 2.2 to 2.9 in Chapter 2. These tables give recipes for 1 pH unit intervals (calculated manually with the aid of the Henderson Hasselbalch equation) and for 2-, 3-, 4-, 5- and

TABLE 3.4
Choice of the gel matrix. A guideline

Protein M_r (upper limit for a given %*T*)	Gel composition
15000	*T*% = 7 *C*% = 5
75000	*T*% = 6 *C*% = 4
150000	*T*% = 5 *C*% = 3
500000	*T*% = 4 *C*% = 2.5

TABLE 3.5
IPG flow sheet

(a) Assemble the gel mold; mark the polarity of the gradient on the back of the supporting plate
(b) Mix the required amounts of Immobilines; fill to one half of the final volume with distilled water
(c) Check the pH of the solution and adjust as required
(d) Add acrylamide, glycerol (0.2–0.3 ml/ml to the 'dense' solution), TEMED and bring to the final volume with distilled water
(e) For ranges removed from neutrality, titrate to ca. pH 7.0, with Tris the acidic, with formic acid the alkaline solution
(f) Transfer the denser solution to the mixing chamber, the lighter solution to the reservoir of a gradient mixer; center the mixer on a magnetic stirrer; check for the absence of air bubbles in the connecting duct
(g) Add AP to the solutions
(h) Pour the gradient into the mold
(i) Allow the gel to polymerize for 1 h at 50 °C
(j) Disassemble the mold, weigh the gel
(k) Wash the gel for 1 h in 1 l of distilled water on a shaking platform
(l) Dry back the gel to its original weight (in front of a blower)
(m) Transfer the gel to the electrophoretic chamber (temperature: 10 °C); apply the electrode strips
(n) Load the samples
(o) Start the run
(p) Stain the gel

6-pH unit intervals obtained with the aid of our computer simulation program. Explanations on the use of these Tables are given directly in Chapter 2, so the reader is referred to this Chapter for selecting the relevant information.

3.4. Gel preparation and electrophoresis

Table 3.5 outlines the series of steps required for an IEF run. The key steps are described in more detail below.

3.4.1. Casting an Immobiline gel

When preparing for an IPG experiment, two pieces of information are required: the total liquid volume needed to fill the gel cassette, and the required pH interval. Once the first is known, this volume

is divided into two halves: one half is titrated to one extreme of the pH interval, the other to the opposite extreme. As the analytical cassette usually has a thickness of 0.5 mm and, for the standard 12×25 cm size, (see Fig. 3.2A-C) contains 15 ml of liquid to be gelled, in principle two solutions, each of 7.5 ml, should be prepared. However, because the volume of some Immobilines to be added to 7.5 ml might sometimes be rather small (i.e., < 50 μl),

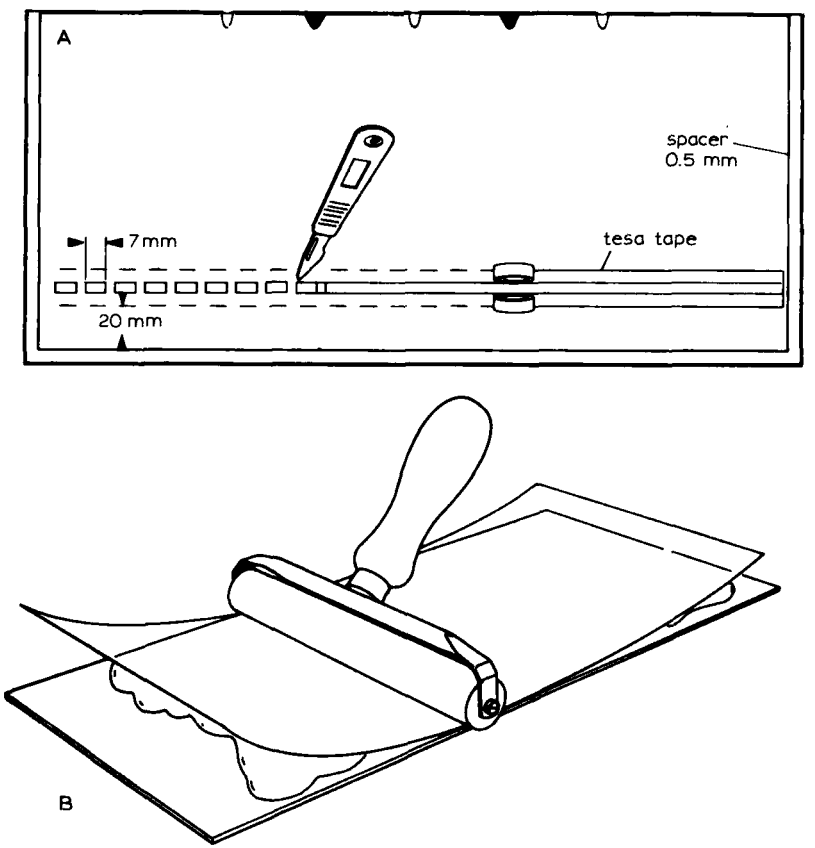

Fig. 3.2. Preparation of the gel cassette. (A) preparation of the slot former: onto the cover plate (bearing the rubber gasket U-frame) is glued a strip of tesa tape out of which rectangular tabs are cut with a scalpel. (B) application of the Gel Bond PAG film to the supporting glass plate. (C) assembling the gel cassette (courtesy of LKB Produkter AB).

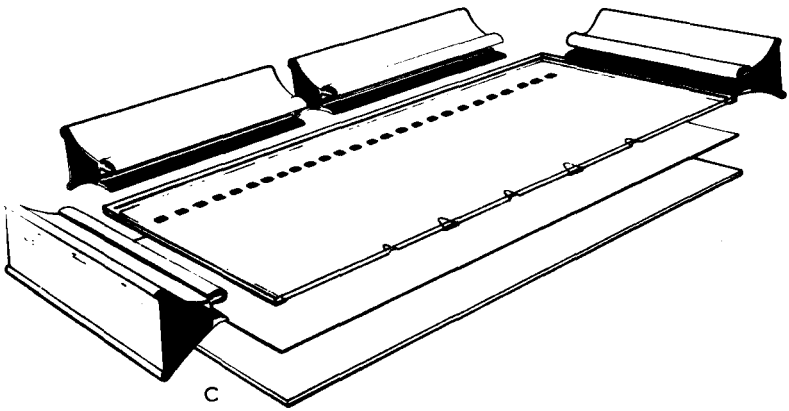

Fig. 3.2 (continued).

Tables 2.2 and 2.3 in Chapter 2 give the required volume (μl) of stock (0.2 M) Immobiline solutions to be added to 15 ml of each starting solution. Clearly this volume will be enough for preparing two gel slabs. The Immobiline solutions (mostly the basic ones) tend to leave droplets on the plastic disposable tips of micropipettes. For accurate dispensing, therefore, we suggest rinsing the tips once or twice with distilled water after each measurement. The polymerization cassette is filled with the aid of a two-vessel gradient mixer and thus the liquid elements which fill the vertically-standing cassette have to be stabilized against remixing by a density gradient. In Tables 2.2 and 2.3 the two solutions are called 'acidic dense' and 'basic light' solutions. This choice is, however, a purely conventional one, and can be reversed, provided one marks the bottom of the mould as the cathodic side. In order to understand the sequence of steps needed, let us refer to Table 3.6 (as a general example of an IPG protocol) and to Fig. 3.3 for the final gel assembly.

Preparation of the gel mould

(i) Wash the glass plate bearing the U-frame with detergent and rinse with distilled water.

(ii) Dry with paper tissue.

TABLE 3.6
Table for preparing starting solutions for one or two gels

Acidic, dense solution		Basic, light solution	
Buffering Immobiline (s) *	μl	Buffering Immobiline (s) *	μl
Non-buffering Immobiline (s) *)	μl	Non-buffering Immobiline (s) *	μl
Add water to a total volume of 7.5 ml		Add water to a total volume of 7.5 ml	
Measure the pH with a pH meter		Measure the pH with a pH meter	
Acrylamide/Bis(A)	2.0 ml	Acrylamide/Bis(A)	2.0 ml
Glycerol (87%)	3.5 ml		
Add water to a total volume of	15 ml	Add water to a total volume of	15 ml

* See Tables 2.2 to 2.9 in Chapter 2. NOTE: The gel solutions are not deaerated, since the gradient mixer is used with both chambers open.
(A): From a stock 30% *T*, 4%. This will give a 4% *T* matrix.

(iii) To mould sample application slots in the gel, apply suitably-sized pieces of Dymo tape to the glass plate with the U-frame; a 5 × 3 mm slot can be used for sample volumes between 5 and 20 μl (this step is only necessary when preparing a new mould or re-arranging an old one; see Fig. 3.2A). To prevent the gel from sticking to the glass plates with U-frame and slot former, coat them with Repel-Silane according to Table 3.1. Make sure that no dust or fragments of gel from previous experiments remain on the surface of the gasket, since this can cause the mould to leak.

(iv) Use a drop of water on the Gel Bond PAG film to determine the hydrophilic side. Apply a few drops of water to the plain glass plate and carefully lay the sheet of Gel Bond PAG film on top with the hydrophobic side down (see Fig. 3.2B). Avoid touching the surface of the film with your fingers. Allow the film to protrude 1 mm over one of the long side of the plate, as a support for the tubing from the gradient mixer when filling the cassette with gel solution (but only if you have a cover plate without any V-indentations; in this last case, the tip of the tubing is lodged snugly in the indentations in the glass cover). Roll the film flat to remove air bubbles and to ensure good contact with the glass plate.

(v) Clamp the glass plates together with the Gel Bond PAG film and slot former on the inside, by means of clamps placed all along the U-frame, opposite to the protruding film. To avoid leakage, the clamps must be positioned so that the maximum possible pressure is applied (see Fig. 3.2C).

Figure 3.3 gives the final assembly for cassette and gradient mixer. Note that inserting the capillary tubing conveying the solution from the mixer into the cassette is greatly facilitated when using a cover plate bearing 3 V-shaped indentations. As for the gradient mixer, it should be noted that one chamber contains a magnetic stirrer, while in the reservoir is inserted a plastic cylinder having the same volume, held by a trapezoidal rod. The latter, in reality, is a 'compensating cone' needed to raise the liquid level to such an extent that the two solutions (in the mixing chamber and in the reservoir) will be hydrostatically equilibrated. In addition, this plastic rod can also be utilized for manually stirring the reservoir after addition of TEMED and persulphate.

Polymerization of a linear pH gradient

It is preferable to use 'soft' gels, i.e., with a low % *T*. Originally, all recipes were given for 5% *T* matrices, but today we prefer 4% *T* or even 3% *T* gels (Righetti and Gelfi, 1984). These 'soft' gels can be easily dried without cracking and allow better entry of larger proteins. In addition, the local ionic strength along the polymer coil is increased, and this permits sharper protein bands due to increased solubility at the pI. A linear pH gradient is generated by mixing equal volumes of the two starting solutions in a gradient mixer. It is a must, for any gel formulation removed from neutrality (pH 6.5–7.5) to titrate the two solutions to neutral pH, so as to ensure reproducible polymerization conditions and avoid hydrolysis of the four alkaline Immobilines. If the pH interval used is acidic, add Tris, if it is basic, add formic acid. We recommend that a minimum of 15 ml of each solution (enough for two gels) is prepared and that the volumes of Immobiline needed are measured with a well-calibrated microsyringe to ensure high accuracy. Prepare the acidic, dense solution and the basic, light solution for the pH gradient as described in Table 3.6 (stock acrylamide solutions are given in Table 3.2; for the catalysts, refer to Table 3.7). If the

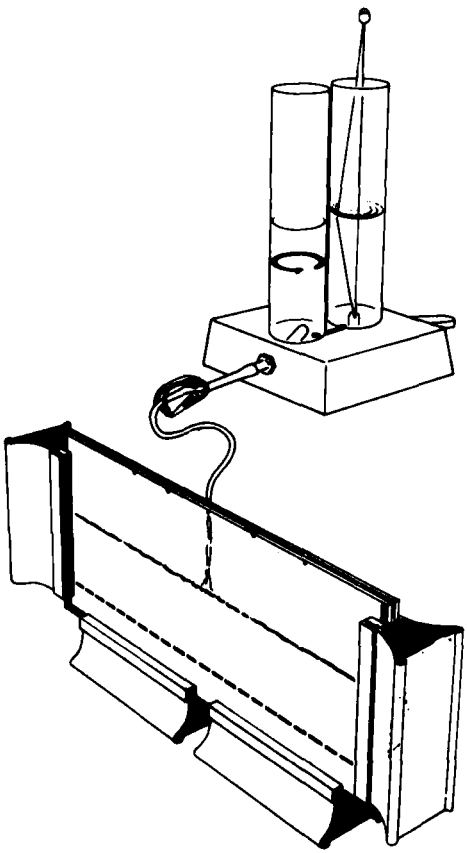

Fig. 3.3. Set-up for casting an IPG gel. A linear pH gradient is generated by mixing equal volumes of a dense and light solution, titrated to the extremes of the desired pH interval. Note the 'compensating' rod in the reservoir, used as a stirrer after addition of catalysts and for hydrostatically equilibrating the two solutions. Insertion of the capillary conveying the solution from the mixer to the cassette is greatly facilitated by using modern cover plates, bearing 3 V-shaped indentations (by courtesy of LKB Produkter AB).

same gradient is to be prepared repeatedly, the buffering and non-buffering Immobiline and water mixtures can be prepared as stock solutions and stored according to the recommendations for Immobiline. Prepared gel solutions must not be stored. However,

TABLE 3.7
Working concentrations for the catalysts

Concentration rating	TEMED (μl/ml)		Persulfate (μl/ml) (40% sol.n)
	acidic pH	basic pH	
Lower limit	0.5	0.3	0.6
Standard, $T\% = 5$ [1]	0.5	0.3	0.8
Standard, $T\% = 3$	0.7	0.5	1.0
For 5–10% alcohol	0.7	0.5	1.0
Higher limit [2]	0.9	0.6	1.4

[1] Righetti, P.G., et al. (1984).
[2] From LKB Application Note #321.

gels with a pH less than 8 can be stored in a humidity chamber for up to one week after polymerization.

(i) Check that the valve in the gradient mixer and the clamp on the outlet tubing are both closed.

(ii) Transfer 7.5 ml of the basic, light solution, to the reservoir chamber.

(iii) Slowly open the valve just enough to fill the connecting channel with the solution, and quickly close it again. Then transfer 7.5 ml of the acidic dense solution to the mixing chamber.

(iv) Place the prepared mould upright on a levelled surface. The optimum flow rate is obtained when the outlet of the gradient mixer is 5 cm above the top of the mould. Open the clamp of the outlet tubing, fill the tubing halfway with the dense solution, and close the clamp again.

(v) Switch on the stirrer, and set to a speed of about 500 rev./min.

(vi) Add the catalysts to each chamber as specified in Table 3.7.

(vii) Insert the free end of the tubing between the glass plates of the mould at the central V-indentation (Fig. 3.3).

(viii) Open the clamp on the outlet tubing, then immediately open the valve between the dense and light solutions so that the gradient solution starts to flow down into the mould by gravity. Make sure that the levels of liquid in the two chambers fall at the same rate. The mould will be filled within 5 min. To assist the mould to fill uniformly across its width, the tubing from the mixer

may be substituted with a 2- or 3-way outlet assembled from small glass or plastic connectors (e.g., spare parts of chromatographic equipment) and butterfly needles.

(ix) When the gradient mixer is empty, carefully remove the tubing from the mould. After leaving the cassette to rest for 5 min, place it on a levelled surface in an oven at 50°C. Polymerization is allowed to continue for 1 h. Meanwhile, wash and dry the mixer and tubing.

(x) When polymerization is complete, remove the clamps and carefully take the mould apart. Start by removing the glass plate from the supporting foil. Then hold the remaining part so that the glass surface is on top and the supporting foil underneath. Gently peel the gel away from the slot former, taking special care not to tear the gel around the slots.

(xi) Weigh the gel and then place it in 0.5 l of distilled water for 1 h to wash out any remaining ammonium persulphate, TEMED and amounts of unreacted monomers and Immobilines. Change the water twice during washing.

(xii) After washing the gel, carefully remove any excess water from the surface with a moist paper tissue. To remove the water absorbed by the gel during the washing step, leave it at room temperature until the weight has returned to within 5% of the original weight. To shorten the drying time, use a non-heating fan placed at about 50 cm from the gel to increase the rate of evaporation. Check the weight of the gel after 5 min and from this, estimate the total weight-reducing time. This step is essential, as a gel containing too much water will 'sweat' during the electrofocusing run and droplets of water will form on the surface. However, if the gel dries too much, the value of % T will be increased, resulting in longer focusing times and a greater sieving effect.

3.4.2. Reswelling dry Immobiline gels

Precast, dried Immobiline gels, encompassing a few acidic ranges, are now available from LKB Produkter AB. They all contain 4% T and they span the following pH ranges: pH 4–7; pH 4.2–4.8 (e.g., for α_1-antitrypsin analysis); pH 4.5–5.4 (e.g., for Gc screening); pH 5.0–6.0 (e.g., for transferrin analysis) and pH 5.6–6.6 (e.g., for

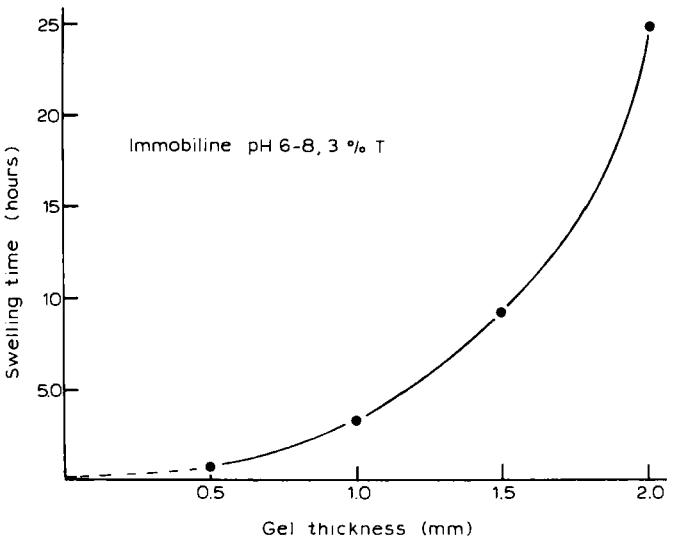

Fig. 3.4. Swelling kinetics of Immobiline gels. The equilibrium swelling times of gels of various thicknesses have been plotted against gel thickness for 3% *T*, pH 6–8 Immobiline gels. Notice how the exponential becomes very steep above 1 mm thickness (from Gelfi and Righetti, 1984; with permission of Verlag Chemie).

phosphoglucomutase screening). Pre-cast, dried IPG gels in the alkaline region have not been introduced as yet, possibly because at high pHs the hydrolysis of both the gel matrix and the Immobiline chemicals bound to it is much more pronounced.

The reswelling properties of an IPG gel depend from many factors: among them, gel thickness, % T (at constant % $C = 4$), temperature of re-hydration, composition of the reswelling medium and pH interval in the IPG matrix (Gelfi and Righetti, 1984). For rapid reswelling, gel thickness and % T play a major role. For example, as shown in Fig. 3.4, already at 1 mm thickness reswelling time is considerably lengthened. For this (and other reasons, like speed of staining and destaining and the like) IPG gels are routinely cast as 0.5 mm thick matrices; however, Pflug (1986) has reported preparation of IPG plates as thin as 250 μm (I do not recommend them, only because of the difficulties in pouring a gradient solution in such a narrow gap in between the two plates of the cassette). At

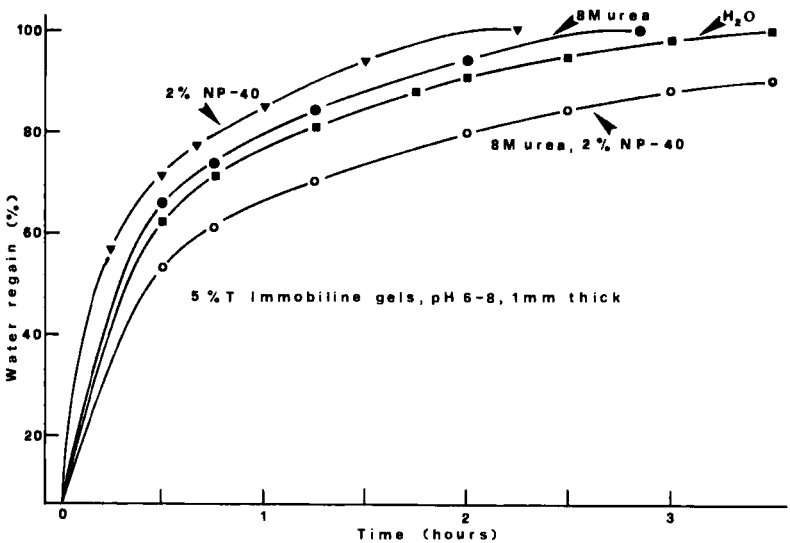

Fig. 3.5. Swelling kinetics of Immobiline gels. 1 mm thick, 3% *T*, 4% *C* IPG gels, pH 6–8 were dried and re-swollen in: plain distilled water (solid squares), 8 M urea (solid circles), 2% Nonidet P-40 (NP-40; solid triangles) and a mixture of 8 M urea and 2% NP-40 (open circles). The swollen gel weight, as taken just after polymerization, was subtracted from the tare (combined weights of Gel Bond PAG and of monomers) and the dried gel was re-swollen to this net weight value. In the case of urea solutions, the solvent uptake was corrected for its density (i.e., the gel was allowed to reswell to 12% more weight, as solvent uptake was evaluated by weighing). Reswelling was here performed in open vessels, rather than in a reswelling cassette (from Gelfi and Righetti, 1984; with permission of Verlag Chemie).

60°C, the reswelling time is reduced by a factor of 2.5 as compared with reswelling at 20°C: thus, whenever possible, reswelling at higher solvent temperature should be adopted (not with urea at alkaline pH values, though, as urea will rapidly decompose and form cyanate: at equilibrium, as much as 20 mM cyanate is present in 8 M urea). In addition to these factors, the composition of the reconstituting medium greatly affects reswelling time: as shown in Fig. 3.5, the most difficult equilibration occurs when reswelling with 8 M urea and 2% detergent, a concoction widely used for 2-D maps of complex samples. In this case, for proper equilibration, the reswelling should be continued at least overnight (at acidic pH

values one can also resort to increases in temperature, which will greatly diminish the viscosity of the reconstituting medium). As an alternative procedure, Field and Lee (1985) have proposed to incorporate directly 8 M urea and 2% detergent into the gelling mixture and then utilize these two additives in the washing solution. In this way, one should be sure that the gel contains uniformly, through its thickness, the correct amount of detergent (owing to the large size of its micelles, it is never guaranteed that, upon incorporation by diffusion into an 'empty' gel, the detergent concentration will be constant through the gel thickness at the end of the reswelling process).

It has been found that the diffusion of water through Immobiline gels does not follow a simple Fick's law of passive transport from high (the water phase) to zero (the dried gel phase) concentra-

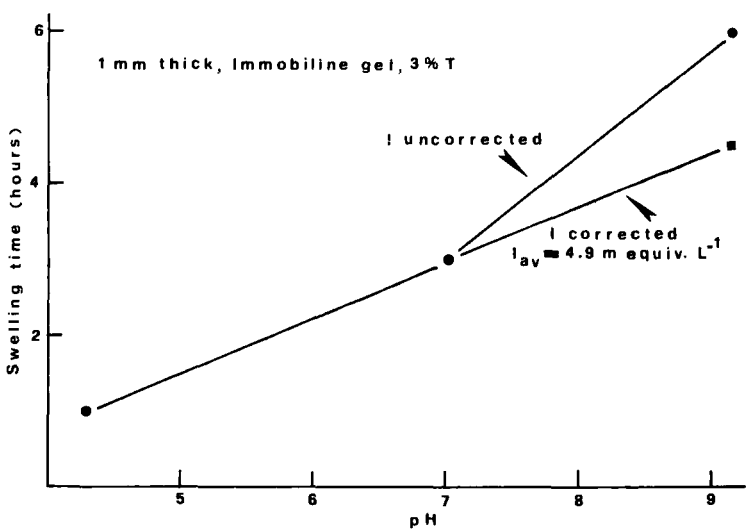

Fig. 3.6. Swelling kinetics of Immobiline gels: effect of the IPG interval. The equilibrium swelling times of three IPG gels (pH 3.5–5, pH 6–8 and pH 8.5–10) have been plotted vs. pH at midpoint. The first two points to the left refer to gels with average ionic strength (I_{av}) of 4.9 mequiv.l^{-1}, while the last point in the uncorrected curve had $I_{av} = 3.1$ mequiv.l^{-1}. In the lower curve, the experiment was repeated by swelling an alkaline gel (pH 8.5–10) with an Immobiline molarity increased by a factor of 1.6, giving an $I_{av} = 4.9$ mequiv.l^{-1}. Thus the lower tracing represents the swelling of iso-ionic strength gels (from Gelfi and Righetti, 1984; with permission of Verlag Chemie).

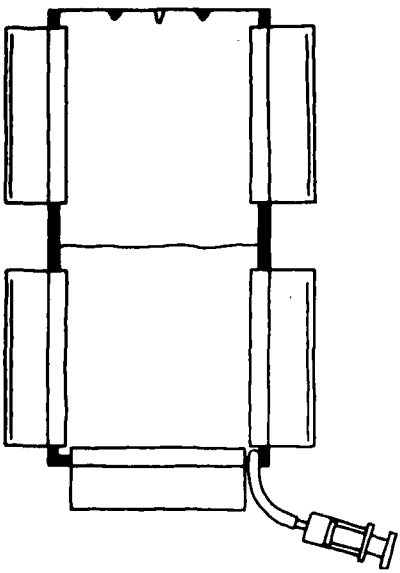

Fig. 3.7. Re-swelling cassette for dry IPG gels. The dried IPG gel (on its plastic backing) is inserted in the cassette, which is then gently filled with any desired re-swelling solution via a bottom hole (by courtesy of LKB Produkter AB).

tion regions, but it is an active phenomenon: even under isoionic conditions, acidic ranges cause swelling 4–5 times faster than alkaline ones (Fig. 3.6). Given these findings, it is preferable to reswell dried Immobiline gels in a cassette similar to the one for casting the IPG gel (Altland et al., 1984). Fig. 3.7 shows the reswelling system produced by LKB. The dried gel is inserted in the cassette, which is clamped and allowed to stand on the short side. The reswelling solution is gently injected into the chamber via a small hole in the lower right side using a cannula, until the cassette is completely filled. As the system is volume-controlled, it can be left to reswell overnight, if needed. Gel drying and re-swelling is the preferred procedure when an IPG gel containing additives is needed. In this case it is always best to cast an 'empty' gel, wash it, dry it and then reconstitute it in presence of the desired additive (e.g., urea, alkyl ureas, detergents, carrier ampholytes and mixtures thereof).

TABLE 3.8
Electrodic solutions

Substance	Use	Concentration	For 100 ml
Glutamic acid	Anolyte	10 mM	147 mg refrigerate
Lysine	Catholyte	10 mM	146 mg refrigerate
Carrier ampholytes [1,2]	Both electrolytes	0.3–1%	0.75–2.5 ml refrigerate
Distilled water [2]	Both electrolytes		

[1] Of the same or of a narrower range than the IPG.
[2] For mixed-bed gels or for samples with high salt concentration. Electrodic strips from Whatmann #17.

3.4.3. Electrophoresis

A list of the electrode solutions in common use can be found in Table 3.8. A common electrophoresis protocol consists of an initial voltage setting of 500 V, for 2–4 h, followed by an overnight run at 2–2500 V. Ultranarrow gradients are further subjected to a couple of hours at 5000 V, or better at about 1000 V/cm across the region containing the bands of interest. Table 3.9 gives some guidelines for voltage settings according to the IPG interval.

TABLE 3.9
Running conditions for one 0.5-mm thick analytical gel

	Voltage	Current	Power	Time
Prerunning	500 V	15 mA	20 W	30–60 min
Electrofocusing	2–3000 V	5 mA	5 W	overnight (for gradients $\leq$ 1 pH unit wide) 3–5 h (for broad gradients)

3.5. General experimental considerations

3.5.1. The use of density agents

When casting an Immobiline gel, a superimposed density gradient is needed in order to stabilize the vertical liquid phase in the gel cassette just prior to the onset of polymerization. However, the addition of some inert chemicals like sucrose or glycerol changes both the density and the viscosity of the solution, affecting the hydrodynamic behavior of the gradient mixer. Assuming that the liquid level in the chambers of the mixer is the same, from Poiseuille's law it follows that the flow is directly proportional to the fluid density (ρ) and, all the geometric factors being equal, inversely proportional to its viscosity (η). Thus, for ideal flow in the two chambers of the gradient mixer, the ratio of the products of density times viscosity in each chamber should be equal to one ($\eta_1\rho_1/\eta_2\rho_2 = 1$). When density and viscosity values relative to water are used, it should be: $\eta_1/\rho_1 = \eta_2/\rho_2 = \eta_{H_2O}/\rho_{H_2O} = 1$, assuming that the solution of acrylamide and Immobiline behaves practically like water.

In reality, as shown in Fig. 3.8, for the most common chemicals used for the generation of a density gradient the η/ρ ratio rapidly diverges from unity with increasing concentration (Weast, 1987). In contrast, a few inert salts, like KCl, NaBr, CsCl, which can be used at concentrations lower than 10% by weight, have a rather constant η/ρ ratio in consequence of their effect on water structure. Thus, if one were to aim at generating a highly linear IPG gradient, an effective way would be to replace the conventional 0–20% glycerol gradient, with a 0–5% KCl gradient as a density agent, since its η/ρ value is quite close to unity (see Fig. 3.8). LKB has tried to overcome this by the use of a compensating cone in the light solution (which, by rising the liquid level in this chamber, tends to hydrostatically re-equilibrate the two chambers). Yet, even the use of this precaution does not guarantee that the more viscous part of the gradient will be linear (in fact, generally, it will deviate from linearity). In a recent study, when trying to form IPG gradients in gel tubes by the use of the principle of rotational centrifugation

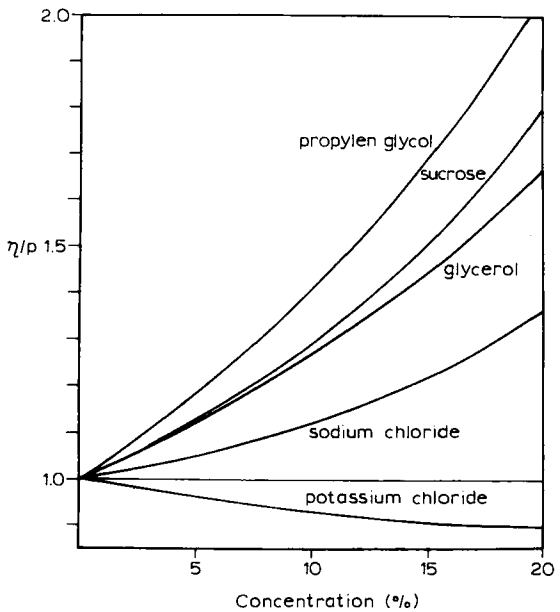

Fig. 3.8. Plot of η/ρ versus concentration for some common chemicals. η, relative viscosity; ρ, relative density. The thin horizontal line is an ideal line with zero slope (from Dossi et al., 1983; with permission of Elsevier).

(Bossi et al., 1988) we could in fact demonstrate that, in presence of a 0–20% glycerol gradient, non-linear IPG gradients were always produced (Fig. 3.9, upper panel, A). Reduction of the gradient to a 0–15% glycerol level gave improved gradients, but still not completely linear (Fig. 3.9, central panel, B), while use of a 10% glycerol gradient gave very linear gradient gels C. Thus, to those scientists requiring rigorously linear IPG gradients we recommend the use of a 0–5% KCl gradient or at least the reduction of the glycerol gradient to a 0–10% level. In this last cases, though, care should be taken to avoid any disturbances during the pouring of the gradient, as the supporting density increments will be very small and thus the liquid stream filling the cassette will be quite sensitive to any disturbances.

3.5.2. On the temperature of polymerization

In copolymerization chemistry, it is often reported that the composition of the copolymer formed differs from the initial input

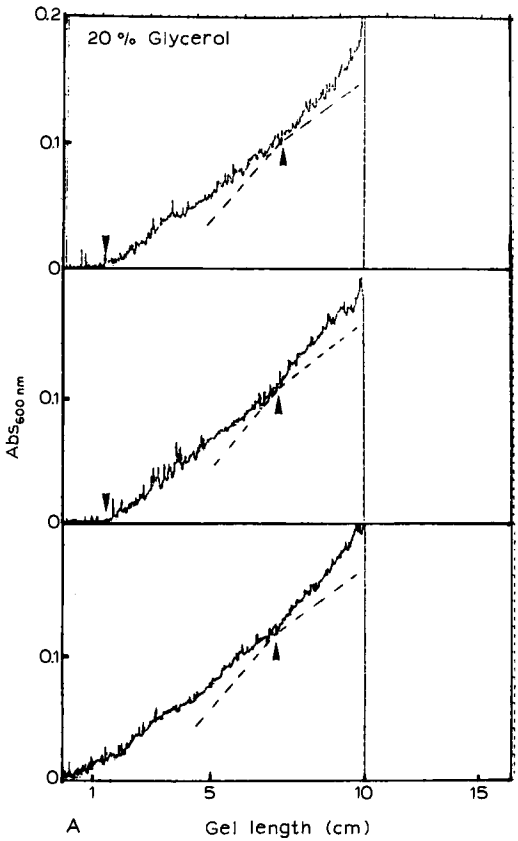

Fig. 3.9. Densitometric profiles of IPG gradients formed in presence of different glycerol concentrations. (A): dense solution containing 20%; (B): 15% and (C): 10% glycerol, respectively. The dense solution contained 0.1% bromophenol blue. The IPG gradient was formed in 2-mm inner diameter tubes by centrifugal rotation at a 2.5° angle. After gelling, the tubes were scanned at 600 nm with an LKB laser densitometer. In B, the amount of bromophenol blue was lowered to $\frac{1}{2}$. Note that in A two curves of different slopes are obtained. If the tubes are rotated immediately after lowering the platform, a plateau is obtained (A, two upper panel), indicating lack of equilibration of the two sliding menisci (from Bossi et al., 1988; by permission of Elsevier).

composition because the monomers differ in reactivity towards free radical addition (Flory, 1953; Aggarwal, 1976; Danusso et al., 1979). Thus, with less than 100% incorporation of monomers into the polymer, there is a possibility that the concentration ratios between the Immobilines built into the gel will differ from the ratios in the starting solution; this could have serious consequences on the pH gradient generated, e.g., by changing its slope and the theoretically computed pH interval. To minimize this effect, all Immobilines are acrylamide derivatives, but even with this precaution it cannot be excluded that the resulting pH values depend to a certain extent on the polymerization efficiency. Using techniques described by Gelfi and Righetti (1981a,b), we have studied the effects of the following parameters on Immobiline gels: (a) level of persulphate, from 0.015 to 0.058%; (b) level of TEMED, from 0.024 to 0.096%; (c) temperature range, from 20 to 60°C and (d) pH of the gelling solution. The optimum polymerization efficiency (in the range 84–88% incorporation for all seven Immobilines) was

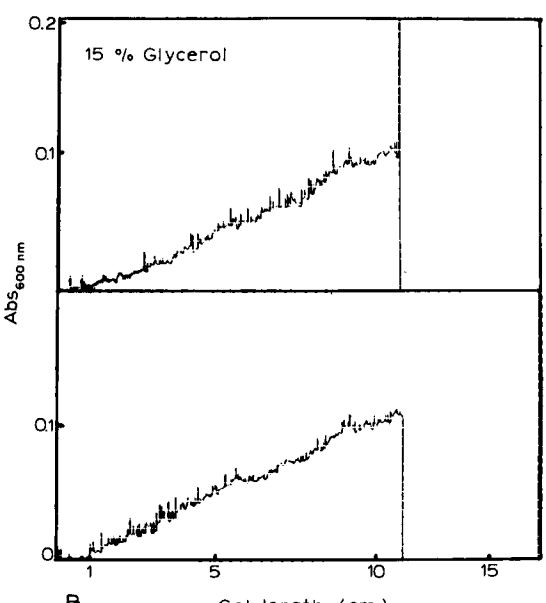

Fig. 3.9 (continued).

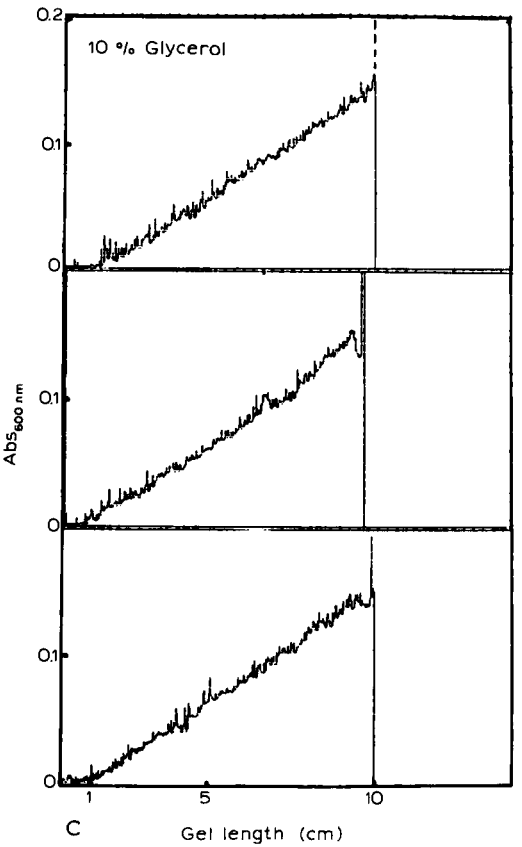

Fig. 3.9 (continued).

found at 0.047% TEMED, 0.033% persulphate, 50°C and pH around neutrality (ca. 7). Fig. 3.10 gives an example of the effect of temperature on the extent and rate of reaction of Immobilines: as the temperature is lowered, the reactivity rate diverges greatly for the different Immobiline chemicals, with a consequent lowering of the incorporation levels in the gel matrix. Curiously, at 60°C, the polymerization efficiency is lowered slightly for some species (the alkaline ones; at the light of the information gathered in Chapter 1, it is quite possible that some degradation takes place). Thus

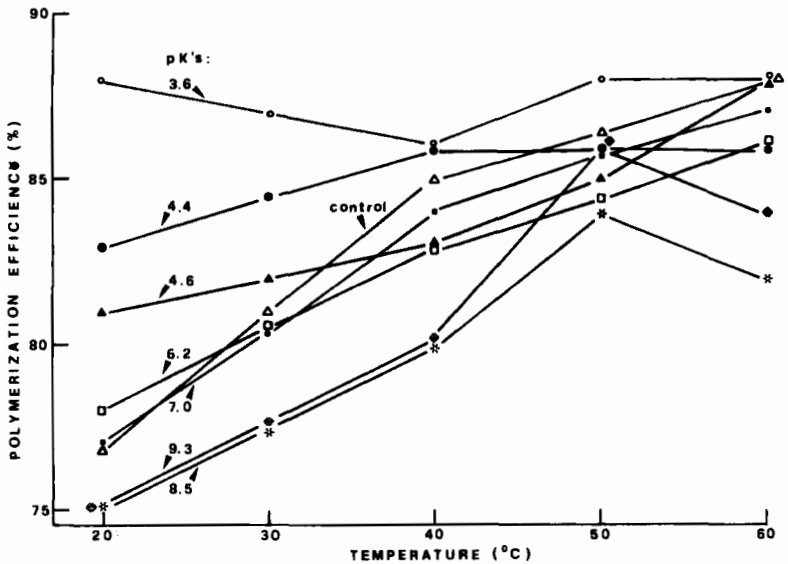

Fig. 3.10. Polymerization efficiency of the seven Immobiline species as a function of temperature. The percentage incorporation in the matrix is putative, as it is based on the ratio between initial and final absorbances at 285 nm (disappearance of double bonds). Experiments performed in a 3 ml thermostated cuvette. Readings taken after 1 h of reaction at the given temperatures. The best convergence (similar reactivity ratios) is only obtained at 50°C (from Righetti et al., 1984; with permission of Elsevier).

polymerization for 1 h at 50°C, as we keep suggesting, appears to be just the right solution: all Immobilines seem to come to a confluence point at this temperature, by exhibiting very similar reactivity ratios and efficiencies (Righetti et al., 1984).

Another important lesson has been learned from these experiments: when casting extended pH gradients, it is imperative that the acidic and basic ends of the pH gradient be titrated around neutrality, the former with Tris, the latter with formic (which, in its protonated form is volatile, thus easily lost from the IPG matrix) or acetic acid. Neutral polymerization conditions ensure maximum stability of all Immobiline chemicals and also good stability of the neutral monomers (acrylamide and Bis), which, at alkaline pH values, would tend to hydrolize too.

3.5.3. On the gradient mixer

When Immobiline gradients are cast as shown in Fig. 3.3, with the two-vessel gradient mixer equilibrated in air, an 84–88% incorporation efficiency is the best that can be achieved, and this for most applications will be adequate. An incorporation efficiency of ca. 95% could be achieved by completely excluding oxygen from the polymerization mixture. To achieve this, the gelling solution should be degassed, equilibrated under argon and transferred to a gradient mixer that provides for anaerobic conditions. We had built such a device (Righetti, 1984), but had never really encouraged its use, as the experimental manipulations become too complex and cumbersome. Recently, however, a similar system, in which the solutions from both vessels are pumped and kept under argon, has been re-proposed by Fawcett et al. (1988). As it is my duty to provide a broad coverage of the field for the reader's interest, I am giving here in Fig. 3.11 a sketch of this set-up; I insist, however, on my original position that the extra labor involved hardly justifies its use. Even if these authors were to achieve a 95% conversion efficiency (which they have not demonstrated) and even though they claim better reproducibility than in all other systems (again, unsubstantiated claims), what is important to bear in mind is that the incorporation ratio among the different Immobilines should be unity, independently from the absolute level of incorporation. The conditions we give in Fig. 3.10 ensure in fact an incorporation ratio close to unity; the fact that the level of incorporation is ca. 85% will only lower by some 15% the average ionic strength and buffering power of the gel, but will still give identical pH intervals to an hypothetical gel in which the incorporation efficiency were 100%. Thus I feel that the methodology we have described here with open vessel gradient mixers is fully adequate in IPG technology.

3.5.4. On the number of washing steps

After standard polymerization (1 h, 50°C, neutral pH values) the gel cassette is recovered from the oven, the clamps removed and the supporting glass plate gently pried open with the tip of a

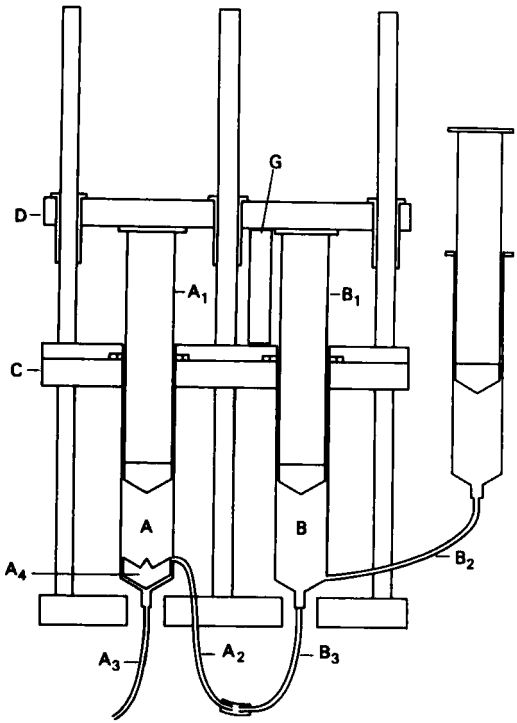

Fig. 3.11. Syringe holder of the gradient maker for casting IPG gels: schematic diagram of the assembly. A,B: 12 ml plastic syringes; A_1, B_1: syringe plungers; A_2, B_3: connecting tubes; A_3: outlet tube (to the gel cassette); B_2: displacement tube with syringe attached; A_4: magnetic stirring bar. C: interchangeable syringe holder plate. D: mobile platform for plunger depression. G: spacer bar of adjustable height. The bar is removed prior to displacement of the syringe (magnetic stirrer and electric motor not shown) (from Fawcett et al., 1988; with permission of Verlag Chemie).

spatula. The Gel Bond PAG foil can now be lifted from one corner and gently peeled off, with the bound polyacrylamide gel layer, from the other glass plate closing the cassette. The first operation to perform at this point is a weighing step (after blotting any traces of liquid around the ridges of the foil, if needed), as the gel has to be washed and will swell in water during this procedure. It is a good idea to mark the weight of the gel on the plastic backing. The

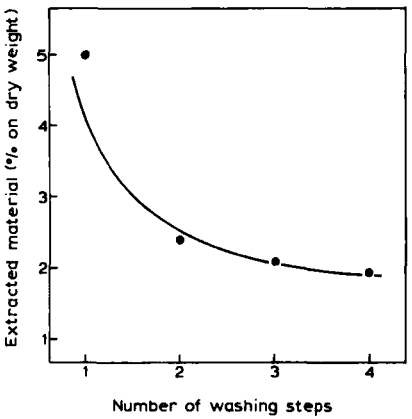

Fig. 3.12. Efficacy of repeated washing steps on the reduction of extractable material from IPGs. IPGs in the pH range 5.4–6.4 were washed in distilled water (500 ml per 20 ml of gel) 1–4 times, 30 min each. The gel was then extracted with 80% acetic acid and the supernatant dried to constant weight on KOH (from Gianazza et al., 1983b; with permission of Elsevier).

gel is now washed in 0.5 l of distilled water for up to 1 h for 0.5 mm thick gels. The washing step is essential: TEMED, persulphate and 12–16% unpolymerized Immobilines (together with the same amount of unreacted neutral monomers, acrylamide and Bis) have to be removed, otherwise huge plateaux of free acids and free bases will form in proximity of the anode and cathode, respectively, and will prevent the protein sample from focusing. In addition, in the absence of washing, the amount of free double bonds contaminating the gel would be extremely high as compared with the level of potentially reacting groups in the proteins under analysis (–SH, $-NH_2$ termini, phenolic –OH, ϵ-amino group of Lys). It might be asked how many washing steps are required for a proper handling of IPG gels. We have studied this by weighing the amount of extracted material after each washing. As shown in Fig. 3.12, at least three washings are recommended for extracting most of the unreacted material from the gel. After that, the amount of extracted material decreases asymptotically. Thus, for analytical purposes, 3 washing steps (at room temperature, on an orbital shaker at ca. 60 rpm, each with 0.5 l of distilled water) are more than

adequate to ensure correct behavior of IPG gels. However, if the gel is used for small scale preparative purposes, it should be subjected to a more drastic washing procedure, since short, oligomeric chains non-grafted into the gel (generally termed liquid, linear polyacrylamide, having apparent M_rs up to 10,000 Da) are eluted at a much slower rate. If the protein to be recovered has to be used for special analyses or for human consumption (like for recombinant DNA products) the gel has to be washed for much longer periods of time, until all leachables become undetectable in the supernantant. For example, with the 'Immobiline membranes' we are using in our new preparative apparatus (the segmented Immobiline principle, see Chapter 5) the washing cycle is protracted for 24 h, with a continuous regeneration of the supernatant. After this period of time, the amount of residual acrylamide in the eluate is less than 1 picomole, the present detection limit of our assay (Faupel and Righetti, unpublished data). It is also my understanding that the precast Immobiline gels presently available from Pharmacia-LKB are subjected to a drastic washing procedure and to a number of cycles definitely greater than 3, as here recommended.

After washing, the gel should be blotted with soft tissue and then, with the aid of a fan, reduced to its original weight. This step is essential, as gels containing too much water will 'sweat' during the IPG run and droplets of water will form on the surface, which will severely disturb the IPG run since locally the conductivity (and thus the field strength) will change.

3.5.5. On sample application

Samples may be applied in a variety of ways to the open surface of an IPG gel slab. For sample application, the general rules given for conventional IEF apply (Righetti, 1983a). Fig. 3.13 indicates some of the ways for applying samples to thin layer plates. The sample can be applied directly on the gel surface simply as a small droplet or as a streak; however, some form of template for sample application, providing physical containement of the liquid is in general preferred. Square (or rectangular) depressions on the gel surface can be produced with the aid of a dymo strip glued to the cover

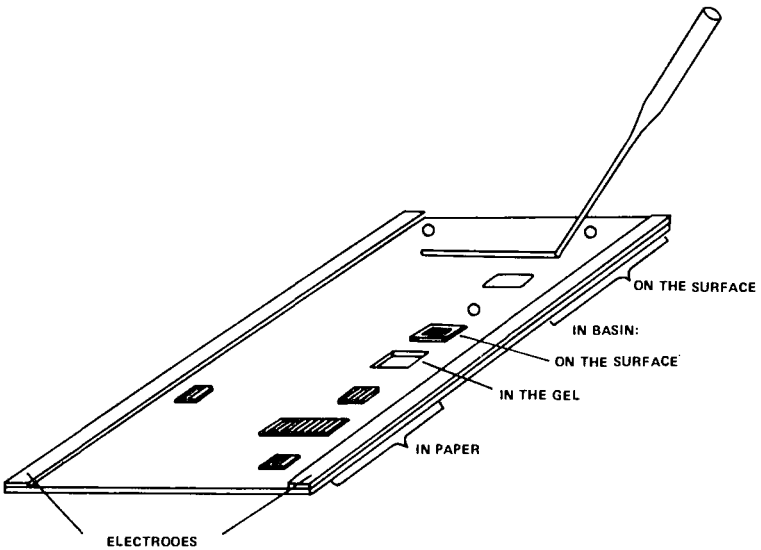

Fig. 3.13. Different ways of applying a protein solution to the gel for isoelectric focusing. From left to right: soaked in a square of chromatographic paper; into a rectangle of the same material, and into two squares, one placed close to each electrode; in a basin dug into the gel; in a basin on the gel surface; as a droplet left on the gel; as a droplet spread on a rectangular area; as a streak; and finally as two droplets, one close to each electrode (from Vesterberg, 1975; with permission of Butterworths).

plate and then cut into pieces of suitable size (see Fig. 3.2). In general these pockets should form a depression in the gel about as deep as one half the gel thickness (e.g., ca. 200 μm deep in a gel of standard 500 μm thickness). In the early days of IPGs, this was the preferred form of sample application, also because the position of the 'pocket' indented in the gel helped to remember the gel polarity (it should be born in mind that, unlike CA-IEF gels, IPG gels have a polarity, and care should be taken to place the anode at the acidic, or less basic, gel end and the cathode at the alkaline, or less acidic, gel extremity). In addition, the 'indentations' in the gel were placed quite apart, since it was customary to cut 'lanes' between adjacent pockets (i.e., to remove a 3–4 mm wide gel strip, going perpendicularly from anode to cathode) so as to prevent lateral sample diffusion and merging of different sample zones. The

problem of lateral sample spreading is still one of the major drawbacks of the IPG technique, and is due to the strong difference in conductivity between the gel matrix and the sample zone (the latter usually containing varying amounts of salts and buffers, up to 100 mM). As it will be discussed below, there are several ways to minimize this lateral band spreading (as an alternative to cutting trenches between adjacent samples). One way is to add a given amount of carrier ampholytes (in general between 0.5 and 1%) to the IPG gel (by re-swelling it in an appropriate CA solution): the CA buffers substantially increase the background conductivity, thus markedly reducing sample spreading. Another way to minimize lateral band spreading, is to equilibrate the gel in 2 mM Tris, in case of cathodic sample application, or in 2 mM acetic acid, in case of anodic sample application (Pharmacia-LKB instruction booklet No. 2355, Uppsala, 1988). In other words, in the case of sample application close to the cathode the gel should contain predominantly mobile cations ($Tris^+$), while for sample application close to the anode, the gel should be equilibrated predominantly with free anions (CH_3COO^-). The reason for that is complex and will be explained in §3.5.7. While we are at it, I must say that, a priori, it is quite impossible to say whether anodic or cathodic sample application should be preferred. There is no general rule, and the site of application will depend on the stability of the protein under analysis. Thus, when dealing with a new protein, it is always best to perform some trial runs in which the same sample is applied at different positions along the focusing path (i.e., close to the anode, close to the cathode and at some positions in between): the quality of the focusing pattern (e.g., absence of precipitates at the application site, number of resolved bands and final quality of the pattern) will give the clue to which site should be selected for protein seeding. Thus, when analyzing phosphoglucomutase isozymes in narrow (pH 5.8–6.8) IPG ranges or acidic phosphatase phenotypes in wider (pH 5.5–7.6) IPG intervals, Sutton and Westwood (1984) and Westwood and Sutton (1984) recommend anodic application either in $10 \times 2 \times 0.2$ mm slots or in circular inserts of 3 mm in diameter. On the contrary, when analyzing some human genetic systems (e.g., α_1-antitrypsin, pH 4.2–4.9; the Gc, group-specific component, pH 4.8–5.2 and the

BF system, B component of complement, pH 5.3–6.0), Charlionet et al. (1984) suggest cathodic application (as much as 15 μl of serum). As a last remedy, Field and Lee (1985) when analyzing tubulin in 8 M urea, 2% Nonidet P-40 IPG gels (pH 5.8–6.4 interval) recommend to load 20% of the protein at the anodal end and 80% at the cathodal end. To quote them verbatim: 'maximal protein entry was obtained when the protein was loaded at both basic and acidic ends of the gel at concentrations of 3 to 5 mg/ml'. However, in some cases, there is already a general consensus: we (Gianazza et al., 1986a,c,d) and others (Görg et al., 1987a,b) have reported that, for 2-D maps of highly heterogeneous samples (e.g., tissue biopsies, cell lysates, total membrane proteins), anodic sample application results in: (a) much better sample entry; (b) much reduced sample streaking from the application point; (c) reduced sample precipitation in the pocket and (d) sharper focusing bands. The reasons for this could be several: (a) hydrophobic interaction with the alkaline end of the IPG matrix; (b) effect of CO_2 adsorption on sample entry and (c) disturbances to the IPG gradient due to the presence of high levels of 2-mercaptoethanol or dithiothreitol (these are buffering groups with pKs around 9.5, which ionize as anions and keep migrating towards the anode) (Righetti et al., 1982).

Today, it appears that one of the best ways to apply the sample to the IPG gel is with the help of applicator strips adhering to the gel surface. Pflug (1988a,b) has described, for CA-IEF, an applicator strip containing funnel-shaped slots, arranged parallel to the pH gradient. He has also reported a modified applicator strip, specifically for IPG gradients, where the slots are separated from each other by a slit in between (Fig. 3.14). According to Pflug and Laczko (1987), such strip prevents or strongly reduces lateral sample spreading. Pharmacia-LKB has now marketed this applicator strip, which consists of 53 adjacent slots, each $5 \times 1 \times 1$ mm, with slits in between adjacent slots 1 mm wide and 0.5 mm deep. Clearly, when applied to the IPG gel surface, the side bearing the slits (which prevent liquid diffusion between adjacent slots by capillary creeping) should face the gel surface. In principle, other ways of applying the sample, as illustrated in Fig. 3.13, can be used: e.g., the sample can be soaked in strips of Paratex (a

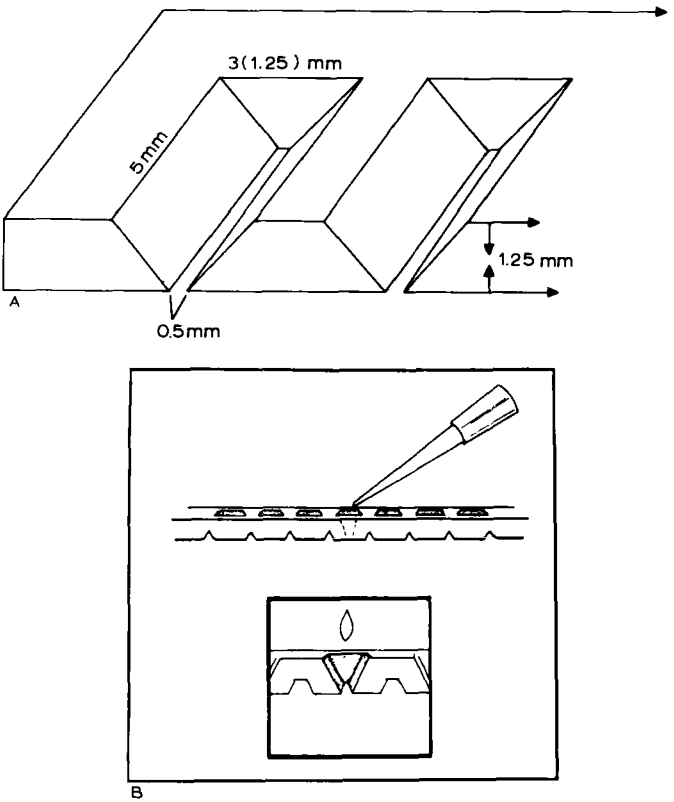

Fig. 3.14. Top (A) and bottom (B) of the sample applicator strip commercially available from Pharmacia-LKB. The applicator contains 53 slots (each 5×1×1 mm) separated by slits (parallel to the slots) 1 mm wide. A: from Pflug (1988b) with permission of VCH; B; by courtesy of Pharmacia-LKB.

non-cellulosic adsorbing tissue) or on granulated Sephadex or polyacrylamide. Or the sample could be contained in an affinity gel column and the resin applied directly for elution under current (Vesterberg, 1976). In general, however, plain filter paper as adsorbent should be avoided (especially when applying the sample at alkaline pH values) since the carboxyl groups contained in the paper will ionize and bind to the sample by strong ionic interaction.

It has been often debated whether the sample should be applied with or without pre-running. It is now a general consensus (Righetti, 1986a,b) that an IPG gel for most samples should *never be pre-run*: in fact, the ionic background present in the gel (even a washed IPG matrix will still contain as much as 0.5–1 mM unbound ions) will help the sample components to enter the gel and will also counteract to some extent lateral band spreading.

3.5.6. Focusing at pH extremes

We have already given in Chapter 2 the appropriate recipes for IPGs at strongly acidic and alkaline pH values (e.g., pH 2.5–3.5 or pH 3–4 and pH 10–11, respectively) together with some general guidelines for successful focusing. In all cases the gels must contain a viscosity gradient (of sorbitol or sucrose) which will act as 'quencher' of both conductivity and electroendosmosis. These gradients (in general at least 0–30%) are arranged so that the dense part falls in the highly conducting gel extreme (thus at pH 2–5 in the acidic ranges and at pH 11 in their basic counterparts). There are two ways in which this can be achieved:

(a) The gel can be already polymerized with the dense part of the viscosity gradient in the correct pH region and used as such, without washing. In this case, the gel should be 'elongated', i.e., it should contain two pH plateaus, one at each extreme of the IPG interval, acting as reservoirs for the electrophoretic depletion of all un-grafted Immobilines and catalysts. Typically, for a 10 cm standard gel length, we add two pH plateaus each 2.5 cm long, so that the final gel length will be 15 cm. At the beginning of the experiment, the gel is run with the electrodic wires at the very extremities of the plateaux; after the salt fronts have been collected in these two gel regions (they will be amply visible due to the strong refractive lines of the moving ion boundaries), the Pt wires can be moved on the two extremes of the IPG intervals, so that the two salt-containing plateaux will be excluded from the electric field and a stronger and more uniform voltage gradient will ensue.

(b) The gel can be polymerized in the usual way, washed, dried, placed back in the cassette and re-swollen with a solution poured with the aid of a gradient mixer, containing the appropriate viscos-

ity gradient needed to counteract the undesired effects of extreme pH values.

In both cases, in any event, it might always be a good idea to have a pH-plateau (i.e., a gel region containing a constant pH value) well removed from the extremes of the narrow pH interval used. This pH plateau will be selected so that the protein to be focused is applied at a pH value well removed from its pI, so that its movement to the pI zone will be accellerated (Ek et al., 1983). In some cases, and for specific samples, one could also apply porosity plateaux (Righetti and Gelfi, 1984) for removing some components by molecular sieving, or affinity plateaux (Gianazza et al., 1985c) for the specific subtraction of some sample component by affinity binding to a ligand.

3.5.7. pH measurements

It is impossible to measure pH values in IPGs either by a surface electrode or by cutting gel slices and equilibrating in 10 mM KCl. As shown in Fig. 3.15, when an IPG gradient (in this case a pH 7–8 interval) is collected in fractions from the gradient mixer (in the absence of gelling agents) and the pH profile measured in solution, its behavior closely follows the expected theoretical curve. However, after gelling, pH measurements in gel slices, even after long equilibration times with the supernantat, are quite erratic and totally meaningless. The use of reversible gels, cross-linked with bisacrylyl cistamine, improves the measurements in the acidic region, but gives false values in the alkaline range, due to the buffering power of added 2-mercaptoethanol or dithiothreitol needed to resolubilize the gel. In a series of papers (Righetti et al., 1986d; Gelfi et al., 1986; Rovida et al., 1986) we have demonstrated that accurate and reliable pH measurements can instead be obtained in mixed-bed CA-Immobiline gels (see also §3.7), the discrepancy between the theoretical IPG slope and the actual pH values obtained by reading the pH of eluted CAs cofocusing in the same gel fragment being less than ± 0.1 pH unit over a 1 pH unit span. It should be appreciated that, in mixed-bed gels, it is the primary, IPG matrix that dictates the width and shape of the pH gradient (as long as the Immobiline chemicals are the prevailing

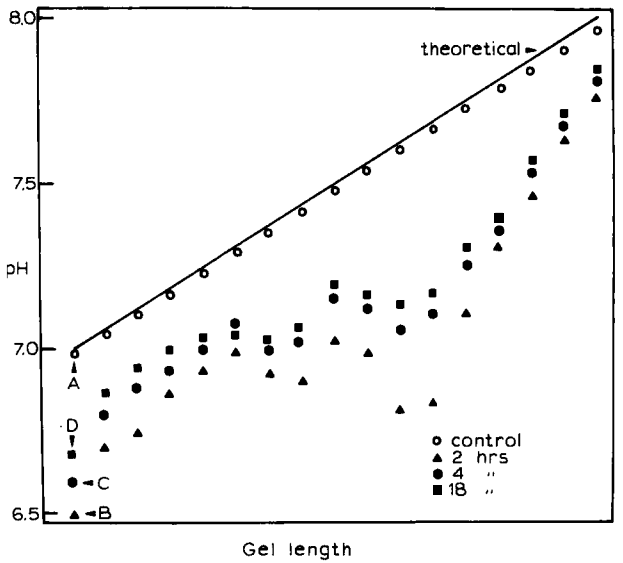

Fig. 3.15. pH gradient determinations in IPG gels in the absence of carrier ampholytes. A pH 7–8 IPG gel was cast and run for 6 h at 2000 V and 10°C. Seventeen gel slices were cut from anode to cathode, 300 μl of 10 mM KCl solution were added and the mixture was allowed to equilibrate under nitrogen for different times. Solid line: theoretical IPG slope. A: gradient measured in unpolymerized gel fractions collected from the gradient mixer into a fraction collector; B, C and D: gradient measured in gel slice eluates after 2 h (triangles) 4 h (solid circles) and 18 h (squares), respectively (from Righetti et al., 1986d; with permission of Elsevier).

species: this is guaranteed up to 2% CA in the gel mixture, at which point the molar ratio Immobiline : CA will be ca. 1 : 1). Thus, if the secondary, CA-generated pH gradient is wider than the former, its width will be reduced to the span of the IPG interval, the excess of CAs with higher and lower pIs collecting at the cathode and anode, respectively. When, however, a wide CA span (2–3 pH unit) is to be converted into a narrow (0.2–0.3 pH unit) span, as often needed in high-resolution analysis, there are two questions to be addressed: what kind of CAs to use and what initial level to add. It turned out (Rovida et al., 1986) that one must use a highly heterogeneous mixture of CAs, obtained by combining several commercial sources, as no single buffering ampholyte cocktail will guarantee an even

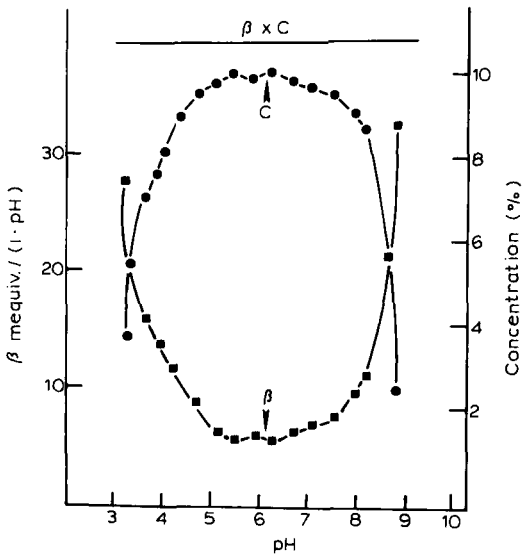

Fig. 3.16. Plot of buffering power (β, in mequiv.$l^{-1}pH^{-1}$, squares) of 1% focused Ampholine in a pH 3–10 range (experimental data from Davies, 1975). The overimposed, bell-shaped profile (circles) represents the reciprocal amount of carrier ampholytes to be added to ultranarrow (0.3 pH unit spans) IPG gradients in order to maintain constant the product β.C (buffering power times the local Ampholine concentration, in %) along the pH axis (upper horizontal line) (from Rovida et al., 1986; with permission of Elsevier).

distribution of different pI species over such a narrow pH range, but will be quite unevenly spread along the pH interval, with several gaps, giving quite erroneous pH readings (Gelfi et al., 1986). In addition, the amount of wide range CAs to be added to narrow IPG spans should vary along the pH axis: taking as a reference point a given CA amount in IPG gels across neutrality, this level should be reduced to about 1/3 in acidic (pH 4 and below) and alkaline (pH 9 and above) pH intervals, since the CA buffers exhibit substantially higher conductivities and buffering capacities (β) and the hydrolytic products of water begin to contribute to the conductivity and β power of the system as well. As shown in Fig. 3.16, the strategy for the amount of CAs to be added to narrow IPG gels is that their concentration (C) should be

the reciprocal of the β power profile (which will be proportional to the conductivity curve) of CAs along the pH axis. By keeping constant the product β.C, i.e., molarity of CAs times their buffering capacity, one can ensure uniform and proper behavior of mixed-bed CA-IPG gels in any narrow interval along the pH axis.

Generally speaking, however, in narrow pH gradients (up to 1 pH unit) it is just as easy to interpolate the pI value of a focused protein simply by its position in the gel matrix, assuming a linear pH course between the two gel extremities (as should be the case if proper handling techniques have been used). In this case, the pI value can be given with an accuracy of two decimal digits. In wide pH intervals, in addition to direct interpolation on the theoretical IPG gradient curve, one can use mixtures of pI standards, as commercially available from most suppliers (e.g., Pharmacia-LKB, Bio-Rad, BDH) or also of carbamylation trains (see Chapter 4).

3.6. Blotting from Immobiline gels

Up to recent times, there has never been an easy solution to the problem of blotting from IPG gels. IPG matrices bind quite tenaciously to the Gel Bond PAG supporting foil and peeling off is simply impossible. This is a highly desirable property, since IPG gels are almost always washed and often dried and re-swollen in different solutions, so they have to stand complex manipulations. In the past we had tried casting them onto a host of porous membranes: denitrated cellulose nitrate; cellulose acetate (including the best IEF brands), cellophane, porous polyethylene, Zeta Probe, Pall Biodyne, just about any commercially available porous membrane; the results though had always been disastrous (Righetti, 1984). A strong electroendosmotic flow at the contact with the membrane gave strong distortion of the focusing pattern, and often the gel and membrane tended to curl severely. So, the only solution adopted was the one proposed by Boss et al. (1984) consisting in polymerizing the gel against the hydrophobic surface of the Gel Bond PAG. The bond was in general so loose that peeling off the gel matrix and tranferring it to the blotting unit was a simple procedure. However, even this solution was not ideal, since during

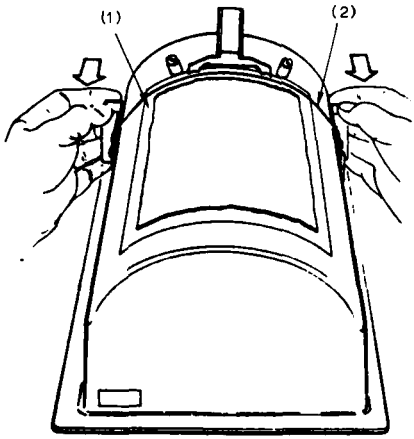

Fig. 3.17. Drawing of the commercial gel slicer from Pharmacia-LKB. The IPG gel, pasted to the Gel Bond PAG foil, is fastened to the curved shield (1). With a quick hand movement, the steel wire (2) is slid at the interface between the IPG matrix and the supporting plastic foil.

gel washing the matrix often tended to peel off the plastic backing. Two additional solutions have now become available: one is a gel slicer, produced by Pharmacia LKB (Fig. 3.17): at the end of the IPG run, the gel is secured to the curved shield, with the gel layer facing up, and then the slicing wire rapidly slided through the contact surface between the plastic foil and the gel. The action is so quick that the gel is effectively cut away from the plastic backing without any tearing action and it can then be trasferred to a porous membrane. The other alternative, just proposed (Knierim et al., 1988; Kinzkofer-Peresch et al., 1988), is the use of a new fabric (called Net-Fix, from Serva, Heidelberg, FRG) hydrophilic and porous, to which the gel adheres and from which it is never detached all throughout the various steps (focusing, blotting etc.). Fig. 3.18 gives a drawing of a typical blotting unit, as commercially available through all suppliers dealing with electrophoretic equipment. As it is not the purpose of this manual to give a detailed information on blotting procedures, the reader is referred to reviews in the field (e.g., Gershoni and Palade, 1983; Towbin and Gordon, 1984; Bjerrum, 1987, editor of an issue of Electro-

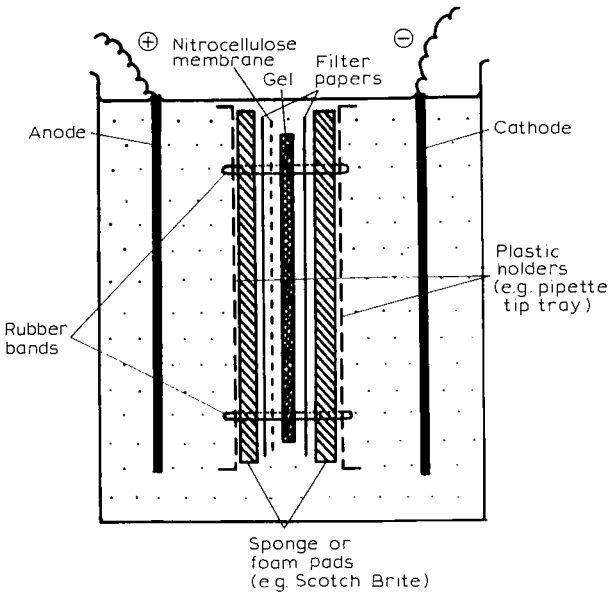

Fig. 3.18. 'Western blotting', i.e. electrophoretic transfer of macromoleculs from a gel slab to an immobilizing membrane. Diagram showing a typical transfer assembly (from Andrews, 1986; by permission of Clarendon Press).

phoresis on this subject). Gelfi et al. (1988) have recently given some general guidelines for blotting from IPG gels, taking as an example a very large protein, α_2-macroglobulin. Blotting is becoming a widely used tool and it appears that it will soon obliterate standard immunochemical techniques (Bjerrum and Heegaard, 1989).

3.7. Mixed-bed, CA-IPG gels

In CA-IPG gels the primary, immobilized pH gradient, is admixed with a secondary, soluble carrier ampholyte driven pH gradient. It sounds strange that, given the problems connected with the CA buffers (discontinuities along the electrophoretic path, pH gradient decay, etc.), which the IPG technique was supposed to solve, one should resurrect this past methodology. In fact, when working with

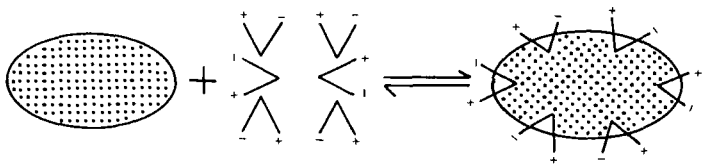

Fig. 3.19. Hypothetical model of a mixed micelle between a neutral detergent (NP-40 or Triton X-100) and carrier ampholytes for IEF. The Ampholine molecules are depicted as 'V'-shaped, with one positive and one negative charge at the extremes (a most likely condition in the isoelectric state; alternatively, they could be represented as 'Y'-shaped, with the charged groups in closer proximity on the prongs of the 'tuning' fork). Upon interaction, the less polar backbone of the Ampholine species could be sorbed within the Debye-Hückel layer of the detergent micelle, leaving a 'zwitterionic' surface. The mixed micelle has been represented as 10% larger than the pure non-ionic species (from Rimpilainen and Righetti, 1985; with permission of Verlag Chemie).

membrane proteins (Rimpilainen and Righetti, 1985) and with microvillar hydrolases, partly embedded in biological membranes (Sinha and Righetti, 1986), we found that the addition of CAs to the sample and IPG gel would increase protein solubility, possibly by forming mixed-micelles with the detergent used for membrane solubilization (Rimpilainen and Righetti, 1985) (see Fig. 3.19) or by directly complexing with the protein itself. It is a fact that, in the absence of CAs, these same proteins essentially fail to enter the gel and mostly precipitate or give elongated smears around the application site (in general cathodic sample loading). It is clear that, on a relative hydrophobicity scale, the four basic Immobilines (pKs 6.2, 7.0, 8.5 and 9.3) are decidedly more hydrophobic than their acidic counterparts (pKs 3.6, 4.4 and 4.6). Upon incorporation in the gel matrix, the phenomenon becomes cooperative and could lead to the formation of hydrophobic patches on the surface of such a hydrophilic gel as polyacrylamide. As the strength of a hydrophobic interaction is directly proportional to the product of the cavity area times its surface tension, it is clear that experimental conditions which lead to a decrement of molecular contact area axiomatically weaken such interactions. Thus, our original idea of CAs as solubilizing ions in IPG matrices has been extended to the hypothesis of CAs as shielding molecules, coating, on one side, the

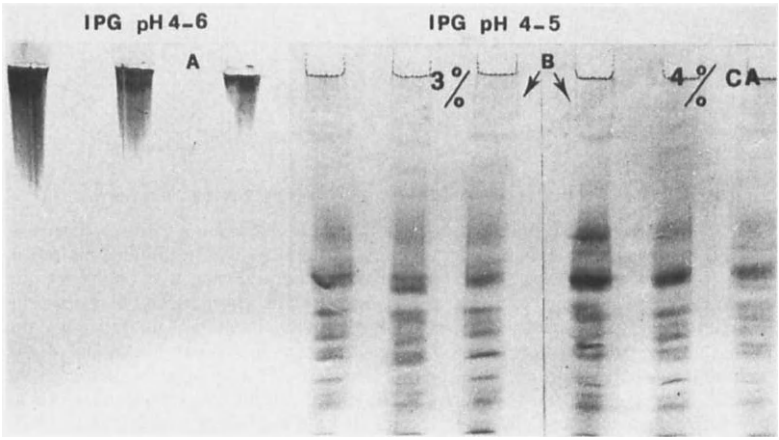

Fig. 3.20. Effect of addition of carrier ampholytes on the hydrophobic protein-IPG matrix interaction. (A): 4% *T* polyacrylamide gel containing a pH 4–6 immobilized gradient in the absence of CAs; (B): 4% *T* gel containing a pH 4–5 IPG, cut into two halves and impregnated with 3% and 4% carrier ampholytes (CA) in the pH 4–6 range. Sample load (from left to right in each gel): 200, 150 and 100 μg horse spleen ferritin. Focusing overnight at 2000 V (final) and 10°C. Staining with Coomassie Blue R-250 (from Righetti et al., 1987d; with permission of Elsevier).

polyacrylamide matrix studded with Immobilines (especially the basic ones) and, on the other side, the protein itself (Righetti et al., 1987c). This strongly quenches the direct hydrophobic protein-IPG matrix interaction, effectively detaches the protein from the surrounding polymer coils and allows good focusing into sharp bands. This phenomenon can be appreciated by considering Fig. 3.20. When horse-spleen ferritin is focused alone in an IPG gel, it gives smears in the proximity of the application site. However, upon addition of 3 to 4% CAs (1.5 to 2% actual gel concentration, as the IPG matrix covers a 1 pH unit interval while the CAs span 2 pH units) a sharp array of ferritin bands is developed in the gel, with essentially no protein remaining in the pocket. For this to happen, the CA shielding species should already be impregnated in the Immobiline gel and present in the sample solution as well. If added afterwards, for example by electrophoretic migration from the electrode strips (Gianazza et al., 1986b), they will be ineffective since, once the hydrophobic protein matrix interaction has oc-

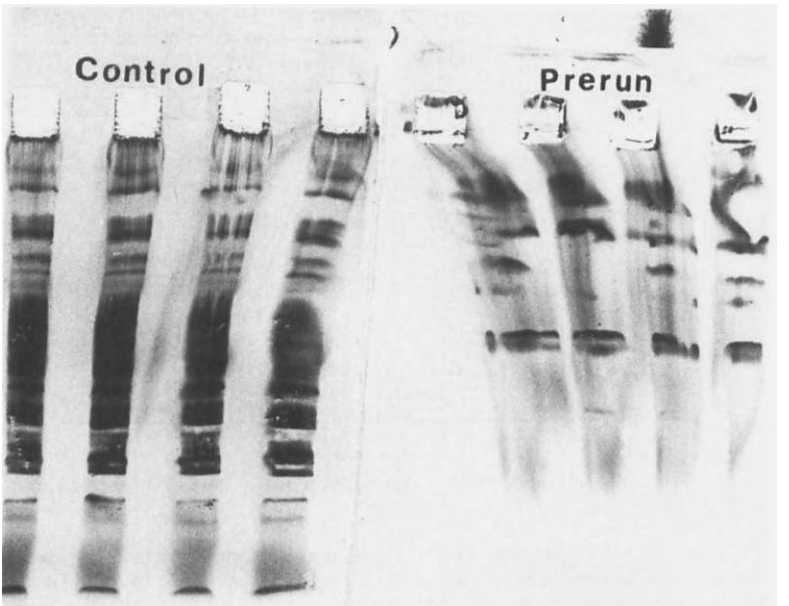

Fig. 3.21. Effect of pre-focusing a mixed-bed, CA-IPG gel. The IPG gel contained a pH 4–5 gradient (made with Immobilines of p*K*s 4.6 and 9.3). 100 μg of ferritin were applied to a pre-focused (right side) or to a control gel in which the protein was focused simultaneously with the background CA (in the IPG gel, at 2% concentration). Note the poor focusing, smearing and sample precipitation in the pre-focused gel. More than 50% of the protein sample (loaded in the same amount as the control in the left panel) was lost by precipitation in the pocket, suggesting that the solubilizing power and shielding effect of CAs is maximal only in the unfocused state (from Rabilloud et al., 1987b; with permission of Verlag Chemie).

curred, the surface which the CAs were supposed to mask will not be available any longer for such shielding action. In other words, CAs can only prevent the phenomenon and cannot cure it a posteriori. The users of the mixed CA-IPG technique should be aware of another fundamental fact: the shielding mechanism is most effective in the unfocused state. If the protein is applied to a prefocused CA bed, severe precipitation and poor protein migration and banding patterns ensue (Fig. 3.21).

A note of caution should be mentioned concerning the indiscriminate use of the CA-IPG technique: At high CA levels (> 1%)

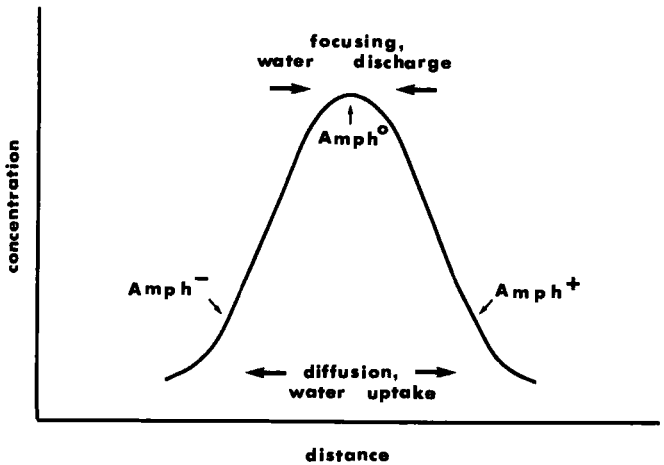

Fig. 3.22. Hypothetical model of the concentration distribution of a focused carrier ampholyte. The peak is subjected to two opposite forces: a focusing process, driven by the electric field, and a diffusion process, driven by the absolute CA concentration in the zone. The diffusion event is depicted as a hydration step, as the anions ($Amph^-$) and cations ($Amph^+$) in equilibrium with the isoelectric species ($Amph^\circ$) acquire more hydration water. The focusing event is represented as a water deposition step at the pI zone (from Astrua-Testori and Righetti, 1987; with permission of Elsevier).

and high voltages (> 100 V/cm) these gels start exuding water with dissolved carrier ampholytes, with severe risks of short-circuits, sparks and burning on the gel surface. The reason for this is shown in Fig. 3.22: the array of focused carrier ampholyte species acts like a chain of mini water-pumps, with water uptake upon diffusion away from the pI and water discharge at the pI zone, due to a regain of the state of zero net charge. This results in accumulation of water droplets at the Ampholine pI zone and dehydration on either side of the peak. This model is corroborated by the findings of Fig. 3.23, which show that the amount of water exuded as droplets on the gel surface is proportional to the molarity of carrier ampholytes present in the IPG gel (Astrua-Testori and Righetti, 1987). The phenomenon is minimized by chaotropes (e.g., 8 M urea) by polyols (e.g., 30% sucrose) and by lowering the CA molarity in the gel. As an answer to the basic question of when and how much CAs to add, we suggest:

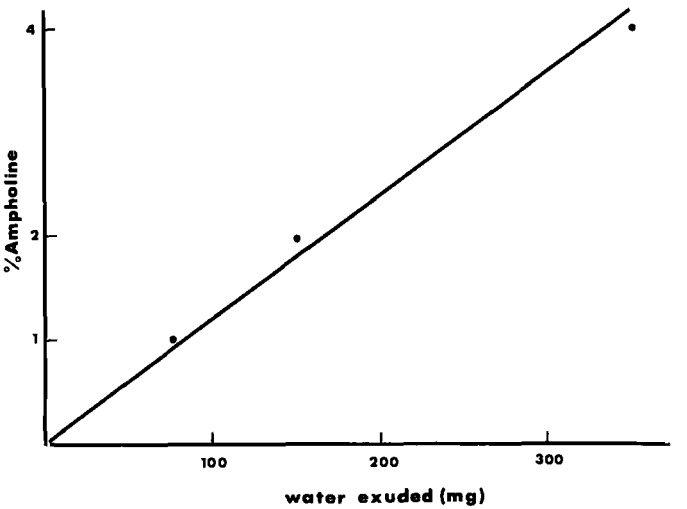

Fig. 3.23. Water exudation as a function of level of carrier ampholyte in the Immobiline gel. A 5% *T*, 4% *C* IPG gel, in the pH 4–8 range, was polymerized, washed, dried, divided into three identical strips (8 cm wide, 11 cm long, 1 mm thick) and re-swollen in 1%, 2% or 4% Ampholine in the pH 4–8 range. After focusing for 6 h at 2000 V (at equilibrium), the total water exuded by each gel was carefully blotted and weighed (from Astrua-Testori and Righetti, 1987; with permission of Elsevier).

(i) if your sample focuses well as such, ignore the mixed-bed technique (which presumably will be mostly needed with hydrophobic proteins and in alkaline pH ranges);

(ii) add only the minimum amount of CAs (in general around 0.5–1%) needed for avoiding sample precipitation in the pocket and for producing sharply focused bands.

As an alternative to the expensive CA chemicals, Polybuffers (inexpensive amphoteric buffers produced by Pharmacia LKB as eluents in chromatofocusing) can be utilized (Rabilloud et al., 1988a).

3.8. Effect of salts on protein patterns in IPG gels

In §3.7 the problem of hydrophobic interaction with the IPG matrix has been debated and as a partial remedy to it addition of

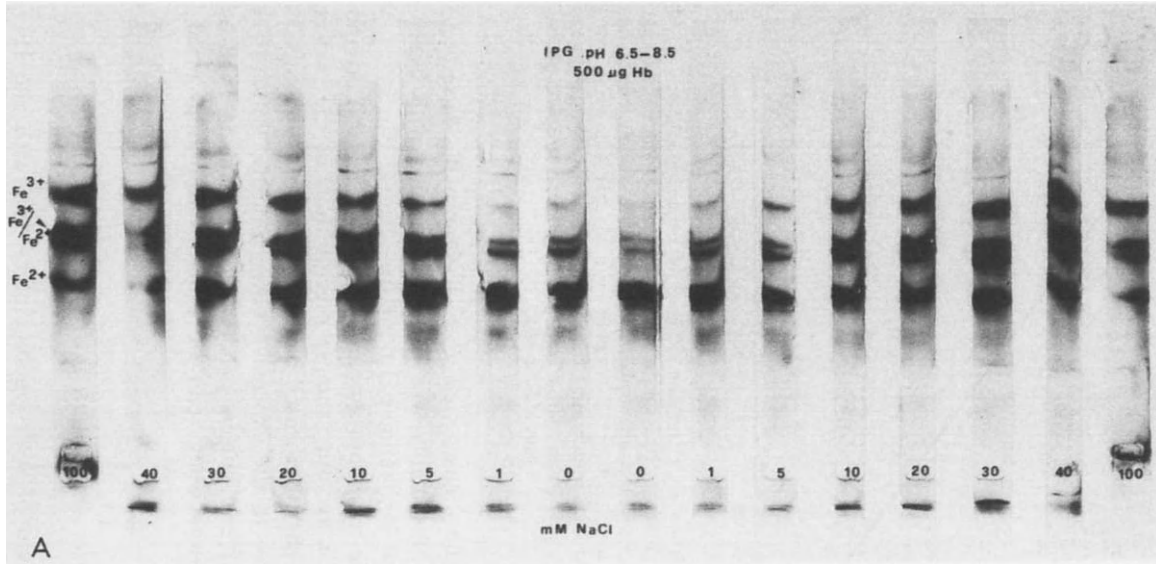

Fig. 3.24. Effects of strong salts, weak electrolytes and carrier ampholytes on proteins patterns in IPGs. A: Hb loaded to a pH 6.5–8.5 IPG gel and added with increasing amounts (up to 100 mM) of NaCl. Reduced (Hb-Fe^{2+}) partially oxidized (Fe^{3+}/Fe^{2+}) and fully oxidized (Fe^{3+}) species are marked on the left side. B: same as A but added with increasing amounts (up to 100 mM) of weak electrolytes (Tris acetate, titrated to pH 7.5). Note the pronounced reduction of oxidized species and the abolition of sample precipitation in the pocket. C: focusing of the same sample added with increasing amounts of NaCl and simultaneously with proportionally increasing levels of carrier ampholytes (pH 6–8 range) so as to keep a constant molar ratio salt : CA of 1 : 1. Note the absence of protein precipitation in the anodic application pockets and the much reduced levels of oxidized species (from Righetti et al., 1988e; with permission of Verlag Chemie).

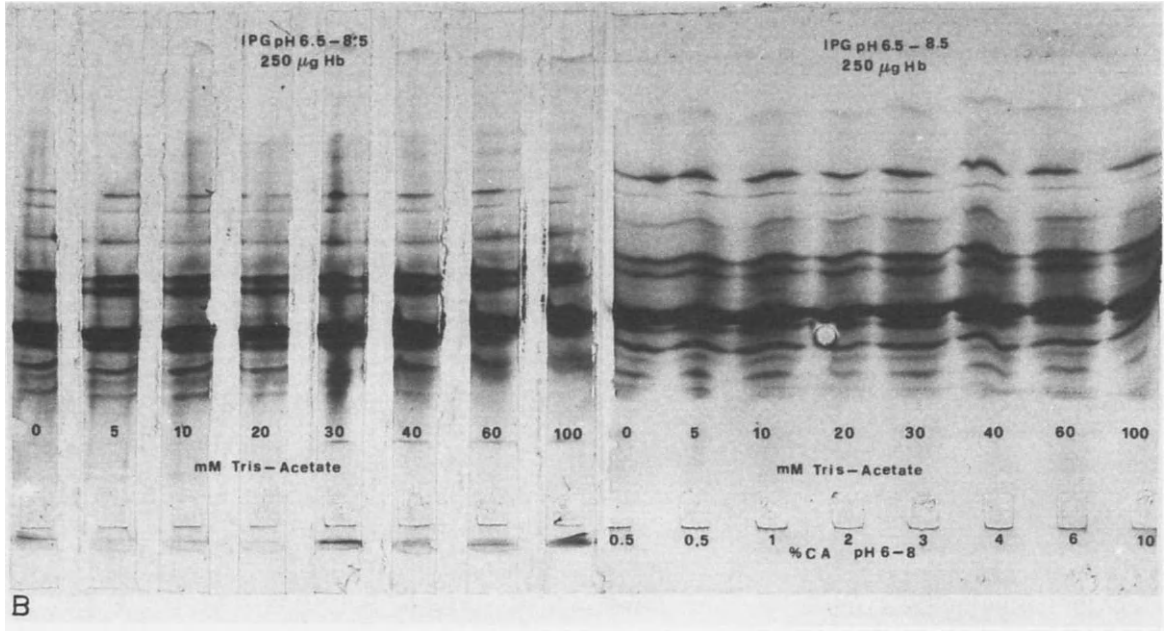

Fig. 3.24 (continued).

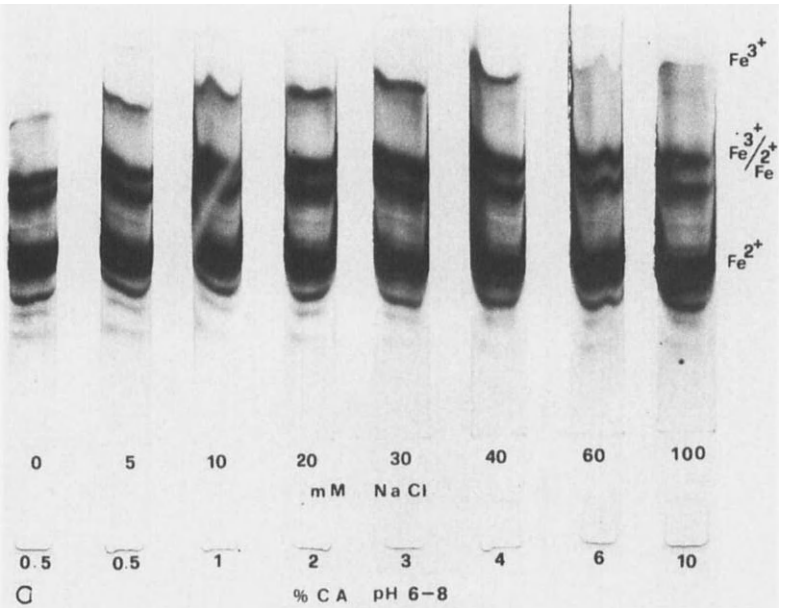

Fig. 3.24 (continued).

ca. 0.5–1% CA buffers has been advocated. With these precautions, can we now assume that IPGs are a trouble-free operation? Yes and no. Read this final section before stretching your sails to the wind. Since its inception, the IPG technique was recognized to be quite tolerant to salt levels present in the sample. This was publicized as one of the greatest advantages of the IPG technique as opposed to CA-IEF, known to be quite sensitive even to low salt levels in the sample. Thus biological samples (containing high salt and dilute proteins) could be run in IPGs without prior dialysis or concentration. This statement is only half the truth: it is true when referring to the IPG matrix which, in principle, can stand any amount of salt; but it is not true when referred to the protein sample. Fig. 3.24A gives us a clue to the phenomenon: salts formed from strong acids and bases (e.g., NaCl, Na_2SO_4, Na_2HPO_4), present in a protein sample applied to an IPG gel, induce protein modification (oxidation of iron moiety in Hb) already at low levels

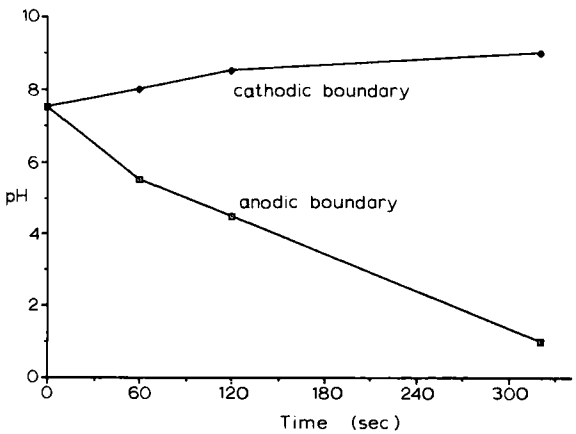

Fig. 3.25. Assessment of pH of salt ion boundaries in the sample zone. Pockets cast in the gel middle (pH 7.5) were filled with 20 μl of 100 mM NaCl. The cathodic and anodic edges were covered with strips of alkaline and acidic pH indicators, respectively. The pH in the two boundaries was assessed by visual inspection of color changes at the given time intervals at constant 2000 V (from Righetti et al., 1988e; with permission of Verlag Chemie).

(5 mM) and irreversible denaturation (precipitation) at higher levels (> 50 mM). This effect is due to production of strongly alkaline cationic and strongly acidic anionic boundaries formed by the splitting of the salt's ion constituents, as the protein zone *is not and cannot be buffered by the surrounding gel until it physically migrates into the IPG matrix.* In order to explain the phenomenon in more detail, Fig. 3.25 shows what happens in the sample liquid droplet, containing high salt levels (in this case, 100 mM NaCl), as soon as the voltage is applied. Within a few minutes, at an applied voltage drop of 200 V/cm, the anodic end of the sample layer reaches a pH as low as 1, with an apparently more modest pH increment in the rear (cathodic) boundary. These extreme pH values generated in the two boundaries are also function of the initial applied voltage (Fig. 3.26): at moderate applied voltages (e.g., 500 V) no adverse pH boundaries are generated, while at progressively higher voltages, strongly adverse pH zones are generated, able to denature and precipitate the protein macroions present in the sample layer. Substitution of 'strong' salts in the sample

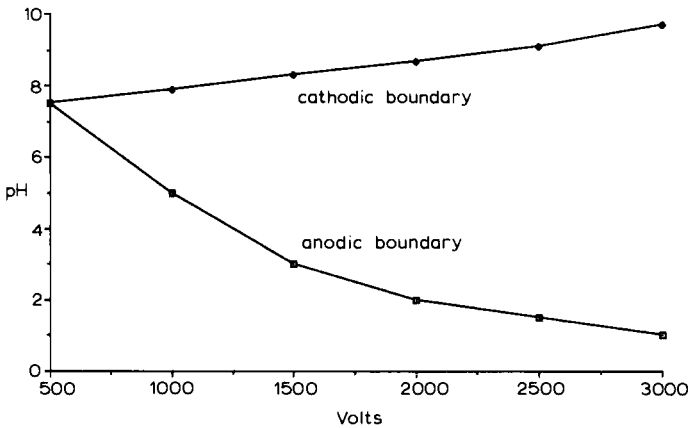

Fig. 3.26. Assessement of pH of salt ion boundaries in the sample zone as a function of applied voltage. The experiment as in Fig. 3.25 was repeated, except that pH estimations were made as a function of different voltage gradients applied (from 500 to 3000 V) after 10 min from application of the electric field. Here and in Fig. 3.23 the alkaline pH estimates must be regarded as approximate since the pH indicators, being negatively charged, move away from the Na^+ boundary towards lower pH values. Conversely, the pH of the anodic boundary is a much better estimate since the pH indicator, when it start leaching out of the filter paper strip, moves with the Cl^- boundary (from Righetti et al., 1988e; with permission of Verlag Chemie).

zone with salts formed by weak acids and bases, e.g., Tris-acetate, Tris-glycinate, Good's buffers, essentially abolishes both phenomena, oxidation and irreversible denaturation (see Fig. 3.24B). Suppression of strong salt effects is also achieved by adding, to the sample zone, carrier ampholytes in amounts proportional to the salt present (e.g., by maintaining a salt : CA molar ratio of ca. 1 : 1) (see Fig. 3.24C). Low-voltage runs for extended initial periods (e.g., 4 h at 500 V) are also beneficial (see Figure 3.26). Table 3.10 summarizes all these recommendations: now you can wander in the proximity of Mount Sinai with your 'pentalogue' under your arm and be a winner.

Note thus that there are two distinct situations requiring different strategies for addition of CA chemicals to an IPG gel: (a) hydrophobic interaction with the matrix and (b) problems of pH control in the sample layer. In the first case, CAs are needed in both sample zone and gel matrix, whereas in the last case CAs are

TABLE 3.10
The 'pentalogue' of IPGs

1	Avoid high salt levels in your sample (> 40 mM).
2	Avoid salt formed strong acids and bases (e.g. NaCl, Na_2SO_4, Na_2HPO_4).
3	In presence of high salt levels, add high levels of CA (e.g. 10% CA to 100 mM salt).
4	If salt is needed for sample solubility, use salts formed from weak acids and bases (e.g. Tris–acetate, Tris-glycinate, any of the Good's buffers (e.g. ACES, ADA, MOPS etc.) titrated around the pK of their amino groups.
5	In presence of high salt levels, run your sample at low voltage for several hours (e.g. 500 V for 4 h) so as to prevent formation of strongly acidic and alkaline boundaries.

only needed in the sample layer, for pH protection during the transient state of sample entry into the gel.

3.9. General staining procedures

Staining for proteins and other macromolecules became a reality with the advent of zone electrophoresis, since in the moving boundary method the only detection possible was by schlieren optics or UV absorption. Early general protein stains included Bromophenol Blue, Amido Black and Ponceau S, all of them characterized by rather low sensitivity, ca. 5–10 μg protein/zone. The development of more sophisticated electrophoretic techniques was paralleled by the introduction of evermore sensitive organic stains, such as the Coomassie Blue stains, which can detect as little as 0.5 μg of protein (Fazekas de St Groth et al., 1963), fluorescent stains (Talbot and Yphantis, 1971), with a sensitivity of 1 ng protein and silvering techniques (Merril et al., 1979), which can detect as little as 0.1 ng protein. We will restrict our discussion to these techniques; for further reading, one should refer to extensive reviews by Righetti (1983a) and by Merril et al. (1986).

3.9.1. Visible organic stains

Coomassie Brilliant Blue R-250 (R stands for a reddish hue while 250 is a dye strength indicator) was the first of the triphenyl-

methane stains to be introduced. It can detect as little as 0.5 $\mu g/mm^2$ of protein and gives a linear response up to 20 $\mu g/mm^2$. Coomassie staining requires an acidic medium for electrostatic interaction between the sulfonated dye molecules and the amino groups of the proteins. Additional dye may be bound by dye-dye interactions to dye molecules that are ionically bound to, or in hydrophobic interaction with, protein molecules (Righetti and Chillemi, 1978). For staining IEF gels, Vesterberg (1972) has introduced a high temperature procedure (60°C) to reduce the interference of ampholytes on the background. Another popular Coomassie is the G-250 (G indicates that this stain has a greenish hue), which is only slightly soluble in 12% TCA. This allows its use as a colloidal dispersion in TCA (or in phosphoric acid/ammonium sulphate), which stains directly the protein zones while leaving a clear background (Neuhoff et al., 1985; 1988). As an example, I will give here a simplified and rapid staining method recently proposed by Neuhoff et al. (1988): at the end of the IEF (or IPG) experiment, fix the gels in the usual way (e.g., 1 h in 12% TCA; this step is not necessary but it is recommended for washing out components causing background staining). Immerse then the gels in a fresh staining solution prepared as follows: 80 ml of 10% ammonium sulphate, 20 ml methanol, 1 ml of 85% phosphoric acid and 2 ml of 5% Coomassie Brilliant Blue G-250 in water. Staining is generally developed in about 20 to 30 min. Wash the gels then briefly with 5×50 ml of 20% methanol in water. Finally, to remove some remaining salts and urea (if used in gel formulations) the gels are briefly rinsed three times with 50 ml distilled water and then dried under an air stream. **Warning**: since Neuhoff's staining results on a surface deposition of colloid dye micelles on the focused protein bands (with no dye penetration within the fibers of the gel matrix), the gel surface should never be rubbed, as customarily done for removing unwanted particulate material precipitated on the gel. Rubbing results in immediate loss of the stained zones. Restaining with fresh dye solution will never reproduce the intensity and quality of the original pattern (Wajcman and Righetti, 1989).

The formula of the two above dyes is given in Fig. 3.27. Also Coomassie Violet R-150 has been reported for staining proteins,

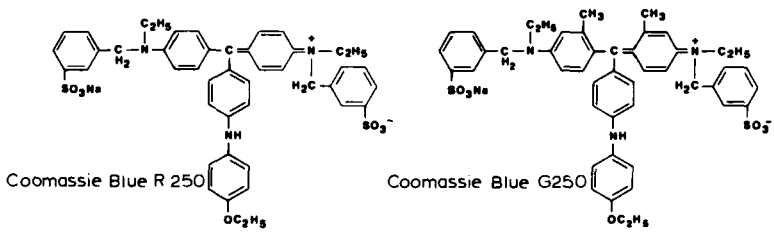

Fig. 3.27. The Coomassie (triphenylmethane dyes) used for protein staining. Note that Coomassie Blue G-250 (b) is a dimethylated form of R-250.

but it has lower sensitivity. Some of these stains can be covalently bound to the protein moiety prior to the electrophoretic run (this is not recommended for IEF analysis, as it would alter the protein charge, but it is in general compatible with an SDS run). Remazol Brilliant Blue R was the first of such reactive stains to be introduced (Griffith, 1972). Bosshard and Datyner (1977) have suggested two additional ones, Drimarene Brilliant Blue K-BL and Uniblue A. These anionic dyes react primarily with the amino groups in proteins as well as with the hydroxyl groups of serine and tyrosine.

3.9.2. Fluorescent stains

In the case of fluorescent dyes, 1-anilinonaphthalene-8-sulphonate (ANS) was the first one to be introduced (Hartman and Udenfriend, 1969), as a post electrophoretic stain, thought to interact with protein's hydrophobic sites. As a pre-electrophoretic fluorescent stain, dansyl chloride was introduced by Talbot and Yphantis (1971): it reacts with proteins in 1–2 min at 100°C, with a sensitivity limit of 8–10 ng. This stain has also been used recently to detect and focus free amino acids in immobilized pH gradients (Bianchi-Bosisio et al., 1986). Other fluorescent dyes utilized include fluorescamine (Pace et al., 1974), 2-methoxy-2,4-diphenyl-3(2H)-furanone (MDPF) (Barger et al., 1976), fluorescein isothiocyanate (Strottmann et al., 1983), tetramethyl rodamine isothiocyanate, rhodamine *x*-isothiocyanate, 4-acetamido-4′-aminostil-

bene-2–2′-disulphonic acid and dichlorotriazinylamino fluorescein (Szewczyk et al., 1987), *o*-phthaldehyde (Weidekamm et al., 1973), 1,3,6-trisulphonyl pyrene-8-isothiocyanate (Tsugita et al., 1982) and bis(8-p-toluidine)-1-naphthalene sulphonate (bis-ANS) (Horowitz and Bowmann, 1987). Fluorescent stains have much greater sensitivity than other organic stains, but the requirement of ultraviolet light for visualization and of sophisticated equipment for quantitation have hampered their utilization on a larger scale. In the case of 2-D maps, Jackson et al. (1988) have recently described a new rapid imaging system for spots labelled with MDPF (after the first IEF dimension) based on a cooled charge-coupled-device (CCD). The CCD photodetector has an array of 385×578 pixels on a single silicon chip and can digitize images focused onto it by a suitable lens system. The characteristic of this CCD system is that it is cooled to $-140°C$. This allows it to have a dark current of ca. 1 photon per pixel per hour. It has extreme sensitivity to low light levels and a detective quantum efficiency of about 50%. The detector has a linear response over a dynamic range of 1 to 10^5.

3.9.3. Silver staining

Perhaps today one of the most popular stains is the silvering technique, first proposed by Merril et al. in 1979, which is said to be 100-fold more sensitive than previous stains. The basic mechanism underlaying all silver stains involves reduction of ionic to metallic silver. There are essentially three different protocols for silvering: (a) diamine or ammoniacal type silver stains; (b) adaptations of photographic chemical development processes and (c) photodevelopment stains. In case (a), silver ions are kept in solution in an alkaline environment by sequestering them in a diamine complex. Thus the concentration of free silver ions in these stains is very low, and there has to be a proper sodium to ammonium ratio in the diamine solution to keep a proper balance of uncomplexed silver ions for proper staining (Allen, 1980). In case (b), silver nitrate reacts with protein sites in acidic conditions, and this is followed by the selective reduction of ionic silver by formaldehyde in alkaline conditions. Sodium carbonate and/or hydroxide are used to maintain an alkaline pH during development (Merril and

Goldman, 1984). In case (c), photodevelopment stains utilize energy from photons of light to reduce ionic to metallic silver. The advantage of this latter stain is its relative rapidity and simplicity, as it can utilize a single staining solution, contrary to other silvering processes which require at least two solutions for processing (Merril et al., 1984). This is particularly useful when staining nitrocellulose membranes after electro-blotting, as they stain very poorly, with e.g., chemical stains, because they retain very little silver nitrate when transferred into alkaline solutions for image developments. Conversely, because the photodevelopment stains contain the silver ions in the image-developing solution, proteins are much better visualized even when bound to thin membranes.

Chemically developed silver stains have been shown to be linear over a 40-fold range in concentration for most proteins. However, protein concentrations greater than 2 $\mu g/mm^2$ generally cause saturation of silver images, resulting in non-linearity above that concentration. In addition, for overloaded spots, (e.g., albumin on a 2-D map of serum) there is always the risk of 'ring-dyeing', i.e., silver deposition only on the spot contour, with little or no staining in the band center. This will render problematic any attempt at quantitation, and would give problems during densitometry, as the single spot could be read as two adjacent peaks. In terms of compatibility of silver stains with autoradiography and fluorography, quenching of ^{14}C-labelled proteins is barely perceptible with most of the non-diamine silver stains. Many diamine stains continue to quench even after treatment with photographic reducing agents, so that fluorographic detection of ^{3}H-labelled proteins is not feasible. In general, however, the detection of tritiated proteins is severely quenched by all silver stains.

3.9.4. Autoradiography and fluorography

Autoradiography is a photographic method for recording the spatial distribution of radioisotope-labelled substances within a specimen material. The radioisotopic emissions release energy to the sensitive silver halide grains in the emulsion layer of the photographic film. The resulting optical density pattern can be used for locating and quantifying the radioactivity distribution. There are

three basic autoradiographic exposure procedures. In the first one (direct exposure) the radioisotope labelled specimen is placed in direct contact with the film detector (Fig. 3.28A). While this procedure generally provides sharper images, it requires longer exposure times than all other methods today employed. Some of the earliest examples of autoradiography can be traced back to the experiments of Becquerel (1896), who studied the blackening of photographic plates (covered with dark paper) in the proximity of crystals of radioactive uranium salts. In the second procedure (fluorographic exposure) (Bonner and Laskey, 1974; Bonner, 1983) the specimen to be analyzed is first overcoated or impregnated with a suitable fluor (Fig. 3.28B). The energy from the radioisotope decay products is converted to light, which becomes then the principal energy source for exposing the film. Either single or double coated film is placed in intimate contact with the treated specimen. Fluorography is almost always used for detection of tritium and for other low-energy beta emitters. The most commonly used fluors are 2,5-diphenyloxazole or sodium salicylate. In the third method (exposure with intensifying screens) (Laskey and Mills, 1977) the photographic film is sandwiched between the radioactive specimen and a radiographic intensifying screen. The ionizing radiation emitted by the specimen (in general gamma or high-energy beta emitters) passes through the film, reaches the screen and is converted into light flashes, resulting in a double film exposure. As a consequence, much shorter exposure times can be used, or lower radioactivity levels can be detected for constant exposure times (Fig. 3.28C). The inorganic phosphors (e.g., calcium tungstate) convert absorbed energy to light in the ultraviolet or blue region of the spectrum. As summarized in Fig. 3.28D, it should be appreciated that intensifying screens only work properly with high-energy emitters, since their radiations are the only ones that can penetrate through the film, its milar support (film base) and excite the phosphor at the bottom. In the case of fluorography, it has been reported that pre-exposure of the film to light produces a two to three-fold increase in the relative densities of faint spots (Laskey and Mills, 1975). Increase in sensitivity is also obtained when the film is exposed at rather low temperatures (e.g., $-70°C$). The minimum amount of radioactivity which can be detected using

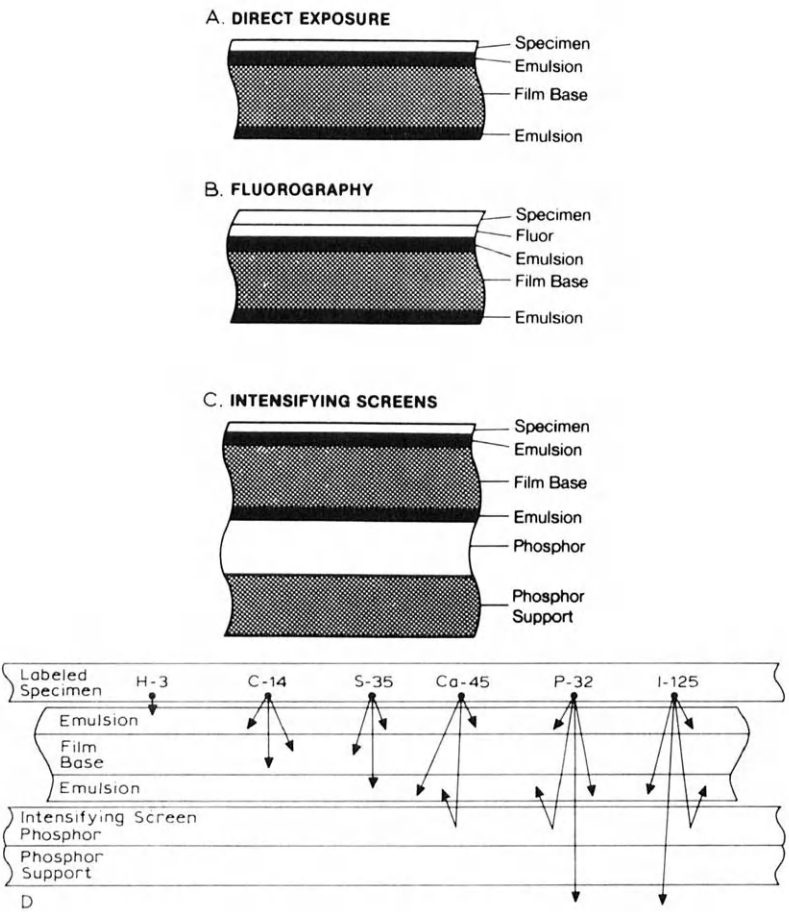

Fig. 3.28. The three classical methods of autoradiography. (A): by direct exposure; (B): by fluorography and (C): with the use of intensifying screens. (D) illustrates the penetration of different radiations into X-ray film. Note that the intensifying screen phosphor method can only be used with high-energy emitters (e.g., gamma radiations) as they can penetrate through the film and excite the phosphor underneath (by courtesy of Eastman Kodak Company).

fluorography with intensifying screen at $-70°C$ and on a pre-exposed film has been evaluated at around 300 d.p.m. for ^{3}H and 30 d.p.m. for ^{14}C in a 1 cm $\times$ 1 mm band in a gel (Laskey and Mills, 1975).

TABLE 3.11
Trouble-shooting guide

Symptom	Cause	Ready
Drifting of pH during measurement of basic starting solution	Inaccuracy of pH glass electrodes (alkaline error)	Consult information supplied by electrode manufacturer
Leaking mold	Dust or gel fragments on the gasket	Carefully clean the gel plate and gasket
The gel consistency is not firm, gel does not hold its shape after removal from the mold	Inefficient polymerization	Prepare fresh AP solution and check that the recommended polymerization conditions are used
Plateau visible in the anodic and/or cathodic section of the gel during electrofocusing, no focusing proteins seen in that part of the gel	High amount of salt in the system	Check that the correct amounts of AP and TEMED are used
Overheating of gel near sample application when beginning electrofocusing	High salt content in the sample	Reduce salt concentration by dialysis or gel filtration
Non-linear pH gradient	Back-flow in the gradient mixer	Find and mark the optimal position for the gradient mixer on the stirrer
Refractive line at pH 6.2 in the gel after focusing	Unincorporated polymers	Wash the gel in 2 L of distilled water; change the water once and wash overnight
Curved protein zones in that portion of the gel which was at the top of the mold during polymerization	Too rapid polymerization	Decrease the rate of polymerization by putting the mold into the freezer for 15 min before filling it with the gel solution, or place the solutions in a refrigerator for 15 min before casting the gel
Uneven protein distribution across a zone	Slot or sample application not perpendicular to running direction	Place the slot or sample application pieces perfectly perpendicular to the running direction
Diffuse zones with unstained spots, or drops of water on the gel surface during electrofocusing	Incomplete drying of the gel after the washing step	Dry the gel until it is within 5% of its original weight
No zones detected	Gel is focused with the wrong polarity	Mark the polarity on the gel when removing it from the mold

3.10. Trouble shooting

One could cover pages with a description of all the troubles and possible remedies in any methodology. However, as LKB has already listed all the major troubles encountered with the IPG technique, we refer the readers to Table 3.11 for all the possible causes and remedies suggested. We should just like to highlight some points:

(i) when the gel is gluey and there is poor incorporation of Immobilines, the biggest offenders are generally the catalysts (e.g., too old persulphate, crystals wet due to adsorbed humidity; wrong amounts of catalysts added to the gel mix); check in addition the polymerization temperature and the pH of the gelling solutions;

(ii) bear in mind the last point in Table 3.11: if you have done everything right, and still you do not see any focused protein, you might have simply positioned the platinum wires on the gel with the wrong polarity. Unlike conventional IEF gel in IPGs the anode has to be positioned at the acidic (or less alkaline) gel extremity, while the cathode has to be placed at the alkaline (or less acidic) gel end.

3.11. Conclusions

I have the feeling that, with all the innovations and recent findings presented in this chapter (particularly the problems connected with sample entry and pH control during the delicate initial phase of the run and guidelines on the addition of CAs), the IPG technique is very well standardized and should perform wonders in any laboratory, without the appearance of the noxious problems which have afflicted the method in the past. It could be asked if we could do better than that. Even though not extensively discussed here, there seems to be a limit in molecular size of the largest protein which could safely enter an IPG gel, this limit being tentatively set at around the size of ferritin (ca. 500,000 Da). Whether this is due to the fact that a large protein can interact cooperatively with the charges (albeit sparse) in the Immobiline matrix or is a pure sieving

phenomenon, remains to be seen. It would be quite attractive to be able to run IPGs in another matrix, e.g., the extremely porous agarose gels, but at the present writing this remains more of a dream than a reality. The technique for reliably grafting Immobilines to agarose matrices (or to cellulose acetate) simply is not there and it might take several years of efforts to develop one. Thus, meanwhile, I think we will have to stick to the present know-how of IPGs in polyacrylamide gels, a technique which still has much to offer to the scientific community.

Two-dimensional maps

4.1. Introduction

According to Giddings (1984) 'two-dimensional (2-D) separations are those techniques in which a sample is subject to two displacement processes oriented at right angles to one another. The displacement steps carry components from their point of application out into a 2-D bed where there is more space for their resolution than in one-dimensional (1-D) separation systems'.

The high intrinsic resolving power of 2-D separations holds great promise for resolving complex biological samples, for which 1-D methods are not powerful enough. In fact the maximum separation power of 2-D systems is described approximately by the multiplicative law:

$$n_2 \approx n_y n_x \approx n_1^2$$

where the subscripts 2 and 1 refer to 2-D and 1-D values, respectively, and n is the peak capacity, i.e., the maximum number of peaks or zones that will fit into the available separation space (Giddings, 1967). 2-D maps, to be highly successful, should be based on completely different separation mechanisms in each single dimension, so as to spread at random the spots in the 2-D plane. If the same methodology is used in the two orthogonal directions, the zones will be simply aligned in a diagonal, with little or no real increment in resolution. Thus Raymonds, who as early as 1964 suggested a 2-D technique called orthogonal acrylamide gel electrophoresis (Orthacryl), cannot legitimately be proposed as the inventor of 2-D methods, as he applied the same electrophoretic principle in both directions, thus generating very nice diagonal patterns (see Figs. 8–12 in Raymonds, 1964). The most modern and powerful method is in fact based on coupled charge-size fractionation,

combining isoelectric focusing in the first dimension (a pure surface charge fractionation) to orthogonal electrophoresis in detergent-laden slabs (sodium dodecyl sulphate, SDS, electrophoresis, i.e., a pure mass-driven separation). This technique was first described by Barrett and Gould in 1973, by MacGillivray and Rickwood in 1974 and subsequently in 1975 by three independent groups (Klose, 1975; O'Farrell, 1975; Scheele, 1975) (the latter, however, utilizing a non-denaturing medium in the second dimension, pore-gradient electrophoresis of native macromolecules). The IEF-SDS technique has been named ISO-DALT (ISO = isoelectric and DALT = Dalton, the unit for mass) by the Anderson's (Anderson and Anderson, 1982a,b), who have pioneered computer modelling of the spots in 2-D maps, standardized the equipment and paved the way, over the years in a series of excellent articles, towards a novel anatomy program, the Human Protein Index.

To be sure, the ISO-DALT is not the only approach to 2-D separations. According to Giddings (1984) there are at least 15 primary displacements for separation of micro- and macro-molecules, based on their different physico-chemical properties: they are listed in Table 4.1. If we note that there are N^2 combinations for N displacements, this means that the 15 primary separation techniques of Table 4.1 can originate 225 different ways of performing 2-D maps. Impressive, isn't it? Yes and no. Giddings notices that this is a much too large number and yet it is much too small since many of the 15 primary 1-D principles can be fractionated into sets of subtechniques, which in turn could generate novel 2-D fractionation principles. Thus Giddings thinks of assembling a grand matrix representing as many as 10^4 to 10^6 distinguishable 2-D techniques. As he is living in the desert of Utah, he might join forces with another giant living in the nearby desert of Arizona, Paolo Soleri, who is spending his life trying to build Arcosanti, the great monoblock city of the future (Soleri, 1969).

I will now discuss a variant of the ISO-DALT technique, which we have nicknamed IPG-DALT, since it utilizes immobilized pH gradients in the first dimension, instead of the conventional CA-IEF methodology. For a wider excursion in the field, the readers are referred to a comprehensive book by Celis and Bravo (1984) and to the proceedings of meetings on 2-D techniques organized by the

TABLE 4.1
One-dimensional displacements which might serve as building blocks for 2-D separation techniques (Giddings, 1984).

Type of displacement	Abbreviation		Property controlling displacement
Bulk	BLK	N	Nonselective
Flow	FLO	N	Nonselective
Chromatographic	CHR	K	Partition coefficient
Field flow fractionation	FFF		Field interaction parameter
Electrophoretic	ELP	u	Electrical mobility
Isoelectric	IEL	pI	Isoelectric point
Isotachophoretic	ITP	u	Electrical mobility
Dielectrophoretic	DEL	k	Dieletric constant
Sedimentation	SED	s	Sedimentation coefficient
Isopycnic sedimentation	IPY		Density
Magnetic gradient	MAG		Magnetic susceptibility
Thermal diffusion	THD	D'	Thermal diffusion coefficient
Thermogravitational	THG		Thermal diffusion factor
Diffusophoretic	DIF		Interfacial energy
Photophoretic	PHO		Photophoretic mobility

Andersons' (1982b, 1984a) and by Galteau and Siest (1986). A manual on 2-D techniques has also recently appeared (Dunbar, 1987). Good reviews can also be found in the manual by Andrews (1986) and in Dunn (1987). After a general survey of the methodology of 2-D maps (gel casting, porosity gradients and the like), I will present different approaches to the IPG-DALT technique, which appears, due to its high reproducibility and very high resolving power, to be a most likely candidate for future expansions in the field of 2-D maps. I apologize for opening such a small window on the almost endless expansion of 2-D techniques; but I must confess that at the present time we are very far from the 10^4 to 10^6 matrix envisioned by Giddings (1984).

4.2. *Sample preparation*

Before entering into the methodology of 2-D maps, a few words should be spent in sample preparation and solubilization, as this will affect the overall performance of the technique. The impor-

tance of protein quantitation in samples should not be overlooked. It should be realized that most protein assays are relative and are based on the measurement of particular amino acid residues and/or peptide bonds. The commonly used methods for determining total protein are the Lowry et al. (1951), based on the combined color developed by Tyr and Trp and by peptide bonds chelating Cu^{2+}, and the Bradford (1976), based on the shift of the leuco-form of Coomassie Blue into the blue-form in presence of protein ions. All these methods have been reviewed by Petersen (1983), who has also presented a detailed list of chemicals, including buffers and deter-

TABLE 4.2
Summary of protein-determination methods

Method	Amino acid residue measured	References
Folin phenol	Aromatic amino acids: (tyrosine and tryptophan) (slower reaction with copper chelates of peptide chain and/or polar side chains)	Lowry et al. (1951); Peterson (1977, 1979, 1983)
UV absorption ($A_{280/260}$ nm) ratio	A_{280}: Tyrosine and tryptophan A_{260}: Nucleic acid interference measurement	Warburg and Christian (1941); Peterson (1983)
UV absorption (244–236 nm)	A_{240}: Tyrosine, tryptophan, phenylalanine, histidine, methionine, cysteine, and peptide bonds A_{230}: Nucleic acid absorption (minimum)	Groves et al. (1968); Petersen (1983)
UV absorption (280/205 nm)	A_{280}: Tyrosine and tryptophan (subject to interference by nucleic acids)	Scopes (1974); Petersen (1983) A_{205}: Peptide bond
Coomassie Blue		Bradford (1976); Read and Northcote (1981)
O-Phthaldehyde fluorescent	NH_2-terminal amino acids and ϵ-amino group of lysine	Butcher and Lowry (1976); Robrish et al. (1978)

gents, which interfere with some of these protein assays. A summary of protein determination methods is given in Table 4.2. Petersen (1983) has recommended that the Folin phenol quantitation method and its modifications be used for general purposes in order to promote consistency in protein measurements between laboratories, since the Lowry et al. (1951) method is the one most frequently used. However, if a rapid method is sought, the Bradford's (1976) is frequently the method of choice. Reagents for this assay are available from Bio Rad Labs. Furthermore, this method has beeen modified so that it can be used directly to measure protein levels in the presence of the solubilizing buffers used for both IEF and sodium dodecyl sulfate-polyacrylamide gel electrophoresis (SDS-PAGE) (Ramagli and Rodriguez, 1985).

4.2.1. Body fluids

Serum, plasma and many other body fluids, such as urine, cerebrospinal fluid (CSF), semen, prostatic and amniotic fluids, acqueous humour of the eye, saliva and suction blister fluid are now routinely analyzed by 2-D PAGE. Samples of these fluids can in general be stored at -20 to $-70°C$ prior to 2-D separation (Tracy et al., 1982a,b), whereas semen samples are quite sensitive to proteolytic degradation (Edwards et al., 1981), so that they should be processed shortly after collection. A peculiar problem with serum samples is the high relative abundance of two classes of proteins, albumin and immunoglobulins, which often mask neighboring minor components on 2-D maps. One approach to this problem is to use a deletion technique, by which serum is subjected to affinity chromatography on Affi-Gel Blue or Sepharose-bound protein A for the selective removal of albumin and immunoglobulins, respectively (Tracy et al., 1982a,b). Albumin removal can also be achieved directly during the IEF step, by incorporating 1% Dextran Blue in a gel layer buffered with Immobilines at pH 9.1 in situ, in front of the sample pocket (Gianazza et al., 1985c). However, these techniques are not fully specific, so that there is always the risk of other protein loss from the 2-D map (Gianazza and Arnaud, 1982).

Most other body fluid samples, however, have a low total protein concentration and contain high levels of salts which usually interfere with the IEF dimension by severely distorting the pH gradient (this, though, is not so critical with the IPG technique, which can tolerate high amounts of salt; see Chapter 3, §3.8). Thus, often, it is necessary, prior to 2-D analysis, to subject a sample to a dialysis and a concentration step; e.g., Merril et al. (1981) have obtained satisfactory 2-D maps by subjecting CSF samples to a 4-fold concentration step by dialysis against 10% polyethylene glycol. In case of urines, however, it is often necessary to concentrate the sample by a factor of up to 1000-fold, coupled with salt removal. Several methods have been proposed: (a) dialysis and gel chromatography (Anderson et al., 1979 a and b; Edwards et al., 1982); (b) gel chromatography coupled to centrifugation (Anderson et al., 1979a); (c) dialysis against polyethylene glycol (Clark et al., 1980); (d) extraction with acidified acetone and gel exclusion chromatography (Guevara et al., 1985). Tracy and Young (1984) have recommended the following procedure: (a) apply 10 ml of urine to a 1.5×60 cm column containing Fracto-Gel HW40-F equilibrated in 0.1 M $HCOO(NH_4)$, pH 6.5, pumped at ca. 0.8 MPa; (b) collect the protein peak, letting the remainder flow to waste; (c) lyophilize the sample, then weigh it; (d) Weigh 1 mg sample, dissolve it in 50 μl dissociation buffer (20 g/liter dodecyl sulphate, 50 ml/liter 2-mercaptoethanol, 100 ml/liter glycerol, 50 mM cyclohexylamine sulfonic acid) and then perform a protein assay. In gels to be silver-stained, 20–30 μg total protein suffice for a 2-D map. Unprocessed human urines have been directly analyzed by Marshall et al. (1985), who could detect > 600 polypeptide spots, but with a poorer resolution than with a desalted sample. Marshall and Williams (1986) have also obtained satisfactory 2-D maps of untreated CSF and amniotic fluid.

Similar methods can be used for other body fluids, except that the desalting step is usually omitted. Salivary proteins have been processed by dialysis and concentration in a centrifuge (Rubin and Penneys, 1983). Other means for sample concentration include a Minicon concentrator (Amicon Ltd.) (Marshall et al., 1985) or precipitation with acetone (Dunn and Burghes, 1986).

4.2.2. Tissue samples

Prior to 2-D PAGE a solid tissue sample is usually disrupted in presence of solubilization buffer. If the size of the tissue allows it, excess fat should be trimmed and the tissue rinsed in physiological saline, so as to remove contaminant blood which otherwise would add to the complexity of the 2-D map (Richardson et al., 1986; Gianazza et al., 1987c). During homogenization proteolytic enzymes, which are normally sequestered into lysosomes, can produce severe protein degradation; in order to minimize that, we routinely add a mixture of 20 μmol of Pepstatin A (4-aminomethylheptanoic acid, a pepsin inhibitor), 2 mmol of phenylmethylsulfonyl fluoride and 2 mmol of benzamidine (Tracy et al., 1982b). Whenever possible, to ensure homogeneity of the tissue for 2-D analysis, the tissue should be monitored by histological, histochemical and immunocytochemical analysis of frozen sections. With the advent of silver staining, it is now possible to perform 2-D PAGE on small amounts of tissue, even on single cryostat sections of frozen biopsy specimens routinely used for histological analysis. In case the tissue cannot be analyzed immediately, the best method for preserving it is to snap freeze each sample by simply immersing it in liquid nitrogen. Rapid freezing tends to be less detrimental than slow freezing, since small rather than large ice crystals form, reducing the amount of lysosome breakdown. In addition, it should be remembered that materials should be frozen to temperatures below $-50°C$ for the most satisfactory long term results, while temperatures above $-20°C$ are quite unsatisfactory for even relatively short periods of storage (avoid thus normal domestic freezers). In order to reduce oxidation, drying and 'freezer burns', samples should be kept in an airtight container with little airspace.

4.2.3. Circulating and cultured cells

A general procedure has been proposed by Neel et al. (1984) for reproducible fractionation of circulating cells. The whole blood sample is first subjected to low-speed centrifugation and the platelet-rich plasma removed. The platelets are then pelleted from the plasma by high-speed centrifugation and the plasma removed and

saved. The platelet pellet is washed with phosphate-buffered saline (PBS) and is now ready for solubilization. The remaining red and white cells are diluted with PBS to the original volume and the non-polymorphonuclear cells separated by centrifugation on Ficoll-Hypaque and recovered. The remaining mixture of polymorphonuclear cells and erythrocytes is then separated into the two cellular components by sedimentation on 3% dextran sulfate. These steps result in the isolation of five fractions: plasma, platelets, non-polymorphonuclear, polymorphonuclear and red cells. The latter fraction, if needed, can be lysed and cytosol and membranes processed separately. For cells cultured in vitro on glass or plastic substrates, the medium should be aspirated and a brief washing performed in PBS, to reduce contamination with medium proteins. The cell layer can then be scraped off with a rubber policemen (avoid the use of proteolytic enzymes to loosen the cell layer). Prior to analysis, large quantities of cells should be treated with DNAase and RNAase, since nucleic acids strongly interfere with the first dimensional IEF separation (Garrels, 1979; Bravo, 1984). In the recommended procedure, cells scraped in 20 mM Tris, pH 8.8, 2 mM $CaCl_2$ and dispersed through a narrow gauge needle are treated with 0.3% w/v SDS to solubilize the proteins. A solution of nucleases (10 × nuclease solution: 1 μl/ml DNAase I, 500 μg/ml RNAase A, 0.5 M Tris, pH 7, 50 mM $MgCl_2$) is then added and the sample left in the cold till no longer viscous. Following freeze drying the sample is resuspended in solubilization buffer and stored at −70°C. Failure to treat with nucleases results in heavy streaking from the application point, sample co-precipitation with nucleic acids and, in case of conventional IEF in CA-buffers, distortion of the pH gradient due to binding of nucleic acids to CAs (carrier ampholytes).

4.2.4. Plant tissues

Plant tissues, such as seeds (Görg et al., 1981; Westermeier et al., 1981) and membranes (Booz and Travis, 1981) can be treated just as animal tissues. However, leaf proteins, prior to 2-D analysis, must first be extracted with acetone to remove phenolic pigments (Hari, 1981).

4.3. Sample solubilization

Ideally, the sample solubilization procedure used in 2-D PAGE should result in the disruption of all non-covalently bonded protein complexes and aggregates to form a mixture of individual polypeptides. When such interactions are not completely disrupted, then proteins in a given sample can be present both in the aggregated state and as individual polypeptides. The final 2-D map could therefore be complicated by the appearance of new spots due to protein complexes. For this reason, solubility and full disaggregation are crucial factors in 2-D PAGE. The most popular solubilization procedure for 2-D runs is that of O'Farrell (1975), which uses a combination of 2% (w/v) of the non-ionic detergent Nonidet P-40 (NP-40) and 9.5 M urea. This procedure gives acceptable results for the majority of samples but not all protein complexes are fully disrupted by this mixture and it is found that not all sample proteins enter the first dimensional IEF gels. These phenomena are particularly evident for more difficult samples such as histones (Willard et al., 1979), ribosomal (O'Farrell, 1975) and membrane (Ames and Nikaido, 1976) proteins. The alternate route would be to solubilize the sample directly in SDS, since this detergent is known to have an extreme solubilizing power, unmatched by any other surfactant. However, since SDS is incompatible with the IEF run, a possible procedure would be to use SDS just in the solubilization procedure, and then perform the IEF run in a detergent compatible with the focusing process. Thus, when dealing with membrane and strongly hydrophobic proteins, it has been suggested to initially solubilize the sample in SDS, followed by dilution in 9.5 M urea, 2% CA, 5% 2-mercaptoethanol and 8% (w/v) NP-40 (Ames and Nikaido, 1976). The ratios of SDS to proteins (1:3) and of SDS to NP-40 (1:8) should be carefully controlled to achieve effective solubilization while minimizing the effects of high levels of SDS on the IEF dimension. The method is based on a competition effect where it is assumed that the lower critical micelle concentration (CMC) of NP-40 compared to SDS and the increased CMC due to urea leads to removal of SDS from the proteins. In the case in which the sample is first solubilized in SDS, it has been suggested that it should be applied to the IEF gel

at the anodic, rather than at the cathodic side, so as to minimize exposure of the entire pH gradient to the released SDS micelles (which would have to migrate through the entire gel length, if applied at the cathode). Migration of SDS through a carrier-ampholyte-generated pH gradient is quite deleterious, since SDS forms mixed micelles with the CA buffers (especially the more alkaline, slightly more hydrophobic species) and depletes the alkaline region of the gradient, in general seriously distorting the pH interval. However, also anodic sample application has its problems, since some SDS-protein micelles, before disruption and detergent exchange with the NP-40 in the gel, could migrate to the anode and be adsorbed by the anodic filter paper strip (in addition, exposure to a harsh acidic environment could result in irreversible protein precipitation). As an alternative to the above, the order of the two dimensions could be reversed, i.e., SDS gels could be used for the first dimension, followed by IEF in a flat bed gel containing 8 M urea and non-ionic detergent (Singer et al., 1978; Siemankowsky et al., 1978; Tuszyncki et al., 1979; Shackelford and Strominger, 1980; Shackelford et al., 1981). However, both systems (SDS solubilization followed by a direct IEF run or by a direct SDS-PAGE) have never become popular, the reason being that it is never guaranteed that, once the proteins have been solubilized by the SDS treatment, they will not become insoluble again once subjected to subsequent procedures not using SDS. A digression on the properties of the many detergents available is thus imperative, so as to offer to the readers a view of the alternatives available in sample solubilization.

4.4. Choice of detergent

Note: the term 'detergent', as commonly used in the field of biochemistry, is a misnomer. All detergents used in the biochemical literature are in fact 'surfactants' (Zeman, 1988). The difference between the term 'surfactant' (or surface active agent) and the term 'detergent' is clearly explained in the Draft International Standard ISO/DIS 862 as follows:

Detergent
A product specially formulated for cleaning through the process of detergency. It comprises a number of components, e.g., surface active agents and additives (builders, etc.).

Surface active agent
A chemical compound including in its molecules at least one group with affinity for polar surfaces, ensuring dissolution in water, and a non-polar group, which has little affinity for water. After dissolution in a liquid, a surfactant lowers the surface tension or interfacial tension by positive adsorption at the liquid-vapour surface or other surfaces.

It is clear from the above that, as no one of us is specially interested in laundering, what we really mean with the term 'detergent' is in fact 'surfactant'. Having cleared the grounds, I will keep sinning like everybody else and stick to the term 'detergent', which I am afraid is here to stay. A large number of detergents are available and hundreds of them have been used in biochemical studies (Helenius and Simons, 1975; Helenius et al., 1979). Some of the chemical and physical properties of those commonly used are presented in Tables 4.3 and 4.4 (Johnstone and Thorpe, 1982). In general, commercially available detergents are chemically impure, especially non-ionic ones. They contain water and other contaminants that vary between batches. After prolonged storage of liquid detergents the composition may vary in different parts of the container. In addition, the chain length of both the hydrophobic and polyoxyethylene portions of the molecule is heterogeneous. Thus, the structure given by the manufacturer and presented in Table 4.3 represents the majority but not all of the molecules.

Ionic detergents (e.g., SDS) tend to denature proteins by destroying their secondary, tertiary and quaternary structure, although in some cases (e.g., antibodies) some activity is retained in low concentration (les than 0.1% SDS). Non-ionic and mildly ionic detergents are less denaturing and can be used to remove a protein from a membrane whilst preserving protein–protein interactions. For example, solubilization of lymphocytes in NP-40 (non-ionic) or plasma membranes in deoxycholate (mildly ionic) releases histocompatibility antigens (HLA in humans) as two polypeptide chains

TABLE 4.3
Structure of some common detergents. Modified from Helenius & Simons (1975) with permission.

Structural formula	Chemical name	Examples of trade names
	*Anionic detergents* Sodium dodecylsulphate	
	*Cationic detergents* Cetyltrimethylammonium bromide	
	Tetradecylammonium bromide	
	*Non-ionic surfactants* Polyoxyethylene isoalcohol	Brij series, Lubrol W, AL series
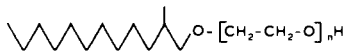	Polyoxyethylene isoalcohol	Sterox AJ, AP series Emulphogen BC series Renex 30 series
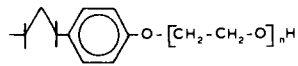	Polyoxyethyelene-*p*-*t*-octyl phenol	Triton X series Igepal CA series Nonidet P 40
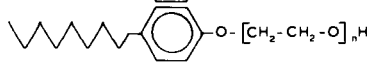	Polyoxyethylene esters of fatty acids	Sterox CO series Myrj series Span series
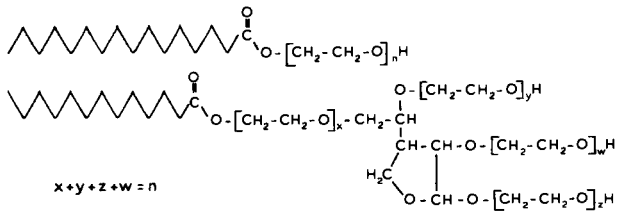	Polyoxyethylene esters of fatty acids	Sterox CO series Myrj series Span series
	Polyoxyethylene sorbitol esters [1]	Tween series Emasol series

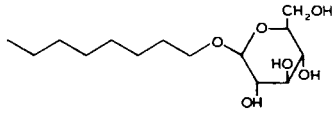

β-D-octylglucoside

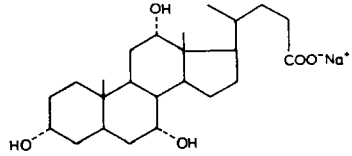

Bile salts
Sodium cholate
(trihydroxy bile salt)

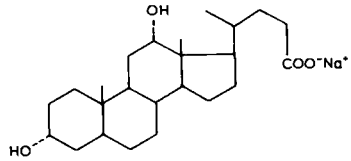

Sodium deoxycholate

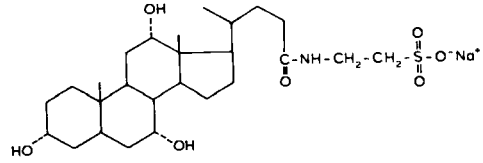

Sodium taurocholate

[1] The formula shown is just one molecular type in a complex mixture of different possible structures, n = average number of ethylene oxide units per molecule.

still held together by non-covalent forces. In addition, the protein detergent micelle is recognized by antibodies directed against the antigens. Several additional factors influence the choice of detergent, as listed below.

4.4.1. Material to be solubilized

An isolated membrane can be solubilized by most detergents. However, with whole nucleated cells it is often desirable to keep the nucleus intact to avoid the problems associated with release of DNA (severe streaks in 2-D maps). This can be accomplished by the use of some polyoxyethylene detergents (e.g., NP-40, Triton X-100, Renex 30) under carefully controlled conditions (e.g., disaggregation of plasma membrane in the cold, in PBS, in 0.5% detergent in the absence of urea, for a short period of time). Some proteins are not solubilized by certain detergents. A useful criterion for solubility is a high yield of a given protein in the supernatant, as measured after centrifugation at 100,000 *g* for 30 min.

4.4.2. Detergent properties detrimental to subsequent procedures

(a) Octyl and nonyl phenol detergents (e.g., Triton X-100 and NP-40) have a high absorbance at 280 nm and hence interfere with protein monitoring during chromatographic elutions. They also induce precipitation in the Lowry et al. (1951) protein assay; they interfere less with the Bradford (1976) assay. (b) Octyl and nonyl phenol detergents are also easily iodinated and therefore should not be present during radioiodination of proteins. In addition, impurities of many other detergents can be iodinated (e.g., any unsaturated alkyl chains). (c) Many detergents have a very high micellar mass (Table 4.4). This makes gel filtration impossible because the variation in proteins size is usually insignificant when compared with the size of the micelle. Also removal of such detergents by dialysis is extremely slow because only the monomers can diffuse out of the dialysis sac, and the concentration of these (i.e., the critical micellar concentration) is usually very low. (d) The solubility of sodium cholate and deoxycholate decreases dramati-

TABLE 4.4
Properties of some common detergents [1]. Modified from Helenius & Simons (1975) with permission.

Detergent	Commercial name	Aggregation number	Micellar mass ($\times 10^{-3}$)	Critical micelle concentration (mM)
Sodium dodecylsulphate (in H_2O)		62	18	8.2
Sodium dodecylsulphate (in 0.5 M NaCl)		126	36	0.52
Tetradecyltrimethyl ammonium chloride		64	19	4.5
Cetyltrimethyl ammonium bromide		169	62	0.92
POG(4,5) *p-t*-octylphenol [2]	Triton X-45			0.11
POG(7–8) *p-t*-octylphenol	Triton X-114			0.20
POG(10)stearyl alcohol	Brij 76			0.03
POG(10)oleyl alcohol	Brij 96			< 0.04
POG(10)cetyl alcohol	Brij 56			0.002
POG(9) *p-t*-octylphenol	Nonidet P40			0.29
POG(9–10) *p-t*-octylphenol	Triton X-100	140	90	0.24
POG(9–10) nonylphenol	Triton N-101			0.085
POG(10) nonylphenol		100	66	00.75
POG(10) tridecyl alcohol		88	56	0.125
POG(12–13) *p-t*-octyl-phenol	Triton X-102			0.3–0.4
POG(14) stearyl alcohol		370	330	0.06
POG(16) *p-t*-octylphenol	Triton X-165			0.43
POG(17) cetyl-stearyl alcohol	Lubrol WX			0.02–0.06
POG(20) sorbitol mono-stearate	Tween 60			0.025
POG(20) sorbitol mono-oleate	Tween 80	60	50–76	0.012
POG(20) sorbitol mono-palmitate	Tween 40			0.027
POG(20) sorbitan mono-laurate	Tween 20			0.059
POG(20) cetyl alcohol	Brij 58			0.077
POG(29) oleyl alcohol	Brij 98			0.025
POG(40) *p-t*-octylphenol	Triton X-405			0.810
β-D-octylglucoside				25
Sodium cholate [3]		2–4	0.9–1.8	13–15
Sodium deoxycholate [3]		4–10	1.7–4.2	4–6
Sodium taurocholate [3]		4	2.2	10–15

[1] Measured at 20–25°C
[2] POG, polyoxyethyleneglycol
[3] pH > 8; ionic strength < 10 mM

cally below pH 7.5 (thus their use in IEF is not recommended) or above an ionic strength of 0.1.

4.4.3. New classes of detergents

It is known that, among the zwitterionic detergents compatible with IEF, linear sulfobetaines have outstanding solubilizing properties (Navarrete and Serrano, 1983; Satta et al., 1984). However, they are not compatible with high levels of urea (they are precipitated in presence of > 4 M urea) and, when used alone, have a poorer performance than the classical urea-NP-40 mix (O'Farrell, 1975). Therefore Gianazza et al. (1987a) and Rabilloud et al. (1988b) have proposed a series of new detergents, having the main features of classical sulfobetaines (SB), i.e., a linear hydrophobic tail and a zwitterionic polar head, but with a hydrophilic amido spacer in order to improve the solubility and thus the urea compatibility. The overall synthetic process is shown in the reaction scheme of Fig. 4.1. The synthesis takes place in two steps, starting from commercial fatty acids. The fatty acids are first reacted with *N*,*N*-dimethyl-1,3-propanediamine to give an amido amine (labelled A in Fig. 4.1). Compound A is then reacted with various reagents to build the polar head. Three different reagents are used, yielding three different series of detergents, according to the scheme in Fig. 4.1. By reaction with propan sultone, the C-series is obtained; with Na 3-chloro 2-hydroxy propanesulfonate the O-series is produced; finally, by reaction with butane sultone, the B-series is generated. Each detergent is therefore labelled C*n*-*X*, where n is the number of C atoms of the starting fatty acid ($n = 10$ to 14) and X is the letter specifying the type of polar head ($X =$ B, C or O). The performances of these detergents, as compared with NP-40, sulfobetaine 3–12 and CHAPS, are given in Table 4.5. It is seen that the best compromise between urea compatibility and solubilization performance stands for an alkyl length of 11–12 C-atoms, depending on the polar head. In turn, it appears that short polar heads (C and O series) result in better intrinsic solubilization than long polar heads (B series). In addition, for short alkyl tails (10 C atoms) both the urea tolerance and solubilization performance resemble closely those of CHAPS.

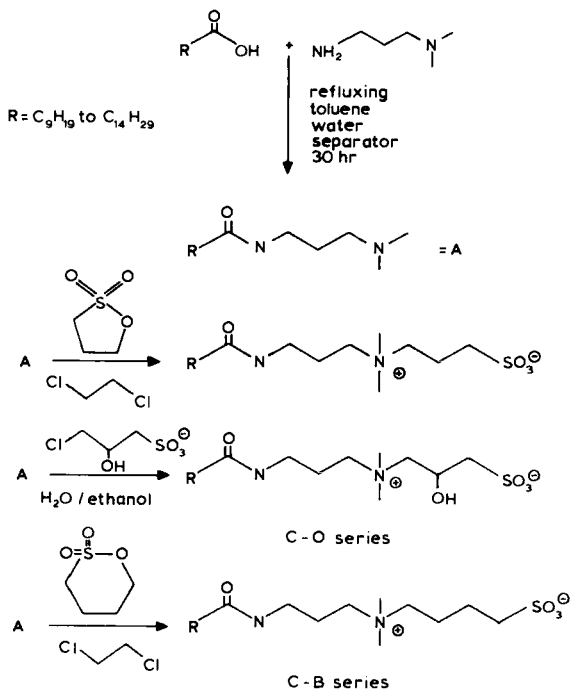

Fig. 4.1. Synthesis of new surfactants. Upper: fatty acids (R-OOH) are reacted with *N,N*-dimethyl 1,3-propanediamine to form an amido amine (A). Compound A is reacted: (I) with propan sultone to produce the C-series; (II) with Na 3-chloro 2-hydroxy propanesulfonate to generate the C-O series and (III) with butane sultone to give the C-B-series (from Rabilloud et al., 1988b; by permission from VCH).

The synthesis of these new detergents has been made possible by some rules-of-thumb known in the field of surfactants. Among them stands the fact that the solubilizing and denaturing powers of a detergent increase with the increasing flexibility and length of the hydrophobic part, and with the increasing polar properties of the polar head. For example, SDS, sarkosyl and SB_{3-14}, which have long, flexible linear alkyl tails and very polar heads are strongly denaturing, whereas Brij (linear alkyl tail but weakly polar head) and taurocholate (non-flexible hydrophobic tail but strongly polar head) are weakly denaturing. Thus, a good denaturing detergent for IEF should combine a very polar but electrically neutral head with

TABLE 4.5
Main features of amidosulfobetaines

Detergent	Urea compatibility		Intrinsic solubilizing power	Electrophoretic efficiency
	at 20°C	at 15°C		
NP-40	9.5 M	9.0 M	91.4	+ +
CHAPS	9.5 M	9.0 M	93.5	−
SB 3-12	4.5 M	< 4 M	96.5	+ + +
C10-C	9.5 M	8.5 M	95.0	−
C12-C	8.5 M	8.0 M	97.0	+ + +
C10-O	9.5 M	8.5 M	93.0	−
C11-O	9.5 M	8.5 M	97.0	+ + +
C12-O	9.5 M	8.5 M	97.0	+
C10-B	9.5 M	8.5 M	82.5	+
C11-B	9.5 M	8.0 M	95.0	+
C12-B	9.5 M	8.0 M	47.0	+ + +

All the data given herein are for 2% solutions of the detergents. The solubilization efficiencies are expressed in percentage of the solubilization achieved by 5% SDS in 0.5 N NaOH. When the detergents have been used in combination with urea, the urea concentration (in M) is indicated in parentheses. The electrophoretic efficiency is defined by the amount of spot A properly focused in the gel and is only estimated.

a long, flexible and linear alkyl tail. The latter introduces an important drawback when urea is required, because linear alkyl compounds are known to form inclusion complexes with urea, which tend to precipitate out of solution, unless the compound is sufficiently hydrophilic (e.g., SDS). Normal sulfobetaines are prone to this phenomenon, and thus cannot be used with urea, whereas the detergents presented in Fig. 4.1 have a sufficiently hydrophilic part to prevent urea precipitation. Among the new detergents, also worth special mention is dodecyl maltoside, which, in combination with SDS, has been proposed in 2-D separations of chloroplast thylakoid membrane proteins (Bass and Bricker, 1988).

4.5. Radiolabelling techniques

In cell culture studies, radiolabelling is still the preferred route for high sensitivity detection of proteins after a 2-D PAGE analysis.

Addition of ^{125}I is one of the most common methods for labelling soluble proteins, because the isotope is cheap and easily detected, and it is possible to obtain preparations of high specific activity. For labelling phosphoproteins, a 'hard' beta emitter (^{32}P) is used, while for total cell proteins in cultures often ^{35}S-Met is adopted. I shall review here some of the widely employed techniques.

4.5.1. Radioiodination

$Na^{125}I$ is a cheap radioisotope than can be obtained with very high specific activity (carrier free, ca. 2000 Ci/matom) and used to radiolabel both soluble proteins and cells. Labelling occurs by electrophilic addition of cationic iodine (I^+) to Tyr residues (Fig. 4.2) and to a lesser extent to His and Trp. The monoiodinated derivative is the major product under the conditions normally used. Alternatively, a small radioiodinated molecule can be conjugated to the protein, usually through the epsilon amino group of Lys (Fig. 4.3). In Fig. 4.3, pathway (a) shows the labelling route of Bolton and Hunter (1973), while scheme (b) shows different iodination protocols, as devised by Sears et al. (1971), Johnstone and Crumpton (1979) and by Hayes and Goldstein (1975). Iodinated proteins, especially with high specific activity, should be analyzed rapidly, since they tend to deteriorate due to several factors: (a) *Radiation destruction*. The products of radioactive decay of ^{125}I can cause

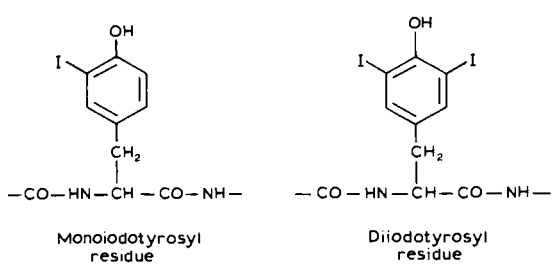

Fig. 4.2. Structure of iodinated Tyr residues in a polypeptide. Under the conditions normally used for radioiodination, though, the mono-iodinated derivative predominates (from Johnstone and Thorpe, 1982; with permission from Blackwell Sci. Publ.).

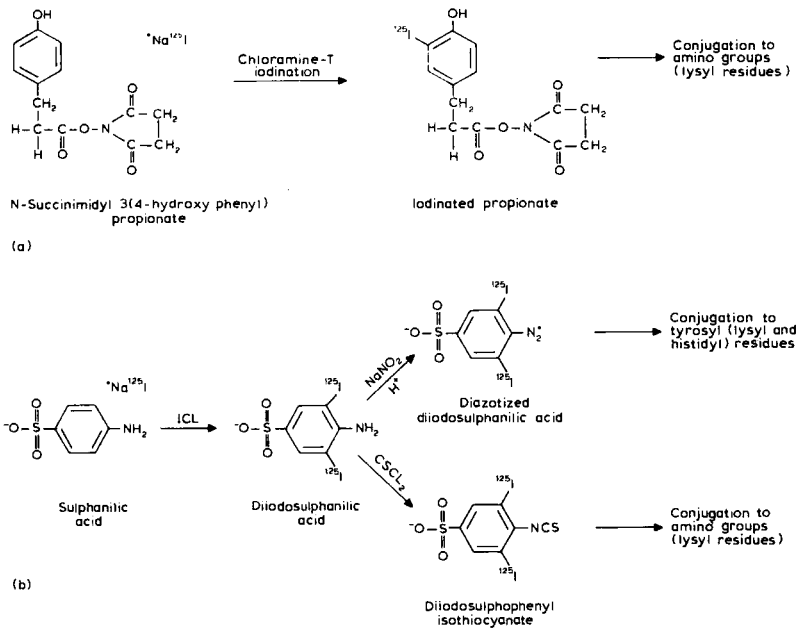

Fig. 4.3. Conjugation methods for radioiodinating proteins. (a) With *N*-succinimidyl 3-(4-hydroxy 5-[^{125}I]-iodophenyl)propionate. (b) With diazo or isothiocyanate derivatives of iodinated sulphanilic acid or aniline. In both cases, the final step is conjugation to amino groups (Lys, His) or to Tyr (from Johnstone and Thorpe, 1982; with permission from Blackwell Sci. Publ.).

damage to the protein. (b) *Loss of iodine*. Iodinated proteins tend to break down to yield free radioiodine and unlabelled protein. (c) *Protein deterioration*. Some proteins tend to aggregate and precipitate upon iodination and subsequent storage. These problems are aggravated in dilute protein solutions, so that often unlabelled carrier protein is added (e.g., 1 mg/ml albumin). Freezing aliquots rapidly and storing at $-70°C$ reduce somewhat the problems.

There are several established methods for radioiodination. The chloramine T method (Greenwood et al., 1963) is used to label soluble proteins to high specific activity. The reaction is virtually instantaneous and the time of contact between the protein and the potentially harmful oxidizing agent should be kept to a minimum. Alternatively, iodogen (1,3,4,6-tetrachloro-3a,6a-diphenylglyco-

luril), a milder oxidizing agent, can be used (Fraker and Speck, 1978). This reagent is practically insoluble in aqueous solutions and the iodination procedes by a solid phase mechanism that damages the protein less, but the reaction is much slower. Iodination via lactoperoxidase (Hubbard and Cohn, 1976) is the mildest procedure available, although it is difficult to obtain preparations with high specific activity. Its major use has been in surface labelling intact cells for structural studies. The enzyme binds all three reactants: $^{125}I^-$, H_2O_2 and Tyr and so, in theory, is the ideal reagent for controlled localized iodination. However, both $^{125}I^+$ and $^{125}I_2$ can be released from the enzyme and diffuse across the membrane. In addition endogeneous cytoplasmic peroxidases can catalyze the iodination of internal Tyr by added $^{125}I^-$ and H_2O_2, both of which are permeant, so that pure cell surface labelling is not quite guaranteed.

4.5.2. Radiolabelling glycoproteins and glycolipids

Carbohydrate residues in proteins can be oxidized under mild conditions to form aldehyde groups which can then be radioactively labelled. Two major reaction schemes are illustrated in Fig. 4.4. The first step involves periodate oxidation of sialic acid (route a) or oxidation of terminal galactose (scheme b). The second step is

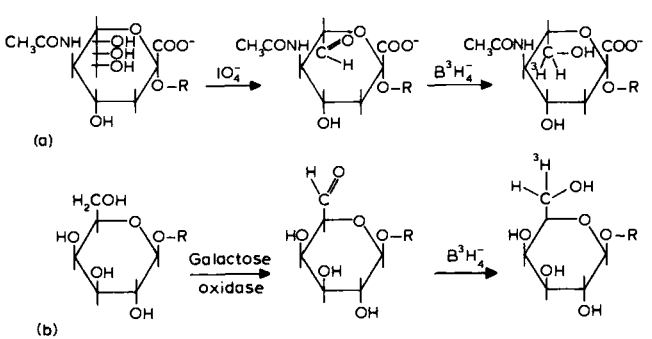

Fig. 4.4. Radiolabelling carbohydrates by oxidation of (a) *N*-acetyl-neuraminic acid (sialic acid) or (b) galactose. In both cases, tritium is introduced by reduction of the aldehyde group back to an alcohol with $NaB[^3H]_4$ (from Johnstone and Thorpe, 1982; with permission from Blackwell Sci. Publ.).

identical in both pathways, and consists in reduction of the aldehyde back to an alcohol by using $NaB[^3H]_4$ to incorporate a tritium label. In the case of scheme (a), low concentrations of Na periodate at neutral pH cleave the alkyl chain of sialic acid between vicinal hydroxyls to generate an aldehyde group which can then be reductively labelled (Gahmberg and Andersson, 1977). The reaction appears to be specific for sialic acid; a higher concentration of periodate ion (45 mM) at a lower pH (in 7% acetic acid) will cleave between vicinal hydroxyls in other sugar groups. In the case of scheme b, galactose oxidase catalyzes the oxidation of the primary hydroxyl group of terminal galactose and *N*-acetylgalactosaminyl residues to generate an aldehyde group which can then be reductively radiolabelled. Neuraminidase is usually also added to remove sialic acid and generate extra terminal galactose residues from the common carbohydrate structure: –Gal–NANA (Gahmberg, 1976).

4.5.3. Biosynthetic labelling

Viable cells in culture will incorporate added radiolabelled precursors into the macromolecules they synthesize. This technique is useful in various metabolic studies, in confirming that a molecule of interest is manufactured by a cell and not passively acquired and in labelling many cellular constituents which are not easily labelled by other procedures (e.g., lipids, internal proteins). Added [^{14}C]acetate and [^{14}C]glucose will label many different macromolecules. Radiolabelling of proteins with mixtures of ^{14}C labelled-amino acids (Bravo and Celis, 1982) has the advantage that multiple amino acids will be incorporated; therefore, any protein deficient in one or more amino acid will still be detected. Theoretically, this method is more optimal for protein quantitation, but in reality, it is generally more time consuming due to the lower specific activity of ^{3}H- or ^{14}C labelled-amino acids. It should be noted that essential amino acids for cells from higher animals (i.e., Leu Ile, Val, Lys, Phe, Trp, Thr, Arg and Met) are incorporated to a greater extent. It seems, however, that the preferred route for radiolabelling is with [^{35}S]Met, when analysis of the synthesis of protein products is carried out by 2-D PAGE (Dunbar, 1987). The reason is that the

high specific activity of this labelled amino acid makes this a sensitive protein detection method and permits reasonably short exposures to autoradiographic films (see Chapter 3, §3.9.4). It should be noted, however, that most commercial preparations of [^{35}S]Met contain dithiothreitol, or 2-mercaptoethanol in order to prevent oxidation of Met to methione sulfoxide, which will not function as a precursor in protein synthesis. Since such reducing agents can greatly alter viability or function of some cell populations, care should be exercised to remove or dilute these reagents before labelling. The major disadvantage of this method is that the detection or quantification of proteins is dependent on the incorporation of a single radiolabelled amino acid precursor. An excellent review and detailed methods for labelling of proteins for use in radiochemical sequence analysis has been outlined by Coligan et al. (1983). Essentially three methods are used for in vivo labelling: (a) *Equilibrium labelling*. Cells or tissue are incubated with large amounts of radioactive material for long time periods, till constant specific activity is reached. (b) *Pulse labelling*. This is used to monitor the rate of synthesis of a given macromolecule (or of a class of proteins) and is carried out by adding the radiolabelled amino acid precursor at varying times throughout an experiment. As the duration of the labelling period decreases to zero, the observed rate of synthesis will approach the true instantaneous rate of synthesis (Cooper, 1977). (c) *Pulse-chase labelling*. This is a variation of the pulse-labelling method, in that the radioactive label is removed and replaced with 500- to 1000-fold of the non-radioactive amino acid. The culture is then sampled at various times after removal of the radiolabelled precursor. This method is used to obtain information on precursor–product relationships.

4.5.4. Post-synthetic labelling

It is clear that all the methods of radio-isotope labelling reported above (except for §4.5.3, where it is done in vivo) are post-synthetic labelling. However, it should be remembered that such post-synthetic radiolabelling procedures, particularly iodination, can introduce charge heterogeneity (Kuhn and Wilt, 1980; Dunn and Burghes, 1983), which will be resolved by the IEF dimension. An

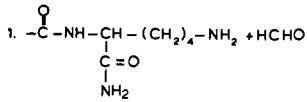

Formaldehyde reacts with amino group to form Schiff's base

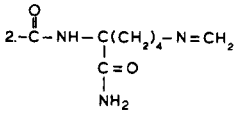

Schiff's base is reduced with $NaBH_4^*$ (*N*-[^{3}H]-methyl derivative of sodium borohydride)

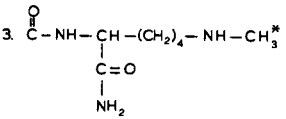

Fig. 4.5. Diagram of the procedure using sodium borohydride (^{3}H) and formaldehyde in the reductive methylation of free amino groups reaction for labelling proteins. adiolabelled group (from Dunbar, 1987; with permission from Plenum Press).

interesting method is the reductive methylation of free amino groups in proteins, as reported by Biocca et al. (1978). The scheme of this reaction is given in Fig. 4.5: here again, like in the case of carbohydrates, tritium is introduced at the end of the procedure by reducing the Schiff base with $NaB[^3H]_4$. It might be argued that this procedure too will introduce charge heterogeneity (no chemical reaction ever goes to 100%), which is anathema for any IEF procedure. This is certainly so, but the novelty of this approach is that Rabilloud et al. (1986) have proposed this radiolabelling procedure at the very end of both dimensions, so that no artefactual polypeptide spots are introduced in the 2-D map. This is a general aspect of labelling techniques, valid also for all the fluorescent tags mentioned in Chapter 3 (§3.9.2). Clearly, no one of these tags (dansyl chloride, MDPF and the like) can be used as pre-labelling, due to the large number of heterogeneous spots generated and resolved during the IEF step, but in fact there is no counter-indication to their use after the IEF dimension; e.g., Jackson et al. (1988) have successfully proposed labelling with MDPF just at the end of the IEF dimension, prior to the SDS-PAGE step.

Thus, all these labels can be introduced in two ways: (a) just in between the IEF and the SDS dimensions (best prior to incubation in the SDS denaturing solution) or (b) at the end of the SDS-PAGE run, just like the reductive methylation or any other staining procedure.

4.6. The first (IPG) dimension

I will briefly reiterate some fundamental parameters of the IPG technique, pertaining to the 2-D methodology. All the recipes for any narrow or extended IPG interval are found in Chapter 2 Tables 2.2 to 2.9. In addition, rules have been given for interpolating any narrower IPG gradient from any wider one (see §2.2.6). For all manipulations concerning IPG gel casting, washing, drying and re-swelling, the reader is referred to Chapter 3 (in particular §3.3 and 3.4).

4.6.1. The gel matrix

It should be emphasized that, since in 2-D maps often highly heterogeneous samples are run (entire cell lysates, total tissue extracts and the like), there is a good chance that most samples will contain a number of very large proteins, which will focus very slowly or even might not be able to enter the gel. It is imperative for 2-D maps that only highly diluted gels are used. In preparative runs, we have described experiments in polyacrylamide matrices as diluted as 2.8% *T* (Righetti and Gelfi, 1984). LKB now sells pre-cast IPG gels of 4% *T*; I suggest that 3% *T* be routinely used. Such gels, when cast onto a Gel-Bond PAG foil, have dimensional stability and can be handled quite safely. At the moment, there is no valid alternative to the classical couple acrylamide-Bis. A good cross-linker is DHEBA, which is highly hydrophilic (Gelfi and Righetti, 1981a and b), but it is prone to hydrolysis at alkaline pH values, so that no strong base should be use as catholyte. Unfortunately, highly cross-linked gels (50–60% *T*), which have an enormous pore size (up to 5–600 nm diam.) cannot be used because they are mechanical unstable and rather hydrophobic

(Bianchi-Bosisio et al., 1980; Righetti et al., 1981; Righetti, 1981). In addition, it seems that Immobilines are not efficiently incorporated into highly cross-linked gels (Righetti, 1984).

4.6.2. Additives

The IEF dimension of high-resolution 2-D PAGE is carried out under denaturing conditions, with both 8 M urea and non-ionic (e.g., NP-40) or zwitterionic (e.g., sulfobetaines, CHAPS) detergent present in the gel. We have given in §4.4 a whole list of detergents to be used. An extensive list of denaturants can be found also in Gordon and Jencks (1963). Tetramethyl- and dimethyl-urea have been used successfully for solubilization of myelin and oligodendroglial proteins prior to 2-D PAGE (Althaus et al., 1983). A combination of urea and n-butyl urea has been used as a denaturant for the analysis of membrane proteins (Steinfeld and Vidaver, 1981). As IPG gels are routinely washed, the best procedure is to polymerize an 'empty' gel, process it through the standard steps (3×500 ml washes), dry it and then re-swell it in the denaturing mixture of choice. Since detergent micelles diffuse rather slowly into the matrix, a suggestion is to let re-swelling proceed overnight (Gelfi and Righetti, 1984). In the original O'Farrell (1975) procedure, the detergent is used at 2% concentration in the IEF gel; however, it seems to be best to reduce the concentration of surfactant, in IPG gels, to 0.5% (while keeping the high level in sample solubilization, though!) (Görg et al., 1987a,b); this considerably reduces sample streaking in the SDS-PAGE.

4.6.3. The IPG gradient. Addition of carrier ampholytes (CA)

As mentioned in Chapter 2 (§2.3.4) the pH slope might need to be altered in pH regions that are overcrowded with proteins. Since, when running 2-D maps of cell lysates or, in general, of complex samples, at least 2/3 of the proteins will focus in the acidic portion of the pH gradient (pH < 7), it is clear that an optimally resolving pH gradient should have a gentler slope in the acidic portion and a steeper course in the alkaline region. Thus, the best results in 2-D maps of complex samples will be obtained with non-linear pH

gradients. Table 2.6 gives such a recipe for a pH 4–10 IPG interval. The next question to be addressed is the optimal total molarity of Immobilines in the IPG gel. It is now generally agreed that, for 2-D maps, the lower is the amount of Immobilines in the gel, the better is the transfer from the IEF to the SDS dimension. This is due to the fact that, in the pI zone, proteins form a salt with the surrounding IPG matrix (Gelfi et al., 1987a) and this could hamper the transfer to the second dimension. In routine IPG analysis, an average buffering power (β) of 3 mequiv.l^{-1} pH^{-1} is generally accepted. When IPGs have to be used in 2-D maps, however, this amount can be lowered to as little as $\beta_{av} = 1$ mequiv.l^{-1} pH^{-1} (Gianazza et al., 1987c), without detrimental effects to the IPG run. A second important question to answer is if and when to add also carrier ampholytes (CA). In principle, adding CAs to an IPG gel can have some disadvantages with respect to equilibrium IEF: e.g., with prolonged focusing time the pattern deteriorates due to liquid exudation (Astrua-Testori and Righetti, 1987) and some electrosmosis is induced. This is a question that cannot have a general answer, since it appears to vary from sample to sample: thus, according to Görg et al. (1988a) yeast cell proteins needed CAs in the first dimension, for better resolution, whereas plant proteins from legume seeds or leaf and stem proteins from barley could be successfully fractionated in the absence of CAs. In any event, it is clear that added CAs should be kept to a minimum, the lowest amount being 0.5%. Moreover, Pharmalytes should be used, as they have the smoothest distribution of species along the pH gradient (see Fig. 4.6).

4.6.4. Sample application

When IEF is performed in IPGs, large sample volumes can be applied at time intervals during the run, without disturbing the pH gradient or the final IEF pattern. Preferably the sample should be applied not in pockets precast in the gel, but on the gel surface, by using different methods for sample containement. Sample applicator strips have been described in Chapter 3 (see Figs. 3.13 and 3.14): it should be emphasized that with applicator strips containing funnel-shaped slots, large sample volumes (up to 100 μl) can be

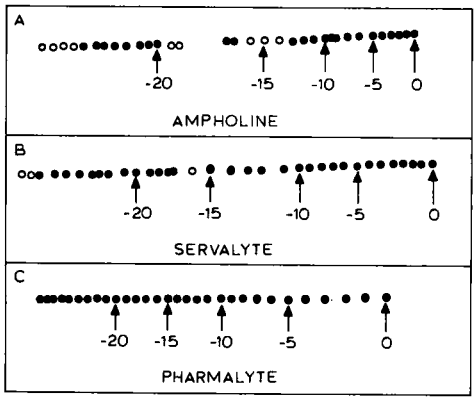

Fig. 4.6. Sections from 2-D gels of human peripheral lymphocytes co-electrophoresed with creatine kinase carbamylation train standards and stained with Coomassie Blue. A: LKB Ampholine pH 3.5–10; B: Servalyte ISO-DALT grade pH 3–10; C: Pharmalyte pH 3–10. 'Zero' represents the unmodified protein; the negative numbers refer to progressively blocked $-NH_2$ residues, originating new spots in the carbamylation train. Solid circles: well-stained protein spots; open circles: fading spots (modified from Tollaksen et al., 1981).

applied at once. Alternatively, Ultrodex can be re-swollen directly into the sample and then this suspension added as such to the gel surface. A typical geometry for an IPG run to be used as first dimension in 2-D maps is given in Fig. 4.7. Two important considerations are:

(a) *Sample viscosity*. For samples, like sera, containing a rather high protein concentration, improved entry is obtained by sample dilution (by a factor of at least 1:1) (Gianazza et al., 1985d);

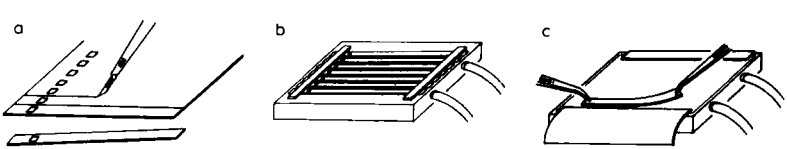

Fig. 4.7. IEF in individual IPG gel strips on Gel Bond PAG film. Strips were cut from the washed and dried IPG gel or ready-made IPG dry plates, rehydrated and placed on the cooling block of the electrophoresis chamber. Sample solution is pipetted into a silicone rubber frame (from Görg et al., 1988b; with permission from VCH).

(b) *Sample application site.* By far, the best application zone for sample in 2-D maps is at the anodic gel side (e.g., 5 mm from the anode) (Gianazza et al., 1985d). This has been found to result in much less sample streaking as compared with cathodic sample application, possibly also due to the higher hydro-

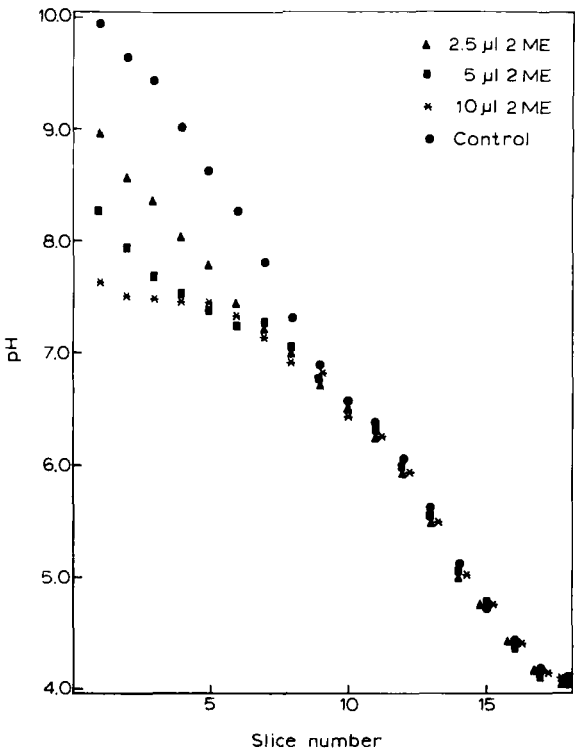

Fig. 4.8. Effect of 2-ME on pH gradients in CA-IEF. 5% *T*, 4% *C* gel tubes were cast to contain 8 M urea, 2% NP-40, 1 mg each of Asp, Lys and Arg and the following Ampholines: 1.6% pH 3.5–10, 0.2% pH 3.5–5 and 0.2% pH 8–10. IEF was run vertically in gel tubes for a total of 5000 V×h at 10°C with 20 mM H_3PO_4 as anolyte and 20 mM NaOH as catholyte. The gels were loaded at the cathodic end with a solution containing 8 M urea, 2% NP-40 and 5% 2-ME but no protein. 50, 100 and 200 µl of this mixture were applied to duplicate gel tubes, corresponding to 2.5, 5 and 10 µl of pure, undilute 2-ME. Note the devastating effects of the thiol compound on the pH gradient (from Righetti et al., 1982; with permission from Elsevier).

phobicity of alkaline pH gradients (Righetti et al., 1987c) and to CO_2 absorption at the cathodic end. There is another important, but often overlooked, reason for anodic sample application: the presence of as much as 5% 2-mercaptoethanol (2-ME). As demonstrated long ago (Righetti et al., 1982), any –S–S– reducing agent is a buffer (pK ca. 9.5 which ionizes by forming an anion) and thus will keep migrating inside the pH gradient and be arrested, by protonation, around pH 7. A steady-state distribution of 2-ME will therefore ensue, which will disrupt a conventional IEF run (see Fig. 4.8). A pH 3–10 gradient can be reduced by as much as 2.5 pH units: this is the real cause of the impossibility, lamented by users of 2-D maps, of obtaining CA-IEF gradients above pH 7.5 (O'Farrell et al., 1977). The situation is ameliorated in IPGs, since 2-ME cannot disrupt the pH gradient. However, due to the impossibility of eliminating 2-ME, the final slope will be altered, since it is like introducing a new Immobiline in the IPG recipe. On the contrary, by adding the sample at the anodic side, no deleterious effects of 2-ME will be produced because at acidic pH, 2-ME cannot buffer nor migrate. Moreover, 2-ME will also be slowly lost by evaporation.

4.6.5. Focusing conditions

As already discussed in Chapter 3 (§3.8) IPGs can stand, in principle, any amount of salt, but the protein applied to an IPG matrix cannot. In Table 3.10 I gave several hints on how to remedy the pH shock on proteins due to ion boundaries leaving the sample zone. If addition of CAs is not desired, good focusing without protein precipitation can still be obtained in presence of as much as 100 mM salt by simply focusing at low voltage gradients for the first few hours. I thus suggest starting the run at 400 V for at least 3–4 h, till all the ions have migrated from the sample zone (Righetti et al., 1988e). At this point, focusing can be continued at high voltages for as long as necessary to establish a steady-state pattern for a given sample. Here again it is quite difficult to give general rules, considering the great variety of samples which can be analyzed. However, as a general guideline, it should be remem-

bered that the combined use of urea and detergent calls for extended focusing times due to an increase of (a) viscosity of the system, (b) gel restrictivity (Gelfi and Righetti, 1981a) and (c) Stokes radius of proteins after urea denaturation (Creighton, 1979). In extended IPG intervals and in presence of low levels of CAs, focusing in IPGs is much faster, thus an overnight run is considered amply adequate for focusing even the largest proteins in the system.

4.6.6. pH gradient estimation

As mentioned in Chapter 3 (§3.5.7) it is impossible to measure pH values in IPGs either by a surface electrode or by cutting gel slices and equilibrating in 10 mM KCl, as customarily done in CA-IEF (Righetti, 1983a). However, accurate and reliable pH measurements can be obtained in mixed-bed CA-Immobiline gels, the discrepancy between the theoretical IPG slope and the actual pH values obtained by reading the pH of eluted CAs cofocusing in the same gel fragment being less than ± 0.1 pH unit over a 1 pH unit span (Righetti et al., 1986d; Gelfi et al., 1986; Rovida et al., 1986). Generally speaking, though, in narrow pH gradients (up to 1 pH unit) it is just as easy to interpolate the pI value of a focused protein simply by its position in the gel matrix, assuming a linear pH course between the two gel extremities. In this case, the pI value can be given with an accuracy of two decimal digits. In wide pH intervals, as customary in 2-D maps, in addition to direct interpolation on the theoretical IPG gradient curve, one can use, as standards, components of the sample itself (e.g., actin, tubulin, tropomyosin, vimentin and lactate dehydrogenase) (Bravo, 1984; Bravo and Celis, 1982), or purified proteins added to the sample to be analyzed (Peters and Comings, 1980). Most commercial pI marker kits are not suitable as landmarks in a 2-D map as they often contain oligomeric proteins which would dissociate in the 2-D denaturing media, producing spots of unknown pI and M_r values. Thus, the best method currently available for calibrating pH gradients in the IPG dimension is the use of carbamylated charge standards (Anderson and Hickman, 1979; Hickman et al., 1980; Tollaksen et al., 1981). These are generated by heating a

suitable protein in 8 M urea for varying lengths of time. The sequential loss of free amino groups below pH 8.5, resulting in unit charge changes, produces in 2-D maps a horizontal row or train of spots of constant mass and spaced apart by ca. 0.1 pH unit. The length of this train depends on the protein amino acid composition, so that β-globin chains form 12 spots, carbonic anhydrase 20 spots, and creatine phosphokinase 30 or more spots. Commercial preparations of such standards are now available as Carbamylyte (Pharmacia); they are: carbonic anhydrase (20 spots, pI 4.8 to 6.7), creatine phosphokinase (34–36 spots, pI 4.9 to 7.1) and glyceraldehyde-3-phosphate-dehydrogenase (34 spots, pI 4.7 to 8.3) (Lizana and Johansson, 1986). An alternative to this approach would be the maleylation (or succinylation) trains generated when treating alkaline proteins with maleic (or succinic) anhydride (Bobb, 1974). In the case of chymotrypsinogen A, the maximum maleylation number (14 residues) produced a train spanning from pI 9.6 to pI 2.8, the M_r increments going from 25.7 kDa (untreated) to 27.1 kDa (14 maleyl residues). In this maleylated train, the ΔpI/charged group appears to be ca. 0.25 pH units, thus the spots are spaced at ca. 0.5 pH unit apart.

4.6.7. Interfacing the 1st to the 2nd dimension

Three methods have been adopted for interfacing IPG to SDS gel slabs, as follows. In one approach (Gianazza et al., 1985d) the IPG gel slab is usually cut into separate lanes before sample application. This prevents lateral spreading and cross-contamination even when running samples with widely different protein concentrations or buffer composition (Fig. 4.9, upper left panel). After the IPG run, the separate gel strips are cut while still bound to the polyester foil. This ensures dimensional stability and thus improves spot reproducibility in the 2-D plane (Fig. 4.9, upper right panel). It is most important here that the plastic on the contact side with the SDS gel is cut flush with the supported IPG strip, so that a good contact between the IPG and SDS gels is ensured. On the contrary, a short length of Gel Bond foil is intentionally left to protrude on the opposite side, for easy handling of the IPG gel when interfacing it with the SDS gel slab. After incubation in the SDS denaturing

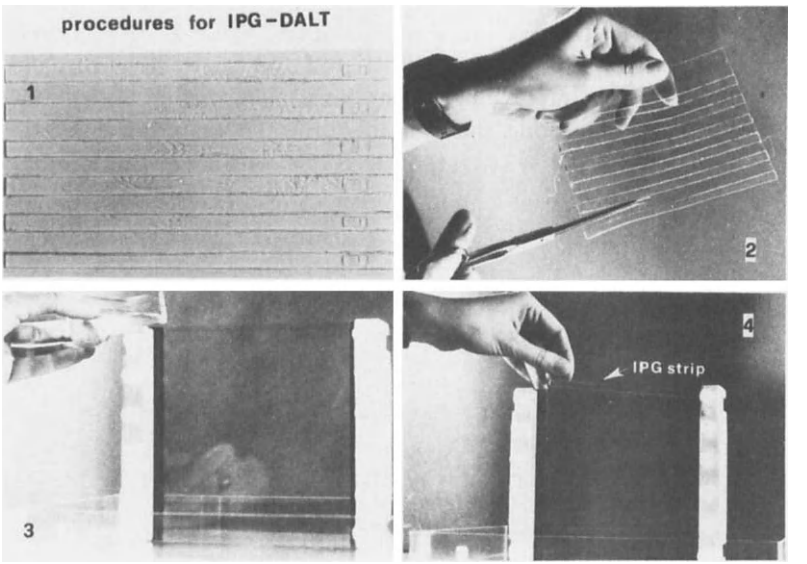

Fig. 4.9. Horizontal to vertical transfer in 2-D maps. Upper left: IPG gel slab with pre-cut lanes onto a single plastic (Gel Bond PAG) support; upper right: cutting individual sample strips after the IPG run (the plastic on the contact side with the SDS gel must be cut flush with the supported IPG strip); lower left: pouring melted agarose on the top of the 2nd-D SDS gel slab; lower right: the equilibrated IPG strip is lowered in situ on the stacking gel before onset of agarose gelation (from Righetti and Gianazza, 1987; by permission from Academic Press).

Fig. 4.10. Procedure for horizontal IPG-DALT. A: dried and washed IPG slab gel or IPG dry plates are cut into individual strips prior to rehydration and IEF. B: IPG gel strips on plastic backing are rehydrated in a cassette containing the desired additives for IEF. C: rehydrated IPG gel strips are blotted and placed on the cooling block side by side, 2 mm apart. Silicone rubber frames for sample application are applied to the IPG gel strip, 5 mm away from the anode. D: after IEF, the IPG gel strips are stored at $-80°C$ or used immediately for the second dimensional run. The IPG strips are transferred into a test tube filled with 10 ml equilibration solution and placed on a shaker. E: the equilibrated and blotted IPG gel strip is placed on the surface of a horizontal SDS gel along the cathodal electrode wick, 1 mm apart. One (18 cm) or two (11 cm each) IPG strips are applied. The IPG strips are removed after 90 min (200 V_{max}) of electrophoresis time, and the cathodal electrode wick moved forward so that it overlaps the former application area of the IPG strips. Electrophoresis is continued with 30 mA max till the Bromophenol Blue front has reached the anodal end of the SDS gel (from Görg et al., 1988b; with permission from VCH).

solution, the vertical gel slab for the 2nd-D is overlaid with 1% melted agarose (dissolved in stacking buffer; lower left panel) and the IPG gel strip immediately transferred and sealed in situ by the gelling agarose (Fig. 4.9, lower right panel). This mixed horizontal-vertical operation mode allows us to run 6–12 slabs in the 2nd-D by utilizing large tanks (e.g., the Bio Rad Protean cell). In another

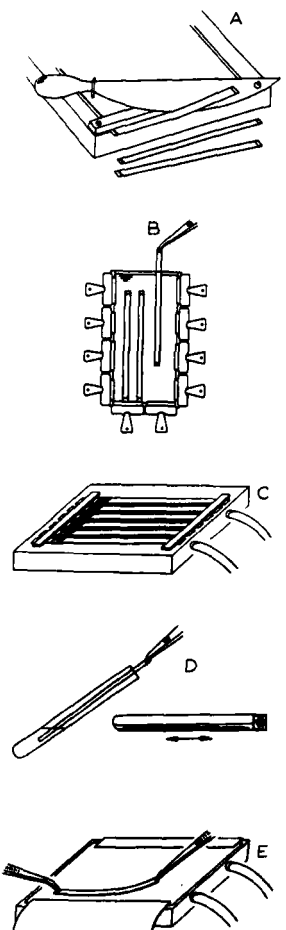

approach (Görg et al., 1988b), the sequence of steps is illustrated in Fig. 4.10(A to E). These authors prefer to cut individual gel strips, separating also the plastic supporting foil at the bottom. The cutting in individual gel strips is thus done on the dried IPG slab (Fig. 4.10A) (whereas in our case, individual gel tracks are obtained by cutting a wet gel and scraping away from the foil the excess gel strips in between). Individual gel strips are then re-swollen and run separately side by side. The equilibration in SDS denaturing buffer is also done individually in test tubes. Finally, the contact between the 1st and 2nd dimension is obtained by a laying-on technique, by reversing (plastic side up) the IPG gel strip on the surface of a horizontal SDS slab. No agarose sealing nor trenches are used for cementing the two dimensions together. In a third approach (Hochstrasser et al., 1986b), the first dimension is performed in gel rods of 1.5 mm diam. This solution was adopted because, when running conventional CA-IEF, the vast majority of 2-D users accepts only gel cylinders and simply refuses to run flat slabs. Being cast in narrow glass tubes, these IPG rods cannot be extruded and washed; thus they **have to be cast with all the denaturants** (urea, detergents etc.) and they **have to contain CAs** (from

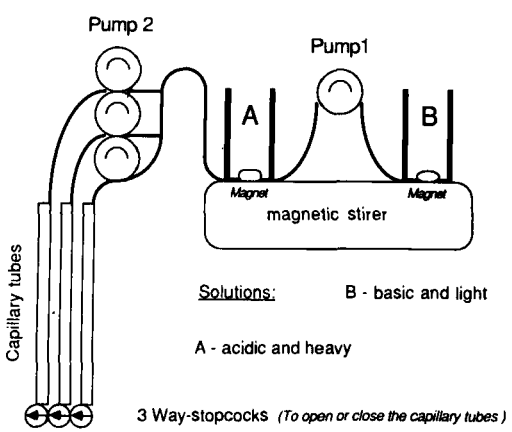

Fig. 4.11. Preparation of cylindrical IPG gels. The solution from reservoir B is transferred by pump 1 to the mixing chamber (A). A multichannel pump (Ismatec, Zurich) conveys the gradient solution simultaneously to the top of 20 glass tubes (200×1.5 mm i.d.) standing vertically (from Hochstrasser et al., 1986b).

0.5 to 1%) for electrophoretic depletion of the ion boundaries during the IEF process. Fig. 4.11 shows the casting process: owing to the small volume in each tube (250 μl), 20 tubes have to be filled simultaneously with a multichannel pump delivering individually the required volume to each tube, from a two-chamber mixing device containing only 2.5 ml of each limiting solution. Subsequent work done in our lab has shown that this latter method has severe limitations. For example dimensional stability is lost, so that reproducibility of spot position in the final 2-D map is severely hampered. In addition, the unwashed salts present during polymerization form boundaries which do not always completely leave the gel (Gianazza et al., 1988). The first two methods offer good reproducibility and experimental flexibility. The horizontal to vertical set-up (Fig. 4.9) allows the simultaneous run of multiple maps in the 2nd dimension. The horizontal to horizontal interfacing (Fig. 4.10) allows only one map at a time, but, due to the open gel geometry in the 2nd dimension, permits large surface areas to be exploited (e.g., first dimension IPG gels as long as 23 cm can be run, if needed).

4.7. The second dimension

The merits and limits of some of the most common methods for preparing the 2nd dimension gel are discussed below.

4.7.1. The interfacing solution

The equilibration buffer for conditioning the 1st dimension gel in preparation for the 2nd dimension run in general consists of 62 mM Tris-base, titrated to pH 6.8 with HCl, in presence of 2% SDS, 5% 2-ME, 10% glycerol and traces of bromophenol blue. 2-ME can be substituted with 0.1% dithioerythritol (DTE) or 0.1% dithiothreitol (DTT). This solution can be made up as such or as a 10 × mix to be diluted just before use. We prefer to store it frozen in case of long term use. **Warning**: for long term use, do not store in presence of thiol reagent, but add it (2-ME or DTE or DTT) fresh every time just prior to use. In aged solutions, the thiol reagent is

oxidized to a disulphide and its reducing power towards proteins is lost. Moreover, it could be responsible for vertical streaking in the 2-D map, as suggested by Marshall and Latner (1981). For the equilibration step, we suggest the use of a volume of denaturant at least 10 times larger than the gel volume. Thus, for each IPG strip, at least a 10 ml volume should be used (discard every time). During this step proteins can diffuse and a certain amount is lost. The quantity depends on the length of incubation time; e.g., if an equilibrium time of 2 h is used, as much as 50% of the total protein in the gel strip can be lost. Therefore, an equilibration time of no longer than 20 min on an orbital shaker is recommended. According to Görg et al. (1988b), if the level of glycerol in the equilibration mix is increased to 30%, this reduces the lateral spreading of the protein spots, due to increased viscosity. Some authors increase the level of DTT from 0.1% to 1% (65 mM). Burghes et al. (1982) use the following equilibration mix: 187.5 mM Tris, titrated with HCl to pH 8.8, 20 mM DTT and 3% SDS; equilibration time: 40 min.

Sealing agarose mix. The overlay agarose recipe consists of: 25 mM Tris-base, 192 mM glycine, 0.1% SDS and 0.8% agarose (traces of bromophenol blue can be added, as above, to mark the leading ion boundary during the SDS run). Large amounts of this can be prepared and then stored frozed in aliquots. Make sure, after removing the IPG gel strip from the interfacing solution, to blot excess liquid with a paper towel.

4.7.2. Solutions for the 2nd-D gel

By and large, the discontinuous SDS gel system described by Laemmli (1970) is used in the second dimension. This consists of a stacking and a running (or separation) gels, whose compositions are given below.

Stacking gel. It should be a wide-pore gel, to allow formation of the isotachophoretic train (Ornstein, 1964), thus its gel strength should not exceed 4 to 5% *T*. It contains 125 mM Tris-base, titrated to pH 6.8 with HCl, and 0.1% SDS. For a proper stacking process, we recommend a length of at least 2 cm. To avoid

excessive diffusion of the stacking/running gel boundary, it is best prepared 1 to 2 h prior to the 2nd dimension run.

Running gel. Most users have adopted a porosity gradient (typical recipes being 5–15% or 5–20% *T*), thus this solution has to be dispensed with a gradient mixer (see below). Both solutions are made to contain 375 mM Tris-base, titrated to pH 8.6 with HCl and 0.1% SDS. The dense solution (the one with the highest % *T* level) will also contain a final concentration of 20% glycerol, while no glycerol will be added to the light solution (the one with the lowest % *T*). An alternate route could be the use of mixed anionic detergent/aliphatic alcohol-polyacrylamide gel electrophoresis, as reported by Brown (1988). This technique, nicknamed MAD-PAGE, consists of running the SDS dimension in a 97.5% mixture of sodium dodecyl-, tetradecyl-, hexadecyl- and octadecyl-sulfates (in a 62 : 23 : 5 : 10 ratio) with 2.5% of their corresponding alkyl alcohols (i.e., dodecanol, tetradecanol, hexadecanol and octadecanol; in a 60 : 20 : 10 : 10 ratio). Interestingly, MAD-PAGE substantially increases the resolution in the 15 to 40 kDa range to a point at which two influenza virus proteins (NS1 and M1) having M_rs of 23,700 and 27,500 Da, respectively, unresolved in SDS-PAGE, can be amply separated in MAD-PAGE. This seems to be connected to a substantial alteration of the respective Ferguson plots (SDS-PAGE vs. MAD-PAGE) in the low M_r region, with a confluence in the higher M_r portion of the two curves. MAD-PAGE has not beed adopted in 2-D mapping as yet, but it could be a valid parallel route.

Tank buffer. Both the anode and cathode compartments contain the same buffer consisting of 25 mM Tris-base (15 g/5 l) added with 192 mM glycine (72 g/5 l) to a final pH of 8.6, and 0.1% SDS (5 g/5 l) (this recipe is given for the Protean tank, which holds this amount of buffer). Note the presence of glycine in this buffer, whereas elsewhere (stacking and running gels) HCl is present. **Do not**, by mistake, **titrate the Tris with HCl**, since the discontinuity Cl^-/Gly^- is needed for the stacking process (Cl^- will be the leading, Gly^- the terminating ion in the isotachophoretic train). The tank buffer can be reused several times, provided at the end of each run anolyte and catholyte are remixed to avoid ion depletion. We keep it up to 3 weeks directly in the lower tank of the Protean

II cell in presence of 0.1% sodium azide, to prevent bacterial and mold growth. Alternatively, packets of powder of the different chemicals can be prepared in advance and diluted just before use.

4.7.3. Gel cassette preparation

The gel is formed between two uniform glass plates, each about 3 mm thick. Typical dimension are rectangular 17×18 cm plates, but this will vary widely according to manufacturer, experimental needs. etc. Spacers are made of perspex or polyvinyl chloride (PVC), in general 1–1.5 mm thick, 1 cm wide and of the desired length (e.g., 20 cm). The spacers must be of uniform thickness to ensure an even gel throughout the slab. The glass plates should be cleaned carefully with detergent followed by several rinses in water and a final wash in ethanol to eliminate any remaining grease that could affect polymerization and gel adhesion. The two glass plates and two spacers are mounted together, the two spacers running down the vertical sides of the plates. The assembled plates are held together with strong clips which are positioned to press over the spacers. The bottom is in general sealed with a clamping device containing a flat rubber sheet against which the end of the cassette is pressed so as to produce a tight seal. In order to prevent leaks, some authors suggest lightly greasing the spacers with vaseline before the assembly, taking care not to grease the glass plates. However, this usually results in difficulty in cleaning the plates, and silver-staining artifacts are increased: for this reason, I do not recommend this procedure. A better method is to pipette melted 2% agarose around the outside of the assembled glass plates and against the spacers to produce a seal.

The running gel is poured in the vertically standing cassette (see §4.7.4) up to 3 cm from the top of the plates. It is then overlaid carefully with water-saturated isobutanol and left to polymerize for at least one hour (the gels can be prepared even the day before and left overnight, with no adverse effects, polymerization slowly continuing to near completion; Gelfi and Righetti, 1981a,b). The overlay is then removed and the gel is rinsed and dried with blotting paper before pouring the stacking gel solution. The stacking gel (usually a 4 or 5% *T* solution) is then poured on top to

occupy a 2 to 2.5 cm height. This leaves a 0.5 to 1 cm empty space for inserting the 1st dimension IPG strip. This gel is also overlaid with isobutanol and left to polymerize for at least 1 h. Two methods for gradient SDS gel casting are detailed below.

4.7.4. Pouring gradient gels

The assembly for casting the SDS-porosity gradient in a block of gel slabs is shown in Fig. 4.12 A (Anderson and Anderson, 1978a,b): the problem in casting identical gels is to arrange for the gradients to flow into the cassettes from below slowly enough so that identical gradients are formed in all holders, but fast enough so that the gradients are completely in place before polymerization occurs. In this system, the assembly (a block of 10 or 20 cassettes can be cast simultaneously) has been mounted on a rotating drum: during filling, the chamber block is kept tilted at 45°, so that the inflowing gradient flows into all gel holders equally and, while flowing up in this orientation, decelerates. As filling proceeds, the chamber is slowly rotated back to an upright position. Once the desired volume has been pumped in, a dense chase solution is introduced via reservoir H till all the gelling solution is purged out of the tubings into the respective cassettes.

For running horizontal, 2-D maps in ultrathin gel layers, the corresponding operation for pouring the SDS-porosity gradient is shown in Fig. 4.12B: as the gels are only 360 μm thick, they are cast one by one to avoid capillary forces and differential filling which would occur in a stack of cassettes as in the system of Fig. 4.12A. In both techniques, a concave exponential gel (e.g., 4% to 22% T) is prepared, even though we now prefer to run the second dimension simply in a linear porosity gradient. While in the ISO-DALT system the first dimension is in a gel cylinder, which is then coupled to a gel slab in the second dimension run (vertically in both cases), in the set up of Görg et al. (1981) both dimensions are run horizontally and they are both in thin layer gels. The 2nd-D SDS gel is cast onto a Gel Bond foil so that, once the cassette is opened, both glass plates are removed and the gel is supported by the plastic sheet.

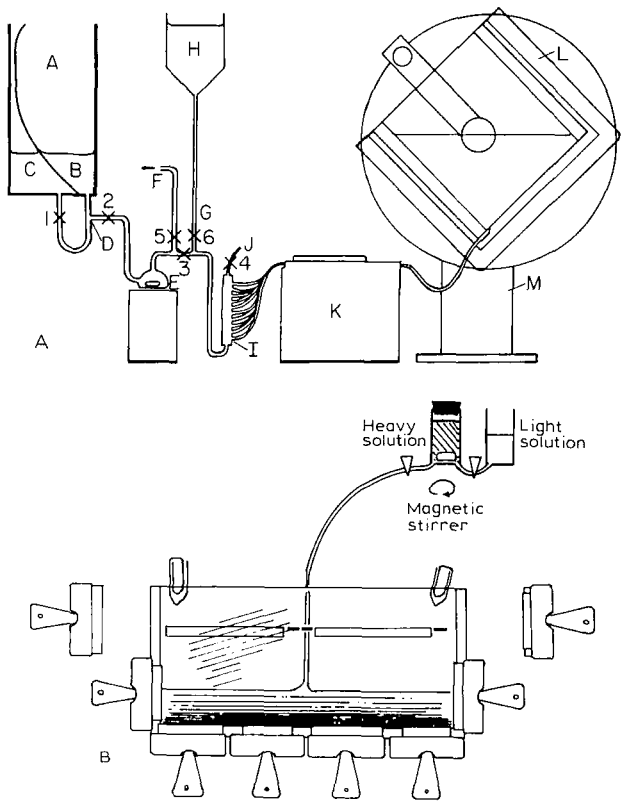

Fig. 4.12. Casting of second dimension slabs. A: schematic drawing of the gel casting apparatus for the DALT system. A: gradient former; B: light acrylamide solution; C: dense acrylamide solution; D: junction where light and dense solutions meet; E: magnetic mixer with input at edge and exit at top to pass air bubbles easily; F: line to vacuum; G: inlet for the dense underlay solution; H: reservoir for underlay; I: 10-exit manyfold; J: opening for air bubble removal; K: peristaltic pump; L: rotatable gel casting chamber (it accepts a set of 10 cassettes); M: apparatus for holding and rotating the gel casting chamber; X: clamping points (initially all are closed except No. 3) (from Anderson and Anderson, 1978a; by permission from Academic Press). B: casting of individual cassettes for a horizontal run (by courtesy of Dr. A. Görg). Note that both systems show the casting of exponential gradients, whereas today they have been abandoned in favor of linear porosity gradients.

A third, fully computerized procedure for casting of SDS-porosity gradients has been described by Altland and Altland (1984). In the original method, four burettes were used, containing, respectively, the dense, the light, the persulfate and TEMED solutions. We have modified the system to use only three burettes, since the TEMED is equally distributed in the dense and light acrylamide solutions forming the gradient. The apparatus is commercially available from Desaga (Heidelberg, FRG): Fig. 4.13A shows the experimental assembly, while Fig. 4.13B gives a close up of the mixing chamber. The burettes are driven by the computer, so that an extreme reproducibility of the gradient shape is ensured from run to run (here too we prefer linear porosity gradients, although any gradient shape can be selected from the program, including exponential convex, concave, sigmoidal, containing plateaus and the like). The mixing chamber is a round, minute (1 cm diam.) vessel, onto whose floor are pumped the eluates from the three burettes (the fourth inlet is kept, in our procedure, permanently sealed). At the center of Fig. 4.13B, we can seee the small, round magnet normally sitting on top of the four inlets, just inside the O-ring sealing the chamber. To the right of Fig. 4.13B is displayed the chamber cover containing in the center a small hole bearing a capillary which will convey the effluent gradient to the polymerization cassette. Once this chamber is assembled, the dead volume of the mixed liquid is barely 200 μl, so that the error in gradient delivery and shape is quite negligible (the total volume of gradient poured in the SDS-gel cassette is 30 ml). Since the three liquid eluates from the burettes meet in the mixing chamber, there is never a risk of premature polymerization of the solutions in the tubings. In the original technique of Altland and Altland (1984), the cassettes were filled from the bottom. Having noticed irregularities in this procedure, we prefer to fill each cassette individually from the top. Thus, the only manual operation in our method is to transfer the capillary from one cassette to the next and then to start again the filling cycle. In our 2-D system, we have adopted a 1 mm thick slab gel for the 1st, IPG dimension, coupled to a vertical 2nd dimension run in a 1.5 mm thick slab, of 14×16 cm size (Protean cell from Bio Rad Labs.) (Righetti and Gianazza, 1985b, 1986). This is not, by all means, the only gel size: dimensions range from

(A)

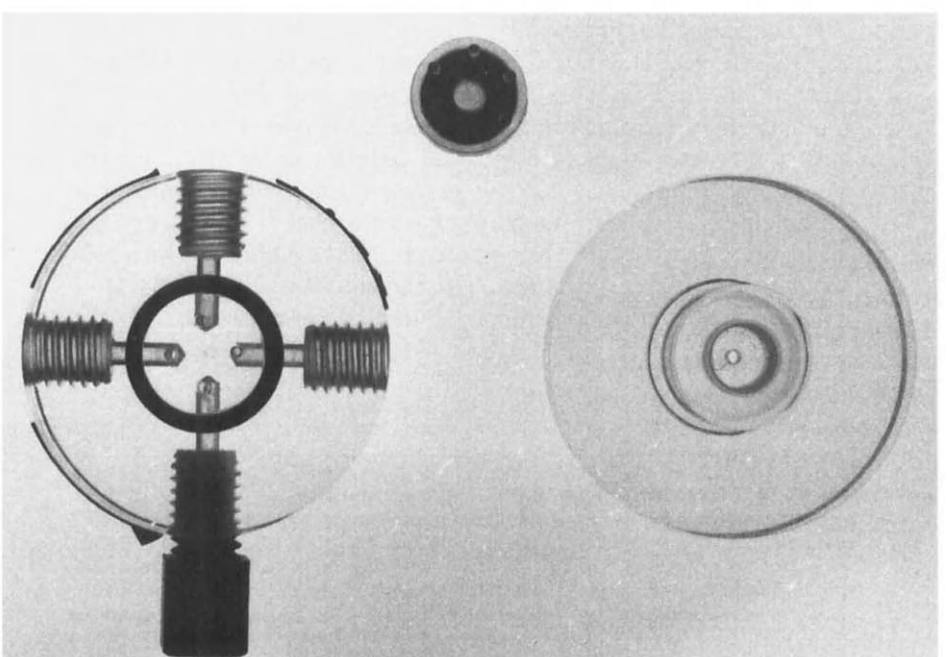

(B)

the 'giant' gels of Colbert et al. (1984; size: 30 × 40 cm) to the mini gel slabs adopted in Japan (Okuyama and Manabe, 1986; size: 3 × 4 cm, as typical of, e.g., the Pharmacia Fast System). Other methods for assembling, casting and running many gels simultaneously have been described by Garrels (1979) and by Jones et al. (1980).

4.7.5. M_r markers

For the SDS dimension, a series of cross-linked polymers of one protein of known M_r could be used as M_r standards (Inouye, 1971); however, they might exhibit anomalous behavior in SDS gels. For this reason, Giometti et al. (1980) have suggested the use of rat heart homogenate as an internal reference standard in the DALT dimension. In the SDS run, this homogenate generates 80 lines, of which 12 are major spots distributed at convenient intervals along the gel pattern covering M_r increments from as little as 300 Da (about 3 amino acid residues) up to 10,000 Da at the upper end of the gel. This homogenate, when extracted with SDS, dispensed in small aliquots in 0.7% agarose and stored frozed at −70°C, gives fully reproducible patterns for over 12 month periods of use. As a simple, tracking colored protein for the IEF-SDS gels, cytochrome C has been suggested (Leader, 1980) while, as a complete set of pI-M_r standards, bacteriophage T4 coat proteins have been proposed by Kurian et al. (1981). Other M_r markers available: lysozyme oligomers (Drozdz and Naskalski, 1988) and photopolymerized hemoglobin subunits (Sato et al., 1988).

Fig. 4.13. Automatic assembly for casting SDS gradient gels. A: general set-up with: (a) Apple II computer; (b) disk drive; (c) three step-motor-driven burettes and (d) mixing chamber. B: close-up of the Desaga gradient assembly. Left: mixing vessel with the four capillary inlets on the chamber floor. The black ring seals the chamber when the cover (extreme right) is placed in situ. Center: cylindrical magnet to be placed inside the O-ring, just above the four inlets in the mixing chamber. Right: chamber cover, with a central hole bearing a capillary for transporting the gradient solution to the gel cassette.

4.8. Reproducibility of spot positions in 2-D maps

The only study appeared in the early days of 2-D maps on reproducibility of spot position was from Hurley et al. (1978). According to these authors (Fig. 4.14A) spot reproducibility is related to their ellipsoidal 95% confidence envelopes in a pI vs. M_r plot. In this study, in which spot distinction by this criterion has been tested, it has not been possible to identify any component within 95% confidence limits by a non-overlapping pI-M_r ellipse. According to these data, 2-D maps are a nonsense procedure and this chapter should only be meant to mourn the technique. Luckily either the data base of Hurley et al. (1978) was deficient or we have improved significantly over the years, since recent data by Fosslien et al. (1984) (Fig. 4.14B) have indeed proved the validity of the 2-D map approach. The solid lines in Fig. 4.14B show the ranges of absolute locations of spots: in the IEF axis, they vary in the range 6–21 mm, while in the SDS dimension the variation is in the range 5–11 mm. If we take relative spot locations (i.e., compared with standards of charge and mass trains) the variation is reduced to the boxes depicted inside the lines. It can be seen that the biggest absolute error is given by the IEF dimension, no doubt due to the instability of the pH gradient and to the variations of batches of carrier ampholytes (these data refer to conventional CA-IEF). If we now compare this to the IPG-DALT technique presented here, it can be seen that the spot positional uncertainty is reduced to a minute ellipse (Fig. 4.14C): note that the variation in absolute spot location is never greater than 3 mm (spots 11 and 12) and in general is much less, of the order of 1 mm. The same applies to the SDS dimension (the gel size being ca. a square of 14×14 cm, excluding the length of the stacking gel from the measurements). Thus, it can be concluded that a 2-D map is just as good as the 1st dimension run, and that IPGs have been instrumental in bringing about this very high reproducibility. The spots of the carbamylation trains in Fig. 4.6(A to C) exemplify how protein spots can shift around in a 2-D map run in conventional CA-IEF simply by changing the type of commercial carrier ampholyte buffers.

4.9. Computer data acquisition

It has rapidly become clear that manual handling of the huge amount of information included in a 2-D map would be quite impossible, since, depending on gel resolution and sample type, up to 3000 spots can routinely be observed on a single gel (Young, 1984). Thus, various authors introduced computerized processing of gel images. The first one appeared already in 1977 and was named Tycho, in honour of the Danish astronomer Tycho Brahe (Anderson and Anderson, 1977, 1978a,b, 1980, 1984). In the meantime, Garrels developed QUEST (Garrels 1979, 1983; Garrels et al., 1984; Garrels and Franza, 1986) and soon after Lemkin (Lemkin and Lipkin, 1981a–d, 1983) and Miller (Bössinger et al., 1979; Vo et al., 1981; Miller et al., 1982, 1984) published details of additional systems, all based on powerful minicomputers. In addition, a large number of less powerful configurations have been described for 2-D image processing. Just to mention a few: Alexander et al., 1980; Amess et al., 1984; Aycock et al., 1981; Bishop et al., 1985; Capel et al., 1979; Kronberg et al., 1984; Okuyama and Manabe, 1986; Potter, 1986; Ridder et al., 1984; Tyson and Haralick, 1986; Vincent et al., 1981 and Zimmer et al., 1980. A summary of all these systems has just been published by Vincens and Tarroux (1988), who have independently developed a powerful, second generation program called HERMeS (Vincens et al., 1986; Vincens, 1986; Vincens and Tarroux, 1987a,b).

There are four steps in computer-assisted gel image processing: (a) gel digitizing and image processing; (b) image cleaning; (c) spot detection and integration and (d) gel matching. I will briefly comment on these procedures, while referring the reader to the excellent review of Vincens and Tarroux (1988) for a deeper treatise. For a better understanding of what follows, Fig. 4.15A and B gives a block diagram of the major hardware components for an image-analysis system. In the Tycho I system (Taylor et al., 1981, 1984) a PDP-11 minicomputer is interfaced with an array processor (AP-120 B) which handles the heavy computational load. Image acquisition is obtained via an Optronics P-1000 rotating drum densitometer, which scans the autoradiographic film. A Grinnell GMR-27 color raster device is used to display the images. It

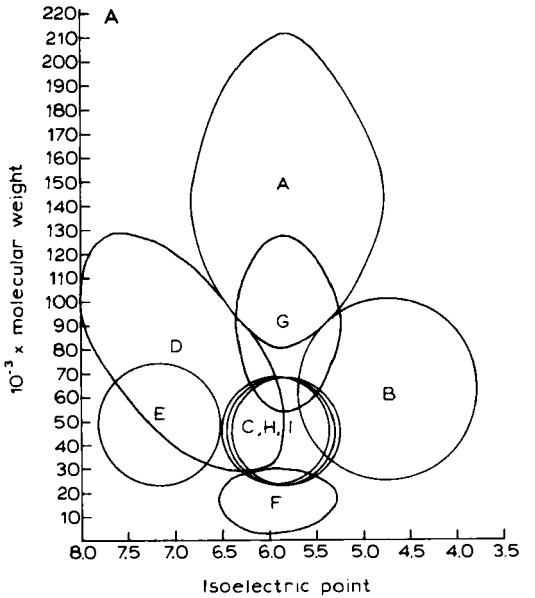
A
220
210
200
190
180
170
160
150
140
130
120
110
100
90
80
70
60
50
40
30
20
10
10^{-3} x molecular weight
A
G
D
B
E
C,H,I
F
8.0 7.5 7.0 6.5 6.0 5.5 5.0 4.5 4.0 3.5
Isoelectric point

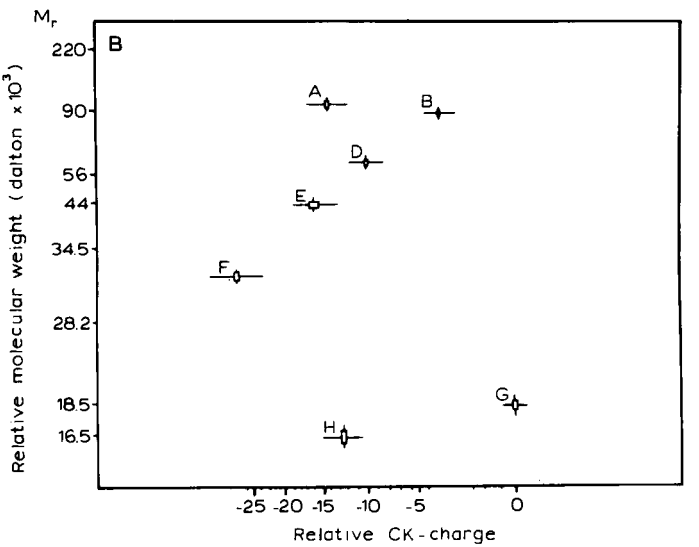
M_r
B
220
90
56
44
34.5
28.2
18.5
16.5
Relative molecular weight (dalton x 10^3)
A
B
D
E
F
G
H
-25 -20 -15 -10 -5 0
Relative CK-charge

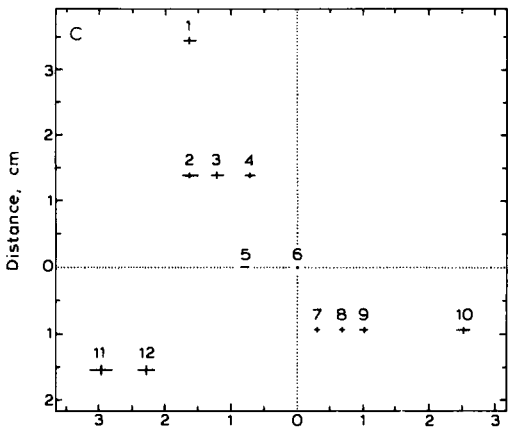

Fig. 4.14. Reproducibility of spot position in 2-D maps. A: 95% confidence ellipses of several subunit species positions in a 2-D map of nuclear chromosomal proteins from aflatoxin-induced liver cancer. Reproducibility was tested by repeating the procedure 6 times with the same control protein sample and determining the mean M_r, pI, standard deviation and variance of each spot. The ellipses were calculated by a computer from the actual position of the subunits in the pI-M_r plane in the six control runs (from Hurley et al., 1978; with permission from Elsevier). B: Solid lines illustrate ranges of absolute locations (in mm) of spots in the x- and y-axes, boxes show ranges of relative spot locations using internal charge and mass standards as references. CK: charge train of creatine kinase. M_r scale: from known markes in a rat heart homogenate (from Fosslien et al., 1984; with permission from VCH). C: IPG-DALT technique. 1st-D: pH 4–8 IPG gel of marker proteins in 8 M urea; 2nd-D: 7.5 to 17.5% T linear porosity gradient in SDS. Each spot is represented by a symmetrical cross with the intersection corresponding to the band average positional value and the arms represent the standard deviation. The S.D. is the average of six different gels (from Gianazza et al., 1986a; with permission from VCH).

contains nine planes of 512×512 bit refresh memory and is equipped with a trackball controlled cursor for interactive work. The system is interfaced to a Tektronix 4025 graphics terminal and a 4663 flatbed plotter for producing a hard copy of the screen images. Hard disks of 300 mega-bytes (Mb) and 14 Mb are available for data storage. The system shown in Fig. 4.15B (Ridder et al., 1984) differs essentially in the image acquisition hardware, which is a television camera. On the other hand most systems commercially available at present (e.g., the Visage 2000 from Bio

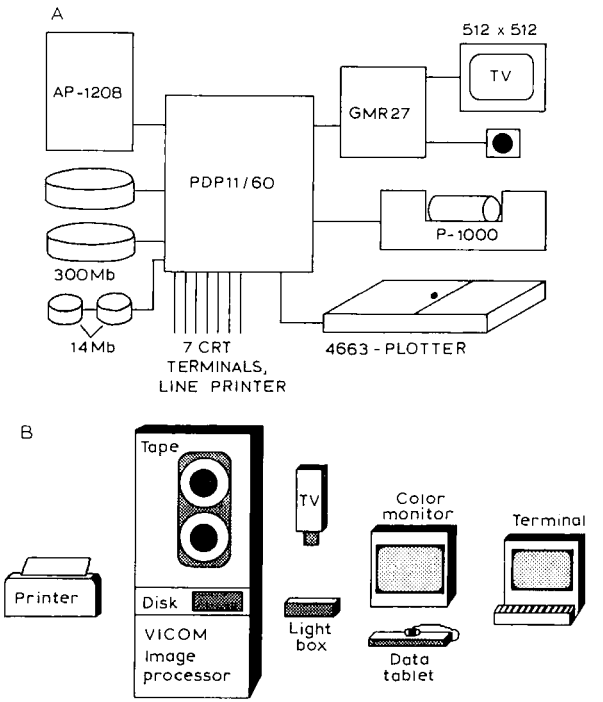

Fig. 4.15. Major hardware components for 2-D image analysis. A: the Tycho I system. P-1000: Optronics rotating drum densitometer; PDP 11/60: minicomputer Digital; AP-1208: array processor (Floating Point System); 300 Mb and 14 Mb: disk storage systems; GMR-27: Grinnel color raster device; 4663: Tektronix flatbed plotter (from Taylor et al., 1982; with permission from Am. Ass. Clin. Chem.). B: image acquisition via video-cameras. TV: model 7120 vidicon television camera, with a 512×512 pixel resolution (from Ridder et al., 1984; with permission from Am. Ass. Clin. Chem.).

Image, Ann Arbor, Mi.) use neither of the two, but rather CCD cameras.

4.9.1. Gel digitizing and image processing

Digitizers must meet two main requirements: adequate resolution and ease of operation. A good sensitivity for such systems seems to be a spatial precision of at least 10 nm, and a digitalization range

of 256 gray levels (8 bits). Todays' scanners offer a resolution of up to 2000 × 2000 points and reach a gray level range of 1024 gray tones (12 bits). In addition, a scanner should cover a dynamic range of at least 0–3 optical density units. Four types of digitizers have been used: roller drum scanners (see Fig. 4.15A) flatbed spot digitizers (Kronberg et al., 1984), flying spot scanners (Spragg et al., 1985), TV (Ridder et al., 1984; see Fig. 4.15B) and CCD (Appel et al., 1986) cameras. It appears that present and future systems will be more and more oriented towards the camera systems, not so much video cameras, which are cheap but offer low image resolution and poor accuracy, but rather CCD cameras which can now digitize images up to 2000 × 2000 pixels.

4.9.2. Image cleaning

Most non-electronically processed pictures of 2-D maps are quite awful to look at: horizontal and vertical streaking are regular features and often the background (especially with silver staining) is highly irregular. These inhomogeneties produce, at the level of image processing, low-frequency noises which must be eliminated. To those, one has to add the high-frequency noise due to film grains in autoradiographic images. A third problem is spot overlap, which leads to poor spot detection and classification in over-crowded regions. Image filtering has thus been proposed by various authors (Lemkin and Lipkin, 1981a; Taylor et al., 1981; Appel et al., 1986). Skolnick and Sternberg have introduced the use of mathematical morphology (Skolnick et al., 1982; Skolnick, 1987), based on the work of Serra (1982) and Matheron (1975). The same approach has been used in the HERMeS program (Vincens et al., 1986; Vincens, 1986), which, by considering the image as the union of different sets of pixels, provides tools for the analysis and contour delineation of each object (i.e., a spot) in the map.

4.9.3. Spot detectors and integrators

The third step in 2-D gel processing is spot detection and integration. The same technique is essentially used to detect spot maxima in almost all the existing systems, whereas spot integration differs

greatly among systems. Two main approaches for integration have been used: spot segmentation and spot modelling. The direct integration method of spot segmentation is chiefly illustrated by the Miller's system (Bössinger et al., 1979). However, most authors currently use a spot model, essentially based on Gaussian surfaces and inspired by chemical diffusion modelling. In addition, the HERMeS program (Vincens, 1986) takes also in account spot disymmetry caused by the protein migration in the X and Y directions. Asymmetric spots are thus memorized as ellipsoids, with the additional values of pitch angle and intensity at the maximum position.

4.9.4. Gel matching

The fourth processing step consists of spot list comparisons to identify homologous spots between gels. The first of such methods was based on geometrical distortions and gel stretching and consisted in spot position correction using a network of landmarks (Taylor et al., 1981). Vincens and Tarroux (1987a) have introduced a different method based on pattern recognition and symbolic computation techniques. Skolnick (1982) has proposed a valuable variant, based on the transformation of the image into specific graphs. In these two latter approaches, spot position is essentially defined by topological considerations, by which a group of closely located spots in a gel is considered as a pattern, to which a similar group of spots in another experimental map has to be matched. It seems that the major improvement associated with the Vincens and Tarroux (1987a) method is the suitability of multiple gel matching. Needless to say, gel matching is of the utmost importance if the overall trend of an experiment has to be decoded (e.g., ontogenic development, appearance of new spots associated with a disease and the like).

Clearly, the present excursus cannot answer all the questions connected with computerized image processing. For more on data handling and processing, and for a glimpse to the future, the reader is referred to the fundamental review of Vincens and Tarroux (1988).

4.10. Silver staining

I have talked at length in Chapter 3 (§3.9.3) of silver staining, but without giving any recipe. The reason being that silvering of IPG gels seldom works, since a rather heavy background is always obtained. Since it is known that amino groups in proteins favour silver deposition, we suspect that the alkaline Immobilines act as nucleation centers for silver, thus strongly increasing the background, to a point at which it is no longer advantageous to perform a silver staining over a Coomassie coloring. While this phenomenon has not been studied in detail, it is a fact that acidic IPG ranges have a lighter background than alkaline IPG intervals. The problem of course does not exist any longer in a 2-D map, as the final SDS gel is devoid of any Immobiline. Thus, I feel that this is the right place for presenting some silvering recipes. I will not comment on the original Merril procedure (Switzer et al., 1979) which is perhaps the best known and the most widely adopted, but rather present some variants which have attained some popularity over the years.

The Oakley procedure. Oakley et al. (1980) have published a variant employing alkaline ammoniacal silver nitrate as the stain and citric acid-formaldehyde as the developer. The recipe is given in Table 4.6. This procedure has become popular in clinical chemistry labs, due to the fact that Tracy and Young (1984) have devised an automatic procedure, by which blocks of gels, held vertically between removable plexiglass separators, are processed simultaneously in a motorized unit. High silver staining throughput is thus ensured, with marked saving of technician time.

The Tunon procedure. The method developed by Tunon and Johansson (1984) and subsequently modified by Johansson and Skoog (1987) is a combination of aspects of several other published variants. The recipe is given in Table 4.7. It has the advantage of requiring only two hours and can be used in daylight.

Variegated silver staining. Sammons et al. (1984) have described a silvering procedure that produces different colors with different classes of proteins, commercially available under the tradename GELCODE. Proteins are stained in four basic colours: yellow, red, brown and blue, with also intermediate hues (e.g., greenish-blue).

TABLE 4.6
Silver stain procedure [1]

Step	Quantity	Time
1. Fix in glutaraldehyde	100 g/liter	30 min
2. Wash (with water)	Several liters	Extensive 15 min
3. Stain in:		
Water	21 ml	
10 *M* NaOH	0.19 ml	
NH_4OH	1.4 ml	
200 g/liter $AgNO_3$	4.0 ml	
total volume (with water) [2]	100 ml	
4. Wash (with water)		5 min, plus a rapid rinse
5. Develop in:		Generally, developing done
Water [2]	100 ml	as 5–10 min
1.0 g/liter citric acid	11 ml	
HCO_3	0.1 ml	

[1] Modification of Oakley et al. (1980); see Tracy et al. (1982b) for details of the procedure.
[2] The actual volumes used will depend upon the gel size, container size, and number of gels; e.g., for 10 standard DALT gels, we use 750 ml of stain when done in boxes and 3000 ml when done in automatic stainer.

According to these authors, this adds a new dimension to 2-D maps, since potentially one could recognize some classes of proteins on a colour base. In addition, if two overlapping spots happen to exhibit different colours, their resolution would be greatly facilitated. The recipe for this peculiar stain is given in Table 4.8.

4.10.1. General comments on silvering

The intensity of silver staining is linear over a 50-fold range in concentration, from 0.02 ng/mm^2 up to 2 ng/mm^2 (Table 4.9). Above this level, the stain density becomes non-linear as spot densities reach saturation (Merril et al., 1982). This non-linearity problem may be alleviated and the dynamic range of the stain extended by recording and analyzing the image during development. With some proteins, as little as 0.02 ng/mm^2 can be detected, in 1 mm thick gels. As shown in Fig. 4.16, the relationship

TABLE 4.7
Rapid silver staining of polyacrylamide gels (Johansson and Skoog, 1987)

A rapid and reproducible silver staining procedure for polyacrylamide gels has been developed. The method is based upon two other silver staining methods (Tunon and Johansson, 1984; Ohsawa and Ebata, 1983). A 2–4 fold increase in sensitivity with only a slight increase of background was obtained when the described method was compared to the one published by Tunon and Johansson (1984). The method presented has a detection limit below 10 ng. It is completed within 2 h and can be performed in daylight.

Staining procedure

Fixatives and solvents are in principal the same as those used by Tunon and Johansson (1984). The ammoniacal silver nitrate solution (mom. 6) was first described by Ohsawa and Ebata (1983).

1. (30 min)	Fix the gel in acetic acid–methanol–water (1 : 4 : 5)
2. (5 min)	Rinse in water
3. (15 min)	Fix in 25% glutardialdehyde–water (1 : 1)
4. (2×10 min)	Rinse in water
5. (15 min)	Rinse in 20% aqueous ethanol
6. (15 min)	Staining solution: 2 ml 20% $AgNO_3$ in water + 2 ml 25% ammonia are added to 10 ml 4% NaOH and
7. (2×5 min)	Rinse in 20% ethanol
8. (2–5 min)	Developer: 200 µl formaldehyde and 50 µl 2.3 M citric acid in 200 ml of 20% ethanol *
9.	Break in glycerol–acetic acid–water (1 : 10 : 89)

* Suitable gel size: ca (150×150×1) mm

between density and concentration of protein, or the slope of the staining reaction, is characteristic for each protein. It can be seen in Fig. 4.16 that, e.g., ovalbumin has a slope nine times that of carbonic anhydrase. Quantitative use of the silver stain is nevertheless possible if constitutive or marker proteins are present on each gel so that densities can be normalized. In addition, it must be stated that protein-specific staining curves have been observed also with organic stains, including Coomassie Blue (Tal et al., 1985) and with most protein assays, such as the commonly used Lowry et al. (1951) assay. A detection method independent from the protein amino acid composition would be only a reading at 210 nm, where the peptide bond would absorb.

Artifacts. Artifactual bands with M_r ranging from 50 to 68 kDa have commonly been observed in silver stained gels. Evidence has been presented indicating that these contaminanting bands are due

TABLE 4.8
Color silver staining procedure for 1.5 mm gel [1,2]

Steps	Solutions	Duration of agitation
Fix	50% EtOH + 5% acetic acid	Overnight (16 h)
Wash	H_2O	1 h
↓	H_2O	1 h
↓	H_2O	1 h
↓	H_2O	1 h
Equillibrate gel	$AgNO_3$ (1.9 g/liter)	1 h
↓		
Rinse	H_2O	10–20 s
↓		
Reduce Silver	HCHO (7.5 ml/liter) in 0.75 N NaOH	10 min
↓		
Enhance color	Na_2CO_3 (7.5 g/liter)	1 h
↓	Na_2CO_3 (7.5 g/liter)	1 h
↓	Na_2CO_3 (7.5 g/liter)	1 h

[1] The silver reduction and color enhancement steps are performed with reagent solutions equilibrated to 25°C.
[2] After the color stained images stabilize (approximately 4 h after last Na_2CO_3 step) the wet gel can be scanned and the image stored on magnetic tape, or the gel may be sorted in an airtight bag with a small amount of 0.75% Na_2CO_3.

TABLE 4.9
Linearity of silver staining

Proteins [a]	Total protein range (ng)	ng protein/ mm^2	Number of bands measured	Slope [2]	Y intercept [2]	Correlation coefficient [1]
Albumin	5.4–270	0.05–2.27	5	101.7	9.0	0.995
Ovalbumin	7.2–360	0.02–1.01	5	231.5	2.7	0.998
Trypsin inhibitor	8.0–200	0.04–0.96	5	165.8	2.4	0.996
Ferritin	25.0–250	0.06–1.60	4	83.3	12.4	0.990
Carbonic anhydrase	4.0–200	0.06–2.85	5	26.0	0.8	0.983
Phosphorylase B	6.4–640	0.06–6.24	5	45.8	3.4	0.998
Catalase	3.6–180	0.03–1.59	5	127.0	8.4	0.990
Lactate dehydrogenase	9.6–240	0.06–1.57	5	107.5	4.4	0.990

[1] Proteins (Pharmacia purified molecular weight markers) were separated in a 10% polyacrylamide gel and densities and band areas determined with computerized microdensitometry.
[2] Slopes, Y intercepts and correlation coefficients were determined by linear regression analysis.

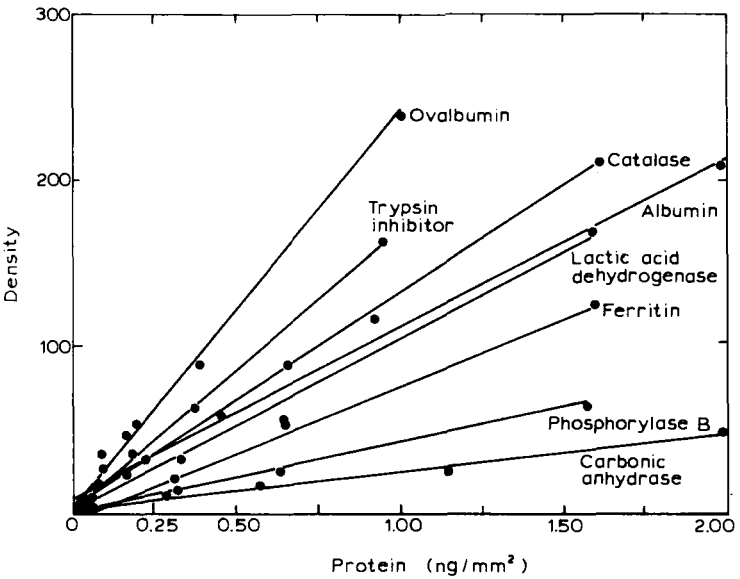

Fig. 4.16. Silver stain density versus protein concentration for purified proteins (Pharmacia markers) electrophoresed in 10% *T* polyacrylamide gels (0.88 mm thick) at 20 mA/gel. The gel images were developed for 9 min in sodium carbonate-formaldehyde solution. Band areas and densities were measured by computerized densitometry (from Merril and Goldman, 1984).

to keratin skin proteins (Ochs, 1983). Thus samples, solutions and equipment should be handled carefully to minimize such artifactual bands. Bacterial and fungal contamination should be strictly avoided and the water used should have a conductivity of less than 1 μmho. **Warning**: silvering is a photographic process, in a way, thus care should be taken to perform all steps at a controlled temperature. Scientists had experienced in the past great variations in stain intensity from the winter to the summer months, no doubt due to fluctuations in 'room temperature'. As a last comment, it appears that the yellowish background, so typical of any silvering procedure, can be strongly reduced if, as a cross-linker, bisacrylyl piperazine (Artoni et al., 1984) is used instead of *N*,*N*′-methylene bisacrylamide (Hochstrasser et al., 1988).

4.11. Blotting of spots from 2-D maps

I have briefly mentioned this technique in Chapter 3 (§3.6); however, since many applications are obtained after 2-D maps, more details are required. Blotting refers to techniques for transferring separated zones of DNA, RNA or proteins from gels to thin sheets of a derivatized paper or membrane matrix such as nitrocellulose, to which they strongly adhere. Many of the advantages of this technique are related to the much greater accessibility of macromolecules adsorbed or bound to the surface of a thin sheet as compared to those buried within a gel matrix. This is quite critical on gels containing a porosity gradient, since in different parts of the gradient the accessibility of reagents can vary greatly. Conversely, when transferred to the blotting membrane all macromolecules will be equally accessible and considerably smaller amounts of reagents will be needed than in the original hydrophilic gel used for the electrophoretic separation. As pointed out by Gershoni and Palade (1983), since the macromolecules are immobilized on the surface of a thin membrane, processing times for staining and destaining reactions, incubations, washings and the like can be much shorter than for gels. In addition, multiple replicas of a single gel can be made, thus allowing for several differential analyses from a single electrophoretic run. There are several types of immobilizing matrices available, but the most widely used is nitrocellulose (NC), in general of 0.45 μm pore size. The mechanism of binding of macromolecules to NC has been found to be by hydrophobic interaction, a minimum contact area of 100 $Å^2$ and a minimum value of free energy of adhesion (ΔG) of -1.5 kT being required for stable fixation to the matrix (Van Oss et al., 1987). In addition to NC, other binding surfaces have been utilized, such as diazobenzyloxymethyl paper (DBM) or paper and cellulose acetate activated with cyanogen bromide, or diethylamino ethyl (DEAE) paper. Also nylon-based membranes have become quite popular, e.g., Gene Screen or Zetabind (also called Zeta Probe, ZB). ZB is derived from nylon 66 and incorporates many tertiary amino groups capable of electrostatic binding to biopolymers such as proteins and nucleic acids. Another attractive membrane appears to be polyvinylidene difluoride (PVDF) (Gültekin and Heermann,

1988). PVDF is a hydrophobic Durapore GVHP membrane with 0.2 μm pore size (a teflon-like polymer which is mechanically strong and chemically inert), available from Millipore as Immobilon-P (Pluskal et al., 1986; Matsudaira, 1987). PVDF membranes are compatible with all stains described, including the india ink stain (Hancock and Tsang, 1983). PVDF appear to offer higher staining sensitivity than nitrocellulose or nylon membranes, and can be rendered transparent, if needed, by washing in dioxane-isobutanol or acetone-tetrahydrofurane. In addition to PVDF, there is a whole series of glass fiber filters (GFF) treated in various ways for proper protein adhesion in electroblotting. In one system (Vandekerckhove et al., 1986, 1987) the GFF sheet is coated with quaternarized ammonium polybases, which increase the protein binding capacity via coulombic attraction. A similar approach has been used by Aebersold et al. (1986) who activate the glass surface with quaternary ammonium groups (QA-GFF). Proteins electroblotted from SDS-PAGE or 2-D gels are used for direct sequence analysis in the Gas-Phase Sequencer (Aebersold et al., 1987; LeGendre and Matsudaira, 1988). In yet another variant, QA-GFF sheets are used for blotting, and the protein link with the membrane is further stabilized by addition of polybrene (an entrapping polymer; in fact a polymeric quaternary ammonium salt) after blotting (Yuen et al., 1986). Kirley (1987) has also proposed coating of GFF sheets, previously activated with trifluoroacetic acid, with polybrene. As a last variant, Bauw et al. (1987) have proposed GFF foils coated with poly (4-vinyl-*N*-methyl-pyridinium) iodide. These membranes have a protein binding capacity ranging from as little as 5–10 (QA-GFF) up to as much as 170 (Immobilon-P) $\mu g/cm^2$. The efficiency of initial coupling (i.e., of protein fixation in the blotting procedure) ranges from 30 to 100% of the amount of protein present in the polyacrylamide gel prior to the transfer, typical values being around 75%. The yield of protein from the GFF filters for microsequencing analysis is in general very high for all types of membranes and approaches 95% (LeGendre and Matsudaira, 1988). It appears that microsequencing can be performed with as little as 10 pmol protein, the preferred amounts being however of the order of at least 100 pmol.

There are three ways by which proteins and nucleic acids are

transported from the electrophoresis gel onto the blotting matrix: simple diffusion, solvent flow or under the influence of an electric field. The concept of transferring macromolecules was first introduced by Southern (1975) and it consisted in a capillary flow migration of DNA to a NC membrane (nicknamed 'Southern blotting'). Thus, when the DMB paper was introduced, still employing solvent flow, the technique became known as 'Northern blotting' (Alwine et al., 1977). By the same token, when Towbin et al. (1979) introduced the electrophoretic transfer of proteins and nucleic acids to NC, it was labelled as 'Western blotting'. The most widely used transfer method today employs electrophoretic elution of the proteins and nucleic acids and it is referred to as 'electroblotting'; the assembly and apparatus has been shown in Fig. 3.18. It has been suggested (Gershoni, 1986) to apply a gradient of field strength along the gel length, with higher voltage gradients in gel regions containing the larger macromolecules, so as to help their transfer (a common drawback is that, during a transfer from a SDS gel, only the smaller polypeptides are sufficiently transferred, anything above 100 kD being poorly extracted from the polyacrylamide gel). A typical general scheme for electroblotting proteins from 2-D gels, onto two different kinds of supports (nitrocellulose and diazo paper) is given in Table 4.10 (Symington, 1984).

For detection after transfer, proteins can be stained with the usual dyes, e.g., Coomassie Blue R-250, or with fluorescent probes (e.g., fluorescamine, fluorescein maleimide), or with colloidal metal particles (gold or iron), which reach a sensitivity of subnanogram/mm^2 (Moeremans et al., 1985; Moeremans et al., 1986). Actually, staining with heavy metal salts seems to be increasingly popular. Thus Lee et al. (1987) have reported a copper chloride stain, while Dzandu et al. (1988) have described additional staining procedures with cobaltous acetate or chlorides of copper, nickel and zinc (this last one being the most sensitive). However, it should be noted that these stain protocols are operative directly in the SDS-gel and they are based on inverse or negative detection, i.e., formation of clear protein zones on a semiopaque gel background. From this point of view, then, a negative gold staining (white zones on a red background) can be obtained, with high sensitivity, directly on a polyacrylamide gel (Casero et al., 1985a) and a negative nitro blue

TABLE 4.10
General scheme for two-dimensional gel protein transfer analysis

0–30 min, size equilibrate	Equilibrate gel in transfer solution	60 min, size equilibrate and remove components that react with diazonium group
10 min, wet in transfer solution	Pretreat transfer sheet	35 min, activate amino form to diazo form and equilibrate in transfer solution
2–22 h, 6–8 V/cm	Electrophoretic transfer of proteins	2–4 h, 8–10 V/cm; cooling for runs > 2 h
1 h, 37°C	Incubate transfer sheet in blocking solution to saturate binding sites	2 h, 37°C
2 h, 22°C	Probe the transfer (e.g., by immunologic techniques.) Bind primary antibody (e.g., rabbit IgG)	2 h, 37°C
40 min: 22°C	Wash sheet	4 h, 37°C
1 h, 22°C e.g., Peroxidase-conjugated goat anti-rabbit IgG	Bind enzyme-conjugated second antibody or radiolabeled tracer	2 h, 37°C e.g., ^{125}I-labeled Protein A
40 min: 22°	Wash sheet	2 h, 37°C
15–30 min: by reaction with chromogenic substrate	Detect specific protein	1–4 h, autoradiography
2 or 3 times	Erase and reprobe	8 or more times

tetrazolium stain has been described for 2-D maps (Bahrman and Thiellement, 1985). In addition, double stains can be performed in the same gel; e.g., a tandem silver-Coomassie stain has been proposed (Dzandu et al., 1984). Macromolecules radiolabelled with ^{32}P, ^{35}S, ^{125}I, or to high specific activity with ^{14}C, are readily and efficiently detected by autoradiography. Ca-binding proteins can be detected with ^{45}Ca followed by autoradiography (Maruyama et al., 1984). Immunological detection of proteins is suitable with all types of immobilizing transfer matrices (see below). After electroblotting, the excess binding sites on the matrix must be blocked

with excess exogenous protein (e.g., casein, whole milk, fish extracts); then a specific antibody is bound and finally a second antibody directed against the first one is allowed to react. This second antibody can be fluorescent labelled, radiolabelled or conjugated to an enzyme such as horse radish peroxidase or alkaline phosphatase. It appears that as little as 100 pg protein can be clearly detected by the enzymatic procedure (Towbin et al., 1979).

4.11.1. Immunochemical labelling after blotting

This is a direct development of the solid-phase enzyme-linked immunosorbent assay, well known in clinical chemistry through the acronym ELISA. The ancestor of this technique is the principle of immunofluorescence (Coons, 1941), by which antigens could be directly visualized in histochemical preparations by using antibodies conjugated with fluorescein isothiocyanate. Subsequently, Nakane and Avrameas (1966) introduced the concept of linking enzymes directly to antibodies, allowing detection of the antigen–antibody complex via a direct enzyme assay (in general, an in situ zymogram development). These immuno-conjugates had relatively small dimensions, so that they had easy access to the antigen structure in the histochemical preparation. By and large, two enzyme immuno-conjugates are preferred: (a) coupling to horseradish peroxidase (HRP) and (b) linking to alkaline phosphatase (AP). Immuno-conjugates have the following advantages over immunofluorescence: greater sensitivity and precision and stability over the time. I will briefly review the different methodologies.

The direct method. In this procedure, the antibody specific for a given antigen (primary antibody) is directly conjugated with peroxidase (or AP) and then reacted with the antigen. This method is the most rapid but also the least sensitive, since the modified antibody can loose affinity for the antigen and, in addition, unlabelled antibody molecules will diminish the yield of enzyme molecules in the complex. Thus, the preferred method is the sequential use of two antibodies (DeLellis, 1981): the first, specific for the antigen to be detected and the second (secondary antibody), conjugated with HRP or AP, specific for the immunoglobulin

fraction of the animal species against which the first antibody had been raised.

Indirect method with peroxidase–antiperoxidase (PAP) complexes. This method sequentially employes three reagents: (1) primary antibody; (2) secondary antibody; and (3) PAP complexes, formed by two molecules of IgG and 3 molecules of enzyme. In this method (Sternberger, 1979) the second antibody acts as a 'bridge', via its Fab fragments, between the primary antibody and the enzyme-linked immuno-complexes. For the bridging action to take place, it is necessary that the primary antibody and the IgG of the PAP complexes are raised in the same animal species; in addition, the 'bridging' antibody must be present in excess (Carrell et al., 1980). The novelty of this approach is that, instead of using antibodies directly conjugated with the enzyme, immuno-complexes formed by antibodies specific for the enzyme are utilized. This renders the PAP system more sensitive and allows thus the use of reduced amounts of primary antibodies.

Indirect method with the avidin–biotin system. This method exploits the extremely high affinity (K_d ca. femto-mol) between an egg-albumen glycoprotein (avidin) and a vitamin (biotin). Guedson et al. (1979) (see also Wilchek and Bayer, 1984) have described two basic variants of this method. In one, the three following steps are utilized: (a) preparation of an antibody conjugated with biotin and specific for a given antigen; (b) incubation with avidin; and (c) application of biotin conjugated with an enzyme (e.g., peroxidase, glucose oxidase, β-galactosidase, alkaline phosphatase). Avidin thus acted as a 'bridge' between the antibody and the enzyme used for detection. In the other variant, after step (a) as above, avidin directly linked to an enzyme was utilized. This method of Guedson et al. (1979) appears to be by far the most sensitive among all indirect methods described. This is due to the fact that in the final complex a high level of enzyme molecules is incorporated, ensuring thus an amplification of the staining reaction. In 1980, Warnke and Levy described a variant of the above method as follows: (a) use of a monoclonal antibody specific for the antigen; (b) application of a secondary (polyclonal, from goat) antibody directed against the primary antibody and conjugated with biotin; and (c) application of the avidin–peroxidase complexes. An additional variant (Hsu

and Raine, 1982) utilizes, in step (b) as above, an antibody conjugated with biotin, followed by incubation first with avidin, then with biotin conjugated with peroxidase. In daily practice, however, in order to speed up the technique, preformed avidin–biotin–peroxidase complexes are directly used. In this last variant of the avidin-biotin system it is possible to substantially amplify the specific enzyme stain, since the large number of avidin and biotin molecules present in the complex form a large network able to incorporate a substantial number of enzyme molecules.

Indirect method with the alkaline phosphatase–anti-alkaline phosphatase (APAAP) complexes. This method is essentially similar to the PAP technique described above. In operational terms, the primary antibody, the 'bridging' antibody and the APAAP complexes are sequentially utilized with the same procedures described for the PAP complexes. This method was first proposed in 1978 by Mason and Sammons and employed polyclonal antibodies. Subsequently Cordell et al. (1984) suggested the use of monoclonal antibodies.

Detection of the enzyme marker. The specific staining reaction for HRP or AP allows visualization of the immuno-complex in the blotted electropherogram, and thus reveals the antigen under study. The enzyme is detected with the aid of solutions containing both the specific substrate and the chromogenic substance (DeLellis, 1981; Mason and Sammons, 1978; Mason, 1985). As a result of the enzyme reaction, the latter is transformed in a stable, colored compound which precipitates in situ, thus indirectly revealing the presence of the antigen.

Peroxidase revelation. The detection of horse radish peroxidase (HRP) in the immuno-complex occurs via the use of its substrate (H_2O_2) and of various chromogens, such as 3,3′-diaminobenzidine (DAB), 3-amino-9-ethyl carbazole (AEC) and 4-chloro-1-naphthol (CN). DAB produces a brown precipitate which can be intensified with osmium tetroxide. AEC gives a purple red precipitate and it is the preferred chromogen, since DAB is a potent carcinogen. CN, after enzyme reaction, generates a dark blue precipitate; however, it is the least sensitive and it is soluble in alcohol, thus its use is not so popular.

Alkaline phosphatase detection. In this reaction, naphthol phos-

phate is generally used as substrate and Fast Red and Fast Blue as chromogens. According to Sinha (1985) the best results are obtained if diethanolamine (pH 10.5) is used as a buffer and if 5-bromo-4-chloro-3-indoxyl phosphate and a tetrazolium salt are used as substrate and chromogen, respectively. This is because they are stable at high pH values and produce relatively insoluble formazans at the site of AP activity (Meyer-Sabellek et al., 1988).

Blotting procedure. Basically, after the electrophoretic separation, the proteins are transferred by a western blot to a thin membrane (e.g., nitrocellulose) to which they are adsorbed by hydrophobic interaction. Following blocking of non-specific sites (by saturation with exogenous proteins, such as milk or fish extracts), the antigens are incubated with a primary antibody, washed and then incubated with a secondary antibody which is conjugated with an enzyme (e.g., alkaline phosphatase, peroxidase). After removing the excess, unbound secondary antibody, an enzyme substrate coupled to a suitable chromogen is used to develop a color reaction. Alternatively, the secondary antibody is biotinylated

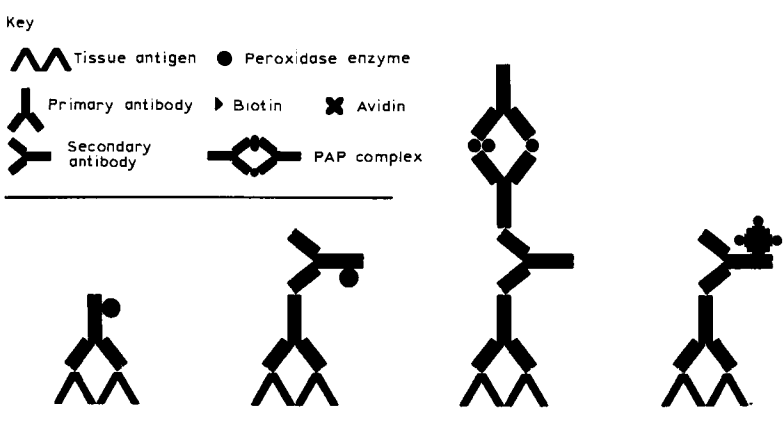

Fig. 4.17. Staining of antigens after blotting by different immuno-techniques. A: by direct coupling with a primary antibody tagged with peroxidase; B: by reaction with a primary antibody and subsequent coupling with a peroxidase-labelled secondary antibody; C: by coupling first to a primary, followed by a secondary antibody and finally by a PAP complex; D: by coupling first to a primary, followed by a biotinylated secondary antibody and final reaction with avidin (by courtesy of Eastman Kodak Company).

and is then made to react with avidin linked to peroxidase. The advantage of these reactions is that they reach very high sensitivities, equalling and even surpassing that of radioisotopes, but without all the drawbacks connected with radiolabelling, such as disposal of noxious isotopes, and long exposure times in autoradiography. In cases in which blotting is done on native enzymes, which however do not yield a colored product which can be precipitated in situ, a technique employing 'auxiliary enzymes' has been described (Sock and Rohringer, 1988). By this method, the 'auxiliary enzymes' are pre-immobilized on membranes of nitrocellulose or positively charged nylon and the reaction they catalyze is coupled with reduction of tetrazolium salt to yield colored formazan on areas of the transfer membrane occupied by the blotted enzyme. For example, different oxidases (glucose, L-amino acid, xanthine, malate oxidases) were used as auxiliary enzymes to detect blotted invertase, leucine amino peptidase, purine nucleoside phosphorylase etc. Fig. 4.17 summarizes some examples of these methods, which are reviewed in more detail in Dunbar (1987).

4.12. General experimental aspects

There are some controversial aspects of 2-D maps which require comment.

Exponential vs linear porosity gradients. At the beginning of 2-D mapping, most porosity gradients in the SDS dimension were exponential, the reason being to allow more space for separation in the lower to medium M_r region, where polypeptides are most abundant (Gianazza and Righetti, 1980). In fact Fig. 4.12A and B shows only exponential gradient devices. Today, this has been largely abandoned: almost all users have adopted linear porosity gradients. Besides being much simpler to cast, these gradients also offer more reliable M_r measurements (Rothe and Maurer, 1986; Rothe, 1988).

Gradient vs non-gradient gels. Some authors have completely abandoned porosity gradients in the 2nd dimension SDS gel slab (Hochstrasser et al., 1986b). Their patterns seem to be quite acceptable; however, since the proposed modification has been applied to only one type of separation (human sera) it may not be

of general applicability. In principle, porosity gradients should offer tighter and less diffuse spots, since the leading edge of the zone will, at any time, be migrating into a slightly higher % T region and thus should be more decelerated than its rear boundary. This should automatically produce sharper spots. In addition, gradient gels should prevent loss of small M_r polypeptides in a prolonged run; therefore, for highly heterogenous samples and long migration times, perhaps one should not abandone porosity gradients.

Stacking vs non-stacking gels. Some authors have also abandoned the use of discontinuous systems (Hochstrasser et al., 1986b) and apply the 1st-D gel directly to the running gel, without a stacking layer. I feel however that, especially in IPG gels were the protein forms a salt with the surrounding Immobilines in the pI zone, a stacking gel layer will be imperative, since the protein could be electroeluted slowly with time, rather than by an on bloc mechanism, and this will automatically provoke vertical streaking. Curiously, the same authors do not even add any SDS to the running gel (instead of the customary 0.1%) and yet they obtain good 2-D maps. Again, there is no way to indicate if this can be generally applied.

Equilibration vs non-equilibration. Some authors (Hochstrasser et al., 1986b) also omit the pre-equilibration step in the SDS-denaturing solution, which seems to be universally adopted. Apparently the proteins in the IPG gel (which however is a tube gel rather than a flat strip) are saturated by the SDS running in from the anodic compartment at the starting of the run. It must be stated, however, that these authors use 1% SDS in the electrolyte buffer, instead of the usual 0.1% level; this could be the secret of the success. If this technique could prove of general applicability, it could be of great interest, since it is known that, during the equilibration step, focused protein zones are both lost and subject to diffusion. Here great care should also be taken when using IPGs, again due to the fact that the proteins are bound to the matrix in the pI zone and certainly the absorbed SDS during the equilibration would help to loosen the bond. One way to reduce lateral band diffusion during equilibration in SDS, could be to add 30% glycerol, as suggested by Görg et al. (1988b). In any event, the equilibration time should be

reduced to a minimum, not more than 20 min. All the above is to indicate that, in principle, any short cut can be taken but there may be a price to pay. Carefully controlled experiments should be performed before abandoning the trodden path. For example, when curtailing the SDS equilibration step, it is essential to recover the 1st dimension gel and subject it to silver staining, to see how much protein has never left the gel.

Thickness of the 2nd-D gel. Most authors have adopted, for the SDS gel run, a gel thickness of 1 to 1.5 mm. In fact, most silver stain recipes are also adapted for this kind of gel thickness. In general, the thickness of the 2nd-D gel should be slightly greater than that of the 1st-D gel, so that sliding the IPG matrix (which always tends to swell a bit in acqueous solvents) into the 2nd-D gel cassette should be facilitated. It is for this reason that we have adopted a 1-mm thickness for the IPG gel and 1.5-mm for the SDS gel. Obviously, if the 2nd dimension is run in open-face gels, these restrictions do not apply any more: in fact, Görg et al. (1988b), who run horizontal 2-D maps, use SDS gel slabs as thin as 360 μm.

Buffer storage. When running multiple gel slabs in large tanks, as much as 10 l buffer are used each time. We have found that it is not necessary to make it fresh each time, but that the same buffer can be re-used, with no detriment to the final pattern in the 2-D map, up to three weeks. It is important, however, that at the end of each run anolyte and catholyte are remixed, to prevent buffer-ion depletion. In addition, contamination by bacteria and moulds should be avoided, otherwise additional protein bands will start appearing in the map. For that, sodium azide (10 mM) is suggested.

4.13. Trouble shooting

The most common problems encountered in 2-D maps are as follows.

Horizontal streaking. This is due to a time-dependent phenomenon occuring during the 1st dimension (IPG), in general due to incomplete focusing time or precipitation and resolubilization cycles at the application point. Check the way the sample has been applied: remember that anodic sample application is far better

than cathodic loading. Check if the pattern is improved by diluting the sample and applying it at time intervals, or by adding CAs to it (up to 2–3%). Check the initial voltage gradient: remember that low initial voltages are greatly beneficial to sample entry (Righetti et al., 1988e). Make sure that the sample does not contain particulate material to start with. In case of incomplete solubilization, it is necessary to clear the solution by a short centrifugation step at high speeds. Particulate material already present in the sample at the start of the experiment will clog the gel pores and favor additional co-precipitation of even soluble proteins. When dealing with samples rich in nucleic acids, check that DNAase and RNAase have been added to remove them by hydrolysis. If all the above steps have been done properly, check that enough running time has been allowed for reaching a steady-state pattern. Remember that (especially in the absence of CAs) IPGs are indefinitely stable so that the focusing time can be prolonged even for days.

Vertical streaking. This indicates incomplete sample solubilization during the SDS equilibration step. Check that the SDS is not precipitated by some additives present in your gel. SDS can also be precipitated by low temperatures. In this case, the Li salt has much higher solubility than the Na salt. The detergent present in the IPG dimension can form mixed micelles with SDS and CAs and give blurred patterns in the SDS-gel. A remedy is to fix the IPG gel in ethanol-acetic acid, washing away the detergent and then equilibrating in SDS buffer (Gianazza et al., 1986d). Alternatively (Görg et al., 1988b) the amount of detergent in the IPG gel can be lowered from the usual 2% level down to only 0.5% (but the normal high level should be used during the sample solubilization step!). If all the above fails, try to lengthen the equilibration time.

Surface streaking. Also called point or vertical micro-streaking, this phenomenon seems to be connected with the use of the thiol-reducing agent present in the 1st dimension gel (remember that if the sample is applied at the cathode the thiol agent will be ionized and effectively migrate in the gel) and/or in the equilibration step. According to Görg et al. (1988b) this can be minimized or completely eliminated by adding, after reduction with DDT (65 mM in their work), an excess of iodoacetamide (260 mM), which will destroy the excess of DTT present in the reaction mixture.

Horizontally elongated spots. Most certainly this is due to a poor contact between the 1st and 2nd dimension gels. For example, if in the contact area some cementing agarose is interposed between the IPG and the SDS gels, during the migration out of the IPG matrix the polypeptide zones will be able to diffuse in the large pore size agarose layer. Check that the 1st-D gel is tightly pressed against the 2nd-D during agarose gelation. If using IPG gel strips, check that the strip is cut flash with the underlaying plastic foil and that the cut is even.

Vertically elongated spots. This could be due to a too wide 1st dimension IPG strip. We prefer, for a proper stacking process, to reduce the 1st dimension gel width to 3 mm. The other cause for this phenomenon could be a stacking gel too short, impeding proper formation of the isotachophoretic train. Remember that, as the IPG gel strip is applied to the 2nd-D gel, the bands appear as vertical lines, and their width has to be reduced to a dot-size in the stacking gel. Accordingly, lengthen the stacking gel and/or use lower inital voltage gradients.

Spot streaking. This phenomenon seems to be connected with the use of SDS gels backed by a plastic foil. It seems that, in Gel Bond PAG production, some substances stick to the surface and provoke distortions of that part of the protein zone migrating next to it. The solution is found simply by washing the Gel Bond PAG (6 times for 10 min) in distilled water just prior to use. This phenomenon could be troublesome also during the IPG run, so check your Gel Bond there too!

Highly diffused spots. This could be due to sample overloading. Check that and reduce the protein load accordingly. Even in a highly heterogeneous sample, with silver staining or isotope labelling, often as little as 20 μg total protein load suffice for detection of all but the very least abundant spots. The other cause of that could be joule heating during the run. Most SDS runs are performed at room temperature. If done in plastic containers, there might not be sufficient heat exchange. In other cases, the entire gel slab containing the running gel is submerged in the cathodic buffer, which thus provides some cooling action. In the latter case, buffer recirculation with a magnetic stirrer could ameliorate the situation. Try running the gel at lower amperage, if needed. In general, we

prefer not to apply more than 50 mA per single slab (14 × 16 cm, 1.5 mm thick).

4.14. Examples of some applications

While this section cannot possibly report all possible applications of 2-D maps, I will list here some applications in different fields, just to show the great potential and versatility of 2-D maps. It should be appreciated that most of the examples here reported refer to conventional 2-D maps, i.e., those maps which utilize soluble carrier ampholyte buffers in the 1st-D. Clearly, the data, if repeated in IPGs, should give similar results and (hopefully) much better resolution and reproducibility in spot position.

4.14.1. Analysis of wheat endosperm and plant proteins

High-resolution 2-D maps have been applied to the analysis of endosperm proteins and used to determine the chromosomal location of a number of different proteins in aneuploid strains of wheat (Brown and Flavell, 1981; Brown et al., 1981; Holt et al., 1981; Gabriel and Ellingboe, 1982; Jackson et al., 1983; Dunbar et al., 1985; Anderson et al., 1985). Prospectively, 2-D mapping of the parent strains and the cultivar registered would define the variety at the outset and would suggest the parental origin of each electrophoretic variant seen. Once a cultivar is defined by 2-D mapping, then it is a simple matter to follow changes occurring with time by mapping small numbers of kernels obtained from many different locations. When a data base of 2-D maps of wheat proteins becomes available, it will be easier to identify contaminating kernels or their genes, to discover new proteins arising from adventitious crosses, and to identify the sources of such accidentally introduced genes (Anderson and Anderson, 1987).

More recently, the applications of 2-D analyses of plant proteins have been reviewed and they include: genetic analysis of organ-specific maize (Goday et al., 1988) and pea (de Vienne et al., 1988) proteins; storage proteins in alfalfa (Krochko and Bewley, 1988); leaf proteins from Barley (Görg et al., 1988); analysis of cereal

prolamins (secalins, gliadins, hordeins, avenins) (Shewry et al., 1988); pollen (from maize) and fungal proteins (Marlow et al., 1988); proteins from tobacco mesophyll protoplasts (Meyer et al., 1988); proteins from seeds of Poaceae (Triticum, Hordeum, Secale) and Fagaceaea (Castanea, Quercus) (Garcia-Olmedo et al., 1988); proteins from barley roots grown under different stress conditions (Hurkman and Tanaka, 1988) and in spinach associated with a cold-acclimation process (Guy and Haskell, 1988).

4.14.2. Serum and plasma proteins

The proteins of normal human plasma and serum have been extensively characterized by 2-D PAGE (Tracy et al., 1982a,b; Anderson and Anderson, 1977; Marshall et al., 1984). Serum protein patterns have been screened by 2-D PAGE in a number of clinical syndromes. Changes have been observed in muscle trauma (Tracy and Young, 1984) in myocardial infarction (Gomo et al., 1983), in cases of alcohol abuse (Marshall et al., 1984) and after chemical exposure (to carbon tetrachloride, trichloroethylene, dimethylformamide; these data refer to rat sera) (Marshall and Vesterberg, 1983; Marshall et al., 1985).

4.14.3. 2-D maps of urines and other body fluids

Reference maps are now available for normal human urines and for such disease conditions as prostatic adenocarcinoma (Edwards et al., 1982a), multiple myeloma (Edwards et al., 1982b), occupational exposure to cadmium (Marshall et al., 1985b), rheumatoid arthritis (Clark et al., 1980) and renal disease (Frearson et al., 1981). A number of other body fluids have also been analysed; they include: cerebrospinal fluid (Harrington and Merril, 1984; Harrington et al., 1984; Wiederkehr et al., 1985; Bergenbraut et al., 1986), semen (Tracy et al., 1982), prostatic fluid (Dermer et al., 1982), amniotic fluid (Burdett et al., 1982),saliva (Marshall and Williams, 1986), sweat (Rubin and Penneys, 1983), aqueous humour (Segers et al., 1984) and suction blister fluid (Jellum and Thorsrud, 1982). They all seem to express a common set of serum components, together with tissue-specific proteins.

4.14.4. 2-D maps in genetic disease

2-D analysis can be instrumental in searching for altered gene products in protein samples of whole cells and tissues from patients suffering from such disorders. For example, in human fibroblasts a mutation in the β-actin gene has been discovered in neoplastic transformation (Leavit et al., 1982). Alterations in 2-D gel profiles (both qualitative and quantitative) associatied to a number of disorders have been described. They include: (a) Duchenne muscular distrophy (Patel et al., 1986; Hughes et al., 1986); (b) Ataxia-Telangioectasia (Murnane and Painter, 1983); (c) Lesch-Nyhan syndrome (Merril et al., 1981); (d) trisomy 21 (Down's syndrome) (Van Keuren et al., 1982; Klose et al., 1982); (e) Joseph disease (Rosenberg et al., 1979); (f) Tangier disease (Visvikis et al., 1986) and (g) cystic fibrosis (Kirkpatrick et al., 1985).

By necessity, this is only a very limited survey of some of the applications of the vast field of 2-D analysis. More information can be found in recent reviews and books specifically dedicated to these topics (Dunn, 1987a,b; Galteau and Siest, 1986; Celis and Bravo, 1984; Dunbar, 1987). Some groups are involved in the heroic effort of establishing databases of protein information derived from the analysis of all the spots in 2-D gels. For example, Celis' group in Aarhus (Celis et al., 1988) is building such data bases for transformed human amnion cells (AMA) and peripheral blood mononuclear cells (PBMC). These authors have assembled a catalogue of a total of 1781 [^{35}S]methionine labelled AMA proteins (1274 separated by IEF, 537 by NEPHGE, i.e., non-equilibrium IEF for alkaline spots) and a catalogue of a total of 1311 spots from PBMC (948 by IEF, 363 by NEPHGE). The information entered in the data base includes: molecular mass, protein name, HeLa protein catalogue number, mouse protein catalogue number, nuclear proteins, phosphorylated proteins, distribution of proteins in Triton X-100 supernantants and cytoskeletons, proliferation- and transformation-sensitive proteins, cell-cycle specific proteins, mitochondrial proteins, proteins matched in normal human embryonal lung MRC-5 fibroblasts and PBMC cells, heat shock proteins, proteins affected by interferons, cytoskeletal proteins, and the presence of antibodies against proteins in human sera. To be

sure, these tables resemble a bit Gruyère cheese, in that holes due to lack of information are quite frequent. But this is a blessing, as it guarantees to the younger generations that there is still plenty of work to do in life sciences.

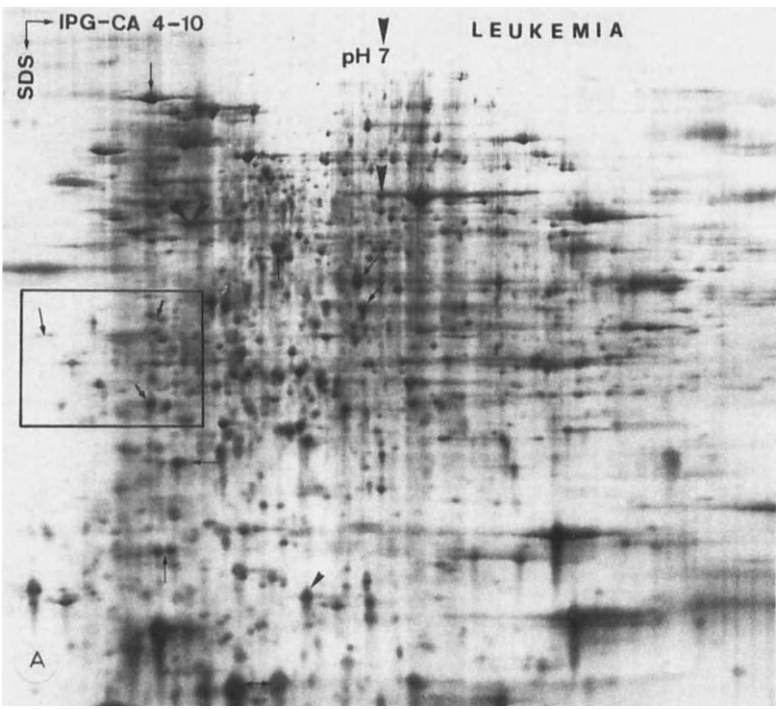

Fig. 4.18. Horizontal 2-D electrophoresis of leukemia proteins in (A) IPG pH 4–10 gradient and (B) IPG pH 4–7. In both gels, the 1st-D strip (4% *T*, 4% *C*) contained 8 mM urea, 0.5% NP-40 and 0.5% CA over the pH 4–10 (A) or pH 4–7 (B). The sample was dissolvd in 9 M urea, 2% NP-40, 2% β-mercaptoethanol, 2% Ampholine pH 3.5–10 and 8 mM protease inhibitor (phenylmethylsulphonyl fluoride). Sample application: 20 μl (100 μg total protein) 5 mm from the anodic side. The IPG gel strip was 5 mm wide. 1st-D: 1 h at 300 V, followed by overnight focusing at 3000 V, 15°C. 2nd-D: stacking gel at pH 6.8 in 125 mM Tris–HCl and 0.1% SDS; running gel: 12–17% *T* in Tris–HCl at pH 8.8. Run at 200 V for 2 h and then an additional 6 h at 600 V, after removal of the 1st-D IPG strip. The boxed area shows improved resolution in the 2-D map when narrowing the IPG gradient from pH 4–10 to pH 4–7. The double arrow indicates actin. Silver stain (from Görg et al., 1987b; by permission from VCH).

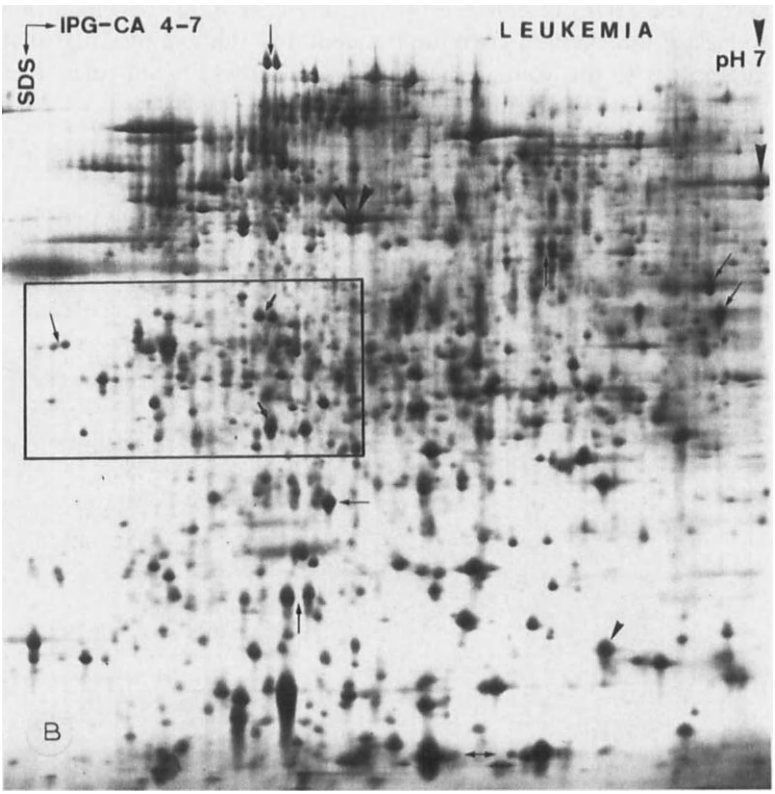

Fig. 4. 18 (continued).

4.15. To be or not to be?

I should like to end this chapter with a pharaphrase of the famous motto of Hamlet: 'to be or not to be' (there)?. So far you have only seen a lot of recipes and recommendations, but you might still wonder whether it will be a good idea to be there, i.e., if it is worthwhile to adopt the IPG technique in your routine work. Like any other transplant, trasferring IPGs in your lab might be too costly and time consuming. Is it worth to take the risk? I will not

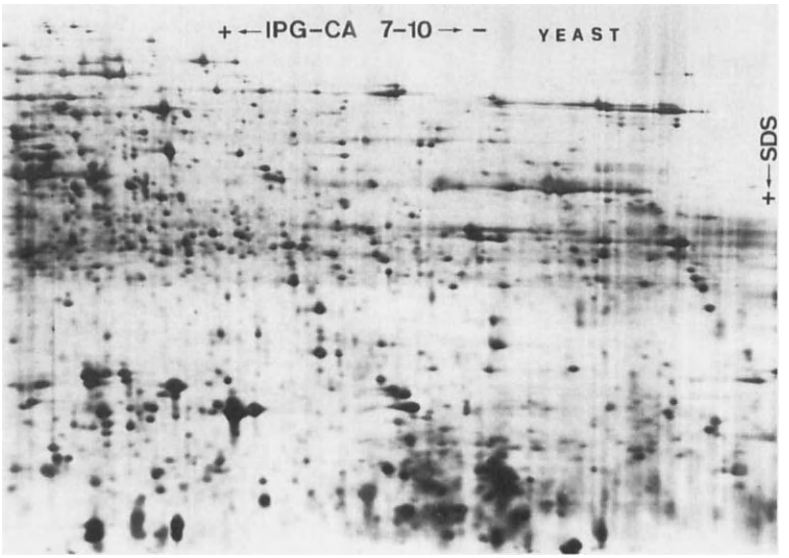

Fig. 4.19. Horizontal 2-D electrophoresis of alkaline yeast cell proteins using IPG CA 7–10 at the steady-state. First dimension: IPG with 0.5% CA, 8 M urea and 0.5% NP-40. Running conditions: 300 V for 1 h, 5000 V_{max}, 2 mA_{max} and 5 W for 18 h. Gel length: 18 cm. The equilibration buffer contained 6 M urea and 30% glycerol. 2nd-D: SDS pore gradient gel, 0.5 mm thick on Gel Bond PAG film. Running gel: 12–15% *T*, 4% *C* in 375 mM Tris–HCl, pH 8.8. Stacking gel: 8% *T*, 4% *C*, 125 mM Tris–HCl, pH 6.8. Silver stain (from Görg et al., 1988a; with permission from VCH).

answer your question, but just present you with the 2-D separations of Figs. 4.18 and 4.19. Compare this patterns with the thousands of published 2-D gels and decide by yourself!

Preparative aspects of immobilized pH gradients

5.1. *Introduction*

Guidelines will be given on the preparative features of immobilized pH gradients, which even in the preparative scale appear to be the most powerful fractionation technique in electrophoresis. The following aspects will be illustrated: (a) explorative runs aimed at defining the load capacity; (b) optimization of experimental parameters, such as ionic strength (I), pH gradient width, and gel thickness; (c) general considerations on the load ability and ionic strength of the milieu; and (d) protein loads as a function of % T in the matrix.

At the methodological level, the following procedures will be detailed: (a) casting of soft and thick Immobiline gels; (b) recovery of protein zones from Immobiline gels by elution into hydroxyapatite beads; (c) recovery by electrophoretic transfer into ion-exchange resins; and (d) the Immobiline-canal technique, with automatic fractionation and recovery in the same gel matrix. At the end of the chapter the latest in preparative work will be presented and will include the idea of 'segmented Immobiline gels' by which the protein of interest is kept isoelectric in the recycling liquid phase, the impurities being focused into anodic and cathodic IPG segments. The latter procedure has been refined into the concept of 'isoelectric, buffering Immmobiline membranes'.

The load ability in IPG gels has been demonstrated to be at least 10 times higher than in conventional isoelectric focusing (IEF) gels, just like at the analytical level, where IPGs seemed to afford a resolution 10 times higher than in CA-IEF. Such a load ability, as we will see, is quite remarkable and matches and even surpasses the load limit of isotachophoresis (ITP) (Svendsen, 1979). According to

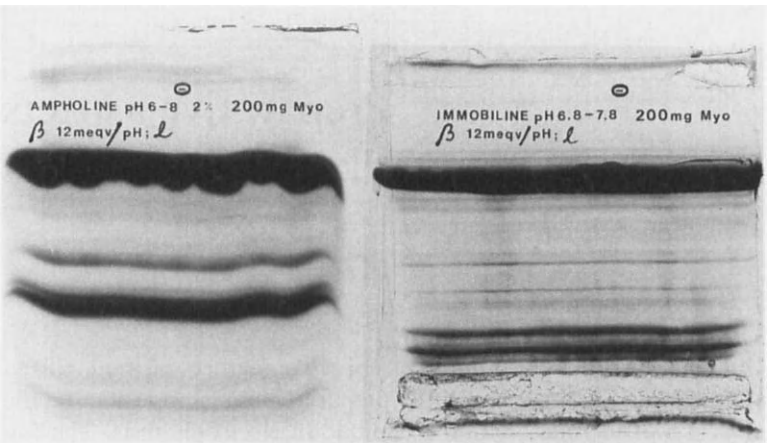

Fig. 5.1. IEF of horse heart myoglobin (Myo) in 5-mm thick polyacrylamide gels. Left: Ampholine gel, field strength 80 V/cm. Right: Immobiline gel at a field strength of 250 V/cm. In both cases, focusing overnight. In order to obtain the same pH slope, since the IPG gel was 1 pH unit wide and the carrier ampholyte buffers 2 pH unit wide, the latter gel was made twice as long as the IPG gel. Only the cathodic half, corresponding to the Immobiline pH gradient, is shown of the CA-IEF gel. Both gels have the same buffering power (β) and the same % T and % C (from Ek et al., 1983; with permission from Elsevier).

this author, ITP can offer high sample loads (75 mg protein/cm^2 per band) at high resolving power, definitely better than CA-IEF. This high sample load is believed to be strictly correlated to the fact that in ITP usually proteins are separated at operational pH values far removed from the pI, so that isoelectric (or near isoelectric) precipitation does not occur (this being the major drawback of preparative CA-IEF runs). IPGs can perform even better than that, in fact with the segmented Immobiline procedure there is virtually no limit to the load capacity of the technique. Fig. 5.1 offers a view of the load capacity of a CA-IEF and a IPG gel, run under identical conditions (same % T, same pH slope, same buffering power, same load). It can be seen that, in CA-IPG gels, as soon as the protein load reaches a critical level, the zones are heavily distorted (the pH gradient is distorted too, in fact) and zone instability shows up as droplets of protein precipitates. On the contrary, the facing IPG gel does not show any disturbance at all.

Clearly, given that the β power and pH gradient slope are identical in both gels, there must be some hidden property of IPG gels that renders them just right for high protein loads.

5.2. *Theory*

While in the past, in preparative electrophoretic or IEF runs, most separations have been performed by trial and error, with no real knowledge of the capacity of the system, it is now possible in IPGs to predict theoretically and from a few analytical runs the load capacity of the system compatible with a given degree of resolution. The various parameters needed for optimizing a preparative IPG run are discussed below.

5.2.1. Prediction of acceptable protein loads in IPGs

For practical preparative work, an equation has been derived correlating the maximum protein load in a single zone to the pI (isoelectric point) distance (ΔpI) with the nearest contaminant and to the slope of the pH gradient. The equation is:

$$M = \left(\frac{\Delta pI}{d(pH)/dx} - L \right) \cdot 2C_M \cdot A \qquad (1)$$

where M = protein load in a single zone (major component) in mg; ΔpI = pI difference between major component and nearest contaminant (in pH units); $d(pH)/dx$ = slope of the pH gradient along the separation track (pH units/cm); L = protein free space, between the major band and the impurity, that is needed to cut the gel without loss of protein or without carrying over the impurity (in general, at least 1 mm is an acceptable distance); C_M = average concentration in the focused zone of the major component (mg/ml); A = cross-sectional area of the gel perpendicular to the focusing direction (in cm^2) (Ek et al., 1983).

It can be seen that the protein load can be maximized by increasing A (the liquid volume available to the focused zone) and by decreasing the slope of the pH gradient (i.e., by focusing in narrow or ultra-narrow pH gradients). Interestingly, Rilbe and

Pettersson (1975) have reached similar conclusions when calculating the maximum tolerated load in conventional CA-IEF, in columns supported by a linear density gradient. According to these authors, the theoretical mass content of a protein zone (M) in sucrose density gradients ranging from 0 to 0.5 g/cm, cannot exceed the following inequality:

$$M < 0.625\, V r^2 \text{ g/cm}^3 \tag{2}$$

where V is the total column volume and r is the zone breadth. Thus, the dependence of protein load on the volume available to the protein once focused in a single zone is clearly recognized in both equations. By further developing Eq. (2) and combining it with the Eq. giving the resolving power of IEF (Eq. 22 in Chapter 2), Rilbe and Pettersson (1975) have derived an inequality in which the mass load of the protein zone is related to the resolving power, as follows:

$$M < \frac{45qD^2(\mathrm{d}c/\mathrm{d}x)}{E^2(\mathrm{pI})^2[\mathrm{d}u/\mathrm{d}(\mathrm{pH})]^2} \tag{3}$$

which bears some similarites with Eq. 1. On the basis of Eq. 1, as a guide, Ek et al. (1983) have constructed a graph correlating these three basic parameters: protein load in a single zone, ΔpI between the band of interest and nearest contaminant and slope of the pH gradient along the separation axis [d(pH)/dx]. This graph is essentially a plot of Eq. (1), taking as a concentration limit (C_M) a common upper limit experimentally found of 40 mg/ml (in reality, as shown ahead, this 'solubility' limit depends on % T; in a 2.5% T matrix, the C_M value can be as high as 90 mg protein/ml gel phase). Fig. 5.2 shows how the graph is laid out: the abscissa reports the ΔpI value (in pH units), and the ordinate the protein load (mg/cm^2) for a given A value. The ΔpI vs. protein load plane is cut by lines of different slopes representing pH gradients of different widths along the IPG gel length. It is seen that ultranarrow pH gradients (e.g., 0.02 pH units/cm) allow for extremely high protein loads (up to 80 mg/cm^2), while still retaining a resolution better than ΔpI = 0.01. At the opposite extreme, broad pH gradi-

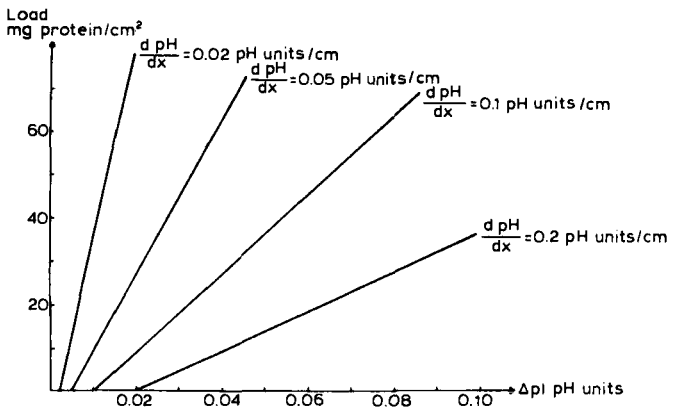

Fig. 5.2. Acceptable protein load (mg/cm^2) as a function of ΔpI for different pH slopes plotted for a mean concentration of 45 mg/ml in the major protein zone. This is a graphical representation of Eqn. (1) (from Ek et al., 1983; by permission from Elsevier).

ents (e.g., 0.2 pH units/cm) would allow a resolution of only $\Delta pI = 0.1$ with a protein load of less than 40 mg/cm^2.

It would be of interest to compare the load ability of the three major electrophoretic systems in use today: CA-IEF, ITP and IPG. No theoretical study is available, but some experimental values can be found in the literature. Thus Radola (1975), by CA-IEF in Sephadex-stabilized layers, has found an upper load limit of ca. 10–12 mg protein/ml gel suspension, with a resolution comparable to that of the same analytical system. Chrambach (1980) has reported upper load limits for different electrophoretic techniques. Thus, for PAGE, the upper limit seems to be 0.1 mg component/cm^2 of gel, while that of CA-IEF is 1–2 order of magnitude higher, and that of ITP 2–3 orders greater than that of PAGE. Thus, maximum protein loads in IEF should be of the order of 1–10 mg of component/cm^2 of gel, while that of ITP should be in the range of 10–100 mg. In general, it seems to be difficult to focus (IEF) or to stack (ITP) more than 100 mg protein/ml in a single zone, because at such high concentrations proteins withdraw water and salt from the medium to such a degree that voltage gradients across the protein zones increase enormously, with concomitant heat

denaturation. Presumably the conductivity within the protein zone becames so low because the buffer constituents and solvent are largely protein bound. Interestingly, the only system which has approached this upper limit is only IPG; in IEF, rarely loads greater than 10 mg/ml have been reported. In ITP, curiously, notwithstanding the much larger protein load-ability reported, in fact only minute amounts of proteins have usually been separated. For example, Brogren and Peltre (1977), who have proposed a flat-bed ITP technique in Sephadex G-75 layers, have separated 40 mg total load of a γ-globulin fraction in a 20×20 cm plate containing 100 ml of gel (30 mM phosphate as leading, 5-amino caproic acid as terminating electrolytes). Considering the high heterogeneity of the applied sample, no more than 2–3 mg protein were present in each zone. There is only a single report (Bier and Kopwillem, 1977) in which fractionation of 2 g plasma proteins was attempted in a Sephadex G-200 bed, in a vertical column (20 cm height, 2.5 cm diam.) with either 20 mM cacodylic acid (pH 8.1) or 20 mM glutamine (pH 8.6) as leading ions and 5-amino caproic acid as terminating electrolyte.

5.2.2. Optimization of environmental parameters

We have performed a thorough study on the optimization of environmental parameters [I (ionic strength), gel thickness, pH gradient width] for maximizing protein loads in Immobiline matrices. These aspects are summarized in Fig. 5.3. By increasing the ionic strength of the gel from 1.25 to 7.5 mequiv./l, a 4-fold increment in load capacity is obtained; above this level, a plateau is abruptly reached around 10–12 mequiv./l. By increasing the gel thickness from 1 to 5 mm, a proportional 5-fold increment in protein load ability is achieved. Although the system does not level off, a 5 mm thickness seems to be optimal because thicker gels would begin to develop thermal gradients in their transverse section, generating skewed zones. Finally, by progressively decreasing the width of the pH interval, there is a linear increase in protein load capability. Here too the system does not reach a plateau. Because of the very long focusing times required by narrow pH

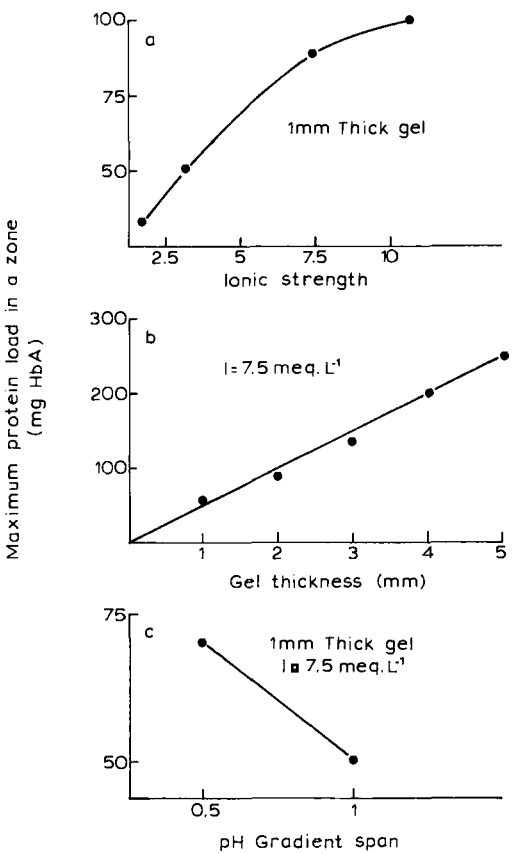

Fig. 5.3. Loading capacity of IPGs. The maximum load in a single protein zone is plotted: (a) as a function of gel thickness at constant ionic strength in a 1 pH unit interval; (b) as a function of gel thickness at constant I in a 1 pH unit interval; (c) as a function of pH gradient width at constant I and constant gel thickness (from Gelfi and Righetti, 1983; with permission from Elsevier).

gradients, aggravated by the high viscosity of protein zones at high loads, it is suggested that fractionation of large protein amounts in pH ranges narrower than 0.5 pH units should not be attempted (Gelfi and Righetti, 1983).

5.2.3. General considerations on the load ability and the ionic strength of the milieu

We have seen above that IPGs have a load ability at least 10 times higher than conventional IEF. I believe this is mostly due to differences in the ionic strength (I) of the two systems. At the very low I values typical of CA-IEF (ca. 1 mequiv./l) (Righetti, 1980) macromolecules will have a very low solubility minimum, and will tend to aggregate and flocculate. An increase of I, ca. 7–10 mequiv./l, as characteristic of IPGs, is thus beneficial since according to the Debye-Hückel equation:

$$-\log \gamma = \log(S/S_o) = 0.51\, Z^2\sqrt{I} \qquad (4)$$

where γ is the activity coefficient of an ion of charge Z, S and S_o are the solubilities of a protein at the pI and at a given ionic strength and as extrapolated to zero ionic strength, respectively. Thus, as the environmental I increases, and the γ values of the ions (both in solution and in the protein) decrease, the protein solubility increases: this is the well-known 'salting in' effect described already in 1936 by Cohn. Because of this I like to equate IPG gels to 'salting in' media and IEF gels to 'salting out' milieus. It might be argued that, as long as the proteins precipitate at their pI, and this material is confined in the isoelectric zone, this should not affect the load capacity in gel matrices, since the precipitate zone is gravitationally stable. This would not be so in the old preparative technique using sucrose density gradients, in vertical columns, where the flocculated material would slowly begin to sediment toward the bottom of the column (Righetti, 1983a). In real cases this does not quite happen. As demonstrated by Grönwall (1942), the solubility of an isoionic protein, plotted against pH near the isoionic point, is a a parabola, with a fairly narrow minimum at relatively high I, but with progressively wider minima, on the pH axis, at decreasing I values.

This phenomenon can be appreciated from Fig. 5.4 (Grönwall, 1942). On the one hand, by increasing the environmental ionic strength from 1 to 20 mM NaCl, the solubility of β-lactoglobulin, at a given pH (ca. 5.3, very close to the pI value), increases by a

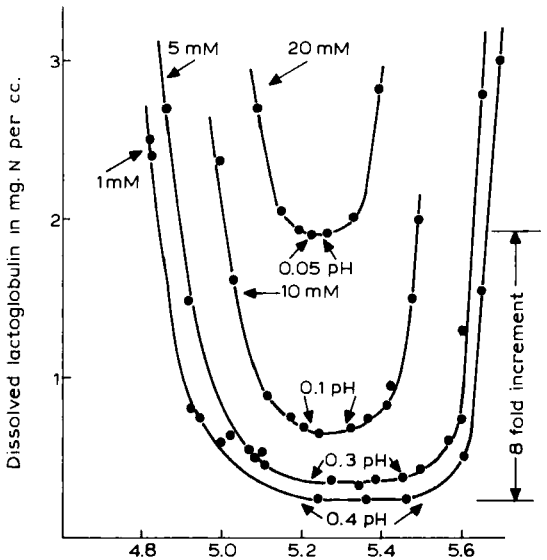

Fig. 5.4. Solubility of β-lactoglobulin in the pH range 4.8–5.6 as a function of the ionic strength of the environment, from 1 mM to 20 mM NaCl. The amount of protein dissolved has been determined as Kjeldhall nitrogen. The pH values on the parabolas give the span of the solubility minimum, centred on a theoretical pI of 5.3 (modified from Grönwall, 1942).

factor of eight. As a second phenomenon, it can be seen that, at moderately high ionic strength (20 mequiv./l), all the protein molecules tend to be isoelectric at a precise point on the pH axis, while at low I values (1 mequiv./l) they are smeared over as much as 0.4 pH unit. For easier appreciation, I have replotted these physical phenomena in the two following graphs: the dependence of the solubility of the isoelectric protein from the environmental ionic strength is depicted in Fig. 5.5, while the width of the apparent pI zone on the pH axis, as a function of the I of the milieu, is plotted in Fig. 5.6, and is seen to vary in a funnel-shaped fashion. It can be seen that, at the prevailing I values typical of conventional IEF (1 mequiv./l), the solubility minimum of β-lactoglobulin spans a 0.4 pH unit interval, while, in IPGs (average $I = 7–10$ mequiv./l, but easily adaptable to any other I value) the pH width of solubility minima is strongly decreased in a funnel-

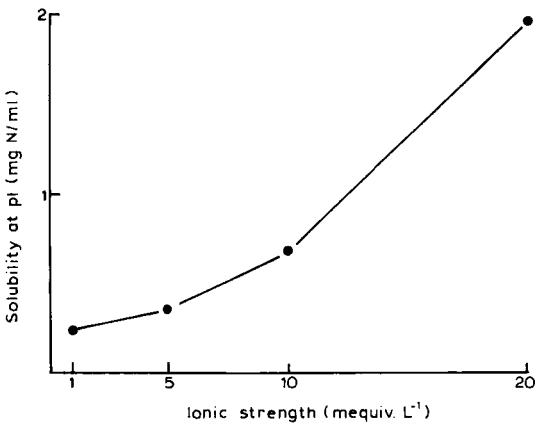

Fig. 5.5. Plot of solubility at pI vs. ionic strength of the milieu for β-lactoglobulin. Data from Fig. 5.4. The solubility increases by a factor of 8 for a 20-fold increase in ionic strength (Gelfi and Righetti, unpublished).

shaped fashion down to only 0.05 of a pH unit. In other words, what is detrimental in conventional, preparative IEF runs is not isoelectric, but near-isoelectric precipitation. The precipitate is not

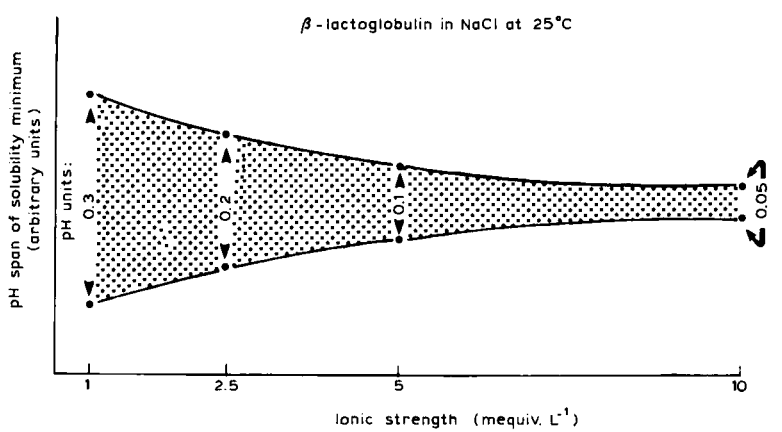

Fig. 5.6. Solubility of a protein in the neighborhood of its pI as a function of the ionic strength of the milieu. At 1 mequiv./l (conditions prevailing in CA-IEF), β-lactoglobulin has a minimum of solubility over a span of > 0.3 pH units; the width of the solubility funnel is markedly decreased at high I values (it is only 0.05 pH unit at 10 mequiv./l, values typical of an IPG milieu) (from Gelfi and Righetti, 1983; with permission from Elsevier).

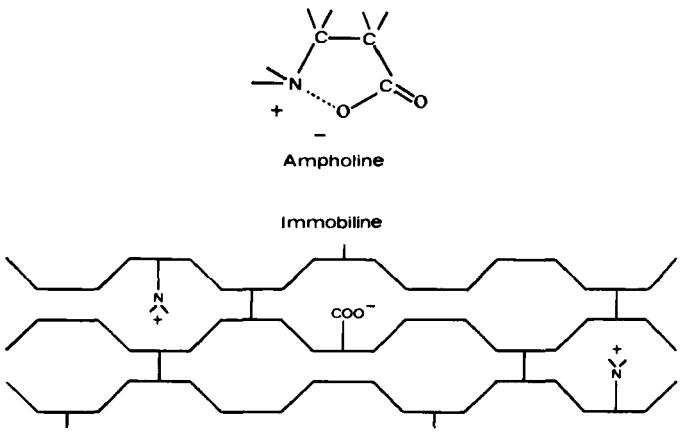

Fig. 5.7. Comparison between ionic strength in Ampholine and Immobiline gels. The upper drawing depicts a segment of an isoelectric Ampholine molecule, while the lower sketch shows a portion of an Immobiline gel. An Ampholine molecule, at its pI, is likely to form an inner salt, which does not contribute to the *I* of the system. The fixed charges in the Immobiline gel, being spaced ca. 50 carbon atoms apart, are believed to behave as point charges in the surrounding space, thus effectively contributing to the *I* of the milieu (from Righetti et al., 1983a; by permission from Elsevier).

confined at the pI position, but is usually smeared over as much as 0.5 pH unit interval, thus being completely detrimental to the resolution of adjacent species. But why, if we have the same molarity of CA-buffers in a gel, or of Immobiline buffers (e.g., a 2% Ampholine gel is ca. equivalent to a 10 mM IPG gel) should there be such a strong difference in the *I* value of the two systems? A potential reason for that is explained in Fig. 5.7: an isoelectric carrier ampholyte molecule, being totally in the form of an inner salt (upper drawing), is completely unable to contribute to the *I* of the solution (only its anionic and cationic species, in equilibrium with the zwitterionic form, will generate any *I* value in the milieu). On the contrary, in an IPG matrix (bottom drawing; in a conventional 4% *T*, 4% *C*, 10 mM Immobiline gel) the grafted ionizable groups, being ca. 50 carbon atoms apart in the polyacrylamide backbone, behave as point charges in the surrounding space, thus fully contributing to the *I* value of the milieu (Righetti et al.,

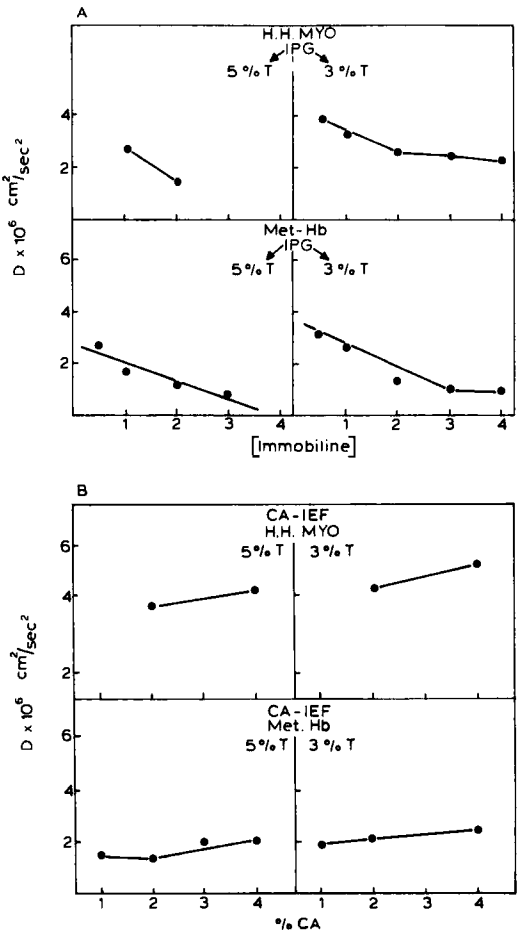

Fig. 5.8. Dependence of the apparent diffusion coefficient (D) of proteins on the Immobiline molarity in an IPG gel (A) or on the carrier ampholyte molarity in a CA-IEF gel (B). A: two upper graphs: D values of horse heart myoglobin (H.H. Myo) in a 5% *T* (left) and a 3% *T* (right) gel. Lower tracings: D values of oxidized hemoglobin (Met-Hb) in a 5% *T* (left) and a 3% *T* (right) gel. The values 1 to 4 on the abscissa (Immobiline concentrations) refer to multiples of the basic molarity (1), taken as 5 mM buffering ion. B: same as A, except that it refers to measurements of D values in CA-IEF gels (CA concentrations from 1 to 4%). Note the positive slopes in CA-IEF, as compared with the negative slopes in IPG gels (from Gelfi et al., 1987a).

1983a). On the basis of these considerations, in an IPG matrix, the protein possibly forms a salt with the surrounding charges in the gel, this greatly contributing to the increment of solubility. On the contrary, the basic concept of CA-IEF (Rilbe, 1973) is that a protein is both isoelectric and isoionic, the latter concept implying that it has to be stripped free of any other ion but the protons which it can bind or release in the pI zone. We now have an experimental proof of this binding mechanism to IPG gels. As shown in Fig. 5.8A, the apparent diffusion coefficients (D) of myoglobin and hemoglobin (Hb) decrease at increasing Immobiline molarities in IPG gels, both in 3% and 5% T matrices. On the other hand, the same proteins exhibit incremental D values at higher carrier ampholyte molarities in the gel (Fig. 5.8B). The reason for IPG matrices being 'salting in' media for isoelectric proteins is now clear: by providing counter ions (different from protons) to an isoelectric macromolecule and allowing for salt formation (concomitant with supplying higher ionic strengths) the protein solubility at the pI is greatly increased (Gelfi et al., 1987a).

5.2.4. Protein load as a function of % T in the matrix

We have seen that three parameters influence the loading ability of a gel (I, gel thickness, pH gradient width). In reality, there is a fourth, hidden parameter, perhaps even more important than the other three, which regulates the load ability in IPG matrices (and I believe in most preparative fractionations in gel systems). According to a theoretical article by Bode (1980) a gel is a visco-elastic matrix which can be imagined as a layer of parallel sheets each of which is composed of fluctuating polymer chains which are inserted into an unspecified backbone. Fluctuations due to thermal agitation are centred symmetrically around the median plane of each sheet. *These motions of polymer give rise to elastic forces directed towards any compact object which tends to invade the volume otherwise available to the polymers for molecular reorientation.*

We have seen above that, no matter how the experimental conditions are optimized, and the ionic strength is increased, a common upper load limit for all proteins investigated has been found, of ca. 40 mg protein/ml gel solution. The key to this

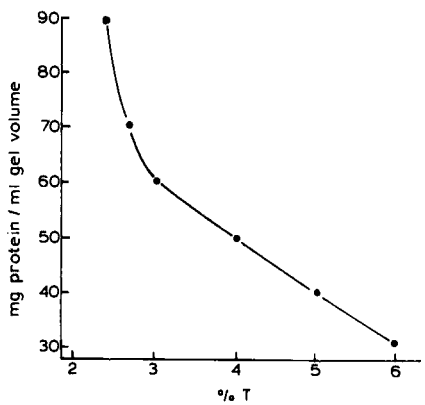

Fig. 5.9. Relation between loading capacity (in terms of mg protein/ml gel volume) and % T (T = grams of acrylamide and cross-linker per 100 ml gel volume) value of the gel matrix. Notice that, while in the range 3% to 6% T the protein load decreases linearly, in softer gels (C 3% T) it increases exponentially (from Righetti and Gelfi, 1984; with permission from Elsevier).

apparent 'solubility limit' is to be found in Fig. 5.9: the amount of protein accepted by a gel matrix is directly related to its composition (% T). The limit of 40 mg protein/ml gel is only valid for a 5% T polyacrylamide matrix: as the amount of fibers in the gel is decreased, progressively more protein can be loaded in the system, so that in a 2.5% T gel as much as 90 mg protein/ml gel can be applied (Righetti and Gelfi, 1984). This experimentally verifies the assumption by Bode (1980), but also introduces an additional parameter, i.e., competition for the available water in the gel structure. Basically, the 'invading' protein macromolecule and the polyacrylamide matrix supporting the 'invasion' are two hydrophilic polymers: both compete for water, and since (in a standard 5% T) the gel chains are one of the most abundant elements, they sequester and coordinate most of the available water, leaving little liquid volume for the protein to be dissolved in. Thus, as the total amount of matrix is decreased, two beneficial effects are obtained: (a) more free water becomes available for the protein, automatically increasing the 'apparent solubility limit'; and (b) the viscoelastic forces of the gel are weakened, allowing the osmotic forces in the protein zone to take over and draw more water from the

surrounding gel regions. This results in an additional increment in load ability within a given protein zone. In fact, given a certain pH slope along the separation axis [d(pH)/dx], a fixed ΔpI between a protein and the nearest contaminant, and a fixed voltage gradient

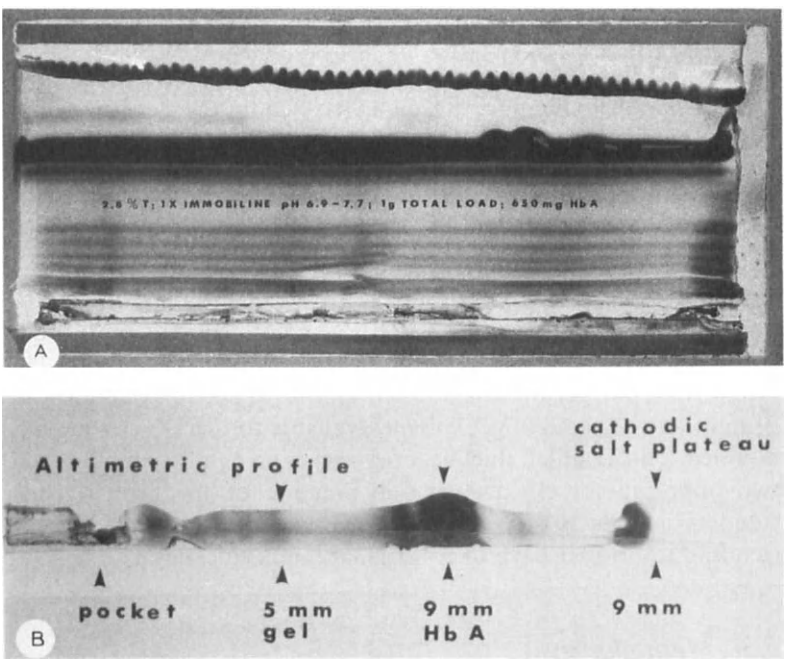

Fig. 5.10. Protein load in soft IPG gels. A: the gel was 5 mm thick, 245 mm long and 110 mm wide. A 2-cm long step (containing 5%T, 2× Immobiline at a constant pH plateau of 5.6) was polymerized around the trench (22 ml total volume). On top of it, 118 ml of an Immobiline pH 6.9–7.7 gradient was poured, in a gel of 2.8% *T*. 1 g total hemoglobin (Hb) was loaded in 7 ml volume. The anodic strip was soaked in 10 mM Glu, while the cathodic strip contained 10 mM NaOH. The slanted Hb A_2 zone with corrugated edges is due to the cathodic salt plateau (see the transverse section in B). Focusing was at 200 V/cm, 10°C, for 18 h. B: transverse section, parallel to the voltage and pH gradients, of A. This altimetric profile shows the considerably swollen Hb A zone and the cathodic salt plateau, with the curled Hb A_2 zone. Notice how a good separation is maintained in all protein zones even throughout the gel thickness. On the lower gel side the plastic backing of the Gel Bond PAG film can be seen (both from Righetti and Gelfi, 1984; with permission from Elsevier).

(which in IPGs can be as high as 250–500 V/cm), there is only a fixed amount of protein which can be loaded per a given gel area (mg/cm^2) (see Fig. 5.2). Above this limit, since the protein cannot diffuse along the x-axis (due to the fixed gel geometry) and is counteracted to move along the y-axis [due to the fixed values of d(pH)/dx and V/cm] any excess protein will simply tend to exude out of the gel into the surface (this in fact happens; see Fig. 8B and F in Righetti and Gelfi, 1984). In soft gels, especially below 3% T, even when this limit is reached, the protein reacts by absorbing water from surrounding gel regions, stretching the gel fibers and moving along the z-axis. An experimental verification of this assumption can be seen in Fig. 5.10A,B: in a 2.8% T gel, 5 mm thick, as much as 1 g protein could be loaded, and the main component (0.6 g of hemoglobin A) could be fully separated from the nearest contaminant (Hb A_{1c}, ΔpI only 0.04 pH units). The secret of this separation (this is really an enormous amount of protein to be loaded in a single zone, of 8 mm width, 25 cm length and 5 mm thickness) can be found in Fig. 5.10B: in reality, in the Hb A zone, the gel thickness has stretched to about twice the size (9 mm) and so the real gel volume available to the Hb A zone has doubled. This doubled thickness represents an equilibrium between two opposing forces: the osmotic pressure of the protein zone (tending to stretch the gel) and the visco-elastic forces of the gel (tending to bring it back to its original 5 mm thickness).

5.3. *Methodology*

The most common procedures for a preparative IPG run in a gel phase are reviewed below (the segmented Immobiline technique is essentially a run where the component of interest is kept in a liquid phase, thus this process will be treated separately).

5.3.1. Gel casting

The equipment needed to cast 5 mm thick Immobiline gels is shown in Fig. 5.11: a tray has been made (LKB 90.01.8623) with a 5 mm thick silicon gasket as one half of the standard gel mould for

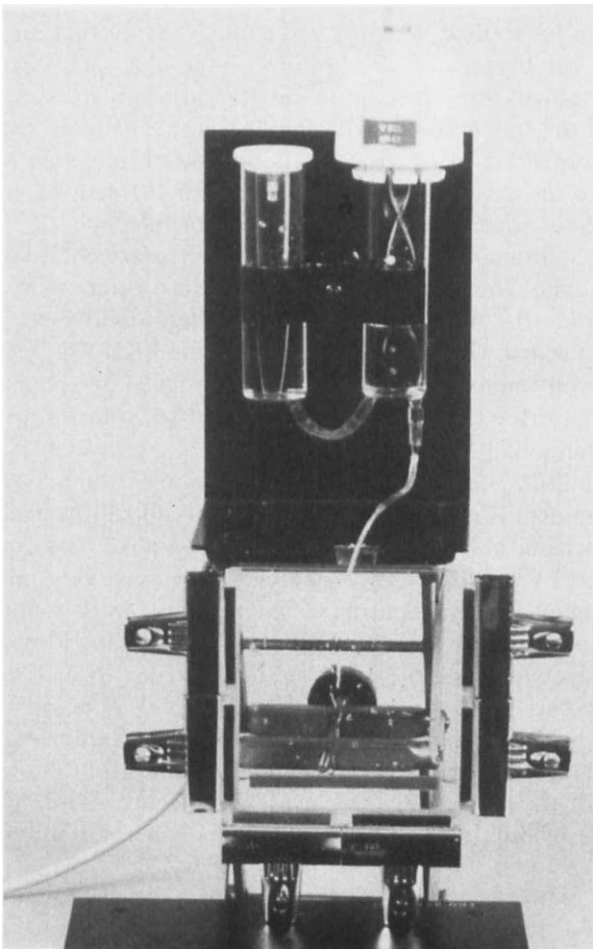

Fig. 5.11. Equipment needed for casting a 5-mm thick IPG gel slab. The glass tray is 1/2 the size of the cooling block of the electrophoresis chamber, and contains a U-gasket of silicone, 5 mm thick. A sample application trench is created by building up layers of embossing tape (10–12 layers of Dymo tape) on the glass. For pouring the gradient, the LKB 8121 Gradient Mixer and 8123 Stirrer Motor from the old sucrose density gradient column for IEF is used (60 ml total volume/chamber).

analytical runs. A sample application slot can be created by building up layers of embossing tape (e.g., Dymo tape) on the glass; 10–12 layers may be needed, depending on the volume of

sample to be applied, but it is essential to ensure that an obvious layer of gel remains at the bottom of the slot after casting. To prevent the gel from sticking to the tray after polymerization, the inside of the tray is coated with Repel Silane. The other half of the mould consists of a sheet of Gel Bond PAG film which has been affixed to the cover plate (see Chapter 3 for the details). Briefly, a few drops of water are placed at one end of the plate, the film laid on top, hydrophobic side down, and then pressed down with a rubber roller. The assembled mould is held together with clamps. For creating the Immobiline gradient, a larger two-vessel gradient mixer is needed. One that can be used is the LKB 8121 mixer and 8123 stirrer motor, which had been designed to pour density gradients for the CA-IEF column designed by Svensson (Svensson and Pettersson, 1968). Two of these mixers are available: one for the 110 ml, the other for the 440 ml Svensson's columns. Although this equipment is not sold any longer, it should still be available in most biochemical laboratories, as these preparative runs in CA-IEF supported by sucrose density gradients have been very popular in the seventies. This gradient mixer is one of the most sophisticated around, and is equipped with a plunger, whose shape is mathematically designed to raise the liquid in the reservoirs to such an extent that the two solutions (mixing chamber and reservoir) will be hydrostatically equilibrated at all times during gradient elution. Each chamber of the mixer will contain 30 ml of solution, the total volume of the mould depicted in Fig. 5.11 being 60 ml. When the mould has been filled, the gel is then polymerized in a oven at 50°C for 90 min.

After removing the polymerized gel from the oven and opening the mould, it is washed overnight in water to remove remaining TEMED, ammonium persulphate and any non-incorporated Immobilines. This procedure is fairly normal for a robust gel (e.g., 5% T) but might be quite delicate for diluted gel matrices (e.g., 3% T) since these gels will tend to swell considerably. In this latter case, it is advisable to leave the gel inside the mould and only lift the glass cover (which will be treated with repel silane and will not contain any binding plastic foil). The gel in the cassette, with only one open face, should then be wrapped up with a dialysis membrane (secured in place with rubber bands) or with a nylon net and then washed.

This will reduce the strong swelling which would occur when removing the gel from the cassette. It should be borne in mind too that such a thick gel will require more extensive washing than a regular 0.5 to 1 mm thick analytical gel. That is why the washing should be continued overnight, with intermittent water changes or in a system provided with a slow water exchange. After washing, as customary for IPG gels (see Chapter 3) the gel should be reduced back to its original weight by removing the gained excess water with a fan. The gel is then placed in the cooling block and strips impregnated of 10 mM glutamic acid and 10 mM NaOH used as anolyte and catholyte, respectively. For the run, all the precautions outlined in Chapter 3, §3.7 and 3.8, should be taken: e.g., start the run at low initial voltages for 3–4 h (max. 400 V), add carrier ampholytes to your sample to prevent any pH shock generated by salt boundaries leaving the sample zone, etc. Alternatively, a prior dialysis step should be taken if the sample contains high salt levels. Remember that the biggest enemy of a protein subjected to an IPG run is the presence of salts formed by strong acids and bases (see Table 3.10). After the initial low voltage run, the sample can be focused to equilibrium by an overnight run with a voltage max. of 2500 V.

Notes. If the sample to be applied is too diluted, it is always possible to apply it batchwise at, e.g., hourly intervals, till the total volume has been processed. In addition, if the sample contains a too high amount of salts, it can be subjected to a rapid desalting step with, e.g., Trisacryl GF-05 or a Sephadex G-25. If for any reason desalting is unwanted, a sample containing high salt levels (> 40 mM) can still be run with the precautions outlined in Chapter 3, §3.7 and 3.8. However, at the end of the run, cations and anions collecting at the electrodes will produce plateaus with extreme pH values, thus reducing the effective separation length of the Immobiline gradient. This problem can be solved by elongating the gel with pH plateaus at the two extremes, where the ion zones can collect just outside the IPG gradient, which will thus be fully available for the separation (Ek et al., 1983). For this, one needs a longer gel mould, e.g., the standard 110×250 mm cassette for analytical runs, to which a new, thicker gasket has been applied. The cassette is clamped and then set to stand vertically on the short

side. First the mould is filled with, e.g., 20 ml of the acidic, dense solution to give one pH plateau, whereupon it is placed in a oven for 15 min at 50°C for a quick polymerization step (alternatively one can heat it in situ with a hair drier). On the top of that, the regular IPG gradient is cast, having its standard length (10 cm; or any desired length for increased resolution). The gel is again subjected to a quick polymerization step as above, and finally the mould is filled to the top with the basic, light solution to give a second pH plateau. At this point the entire assembly is subjected to a final polymerization procedure (1 h at 50°C) and then processed as usual. The same protocol can be adopted when casting a 'soft' gel: this will require a stronger gel around the sample application trench (e.g., 5% *T* in the loading zone and 3% *T* in the separation area). Again, the gel can be polymerized by a two-step procedure as above. In addition, the higher % *T* plateau can be prepared as a pH plateau as well. In fact, there is no reason why around the sample application trench there should be a pH gradient as well, unless it is known a priori that some proteins will focus in this region.

5.3.2. Protein detection

At the end of the preparative run, the pattern of separated protein zones should be revealed, so that the band of interest can be excised and eluted from the IPG matrix by suitable means. There are two ways to obtain this. In one simple approach, a strip is cut from each edge of the gel, parallel to the pH gradient and including part of the area were the sample was applied. The two strips are then fixed and stained to reveal the protein zones. During this process, the voltage is maintained over the rest of the gel, to ensure the continuing sharpness of the bands (since there is no cathodic drift, there is no danger that this will result in a change of band position). By then replacing the stained strips of gel in their original positions, the zone of interest in the major part of the gel can be located, and the section of gel containing it cut out. This process is shown in Fig. 5.12A. Alternatively, one could use the naked eye as a refractometer: as discovered by Kolin (1958) long ago, a protein condensed at its pI will exhibit a sufficiently steep refractive index gradient to be detected by visual inspection. This

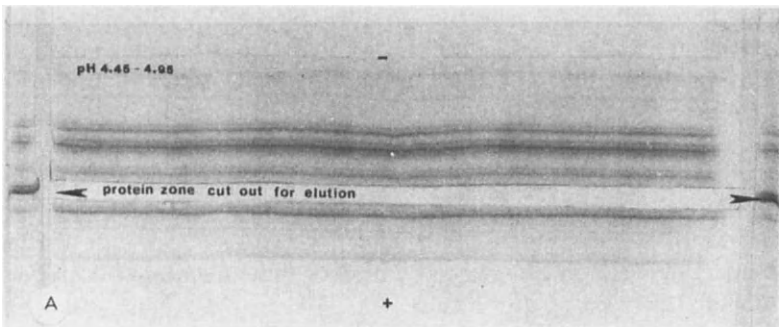

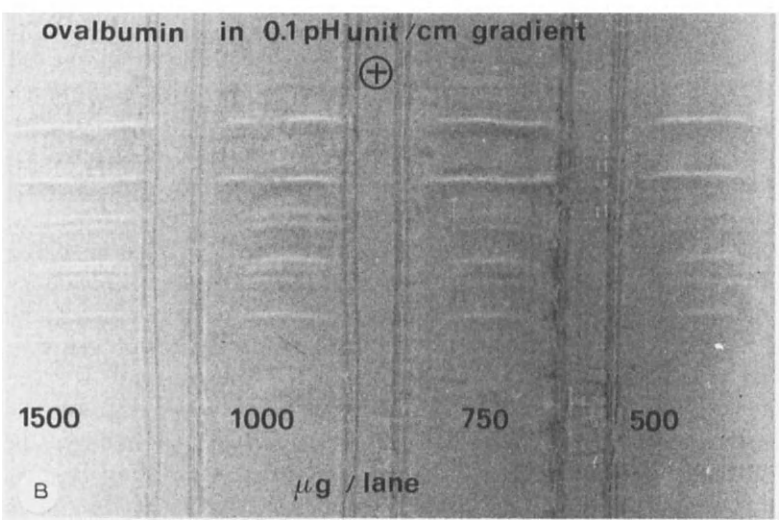

Fig. 5.12. Zone detection in preparative IPGs. A: by lateral strip excision. In this case, ovalbumin was focused in an IPG pH 4.45–4.95 interval (20 mg total sample applied in a cathodic trench of a 0.5 mm thick gel). At the end of the run, two lateral strips (1 cm wide) are cut and stained in Coomassie Blue. After reassembling the two strips in situ, the protein zone indicated by the two lateral arrow heads was cut out and the protein eluted electrophoretically. In this picture, the empty gel zone was stained and placed back in its original position, to show that it does not contain any detectable protein. B: detection of unstained protein zones by refractive index gradients. Here ovalbumin was loaded (amounts given under each track) in slots at the cathode in 0.5-mm thick gels in an IPG pH 4.2–5.2 interval. Focusing: overnight, 2000 V, 10°C. The gel was photographed directly after switching off the voltage with a shallow side illumination (both figures from Ek et al., 1983; with permission from Elsevier).

ingenious detection principle, totally lost in CA-IEF, since the carrier ampholytes themselves would give such a complex striation pattern (Righetti et al., 1975), is again fully operative in Immobiline gels. As shown in Fig. 5.12B, the focused ovalbumin zones are quite visible as refractive lines, the detection limit being possibly as low as 5–10 μg/band (Ek et al., 1983). One limit of this latter technique, however, is that it is quite difficult to see the boundaries of the different zones, i.e., to detect where one zone terminates before the onset of the adjacent one. For that, a staining technique would clearly give better results.

5.3.3. Protein elution

There are several ways for eluting a protein zone from an excised IPG gel strip: (a) electrophoretic recovery into a hydroxyapatite layer; (b) electrophoretic recovery into ion exchangers (DEAE-Sephadex for acidic to mildly alkaline proteins; CM-Sephadex for strongly basic proteins); (c) electrophoretic elution into a dialysis sac tied at the bottom of a zone electrophoresis gel; (d) electrophoretic retrieval into a sucrose density gradient. It must be stated that, since Immobiline gels have positive and negative charges incorporated into the matrix, electrophoretic elution of the separated proteins gives the best results; elution by diffusion can give decreased yields because of swelling of the IPG gel and of some ion-exchange action. In the early days of preparative electrophoresis, it was customary to slice the gel, grind the slice and recover the protein by diffusion into a large volume of eluant buffer. It soon turned out, however, that non-cross-linked polyacrylamide chains (i.e., liquid linear polyacrylamide) would also diffuse out and contaminate the sample. Often, the amount of contaminant recovered was greater than the amount of protein applied. It might be argued that this should not be a problem in IPGs, since the gel is washed prior to use. Yet, even in washed gels, possibly because of the extremely large surface area of finely ground pieces, fragments are eluted which, at the ultracentrifuge, exhibit an apparent M_r of 8 to 10 kDa (Ek and Righetti, unpublished). A second reason to avoid diffusion-driven elution is the fact that, in an electric field, the ion linkages between the protein and the IPG matrix are easily

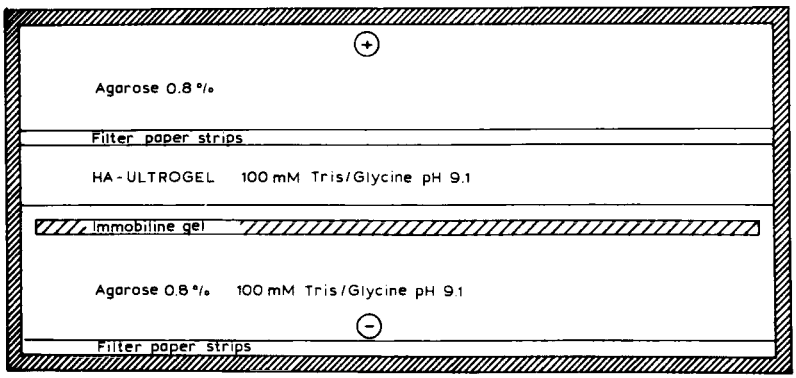

Fig. 5.13. Assembly for eluting electrophoretically protein zones from IPG gel strips. The tray is filled with 100 ml of molten 0.8% low-gelling agarose (in 100 mM Tris–Gly, pH 9.1). Upon cooling at ca. 42°C, the IPG gel strip, excised from the preparative run, is embedded in the agarose layer. A 2-cm wide trough is cut in front of the IPG strip, to accomodate the HA-Ultrogel. Essentially the same set up is used when eluting into DEAE- or CM-Sephadex (from Ek et al., 1983; with permission from Elsevier).

disrupted, whereas in the absence of it a substantial amount of protein might stay bound to the ground IPG fragments. As a third reason, as just stated above, ground pieces of IPG gel, being charged, would swell ominously in the elution buffer, thus re-adsorbing the protein which had just leached out. As a conclusion, electrophoretic retrieval is to be preferred: here follows a review of these different procedures.

Hydroxyapatite beads. This retrieval method has been adapted from Ziola and Scraba (1976) and from Guevara et al. (1982). The recovery step consists of the electrophoretic transport of the focused protein out of the gel strip into a zone of HA-Ultrogel (hydroxyapatite crystals immobilized in spherical agarose beads), through a contact zone made of a bed of agarose. Fig. 5.13 shows the experimental assembly: the electrophoresis is performed in an LKB 90.000.157 glass tray (provided with a gasket of 5 mm height). Three IEF strips, soaked in 100 mM Tris–Gly buffer, pH 9.1, and cut to length, are placed one on top of the other against the silicone rubber frame at the cathodic side of the tray; three more strips, likewise treated, are placed 40 mm from and parallel to the anodic

side of the tray. A molten solution of a 0.8% of low-gelling agarose, in 100 mM Tris–Gly buffer, pH 9.1, is poured into the tray and allowed to set. A 20 mm wide strip of agarose is then removed along the anodic side filter paper strip and replaced by a slurry of HA-Ultrogel. The Immobiline strip containing the protein of interest is now placed 5 mm away from, and on the cathodic side of, the HA-Ultrogel. If the IPG gel strip is 0.5–2 mm thick, it can simply be laid on the surface of the agarose gel layer (with the gel side facing down and the supporting Gel Bond PAG film facing the operator). For 5 mm thick gels, there are two ways for making the contact: one is to cut a trough of the same size out of the agarose gel bed and force the IPG gel strip into this trench, so as to make a good electric contact throughout the whole depth of the gel strip. The other is to fuse the IPG gel strip directly with the agarose layer just prior to gelation. For this last method (to be preferred, since the contact is not lost due to uneven heating at the level of the cut between the agarose/polyacrylamide gels) only low-melting (37°C) agarose is used, and, when the poured liquid reaches ca. 40–42°C, the IPG strip is quickly embedded in the molten agarose layer.

The HA-Ultrogel is prepared as follows: it is re-swollen and washed in distilled water, then reduced to a semi-dry cake under suction in a Buchner funnel. It is then transferred to a beaker and equilibrated in 100 ml Tris–Gly buffer, pH 9.1. The gel slurry is again transferred to a Buchner funnel and brought to a consistency which allows it to be applied directly with a spatula to the trench in the agarose gel bed. If the gel had been already used for a prior eletrophoretic elution, it can be regenerated by washing, under suction in a Buchner funnel, with 1 M phosphate buffer, pH 6.8 (100 ml buffer to 10 g gel), to remove any traces of proteins remaining from previous experiments.

After the sequence of operations described above, the electrical circuit is now closed with paper wicks connecting the gel to 0.2 M Tris–Gly buffer, pH 9.1, in the buffer chambers of a suitable horizontal cell (e.g., the Pharmacia-LKB 2117 Multiphor II unit). Electrophoresis is performed at 30 W constant power for 1 h at 10°C, with an initial voltage of approx. 420 V. At this point, the protein zone contained into the IPG strip has been electrophoretically transferred and adsorbed onto the HA-Ultrogel grains (they

TABLE 5.1
Protein recovery after preparative electrofocusing in immobilized pH gradients

Protein	Total protein recovery (%)
Haemoglobin	98
Myoglobin (horse heart)	98
Albumin (bovine serum)	76
Carbonic anhydrase	81
Ovalbumin	89
Transferrin	87

are concentrated there and retained by a weak ion exchange property of these gels). A second transfer is now needed, in order to recover the protein in a free liquid phase. Thus, the hydroxyapatite grains are transferred with a spatula to a 25 ml plastic syringe, plugged at the bottom with cotton wool or a disc of filter paper. The protein is eluted with aliquots of 0.2 M phosphate buffer, pH 6.8. In addition to the first fraction, 5×7 ml of buffer are normally sufficient to remove all the proteins from the HA-Ultrogel. The aliquots of buffer are pipetted into the barrel of the syringe, the gel briefly stirred with a glass rod, and the buffer eluted into a test tube with the aid of the plunger: this helps to squeeze all the liquid out of the gel. As stated above, the gel can then be regenerated by washing in 1 M phosphate buffer, pH 6.8. A set of six proteins were used as a test for recovery (see Table 5.1). The recovery is expressed as a fraction of the total amount of each protein loaded onto a 1 pH unit-wide Immobiline gel. Recoveries range from 76% (BSA) up to 98% (Hb and myoglobin), typical values being of the order of 85%. These yields from Immobiline matrices are of the same order of magnitude as protein recoveries from the granulated dextran gels (Sephadex) used in the conventional preparative IEF technique of Radola (1975). Recoveries are optimized by working in the range 0.2–0.25 M phosphate as eluent: at lower (0.1 M) or higher (0.5 M) concentrations there is a loss of protein (see Fig. 5.14), in the former case due to ionic binding and in the latter case most probably because of hydrophobic interactions with the agarose matrix of the HA-Ultrogel (Hjertèn, 1976).

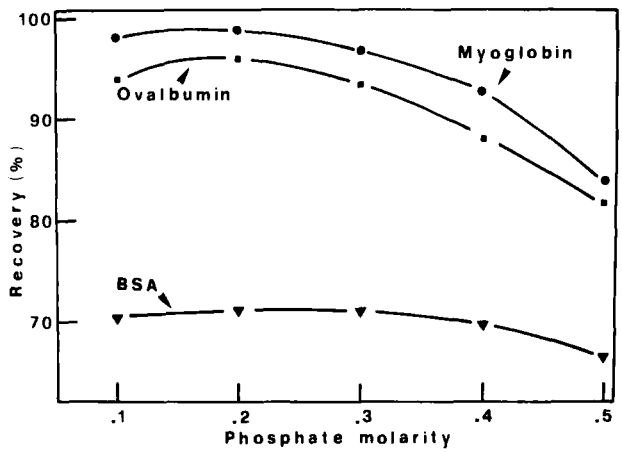

Fig. 5.14. Recovery of protein fractions from HA-Ultrogel as a function of phosphate eluant molarity. Myoglobin (circles), ovalbumin (squares) and BSA (triangles) were separately adsorbed onto hydroxyapatite, equilibrated in 100 mM Tris–Gly buffer, pH 9.1, and eluted with increasing molarities (from 0.1 to 0.5) of pH 6.8 phosphate buffer (from Ek et al., 1983; with permission from Elsevier).

DEAE- and CM-Sephadex. The HA-beads transfer technique would work satisfactorily for small protein loads (in the mg/ml range), but it would not perform properly on a larger scale (tens of mg/ml range), i.e., at loads compatible with the high through-put of Immobiline matrices. At these high loads, the HA grains would be quickly saturated, and the protein zone would cross the entire layer of resin and be lost in the anodal agarose zone embedding it. The reason is that calcium phosphate crystals are an excellent ion-exchange material for separation of nucleic acids (Bernardi, 1971), but they have rather poor sorption capacity for proteins (barely 0.5–1 mg/ml resin). For this reason, Casero et al. (1985b) described a new transfer system based on electrophoretic recovery into true ion-exchangers, as utilized for routine protein separations (average capacity for 40 to 60 kDa proteins: 50–80 mg protein/ml exchanger). The IPG gel strip is still transferred to the horizontal tray of Fig. 5.13, embedded in low gelling agarose and eluted electrophoretically, but this time against either DEAE- or CM-Sephadex. For acidic to neutral proteins (up to pI 7.7) the electro-

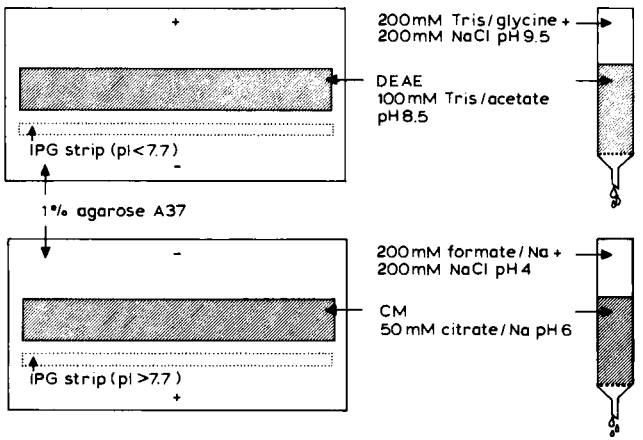

Fig. 5.15. Recovery of protein zones from IPG gels into ion exchangers. Left side: after IEF, the IPG gel strip is cut out along the protein contour (still supported by the Gel Bond foil) and embedded in a 5-mm thick layer of 0.8 % agarose A-37. In front of it, a 2-cm wide trench, as long as the IPG strip, is dug into the gelled agarose and filled with the ion exchanger (the distance between the IPG gel and the resin should be barely 3–5 mm). For proteins with pIs < 7.7, a DEAE-Sephadex, in 100 mM Tris–acetate, pH 8.5, is used; for proteins with pI > 7.7, a CM-Sephadex in 50 mM citrate, pH 6.0, is utilized for electrophoretic retrieval (cathodic migration). The surrounding agarose layers are equilibrated in the corresponding buffers. Electrophoretic elution lasts in general 700 V×h. Right side: after electrophoresis, the resins are transferred to short columns or to plastic syringes, and then the protein is eluted either with 200 mM Tris–Gly, pH 9.5+200 mM salt (anionic species) or with 200 mM Na-formate, pH 4.0, +200 mM NaCl (cationic species) (from Righetti and Gianazza, 1987; by permission from J. Wiley).

phoretic transfer is from the IPG strip into a layer of DEAE-Sephadex, buffered at pH 8.5 in 100 mM Tris–acetate (Fig. 5.15, upper). Recovery (better than 90% in all cases studied) was achieved by transferring the resin to a column and titrating it at pH 9.5 (the pK of the exchanger), in 200 mM Tris–Gly buffer, containing 200 mM salt. For basic proteins (pI > 7.7), the electrophoretic retrieval is from the IPG strip into a zone of CM-Sephadex, buffered at pH 6.0, in 50 mM citrate (cathodic migration; Fig. 5.15 lower). Recovery (again better than 90%) is accomplished by titrating the exchanger at pH 4.0, in 200 mM formate buffer, containing 200 mM NaCl. By this technique it was demonstrated that Immobiline gels, even when incorporating five times the standard amount of

TABLE 5.2
Recovery of proteins from DEAE-Sephadex [1]

Protein	Applied (mg)	Recovered (mg)	Recovery (%)
β-Lactoglobulin	31.3	28.0	89.5
Transferrin	34.5	32.0	91.8
Ovalbumin	38.9	36.3	93.3
Bovine serum albumin	29.8	25.6	86.0
Hemoglobin	37.0	36.7	99.0

[1] Eluant: 0.2 M Tris–Gly, pH 9.5 in 0.2 M NaCl.

buffer (75 mM Immobiline at pH = pK, i.e., 50 mM buffering ion and 25 mM titrant) exhibit, in the electric field, negligible ion-exchange properties, thus ensuring ideal supports for isoelectric focusing. Tables 5.2 and 5.3 give the recoveries of standard proteins from the two types of titrants. While these data refer only to the total amount of applied sample, Casero et al. (1985b) have also investigated the recovery of enzyme activity after these various treatments. If proper guidelines are followed, also enzymatic activity yields can be high: in particular, elution from the exchanger should be done in presence of substrate (e.g., 20 mM) and by quickly titrating the eluate to physiological pH. With these two precautions, 70 to 80% recovery of enzyme activity could be obtained. It should be noted that the strategy here adopted for eluting proteins from the exchanger is quite different from that used in ion-exchange chromatography. In the latter technique, proteins, bound to the resin at a suitable pH, are generally desorbed

TABLE 5.3
Recovery of proteins from CM-Sephadex [1]

Protein	Applied (mg)	Recovered (mg)	Recovery (%)
Myoglobin HH	31.4	22.9	73
Myoglobin SW	36.2	32.7	91
Bromelain	23.4	20.2	86
Ribonuclease	30.5	30.0	98
Cytochrome *c*	37.0	36.7	99

[1] Eluant: 0.2 M Formate, pH 4.0 in 0.2 M NaCl.

by progressive titration to their respective pI values. It is known in fact that an isoelectric protein should have minimal or no interaction with an ion-exchanger. In fact, a general technique, called 'isoelectric chromatography' (Petrilli et al., 1977) has been reported, by which a protein, contaminated by other species, is sequentially eluted through an anion and cation exchanger, both buffered at their pI. Under ideal conditions, the protein should flow unbound through the two exchangers, while higher and lower pI contaminants should be retained by one or the other resin beds. In the present case, on the contrary, a new strategy can be adopted, namely the titration of the weak buffering groups on the resin, above the pK for DEAE-, below the pK for CM-Sephadex. By substantially lowering the average charge density on the resin, high protein recoveries are guaranteed.

Dialysis sacs. The elution procedures described so far are two-step, sequential methods, requiring two successive elutions. It would be preferable, whenever possible, to perform the transfer in a single step. This can be achieved, provided an additional electrophoretic cell is utilized. In one approach, electrophoretic retrieval can be performed in the cell of Fig. 5.16: it is the preparative adaptation of an earlier analytical gel focusing chamber (Righetti and Drysdale, 1973). The central unit (core) accomodates 3 glass tubes of 50 ml capacity (1.8 cm i.d.) and 2 tubes of 20 ml capacity (1.2 ml i.d.), both 15 cm long, resting on 2 rubber grommets sealing the central cooling chamber (the water inlets and outlets are indicated by arrows). A sixth position is occupied by an analytical gel of 2 ml capacity (0.6 cm i.d.), generally left sealed by conical plugs. The top (TE) compartment is a shallow chamber (3 cm in height) with circular platinum electrodes, with a total volume of 100 ml, while the bottom chamber (BE) can be filled with up to 500 ml of chilled buffer. The set-up for electrophoretic elution is shown in Fig. 5.17A. The basic idea was from Suzuki et al. (1973): the bottom of the glass tube (anodic side) is sealed with a dialysis membrane and filled with 20% sucrose in 100 mM Tris–acetate buffer, pH 8.5 (this will be the elution chamber; its height can be chosen according to experimental needs; in general, 1–2 cm are sufficient for eluting 100–200 mg protein). On top of it, a 5% T gel is cast, prepared in the above buffer, having a minimum height of 6 mm. Once the strip

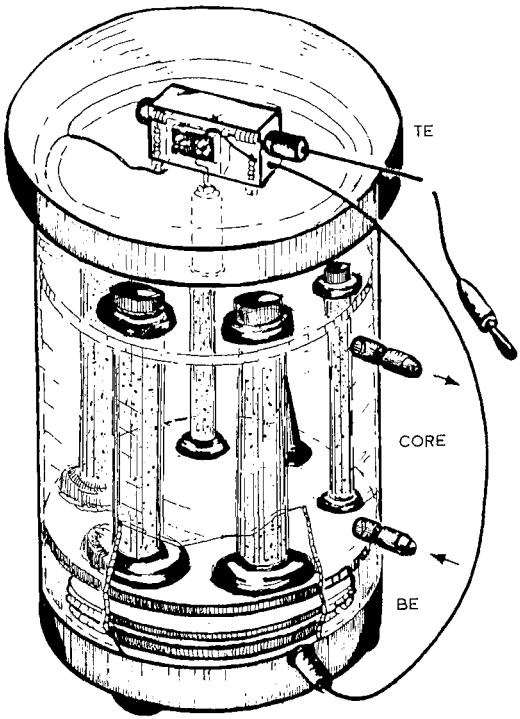

Fig. 5.16. Drawing of the electrophoretic elution chamber from IPG gels strips. BE and TE: bottom and top electrodic chambers, respectively. CORE: central cooling chamber, accomodating 3 large-bore tubes (1.8 cm diam.), 2 medium-bore tubes (1.2 cm diam.) and one analytical gel of 0.6 cm diam. The glass tubes are held in place between two rubber grommets, with a snug fit ensuring electrical insulation between the central coolant and the electrodes at the two extremities. In the actual apparatus, the height of the bottom anodic chamber has been increased from 2 to 10 cm, to avoid anodic oxidation of eluted proteins (from Righetti et al., 1986c; by permission from Elsevier).

of IPG gel containing the band of interest has been excised, it is chopped to pieces which are loaded on top of the stacking gel soaked in the same buffer as above, containing 6% sucrose. By absorbing sucrose, the pieces of IPG gel become denser than the electrodic buffer (200 mM Tris–acetate, pH 8.5) and are thus prevented from floating. The tube is now assembled in the electrophoretic apparatus of Fig. 5.16 and the protein electrophoresed out

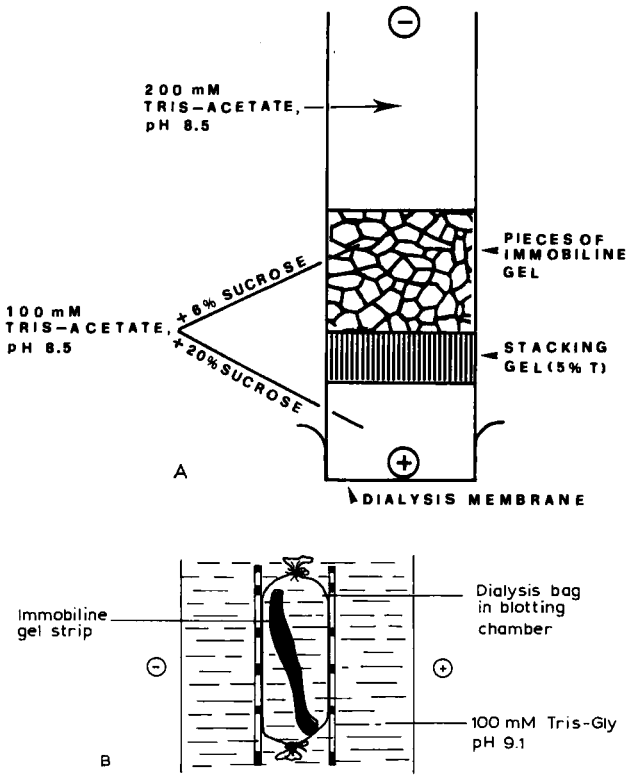

Fig. 5.17. Elution into dialysis sacs. A: from a gel layer into a dialysis bag. A glass tube, coated with Bind Silane, is sealed with a dialysis membrane fitting around it as a sleeve. A 6–10 mm high stacking polyacrylamide gel (5% *T*) is polymerized on top of a chamber filled with 20% sucrose in 100 mM Tris–acetate, pH 8.5. The pieces of Immobiline gel, containing the protein to be eluted, are accomodated on top of the stacking gel in 6% sucrose solution. B: with an IPG gel trapped inside a dialysis bag. The Immobiline gel strip containing the band of interest is cut and placed in a dialysis sac. The bag is sandwiched between the two porous pads of a blotting chamber and a transverse electric field applied. A: from Righetti et al., 1986c; with permission from Elsevier. B: from Righetti et al., 1986e; with permission from VCH.

at 10 W constant power for 30–60 min. Also with this set up good recoveries, similar to those described in Tables 5.2 and 5.3, are obtained.

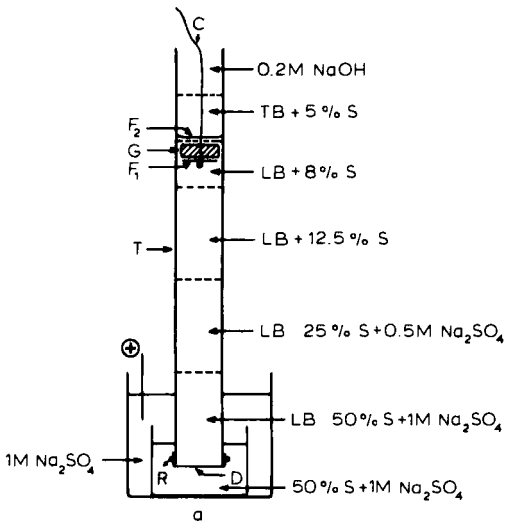

Fig. 5.18. Elution of protein bands by a combination of displacement electrophoresis and electrophoresis in a conductivity gradient. TB: terminating buffer; LB: leading electrolyte; S: sucrose solution; G: Immobiline gel slice; E_1: and E_2: electrode vessels; D: dialysis membrane; R: rubber band; F_1: filter paper; C: cotton thread (adapted from Hjertèn et al., 1983; with permission from Elsevier).

Note: for proper gel adhesion, the glass tube should be coated with bind silane, otherwise the osmotic pressure of the protein eluted in the dialysis sac could displace the stacking gel (see Fig. 5.17A). In another approach (Righetti et al., 1986e), the Immobiline gel strip, with the protein band of interest, could be trapped directly into a dialysis bag, which would then be placed in a vertical position between the two porous pads of a blotting chamber. Upon application of a transverse electric field, the protein will migrate out and, upon collecting against the anodic wall of the bag, sediment at the bottom of the sac by electrodecantation (Fig. 5.17B).

Conductivity gradients. This is an adaptation of a method described by Hjertèn et al. (1983) Fig. 5.18: the Immobiline gel strip could be hanged (via cotton thread C and a filter pad F_1) on the cathodic extremity of a discontinuous sucrose density gradient coupled to a conductivity gradient in a vertical column and eluted

by displacement electrophoresis (isotachophoresis). The protein will be stacked between the terminating buffer (TB) and the leading ion (LB) into a highly concentrated zone. The underlying density gradient will also help to further sharpen the bands, so that the protein will be recovered into a small liquid volume. Recovery can then be obtained by emptying the column with the aid of a fraction collector.

5.3.4. An example of a purification protocol

A practical example of a purification protocol, uses as a model the elimination from hemoglobin A (Hb A) of its main contaminant, Hb_{1c}, a glycated form present at a 2–3% level in normal human adults (and at a 5–15% level in diabetic patients) having a ΔpI of only 0.04 pH units from the main component. In addition, umbilical cord blood will be separated into its three main components, fetal and adult Hbs. The preparative run takes place over a two-day period, as follows: (a) day one: gel casting, washing, weight-reconstitution, sample application and overnight run; and (b) day two: excision of the major Hb zone, casting of the agarose plate, preparing a trench with either hydroxyapatite or DEAE-Sephadex, electrophoretic transfer and protein elution from the exchanger beads. For a check list of materials required, see Chapter 3. In addition, low-gelling agarose (A-37) is used and for protein recovery two different methodologies: adsorption on a weak (hydroxyapatite) or a stronger (DEAE-Sephadex) ion-exchanger. For the preparative run, use is made of a 2 mm thick gel, one half the size of the cooling block of the Ultrophor (11 × 11 cm), over a 1 pH unit interval (pH 6.8–7.8), of low matrix content (3% T), to enable fractionation of at least 150 mg total sample. Two different types of red cell lysates are used: an adult, containing 95% Hb A and a cord blood lysate, containing three major Hb species: Hb F (fetal, 70%), Hb A (20%) and Hb F_{ac} (acetylated fetal, 10%). The operative steps are outlined below. The gel composition for the IPG run is given in Table 5.4, while two alternate formulations for the electrophoretic elution are listed in Table 5.5. The Hb lysate is prepared as follows: the red cells are washed 3 times in normal saline and lysed in two volumes of distilled water (so the final

TABLE 5.4
Formulation for a preparative pH 6.8–7.8 IPG run (gel thickness 2 mm, size 11 × 11 cm)

Chemicals	Acidic (heavy) sol.	Basic (light) sol.
Immobiline pK 3.6 [1]	387.5 μl	103 μl
Immobiline pK 7.0 [1]	569 μl	781 μl
Acrylamide stock (30%T, 4%C) (for $T\% = 3$)	1.25 ml	1.25 ml
Glycerol (87%)	2.50 ml	
Water	7.79 ml	10.36 ml
Total Volume	12.5 ml	12.5 ml
TEMED	9 μl	9 μl
Persulfate (40% sol)	12 μl	12 μl

[1] From stock 0.2 M solutions.

concentration is ca. 8% Hb). The stroma is removed by shaking the lysed cells with one volume of CCl_4 and centrifuging at full speed in a bench centrifuge (approx. 3000 g) for 20 min. It is preferable not to add KCN, as often the excess salt disturbs the run. It is best to gas the sample with CO for 30 s and then store in 30% ethylene glycol at −20°C. The stability is guaranteed for at least one year.

First day:

- assemble the cassette (15 min);
- mix the IPG solutions, check the pH (30 min);
- pour the gradient, rinse carefully the apparatus, dry the outlet with ethanol (20 min);
- polymerize the gel (1 h in a forced ventilation oven at 50°C);
- weigh the gel and mark the weight on the plastic backing;
- wash the gel (3 × 1 h) in 0.5 l distilled water each time;
- blot the gel surface with soft tissue and reconstitute to its original weight (1 h);
- apply the sample (150 mg in 0.9 ml) and start the experiment (15 min). Run initially at low V (e.g., 3 to 400 V) for 3 to 4 h. Continue the run overnight at 200 V/cm;
- re-swell the ion exchanger overnight (if DEAE-Sephadex is chosen for elution).

Second day:

- wash the ion exchanger (30 min);
- boil the agarose in buffer (15 min);

TABLE 5.5
Eluting systems for proteins from an Immobiline matrix

	HA-Ultrogel		DEAE-Sephadex	
Agarose	M, 0.8%	800 mg	A-37, 1%	1 g
Buffer	[1] 100 mM Tris-Glycine pH 9.1	12.1 g Tris + 4.1 g Gly in 1 l final volume (20°C)	[2] 100 mM Tris–Acetate pH 8.5	12.1 g Tris + 35 ml 1 M CH_3COOH in 1 l final volume (20°C)
Ion-exchanger	HA-Ultrogel	15 ml equilibrated in 150 ml Tris–Gly buffer pH 9.1 to fill a 12.5 × 1 × 0.5 cm trench	DEAE-Sephadex	500 mg swollen and equilibrated in 100 ml of Tris–acetate buffer, pH 8.5, to fill a 12.5 × 1 × 0.5 cm trench
Elution buffer	0.2 M Phosphate buffer, pH 6.8	2.84 g Na_2HPO_4 + 1.75 g NaH_2PO_4 in 100 ml final volume (20°C)	0.2 M Tris-Glycine pH 9.5 in 0.2 M NaCl	2.42 g Tris + 0.21 g Gly + 1.168 g NaCl in 100 ml final volume (20°C)

[1] Electrode Buffer: double molarity; same pH
[2] Electrode Buffer: same molarity and pH

- cut the IPG gel strip with the protein band of interest (the matrix stays bound to the plastic foil);
- pour the agarose into the tray and allow to cool at 42°C;
- embed the IPG gel strip into the melted agarose A-37 plate, plastic backing against the glass bottom of the tray (visualize this operation and the following ones in Fig. 5.13);
- cut a trench (2 cm wide, 24 cm long) anodic to the IPG gel strip;
- fill this trench with a slurry of ion-exchanger (DEAE-Sephadex or HA-Ultrogel, according to the elution system chosen);
- start the experiment (1 h at 30 W, ca. 300 V, 5°C);
- remove the ion-exchanger and transfer to a syringe (5 min);
- wash with elution buffer (20 min; in case of DEAE-Sephadex, refer to Fig. 5.17);
- for testing protein recovery, read the eluate at 546 nm (for Hb).

General comments. Remember it is essential to start the run at low voltage gradients for a few hours. If the sample contains medium to high salt levels (> 40 mM) the ionic boundaries will form strongly acidic and strongly alkaline zones which will denature the protein. Low voltage gradients will prevent formation of strong pH boundaries due to a dilution of the ion fronts. The sample can also be protected by adding CA buffers, or by a prior dialysis step, or by equilibration in **buffers formed from weak acids and bases**. For all these precautions, refer to Chapter 3, §3.7 (Righetti et al., 1988e). The advantage of 'soft' gels will be apparent during the run: as the visco-elastic forces of the matrix are weakened, the osmotic force in the protein zone will take over, so that, proportionally to the amount loaded in a single zone, the gel will stretch locally forming a peak in the focused protein band, the peak height representing an equilibrium between the two opposite forces.

5.4. Immobiline canal technique

For small-scale protein loads in IPGs, an interesting method was described by Bartels and Bock (1984) who recovered the protein of interest focused in the Immobiline gel directly into gel filtration media: this was performed by collecting the protein of choice into

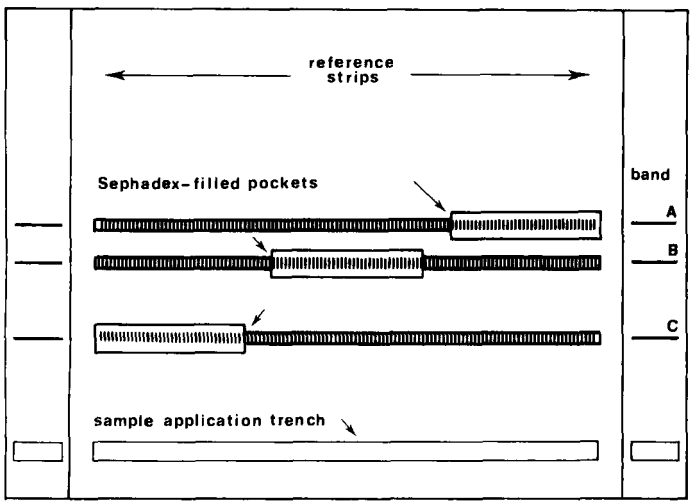

Fig. 5.19. Recovery of proteins in gel filtration media (Immobiline-canal technique). After prepararing the IPG gel, the sample to be purified is applied only in two lateral, reference strips and focused. The strips are stained and re-aligned with the intact IPG gel. In the latter, in correspondence with the focusing positions of the desired proteins (here three major bands, A, B and C are considered), three trenches are dug, scraped free of Immobiline matrix and filled with Sephadex G-200. The sample for the preparative run is now loaded into the application trench. Upon completion of the IEF step, the proteins of interest are eluted from the Sephadex grains (from Righetti and Gianazza, 1987; with permission from J. Wiley).

a layer of Sephadex G-200, inserted into a channel cut into the IPG matrix.

The principle of the technique is illustrated in Fig. 5.19, while a practical example is given in Fig. 20A and B. The IPG plate is first run by applying the sample only in two lateral tracks (C and C′ in Fig. 20A); after reaching equilibrium conditions, the two zones are cut away and stained for proteins. The developed analytical strips are then aligned back into their original position, and in the middle preparative surface of the IPG gel, areas are selected where the protein bands of interest would focus. A channel is cut away with the aid of a scalpel and a spatula in these areas, and the trench is filled with a slurry of Sephadex G-200 equilibrated in distilled water. Then the sample for the preparative run is applied in tracks

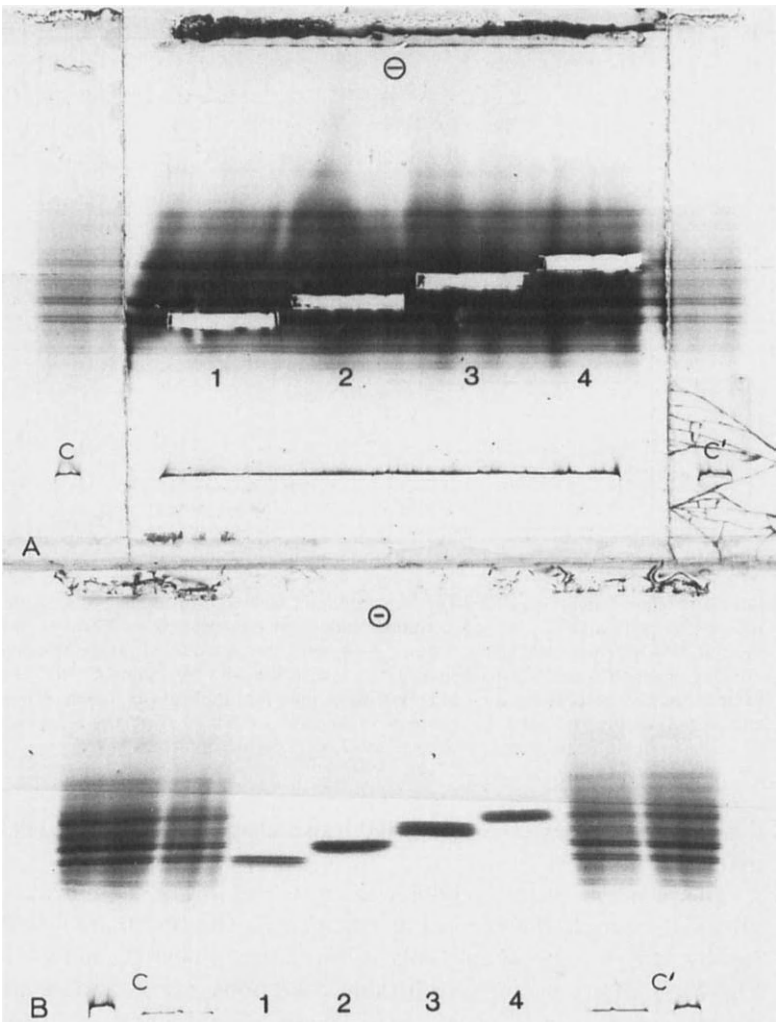

Fig. 5.20. Immobiline-canal technique. (A): IEF of ovalbumin. Gel: 185×125×0.5 mm, pH 4.3–5.3 IPG gradient; 4°C, 8 kV×h, max 5 W and 5 kV. Fixing and staining in Coomassie Blue. C and C′: lateral edges for analytical pre-run; 1–4: channels for the collection of proteins, filled with an aqueous slurry of Sephadex for IEF. The sample application trench is at the anode. (B): Re-focusing of the four protein samples collected in the channels 1–4 of (A). The IEF-Sephadex from the different channels of the previous gel was directly inserted into pockets at the anode and rerun under the same conditions of the analytical experiment. Lanes C and C′: control, unfractionated ovalbumin; channels 1–4: single fractions eluted from gel (A) (from Bartels and Bock, 1984; with permission of VCH).

corresponding to the different cut-out channels, and the IPG run is performed under the same conditions used for the analytical pre-run. On reaching equilibrium, the desired protein will collect in the Sephadex-filled channel and will be forced to stay there by the electric field. At the termination of the run, the Sephadex grains are quickly removed from the different channels and individually transferred into suitable micro-columns, where the different protein zones are recovered by gel filtration.

The difference between the present method and the systems of Ek et al. (1983) and Casero et al. (1985b) is that both the electrophoretic fractionation and the protein recovery are performed simultaneously in the same mixed Immobiline–Sephadex gel rather than sequentially in two different gel layers by two separate experiments. The efficiency of the separation is shown in Fig. 20B: here the fractions eluted in the (now empty) channels of Fig. 20A are rerun in the same Immobiline pH interval under analytical conditions, side by side with the unfractionated mixture as a control. Fractions 1 to 4 appear now as homogeneous, single protein zones. I believe that the different techniques are indeed complementary: canal-Immobiline would be adequate for small scale sample loads, whereas the two step methodology of Ek et al. (1983) and Casero et al. (1985b) is the only choice for large-scale preparations.

5.5. Reversible polyacrylamide gels

The same two authors (Bartels and Bock, 1988) have recently introduced a new preparative variant, called BAC-IPG, consisting of the use of soluble polyacrylamide gels. This is based on a technique developed by Hansen (1976) for nucleic acid, consisting in substituting the common cross-linker (Bis) with a disulfide containing agent, bis-acrylyl cistamine (BAC). Gels cross-linked with BAC are reversible, i.e., they can be solubilized after the preparative electrophoretic step simply by incubation in an excess thiol agent (e.g., dithiothreitol, DTT). The methodology is similar to the one illustrated in Fig. 5.12A: at the end of the IPG run, two narrow lateral strips are cut and stained for protein, while leaving

the remaining of the gel under voltage. The two stained strips are then re-aligned to the intact gel and the zones of interested identified and cut away with the aid of a scalpel. The excised gel strips are now separately treated with excess DTT at a slightly alkaline pH, till the matrix has been dissolved. Now the desired protein is separated from the accompanying liquified gel phase by column chromatographic procedures, e.g., affinity, hydrophobic interaction or ion-exchange chromatography. Some caution should be exercised with this technique. First of all, the solubilized sample zone will be rather viscous, thus the chromatographic step might be quite difficult to perform. The sample will thus have to be diluted or, alternatively, the protein could be pricipitated with saturating levels of ammonium sulphate, so as to eliminate the viscous gel phase. Secondly, the copolymerization conditions with BAC will not be the same as with Bis, therefore, proper gelling conditions will have to be studied in order to obtain optimal Immobiline incorporation (Bartels and Bock, 1988). Finally, and most critical, it should be remembered that quite a few proteins will not stand the harsh treatment with DTT: –S–S– bridges in proteins will be reduced as well, and it is not guaranteed that, after DTT removal, full enzymatic activity will be recovered. In addition, if impurities are still present in the zone, upon –S–S– bond re-formation, mixed disulphides could form, resulting in spurious protein zones. This is in fact what seems to occur to Bartels and Bock (1988): loss of enzyme activity and spurious bands are clearly visible in their data. Neverthelss, for proteins resistant to thiol treatment this could be an interesting method to explore.

5.6. Segmented immobilized pH gradients

We have seen in Fig. 5.9 that the amount of protein which can be focused in a single zone is inversely proportional to gel strength: at high gel dilutions, progressively higher sample loads can be applied. Theoretically, if one were to extrapolate the curve of Fig. 5.9 to zero gel strength, possibly protein concentrations as high as 30% (e.g., as typical of Hb in the red blood cell) could be arrived at. On the basis of this observations, we have carried preparative IPGs to

what could be the ultimate development: the concept of segmented IPG matrices. The idea of this latter approach is to leave the protein of interest, at any given time during the purification process, outside the IPG matrix, in the liquid stream feeding the IPG support, while focusing in the Immobiline gel only the impurities. This is made possible by a novel design of the electrophoretic chamber, coupling orthogonally a liquid sample flow to an electric field in a segmented Immobiline matrix (Faupel et al., 1987). This allows processing of large sample volumes and extremely high sample recoveries in a simple experimental set-up, requiring only a single electrophoretic step. It should also be noted that the other techniques described above require in general quite a cumbersome handling and lengthy purification protocols; in addition, when focusing slightly hydrophobic or membranaceous proteins into IPG matrices, recoveries are in general rather poor (Davis et al., 1986).

5.6.1. Vertical chambers

Fig. 5.21 gives an idea of the electrophoretic apparatus: a central flow chamber (2 cm diam., 3 cm in height) is connected to a sample reservoir (which, in principle, can hold any volume for processing) and to a pump recirculating the feed through the electric field (in general, operated at maximum speed). Perpendicular to the hydraulic flow, an electric field is activated between two platinum plates (25 cm distance between anode and cathode) which serves to remove electrophoretically, from the flow chamber, any charged monovalent ion or non-isoelectric amphoteric species. The flow chamber is connected, via upper and lower O-ring seals, to 2 polyacrylamide gel cylinders held in short (2 cm diam., 8 cm in height) glass tubes fitted with jackets for coolant flow. The upper tube is sealed, via an O-ring, to the cathodic chamber, containing in general a diluted base (e.g., 50 mM NaOH or ethanolamine, ethylendiamine, isoionic Lys or Arg) as customary in conventional IEF. The lower tube bathes its extremity directly into the anodic chamber, in general containing a diluted acid (strong or weak) such as acetic, phosphoric or sulfuric acids or isoionic Asp or Glu solutions. The novelty of this fractionation technique is that the flow chamber is delimited by a floor and a ceiling which are, in

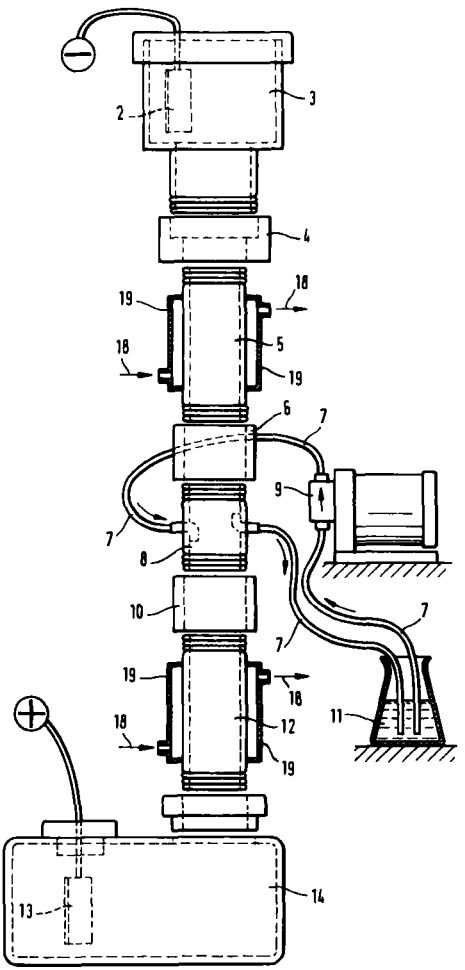

Fig. 5.21. Sketch of the segmented, IPG gel apparatus. 2 and 13: platinum electrodes; 3 and 14: cathodic and anodic compartments, respectively; 4, 6 and 10: connecting pieces holding an upper and lower O-ring seal for leak-free connections; 5 and 12: glass cylindes for the upper and lower IPG gel segments; 7: tubing for recycling the sample solution from the reservoir (11); 8: central sample flow-chamber; 9: peristaltic pump; 18: inlets and outlets for coolant flow; 19: column jackets (modified from Faupel et al., 1987).

fact, the extremities of a lower and a upper polyacrylamide gel containing an immobilized pH gradient. By arranging the extremities of these 2 gel segments bathing the flow chamber to have pIs just below (on the anodic side) and just above (on the cathodic side) the pI of the protein of interest under purification, this protein will in practice be continuously titrated to its pI and as such will never be able to leave the flow chamber. Conversely, all proteinaceous impurities accompanying the protein under purification will automatically be (at the pH prevailing in the flow chamber) either above or below their respective pIs, and thus be forced to leave the chamber and focus either in the lower or upper segments of the Immobiline gel. Given sufficient recycling time under a voltage gradient, all impurities will leave the flow chamber and the pure, isoelectric protein simply recovered in the sample reservoir containing the original feed. No further manipulations or sample extractions will be needed, as the protein of interest has been kept all the time in the liquid phase and has never entered the gel.

Fig. 5.22 gives a sketch of the experimental set-up needed: the assembled vertical apparatus is connected to a power supply (from any commercial source, provided it can deliver at least 1000 V). As the sample flow chamber is not refrigerated, the feed is kept in a larger, jacketed reservoir, coupled to a thermostat. It is best to keep the sample vessel under continuous, gentle stirring, otherwise, with time, a denser stratum could separate from a lighter one. Recycling is in general done at high speed, so as to reduce to a minimum the sample residence time in the flow chamber, thus avoiding any risk of thermal denaturation. This is the simplest set-up for operation. In principle, any other probe or metering device can be built around this apparatus: e.g., by fitting it with a flow electrode for pH measurements and a flow cell for conductivity monitoring. As a variant of the system shown in Fig. 5.22, in case that more than 1 component has to be simultaneously purified from the same protein feed, the apparatus can be easily modified from the mono-segmented version of Fig. 5.21 to a multi-segmented assembly, as shown in Fig. 5.23. Suppose that 2 (or more) proteins having known pIs have to be separated and simultaneously harvested, 2 (or more) flow chambers can be stacked up in the same apparatus,

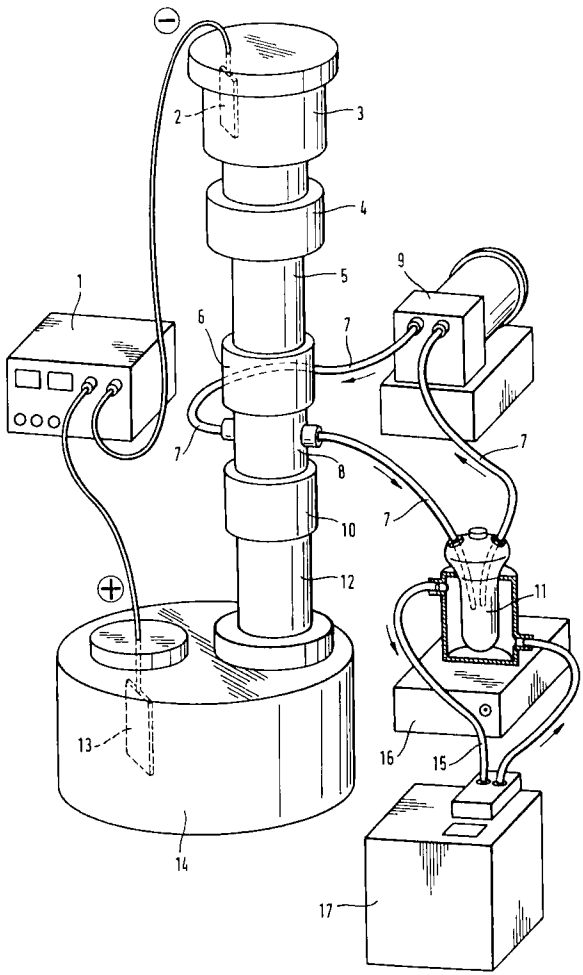

Fig. 5.22. Experimental assembly of a preparative IPG run in a segmented gel apparatus. 1: power supply; 15: tubing for the coolant flow to the sample reservoir (11); 16: motor for magnetic stirring; 17: thermostat. All other numbers as in Fig. 5.21 (modified from Faupel et al., 1987).

separated by short gel blocks containing immobilized pH gradients of the appropriate pH span between the pI values of the different proteins to be purified. The sample feed can be divided into 2 (or

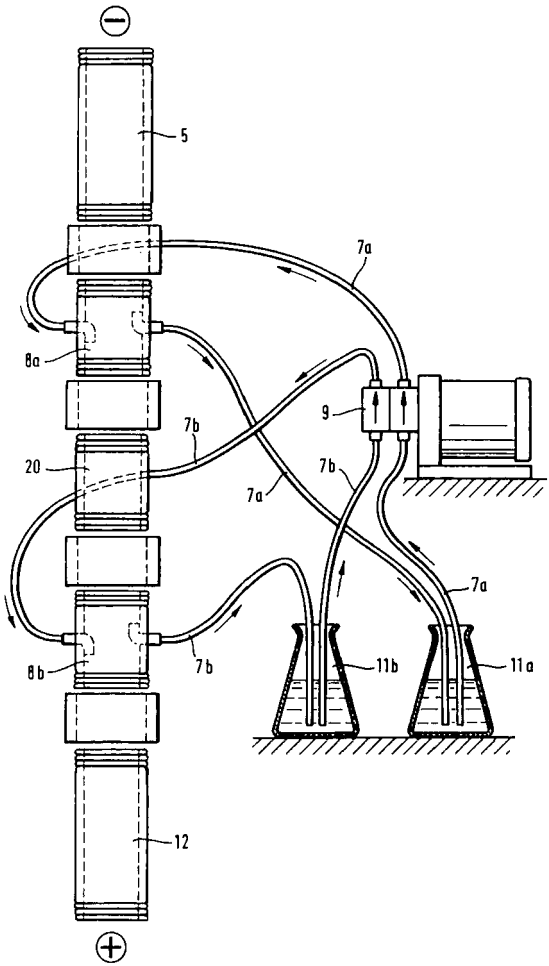

Fig. 5.23. Sketch of a recycling, segmented IPG column. It is hypothesized that 2 major components have to be purified and the apparatus is modified to contain two flow chambers. In principle, several flow chambers cam be added according to experimental needs. 20: third segment of Immobiline gel defining the isoelectric conditions between the higher pI component remaining in chamber 8a and the lower pI species collecting in chamber 8b. For all other numbers refer to Fig. 5.21 (modified from Faupel et al., 1987).

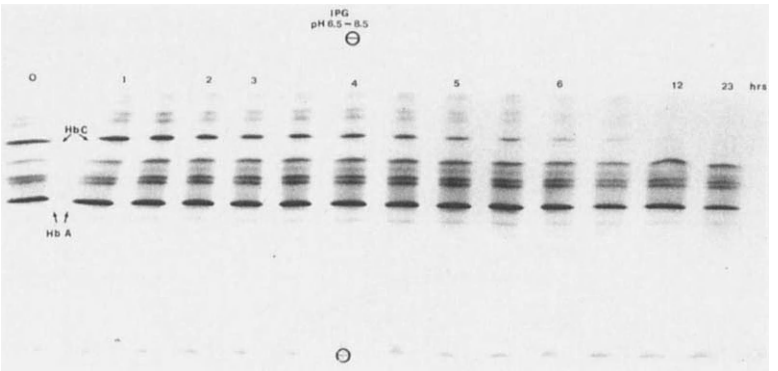

Fig. 5.24. Purificaton of Hb A from Hb C in the recycling, segmented IPG apparatus. The sample reservoir and central-flow chamber contained 25 ml of 0.5% Ampholine (pH 6–8) and a total of 70 mg hemoglobin from a heterozygous for Hb C (approx. 60% Hb A and 40% Hb C). Recycling was continued for 12 h at 1000 V, 3 mA, 3 W and then overnight at 500 V. 30 μl sample were harvested at the given time intervals and analyzed in a 0.5 mm thick IPG gel in the pH 6.5–8.5 range. The run was over after 3 h at 2000 V. Coomassie staining. Note the constant level of Hb A (kept isoelectric in the flow chamber) and the progressive loss of Hb C (from Faupel et al., 1987; with permission from Elsevier).

more) identical volumes, kept into separate sample reservoirs, and simultaneously recycled through the system. Given enough time under voltage, each protein species will collect into the appropriate flow chamber in which it is titrated to its isoelectric point.

Some examples of separations obtained are given as follows. In Fig. 5.24, purification of Hb A from Hb C in the blood of heterozygous carriers is shown. The figure represents the analytical run, in a kinetic experiment, of the removal of Hb C, under IPG conditions defined to keep isoelectric Hb A. For that, the lower IPG segment of the column in Fig. 5.21 was made to contain a pH 3.5–7.2 IPG interval, in presence of 1% carrier ampholytes, in a 5% *T*, 4% *C* gel. The upper IPG gel is cast in the pH 7.4–10 range and contains 1% *C*A in the same pH interval and the same matrix value as above. Thus the central flow chamber is confined to a narrow pH interval (pH 7.2–7.4) centred on the pI (7.3) of Hb A. A 70 mg total sample load in 25 ml of 0.5% Ampholine pH 6–8 was recycled in a prefocused apparatus under 1000 V constant. At 30 min

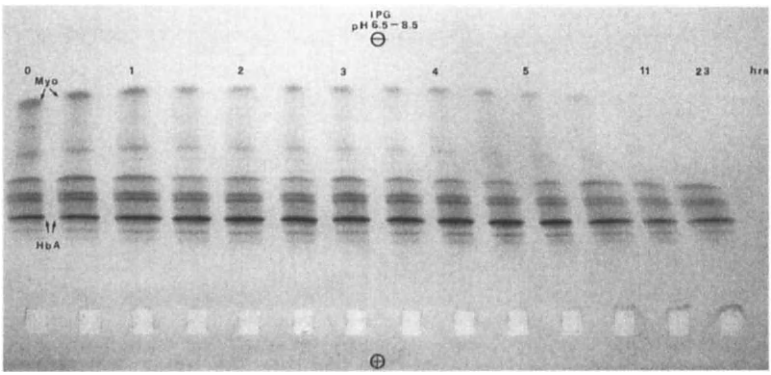

Fig. 5.25. Purification of Hb A from myoglobin in a segmented IPG gel. An experiment similar to that of Fig. 5.24 was run. Purified Hb A (50 mg) was mixed with 20 mg of sperm whale myoglobin (Myo) and recycled for 23 h at 1000 V, 3 mA, 3 W. 30 μl aliquots were analyzed at the given time intervals in an analytical IPG gel in the pH 6.5–8.5 range (from Faupel et al., 1987; with permission from Elsevier).

intervals 30 μl are sampled and kept at 4°C for subsequent analysis. The experiment is terminated with the last sampling after 23 h. The aliquots are analyzed in a 5% T IPG gel in the pH 6.5–8.5 span. As shown in Fig. 5.24, while Hb A stays constant for the duration of the run, Hb C is progressively removed till, at 23 h, it cannot any longer be detected. Similar results can be seen in Fig. 5.25, in which a mixture of Hb A and myoglobin are separated. Owing to the larger ΔpI between the two species (and thus to the higher mobility of myoglobin at the boundary conditions set), the contaminant is completely removed from Hb A after only 10 h of recycling.

5.6.2. Horizontal chambers

It was soon understood that the chamber described in Fig. 5.21 had some inherent problems: (a) due to its vertical mode of operation, air bubbles tend to accumulate in the ceiling of the flow chamber, this resulting in uneven trasport of impurities and hindrance of electric current flow; and (b) the lower IPG segment, immersed in the lower electrolyte reservoir (in general the anode) tends to swell

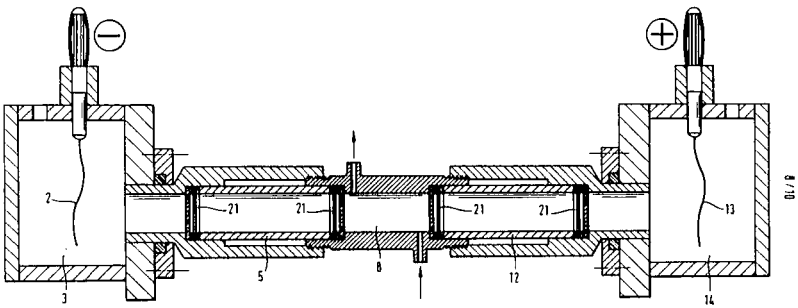

Fig. 5.26. Sketch of the horizontal, segmented IPG apparatus. 2 and 13: platinum wires; 3 and 14: electrolyte reservoirs; 5 and 12: plastic cylinders for holding the IPG gel segments (polymerized in glass tubes and subsequently inserted in these sleeves); 8: sample flow chamber; 21: membranes bound to the extremities of the IPG gel segments (modified from Righetti et al., 1987f).

ominously, this forcing the gel to protrude from the supporting tube and eventually detach from the glass wall and fall out from its lodging. In order to eliminate these problems, a new apparatus was described by Righetti et al. (1987f), based on a horizontal chamber provided with filters at all extremities of the IPG segments, for blocking in situ the Immobiline gel phases. As shown in Fig. 5.26, in this new orientation any air bubble flowing into the recycling chamber will be carried out by the liquid stream. In addition, the two gel phase delimiting the flow chamber are blocked by porous membranes (e.g., polypropylene filters, porous glass disks) which are pressed in appropriate lodgings machined into the supporting plexiglass tubes during the apparatus assembly. The IPG gel segments are first polymerized into glass tubes, which are then inserted, together with the membranes (21 in Fig. 5.26) at the two extremities, into two plastic cylinders (5 in Fig. 5.26). The central flow chamber (8) is screwed together with the two IPG gel segments and the horizontal block inserted in a slightly conical mounting connecting the gel tubes to the electrode reservoirs. Leakage is prevented by O-ring seals in the connection between each gel tube and the electrolyte chambers.

The performance of this horizontal apparatus was much improved as compared with the vertical version. In reality, however, the reason why this system works is shown in Fig. 5.27: it is

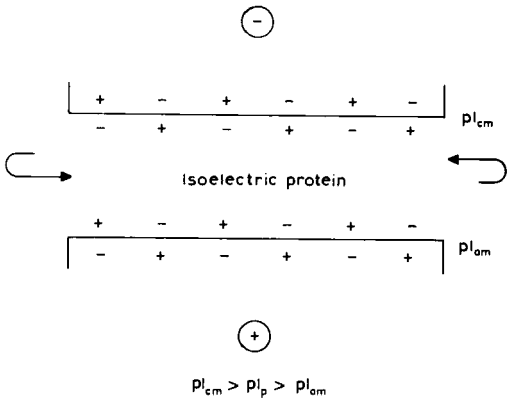

Fig. 5.27. Mechanism of the process of segmented IPGs. It is hypothesized that the two IPG gel extremities facing the recycling chamber act like isoelectric membranes titrating the protein of interest to its isoelectric point (pI), thus keeping its mobility constant and equal to zero throughout the purification process. For this to occur, it is necessary that $pI_{cm} > pI_p > pI_{am}$, where the subfixes indicate cathodic membrane, protein and anodic membrane, respectively. In addition, the two Immobiline membranes satisfy the condition of having high buffering power at their pI value. The curved arrows indicate protein recycling in the flow chamber (from Righetti et al., 1987e; with permission from Elsevier).

hypothesized that the two IPG gel extremities facing the recycling chamber act like two isoelectric membranes titrating the protein of interest to its isoelectric point. Thus these gel extremities can be envisaged like highly selective membranes, which retain any protein having pIs in between their limiting values, and which will allow transmigration of any non-amphoteric, non-isoelectric species. For that, the only condition required is that $pI_{cm} > pI_p > pI_{am}$, where the subscripts cm and am denote cathodic and anodic membranes, respectively, and p is the protein having a given isoelectric point between the two membranes (Righetti et al., 1987e). For this mechanism to be operative, it is necessary that the two gel extremities, idealized here as isoelectric membranes, possess good conductivity and good buffering capacity, so as to be able to effectively titrate the protein present in the flow chamber to its pI, while ensuring good current flow through the system. Wenger et al. (1987) had in fact synthesized amphoteric, isoelectric Immmobiline membranes and demonstrated that indeed (see Fig. 5.28) they are

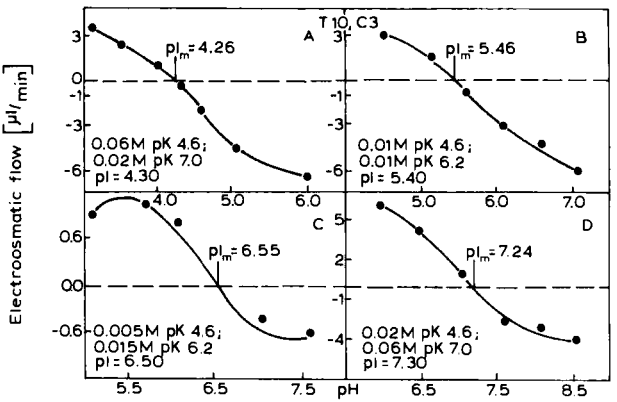

Fig. 5.28. Electrosmotic flow properties of Immobiline-based polyacrylamide membranes. Four different membranes have been made with the following theoretical isoelectric points: 4.30 (A), 5.40 (B), 6.50 (C) and 7.30 (D). The electrosmotic flow was measured in a chamber divided into two compartments by the IPG membrane and fitted with two capillaries for assessing water transport as a function of the prevailing pH in the two sectors. The pH of null flow is the measured pI (pI_m) of the membrane. Note the excellent agreement between experimental and theoretical pI values. The capacity of the IPG membranes of reversing the electrosmotic flow upon crossing the pI value is an indication of their good buffering power (from Wenger et al., 1987; with permission from Elsevier).

good conductors and good buffers at their pI. On the basis of these observations, a third type of apparatus has been built, based on the concept of isoelectric Immobiline membranes.

5.6.3. Membrane apparatus

Given the above considerations, we have built a scaled-up version of the segmented, recycling IPG apparatus (Fig. 5.29). The salient features are: (a) the immobilized pH gradients facing the sample flow chamber are reduced to membranes possessing a single pH value. These membranes are barely 2–3 mm thick (gel phase), are cast onto glass filters and are lodged in a housing (22, 24) against rigid disks of porous polypropylene. O-rings ensure flow-tight connections with the adjacent electrodic chambers (3 and 14); (b) the apparatus is horizontal, as above, so that the presence of air bubbles in the liquid stream does not hamper the electrophoretic

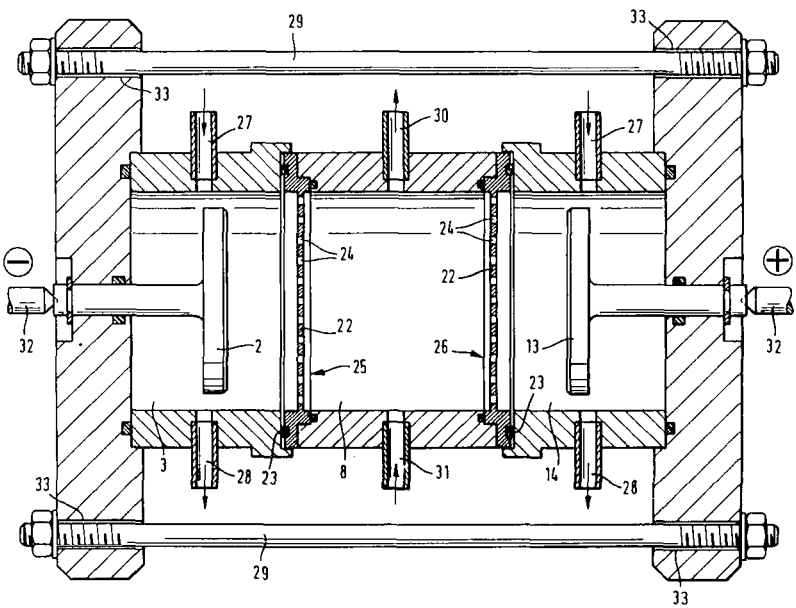

Fig. 5.29. Sketch of the membrane IPG apparatus. 2 and 13: platinum disk electrodes; 3 and 14: electrolyte chambers; 8: sample recycling chamber; 22: rigid polypropylene disks for housing the IPG membrane; 23: O-ring seals; 24: holes bored in the rigid disk (22) for current flow; 25 and 26: cathodic and anodic IPG membranes, respectively. These membranes are 2 mm thick and are polymerized onto a glass filter. 27 and 28: inlets and outlets, respectively, for recycling the electrolyte solutions; 29: steel rods for assembling the chambers of the electrophoretic apparatus; 30 and 31: outlet and inlet, respectively, for sample recycling; 32: connections to power supply; 33: holes bored in the two plastic feet for passage of the steel bars 29. The apparatus houses an IPG gel membranes with a surface area available for fractionation of 63.6 cm^2 (9 cm diam.) (modified from Righetti et al., 1988d).

process; (c) the electrodes are movable and can be positioned as close as 5 cm distance; and (d) the IPG membranes and the two Pt electrodes have a large diameter (9 cm) so as to ensure an even current flow and large transport rates of non-isoelectric proteins.

The membrane housing unit is shown in more detail in Fig. 5.30: once the IPG membrane, having the desired pI value, has been cast against a glass filter, it is throughly washed, so as to remove toxic unpolymerized contaminants, and then transferred to the lodging unit. This unit is made of two disks, consisting of a rigid Lucite

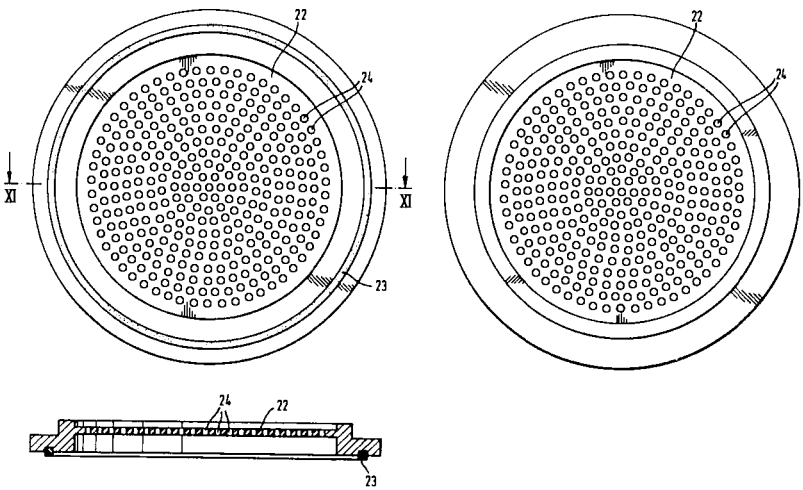

Fig. 5.30. Polypropylene disks for IPG membrane housing. Numbers as in Fig. 5.29. The figure represents the base (left) disk and the cover plate (right) into which the IPG membrane is sandwiched. The IPG fixed pI gel is polymerized separately in a closed chamber onto a glass fiber filter as a support. The IPG membrane protrudes ca. 1 mm on either side of the glass membrane. Note the O-ring (23) resting in a groove on the outer rim of the left disk. When the IPG membrane is housed in the two disks (whose transverse section can be seen in the lower left drawing) and assembled in situ (see Fig. 5.29), upon tightening the bolts in the assembled apparatus, a water-tight connection between the sample flow chamber and the electrolyte reservoirs is formed (Faupel and Righetti, unpublished).

round frame supporting a perforated polypropylene screen, with an O-ring on one side and a corresponding groove on the facing disk. The membrane is sandwiched in between these two support disks, and a flow-tight connection is ensured when the two membranes, with their lodging units, are assembled in the recycling chamber and the different blocks of the apparatus are bolted together with the aid of the four threaded metal rods and the corresponding winged nuts (see Fig. 5.29).

In the apparatus of Fig. 5.29, we have purified (Righetti et al., 1988d) 5 g of *N*-acetyl Eglin C (prepared at Ciba Geigy as a recombinant DNA product and ca. 80% pure) dissolved in 250 ml volume. Eglin C has a pI of 5.5, an M_r of 8300 Da and is a protease inhibitor produced by leeches. Its potential pharmacologi-

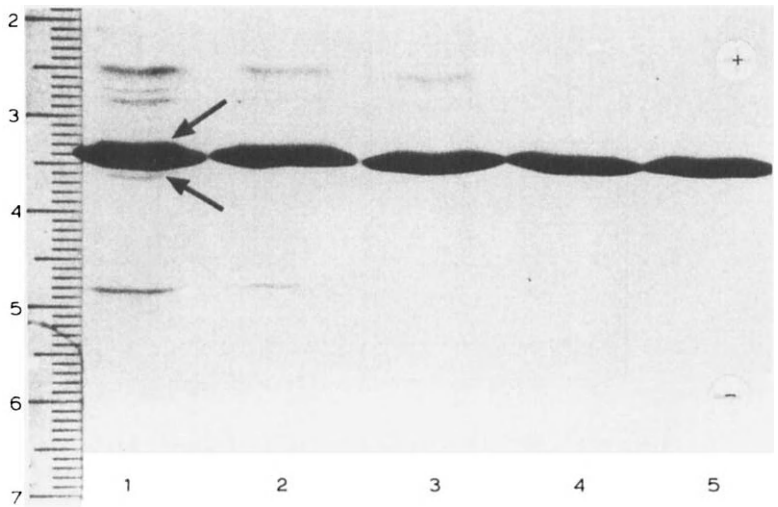

Fig. 5.31. Purification of Eglin C in the large scale membrane apparatus of Fig. 5.29. 5 g of *N*-acetyl Eglin C (produced at Ciba Geigy by recombinant DNA manipulations), dissolved in 250 ml distilled water, were purified in the apparatus of Fig. 5.29 at 500 V, 12 W constant, with 1 M acetic acid as anolyte and 1 M NaOH as catholyte, at 15°C. The boundary conditions were $pI_{cm} = pI_p = pI_{am} = 5.5$. At hourly intervals, 100 μl aliquots were collected and analyzed in an Ampholine PAG plate pH 3.5–9.5 (4% *T*, 3% *C*) for 3 h at 1000 V. The plate has been stained with Coomassie Blue in Cu^{2+}. Note that no impurities can be detected after 5 h of recycling (Faupel and Righetti, unpublished).

cal use could be in those inflammatory states in which extensive tissue breakdown occurs as a result of excessive activity of proteolytic enzymes. The experiment was run for 5 h at 500 V, 12 W constant, at 15°C, and 100 μl aliquots were collected and analyzed by CA-IEF in an Ampholine PAG plate. As shown in Fig. 5.31, after 5 h recycling, no impurities can be detected in the sample stream. It should be noted that in this separation, a new principle has been adopted: namely the boundary conditions have been set so that $pI_{cm} = pI_{am} = pI_p$ (all values being pH 5.5). In other words, the ΔpI between the two membranes was set at zero. This was rendered necessary by the fact that the nearest contaminant present in the Eglin C preparation had a $\Delta pI = 0.01$ pH unit. In this way, also this impurity was removed; however, the price to pay was a

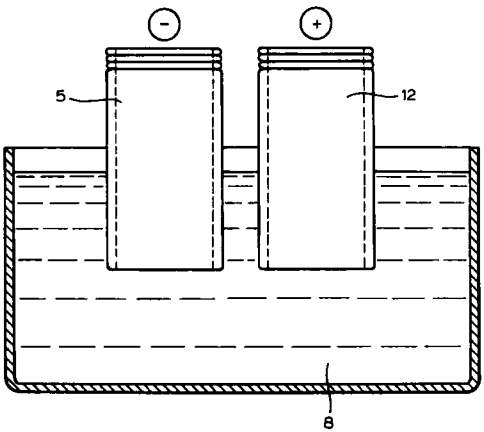

Fig. 5.32. Sketch of a 'tower' IPG apparatus. The sample is kept in a large, stirred and cooled reservoir (8), into which two cylinders (5 and 12) are lowered, containing either IPG gel intervals or IPG pH plateaus (membranes) for removal of non-isoelectric impurities. The catholyte and anolyte are poured on top of the IPG gel layers in cylinders 5 and 12; the Pt electrodes are not shown (Righetti and Faupel, unpublished).

small loss (ca. 15%) of Eglin C in the two electrodic compartment since the isoelectric protein, even though it could not be trasported electrophoretically out of the flow chamber, it could be lost by diffusion, since the two membranes facing it had the same pI as Eglin C.

A 'tower'-type apparatus could also be built, which, in principle, resembles the U-tube electrophoretic cell of the Tiselius (1937) moving boundary process. Fig. 5.32 gives a sketch of such an instrument. It consists of a large sample container accommodating, on the cover, IPG membranes coupled to towers containing the electrodic solutions and the Pt wire for connection to the power supply. The IPG membrane will be facing on one side the sample feed and, on the opposite side, the anolyte and catholyte solutions bathing the Pt wire for electric contact. The entire sample feed could be contained in this reservoir, which will be provided with cooling coils and with stirring. While Fig. 5.32 shows only two such towers, in reality one could build a battery of anodic and cathodic towers, coupled in series each one to its respective electrode. Such a

battery would have some important advantages: (a) it would provide a very large cross-flow area without having to resort to single, very large IPG membranes which could collapse under the hydraulic pressure or would be in any event quite difficult to handle; and (b) it could enable pharmaceutical industries to process several liters of sample stream and a handling rate close to the kg/day, which could be of extreme interest for purification of recombinant DNA products. Finally, a multi-membrane apparatus has recently been described (Righetti et al., 1989c).

5.6.4. On the upper load limit in electrokinetic processes

The following inequality can be derived for the upper load limit on the mass processing rate (M) in an electric field:

$$M < (\Delta\mu) E A_c C_\infty$$

where A_c is the lateral cross-sectional area and C_∞ is the far-field protein concentration in the chamber (i.e., the solute concentration at a sufficient distance from the feed port) in grams per cubic centimeter. For $\Delta\mu$ of ca. 10^{-4} (cm/s)/(volt/cm) (as typical of protein ions), E (voltage gradients) of ca. 25 V/cm and C_∞ of ca. 10 mg/ml (i.e., 1% protein solution), a minimum of one square centimeter cross-sectional area is needed to process 0.1 g protein/h. Thus, with the membrane apparatus of Fig. 5.29 (having a cross-sectional area of 63.5 cm^2) there is the potential of processing 6 g protein/h, a definitely interesting amount of protein to deal with.

5.7. Alternative preparative methods

Some alternative preparative electrokinetic processes are also described in the literature and are reviewed briefly below. For a more extensive survey, refer to Righetti (1983a).

5.7.1. The Biostream separator

In the late thirties, Philpot (1940) attempted to extend the scale of the Tiselius' (1937) U-tube by adapting it to continuous sep-

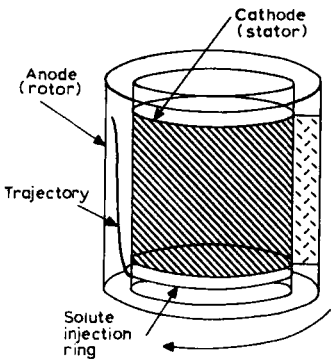

Fig. 5.33. Scheme of the Biostream separator. Protein separation occurs in an annulus between a static cathode and a rotating anode. Carrier fluid flows axially upwards through the annulus and feed is injected through a ring-shaped opening just below the electrodes. The liquid is collected into 50 fractions at the top.

arations. However, it was not until the mid seventies that he finally designed a chamber which achieved stable operation (Philpot, 1973). This was accomplished by rotating the outer wall to apply a transverse stress field across a thin annulus formed between two concentric cylinders (see Fig. 5.33). The two cylindrical walls which delimit the separation chamber act also as electrodes and the annulus in between is the sample processing chamber. In this equipment the inner cylinder is fixed and generally is utilized as cathode, while the outer cylinder, which functions as anode, rotates at a speed of ca. 150 rev./min, generating a liquid-stabilizing velocity gradient. The carrier fluid flows axially through the annulus and the feed is injected through a O-shaped opening just below the electrodes. This configuration allows operation at through puts in excess of 1 l/h, three orders of magnitude greater than classical 'thin-film' devices [e.g., the continuous flow chamber of Hannig (1967)]. In terms of protein load, as much as 10 g/h have been processed. A commercial version of this device is now available as the Biostream separator (Mattock et al., 1980). In the Biostream chamber, a counter-current flow (the buffer film is pumped upwards) is used to discourage unstable convection, with the radial stress field (generated by rotating the outer, anodic wall) producing added stability by dumping unstable convection driven

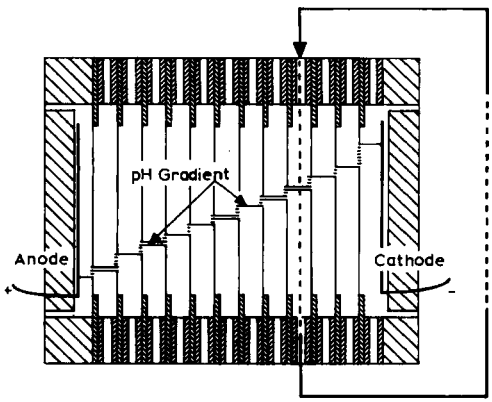

Fig. 5.34. Scheme of the recycling isoelectric focusing (RIEF) apparatus. The focusing cell consists of a stack of nylon membranes, delimiting narrow channels (2 mm wide) into which the sample and carrier ampholyte solution is continuously recycled from a large and cooled reservoir. Given sufficient time under voltage, a pH gradient is established between the electrodes. In the Rotophor, all the sample feed is contained in the focusing cell, which is made of 20 compartments, is cooled by a central finger and rotates slowly on its axis to prevent protein decantation.

by radial and axial temperature gradients. In addition, the parabolic velocity profile of the carrier fluid is used to advantage to sharpen the solute bands during separation. Finally, because the electric field in the Biostream runs perpendicular to the transverse annular surfaces, there is no electrosmosis and dispersion is, in principle, controlled by the slow diffusive process. The apparatus looks promising and the through put is definitely the highest so far reported in any electrokinetic process. However, the examples given in the literature only show separations of proteins differing by large ΔpI values (e.g., ΔpI of 2–3 pH units).

5.7.2. Recycling isoelectric focusing (RIEF)

The application of recycling to continuous electrophoretic processing was pioneered by Bier and coworkers (1979, 1986a,b) for IEF. Fig. 5.34 shows the central flow chamber of this instrument. The heart of the apparatus is an adiabatic, multichannel slit which is partitioned into compartments by closely-spaced, fine

porosity nylon screens which act to damp convection but which freely transmit macroions as they move in the electric field. The sample feed (dissolved in 2% carrier ampholytes) is kept in a large, cooled reservoir divided into as many compartments as there are slits into the focusing chamber. During a run each of the compartments develops a characteristic pH which is highest at the cathode and lowest at the anode and which changes sharply at the nylon mesh screens. Once the pH gradient is established, the proteins present in the system will migrate, at their characteristic velocities (depending on the slope of their pH/mobility curves), to their pI position. The electric field is then switched off and the apparatus and reservoirs drained of product. In a recent commercial version, called the Rotophor (Bio Rad Labs, Richmond, CA) all the unit is assembled in a single piece, a rotating chamber provided with a cooling finger and divided into 20 compartments. All the mixture to be fractionated is present in the chamber which rotates slowly on its axis to prevent electrodecantation. At the end of the separation process, all the chambers are simultaneously emptied with the help of 20 suction needles connected to a vacuum port. This apparatus cannot process large amounts of proteins (max. 100–150 mg) nor large liquid volumes (max. 50 ml) but it has the advantage of allowing quick separations and is quite 'user friendly'.

5.7.3. Free-flow field step focusing

An idea which makes optimal use of commercial thin-film electrophoresis technology was advanced by Wagner and Kessler (1983) and by Wagner et al. (1984). This process, known as field step focusing (FSF), introduces a sample zone into a continuous flow-curtain apparatus, such as the Bender & Holbein's Elphor VaP 21, as a broad, low-conductivity layer of buffer spanning the central portion of the cell and running between two curtains of substantially higher conductivity. Typically, the central curtain is 3–5 cm across and 0.5–1 mm thick, the conductivity of the central curtain is 10–5 mho/cm and the conductivities of the outer curtains are some 10–100 times higher. The pH of the central curtain is adjusted so that it is intermediate to the pIs of two 'key' components and, when the electric field is applied, these compo-

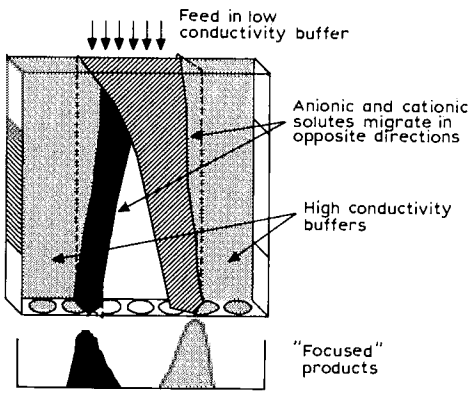

Fig. 5.35. Scheme of the Wagner's apparatus for field step focusing. The sample is introduced in a thin electrophoresis cell (continuous flow, curtain type) as a broad, low conductivity curtain. Sample components are forced to 'focus' against two lateral, high conductivity buffers. The pH of the central curtain is adjusted so that it is intermediate between the pIs of two 'key' components whose purification is sought.

nents migrate to opposite sides of the central curtain (Fig. 5.35). Upon contact with the high-conductivity curtains, whose pH may be optimally adjusted to discourage further migration, the electrophoretic velocity decreases by at least the fraction

$$\sqrt{\sigma_{high}/\sigma_{low}}$$

where σ is the electrical conductivity. Thus the solutes slow down and 'focus' at the interfaces between the two buffer curtains. According to Wagner et al. (1984) the four addvantages of FSF are: (a) focusing is achieved without ampholytes; (b) through put is high; (c) separation is optimized by simply adjusting the buffer pH; and (d) separation is conducted at pH values removed from protein pIs, so that precipitation is avoided. According to Wagner et al. (1984) the volumetric flow rate processing can be of ca. 500 ml/h and the maximum protein processing rate of the order of 0.6 g/h. Here again, though, separations have only been made among artificial mixtures of standard proteins, with well separated pI values (ΔpI ca. 2–3 pH units) so that there is really no way to

know how the FSF technique would work under conditions comparable to those achieved in the IPG membrane apparatus, i.e., high sample through puts (1 g/h) but with ΔpIs as low as 0.01 pH units.

5.8. Conclusions

It seems that preparative electrokinetic processes are now becoming a reality, not only in the specific field of IPGs, but also in free-flow systems, such as the Rotophor apparatus and the FSF method we have just analyzed. Of all these preparative systems, IPGs however appear outstanding, since they seem to be the only ones offering a high through put coupled with a high resolving power, a condition often overlooked in all other electrokinetic processes. In addition, the new IPG membrane apparatus offers another remarkable advantage: the possibility of obtaining clean proteins which are also free from contaminants leached out from polyacrylamide gels. In all gel electrophoretic systems of the past, often the major contaminants in a purified sample zone were monomers and oligomers extruded from the matrix during the elution step. With the membrane apparatus we have developed (Fig. 5.29), after a 24 h washing cycle of the membranes, it was impossible to detect the presence of gel monomers down to the picomole level. Clearly, this is of extreme importance in the pharmaceutical industry when purifying recombinant DNA proteins for human consumption. It does not seem to be right to administer a drug on one hand free from other protein contaminants but on the other hand contaminated by neurotoxins such as acrylamide and Bis.

Some applications of IPGs

Due to the fact that IPGs have still not found wide applications as yet, since the inherent problems of the technique have been solved only recently, the survey I will make of the applications of the technique will be quite extensive. It is clear, however, that, since the technique is rapidly spreading and it will soon be a standard method in laboratories arounds the world, the new edition of this book will only contain some examples of applications of IPGs, or else an entire new book on applications will have to be written.

6.1. Analysis of hemoglobins

As usual, hemoglobins (Hb) always have the lion's share in the development of a new technique. They are highly soluble, easily available in pure form, colored and they never behave 'badly' in any separation technique. It is only natural, thus, that IPGs would be extensively applied to their analysis. Already in the case of conventional IEF, Hb analysis in carrier-ampholyte-driven pH gradients had become a standard tool in hematology departments for mass screening of blood samples and for diagnosis of hemoglobinopathies (Righetti, 1983a). CA-IEF had been instrumental in the discovery of a substantial number of new, previously undetected Hb mutants (Basset et al., 1982). In addition, it had proven to be a fine tool for physico-chemical investigation of Hb structure and function. Thus, CA-IEF could be used for an accurate measurement of the intrinsic alkaline Bohr effect of normal and mutant human Hbs (Poyart et al., 1981); as a probe of the red-ox state of the iron in the ligand heme (Bunn et al., 1977); as a probe for studying subunit exchange (e.g., hybrid hemoglobins in the same species, Hb A with Hb C; Bunn and McDonough, 1974). As an additional variant, CA-IEF at sub-zero temperatures ($-23°C$, in

gels containing a hydro-organic solvent) has allowed the resolution of all the possible intermediates of oxidation between fully reduced and fully oxidized Hb tetramers (eight intermediates plus the two extremes) and to calculate the dissociation constants of all the intermediate species (Perrella et al., 1981). I will review here what additional benefits have come from IPGs.

6.1.1. Detection of charged variants

In principle, this should pose no problems in electrophoretic analysis, since charged mutants produce a sufficiently high ΔpI to allow, in most cases, for clear cut separations not only in CA-IEF, but often even in cellulose acetate or agarose electrophoresis. Thus, the separation I am proposing in Fig. 6.1 could appear to be trivial, since the different charged mutants (S, a β6 Glu → Val, C, a β6 Glu → Lys and J-Baltimore, a β16 Gly → Asp, in addition to fetal, F, tetramers) can be easily detected by almost any technique. Yet, we begin to see already some differences: the bands are usually razor sharp, even at high-protein loads. In addition, a most interesting phenomenon occurs with the sample from umbilical cord

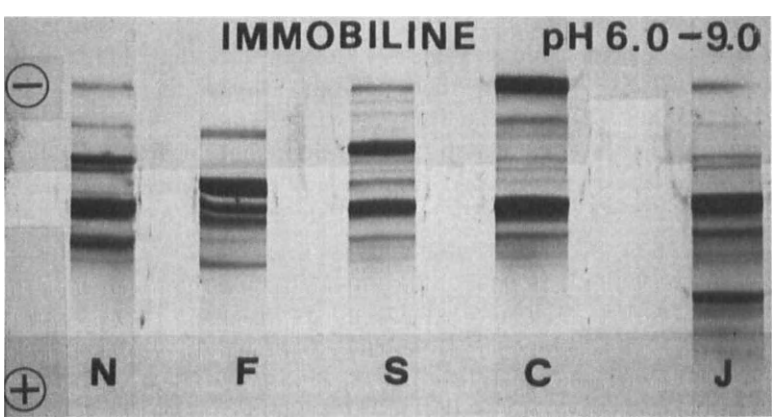

Fig. 6.1. Hemoglobin separation in an Immobiline pH 6–9 gradient. N: normal human adult; F: umbilical cord blood lysate; S, C and J: samples from patients heterozygous for hemoglobins S, C, and J, respectively. Anodic sample application (3 mg each). Focusing for 4 h at 10°C and 2500 V. Unstained gel. Unpublished experiments with Dr. T. Hebbell.

blood: in a 3 pH unit interval, the separation between the three major Hb samples (F, ca. 70%, A, ca. 20% and F_{ac}, ca. 10%, this latter species being an acetylated derivative of the fetal band) is much better than in a 2 pH unit CA-IEF gradient (compare with Fig. 1 in Manca et al., 1986).

Some separations of charged Hb mutants, in addition, are not trivial at all since the pI of the mutant could overlap with the pI of a normal Hb already present in the red blood cell. A case in point is Hb E, a β26 Gly → Lys variant already discovered in 1961 by Hunt and Ingram. HbE is one of the most prevalent Hb variants in man; its occurrence is virtually confined to South East Asia, where it has been estimated to affect about 30 million people (Fairbanks et al., 1979). In this part of the world other hemoglobinopathies, mostly α- and β-thalessemias, are also very frequent (Sicard et al., 1979). Hb E is, in addition, characterized by a decreased level of biosynthesis, giving rise to a β^+-thalassemia. Thus, individuals homozygous for Hb E present a constant anemia and the phenotype of a mild homozygous thalassemia. Heterozygous individuals (Hb E trait) have smaller amounts (ca. 35%) of Hb E than of Hb A. In addition, when some α-thalassemia coexists, in relation with preferential subunit association of α-chains with normal β-chains, the amount of Hb E may be as low as 10% or even less. The electrophoretic and haematological pattern is then very similar to that observed in the case of β-thalassemia trait in which Hb A_2 (a normal component of adult blood, present at a ca. 2–4% level) is increased. An accurate diagnosis between these two haemoglobinopathies would thus require an electrophoretic test discriminating Hb E from Hb A_2. It just so happens, however, that, as a result of the mutation, Hb E exhibits an almost identical pI as Hb A_2, rendering the discrimination by CA-IEF of these two bands virtually impossible (Basset et al., 1982). As shown in Fig. 6.2, very shallow IPG gradients (a pH 7.55–7.65 interval) covering barely 0.1 pH unit, are able to fully separate mixture, of Hb A_2 and Hb E in any proportion (the ΔpI being barely 0.004 pH unit).

6.1.2. Detection of neutral mutations

In a recent survey (Wrightstone, 1986), as many as 457 Hb variants were listed. Of the 134 α-chain mutants, only 11 bear neutral →

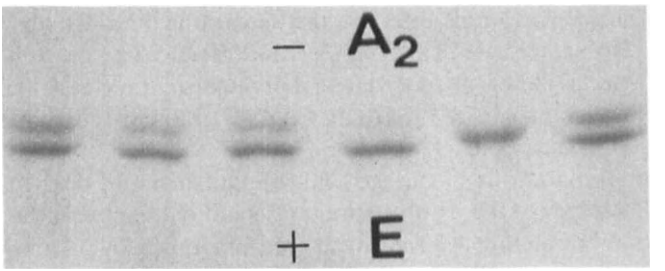

Fig. 6.2. Separation of Hb E from Hb A_2 in immobilized pH gradients. The IPG gel was a 4% *T*, 4% *C* matrix containing a pH 7.55–7.65 pH interval. Sample: a 6:4 mixture of chromatographically pure Hb E and Hb A_2 (two lateral lanes; the others contained from 0 to 3% A_2, starting at the second lane from the right). Run: 2500 V, 0.3 mA, 20 h at 10°C. Staining wiht Coomassie Blue (from Bianchi-Bosisio et al., 1985; with permission from Elsevier).

neutral substitutions; in the case of β-chains, out of 229 variants only 59 are neutral. Of the δ chains, no neutral mutants are described among the 15 reported and, in the case of γ-chains, only four neutral mutants out of a total of 39 have been detected. By averaging these data, it appears that barely 15% of all Hb mutants listed are neutral substitutions, the remaining 85% involving charged amino acids. However, on the assumption that nucleotide substitutions in human genes occur at random, a preponderance of neutral mutants would be expected so that, in a population at equilibrium, ca. 70% of the variants should be neutral and ca. 30% charged (this reflecting the ratio neutral/charged amino acids in proteins). Thus, if the total number of charged Hb mutants is 383, there should be at least of the order of 893 neutral ones and close to a total of 1276 overall existing Hb phenotypes, rather than the value of 457 reported. The reason for this odd ratio probably stems from the fact that most of these variants have been detected by conventional electrophoretic techniques, like cellulose acetate, starch, citrate-agar or polyacrylamide gel electrophoresis, which would be generally unable to detect neutral mutants. Conventional IEF has substantially increased our ability to resolve mutants with similar pI values, but is still unable to separate anything having ΔpIs of less than 0.01 pH units, the present resolution limit of CA-IEF. With IPGs, claimed to have a resolving power of $\Delta pI = 0.001$ pH unit, the situation was bound to change.

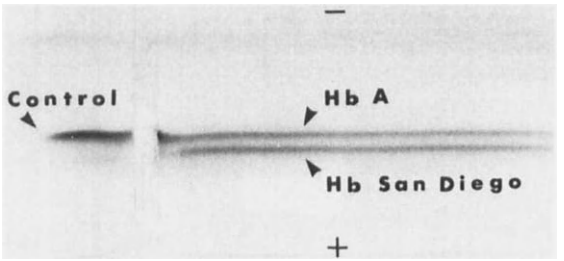

Fig. 6.3. Separation of Hb A–Hb San Diego in IPGs. The gel was 125×110 mm, 1 mm thick, in a 5% *T*, 4% *C* matrix containing an IPG pH 6.9–7.7 interval. About 8 mg total protein were loaded on the right-hand trench. In the left-hand pocket, 1.5 mg of Hb from a normal human adult lysate were applied. The ΔpI between Hb A and Hb San Diego was calculated to be 0.01 pH unit. Unstained gel (from Rochette et al., 1984; with permission from Elsevier).

A case in point is given in Fig. 6.3, which shows the separation between Hb A and Hb San Diego (β109 Val → Met) (Rochette et al., 1984). Even though the analysis was performed on an IPG pH 6.9–7.7 gradient (thus spanning a 0.8 pH unit interval), ample separation was obtained between the two phenotypes. Interestingly, when first described (Nute et al., 1974), it was reported that this mutant could not be resolved from Hb A by any known chromatographic or electrophoretic technique (including CA-IEF). Another example is offered in Fig. 6.4, which shows the separation between Hb Beirut (β126 Val → Ala) and Hb A (Cossu et al., 1986a). When a red cell lysate from the carrier was analyzed by CA-IEF, in 2% Ampholine pH 6–8 added with an equimolar mixture of β-Ala and 6-amino caproic acid (which flatten this pH gradient in the pI region of Hb A; Cossu et al., 1984), no separation was obtained between the two species, but barely a thickening of the Hb A zone (Fig. 6.4A). The quality of the separation can be judged by the fact that a minor, glycated Hb (Hb A_{1c}) is well resolved from Hb A. However, when the same analysis was attempted in an IPG pH 7.2–7.6 interval, the two species were well separated (Fig. 6.4B). I do not want to insist in producing *n* examples of separations of 'electrophoretically silent' mutants, as this would resemble a mere academic exercise at this point. However, an interesting case is certainly the separation of foetal hemoglobins (Hb F). There exists

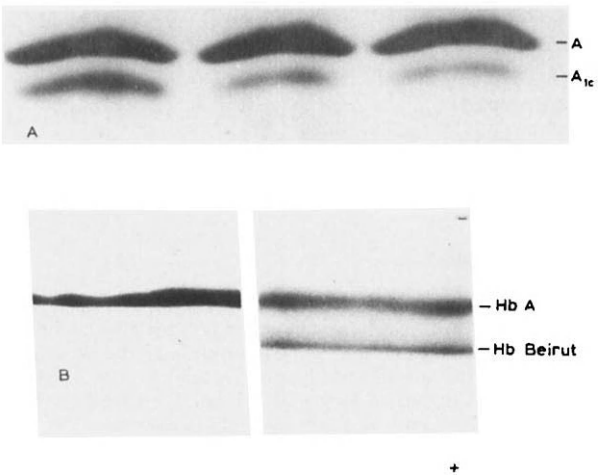

Fig. 6.4. Separation of Hb Beirut from Hb A. A: CA-IEF of Hb A and Hb Beirut in a 5% *T*, 4% *C* polyacrylamide gel containing 2% Ampholine pH 6–8 and an equimolar (0.2 M) mixture of β-Ala and 6-amino caproic acid. Left: control lysate from a diabetic patient. Centre: 1:1 mixture of Hb A and Hb Beirut. Right: lysate containing blood from a Hb Beirut heterozygous. Conditions: 15 min at 400 V, sample application at the cathode (50 μg protein per track), followed by 90 min at 1500 V. The gel was stained with 0.1% bromophenol blue in 50% methanol and 10% acetic acid. Note the thickening of the A band but the absence of any separation. B: IPG gel of 4% *T*, 4% *C* containing an IPG spanning a pH 7.20–7.35 gradient. The washed gel was re-swollen in 4% Ampholine pH 6–8, in order to improve the background conductivity across neutrality and shorten the focusing time. Running conditions: 6 h at 4000 V at 10°C. Total sample load: 200 μg (unstained gel). Both gels from Cossu et al. (1986a); with permission from Elsevier.

a neutral mutant, called Hb F Sardinia, carrying a Ile → Thr substitution in position 75 of the β chains. When analyzing the cord blood of a newborn heterozygous for Hb F Sardinia (Fig. 6.5A, left side) barely a thickening of the F zone was observed, but this condition could be hardly diagnosed if confronted with a normal newborn (Fig 6.5A, right track) (Cossu et al., 1986b). When the same separation was performed in an IPG pH 6.9–7.5 interval, now the Hb F Sardinia band was clearly seen splitting from Hb F as a more alkaline band (Fig. 6.5B), whereas this splitting was not observed in the normal newborn (Fig 6.5B, right track). Obviously, when the separation was repeated in a shallower IPG gradient (pH 7.33–7.55) the two zones were further split apart (Fig. 6.5C). In

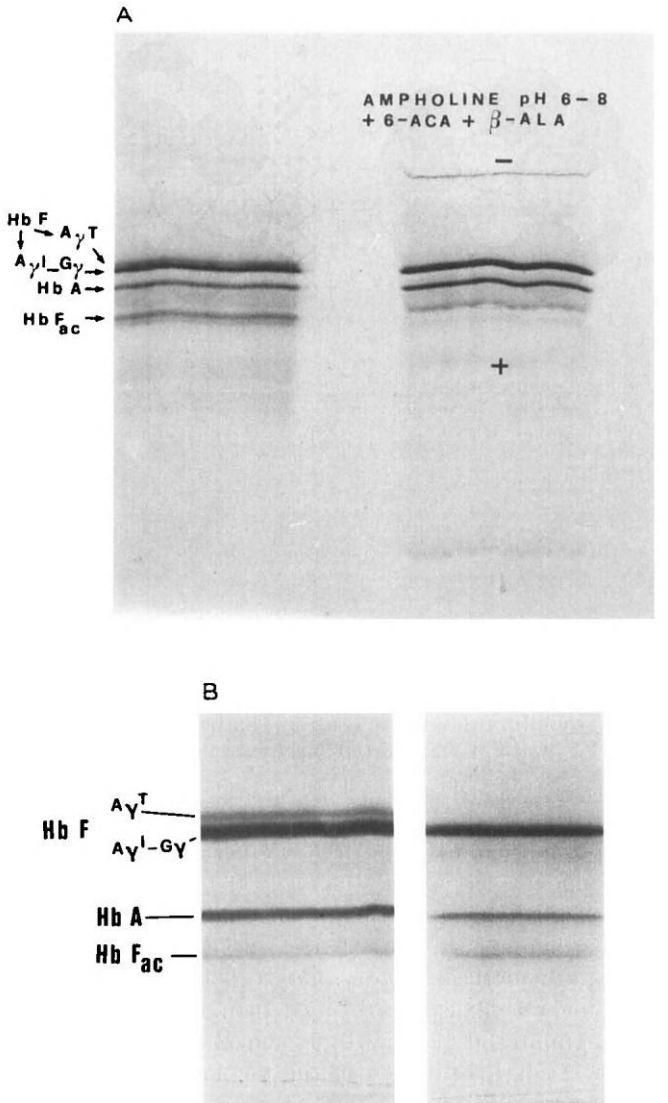
A
AMPHOLINE pH 6–8
+ 6-ACA + β-ALA
–
+
Hb F
$A_\gamma T$
$A_\gamma I$–G_γ
Hb A
$Hb F_{ac}$
B
Hb F
$A_\gamma T$
$A_\gamma I$–G_γ
Hb A
$Hb F_{ac}$

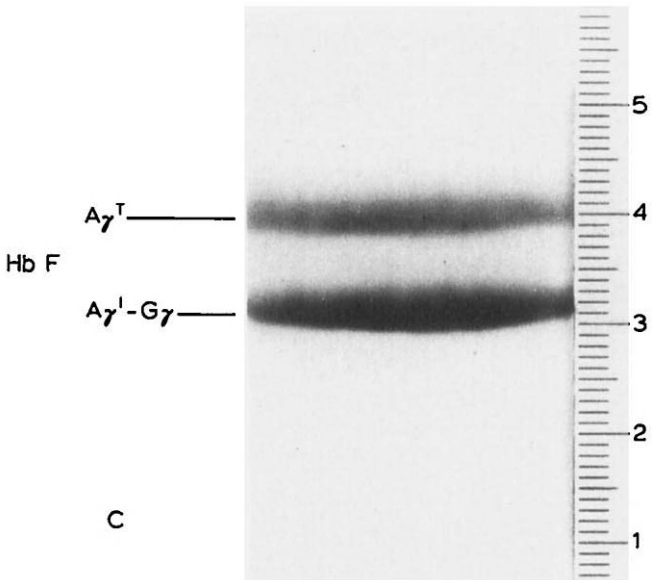

Fig. 6.5. IEF of cord blood lysates from newborns. A: 5% *T*, 4% *C* polyacrylamide gel containing 2% Ampholine pH 6–8. Sample load: 50 μg total Hb, applied at the cathode. Running conditions: pre-run for 15 min at 400 V, then sample application, followed by 90 min at 15 W (1500 V at equilibrium). Left: newborn heterozygous for the AγT condition; right: normal newborn, containing 70% Hb F, 20% Hb A and 10% Hb F_{ac}. B: IEF of the same two samples as in A, but utilizing an IPG pH 6.9–7.5 gel. Note the partial separation between Hb F Sardinia and normal Hb F. C: IEF of the heterozygous sample in an IPG pH 7.3–7.55 gradient. Note the complete separation of the AγT tetramer from the zone containing the AγI and Gγ tetramers. Running conditions: 5 h at 4000 V at 10°C. In (C), due to the shallow pH gradient generated, Hb A and Hb F_{ac} focus outside the fractionation range, collecting at the anode (from Cossu et al., 1986b; with permission from VCH).

reality, the situation is more complex than that: even normal newborns contain in their cord blood two Hb F tetramers, called A_γ and G_γ (in a ratio of ca. 1 : 4) produced by two genes carrying an Ala-136 → Gly substitution in the γ-chains. The latter species have not been resolved by any chromatographic (including HPLC) or electrophoretic technique but now, in a 0.1 pH unit interval IPG run, they could be fractionated into single components (Fig. 6.6) (Cossu and Righetti, 1987). The identity of these two bands was

Fig. 6.6. Resolution of the two Hb F phenotypes in a 3% *T*, 4% *C* polyacrylamide gel containing an IPG pH 7.35–7.55 gradient over a 20 cm distance. The gel was added with 6% Pharmalyte pH 5–8. Focusing time: 6 h at 5000 V, 10°C. Unstained gel. The cathode is uppermost (from Cossu and Righetti, 1987; with permission from Elsevier).

confirmed by eluting the two zones from the IPG gel, by preparing heme-free chains and by analyzing the γ-chains by conventional IEF in 8 M urea and 2% neutral detergent (Nonidet P-40) (Righetti et al., 1979). It was shown that the higher pI band contained only the A_γ fetal chain, while the lower pI species essentially comprised only G_γ chains. In addition, the ratio between the two bands was 1 : 4, as expected from genetic expression of these two Hbs. Note that the difference in isoelectric points between the two species is barely 0.003 of a pH unit (pI 7.450 for G_γ vs. 7.453 for A_γ) which means that IPGs can indeed attain a resolution of $\Delta pI = 0.001$ pH unit, as predicted (Bjellqvist et al., 1982).

Why should IPGs be able to separate what up to now had been believed to be species unseparable by electrokinetic methodologies (thus called 'electrophoretically silent' mutants)? I propose here a likely mechanism for these separations which, by involving non-charged amino acids, should normally be the province of HPLC rather than of electrophoretic techniques. There has to be a 'transducing element' which converts a hydrophobic (non-polar or non-charged) signal into an electric signal, which is reflected as a feeble change in the net charge at the surface of the polymer. This 'transformer' can only be another amino acid, with an ionizable side group, bordering the mutation side, which senses the hydrophobicity change brought about by the mutation, and changes its p*K* accordingly. If this hypothesis is correct, it is not true that a neutral → neutral amino acid substitution is 'electrophoretically silent' (in the sense that it does not alter the protein mobility in an electric field): it does indeed alter the net surface charge of the native macromolecule, but to such a minute extent as to be

generally undetected by conventional electrophoretic techniques and often even by more sophisticated ones, like conventional IEF. As these surface charge changes are in general quite minute, often well below 0.01 pH unit in pI changes, it follows that the only correct probe today available to detect them is the IPG technique, which indeed affords such resolution.

There is another general conclusion that can be drawn from the above experiments. With a resolution of $\Delta pI = 0.001$ pH units, it should be possible, in principle, to separate 1000 proteins in a 1 pH unit span. Given the fact that we can now utilize pH 2.5–11 IPGs (over 8.5 pH units), if the proteins had pH values evenly distributed along the pH axis, we should be able to separate at least 8000 protein bands. In fact, this is not the case, as 60% of all possible phenotypes focus in the pH 4–7 range (Gianazza and Righetti, 1980); thus, this capability is reduced to about 4000 bands over the entire pH axis. Eukariotic cells are thought to be able to express 40–60,000 different polypeptide chains (Holland et al., 1980). However, in practice, at any given time no more than 4000 spots are detected in two-dimensional maps (Klose and Zeindl, 1982), suggesting that, during normal activity, the cells express only 10% of their potential gene products (the other alternative being that many more are expressed, but in such low amounts as to be undetectable even by highly sensitive staining techniques, such as silver stain or autoradiography). If this is so, when working in ultra-shallow IPG gradients (0.1 pH unit spans), with a resolution of $\Delta pI = 0.001$, a band focusing in a given position is likely to be truly homogeneous, i.e., uncontaminated by a different protein band co-focusing in the same position.

6.1.3. Thalassemia screening

For a correct evaluation of thalassemia syndromes, heme-free globins have to be separated by chromatographic or electrophoretic means and their relative ratio assessed. Already in 1979 Righetti et al. had devised a method for globin chains separation by CA-IEF in the presence of urea and detergents. The detergent, probably by binding to denatured globins, greatly increases the separation between γ- and β-chains, thus allowing for a proper densitometric or

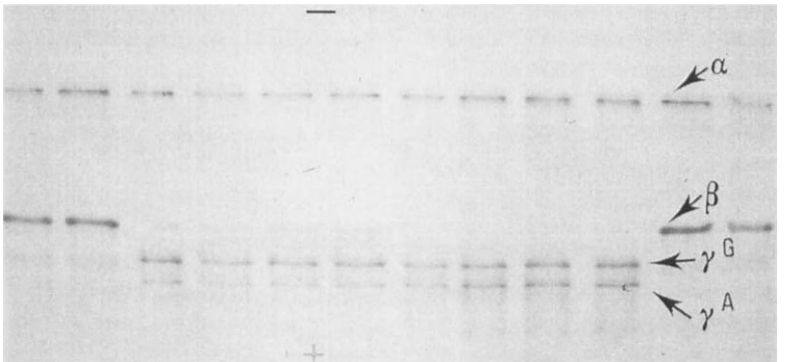

Fig. 6.7. Separation of human globin chains by CA-IEF. The gel (5% *T*, 4% *C* matrix, 0.5 mm thick) contained 2% Ampholine pH 6–8, 8 M urea and 1% Nonidet P-40 (NP-40). The globin chains were dissolved in the same solvent and were applied at the anode in 50 μg/track load. Focusing was for 3 h at 1500 V and 10°C. Staining with Coomassie Blue (modified from Righetti et al., 1979; with permission from Elsevier).

fluorographic quantitation of their relative ratios (Fig. 6.7). In addition, the detergent splits the γ-zone into two bands, which have been demonstrated to be the two phenotypes of the human fetal γ-globin chains, called A_γ and G_γ. According to Righetti et al. (1980) this NP-40 effect might be due to preferential binding of the detergent micelle to the hydrophobic stretch ^{133}Met to ^{141}Leu in A_γ chains. Upon binding, the detergent could sorb the ^{132}Lys in this stretch into its Stern layer or bury it within the micelle, thus inducing a total loss of one proton from otherwise identical-charge phenotypes. This unique separation between A_γ- and G_γ-chains has made possible studies on the switch from G_γ- to A_γ-chain synthesis during development and maturation of erythroblasts (Papayannopoulou et al., 1981).

With the advent of IPGs, due to the high resolution intrinsic to the technique, it has been possible to perform diagnosis for thalassemias directly on umbilical cord lysates in newborns and in fetuses. In reality, diagnosis of β-thalassemia in newborns could be performed also quite well with the CA-IEF technique in presence of separators, able to flatten the pH gradient in the region where Hb F, A and F_{ac} focus (Cossu et al., 1982). For antenatal diagnosis,

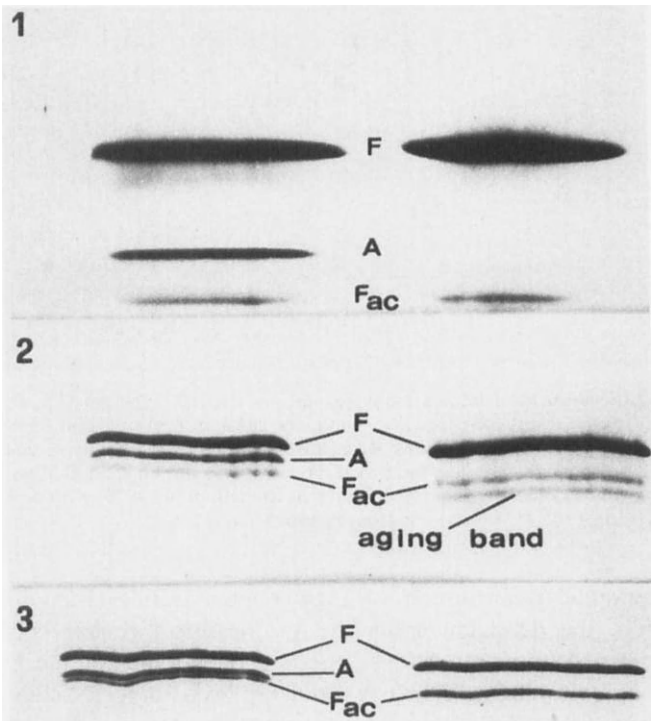

Fig. 6.8. Separation of Hb F, Hb A and Hb F_{ac} from foetal cord blood (week 18 of pregnancy). Panel 1: IPG gel, pH 6.8–7.8 range; panel 2: pH 6–8 Ampholine range added with 0.2 M β-alanine and 0.2 M 6-amino caproic acid; panel 3: conventional pH 6–8 Ampholine range. Left: normal foetus; right: homozygous β°-thalassemic foetus. Staining: Coomassie Brilliant Blue R-250 in Cu^{2+} (from Manca et al., 1986; by permission from A. Liss).

however, because of the ethic problems connected with genetic counselling of couples at risk, and the possibility of abortion, a foolproof screening technique coupling a high resolving power with a high sensitivity for the detection of even minute amounts of Hb A in fetal blood is necessary. IPGs have proven to fulfill these requirements. Fig. 6.8 shows the separation of the three main components of cord blood (foetal, adult and acetylated foetal) in foetuses at the 18th week of pregnancy. Normal foetuses produce

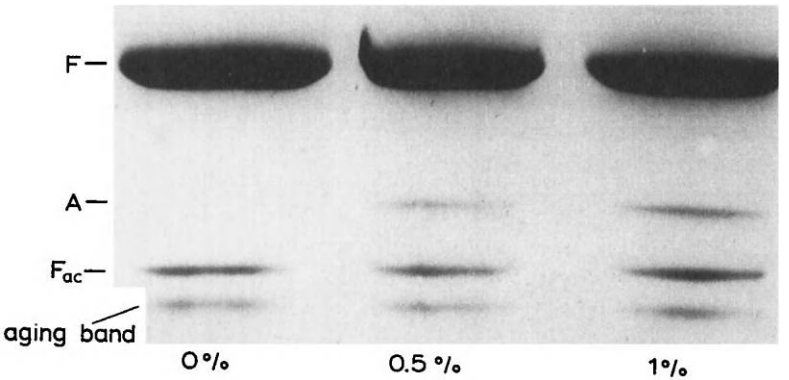

Fig. 6.9. Minimum detectability of Hb A in fetal cord blood. A homozygous β°-thalassemic umbilical lysate was added with increasing amounts of purified Hb A (from 0.5 to 1%). A total amount of 1.2 mg protein/track was applied to a 0.5-mm-thick Immobiline gel, pH 6.8–7.6. By this overloading technique, the minimum detectability appears to be better than 0.5% Hb A without disruption of the pH gradient or distortion of protein bands (from Manca et al., 1986; with permission from A. Liss).

already substantial amounts of Hb A (left track), while a homozygous β°-thalassemic foetus (right sample) had none. The diagnosis was quite simple when utilizing IPGs (upper panel), barely acceptable in conventional IEF in presence of separators (central panel) and definitely unsatisfactory in CA-IEF alone, due to the poor resolution afforded (lower panel). In this last case, a correct diagnosis of the homozygous condition would be extremely difficult, especially at earlier weeks of pregnancy, when the amount of adult Hb could be below 1%. Just to check how accurate the assessement would be when using IPGs, a homozygous β°-thalassemic umbilical lysate was added with increasing amounts of purified Hb A. As shown in Fig. 6.9, with the IPG methodology as little as 0.5% Hb A could be clearly detected in the focusing pattern. Such a high sensitivity was made possible by grossly overloading this analytical gel. In the case of Fig. 6.9, as much as 1.2 mg protein was applied per track, in an analytical gel of barely 0.5 mm thickness. In CA-IEF such a high sample load would have produced pH gradient distortion, sample smear and precipitation all along the separation track.

6.1.4. Animal hemoglobins

Braend's group has extensively analyzed animal Hbs in IPGs covering the following pH intervals: 6.7–7.7, 6.9–7.6, 6.9–7.5 and 7.1–7.7 (Braend, 1988a,b; Braend and Tucker, 1988; Braend et al., 1987a–c). Their results can be summarized as follows:

(a) In the case of cattle Hb, an analysis of 140 animals has revealed a new Hb variant, previously non-separable by various methods of electrophoresis. Chemical analysis of this variant is not available as yet, thus it is not known if it is a completely new species or if it could be the same as Hb Zebu, a recently described Hb mutant having a Thr instead of a Ser in $\beta 43$ (Namikawa et al., 1987).

(b) In domestic dog, a new Hb polymorphism was detected by the Immobiline technique. Interestingly, only in Japanese dogs a variant, called Hb A, had been described (Tanabe et al., 1978); in other breeds, no Hb polymorphism could be detected by any electrophoretic technique, including CA-IEF. Again, this new Hb has not been analyzed yet, but its existence is in agreement with the multiplicity of Hb α-chains in dogs, with one form having Thr at position 130 and the other having Ala (Dresler et al., 1974).

(c) In sheep, the extensive Hb polymorphism detected by the IPG technique (16 different Hb phenotypes observed in 61 English Saanen goats) has allowed Braend and Tucker (1988) to propose a genetic theory of 5 β-globin genes (A_4, A_6, A_8, E and D) and two closely-linked α-globin loci ($'\alpha$ and $''\alpha$) of which the $''\alpha$ has a variant allele, called $''\alpha^x$. It should be noted that previous electrophoretic and chromatographic analysis had disclosed only five different types of goat Hbs (called Hb A, Hb B, Hb D, Hb D Malta and Hb E). The extensive Hb A phenotype polymorphism described by Braend and Tucker (1988) is a typical 'bonus' of the IPG technique.

An example of IPG analysis of short tail race sheep is given in Fig. 6.10: the bands are razor sharp and the different haplotypes are recognized at a glance.

In addition to this work on animal Hbs, Whitney III et al. (1985) have studied the genetic polymorphism of mouse Hbs. Up

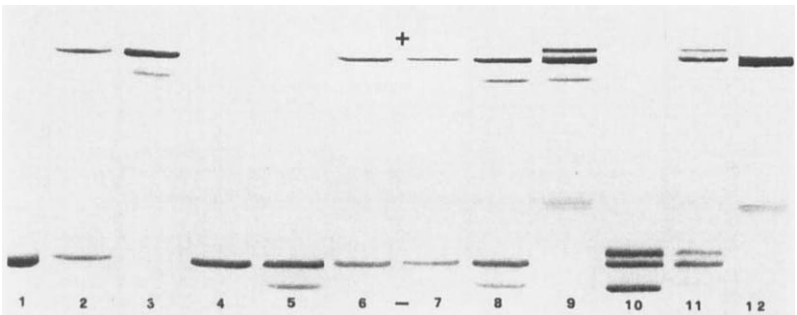

Fig. 6.10. Immobiline gel, pH range 6.7–7.7, showing selected Hb phenotypes in short tail land race sheep. Samples: 1: $B\alpha^{Le}$; 2: $AB\alpha^{Le}$; 3: $A\alpha^{Le}\alpha^{Hi}$; 4: $B\alpha^{Le}\alpha^{Hi}$ (α^{Hi} weak); 5: $B\alpha^{Le}\alpha^{Hi}$; 6 & 7: $AB\alpha^{Le}\alpha^{Hi}$ (α^{Hi} weak); 8: $AB\alpha^{Le}\alpha^{Hi}$; 9: $A\alpha^{A1Le}\alpha^{Hi}\alpha^{Le}$; 10: $B\alpha^{A1Le}\alpha^{Hi}\alpha^{Le}$; 11: $AB\alpha^{A1Le}\alpha^{Hi}\alpha^{Le}$ (α^{Hi} weak); 12: $A\alpha^{Le}$ (reproduced by permission from Braend et al., 1987c).

to 1977, five genetic variants of mouse Hb α chains were known from studies of Hb solubility and sequence analyses. None of these genetic variants is distinguishable from any other by standard electrophoresis because neutral amino acid replacements are involved. Four structurally distinct α-globin chains were characterized among mice of these five Hb A genotypes or haplotypes. Through the use of IEF in a pH 7–9 Ampholine interval, several of these Hbs could be resolved, but discrimination was not complete for quite a few species. Thus chain 5 Hb is often not fully split from chain 1 Hb, and accurate discrimination among the Hb A^a, Hb A^g, Hb A^i and Hb A^f Hbs, especially in heterozygous combinations, was frequently difficult. Likewise, the resolution of Hbs with chains 2, 3 and 4 was also incomplete. With IPGs (the best interval being 7.2–7.55) full resolution of all these different chain types could be obtained. In particular, ample discrimination between Hbs with α-globin chains 5 and 1 or with chains 2 and 3 is achieved, allowing assessment of the phenotypes commonly found in laboratory mice.

6.1.5. Leghemoglobins

Leghemoglobins (Lb) are monomeric heme proteins which play an important role in legume nodules: they ensure an adequate flux of

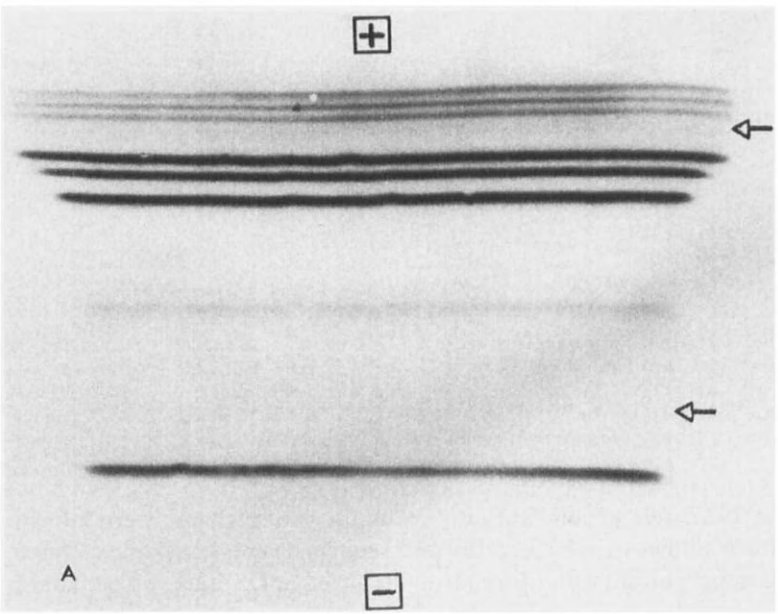
+
A
−

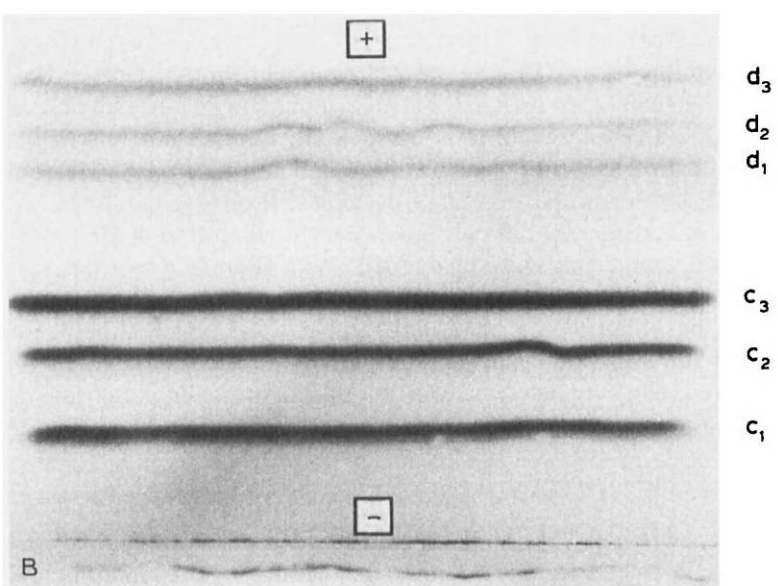
+
d3
d2
d1
c3
c2
c1
−
B

oxygen to the bacteroids requiring energy for nitrogen fixation without affecting their oxygen-sensitive nitrogenase. In soybean nodules, four isoproteins are synthesized from four genetic loci and are called, according to their pIs, Lba, Lbc_1, Lbc_2 and Lbc_3 (Fuchsmann and Appleby, 1979). In addition, each of these proteins also exists in an NH_2-terminal acetylated form giving rise to Lbb, Lbd, Lbd_2 and Lbd_3. Thus eight Lb components can be separated by flat bed CA-IEF in polyacrylamide gels.

With the advent of IPGs, the eight components of soybean Lb could be separated with good resolution and reproducibility in a pH 4.2–5.2 interval (Fig. 6.11a) (Puppo and Rigaud, 1987). Due to the high loading capacity of IPGs, it was possible to analyze Lb samples from a single mature nodule and to detect minor components by overloading the major zones. In addition, by using progressively narrower IPG intervals, it was possible to obtain resolution of the Lbc and Lbd subcomponents (Fig. 6.11b). The technique could be scaled up to small scale preparative runs, with recovery of homogeneous zones at a $> 90\%$ level.

6.2. *Polymorphism of human proteins*

A host of human proteins have been found to be microheterogenous by electrophoretic analysis, i.e., to exhibit a multiple banding pattern in an electrokinetic system. Strictly speaking, the term 'polymorphic' should be confined to known products of altered genes. For example, if, as a result of a mutation, there is more than one form of DNA available for a particular locus within a species, such gene is said to be polymorphic. Each of these alternative forms is called an allele. Alleles are often distinguished by differences in the final phenotype; thus, only after chemical and

Fig. 6.11. A: separation of the eight soybean Lbs on analytical IPGs in the pH 4.2–5.2 interval. Sample application near the cathode. Major components from cathode to anode: Lba, Lbb, Lbc_1, Lbc_2, Lbc_3, Lbd_1, Lbd_2 and Lbd_3. Minor components are indicated by arrows between Lba and Lbb and between Lbc_3 and Lbd_1. B: Separation of Lbc and Lbd subcomponents by IPGs. Same conditions as in A, except that the IPG interval was a pH 4.3–4.7 range (both figures from Puppo and Rigaud, 1987; by permission from VCH).

sequence analysis an electrophoretic variant can be properly called 'polymorphic' if it can be related to an altered gene. Therefore, most biochemists, when lacking direct chemical evidence of such a gene alteration, prefer to speak in more vague terms of 'microheterogenous' protein pattern. I will give here examples of IPG analysis of a host of human proteins, taking as an example the analysis of serum proteins, as they assume particular importance as biochemical indicators in a host of diseases and are important markers in genetic analysis, due to their easy availability in a pure form and to the facility of obtaining specific antibodies from commercial sources.

6.2.1. α_1-acidic glycoprotein

This protein (also known as orosomucoid, ORM) is an acute phase reactant with a molecular mass of ca. 40,000 Da, a high carbohydrate content (up to 55% of neutral sugars) and a large number of sialyc acid residues (up to 11%) (Schmid, 1975). After desialylation, the electrophoretic pattern of ORM shows three phenotypes, determined by two codominant autosomal alleles OR^F and OR^S. By CA-IEF, a third allele for OR^F was described by Thymann and Eiberg (1986) in a Danish population. ORM levels increase upon infection, inflammation or malignancy and also during pregnacy or under pharmacological treatment. In biological terms, ORM shares about 50% sequence homology with immunoglobulins; it affects immuno responses by inhibiting lymphocyte mitogenesis and mixed lymphocyte reaction. ORM has been linked to ABO and adenylate kinase, and it has been assigned to human chromosome 9. By IPG analysis in a pH 2.8–4.5 gradient, ORM is fractionated into six bands, with pIs in the pH 3.4–3.8 range (Gianazza et al., 1987b) (see Fig. 12). The sera we have screened had a titer in ORM ranging from 0.17 to 3.02 mg/ml: as the gels were stained with Coomassie Blue, ca. 15 μl of the high titer samples were enough for band visualization. However Eap and Baumann (1988), who performed IPG runs of the desialylated forms (which exhibit the same polydisperse spectrum, only shifted at ca. 1 pH unit higher values) could still detect the protein, after

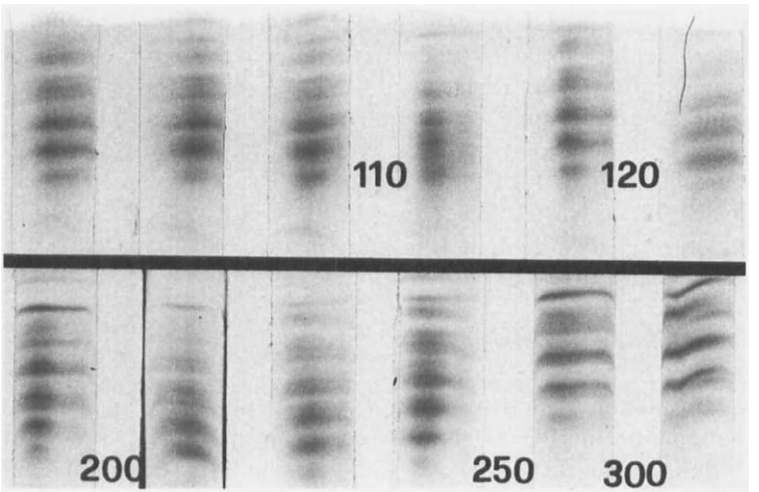

Fig. 6.12. α_1-acidic glycoprotein patterns of some serum samples on pH 2.8–4.5 IPG matrices, ordered according to their increasing protein titer. The gel was a 3% *C*, 4% *T* polyacrylamide matrix, the average buffering power of grafted Immobilines being 9 mequiv.$l^{-1}pH^{-1}$. Run: overnight at 200 V, then 90 min at 1500 V, at 6°C. Staining with Coomassie Brilliant Blue (from Gianazza et al., 1987b; with permission from VCH).

blotting and staining with an alkaline phosphatase-linked secondary antibody system, at a dilution of 1 : 28672.

6.2.2. Acid phosphatase

Phenotyping of human erythrocyte acid phosphatase (ACP1) is widely applied in forensic science for, e.g., paternity cases and the like. ACP1 polymorphism was first demonstrated in 1963 by Hopkinson et al., using starch gel electrophoresis. Today, however, CA-IEF is routinely used for screening ACP1, either in conventional gels (Burdett and Whitehead, 1977) or in ultrathin matrices (Randall et al., 1980; Divall, 1981). Westwood and Sutton (1984) have recently applied the IPG methodology to the analysis of ACP1, in pH 5.5–7.6 ranges, since most ACP1 isoforms have pIs in the pH 5.8–7.5 interval. For enzyme visualization, the IPG gel, after the run, is overlaid with a foil of cellulose acetate soaked in

0.5 M citric acid, pH 5.0, containing 1 mg/ml 4-methylumbelliferyl phosphate. Development occurs in the dark at 37°C for 30 min and the gels are viewed under long-wave UV-light. Successful runs require anodic sample application in slots. It is also possible to type 7-week-old blood stains by extracting the enzyme in presence of freshly prepared 1% dithioerythritol. The six common phenotypes in blood lysates and stains (ACP1 A, B, C, CB, BA and CA) were readily identified in IPG gels; in fact band separation was greater than in CA-IEF.

6.2.3. Albumin and prealbumin

Perhaps albumin is one of the few proteins not easily amenable to fractionation in IPGs. It is believed (Gianazza et al., 1984c) that albumin recognizes two of the acidic Immobilines (the pK 4.4 and 4.6 species) as analogues of physiological ligands (mini-fatty acids) and thus, during a standard IPG run, it forms a curtain of macro-ions smearing down from the application site. This is quite undesirable, since it often masks neighboring proteins (e.g., α_1-antitrypsin), impeding a proper analysis. However, if the run is performed under denaturing conditions (8 M urea) the unfolded protein focuses in the correct place, leaving a clear background. Gianazza et al. (1985c) have also described a method for selective removal of albumin in an IPG run by in situ adsorption on Dextran Blue. 0.5% Dextran Blue is incorporated in an alkaline plateau (pH 8.5) containing the pockets for sample application. Essentially all albumin is trapped at the seeding site, leaving a clear pattern of other serum proteins. This procedure is more efficient than adsorption on the resin Affigel Blue, usually adopted for pseudo-ligand affinity-chromatography. However, it should be appreciated that, due to the low selectivity of this adsorption procedure, additional serum proteins are subtracted as well, so that great caution should be exerted when adopting this subtraction method.

As for prealbumin (also called transthyretin, TTR) Altland and Banzhoff (1986) have demonstrated inherited variants by IPG in a pH 4–7 gradient rehydrated in presence of 8 M urea, 50 mM DTT, 0.5% CA and 6% Dextran 8. In order to clarify the region where TTR focuses, they use a technique called double one-dimensional

electrophoresis, consisting in first subjecting the sample to a CA-IEF step, locating the band of interest, cutting it out of the gel with a blade and re-submitting the gel block to a second, IPG run. In this way, the protein of interest is already desalted and free from neighboring contaminating macro-ions. By this method they were able to detect a mutant (called TTR-Met^{30}) differing from the normal (TTR-Val^{30}) for a Met substituting a normal Val residue at position 30 from the amino end. This variant is consistently found in individuals with familial amyloidotic polyneuropathy of Portuguese type I.

6.2.4. α_1-antitrypsin (α_1-AT)

Also called PI (protease inhibitor), it is one of the highly polymorphic plasma proteins. Genetic variation was observed first in 1963 by Laurell and Eriksson, who reported an inherited deficiency of PI associated with chronic obstructive pulmonary disease. This abnormality is transmitted with an autosomal recessive mode of inheritance. This genotype is now known as PI-ZZ, and is associated with progressive liver disease in infancy and early childhood. Laurell and Eriksson (1963) detected these early variants by agarose gel electrophoresis, while Fagerhol and Braend (1965) used an acid-starch gel method. It was only in 1975 that Arnaud et al. and Constans and Viau, independently suggested the use of CA-IEF in narrow pH ranges for screening of PI polymorphism and with that reported the first discovery of PI subtypes. Since then, CA-IEF has been the method of choice for the classification of PI variants. The most common allele is PI*M; several subtypes can be distinguished by IEF, which have the notations PIM1, PIM2, PIM3 and PIM4. It has become customary to take the PIM allele as a reference point and thus designate the anodal variants from B to L and the cathodal variants from N to Z.

IPGs were first applied by Görg et al. (1983, 1985) and by Weidinger and Cleve (1984) to the analysis of the PI system. It was immediately apparent that: (a) the classification of the six common PIM1, M1M3, M3, M1M2, M2M3 and M2 could be readily and reliably accomplished; (b) the less frequent PI variants could be demonstrated with a high degree of resolution; and (c) the PIZ

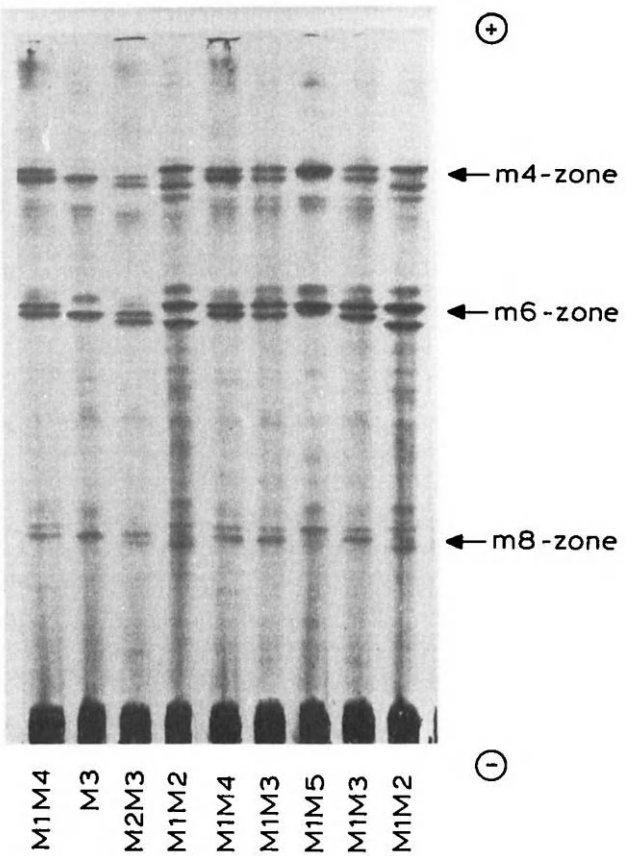

Fig. 6.13. Demonstration of PI-M subtypes as analyzed by IEF in IPGs, in a pH 4.3–4.8 range, over a 17 cm electrode distance, giving a $\Delta pH = 0.025/cm$. Cathodic sample application in $6 \times 6 \times 0.25$ mm slots. Coomassie Blue staining (from Görg et al., 1985a; with permission from the Amer. Soc. Hum. Genet.).

variant could also be clearly identified in a somewhat wider IPG interval. Görg et al. (1983a,b) have proposed two IPG intervals for best resolution: a pH 4.5–4.7 gradient to optimize the pattern of PIM types and subtypes and a pH 4.4–4.8 range to differentiate anodically and cathodically located PI variants. Fig. 6.13 gives an example of the resolution afforded by the IPG method in PI

analysis. At the time of these studies, no new variants were reported, but simply an improved and much more reliable screening methods. Soon, however, Weidinger et al. (1985) reported evidence for a fifth PIM subtype and for a new deficiency allele, called PI*Z Augsburg. Contemporarily, Yuasa and Okada (1985) discovered a new PI allele, called PI*Poki. More recently, Weidinger and Cleve (1986) have reported two additional PIM subtypes, termed PI Mpassau and PI Mlarisse (observed in an IPG pH 4.45–4.75 interval), while, in japanese populations, a PI Mtoyoura, has been discovered by Yuasa et al. (1988) (in an IPG 4.35–4.65 range).

An interesting application of PI screening for forensic hemogenetics comes from Skoda et al. (1988). These authors, over a period of 3 years, have analyzed PI types in 347 putative paternity cases: due to the reproducibility and accuracy of the IPG technique, 54 men were excluded from paternity on the sole PI evidence. Even though the number of excluded men in paternity cases was below the theoretical single exclusion chance for non-father, for this particular polymorphism (the single exclusion chance in the case of PI should be 27%, vs. a found value of 15.6%, i.e., 54 cases out of a total of 347) this was remarkably superior and more accurate than when using CA-IEF, even in presence of separators. On the basis of these analyses, these authors have concluded that the allele frequency from non-related individuals did not deviate from the Hardy-Weinberg equilibria and corresponded well to known frequencies from West Germany and other Caucasoid populations. They concluded from their experience with PI phenotyping that the method of IPG gels, despite its increased technological demands, represents a major improvement over conventional IEF in the distinction of phenotypes.

6.2.5. Apoliproteins

Polymorphic forms of human apoliproteins have been described for apo A (Utermann et al., 1975), apo C-III (Brown et al., 1970), apo C-II (Havel et al., 1979), apo A-I (Menzel et al., 1982) and apo A-IV (Utermann et al., 1982), simply with the use of CA-IEF. Some of these forms exist due to differences in sialic acid content,

as in the case of apo C-III (Brown et al., 1970), while apo E also demonstrates genetic polymorphism due to variation in primary structure (Weisgraber et al., 1981). Human apo A-I exhibits a few rare mutant forms, such as $A\text{-}I_{Milano}$ (Franceschini et al., 1980), A-I-Marburg and A-I-Giessen (Utermann et al., 1982) and A-I-Munster (Menzel et al., 1982). In the latter case, Menzel et al. (1984) have recently described three apo A-I-Munster-3 variants, which were designated as apo A-I($Asp_{103} \rightarrow Asn$), apo A-I($Pro_4 \rightarrow$ Arg) and apo A-I($Pro_3 \rightarrow His$), to indicate the position in the chain and the type of mutation occurring. As these mutations involve charged amino acids, they could easily be identified by CA-IEF; however, the sequencing and chemical analysis were made possible by purifying each mutant in a preparative Immobiline gel in the pH 4.9–5.9 gel. Enough protein (ca. 25 mg) could be applied to the IPG gel to allow for recovery of purified zones. Interestingly, since the IPG run was performed in 6 M urea, the focused bands could be visualized by simply immersing the gel for a few minutes in distilled water, whereby the isoforms appeared as opaque bands. Preparative IPG for purification of apo A-I was also successfully used by Jabs et al. (1986).

For identification of apo A-I in analytical IPG gels, Holmquist (1988) has proposed an interesting variant of a blotting procedure. We have seen (Chapter 3, Fig. 3.15) that it is possible to perform blotting from an IPG gel by placing the matrix (still bound to the Gel Bond PAG) in the LKB Film Remover, which allows sharp gel-film separation by a guillotine procedure (perhaps the bi-centennial of the French revolution helped in the design!). However, when utilizing commercial Immobiline Dry Plates (possibly due to their poor mechanical strength for their low % T) this procedure produces a crumpled gel. Holmquist (1988) has thus proposed, for blotting purposes, that, after the IEF run, the IPG gel be covered by a thin (ca. 1 mm) layer of 1% agarose (Litex LSL). Thus, after slicing away the plastic backing, an agarose-IPG gel sandwich is obtained with excellent mechanical properties allowing electroblotting and immunoreactions to be performed without distortion of band patterns. In addition, the agarose layer prevents adhesion of the IPG gel to the nitrocellulose membrane, a most common problem when blotting from IPG matrices.

Another class which has been extensively studied is the apolipoprotein C (apo C) family. Apo Cs are components of both very low density lipoproteins (VLDL) and high density lipoproteins (HDL), the group being composed of apo C-I, apo C-II, apo $C\text{-}III_{0,1,2}$, apo C-IV and apo C-V (Catapano et al., 1978). The apo Cs are polypeptides with different amino acid sequences and molecular mass values between 6600 and 9700. Apo C-III is composed of three isoforms, designated $C\text{-}III_0$, $C\text{-}III_1$ and $C\text{-}III_2$, which have a sugar chain at threonine-74 consisting of one galactose, one galactosamine and 0, 1 or 2 neuraminic acid residues (Vaith et al., 1978). Apo C-I is an activator of lecithin cholesterol acyltransferase (Kostner, 1983), apo C-II activates extrahepatic lipoprotein lipase, while apo C-III is an inhibitor thereof (Ott and Shore, 1983). Apo C-II also inhibits hepatic lipase (Jahn et al., 1981). Apo C-II and Apo C-III are, therefore, important regulators

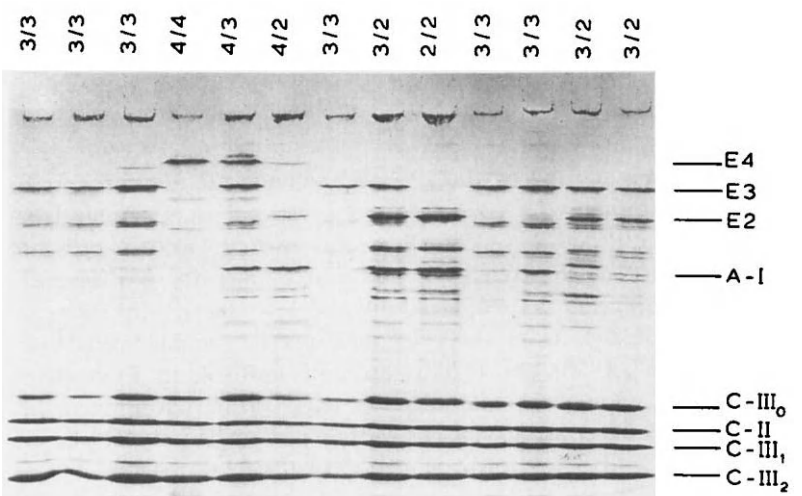

Fig. 6.14. IEF of apoliproteins from VLDL in a CA-IPG system. For each lane, apo E phenotypes are indicated. Staining with Coomassie Brilliant Blue R-250. The gel (pH 4–7 range) was re-swollen in 8 M urea, 30% glycerol, 2 mM Tris and 1% Servalyt pH 4–7. Cathodic sample application (at the top in the figure). Focusing conditions: overnight at 5000 V, 3 mA, 3 W with a Macrodrive power supply at 15°C (from Baumstark et al., 1988; with permission from VCH).

of lipolysis, and an apo C-II deficiency can give rise to severe hypertriglyceridemia. Most analyses performed so far on apo Cs have utilized CA-IEF; in fact, Bugugnani et al. (1984) give the following pI values for apo Cs: apo $C\text{-}III_0$: 5.10; apo C-II: 5.01; apo $C\text{-}III_1$: 4.92 and apo $C\text{-}III_2$: 4.84. Recently, Haase et al. (1988) have applied IPGs, in the pH 4.8–5.7 range, to the analysis of apo Cs: an example of the separations obtained is given in Fig. 6.14. According to these authors, the advantages of IPGs lie not only in higher resolution and sharper bands, but also in the better reproducibility from run to run. Weisgraber et al. (1985) have also utilized IPGs for the preparative fractionation of apo E_3 (in a pH 4.9–5.9 gradient) and of apo Cs (in a pH 4.0–5.0 interval; the discrepancy with Haase et al. being only apparent, as in this latter case the IPG gradient is corrected for the presence of 7 M urea in the gel, shifting the apparent pH interval from 4.0–5.0 to 4.8–5.7). As described above, in preparative IPGs the apoliprotein isoforms are simply detected by soaking the gels in distilled water; after excising and mincing the bands, the apo E and apo Cs are extracted at 4°C in 100 mM Tris–HCl, 4 M guanidium chloride and 1 mM EDTA (pH 7.4) for a total of ca. 24 h (by this procedure, though, recoveries are rather low, barely 40 to 60% of applied sample).

A last class studied by the IPG technique is the apoliprotein E (apo E). Although the concentration of apo E in serum is low compared with the other classes (apo A-I and apo B), it is present in all lipoprotein density classes in variable amounts (Koffigan et al., 1987). Since it is recognized by the low density lipoprotein (LDL) receptor (Pitas et al., 1979) and specific remnant receptors (Sherrill et al., 1980), apo E plays an important role in lipoprotein metabolism, namely the catabolism of triglyceride rich lipoprotein particles (Brown et al., 1981). The protein is a single polypeptide of 299 amino acids of known sequence (Rall et al., 1982). Three common alleles, E2, E3 and E4, exist at a single gene locus, leading to six different phenotypes that can be distinguished by IEF (Zannis and Breslow, 1981). A number of less frequently occurring genetic apo E isoforms have been described (Menzel and Uterman, 1986; Steinmetz, 1987). In addition, each apo E isoform is found in plasma in a number of minor species, differing in their sialic acid

content. In general, this produces a train of spots of progressively higher M_r and lower pIs.

Baumstark et al. (1988) have applied the IPG technique to the routine screening of apo Es. The runs are performed in Immobiline Dry Plates, pH 4–7 (which allow the simultaneous screening of both apo Es and apo Cs), re-swollen in 8 M urea, 30% glycerol and 0.5% carrier ampholytes. Interestingly, addition of CAs to the rehydration solution was found necessary to ensure the entrance of apo E molecules (applied in tabs at the cathodic gel edge). CAs were not necessary to focus apo A-I, apo A-II, apo A-IV, apo C-III and apo C-II isoforms. An example of their separations is shown in Fig. 6.15. These authors too found the IPG technique to be superior than CA-IEF for resolution, reproducibility and (quite surprising) even for simplicity (no doubt due to the availabilily of precast gel plates).

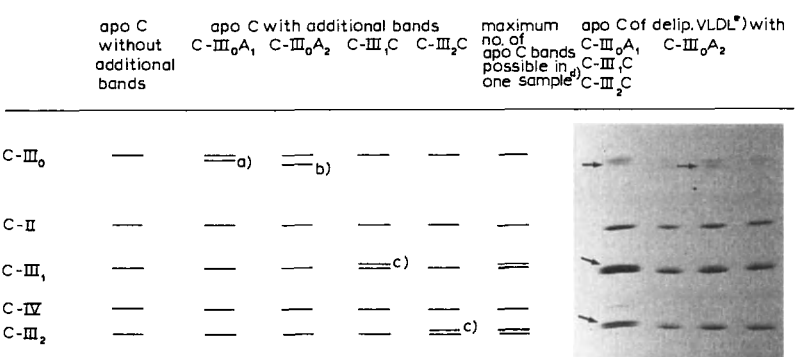

a) C-III$_0$A$_1$ focused 1 mm anodal to C-III$_0$
b) C-III$_0$A$_2$ focused 1.5 mm anodal to C-III$_0$
c) C-III$_1$C and C-III$_2$C focused cathodal to C-III$_1$ and C-III$_2$, respectively
d) additional band at C-III$_0$: either C-III$_0$A$_1$ or C-III$_0$A$_2$
e) the VLDL was isolated from 3 patients with hypertriglyceridemia; the 2nd sample was applied in two differend concentrations

Fig. 6.15. Examples of apo C patterns of delipidated VLDL obtained with IEF on an immobilized pH gradient from 4.8–5.7 in 7 M urea (corresponding to a pH 4.0–5.0 gradient in water). Left: schematic representation; right: part of a gel (additional bands are indicated by arrows) (from Haase et al., 1988; by permission from VCH).

6.2.6. C3

C3 is the most abundant complement component in human serum. It is a 185 kDa protein consisting of two non-identical polypeptide chains, called α (110 kDa) and β (75 kDa). The native C3 molecule is the specific substrate for the classical and the alternative C3/C5 convertases, the proteolytic cleavage of C3 being the critical step in the activation of the complement system. A genetic polymorphism of human C3 was demonstrated by Wieme and Demeulenaere in 1967 and later on confirmed by Alper and Propp (1968) and Azen and Smithies (1968). They used electrophoresis either in starch or in agarose gels. These authors described a system with two codominant alleles, C3*S (slow) and C3*F (fast). Additional studies revealed 22 less common variants (Rittner and Rittner, 1974). The C3 locus has recently been located on human chromosome 19 (Whitehead et al., 1982) and shown to segregate independently from the major histocompatibility complex in man. A linkage has also been described between the C3 locus and the loci for apo E, ABH secretion, Lewis secretion and Lutheran blood group (Eiberg et al., 1983). Like other genetic markers in human blood, C3 polymorphism has been mainly used in forensic medicine and in anthropological studies (Davrinche and Rivat, 1982). Recently, Charlionet et al. (1985) have applied the IPG technique for a potential subtyping of the C3 system. Analysis was performed in very narrow IPG gels (pH 5.5–5.7) equilibrated in 10% saccharose, since this sugar seems to stabilize the C3 component in the proximity of its pI. These gels are quite unique in that these authors seem to be particularly allergic to commercial Immobilines, so that they use itaconic acid as buffering group and DMAPMA (dimethylaminopropyl methacrylamide) as a titrant base. Detection is made by capillary transfer to a nitrocellulose membrane, incubation with rabbit antiserum anti-C3, subsequent reaction with a secondary, peroxidase-labelled goat anti-rabbit IgG and final zymogramming in O-dianisidine and H_2O_2. The aim of this subtyping is to find a correlation between potential C3 variants and certain diseases corresponding to the disfunction of the components of complement, as suggested by Porter (1983).

6.2.7. *Factor B*

The factor B of human complement is genetically polymorphic in most human populations, as first reported by Alper et al. (1972). These authors concluded that the factor B variants are coded by a series of codominant alleles at an autosomal locus BF. Two common alleles, BF*S and BF*F, predominate whereas two others, BF*SO7 and BF*F1, appear with a lower incidence in most populations. About ten other alleles were described later on and appear to be restricted to particular cases (Mauff et al., 1978). The method commonly used to detect factor B variants is high-voltage agarose gel electrophoresis at pH 8.6, followed by immunofixation (Alper and Johnson, 1969). More recently, factor B polymorphism has been studied by CA-IEF in polyacrylamide (Geserick et al., 1983) or in agarose gels (Teng and Tan, 1982), both followed by immunofixation. Davrinche et al. (1985) have recently applied the IPG technique to the screening of factor B polymorphism. They use two types of IPG ranges, either a pH 5.2–6.1, or a pH 5.4–5.9 interval. Again, due to the same allergy reported in the case of C3, they refuse to use Immobiline chemicals, and produce their gradients by utilizing itaconic and methacrylic acids as buffering ions and DMAPMA as a titrant base. After focusing, the bands are transferred to nitrocellulose by a quick capillary blotting (10 min), followed by a primary and a secondary immunofixation step, the latter utilizing horse-radish peroxidase, which is then revealed by 3,3′-diamino benzidine and H_2O_2. No new subtypes have been found, at present, even with the IPG technique.

6.2.8. *Factor XIIIB*

In plasma, most of the coagulation factor XIIIB (FXIIIB), also known as fibrin stabilizing factor, exists as a proenzyme with two A- and two B-polypeptide chains (A_2B_2). After activation with thrombin the B-subunits are cleaved off. Only the A-subunits have enzymatic activity and take part in the coagulation process. The B-subunit, also designated as FXIIIB, F13B, B-protein or S-subunit, acts as a carrier protein for the A-chain and is also found in serum. FXIIIB is a glycoprotein with a molecular mass of 87,800

(Schwartz et al., 1973); the carbohydrate moiety contains neuraminic acid. The pI is in the pH 5.1–5.6 range and after desialylation is increased between pH 5.6–8.8 (Kera et al., 1981). The genetic polymrphism of FXIIIB was first described by Board (1980) using agarose gel electrophoresis. Subsequently, by IEF, a series of new rare variants was discovered (Nakamura et al., 1986). Leifheit and Cleve (1988) have recently applied IPGs (in the pH 5.6–6.6 range) to the analysis of FXIIB. After focusing, the zones are transferred to nitrocellulose by capillary blotting, precipitated with a primary antibody and then detected with a peroxidase-conjugated anti-rabbit IgG-antiserum. The bands are revealed with 4-chloro-1-naphthol in ethanol and H_2O_2 at pH 7.3. By this method, all common FXIIIB phenotypes: 1, 2–1, 2, 3–1, 3–2 and 3 could be revealed with good precision and reproducibility. As this phenotyping is used in forensic hemogenetics, it was found that the exclusion rate in cases of disputed paternities, for non-fathers, with this system alone, is 20.35%.

6.2.9. Group specific component

The group specific component (GC) of human serum was discovered in 1959 by Hirschfeld. Simultaneously and independently a vitamin D binding protein (DBP) was found in human serum (Thomas et al., 1959). The identity of the two proteins was established only in 1975 by Daiger et al. Since then, the system is referred to as GC/DBP. The genetic variants of this protein were originally classified by immunoelectrophoresis on agarose gels (Alper and Johnson, 1969). A major advance was the application of IEF in polyacrylamide gels, with subsequent immunoprint, allowing the separation of GC subtypes (Constans and Viau, 1977). The currently employed methods for the analysis of the GC-DBP are CA-IEF, PAGE and IEF in presence of 3 M urea (Constans et al., 1983). Routine classification of the different genetic types of the GC/DBP system for studies in population genetics, for investigation of disputed paternities and for twin diagnosis is usually carried out by CA-IEF. Six common GC phenotypes are distinguished, corresponding to six genotypes, determined by three alleles: GC*1F, GC*1S and GC*2. The notations for the six

common GC types are thus 1F, 1S, 2, 1F-1S, 2–1F and 2–1S. Their mode of inheritance is autosomal co-dominant and the gene locus is mapped on the long arm of chromosome 4 at 4q12. In addition to the six common GC types, a total of more than 120 uncommon GC variants has been identified (Cleve and Constans, 1988).

A number of authors have proposed IPGs for the analysis of GC/DBP. The first report to appear was from Cleve et al. (1982). After that, Westwood (1985), Pflug (1986, 1988a), Pflug and Laczko (1987) and Constans and Cleve (1988) have investigated various aspects of GC screening by the IPG technique. In particular, Pflug (1986) has proposed an IPG method based on pouring barely 250 μm thick gels (against a customary 0.5 mm thickness) and has suggested to re-use the same gel, after washing and drying, up to six times, for improved reproducibility. Pflug (1986) has also investigated detection of the focused GC zones by direct immunofixation on cellulose acetate membranes overlaid on the IPG gel, as opposed to capillary blotting on nitrocellulose. According to this author, the sensitivity of the former method is much better than that of the latter. By detection with an alkaline phosphatase linked secondary antibody, Pflug (1986) has demonstrated a sensitivity of about 150 pg of GC in a 1 : 12,800-fold diluted serum samples. Even in 6-year-old badly soluble bloodstains kept at room temperature, GC could be phenotyped (I wonder if they have performed it in mummies!). Here too, I am afraid we will have to apply the usual litany: IPGs perform better than IEF etc. One point is noteworthy: according to Constans and Cleve (1988), some rare variants, like 1A23, 1A28, 1A30 and 1C53, which cofocus in CA-IEF, could only be separated in IPG gels. An interesting point (which applies too to focusing of α_1-AT) is that the order of pIs in CA-IEF vs. IPGs varies for some of the mutants. The phenomenon is unexplained but a likely cause is that, since the two techniques act on the same principle, in CA-IEF some variants might not focus as 'stripped' forms, but as complexes with carrier ampholytes: this outer CA-coating would then be responsible for the observed pI in CA-IEF (P.G. Righetti, personal observation; see also Righetti, 1983a).

Pflug et al. (1988) and Pötsch-Schneider and Klein (1988) have also applied IPGs to the typing of GC in human semen and vaginal

fluid. This GC screening in semen stains seems to be of practical value in criminal investigations of sexual delinquencies. GC is present in normospermia and azoospermia seminal fluids and found in about 20% of the vaginal secretions. The GC patterns in these fluids were similar and in accordance with the bands of the individual GC type in plasma/serum.

6.2.10. Lecithin : cholesterol acyltransferase

The esterification of the free cholesterol of human plasma lipoproteins is catalyzed by lecithin : cholesterol acyltransferase (LCAT, EC 2.3.1.43). In this reaction a fatty acid acyl moiety of lecithin is transferred to the 3-β-hydroxyl group of cholesterol, with the ultimate formation of cholesterol ester (Glomset, 1968). LCAT is a key component in the cholesterol transport process between plasma and tissue. Purified LCAT shows charge polymorphism in CA-IEF (Albers et al., 1979). This micro-heterogeneity reflects the presence of molecular species of the enzyme with a different number of sialic acid residues (Doi and Nishida, 1983), even though there are discrepancies in the literature on the number of isoforms and on their respective pI values. Holmquist and Bjellqvist (1988) have applied the IPG technique to the analysis of LCAT polymorphism. Due to the strong tendency of purified LCAT to aggregate in the absence of dissociating agents, the IPG run (in the pH 4.2–4.9 interval) had to be performed in presence of 8 M urea, 0.5% Triton X-100 and 2 mmol/l of 2-mercaptoethanol. Seven isoforms were characterized, having the following pIs (at 15°C): 4.37; 4.42; 4.48; 4.53; 4.60; 4.67 and 4.74 (SD = $\pm$0.03 for all); of those, the pI 4.48 isoform was the most abundant species.

6.2.11. Phosphoglucomutase

Phosphoglucomutase 1 (PGM1) polymorphism was first demonstrated by Spencer et al. (1968) using starch gel electrophoresis. They discovered three different phenotypes: PGM1 1, PGM1 2–1 and PGM1 2. These phenotypes are coded for by two autosomal codominant alleles PGM1*1 and PGM1*2. By IEF, Bark et al. (1976) demonstrated that the PGM1 polymorphism is determined

by four alleles, thus resulting in ten different PGM1 phenotypes. Sutton and Burgess (1978), Kühnl et al. (1977) and Kühnl and Spielmann (1978a) confirmed the existence of the common PGM1 phenotypes. Up to recent times, for routine forensic analysis of blood stains, PGM1 subtyping was performed essentially by CA-IEF in ultra-thin polyacrylamide or agarose gels. It was in 1984 that Sutton and Westwood proposed the use of IPGs in the pH 5.8–6.8 interval. In this pH range, the best separation of the four main PGM1 bands: 1A, 1B, 2A and 2B* is achieved. At the end of the run, the enzyme is visualized by a zymogramming procedure, consisting on a 2% agarose overlay, containing 8 mg NADP, 45 mg glucose-1-phosphate (the latter in presence of 1% glucose-1,6-di-phosphate), 1.5 mg phenazine methosulphate, 1.5 mg MTT and 8 U glucose-6-phosphate dehydrogenase in 10 ml buffer (consisting of 0.3 M Tris, 2.5 mM EDTA, 4.9 mM $MgCl_2$ and 5 mM histidine HCl, adjusted to pH 8.0). According to Pflug (1988b), by this method it is also possible to determine the PGM1 subtypes of semen stains, vaginal secretions and mixtures of both. In addition, it is possible to obtain PGM1 patterns directly from hair root cells. The hair roots are cut from pulled hairs and deposited directly on the IPG gel surface, whereby the enzyme forms are electroeluted during the run. Although not explicitly stated in this scientific report (Pflug, 1988b), it seems that bald delinquents, e.g. à la Terry Savalas, have a distinct advantage over hirsute criminals in court cases.

6.2.12. Protein C

Protein C (PC) is a vitamin K dependent plasma component that is a precursor of a serine protease (Kisiel, 1979). It is a glycoprotein containing 23% carbohydrate, with an M_r of 62,000 Da, composed of a heavy chain (M_r 41,000 Da) and a light chain (M_r 21,000 Da) held together by disulphide bonds. Incubation of PC with human α-thrombin results in the cleavage of a dodecapeptide (M_r 1400) from the amino terminal region of the heavy chain and in the formation of activated PC, an enzyme with serine amidase activity that has strong anticoagulant properties due to selective inactivation of the active forms of factor V and VIII in plasma. There is

evidence (Discipio and Davie, 1979) that protein C contains 10 γ-carboxyglutamic acid residues/mole of protein, the two carboxyls in the γ-position being necessary for Ca^{2+} binding and for acting on the surface of biological membranes. The importance of PC as a major regulator of blood coagulation is now established by the finding that patients with hereditary deficiencies of this protein often develop venous thromboembolic disorders (Griffin et al., 1981), and by the discovery of low PC levels in acquired conditions associated with thrombosis, such as disseminated intravascular coagulation syndrome and the postoperative period (Mannucci and Vigano', 1982). Due to the lack of a properly purified preparation of PC and of specific antibodies, no studies had been performed on the surface charge properties of PC and on the possible existence of isoforms. Gelfi et al. (1985) have applied directly the IPG technique to the study of PC. The protein has been analyzed in IPG gels in the pH 4–6 interval, in presence of 8 M urea and of 2 mM EDTA (the latter present initially in the gel and sample zone). After IEF, the IPG gel is separated from the plastic foil and electroblotted against a nitrocellulose sheet. After fixation with a primary antibody, the membrane is confronted with a peroxidase-labelled secondary antibody, which is then revealed with 4-chloro-1-naphthol and H_2O_2. PC is thus resolved into six isoforms, having the following pIs (corrected for the presence of 8 M urea): 4.80; 4.86; 4.92; 4.96; 5.02 and 5.1. If PC is activated (thus loosing the amino terminal dodecapeptide) it still shows the same group of six bands, with pIs ca. 0.5 units higher. At present, no studies are available on the genetic background of these bands, nor on the possible linkage of some isoforms with coagulation disorders.

6.2.13. Transferrin

Transferrin (Tf, also called siderophilin) is an iron binding, monomeric glycoprotein found in the biological fluids of invertebrates (Martin et al., 1984) and of vertebrates (Aisen and Listowsky, 1980). The encoding gene for human Tf is on chromosome 3 (Yang et al., 1984); also its complete amino acid sequence has been established (MacGillivray et al., 1983). Human Tf consists of a single polypeptide chain containing 679 amino acid residues and

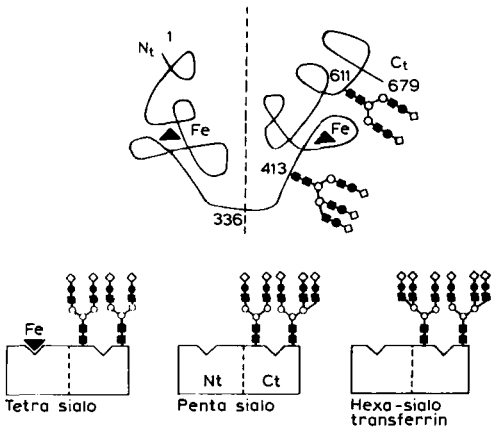

Fig. 6.16. Schematic representation of the polypeptide chain and two N-linked glycans in the C-terminal domain of three michroheterogeneous forms uf human transferrin. The dashed line indicates the division between the two globular domains, N_t and C_t, each of which can bind one ferric iron (from de Jong and van Eijk, 1988; with permission from VCH).

two N-linked complex type oligosaccharide chains, which results in a calculated molecular mass of 79,570. The Tf molecule can be divided into two homologous domains, the N-terminal (residues 1–336) and the C-terminal domain (residues 337–679), with both sites of glycosylation in the carboxyl-terminal domain at positions 413 and 611 (see Fig. 6.16). Each domain contains a metal binding site, binding a ferric ion with a K_m of approximately 10^{22} M^{-1}. The concomitant binding of an anion (carbonate or bicarbonate) is essential for metal binding at each site. The bilobal structure together with the existence of a high degree of internal homology between the two domains (Park et al., 1985) has led to the hypothesis (Greene and Feeney, 1968) that mammalian two-lobed transferrins arose during the course of evolution by duplication and fusion of a gene specifying a simpler single-domain protein.

The first factor determining the electrophoretic behavior of transferrin is its iron content. Under physiological conditions serum Tf is ca. 30% saturated with Fe; consequently, in fresh serum four different forms of Tf with respect to Fe content can be distinguished and isolated electrophoretically; apo Tf, (Fe)NtTf,

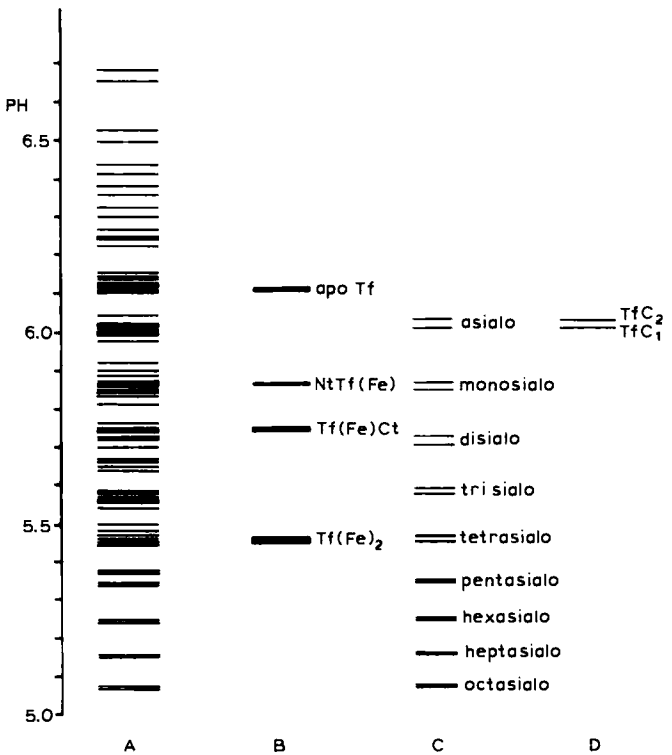

Fig. 6.17. Diagramatic representation of transferrrin microheterogeneity of an individual with the C_1C_2 genotype detectable on IEF. A: total number of bands than can theoretically be distinguished on an Immobiline gel (as many as 72!). B: major bands as revealed by CA-IEF. Before the introduction of Immobilines, these bands, together with their genetically determined variations, were believed to comprise the total spectrum of transferrin heterogeneity. They correspond to the tetrasialotransferrins that can be separated because of differences in iron content. C: microheterogeneous forms of transferrins that can be separated and isolated from an iron-saturated serum sample. D: reduction of the number of bands from 72 (in A) to 2 by iron-saturation and neuraminidase treatment of the serum sample, a procedure that can be useful in the assessment of genotypic variations (from de Jong and van Eijk, 1988; with permission from VCH).

Tf(Fe)Ct and diferric transferrin (see Fig. 6.17, track B). The second determinant of electrophoretic behavior, genetic polymorphism, is best revealed by CA-IEF of serum samples that have been

saturated with iron and then desialylated by neuraminidase treatment. In fact, genetic polymorphism of Tf was already reported in 1957 by Smithies, simply by zone electrophoresis in starch gels. The most common phenotype in all human populations has been designed TfC, the more anodal variant (lower pI) TfB and the more cathodal form (higher pI) TfD. Up to 1978, TfC was considered to be a single variant. By IEF, however, TfC was shown to consist of two subtypes, Tf^{C1} and Tf^{C2} (Kühnl and Spielmann, 1978b; Thymann, 1978). Subsequently, a third, relatively common allele (Tf^{C3}) was reported by Kühnl and Spielmann (1979); additional C variants were then detected by IEF, bringing the total number to 13 (Kamboh and Ferrell, 1987). The third determinant of Tf electrophoretic behavior is the carbohydrate moiety. The two N-linked oligosaccharide chains of transferrin have been shown to be structurally variable (Marz et al., 1982). The glycans can differ in their degree of branching since biantennary, triantennary and tetrantennary structure have been shown to exist (see also Fig. 6.16). As a result, nine different Tf variants, with pIs ranging from 5 to 6 can be distinguished electrophoretically due to differences in sialic acid content (Van Eijk et al., 1987; see Fig. 6.17, track C).

The first to utilize IPGs for analysis of Tf variants were Görg et al. (1983b). In a subsequent study, Weidinger et al. (1984), by screening 1125 unrelated individuals in Southern Germany, could determine the following allele frequency for TfC: $Tf*C1 = 0.787$; $Tf*C2 = 0.136$ and $Tf*C3 = 0.067$. A new subtype, called C10, was observed and identified for the first time by the IPG technique. Evidence for a Tfnull allele was obtained in a child and the putative father. By IPG analysis, Weidinger et al. (1984) could calculate a theoretical exclusion rate for paternity examinations, in the case of the Tf system, of 17.95%. The above data agree quite well with the frequencies proposed by Scherz et al. (1985), who have also given essentially the same value for the average chance of exclusion in case of disputed paternity (18.19%). In addition, these authors have found three new variants located in the cathodal region of Tf bands, and thus considered to be D variants. These three new Tf species have been given the names of the towns of origin of the families of the carriers, and thus have been called: $D_{Mortsel}$, D_{Sorens} and $D_{Bellegarde}$. Scheffrahn et al. (1985) have ad-

ditionally reported the analysis of Tf subtypes among Brazilian indians. Pascali et al. (1988) also analyzed Tf in human sera, and gave guidelines for proper sample handling in IPGs. According to D'Alessandro et al. (1988), CA-IEF has a distinct disadvantage over IPGs, in that the former technique produces always a multiplicity of bands, possibly due to a whole series of partially saturated Tf molecules, in which the iron is partially depleted during the run, due to the rather strong chelating power of CAs. In fact, if we sum all the potential sources for microheterogeneity (genetic variability, partial iron saturation and differences in the carbohydrate moiety) they could potentially produce, in an individual, as many as 72 discrete zones focusing in the pH 5.0–6.8, fully resolvable by the IPG technique (see Fig. 6.17) (de Jong and van Eijk, 1988). Thus, analysis of Tf under uncontrolled conditions, could lead to disaster. However, it is comforting to note that, if all the sources of this microheterogeneity are eliminated (by complete desialylation and full iron saturation) an individual with a C_1C_2 genotype should produce by IEF analysis only 2 (as opposed to 72!) zones (see Fig. 6.17, track D).

6.3. Zymograms

Görg's group (Görg et al., 1985) and my own (Sinha and Righetti, 1986; Kilias et al., 1988) have extensively investigated the feasibility of performing zymograms directly on an IPG gel after the IEF run. While Görg et al. (1985c) have mostly worked with soluble enzymes from vegetable extracts (e.g., esterase and hydrolases from barley cultivars) we have attempted to detect enzyme anchored to membranes. We have particularly analyzed microvillar hydrolases, which are a group of enzymes, with hydrolytic activity, present in the brush borders of the kidney and intestine. These enzymes are integral membrane proteins which possess a set of common, distinct characteristics in their structure and topology: (a) they are in general made of large subunits; (b) they are often dimeric; (c) the bulk of the protein is hydrophilic and glycosylated; (d) only a small domain is involved in hydrophobic interactions with the membrane lipids and this domain is located near the NH_2-terminal sequence

(sometimes also near the C-terminal) and (e) they in general contain metal ions (Kenney and Maroux, 1982). While most of these enzymes have been shown to be transmembrane, their orientation across the membrane is markedly asymmetric, so that almost the whole mass is at the external or luminal surface. The anchoring domain and the region accessible at the cytoplasmic surface contribute only 2.5–5% of the mass of the active protein. These enzymes are usually extracted from membranes by two procedures: proteinase treatment or with detergents. Only in the detergent extracted form is the native primary structure preserved; the protease-solubilized form inevitably lacks the domain originally associated with the lipids of the membrane.

By CA-IEF, most of these enzymes have been demonstrated to be extensively microheterogeneous: thus human kidney γ-glutamyl transferase (GGT) has been resolved into 12 bands (Tate and Ross, 1977); multiple banding patterns are given also by rat intestinal amino peptidase N and by lactase-glycosyl ceramidase (Cousineau and Green, 1980). The IEF analysis of these enzymes is quite important in biochemistry and clinical chemistry, as the microheterogeneous spectrum of bands has been demonstrated to be tissue- and tumor-specific. Thus, some isoforms of alkaline phosphatase (AlP) in serum have been associated weith bone tumors (Fishman, 1974). We have analyzed these enzymes by the IPG technique (Sinha and Righetti, 1986; Sinha et al., 1986; Sorroche et al., 1987) and have had some most instructive results worth commenting. First of all, most analyses were performed in IPG pH 4.0–7.0 (in some cases pH 4.8–7.2) gradients, supplemented with 1% carrier ampholytes. Absence of CA in both, sample and gel phase, usually results into smears, precipitation at the origin or loss of enzyme activity. At the time of these analyses, we had not yet discovered the undesired phenomena of IPGs, notably the presence in the alkaline species of oligomers able to precipitate proteins by a mixed ionic/hydrophobic interaction. As most of these enzymes were of membrane origin, it is quite possible that some of the problems encountered were indeed due to oligomers in the Immobiline solutions. It is also quite possible that the precipitates often obtained in the application pocket could have been produced by salts in the sample (the unwanted phenomena of strong salts in

the sample zone were discovered only recently; Righetti et al., 1988e). Nevertheless, the results obtained with zymogramming in IPGs are extremely interesting for validating the methodology. It is known that, whenever a new technique is introduced, especially if possessing a strong resolving power, the immediate reaction of the academic community at large is a strong rejection crisis. Even though despicable, such a refusal can be understood: imagine a poor old biochemist, who has spent half of his life purifying his pet protein, and demonstrating its homogeneity by the criteria of his times, finding suddenly a tremendous microheterogeneity with next-day analytical techniques. Quite a damnation, isn't it? CA-IEF and IPGs were immediately attacked, as soon as proposed, on the grounds of producing artefactual heterogeneity in an otherwise homogeneous protein preparation. The controversy, in the case of CA-IEF, continued for a good 20 years, and has quite never subsided. So, it was important, in the case of IPGs, to stop this nonsense at its very origin. We thus used the zymogramming technique, coupled to a bit of genetic analysis, to have a clear cut view of the phenomena occurring in IPGs.

Fig. 6.18 shows the zymogramming (in this and the following figures, staining was by the azo-coupling technique described by Sinha and Gossrau, 1984 for CA-IEF gels) of GGT extracts from a number of rat tissues: it is seen that the isoforms of GGT are tissue specific. The kidney is the source of the most polydisperse spectrum, with an array of at least 20 isoforms focusing in the pH 4–6 range, whereas semen and epididymus extracts contain only the acidic part of the spectrum, and the jejunum the more basic counterpart. Conversely, tissues known not to contain any GGT activity (notably the lung and the colon) were devoid of any enzyme isoform. Such a clear-cut tissue specificity within a single animal is comforting and tends to give a biochemical evidence against potential artefacts generated by the IPG technique per se. The same applies to the zymogramming of amino peptidase M, extracted from a number of human and rat organs and run in parallel in the same gel matrix (Fig. 6.19). It is now seen that the spectrum of bands is this time both, tissue and species specific, this being the best safeguard against any potential artefact of the IPG method. This seems to be quite a general phenomenon: when the

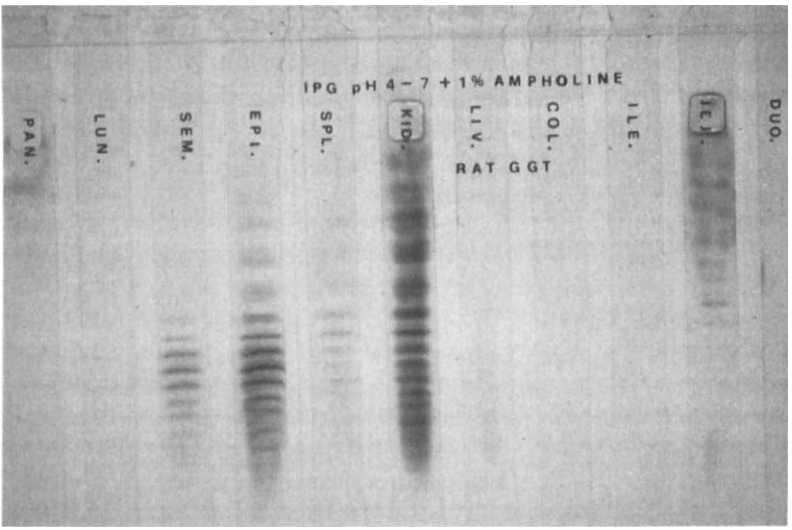

Fig. 6.18. Zymograms of rat tissue's gamma-glutamyl transferase (GGT) from microvillar membranes. Gel: pH 4–7 IPG, 4% *T*, 4% *C*, supplemented with 1% Ampholine in the same pH interval. Focusing for 5 h at 3000 V (at equilibrium), 10°C. Pan.: pancreas; Lun.: lung; Sem.: semen; Epi.: epididimus; Spl.: spleen; Kid.: kidney; Liv.: liver; Col.: colon; Ile.: ileum; Jej.: jejunum and Duo.: duodenum. After scraping the villi (where applicable) the enzyme was released by a short protease treatment, clarified by centrifugation and applied as such in pockets at the cathode. Staining by the azo-coupling technique using γ-glutamyl MNA as a substrate (Sinha and Righetti, just published).

same analysis was repeated with dipeptidyl peptidase IV (DPP IV) of rat (Fig. 6.20A) and human origin (Fig. 6.20B), it was comforting to see that here too the isoforms were tissue and species specific. The picture, however, changes, if we now compare CA-IEF with the IPG methodology. As shown in Fig. 6.21, the patterns of DDP IV in the two systems are completely different. While in CA-IEF alone the DDP IV isoforms are compressed in the pH 4.0–4.5 region, in IPGs (added with 1% CA) the spectrum is spread over the pH 4.3–5.5 region, thus encompassing pI values on the average higher by 1 pH unit. In addition, it is quite difficult to reconcile the two pattern (which, however, are both highly heterogeneous). The clue to what is happening here is given to us by the

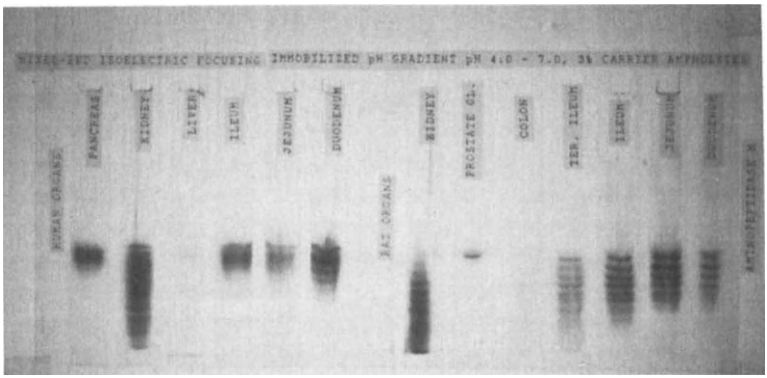

Fig. 6.19. Zymograms of rat and human organs' aminopeptidase M. Gel: pH 4–7 IPG, in presence of 3% carrier ampholyte. Sample application in pockets at the cathode. All other conditions as in Fig. 6.18. Gl.: gland; Ter.: terminal (Sinha and Righetti, just published).

last track to the right, showing an IPG run in presence of 4% CA. Here it is seen that the most alkaline bands begin to disappear, and more of the acidic zones are produced. We thus concluded (Sinha and Righetti, 1986) that indeed in CA-IEF alone enzymes solubilized from membranes form complexes with carrier ampholytes: the pI spectrum thus generated gives pI values produced by the CA chemicals coating the protein species. In addition to altering the original pI values, this could generate also additional bands representing multiple equilibria of enzymes bound and free of CA species. Conversely, in IPGs, the spectrum of bands generated should represent the true spectrum of 'stripped' enzyme molecules, uncomplexed by any potential complexing agent. It is only when adding very high levels of CAs (4%) that the equilibrium begins to be shifted towards the complexed form, thus producing the more acidic species. This phenomenon was observed with all the microvilli enzymes we have analyzed (GGT, DPP IV, AlP, aminopeptidase M). Thus, if it is true that in CA-IEF (in a very limited number of cases, though, and for very peculiar structures; see Righetti, 1983a) there could be occasionally some artefacts, due to complexation with carrier ampholyte species, this is a phenomenon which is most unlikely to occur in the IPG technique. So far, in

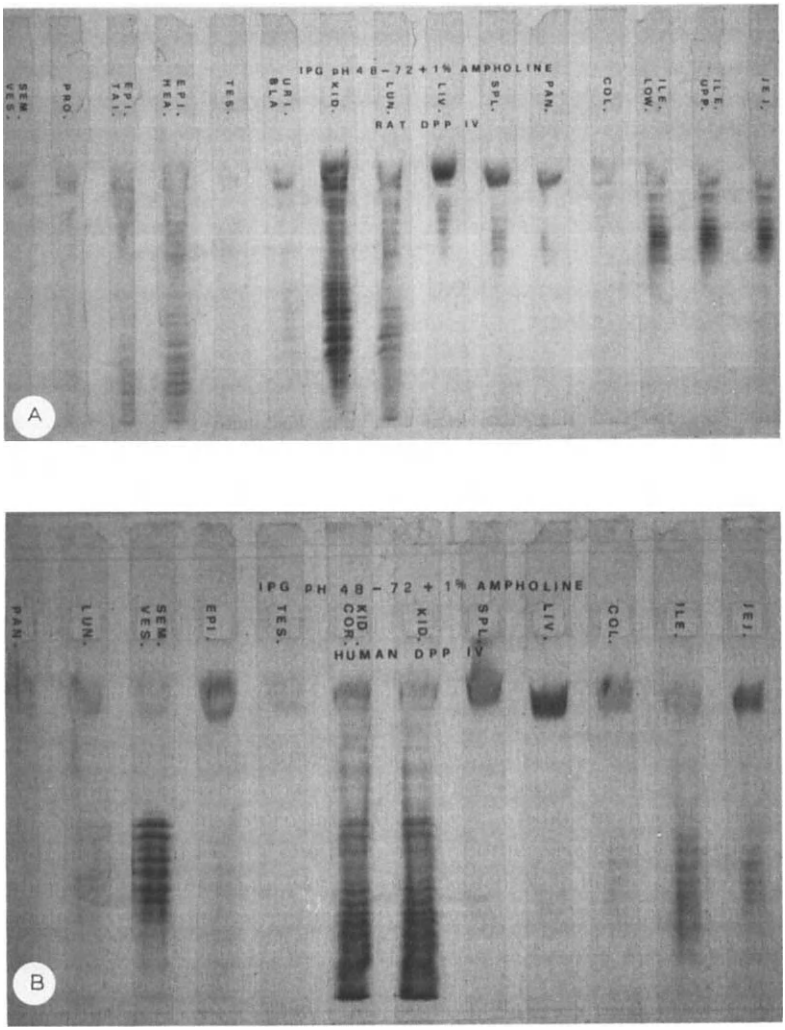

Fig. 6.20. Zymograms of rat (A) and human (B) organs' dipeptidyl peptidase IV (DPP IV). Gel: pH 4.8–7.2 IPG, 4% *T*, 4% *C*, added with 1% Ampholine pH 4–7. Sample application in pockets at the cathode. All other conditions and abbreviations as in Fig. 6.18, with the addition of: Sem. Ves.: semen vescicles; Pro.: prostate; Epi. tai.: epididimus tail; Epi. Hea.: epididimus head; Tes.: testicles; Uri. Bla.: urinary bladder; Low. Ile.: lower ileum; Upp. Ile.: upper ileum; Kid. Cor.: kidney cortex (Sinha and Righetti, just published).

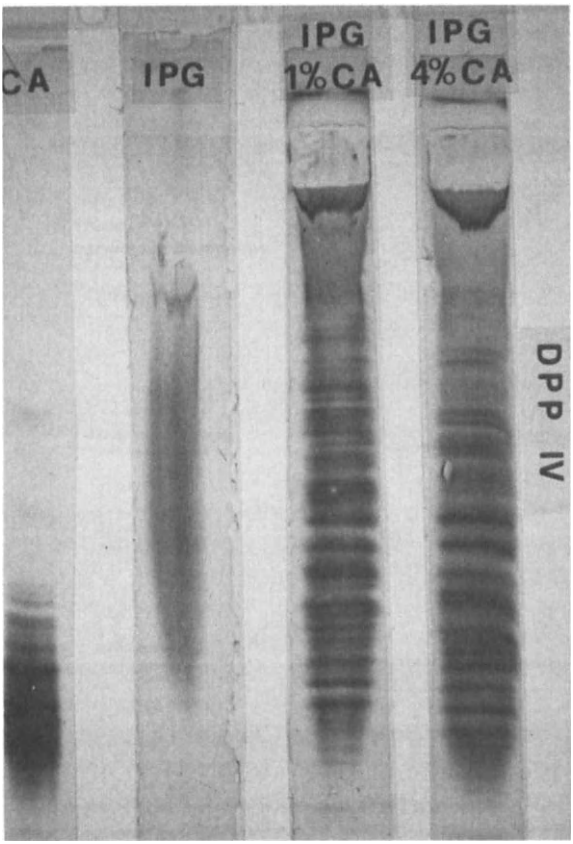

Fig. 6.21. Comparison of focusing DPP IV in carrier ampholytes (CA) and in Immobiline (IPG) gels. CA: conventional IEF with carrier ampholytes in the pH 4–6.5 range; IPG: immobilized pH gradient in the pH 4–6.5 range; mixed IPGs (pH 4–6.5) with an added 1% Ampholine (IPG-1% CA) and mixed-bed IPG (pH 4–6.5) with an added 4% Ampholine (IPG-4% CA). Cathode at the top, anode at the bottom. IEF for 12 h at 2000 V (max) at 10°C with 10 mM Glu as anolyte and 10 mM Lys as catholyte. Staining by the azo coupling technique using Gly-Pro-MNA as substrate (from Sinha and Righetti, 1986; by permission from Elsevier).

fact, the only report we know off is the binding of albumin to the pK 4.4 and 4.6 acids (this producing a smear, though, and not distinct bands; the result is a sort of an affinity electrophoresis).

The other interesting aspect of zymogramming with the IPG technique is the maintenance of band sharpness all throughout the staining procedure, even when the incubation is protracted for more than an hour. Again, we attribute this to the fact that the protein, at its pI, forms a salt with the surrounding Immobiline chemicals (Gelfi et al., 1987). As the latter are grafted to the matrix, the isoelectric protein has difficulties in diffusing away from the pI zone (for more on this phenomenon, see Chapter 5, §5.2.3 and Fig. 5.8A and B).

6.4. Focusing at pH extremes

We have seen in Chapter 2 (see §2.9) that, notwithstanding the presence of huge amounts of a 'buffering Immobiline' in the extreme pH regions (water, constantly present at the 55.56 M level), it is possible, with due precaution, to extend the fraction range to as low as pH 2.5 and as high as pH 11, i.e., in regions 'forbidden' by physical laws. As shown in Fig. 2.17, in these regions (and of course, even more so at progressively lower and higher pH values) water acts as a good buffer and a good conducting species, i.e., it fulfills the fundamental requirements defined by Rilbe (1973) for a carrier buffer to be used in IEF. However, due to the enormous differences in conductivity between the Immobiline matrix and the bulk water, connected with severe electrosmosis at these rather extreme pH regions, it did not seem feasible to perform IPG fractionations at extreme pH values. On the contrary, we have shown that, with the use of 'conductivity and electrosmosis quenchers', i.e., with the incorporation of strong density gradients of polyols (sucrose and sorbitol) with the dense part in the highly-conducting region (pH 2.5 in acidic, pH 11 in basic gradients) it is possible to obtain more than satisfactory IPG patterns.

Fig. 6.22 gives an example of a separation in an IPG pH 3–4 interval. There are some interesting aspects of this separation of dansylated amino acids worth mentioning. First of all, at the time this separation was performed (Bianchi-Bosisio et al., 1986) it was believed that no IPG runs could be made operative below pH 4.

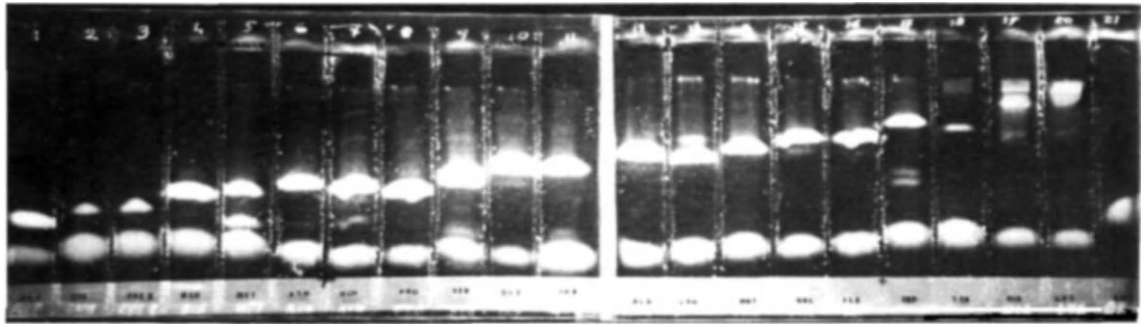

Fig. 6.22. IEF of 21 dansyl amino acids in a pH 3.1–4.1 Immobiline gel. Conditions: 6% *T*, 4% *C* Immobiline gel with three times the standard amount of Immobiline (ca. 30 mM buffering ion). Run: 5 h at 1200 V (at equilibrium) 5 W_{max} at 4°C. Detection by fluorescence (from Bianchi-Bosisio et al., 1986; with permission from VCH).

Secondly, by transforming free amino acids into dansylated species, it is possible to focus even the 15 mono-amino, mono-carboxylic acids, which, according to Rilbes' law should not be amenable to IPG fractionations since they exhibit too high ΔpK values (ca. 7 pH units). In this case, the primary amino group (pK ca. 9.6) is substituted with the tertiary amino group in the dansyl moiety (pK 5.11) and now the derivatized species have sharp isoelectric points (ΔpKs ca. 2.8). Thirdly, it was shown that IPGs could be used as a physico-chemical probe, since they allowed accurate measurements of the pK value of the dansyl amino group, not reported in the literature. This was made possible by knowing the pK value of the carboxyl group of each amino acid and by measuring its pI value in the IPG gel: thus pK_2 (tertiary amino group) was derived from the equation: $pK_2 = (2pI - pK_1)$.

Fig. 6.23 shows the pattern of pepsin from pig stomach mucosa, separated in an IPG pH 2.5–3.5 interval (the physico-chemical parameters of this very acidic gradient are shown in Fig. 2.20): after IEF, the gel was overlaid with a casein-agar and a zymogram was taken: the four bands labelled with pI values exhibited full enzymatic activity. It should be noted that this is the first time that such an acidic separation has been performed in IEF: it is true that in the past, in CA-IEF, attempts have been made at focusing in such acidic regions by creating a gradient formed by a mixture of weak and strong acids (Stenman, 1975), but true steady-state patterns were never obtained, and the pH gradient kept drifting severely. It should also be noted that pI values can be given with much greater accuracy than in CA-IEF. What is important to stress here is that, although the pH gradient is very stable with time, the protein might not stand for long periods such a harsh pH environment: this is not the case of pepsin but, e.g., with orosomucoid (pH 3–4 IPG interval), we noticed that, if focusing was performed overnight, the pattern was blurred and unreproducible, whereas if focusing was allowed for a short time (4–5 h) sharp and constant patterns were obtained. We attribute this to the slow hydrolysis of the protein moiety (or of its carbohydrates) with time.

At the opposite extreme of the pH scale, very good separation was obtained of strongly basic proteins, such as cytochrome *c* and lysozyme, in an IPG pH 10–11 interval (Fig. 6.24) (Gelfi et al.,

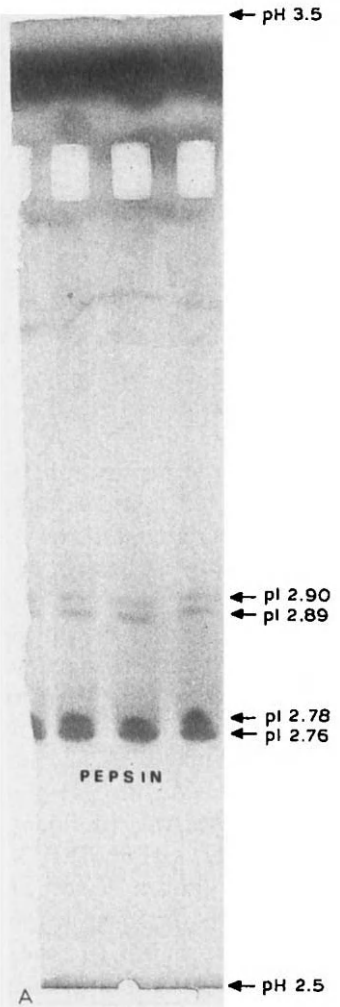

Fig. 6.23. IEF of pepsin. A 4% *T*, 4% *C* IPG matrix in the pH 2.5–3.5 interval was made, containing 20 mM AGA as buffering ion and the p*K* 9.3 Immobiline as titrant. The gel was polymerized in presence of 0.5% Ampholine pH 2.5–4 and was 0.5 mm thick and 18 cm long. 30 μg of pepsin from pig stomach mucosa were loaded in pockets precast at the cathode. The gel was not pre-focused. Running conditions: 3 h at 300 V followed by 4 h at 1000 V, 10°C. Staining with Coomassie Brilliant Blue R-250 in copper sulphate. The pIs were derived by linear interpolation from the known gradient slope. A: picture of the entire gel over the 18 cm separation axis; B: close-up of the 4 focused pepsin bands.

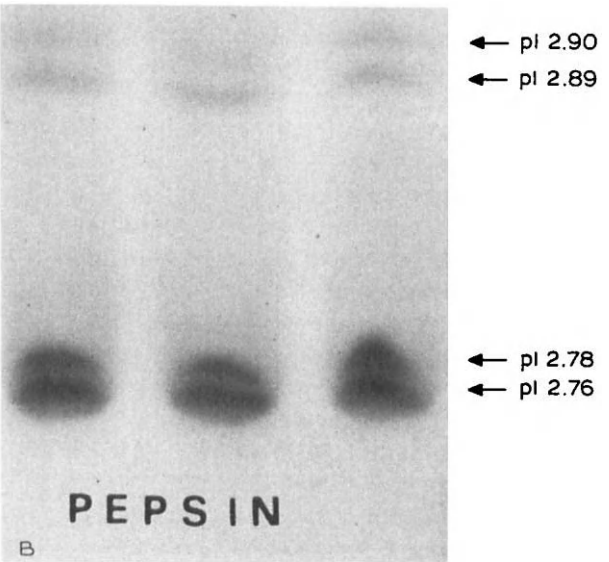

Fig. 6.23 (continued).

1987). Note that in fact cytochrome *c* (which is usually lost in the cathodic compartment after a short focusing time in CA-IEF) is not a single band, but contains an additional two more acidic isoforms. The heterogeneity of cytochrome *c* was also reported long ago by Vesterberg and Svensson (1966). What is of interest is that lysozyme, believed to have a pI of ca. 9.5, here behaves as a species with pI 10.6, i.e., greater by at least one pH unit. This is not the only discrepancy we have found: e.g., human α-globin chains give a pI of ca. 8 in CA-IEF, but in IPGs have a pI > 9. This last value seems to be the correct one, since, by calculating the theoretical pI value from the known sequence of the α-chains with the Linderstrøm-Lang equation, one expects to obtain a pI value of ca. 9. Perhaps, as we have stated above in the case of DPP IV focusing (see Fig. 6.21), the lower pI values in CA-IEF are due to binding of CA species to the protein coil. However, it should also be noted that part of this pI discrepancy could be due to temperature differences in pI measurements (10°C in IPG as opposed to

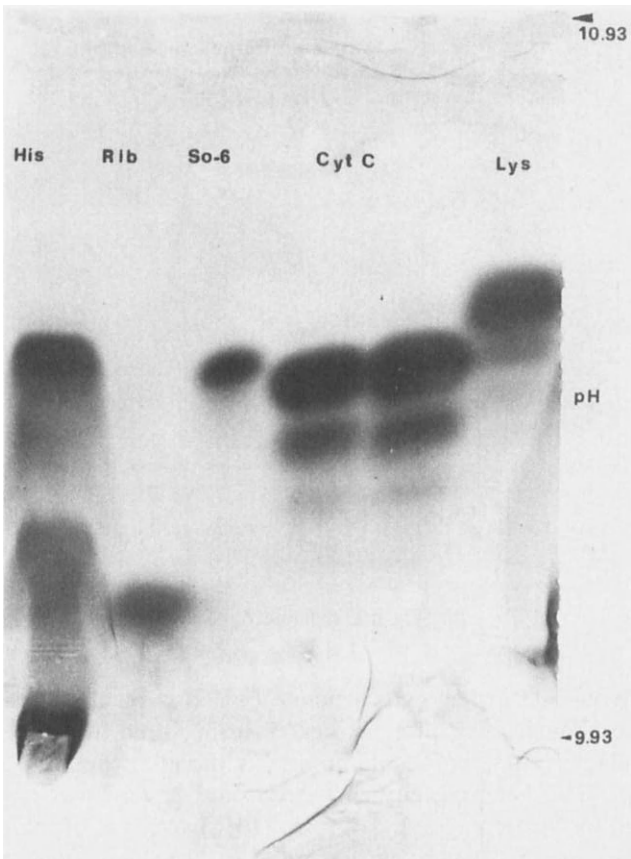

Fig. 6.24. IEF of different proteins in an IPG pH 10–11 gel. The matrix contained 4% *T*, 4% *C* and 0.5% Pharmalyte pH 8–10.5+0.5% Ampholine pH 9–11. His: histones; Rib: ribonuclease; So-6: purified leaf protein from Saponaria officinalis; Cyt C: cytochrome *c*; Lys: lysozyme. Eahc protein was loaded at the anode (a total of 30 μg except for histones, for which 200 μg were applied). Stain: colloidal dispersion of Coomassie Blue G-250. Focusing: overnight at 300 V, then 3 h at 2000 V at 10°C (from Gelfi et al., 1987; by permission from Elsevier).

20–25°C in most CA-IEF runs; the increment in pI could be as high as 0.3–0.4 pH units in the case of IPGs).

What happens to enzymes in such alkaline pH ranges is shown in Fig. 6.25: elastase was focused and revealed by in situ zymo-

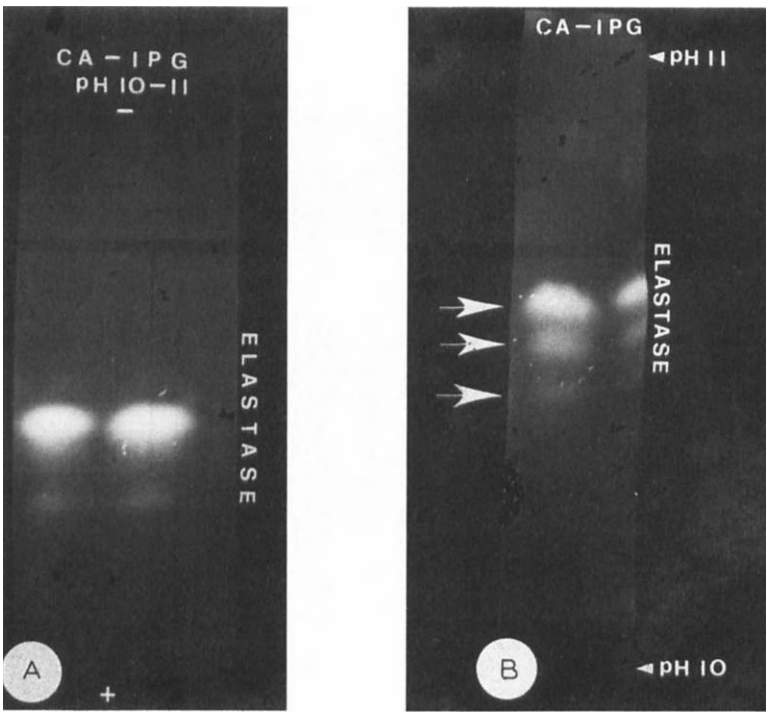

Fig. 6.25. Focusing and in situ zymogramming of elastase. A: 10 μg/lane of elastase (from porcine pancreas) focused in a pH 10–11 IPG gel containing 1% CA and visualized with glutaryl-$(Ala)_3$-MNA impregnated cellulose acetate overlay in 50 mM Tris–acetate buffer at pH 8.0. Focusing: 500 V for 6 h and zone sharpening for 1 h at 2000 V, 10°C. Anodic sample application in a pH 8.0 IPG pH plateau. B: same as A except that 30 μg/lane was applied and zone sharpening was continued for 3 h at 2000 V (limiting) (from Sinha and Righetti, 1987; with permission from Elsevier).

gramming with fluorogenic substrates. It seems that the three isoforms separated are fully enzyme active (Sinha and Righetti, 1987). Here too it should be stated that focusing should be run for short times, so as to prevent potential harmful effects of such high pH values. We had reported in both of these articles that, for a proper performance of such alkaline ranges, one should bind the IPG matrix to silanized glass surfaces (coated with bind-silane),

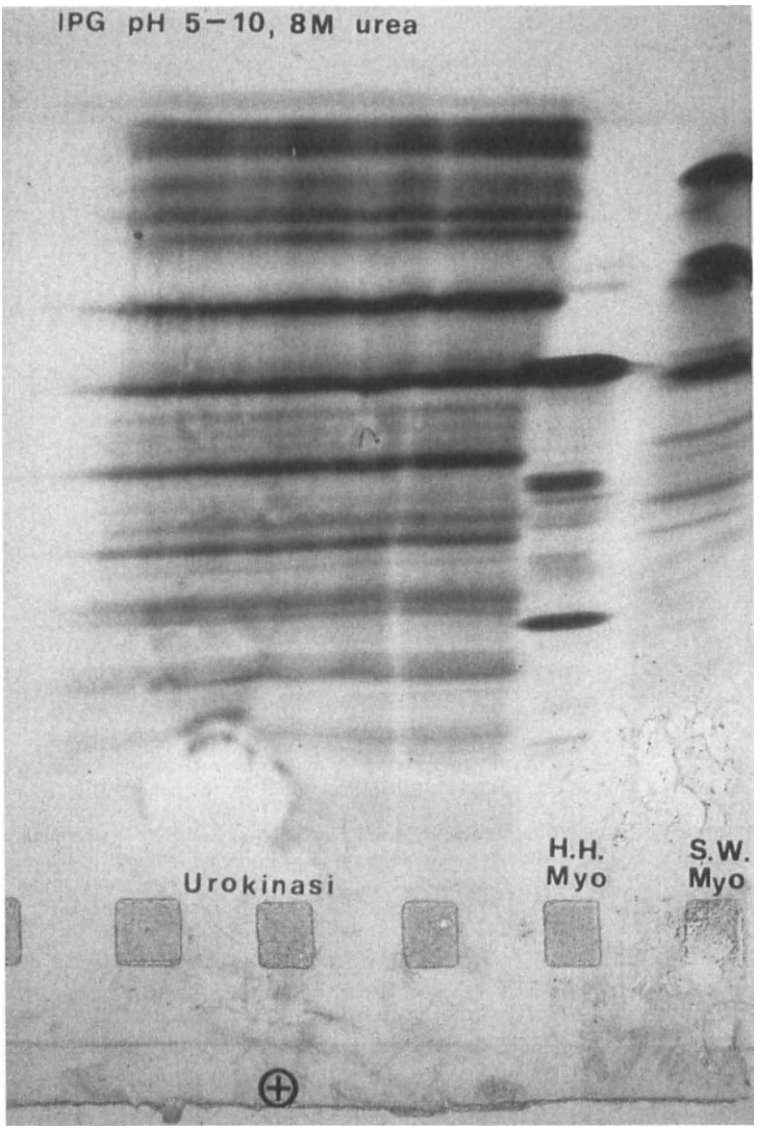
IPG pH 5–10, 8M urea
Urokinasi
H.H. Myo
S.W. Myo
⊕

since apparently Gel Bond foils would not stick to it. We have now found (as reported by many investigators; e.g., Ostergren et al., 1988) that indeed Gel Bond contains noxious impurities which prevent good binding of the gel matrix and often ruin the separation by interfering with the pH gradient. If the plastic foil is washed four times (15 min each) in distilled water and let dry, good binding will be possible, even at alkaline pH values (but never touch with your fingers the plastic surface, as you will deposit a fat layer on it and prevent binding!).

6.5. Conclusions. On protein heterogeneity

I believe I have covered the grounds perhaps a bit better than the father who explained sex to his son in a famous song of Harry Belafonte, which had the son concluding: 'it was as clear as mud, but it covered the ground'. If I happened to give to you such a disastrous account, perhaps I will go down to history not as a biochemist, but as a relative of a blues musician, the well-known 'Muddy Waters'. But even a muddy river can produce a crystal-clear lake, once the silt has deposited at the bottom. So paddle gently down the river, hoping to get to the lake.

I do not want to leave you with the impression that IPGs are a trouble-free technique. Otherwise a snowball will become an avalanche (of too many users of the technique, a most undesirable event, which will force me to waste my life away trying to catch up). There might be some problems, after all. An example is offered in Fig. 6.26: pure urokinase, showing a single band in SDS, and cleaned with an affinity column containing specific antobod-

Fig. 6.26. Analysis of urokinase by IEF in IPG. A 4% *T*, 4% *C* polyacrylamide gel was prepared, containing a pH 5–10 immobilized gradient. The gel was washed, dried and re-swollen in 8 M urea and 1% carrier ampholytes in the same pH 5–10 range. Samples were applied in pockets precast at the anodic side. Run: overnight at 2000 V, 10°C. The three urokinase lanes contained a total of 100 μg protein, while the two pH indicators were 20 μg each. HH Myo and SW Myo: horse heart and sperm whale myoglobins, respectively. Staining: Coomassie Brilliant Blue R 250 in presence of copper sulphate (from Righetti et al., 1989b; with permission from Elsevier).

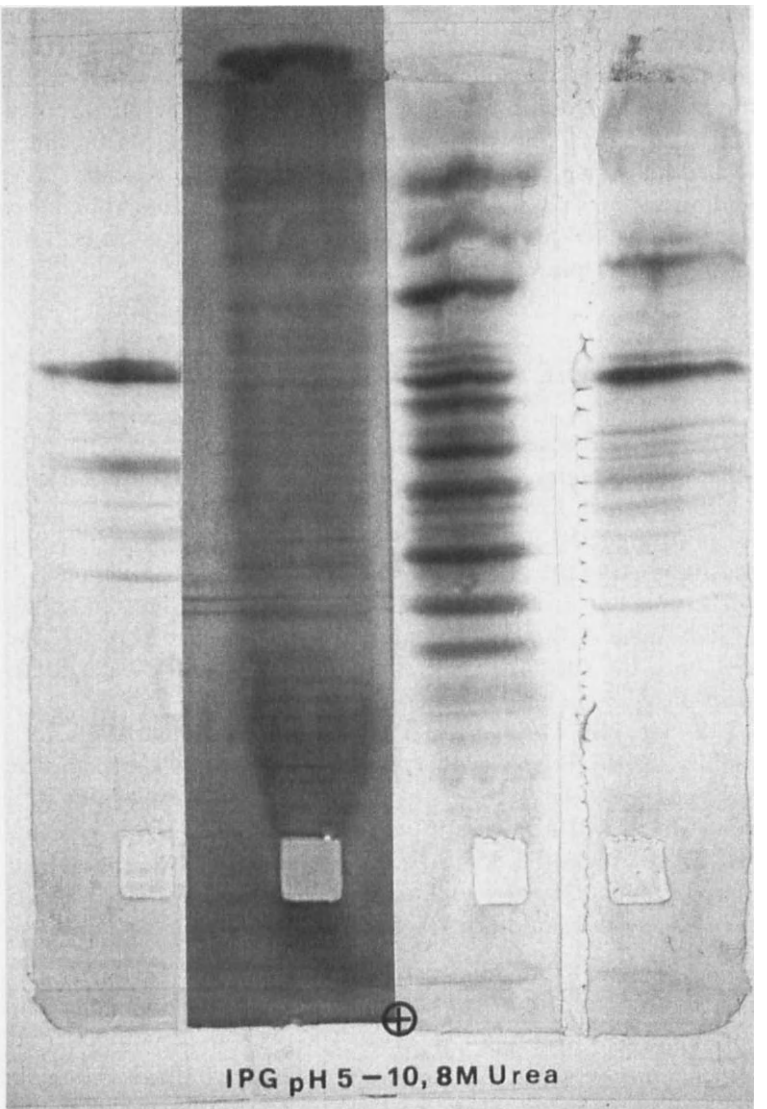

Fig. 6.27. IEF in IPG of pro-urokinase (pro-uro) (2nd track from the left) and of urokinase (3rd track from the left). All conditions as in Fig. 6.26. Due to the low amount loaded, the pro-uro strip was stained with silver, while the others were dyed with Coomassie Blue. Note the strongly alkaline major band in the pro-uro preparation. Track 1: horse heart myoglobin; track 4: sperm whale myoglobin (from Righetti et al., 1989b; with permission from Elsevier).

ies, in fact already used in human therapy, when analyzed in IPGs gave a frightening multitute of bands (> 20), many more in fact than one could see in CA-IEF. It turned out, in this case, that this phenomenon should not be attributed to the higher resolving power of IPG over CA-IEF. When the smaller and higher M_r fragments were analyzed in IPGs, they also exhibited considerable heterogeneity; even a pure preparation of pro-urokinase, in IPGs, gave an astonishing number of bands (when counting the major and minor, ca. 50!) (Fig. 6.27). Had we been poisoning then our patients? Curiously, even though never published, also tissue plasminogen activator (tPA) from Genentech (a rDNA protein also used as a drug in human therapy) shows this incredible array of bands. It turns out that these proteins contain an extremely high number of Cys residues (24 in the case of UK, 28 for tPA); to make things worse, both proteins have rather high pIs (ca. 10 for pro-UK). As focusing in IPGs is conducted for long times (often overnight), at these high pH values –SH groups can undergo all sort of oxidation reactions, easily to –S–S– bridges, possibly even to cysteic acid residues. In the case of –SH/–S–S– equilibria, 'scrambled' molecules could form, producing statistically several million different species with any possible –S–S– combination. We have already discussed this phenomenon in Chapter 1 (see also Figs. 1.15 to 1.17) but it is clear that, even when the matrix is devoid of noxious N-oxides, oxidation can still occur simply via atmospheric oxygen. Thus, it might turn out that, for alkaline proteins rich in –SH groups, focusing in IPGs might be the worst of all possible choices. I suggest that, in these cases, analysis should be performed by capillary zone electrophoresis (CZE) at close to neutral pH values (pH 6 to 7): these pH values will prevent auto-oxidation during the run; in addition the very short runs typical of CZE (10 to 15 min) should also minimize any oxidative phenomena. With the peace of mind of my friends at Genentech (tPA) and at Lepetit (urokinase) who for years have ben hiding away their IEF patterns from nosy FDA officials.

Post scriptum: Maestro Volta

Alessandro Volta (Camnago, 1745–Como, 1827) became Professor of Physics at the University of Pavia in 1799. We have left him in the Introduction quarreling with Galvani and experimenting with metals above and below his tongue. It was in the course of these experiments that Volta was to perfect an instrument whose effects seemed extraordinary. He placed round plates of silver and zinc on top of each other, with little rounds of a spongy substance soaked in salt water or acid solution. This 'pile' produced electricity, and of quite a peculiar kind, in fact continuous electricity. In his famous letter addressed on March 20, 1800 to the London Royal Society, Volta thus spoke of his invention: 'I should like to call this apparatus, which is more like the natural electric organ of electric fish, than the Leyden bottle of known electric batteries, an artificial electric organ'. Received by the Paris Academie des Sciences, Volta presented his invention to Bonaparte, who was a member of the Institute, on Brumaire 16 in the year 9. Napoleon was quite impressed and had the following notice published in the Moniteur: 'I wish to donate the sum of 60,000 francs as an encouragement to the person whose experiments and discoveries shall help to develop electricity and galvanism in a manner comparable to the furtherance of these sciences by Franklin and Volta'. Ampère, who was a young assistant at the Ecole Polytechnique, and already passionately interested in electricity, must have dreamt and worked hard for that prize money which, however, was awarded to Humphry Davy for his work on the electric decomposition of potash and soda. It was an imperial gesture on the part of Napoleon to offer such a prize to an English scientist at a time when it was common knowledge that the British Cabinet was preparing a fifth coalition: his personal reward, a few years later, was Waterloo.

Let us hear from H. Davy how he performed the crucial experiment which led to the discovery of two new elements. 'I placed', he

said, 'a fragment of potash on a platinum disc connected to the negative side of a 225-plate 'pile' in full operation. A platinum wire linked to the positive side was connected to the upper side of the potash. The entire apparatus functioned in contact with the air. The potash began to melt at the two points of electrification. On the underside appeared a series of small globules exactly like drops of mercury. Identical results were obtained with soda'. He observed that, because of their opacity, brightness and malleability and the fact that they conducted both heat and electricity, these new substances resembled metals. 'I therefore ventured', he concluded, 'to call these new substances potassium and sodium'. Thus, it is seen that with Volta not only electrophoresis was born, but also modern chemistry.

References

Abramson, H.A. (1934) Electrokinetic Phenomena and Their Application in Biology and Medicine, Am. Chem. Soc. Monograph Ser., Chem. Cat. Co., New York.

Aebersold, R.H., Teplow, D.B., Hood, L.E. and Kent, S.B.H. (1986) J. Biol. Chem. *261*, 4229–4238.

Aebersold, R.H., Leavitt, J., Hood, L.E. and Kent, S.B.H. (1987) in: Methods in Protein Sequence Analysis (Walsh, K., ed.) Humana Press, Clifton, pp. 277–294.

Aggarwal, S.L. (1976) Polymer *17*, 38–56.

Aisen, P. and Listowsky, I. (1980) Ann. Rev. Biochem. *49*, 357–393.

Albers, J.J., Lin, J. and Roberts, G.P. (1979) *5*, 61–75.

Alexander, A., Cullen, B., Emigholz, K., Norgard, W.M. and Monahan, J.J. (1980) Anal. Biochem. *103*, 176–183.

Allen, R.C. (1980) Electrophoresis *1*, 32–37.

Alper, C.A. and Propp, R.P. (1968) J. Clin. Invest. *47*, 2181–2191.

Alper, C.A. and Johnson, A.M. (1969) Vox Sang. *17*, 445–452.

Alper, C.A., Boenish, T. and Watson, L. (1972) J. Exp. Med. *135*, 68–80.

Altland, K. and Kaempfer, M. (1980) Electrophoresis *1*, 57–62.

Altland, K. and Altland, A. (1984) Clin. Chem. *30*, 2098–2103.

Altland, K., Banzhoff, A., Hackler, R. and Rossmann, U. (1984) Electrophoresis *5*, 379–381.

Altland, K. and Rossmann, U. (1985) Electrophoresis *6*, 314–325.

Altland, K. and Banzhoff, A. (1986) Electrophoresis *7*, 529–533

Almgren, M. (1971) Chem. Scripta *1*, 69–75.

Althaus, H.H., Klöppner, S., Poehling, H.M. and Neuhoff, V. (1983) Electrophoresis *4*, 347–353.

Alwine, J.C., Kemp, D.J. and Stark, G.R. (1977) Proc. Natl. Acad. Sci. USA *74*, 5350–5355.

Ames, G.F.L. and Nikaido, K. (1976) Biochemistry *15*, 616–623.

Amess, R., Ramasamy, R. and Spragg, S.P. (1984) in: Electrophoresis '84 (Neuhoff, V., ed.) VCH, Weinheim, pp. 297–300.

Anderson, N.G. and Anderson, N.L. (1977) Proc. Natl. Acad. Sci. USA *74*, 5421–5425.

Anderson, N.G. and Anderson, N.L. (1978a) Anal. Biochem. *85*, 331–340.

Anderson, N.G. and Anderson, N.L. (1978b) Anal. Biochem. *85*, 341–354.

Anderson, N.L. and Hickman, B.J. (1979) Anal. Biochem. *93*, 312–320.

Anderson, N.G., Anderson, N.L. and Tollaksen, S.L. (1979) Clin. Chem. *25*, 1199–1210.

Anderson, N.G., Anderson, N.L., Tollaksen, S.L., Hahn, H., Giere, F. and Edwards, J. (1979) Anal. Biochem. *95*, 48–61.

Anderson, N.G. and Anderson, N.L. (1980) J. Automatic Chem. *2*, 177–178.

Anderson, N.G. and Anderson, N.L. (1982a) Clin. Chem. *28*, 739–745.

Anderson, N.G. and Anderson, N.L. (Eds.) (1982b) Clin. Chem. *28*, 737–1029.

Anderson, N.G. and Anderson, N.L. (Eds.) (1984a) Clin. Chem. *30*, 1897–2108.

Anderson, N.G. and Anderson, N.L. (1984b) Clin. Chem. *30*, 1898–1905.

Anderson, N.G., Tollaksen, S.L., Pascoe, F.H. and Anderson, N.L. (1985) Crop Science *25*, 667–674.
Anderson, N.G. and Anderson, N.L. (1987) In: New Directions in Electrophoretic Methods, Jorgenson, J.W. and Phillips, M. eds. (Am. Chem. Soc. Symp. Ser., Washington) *335*, pp. 132–142.
Andrews, A.T. (1986) Electrophoresis: Theory, Techniques and Biochemical and Clinical Applications, Clarendon Press, Oxford.
Appel, R., Funk, M., Hochstrasser, D., Muller, F. and Pellegrini, C. (1986) in: Recent Progresses in Two-Dimensional Electrophoresis (Galteau, M. and Siest, G., eds.), Presses Universitaires de Nancy, pp.108–116.
Arnaud, P., Chapuis-Cellier, C. and Creyssel, R. (1975) Prot. Biol. Fluids *22*, 515–520.
Artoni, G., Gianazza, E., Zanoni, M., Gelfi, C., Tanzi, M.C., Barozzi, C., Ferruti, P. and Righetti, P.G. (1984) Anal. Biochem. *137*, 420–428.
Astrua-Testori, S., Pernelle, J.J., Wahrmann, J.P. and Righetti, P.G. (1986) Electrophoresis *7*, 527–529.
Astrua-Testori, S. and Righetti, P.G. (1987) J. Chromatogr. *387*, 121–126.
Aycock, B.F., Weil, D.E., Sinicropi, D.V. and McIlwain, D.L. (1981) Comput. Biomed. Res. *14*, 314–326.
Azen, E.A. and Smithies, O. (1968) Science *162*, 905–907.
Bahrman, N. and Thiellement, H. (1985) Electrophoresis *6*, 357–358.
Barger, B.O., White, F.C., Pace, J.L., Kemper, D.L. and Ragland, W.L. (1976) Anal. Biochem. *70* 327–335.
Bark, J.E., Harris, M.J. and Furth, M.J. (1976) J. Forens. Sci. *16*, 115–120.
Barrett, T. and Gould, H.J. (1973) Biochim. Biophys. Acta *294*, 165–175.
Bartels, R. and Bock, L. (1984) in: Electrophoresis '84 (Neuhoff, V., ed.) VCH, Weinheim, pp. 103–106.
Bartels, R. and Bock, L. (1988) in: Electrophoresis '88 (Schafer-Nielsen, C., ed.) VCH, Weinheim, pp. 289–294.
Barzaghi, B., Righetti, P.G. and Faupel, M. (1987) J. Biochem. Biophys. Methods *15*, 177–188.
Bass, W.T. and Bricker, T.M. (1988) Anal. Biochem. *171*, 330–338.
Bassett, P., Braconnier, F. and Rosa, J. (1982) J. Chromatogr. *227*, 267–304.
Bauer, H., Nagel, J. and Franz, H.E. (1986) in: Electrophoresis '86 (Dunn, M.J., ed.) VCH, Weinheim, pp. 677–679.
Baumstark, M.W., Berg, A., Halle, M. and Keul, J. (1988) Electrophoresis *9*, 576–579.
Bauw, G., DeLoose, M., Inze, D., Van Montagu and Vandekerckhove, J. (1987) Proc. Natl. Acad. Sci. USA *84*, 4806–4810.
Becquerel, A.H. (1896) C.R. Acad. Sci. Paris *122*, 420–421.
Bergenbraut, S., Gallo, P., Gudmunson, C. and Siden, A. (1986) Prot. Biol. Fluids *34*, 855–858.
Bernardi, G. (1971) Methods Enzymol. *21*, 95–140.
Bianchi-Bosisio, A., Loherlein, C., Snyder, R.S. and Righetti, P.G. (1980) J. Chromatogr. *189*, 317–330.
Bianchi-Bosisio, A., Rochette, J., Wajcman, H., Gianazza, E. and Righetti, P.G. (1985) J. Chromatogr. *330*, 299–306.
Bianchi-Bosisio, A., Righetti, P.G., Egen, N.B. and Bier, M. (1986) Electrophoresis *7*, 128–133.

Bier, M. and Kopwillem, A. (1977) in: Electrofocusing and Isotachophoresis (Radola, B.J. and Graesslin, D., eds.) de Gruyter, Berlin, pp. 567–576.
Bier, M. and Egen, N. (1979) in: Electrofocus '78 (Haglund, H., Westerfeld, J.C. and Ball, J.T., Jr., eds.), Elsevier, Amsterdam, pp. 35–48.
Bier, M., Egen, N.B., Allgyer, T.T., Twitty, G.E. and Mosher, R.A. (1979) in: Peptides: Structure and Biological Function (Gross, E. and Meienhofer, J. eds.), Pierce Chem. Co., Rockford, Il., pp. 79–89.
Bier, M., Mosher, R.A., Thormann, W. and Graham, A. (1984) In: Electrophoresis '83 (Hirai, H., ed.), de Gruyter, Berlin, pp. 99–107.
Bier, M. (1986a) in: Separation, Recovery and Purification in Biotechnology (Asenjo, J. and Hong, eds.) ACS Symp. Ser. *314*, Am. Chem. Soc., Washington, pp. 320–330.
Bier, M., Egen, N.B., Twitty, G.E., Mosher, R.A. and Thormann, W. (1986b) in: Chemical Separations, vol. 1 (King, C.J. and Navratil, J.D., eds.) Litarvan Literature, Denver, pp. 220–230.
Biocca, S., Calissano, P., Barra, D. and Fasella, P.M. (1978) Anal. Biochem. *87*, 334–342.
Bishop, C.W., Kendrick, N.C., Santek, D.A., Thomson, R.G. and Deluca, H.F. (1985) Anal. Biochem. *148*, 133–148.
Bjellqvist, B., Ek, K., Righetti, P.G., Gianazza, E., Görg, A., Postel, W. and Westermeier, R. (1982) J. Biochem. Biophys. Methods *6*, 317–339.
Bjerrum, O.J. (ed.) (1987) Protein Blotting, Electrophoresis *8*, 377–464.
Bjerrum, O.J. and Heegaard, N.H. (1989) J. Chromatogr., *470*, 351–367.
Board, P.G. (1980) Am. J. Hum. Genet. *32*, 348–353.
Bode, J.H. (1980) in: Electrophoresis '79 (Radola, B.J., ed.), de Gruyter, Berlin, pp. 39–52.
Bobb, D. (1974) Ann. N. Y. Acad. Sci. *209*, 225–236.
Bolton, A.E. and Hunter, W.M. (1973) Biochem. J. *133*, 529–538.
Bonner, W.M. and Laskey, R.A. (1974) Eur. J. Biochem. *46*, 83–88.
Bonner, W.M. (1983) Methods Enzymol. vol. *96*, Academic Press, New York, pp. 215–225.
Booz, M.L. and Travis, R.L. (1981) Phytochemistry *20*, 1773–1779.
Boschetti, E. (1985) In: Affinity Chromatography (Dean, P.D.G., Johnson, W.S. and Middle, F.A., eds.), IRL Press, Oxford, pp. 11–15.
Bos, E.S., Van der Doelen, Van der Struick, E., Bergink, E.N. and Schurrs, A.H.W.M. (1984) In: Electrophoresis '84 (Neuhoff, V., ed.) VCH, Weinheim, pp. 93–93
Bosshard, H.F. and Datyner, A. (1977) Anal. Biochem. *82*, 327–333.
Bossi, M.L., Bossi, O., Gelfi, C. and Righetti, P.G. (1988) J. Biochem. Biophys. Methods *16*, 171–182.
Bössinger, J., Miller, M.J., Vo, K.P., Geisduschek, E.P. and Xuong, N.H. (1979) J. Biol. Chem. *254*, 7986–7998.
Bradford, M.M. (1976) Anal. Biochem. *72*, 248–254.
Braend, M. (1988a) Anim. Genet. *19*, 59–62.
Braend, M. (1988b) J. Hered. *33*, 211–212.
Braend, M., Nesse, L.L. and Efremov, G.D. (1987a) Anim. Genet. *18*, 223–231.
Braend, M., Tucker, E.M. and Clarke, S.W. (1987b) Anim. Genet. *18*, 75–79.
Braend, M., Aursjo, J. and Austbo, O. (1987c) Acta Vet. Scand. *28*, 121–123.
Braend, M. and Tucker, E. (1988) Biochem. Genet. *26*, 511–518.
Bravo, R. and Celis, J.E. (1982) Clin. Chem. *28*, 766–781.

Bravo, R. (1984) in: Two-Dimensional Gel Electrophoresis of Proteins (Celis, J.E. and Bravo, R., eds.) Academic Press, Orlando, pp. 3–36.
Brogren, C.H. and Peltre, G. (1977) in: Electrofocusing and Isotachophoresis (Radola, B.J. and Graesslin, D., eds.) de Gruyter, Berlin, pp. 587–599.
Brown, W.V., Levy, R.I. and Fredrickson, D.S. (1970) J. Biol. Chem. *245*, 6588–6594.
Brown, R.K., Caspers, M.L., Lull, M.J., Vinogradov, S.N., Felgenhauer, K. and Nekic, M. (1977) J. Chromatogr. *131*, 223–232.
Brown, E., Racois, A., Boschetti, E. and Corgier, M. (1978) J. Chromatogr. *150*, 101–110.
Brown, J.W.S. and Flavell, R.B. (1981) Theor. Appl. Genet. *59*, 349–359.
Brown, J.W.S., Law, C.N., Worland, A.J. and Flavell, R.B. (1981) Theor. Appl. Genet. *59*, 361–371.
Brown, M.S., Kovanen, P.T. and Goldstein, J.L. (1981) Science *212*, 628–655.
Brown, E.G. (1988) Anal. Biochem. *174*, 337–348.
Bugugnani, M.J., Koffligan, M., Kora, I., Ouvry, D., Clavey, V. and Fruchart, J.C. (1984) Clin. Chem. *30*, 349–351.
Bunn, H.F. and McDonough, M. (1974) Biochemistry *13*, 988–993.
Bunn, H.F., Forget, B.G. and Ranney, H.M. (1977) Hemoglobinopathies, Saunders, Philadelphia.
Burdett, P. (1982) Isoelectric Focusing, Principles and Methods (Pharmacia, Uppsala) pp. 31–36.
Burdett, P., Lizana, J., Eneroth, P. and Bremme, K. (1982) Clin. Chem. *28*, 935–940.
Burdett, P. and Whitehead, P.H. (1977) Anal. Biochem. *77*, 419–428
Burghes, A.H.M., Dunn, M.J. and Dubowitz, V. (1982) Electrophoresis *3*, 354–363.
Butcher, E.C. and Lowry, O. H. (1976) Anal. Biochem. *76*, 502–523.
Capel, M., Redman, B. and Bourque, D.P. (1979) Anal. Biochem. *97*, 210–228.
Carrell, S., Accolla, R.S., Carmagnola, A.L. and Mach, J.P. (1980) Cancer Res. *40*, 2523–2530.
Casero, P., Del Campo, G.B. and Righetti, P.G. (1985a) Electrophoresis *6*, 367–371.
Casero, P., Gelfi, C. and Righetti, P.G. (1985b) Electrophoresis *6*, 59–69.
Catapano, A.L., Jackson, R.L., Gillian, E.B., Gotto, A.M., Jr. and Smith, L.C. (1978) Lipid Res. *19*, 1047–1052.
Celentano, F., Gianazza, E., Dossi, G. and Righetti, P.G. (1987) Chemometr. Intel. Lab. Systems *1*, 349–358.
Celentano, F., Tonani, C., Fazio, M., Gianazza, E. and Righetti, P.G. (1988) J. Biochem. Biophys. Methods *16*, 109–128.
Celis, J.E. and Bravo, R. (Eds.) (1984) Two-dimensional Gel Electrophoresis of Proteins, Academic Press, Orlando.
Celis, J.E., Ratz, G.P., Celis, A., Madsen, P., Gesser, B., Kwee, S., Madsen, P.S., Nielsen, H.V., Yde, H., Lauridsen, J.B. and Basse, B. (1988) Leukemia *2*, 561–601.
Challis, B.C. and Butler, A.R. (1975) in: The Chemistry of the Amino Group (Patai, S., ed.) Wiley, Interscience, NY, pp. 326–327.
Charlionet, R., Sesboüè, R. and Davrinche, C. (1984) Electrophoresis *5*, 176–178.
Charlionet, R., Davrinche, C. and Rivat, C. (1985) Electrophoresis *6*, 423–427.
Chiari, M., Casale, E., Santaniello, E. and Righetti, P.G. (1989a) Theor. Applied Electr. *1*, 99–102.
Chiari, M., Casale, E., Santaniello, E. and Righetti, P.G. (1989b) Theor. Applied Electr. *1*, 103–107.

Chrambach, A. (1980) Mol. Cell Biochem. *29*, 23–46.
Chrambach, A. and Hjelmeland, L.M. (1984) In: Electrophoresis '83 (Hirai, H., ed.), de Gruyter, Berlin, pp. 81–97.
Clark, P.M.S., Kricka, L.J. and Whitehead, T.P. (1980) Clin. Chem. *26*, 201–204.
Cleve, H., Patutschnick, W., Postel, W., Weser, J. and Görg, A. (1982) Electrophoresis *3*, 342–345.
Cleve, H. and Constans, J. (1988) Vox Sang. *54*, 215–225.
Cohn, J.E. (1936) Chem. Rev. *19*, 241–255.
Colbert, R.A., Amatruda, J.M. and D.S. Young (1984) Clin. Chem. *30*, 2053–2058.
Coligan, J.E., Gates, F.T., III, Kimball, E.S. and Maloy, W.L. (1983) Methods Enzymol. *91*, 413–434.
Constans, J. and Viau, M. (1975) C.R. Acad. Sci., Ser D, *281*, 1361–1364.
Constans, J. and Viau, M. (1977) Science *198*, 1070–1071.
Constans, J. and Cleve, H. (1988) Electrophoresis *9*, 599–602.
Constans, J., Cleve, H., Dykes, D., Fischer, M., Kirk, R.L., Papiha, S.S., Scheffrahn, W., Scherz, R., Thymann, M. and Weber, W. (1983) Hum. Genet. *65*, 176–180.
Cooper, T.G. (1977) in: The Tools of Biochemistry, Wiley & Sons, New York, pp. 113–135.
Cordell, J.L., Falini, B., Erber, W.N., Ghosh, A.K., Abdulaziz, Z., MacDonald, S., Pulford, K.A.E, Stein, H. and Mason, D.Y. (1984) J. Histochem. Cytochem. *32*, 219–227.
Cossu, G., Manca, M., Gavina-Pirastru, M., Bullitta, R., Bianchi-Bosisio, A., Gianazza, E. and Righetti, P.G. (1982) Am. J. Haematol. *13*, 149–157.
Cossu, G., Manca, M., Gavina-Pirastru, M., Bullitta, R., Bianchi-Bosisio, A. and Righetti, P.G. (1984) J. Chromatogr. *307*, 103–110.
Cossu, G., Manca, M., Strahler, J.R., Hanash, S.M. and Righetti, P.G. (1986a) J. Chromatogr. *361*, 223–229.
Cossu, G., Manca, M., Righetti, P.G., Gianazza, E., Baudin, V., Wajcman, H. and Bianchi-Bosisio, A. (1986b) Electrophoresis *7*, 213–216.
Cossu, G. and Righetti, P.G. (1987) J. Chromatogr. *398*, 211–216.
Cousineau, J. and Green, J. (1980) Biochim. Biophys. Acta *615*, 147–157.
Creighton, I.E. (1979) J. Mol. Biol. *129*, 235–264.
Daiger, S.P., Schanfield, M.S. and Cavalli-Sforza, L.L. (1975) Proc. Natl. Acad. Sci. USA *72*, 2076–2080.
D'Alessandro, A., D'Andrea, G. and Oratore, A. (1988) Electrophoresis *9*, 80–83.
Danusso, F., Ferruti, P., Peruzzo, G. and Natta, G. (1966) Chimica & Industria *48*, 466–470.
Danusso, F., Tieghi, G. and Ricco, T. (1979) Polymer *20*, 805–812.
Davies, H. (1970) Prot. Biol. Fluids *17*, 389–396.
Davis, J.M., Bartley, T., Parker, C.G., Lai, P., Righetti, P.G. and Goldstein, L. (1986) Prot. Biol. Fluids *34*, 859–862.
Davrinche, C. and Rivat, C. (1982) Blood Transf. Immunohaem. *25*, 199–213.
Davrinche, C., Charlionet, R. and Rivat, C. (1985) Electrophoresis *6*, 556–559.
Debye, P. and Hückel, E. (1924) Physik Z. *24*, 305–330.
de Jong, G. and Van Eijk, H.G. (1988) Electrophoresis *9*, 589–598.
DeLellis, R.A. (1981) In: Diagnostic Immunohistochemistry (DeLellis, R.A., ed.) Masson Publ., New York, pp. 7–17.
Delincée, H. and Radola, B.J. (1978) Anal. Biochem. *90*, 609–623.
Dermer, G.B., Silverman, L.M. and Chapman, J.F. (1982) Clin. Chem. *28*, 759–765.
Descartes, R. (1637) Le discours de la Méthode, Hachette, Paris.

de Vienne, D., Leonardi, A. and Damerval, C. (1988) Electrophoresis *9*, 742–750.
Discipio, R.G,. and Davie, E.W. (1979) Biochemistry *18*, 899–903.
Divall, G. B. (1981) Forensic Sci. Int. *18*, 67–68
Doi, Y. and Nishida, T. (1983) J. Biol. Chem. *258*, 5840–5846.
Dossi, G., Celentano, F., Gianazza, E. and Righetti, P.G. (1983) J. Biochem. Biophys. Methods *7*, 123–142.
Dresler, S., Runkel, D., Stenzel, P., Brimhall, B. and Jones, R.T. (1974) Ann. N.Y. Acad. Sci. *241*, 411–415.
Drozdz, R. and Naskalski, J.W. (1988) Anal. Biochem. *171*, 419–422.
Dunbar, B.D., Bundman, D.S. and Dunbar, B.S. (1985) Electrophoresis *6*, 39–43.
Dunbar, B.S. (1987) Two-Dimensional Electrophoresis and Immunological Techniques. Plenum Press, New York, pp. 148–156.
Dunn, M.J. and Burghes, A.H.M. (1983) Electrophoresis *4*, 173–189.
Dunn, M.J. and Burghes, A.H.M. (1986) in: Gel Electrophoresis of Proteins (Dunn, M.J., ed.) Wright, Bristol, pp. 203–261.
Dunn, M.J. (1987) J. Chromatogr. *418*, 145–185.
Dzandu, J.K., Deh, M.E., Barratt, D. and Wise, G.E. (1984) Proc. Natl. Acad. Sci. USA *81*, 1733–1737.
Dzandu, J.K., Johnson, J.F. and Wise, G.E. (1988) Anal. Biochem. *174*, 157–167.
Eap, C.B. and Baumann, P. (1988) Electrophoresis *9*, 650–654.
Edwards, J.J., Tollaksen, S.L. and Anderson, N.G. (1981) Clin. Chem. *27*, 1335–1340.
Edwards, J.J., Tollaksen, S.L. and Anderson, N.G. (1982a) Clin. Chem. *28*, 941–948.
Edwards, J.J., Anderson, N.G., Tollaksen, S.L., von Eschenbach, A.C. and Guevara, J. (1982b) Clin. Chem. *28*, 160–163.
Eiberg, H., Mohr, J., Staub-Nielsen, L. and Simonsen, N. (1983) Clin. Genet. *24*, 159–170.
Ek, K., Bjellqvist, B. and Righetti, P.G. (1983) J. Biochem. Biophys. Methods *8*, 134–155.
Fagerhol, M.K. and Braend, M. (1965) Science *149*, 986–987.
Fairbanks, V.F., Gilchrist, S.G., Brimhall, B., Jereb, J.A. and Goldsten, E.C. (1979) Blood *53*, 109–115.
Faupel, M., Barzaghi, B., Gelfi, C. and Righetti, P.G. (1987) J. Biochem. Biophys. Methods *15*, 147–162.
Fawcett, J.S. and Chrambach, A. (1986) Electrophoresis *7*, 266–272.
Fawcett, J.S., Sullivan, J.V., Chidakel, B.E. and Chrambach, A. (1988) Electrophoresis *9*, 216–221.
Fazekas de St. Groth, S., Webster, R.G. and Datyner, A. (1963) Biochim. Biophys. Acta *71*, 377–391.
Field, D.J. and Lee, J.C. (1955) Anal. Biochem. *144*, 584–592.
Fishman, W.H. (1974) Am. J. Med. *56*, 617–650.
Flory, P.J. (1953) Principles of Polymer Chemistry, Cornell University Press, Ithaca.
Fosslien, E., Prasad, R. and Stastny, J. (1984) Electrophoresis *5*, 102–109.
Fraker, P.J. and Speck, J.C. (1978) Biochem. Biophys. Res. Commun. *80*, 849–854.
Franceschini, G., Sirtori, C.R., Capurso, A., Weisgraber, K.H. and Mahley, R.W. (1980) J. Clin. Invest. *66*, 892–900.
Fredriksson, S. (1977) In: Electrofocusing and Isotachophoresis, Radola, B.J. and Graesslin, D., eds. (de Gruyter, Berlin) pp. 71–83.
Friedli, W. and Schumacher, E. (1961) Helv. Chim. Acta *44*, 1829–1856.
Fuchsmann, W.A. and Appleby, C.A. (1979) Biochim. Biophys. Acta *579*, 314–324.
Gabriel, D.W. and Ellingboe, A.H. (1982) Physiol. Plant Pathol. *20*, 349–357.

Gahmberg, C.G. (1976) J. Biol. Chem. *251*, 510–514.
Gahmberg, C.G. and Andersson, L.C. (1977) J. Biol. Chem. *252*, 5888–5893.
Galante, E., Caravaggio, T. and Righetti, P.G. (1975) In: Progress in Isoelectric Focusing and Isotachophoresis (Righetti, P.G., ed.), Elsevier, Amsterdam, pp. 3–12.
Galteau, M.M. and Siest, G. (Eds.) (1986) Recent Progresses in Two-Dimensional Electrophoresis, Presses Universitaires de Nancy.
Garcia-Olmedo, F., Salcedo, G., Aragoncillo, C., Sanchez-Monge, R., Collada, C. and Gomez, L. (1988) Electrophoresis *9*, 719–726.
Garrels, I.J. (1979) J. Biol. Chem. *254*, 7961–7977.
Garrels, I.J. (1983) Methods Enzymol. *100*, 411–423.
Garrels, I.J., Farrar, J.T. and Burwell IV, C.D. (1984) in: Two Dimensional Gel Electrophoresis of Proteins (Celis, J.E. and Bravo, R., eds.) Academic Press, Orlando, pp. 37–91.
Garrels, I.J. and Franza Jr., B.R. (1986) in: Recent Progresses in Two-Dimensional Electrophoresis (Galteau, M. and Siest, G., eds.), Presses Universitaires de Nancy, pp. 85–90.
Gasparic, V., Bjellqvist, B. and Rosengren, A. (1975) Swedish Patent No. 7514049–1.
Gåveby, B.M., Pettersson, P., Andrasko, J., Ineva-Flygare, L., Johannesson, U., Görg, A., Postel, W., Domscheit, A., Mauri, P.L., Pietta, P., Gianazza, E. and Righetti, P.G. (1988) J. Biochem. Biophys. Methods *16*, 141–164.
Gelfi, C. and Righetti, P.G. (1981a) Electrophoresis *2*, 213–219.
Gelfi, C. and Righetti, P.G. (1981b) Electrophoresis *2*, 220–228.
Gelfi, C. and Righetti, P.G. (1983) J. Biochem. Biophys. Methods *8*, 156–171.
Gelfi, C. and Righetti, P.G. (1984) Electrophoresis *5*, 257–262.
Gelfi, C., Righetti, P.G. and Mannucci, P.M. (1985) Electrophoresis *6*, 162–170.
Gelfi, C., Morelli, A., Rovida, E. and Righetti, P.G. (1986) J. Biochem. Biophys. Methods *13*, 113–124.
Gelfi, C., Bossi, M.L. and Righetti, P.G. (1987a) J. Chromatogr. *390*, 225–236.
Gelfi, C., Bossi, M.L., Bjellqvist, B. and Righetti, P.G. (1987b) J. Biochem. Biophys. Methods *15*, 41–48.
Gelfi, C., Righetti, P.G., Rovida, E. and Samaja, M. (1987c) J. Biochem. Biophys. Methods *14*, 139–147.
Gelfi, C., Righetti, P.G., Cattò, N., Bontempi, L. and Gianazza, E. (1988) J. Biochem. Biophys. Methods *16*, 193–204.
Gershoni, J.M. and Palade, G. (1983) Anal. Biochem. *131*, 1–28.
Gershoni, J.M. (1986) in: Electrophoresis '86, Dunn, J.M. (Ed.), VCH, Weinheim, pp. 305–313.
Geserick, G., Patzelt, D., Schrodez, H. and Nagai, T. (1983) Vox Sang. *44*, 178–182.
Gianazza, E., Astorri, C. and Righetti, P.G. (1979) J. Chromatogr. *171*, 161–169.
Gianazza, E. and Righetti, P.G. (1980) J. Chromatogr. *193*, 1–8.
Gianazza, E. and Arnaud, P. (1982) Biochem. J. *201*, 129–136; Ibid. *203*, 637–641.
Gianazza, E., Dossi, G., Celentano, F. and Righetti, P.G. (1983a) J. Biochem. Biophys. Methods *8*, 109–133.
Gianazza, E., Chillemi, F., Duranti, M. and Righetti, P.G. (1983b) J. Biochem. Biophys. Methods *8*, 339–351.
Gianazza, E., Artoni, F. and Righetti, P.G. (1983c) Electrophoresis *4*, 321–326.
Gianazza, E., Celentano, F., Dossi, G., Bjellqvist, B. and Righetti, P.G. (1984a) Electrophoresis *5*, 88–97.
Gianazza, E., Frigerio, A., Astrua-Testori, S. and Righetti, P.G. (1984b) Electrophoresis *5*, 310–312.

Gianazza, E., Frigerio, A., Tagliabue, A. and Righetti, P.G. (1984c) Electrophoresis *5*, 209–216.
Gianazza, E., Giacon, P., Sahlin, B. and Righetti, P.G. (1985a) Electrophoresis *6*, 53–56.
Gianazza, E., Astrua-Testori, S. and Righetti, P.G. (1985b) Electrophoresis *6*, 113–117.
Gianazza, E., Giacon, P., Astrua-Testori, S. and Righetti, P.G. (1985c) Electrophoresis *6*, 326–331.
Gianazza, E., Astrua-Testori, S., Giacon, P. and Righetti, P.G. (1985d) Electrophoresis *6*, 332–339.
Gianazza, E., Astrua-Testori, S., Caccia, P., Giacon, P., Quaglia, L. and Righetti, P.G. (1986a) Electrophoresis *7*, 76–83.
Gianazza, E., Quaglia, L., Caccia, P. and Righetti, P.G. (1986b) J. Biochem. Biophys. Methods *12*, 227–237.
Gianazza, E., Astrua-Testori, S., Righetti, P.G. and Bianchi-Bosisio, A. (1986c) Electrophoresis *7*, 435–438.
Gianazza, E., Caccia, P., Quaglia, L., Righetti, P.G., Rimpilainen, M. and Righetti, P.G. (1986d) Electrophoresis *7*, 537–543.
Gianazza, E., Rabilloud, T., Quaglia, L., Caccia, P., Astrua-Testori, S., Osio, L., Grazioli, G. and Righetti, P.G. (1987a) Anal. Biochem. *165*, 247–257.
Gianazza, E., Cattò, N., Righetti, P.G. and Bianchi-Bosisio, A. (1987b) Electrophoresis *8*, 538–540.
Gianazza, E., Osio, L., Grazioli, G., Astrua-Testori, S., Righetti, P.G., Accinni, R., Renoldi, I. and Repossini, A. (1987c) Clin. Chem. *32*, 2011–2018.
Gianazza, E., Tedesco, G., Cattò, N., Bontempi, L. and Righetti, P.G. (1988) Electrophoresis *9*, 172–182.
Giddings, J.C. (1967) Anal. Chem. *39*, 1927–1932.
Giddings, J.C. (1984) Anal. Chem *56*, 1258–1262.
Giometti, C.S., Anderson, N.G., Tollaksen, S.L., Edwards, J.J. and Anderson, N.L. (1980) Anal. Biochem. *102*, 47–58.
Glomset, A. (1968) J. Lipid Res. *9*, 155–167.
Goday, A., Torrent, M., Ludevid, M.D. and Puigdomenech, P. (1988) Electrophoresis *9*, 738–741.
Gomo, Z.A.R., Clark, P.M.S., Kricka, L.J., Woods, K., Buckley, B. and Whitehead, P.T. (1983) Electrophoresis *4*, 298–301.
Gordon, J.A. and Jencks, W.P. (1963) Biochemistry *2*, 47–57.
Görg, A., Postel, W., Westermeier, R. (1978) Anal. Biochem. *89*, 60–70.
Görg, A., Postel, W., Westermeier, R., Gianazza, E. and Righetti, P.G. (1980) J. Biochem. Biophys. Methods *3*, 273–284.
Görg, A., Postel, W. and Westermeier, R. (1981) in: Electrophoresis '81 (Allen, R.C. and Arnaud, P., eds.) de Gruyter, Berlin, pp. 259–270.
Görg, A., Postel, W., Weser, J., Weidinger, S., Patutschnick, W. and Cleve, H. (1983a) Electrophoresis *4*, 153–157.
Görg, A., Weser, J., Westermeier, R., Postel, W., Weidinger, S., Patutschnick, W. and Cleve, H. (1983b) Hum. Genet. *64*, 222–226.
Görg, A., Postel, W., Weser, J., Patutschnick, W. and Cleve, H. (1985a) Am. J. Hum. Genet. *37*, 922–930.
Görg, A., Postel, W., Günther, S. and Weser, J. (1985b) Electrophoresis *6*, 599–604.
Görg, A., Postel, W. and Johann, P. (1985c) J. Biochem. Biophys. Meth. *10*, 341–350.

Görg, A., Postel, W., Weser, J., Günther, S., Strahler, J.R., Hanash, S.M. and Somerlot, L. (1987a) Electrophoresis *8*, 45–51.
Görg, A., Postel, W., Weser, J., Günther, S., Strahler, J.R., Hanash, S.M. and Somerlot, L. (1987b) Electrophoresis *8*, 122–124.
Görg, A., Postel, W., Günther, S., Weser, J., Strahler, J.R., Hanash, S.M. Somerlot, L., and Kuick, R. (1988a) Electrophoresis *9*, 37–46.
Görg, A., Postel, W. and Günther, S.(1988b) in: Electrophoresis '88 (Schafer-Nielsen, C., ed.) VCH, Weinheim, pp. 57–72.
Görg, A., Postel, W., Domscheit, A. and Günther, S. (1988) Electrophoresis *9*, 681–692.
Greene, F.C. and Feeney, R. (1968) Biochemistry *7*, 1366–1370.
Greenwood, F.C., Hunter, W.M. and Glover, J.S. (1963) Biochem. J. *89*, 114–119.
Griffin, J.H., Evatt, B., Zimmermann, T.S., Kleiss, A.J. and Wideman, C. (1981) J. Clin. Invest. *68*, 1370–1373.
Griffith, I.P. (1972) Anal. Biochem. *46*, 402–412.
Grönwall, A. (1942) Com. Rend. Lab. Carlsberg, Ser. Chem. *24*, 185–195.
Groves, W.E., Davis, F.C., Jr. and Sells, B.H. (1968) Anal. Biochem. *22*, 195–210.
Guedson, J.L., Ternynck, T. and Avrameas, S. (1979) J. Histochem. Cytochem. *27*, 1131–1138.
Guest, J., Patel, K. and Dunn, M.J. (1986) in: Electrophoresis '86 (Dunn, M.J., ed.), VCH, Weinheim, pp. 658–661.
Guevara, J., Jr., Chiocca, E.A., Clayton, L.F., von Eschenback, A.L. and Edwards, J.J. (1982) Clin. Chem. *28*, 756–758.
Guevara, J.G., Herbert, B.H. and Martin, B.A. (1985) Electrophoresis *6*, 613–619.
Gültekin, H. and Heermann, K.H. (1988) Anal. Biochem. *172*, 320–329.
Guy, C.L. and Haskell, D. (1988) Electrophoresis *9*, 787–796.
Haase, R., Menke-Mollers, I. and Oette, K. (1988) Electrophoresis *9*, 569–575.
Hanash, S.M., Strahler, J.R., Somerlot, L., Postel, W. and Görg, A. (1987) Electrophoresis *8*, 229–234.
Hancock, K. and Tsang, V. (1983) Anal. Biochem. *133*, 157–162.
Hannig (1967) in: Electrophoresis, vol. II (Bier, M., ed.) Academic Press, New York, pp. 423–471.
Hansen, J.N. (1976) Anal. Biochem. *76*, 37–48.
Hari, V. (1981) Anal. Biochem. *113*, 332–335.
Harrington, M. and Merril, C.R. (1984) Clin. Chem. *30*, 1933–1937.
Harrington, M., Merril, C.R., Goldman, D., Xu, X.H. and McFarlin, D. (1984) Electrophoresis *5*, 236–245.
Hartman, B.K. and Udenfriend, S. (1969) Anal. Biochem. *30*, 391–394.
Havel, R.J., Kotite, L. and Kane, J.P. (1979) Biochem. Med. *21*, 121–138.
Hayes, C.E. and Goldstein, I.J. (1975) Anal. Biochem. *67*, 580–588.
Helenius, A. and Simons, K. (1975) Biochim. Biophys. Acta *415*, 29–75.
Helenius, A., McCaslin, D.R., Fries, A. and Tanford, C. (1979) Methods Enzymol. *56*, 734–754.
Hickman, B.J., Anderson, N.L., Willard, K.E. and Anderson, N.G. (1980) in Electrophoresis '79 (Radola, B.J., ed.) de Gruyter, Berlin, pp. 341–360.
Hirschfeld, J. (1959) Acta Pathol. Microbiol. Scand. *47*, 160–168.
Hjertèn, H. (1976) in: Methods of Protein Separation (Catsimpoolas, N., ed.) Plenum Press, New York, vol. II, pp. 58–70.
Hjertèn, H., Liu, Q.Z. and Zhao, S.L. (1983) J. Biochem. Biophys. Methods *7*, 101–113.

Hochstrasser, D., Augsburger, V., Funk, M., Appel, R., Pellegrini, C. and Muller, A.F. (1986a) In: Electrophoresis '86 (Dunn, M.J., ed.) VCH, Weinheim, pp. 566–568

Hochstrasser, D., Augsburger, V., Funk, M., Appel, R., Pellegrini, C. and Muller, A.F. (1986b) Electrophoresis *7*, 505–511.

Hochstrasser, D., Harrington, M.G, Hochstrasser, A.C. and Merril, C.R. (1988) in: Electrophoresis '88 (Schafer-Nielsen, C., ed.) VCH, Weinheim, pp. 245–248.

Holland, C.A., Mayrand, S. and Pederson, T. (1980) J. Mol. Biol. *138*, 775–778.

Holmberg, E.A., Campeau, J.D., Devereaux, D.L., Ono, T. and diZerega, G.S. (1986) Prep. Biochem. *16*, 275–295.

Holmquist, L. (1988) Electrophoresis *9*, 511–513.

Holmquist, L. and Bjellqvist, B. (1988) Electrophoresis *9*, 580–582.

Holt, L.M., Astin, R. and Payne, P.I. (1981) Theoret. Appl. Genet. *60*, 237–243.

Hopkinson, D.A., Spencer, W. and Harris, H. (1963) Nature *27*, 969–971

Horowitz, P.M. and Bowman, S. (1987) Anal. Biochem. *165*, 430–434.

Hsu, S.M. and Raine, L. (1982) J. Histochem. Cytochem. *30*, 157–165.

Hubbard, A.L. and Cohn, Z.A. (1976) in: Biochemical Analysis of Membranes (Maddy, A.H., ed.) Chapman & Hall, London, pp. 427–501.

Hughes, A.E., Graham, C.A., McLean, W.H.I., Burn, J. and Nevin, N.C. (1986) in: Electrophoresis '86 (Dunn, M.J., ed.), VCH, Weinheim, pp. 723–726.

Hunt, J.A. and Ingram, V.M. (1961) Biochim. Biophys. Acta *49*, 520–530.

Hurkman, W.J. and Tanaka, C.K. (1988) Electrophoresis *9*, 781–786.

Hurley, P.M., Catsimpoolas, N. and Wogan, G.N. (1978) in: Electrophoresis '78 (Catsimpoolas, N., ed.) Elsevier, Amsterdam, pp. 283–296.

Inouye, M. (1971) J. Biol. Chem. *246*, 4834–4838.

Jabs, H.U., Assmann, G., Greifendorf, D. and Benninghofen, A. (1986) J. Lipid Res. *27*, 613–621.

Jackson, P., Urwin, V.E. and Mackay, C.D. (1988) Electrophoresis *9*, 330–339.

Jackson, E.A., Holt, L.M. and Payne, P.I. (1983) Theor. Appl. Genet. *66*, 29–37.

Jacobs, S. (1971) Prot. Biol. Fluids *19*, 499–502.

Jacobs, S. (1973) Analyst *98*, 25–33.

Jahn, C.E., Osborne, J.C., Schaefer, E.J. and Brewer, H.B., Jr. (1981) FEBS Lett. *131*, 366–368.

Jellum, E. and Thorsrud, A.K. (1982) Clin. Chem. *28*, 876–883.

Johansson, S. and Skoog, B. (1987) J. Biochem. Biophys. Methods 14 (Suppl.), 33–33.

Johnstone, A. and Crumpton, M.J. (1979) FEBS Lett. *108*, 119–124.

Johnstone, A. and Thorpe, R. (1982) Immunochemistry in Practice, Blackwell Sci. Publ., Oxford.

Jokl, V., Dolesovà, J. and Matusovà, M. (1979) J. Chromatogr. *172*, 239–248.

Jones, M.I., Massingham, W.E. and Spragg, S.P. (1980) Anal. Biochem. *106*, 446–449.

Jorgensson, J.W. (1987) In: New Directions in Electrophoretic Methods, Jorgenson, J.W. and Phillips, M. eds. (Am. Chem. Soc. Symp. Ser., Washington) *335*, pp. 182–198.

Kamboh, M.I. and Ferrell, R.E. (1987) Hum. Hered. *37*, 65–81.

Kauman, W.G. (1957) Clas. Sci. Acad. Roy. Belg. *43*, 854–868.

Kenny, A.J. and Maroux, S. (1982) Physiol. Rev. *62*, 91–128.

Kera, Y., Nishimukai, H. and Yamasawa, K. (1981) Hum. Genet. *59*, 360–364.

Kilias, H., Gelfi, C. and Righetti, P.G. (1988) Electrophoresis *9*, 187–191.

Kinzkofer-Peresch, A., Patestos, N.P., Fauth, M., Kögel, F., Zok, R. and Radola, B.J. (1988) Electrophoresis *9*, 497–501.
Kiowsky, T.E. and Pincock, R.E. (1966) J. Am. Chem. Soc. *88*, 4704–4710.
Kirkpatrick, C., Lecocq, R., Lamy, F., Defleur, V., Dedobeleer, G., Baran, D., Rodesch, F. and Dumont, J.E. (1985) Pediat. Res. *19*, 1341–1345.
Kirley, T. (1987) in: Methods in Protein Sequence Analysis (Walsh, K., ed.) Humana Press, Clifton, pp. 303–310.
Kisiel, W. (1979) J. Clin. Invest. *64*, 761–769.
Klose, J. (1975) Humangenetik *26*, 231–235.
Klose, J., Zeindl, E. and Sperling, K. (1982) Clin. Chem. *28*, 987–992.
Klose, J. and Zeindl, E. (1982) Clin. Chem. *30*, 2014–2020.
Knierim, M., Buchholz, J. and Pflug, W. (1988) Anal. Biochem. *172*, 139–144.
Knisley, K.A. and Rodkey, L.S. (1988) Electrophoresis *9*, 183–186.
Koffigan, M., Kora, I., Clavey, V., Bard, J.M., Chapman, J. and Fruchart, J.C. (1987) Clin. Chim. Acta *163*, 245–256.
Kolin, A. (1954) J. Chem. Phys. *22*, 1628–1629.
Kolin, A. (1955a) J. Chem. Phys. *23*, 407–410.
Kolin, A. (1955b) Proc. Natl. Acad. Sci. USA *41*, 101–110.
Kolin, A. (1958) in: Methods of Biochemical Analysis (Glick, D., ed.) Wiley, Interscience, New York, pp. 259–288.
Kolin, A. (1977) In: Electrofocusing and Isotachophoresis, (Radola, B.J. and Graesslin, D., eds.), de Gruyter, Berlin, pp. 3–33.
Kostner, G.M. (1983) Adv. Lipid Res. *20*, 1–43.
Krishnamoorthy, R., Bianchi-Bosisio, A., Labie, D. and Righetti, P.G. (1978) FEBS Lett. *94*, 319–323.
Krochko, J.E. and Bewley, J.D. (1988) Electrophoresis *9*, 751–763.
Kronberg, H., Zimmer, H.G. and Neuhoff, V. (1984) Clin. Chem. *30*, 2059–2062.
Kuhn, O. and Wilt, F.M. (1980) Anal. Biochem. *105*, 274–280.
Kühnl, P., Schmidtmann, U. and Spielman, W. (1977) Hum. Genet. *35*, 219–223.
Kühnl, P. and Spielmann, W. (1978a) Hum. Genet. *43*, 57–67.
Kühnl, P. and Spielmann, W. (1978b) Hum. Genet. *43*, 91–95.
Kühnl, P. and Spielmann, W. (1979) Hum. Genet. *50*, 193–198.
Kurian, P., Gersten, D.M., Suhocki, P.V. and Ledley, G. (1981) Electrophoresis *2*, 184–186.
Låås, T. and Olsson, I. (1981) Anal. Biochem. *114*, 167–172.
Laemmli, U.K. (1970) Nature *277*, 680–682.
Laskey, R.A. and Mills, A.D. (1975) Eur. J. Biochem. *56*, 335–341.
Laskey, R.A. and Mills, A.D. (1977) FEBS Lett. *82*, 314–316.
Laurell, C.B. and Eriksson, S. (1963) Scand. J. Clin. Lab. Invest. *15*, 132–140.
Leader, D.P. (1980) J. Biochem. Biophys. Methods *3*, 247–248.
Leavitt, J., Goldman, D., Merril, C. and Kakunaga, T. (1982) Clin. Chem. *28*, 850–860.
Lee, C., Levin, A. and Branton, D. (1987) Anal. Biochem. *166*, 308–312.
Leifheit, H.J. and Cleve, H. (1988) Electrophoresis *9*, 426–429.
LeGendre, N. and Matsudaira, P. (1988) Bio Techniques *6*, 154–159.
Lemkin, P.F. and Lipkin, L.E. (1981a) Comput. Biomed. Res. *14*, 272–297.
Lemkin, P.F. and Lipkin, L.E. (1981b) Comput. Biomed. Res. *14*, 355–380.
Lemkin, P.F. and Lipkin, L.E. (1981c) Comput. Biomed. Res. *14*, 407–446.
Lemkin, P.F. and Lipkin, L.E. (1981d) in: Electrophoresis '81 (Allen, R.C. and Arnaud, P., eds.) de Gruyter, Berlin, pp. 401–411.

Lemkin, P.F. and Lipkin, L.E. (1983) Electrophoresis *4*, 71–82.
Lizana, J. and Johansson, K.E. (1986) Prot. Biol. Fluids *34*, 741–744.
Lowry, O.H., Rosebrough, N.J., Farr, A.L. and Randall, R.J. (1951) J. Biol. Chem. *193*, 265–275.
MacGillivray, A.J. and Rickwood, D. (1974) Eur. J. Biochem. *41*, 181–191.
MacGillivray, R.T.A., Mendez, E. Shewale, J.G., Sinha, S.K., Linebak-Zins, J. and Brew, K. (1983) J. Biol. Chem. *258*, 3543–3553.
Manca, M., Cossu, G., Angioni, G., Gigliotti, B., Bianchi-Bosisio, A., Gianazza, E. and Righetti, P.G. (1986) Am. J. Haematol. *22*, 285–293.
Mannucci, M. and Vigano', S. (1982) Lancet *2*, 463–467.
Marlow, G.C., Wurst, D.E. and Loschke, D.C. (1988) Electrophoresis *9*, 693–703.
Marshall, T. and Latner, A.L. (1981) Electrophoresis *2*, 228–235.
Marshall, T. and Vesterberg, O. (1983) Electrophoresis *4*, 363–368.
Marshall, T., Williams, K.M. and Vesterberg, O. (1984a) Clin. Chem. *30*, 2008–2011.
Marshall, T., Vesterberg, O. and Williams, K.M. (1984b) Electrophoresis *5*, 122–126.
Marshall, T., Williams, K.M. and Vesterberg, O. (1985a) Electrophoresis *6*, 47–52.
Marshall, T., Williams, K.M. and Vesterberg, O. (1985b) Electrophoresis *6*, 392–396.
Marshall, T. and Williams, K.M. (1986) in: Electrophoresis '86 (Dunn. M.J., ed.) VCH, Weinheim, pp. 523–537.
Martin, A.W., Huebers, E., Finch, C.A., Martin, A.W. and Webb, J. (1984) Prot. Biol. Fluids *32*, 59–61.
Maruyama, K., Mikawa, T. and Ebashi, S. (1984) J. Biochem. *94*, 511–518.
Marz, L., Hatton, M.W.C., Berry, L.R. and Regoeczi, E. (1982) Can. J. Biochem. *60*, 624–630.
Mason, D.Y. and Sammons, R. (1978) J. Clin. Pathol. *31*, 454–460.
Mason, D.Y. (1985) in: Techniques in Immunochemistry (Bullock, G.R. and Petrusz, P. eds.) Academic Press, London, vol. *3*, pp. 25–50.
Matheron, G. (1975) Random sets and Integral Geometry, Wiley, New York.
Matsudaira, P. (1987) J. Biol. Chem. *262*, 10035–10038.
Mattock, P., Aitchison, G.F. and Thompson, A.R. (1980) Separ. Purif. Methods *9*, 1–40.
Mauff, G., Hauptmann, G., Hitzeroth, W., Gauchel, C.F. and Scherz, R. (1978) Z. Immunforsch. Exp. Ther. *154*, 115–120.
Menzel, H.J., Kladetszky, R.G. and Assmann, G. (1982) J. Lipid Res. *23*, 915–922.
Menzel, H.J., Assmann, G., Rall, S., Jr., Weisbraber, K.H. and Mahley, R.W. (1984) J. Biol. Chem. *259*, 3070–3076.
Menzel, H.J. and Utermann, G. (1986) Electrophoresis *7*, 492–495.
Merril, C.R., Switzer, R.C. and Van Keuren, M.L. (1979) Proc. Natl. Acad. Sci. USA *76*, 4335–4339.
Merril, C.R., Goldman, D., Sidman, S.A. and Ebert, M.H. (1981a) Science *211*, 1437–1438.
Merril, C.R., Goldman, D. and Ebert, M.H. (1981b) Proc. Natl. Acad. Sci. USA *78*, 6471–6475.
Merril, C.R., Goldman, D. and Van Keuren, M.L. (1982) Electrophoresis *3*, 17–23.
Merril, C.R., Harrington, M. and Alley, V. (1984) Electrophoresis *5*, 289–297.
Merril, C.R. and Goldman, D. (1984) in: Two-dimensional Gel Electrophoresis of Proteins, Celis, J.E. and Bravo, R. (Eds.), Academic Press, New York, pp. 93–109.
Merril, C.R., Harasewych, M.G. and Harrington, M.G. (1986) in: Gel Electrophoresis of Proteins, Dunn, M.J. (Ed.), Wright, Bristol, pp. 323–362.

Meyer, Y., Grosset, J., Chartier, Y. and Cleyet-Marel, J.C. (1988) Electrophoresis *9*, 704–711.
Meyer-Sabellek, W., Sinha, P.K. and Köttgen, E. (1988) J. Chromatogr. *429*, 419–444.
Michl, H. (1952) Monatsh. Chem. *83*, 210–220.
Miller, M.J., Vo, P.K., Nielsen, C., Geiduschek, E.P. and Xuong, N.H. (1982) Clin. Chem. *28*, 867–875.
Miller, M.J., Olson, A.D. and Thorgeirsson, S.S. (1984) Electrophoresis *5*, 287–303.
Moeremans, M., Daneels, G. and De Mey, J. (1985) Anal. Biochem. *145*, 315–321.
Moeremans, M., De Raeymaeker, M., Daneels, G. and De Mey, J. (1986) Anal. Biochem. *153*, 18–22.
Mosher, R.A., Bier, M. and Righetti, P.G. (1986) Electrophoresis *7*, 59–66.
Murnane, J.P. and Painter, R.B. (1983) Biochemistry *22*, 1217–1222.
Nakamura, S., Ohue, O. and Abe, K. (1986) Hum. Genet. *73*, 183–185.
Namikawa, T., Nagai, A., Takenaka, O. and Takenaka, A. (1987) Anim. Genet. *18*, 133–141.
Navarrete, R. and Serrano, R. (1983) Biochim. Biophys. Acta *728*, 403–408.
Neel, J.V., Rosenblum, B.B., Sing, C.F., Skolnick, M.M., Hanash, S.M. and Sternberg, S. (1984) in: Two-Dimensional Gel Electrophoresis of Proteins (Celis, J.E. and Bravo, R., eds.) Academic Press, Orlando, pp. 259–306.
Neuhoff, V., Stamm, R. and Eibl, H. (1985) Electrophoresis *6*, 427–448.
Neuhoff, V., Arold, N., Taube, D. and Ehrhardt, W. (1988) Electrophoresis *9*, 255–262.
Nute, P.E., Stamatoyannopoulos, G., Hermodson, M.A. and Roth, D. (1974) J. Clin. Invest. *53*, 320–328.
Oakley, B.R., Kirsch, D.R. and Morris, R.N. (1980) Anal. Biochem. *105*, 361–363.
Ochs, D. (1983) Anal. Biochem. *135*, 470–474.
O'Farrell, P. (1975) J. Biol. Chem. *250*, 4007–4021.
O'Farrell, P.Z., Goodman, H.M. and O'Farrell, P.H. (1977) Cell *12*, 1133–1140.
Ohsawa, K. and Ebata, N. (1983) Anal. Biochem. 135, 409-415.
Okuyama, T. and Manabe, T. (1986) in: Recent Progresses in Two-Dimensional Electrophoresis, Presses Universitaires de Nancy (Galteau, M.M. and Siest, G. (Eds.), pp. 131–140.
Ornstein, L. (1964) Ann. N.Y. Acad. Sci. *121*, 321–349.
Ott, G.S. and Shore, V.G. (1983) in: Lewis, L.A. (ed.) Handbook of Electrophoresis, CRC Press, Boca Raton, Florida, pp. 105–132.
Pace, J.L., Kemper, D.L. and Ragland, W.L. (1974) Biochem. Biophys. Res. Commun. *57*, 482–488.
Papayannopoulou, Th., Kurachi, S., Brice, M., Nakamoto, B. and Stamatoyannopoulos, G. (1981) Blood *57*, 531–536.
Park, I., Schaeffer, E., Sidoli, A., Baralle, F.E., Cohen, G.N. and Zakin, M.M. (1985) Proc. Natl. Acad. Sci. USA *82*, 3149–3153.
Pascali, L.V., Dobosz, M., Destro-Bisol, G. and D'Aloja, E. (1988) Electrophoresis *9*, 411–417.
Pernelle, J.J., Chafey, P., Lognonne, J.L., Righetti, P.G., Bianchi-Bosisio, A. and Wahrmann, J.P. (1986) Electrophoresis *7*, 159–165.
Pernelle, J.J., Righetti, P.G. and Wahrmann, J.P. (1988) J. Biochem. Biophys. Methods *16*, 227–236.
Perrella, M., Cremonesi, L., Benazzi, L. and Rossi-Bernardi, L. (1981) J. Biol. Chem. *256*, 11098–11103.

Peters, K.E. and Comings, D.E. (1980) J. Cell. Biol. *86*, 135–155.
Peterson, E.A. and Sober, H.A. (1959) Anal. Chem. *31*, 857–862.
Peterson, G.L. (1977) Anal. Biochem. *83*, 346–356.
Peterson, G.L. (1979) Anal. Biochem. *100*, 201–220.
Peterson, G.L. (1983) Methods Enzymol. *91*, 95–119.
Petrilli, P, Sannia, G. and Marino, G. (1977) J. Chromatogr. *135*, 511–513.
Pflug, W. (1986) Electrophoresis *7*, 273–278.
Pflug, W. and Laczko, B. (1987) Electrophoresis *8*, 247–248.
Pflug, W. (1988a) Electrophoresis *9*, 443–448.
Pflug, W. (1988b) Electrophoresis *9*, 438–443.
Pflug, W., Eberspächer, B. and Bäβler, G. (1988) Electrophoresis *9*, 239–240.
Philpot, J. St. L. (1940) Trans. Faraday Soc. *39*, 38–50.
Philpot, J. St. L. (1973) in: Developments in Biochemistry, vol. 2 (Reid, E., ed.) Longmans, London, pp. 180–200.
Pietta, P.G., Pocaterra, E., Fiorino, A., Gianazza, E. and Righetti, P.G. (1985) Electrophoresis *6*, 162–170.
Pitas, R.E., Innerarity, T.L., Arnold, K.S. and Mahley, R.W. (1979) Proc. Natl. Acad. Sci. USA *76*, 2311–2315.
Pluskal, M.F., Przekop, M.B., Kavonian, M.R., Vecoli, C. and Hicks, D.A. (1986) Bio Techniques *4*, 272–282.
Porter, R.R. (1983) Mol. Biol. Med. *1*, 161–168.
Pötsch-Schneider, L. and Klein, H. (1988) Electrophoresis *9*, 602–605.
Potter, D.J. (1986) Comp. Biomed. Res. *19*, 565–575.
Poyart, C.F., Guesnon, P. and Bohn, B.M. (1981) Biochem. J. *195*, 493–501.
Puppo, A. and Rigaud, J. (1987) Electrophoresis *8*, 212–214.
Rabilloud, T., Hubert, M. and Tarroux, P. (1986) J. Chromatogr. *351*, 77–89.
Rabilloud, T., Pernelle, J.J., Wahrmann, J.P. Gelfi, C. and Righetti, P.G. (987a) J. Chromatogr. *402*, 105–113.
Rabilloud, T., Gelfi, C., Bossi, M.L. and Righetti, P.G. (1987b) Electrophoresis *8*, 305–312.
Rabilloud, T., Barzaghi, B. and Righetti, P.G. (1988a) J. Biochem. Biophys. Methods *16*, 237–241.
Rabilloud, T., Gianazza, E., Tarroux, P. and Righetti, P.G. (1988b) in: Electrophoresis '88 (Schafer-Nielsen, C., ed.) VCH, Weinheim, pp. 89–94.
Radola, B.J. (1975) in: Isoelectric Focusing (Arbuthnott, J.P. and Beeley, J.A., eds.) Butterworths, London, pp. 182–197.
Rall, S.C., Jr., Weisgraber, K.H. and Mahley, R.W. (1982) J. Biol. Chem. *257*, 4171–4178.
Ramagli, L.S. and Rodriguez, L.V. (1985) Electrophoresis *6*, 559–563.
Randall, T., Harland, W.A. and Thorpe, J. W. (1980) Med. Sci. Law *20*, 43–47.
Raymonds, S. (1964) Ann. N.Y. Acad. Sci. *121*, 350–370.
Read, S.M. and Northcote, D.H. (1981) Anal. Biochem. *116*, 53–64.
Richardson, B.J., Baverstock, P.R. and Adams, M. (1986) Allozyme Electrophoresis, Academic Press Australia, North Ryde.
Ridder, G., Von Bargen, E., Burgard, D., Pickrum, H. and Williams, E. (1984) Clin. Chem. *30*, 1919–1924.
Righetti, P.G. and Drysdale, J.W. (1973) Ann. N.Y. Acad. Sci. *209*, 163–186.
Righetti, P.G. (ed.) (1975) Progress in Isoelectric Focusing and Isotachophoresis, Elsevier, Amsterdam.
Righetti, P.G., Pagani, M. and Gianazza, E. (1975) J. Chromatogr. *109*, 341–356.
Righetti, P.G. and Drysdale, J.W. (1976) Isoelectric Focusing, Elsevier, Amsterdam.

Righetti, P.G., Balzarini, L., Gianazza, E. and Brenna, O. (1977) J. Chromatogr. *134*, 279–284.
Righetti, P.G. and Chillemi, F. (1978) J. Chromatogr. *157*, 243–251.
Righetti, P.G., Gianazza, E., Gianni, A.M., Comi, P., Giglioni, B., Ottolenghi, S., Secchi, C. and Rossi-Bernardi (1979) J. Biochem. Biophys. Methods *1*, 45–57.
Righetti, P.G. (1980) J. Chromatogr. *190*, 275–282.
Righetti, P.G., Gianazza, E. and Bianchi-Bosisio, A. (1980) in: Recent Developments in Chromatography and Electrophoresis (Frigerio, A. and McCamish, M., eds.), Elsevier, Amsterdam, vol. *10*, pp. 89–117.
Righetti, P.G. (1981) In: Electrophoresis '81 (Allen, R.C. and Arnaud, P., eds.), de Gruyter, Berlin, pp. 3–16.
Righetti, P.G. and Gianazza, E. (1981) In: Electrophoresis '81 (Allen, R.C. and Arnaud, P., eds.), de Gruyter, Berlin, pp. 655–665.
Righetti, P.G. and Hjertèn, S. (1981) J. Biochem. Biophys. Methods *5*, 259–272.
Righetti, P.G., Brost, B.C.W. and Snyder, R.S. (1981) J. Biochem. Biophys. Methods *4*, 347–363.
Righetti, P.G. and Macelloni, C. (1982) J. Biochem. Biophys. Methods *6*, 1–15.
Righetti, P.G., Tudor, G. and Gianazza, E. (1982) J. Biochem. Biophys. Methods *6*, 217–227.
Righetti, P.G. (1983a) Isoelectric Focusing: Theory, Methodology and Applications, Elsevier, Amsterdam.
Righetti, P.G. (1983b) Trends Anal. Chem. *2*, 193–196.
Righetti, P.G., Gianazza, E. and Bjellqvist, B. (1983a) J. Biochem. Biophys. Methods *8*, 89–108.
Righetti, P.G., Delpech, M., Moisand, F., Kruh, J. and Labie, D. (1983b) Electrophoresis *4*, 393–398.
Righetti, P.G. (1984) J. Chromatogr. *300*, 165–223.
Righetti, P.G. and Gelfi, C. (1984) J. Biochem. Biophys. Methods *9*, 103–119.
Righetti, P.G., Ek, K. and Bjellqvist, B. (1984) J. Chromatogr. *291*, 31–42.
Righetti, P.G. and Gianazza, E. (1985a) J. Chromatogr. *334*, 71–82.
Righetti, P.G. and Gianazza, E. (1985b) Bull. Mol. Biol. Med. *10*, 387–402.
Righetti, P.G. (1986a) Sci. Tools *33*, 1–4.
Righetti, P.G. (1986b) Trends Anal. Chem. *5*, 16–20.
Righetti, P.G. and Cossu, G. (1986) Trends Anal. Chem. *5*, 147–151.
Righetti, P.G. and Gianazza, E. (1986) in: Recent Progresses in Two-Dimensional Electrophoresis (Galteau, M.M. and Siest, G., eds.) Presses Universitaires de Nancy, pp. 11–20.
Righetti, P.G., Gelfi, C. and Gianazza, E. (1986a) In: Analytical Gel Electrophoresis of Proteins, Dunn, M.J., ed. (Wright, Bristol) pp. 141–202.
Righetti, P.G., Gianazza, E., Bianchi-Bosisio, A. and Cossu, G. (1986b) In: The Hemoglobinopathies, Huisman, T.H.J., ed. (Churchill Livingstone, Edinburgh) pp. 47–71.
Righetti, P.G., Gianazza, E. and Celentano, F. (1986c) J. Chromatogr. *356*, 9–14.
Righetti, P.G., Morelli, A., Gelfi, C. and Westermeier, R. (1986d) J. Biochem. Biophys. Methods *13*, 151–159.
Righetti, P.G., Morelli, A. and Gelfi, C. (1986e) J. Chromatogr. *359*, 339–349.
Righetti, P.G., Gianazza, E., Gelfi, C. and Sinha, P.K. (1986f) In: Electrophoresis '86, Dunn, M., ed. (VCH, Weinheim) pp. 419–434.
Righetti, P.G. and Gianazza, E. (1987) In: Methods of Biochemical Analysis, Glick, D., ed. (Wiley, New York) *32*, pp. 215–278.

Righetti, P.G., Gelfi, C. and Gianazza, E. (1987a) In: New Directions in Electrophoretic Methods, Jorgenson, J.W. and Phillips, M. eds. (Am. Chem. Soc. Symp. Ser., Washington) *335*, pp. 33–53.
Righetti, P.G., Gianazza, E. and Gelfi, C. (1987b) Separ. Purif. Methods *16*, 105–169.
Righetti, P.G., Gelfi, C., Bossi, M.L. and Boschetti, E. (1987c) Electrophoresis *8*, 62–70.
Righetti, P.G., Gelfi, C. and Bossi, M.L. (1987d) J. Chromatogr. *392*, 123–132.
Righetti, P.G., Barzaghi, B. and Faupel, M. (1987e) J. Biochem. Biophys. Methods *15*, 163–176.
Righetti, P.G., Barzaghi, B., Luzzana, M., Manfredi, G. and Faupel, M. (1987f) J. Biochem. Biophys. Methods *15*, 199–206.
Righetti, P.G. (1988) J. Biochem. Biophys. Methods *16*, 99–108.
Righetti, P.G., Fazio, M., Tonani, C., Gianazza, E. and Celentano, F. (1988a) J. Biochem. Biophys. Methods *16*, 129–140.
Righetti, P.G., Chiari, M., Sinha, P.K. and Santaniello, E. (1988b) J. Biochem. Biophys. Methods *16*, 185–192.
Righetti, P.G., Gianazza, E. and Gelfi, C. (1988c) TIBS *13*, 335–338.
Righetti, P.G., Barzaghi, B. and Faupel, M. (1988d) Tib. Tech. *6*, 121–125.
Righetti, P.G., Chiari, M. and Gelfi, C. (1988e) Electrophoresis *9*, 65–73.
Righetti, P.G., Chiari, M., Casale, E. and Chiesa, C. (1989a) Appl. Theor. Electrophoresis *1*, 115–121.
Righetti, P.G., Barzaghi, B., Sarubbi, E., Soffientini, A. and Cassani, G. (1989b) J. Chromatogr. *470*, 337–350.
Righetti, P.G., Wenisch, E. and Faupel, M. (1989c) J. Chromatogr. *475*, 293–309.
Rilbe, H. (1973) Ann. N.Y. Acad. Sci. *209*, 11–22.
Rilbe, H. and Pettersson, S. (1975) in: Isoelectric Focusing (Arbuthnott, J.P. and Beeley, J.A., eds.) Butterworths, London, pp. 44–57.
Rilbe, H. (1976a) Sci. Tools *23*, 18–22.
Rilbe, H (1976b) In: Isoelectric Focusing, Catsimpoolas, N., ed. (Academic Press, New York) pp. 14–52.
Rilbe, H. (1978) J. Chromatogr. *159*, 193–205.
Rimpilainen, M. A. and Righetti, P.G. (1975) Electrophoresis *6*, 419–422.
Rittner, C. and Rittner, B. (1974) Vox Sang. *27*, 464–472.
Robrish, S.A., Kemp, C. and Bouen, W.H. (1978) Anal. Biochem. *84*, 196–204.
Rochette, J., Righetti, P.G., Bianchi-Bosisio, A., Vertongen, F., Schneck, G., Boissel, J.P., Labie, D. and Wajcman, H. (1984) J. Chromatogr. *285*, 143–152.
Rosenberg, R.N., Thomas, L., Baskin, F., Kirpatrick, J., Bay, C. and Nyhan, W.L. (1979) Neurology *29*, 917–926.
Rothe, G.M. and Maurer, W.D. (1986) in: Gel Electrophoresis of Proteins (Dunn, M.J., ed.) Wright, Bristol, pp. 37–140.
Rothe, G.M. (1988) Electrophoresis *9*, 307–316.
Rovida, E., Gelfi, C., Morelli, A. and Righetti, P.G. (1986) J. Chromatogr. *363*, 159–171.
Rubin, R.W. and Penneys, N.S. (1983) Anal. Biochem. *131*, 520–524.
Sammons, D.W., Adams, L.D., Vidmar, T.J., Hatfield, C.A., Jones, D.H., Chuba, P.J. and Crooks, S.W. (1984) in: Two-Dimensional Gel Electrophoresis of Proteins (Celis, J.E. and Bravo, R., eds.) Academic Press, Orlando, pp. 111–126.
Sato, H., Aono, S., Semba, R. and Kashiwamata, S. (1988) Electrophoresis *9*, 352–353.

Satta, D., Shapira, G., Chafey, P., Righetti, P.G. and Wahrmann, J.P. (1984) J. Chromatogr. *299*, 57–72.
Scheele, G.A. (1975) J. Biol. Chem. *250*, 5375–5380.
Scheffrahan, W. (1985) Ann. Hum. Biol. *12*, 551–552.
Scherz, R., Reber, B., Pflugshaupt, R. and Butler, R. (1985) Electrophoresis *6*, 569–571.
Schmid, K. (1975) in: The Plasma Proteins (Putnam, F.W., ed.) Academic Press, New York, Vol. 1, pp. 183–228.
Schouteeten, A., Christidis, Y. and Mattioda, G. (1978) Bull. Soc. Chim. France II, 248–254.
Schumacher, E. (1957) Helv. Chim. Acta *40*, 221–228.
Schwartz, M.L., Pizzo, S.V., Hill, R.J. and McKee, P.A. (1973) J. Biol. Chem. *248*, 1395–1407.
Scopes, R.K. (1974) Anal. Biochem. *59*, 277–282.
Sears, D.A., Read, C.F. and Helmkamp, R.W. (1971) Biochim. Biophys. Acta 233, 716–719.
Segers, J., Rabaey, M. and Van Oye, R. (1984) Electrophoresis *5*, 48–53.
Serra, J. (1982) Image Analysis and Mathematical Morphology, Academic Press, New York.
Shackelford, D.A. and Strominger, J.L. (1980) J. Exptl. Med. *151*, 141–165.
Shackelford, D.A., Mann, D.L., Van Rood, J.J., Ferrara, G.B. and Strominger , J.L. (1981) Proc. Natl. Acad. Sci. USA *78*, 4566–4570.
Sherrill, B.C., Innerarity, T.L. and Mahley, R.W. (1980) J. Biol. Chem. *255*, 1804–1807.
Shewry, P.R., Parmar, S. and Field, J.M. (1988) Electrophoresis *9*, 727–737.
Sicard, D., Lierzou, Y., Lapomeroulie, C. and Labie, D. (1979) Human Genet. *50*, 327–336.
Siemankowski, R.F., Giambalvo, A. and Dreizen, P. (1978) Physiol. Chem. Phys. *10*, 415–434.
Singer, B.S., Morrisset, H. and Gold, L. (1978) Anal. Biochem. *85*, 224–229.
Sinha, P.K. and Gossrau, R. (1984) Histochemistry *81*, 161–167.
Sinha, P.K. (1985) J. Biochem. Biophys. Methods *11*, 327–340.
Sinha, P.K. and Righetti, P.G. (1986) J. Biochem. Biophys. Methods *12*, 289–297.
Sinha, P.K., Bianchi-Bosisio, A., Meyer-Sabellek, W. and Righetti, P.G. (1986) Clin. Chem. *32*, 1264–1268.
Sinha, P.K. and Righetti, P.G. (1987) J. Biochem. Biophys. Methods *15*, 199–206.
Skoda, U., Fassbender, L., Handler, C., Mauff, G. and Pulverer, G. (1988) Electrophoresis *9*, 606–609.
Skolnick, M.M., (1982) Clin. Chem. *28*, 979–986.
Skolnick, M.M., Sternberg, S.R. and Neel, J.V. (1982) Clin. Chem. *28*, 969–978.
Skolnick, M.M. (1987) Comput. Vision Graphics Image Proc. *5*, 448–468.
Smithies, O. (1957) Nature *180*, 1482–1483.
Sock, J. and Rohringer, R. (1988) Anal. Biochem. *171*, 310–319.
Soleri, P. (1969) Arcology: the City in the Image of Man; MIT Press, Cambridge.
Sorroche, P., Bianchi-Bosisio, A., Sinha, P.K., Gelfi, C. and Righetti, P.G. (1987) Clin. Chem. *33*, 653–657.
Southern, E.M. (1975) J. Mol. Biol. *98*, 503–510.
Spencer, H., Hopkinson, D.A. and Harris, H. (1968) Ann. Hum. Genet. *32*, 9–14.
Spragg, S.P., Amess, R., Jones, M.I. and Ramasamy, R. (1985) Anal. Biochem. *147*, 120–127.

Stahl, E. (1964) Angew. Chem. Int. Ed. *3*, 784–791.
Stahl, E. and Miller, J. (1981) J. Chromatogr. *209*, 484–488.
Steinfeld, R.C. and Vidaver, G.A. (1981) Biophys. J. *33*, 185–185.
Steinmetz, A. (1987) J. Lipid Res. *28*, 1364–1370.
Sternberger, L.A. (1979) Immunocytochemistry, J. Wiley, New York.
Strahler, J.R., Hanash, S.M., Somerlot, L., Weser, J., Postel, W. and Görg, A. (1987) Electrophoresis *8*, 165–173.
Strahler, J.R., Hanash, S.M., Somerlot, L., Bjellqvist, B. and Görg, A. (1988) Electrophoresis *9*, 74–80.
Strottmann, J.M., Robinson, J.B., Jr. and Stellwagen, E. (1983) Anal. Biochem. *132*, 334–337.
Sutton, J.G. and Burgess, R. (1978) Vox. Sang. *34*, 97–103.
Sutton, J.G. and Westwood, S.A. (1984) Electrophoresis *5*, 252–253.
Suzuki, T., Benesch, R.E., Yung, S. and Benesch, R. (1973) Anal. Biochem. *55*, 249–254.
Svendsen, P.J. (1979) in: Electrophoresis (part A), vol. 18 of J. Chromatogr. Library (Deyl, Z., ed.) Elsevier, Amsterdam, pp. 345–362.
Svensson, H. (1961) Acta Chem. Scand. *15*, 325–341.
Svensson, H. (1962a) Acta Chem. Scand. *16*, 456–466.
Svensson, H. (1962b) Arch. Biochem. Biophys., Suppl. *1*, 132–140.
Svensson, H. and Pettersson, S. (1968) Separ. Sci. *3*, 209–234.
Switzer, R.C., Merril, C.R. and Shifrin, S.A. (1979) Anal. Biochem. *98*, 231–237.
Symington, J. (1984) in: Two-Dimensional Gel Electrophoresis of Proteins (Celis, J.E. and Bravo, R., eds.) Academic Press, New York, pp. 127–168.
Szewczyk, B., Bienkowska-Szewczyk, K. and Kozloff, L.M. (1987) Electrophoresis *8*, 25–28.
Tal, M., Silberstein, A. and Nusser, E. (1985) J. Biol. Chem. *260*, 9976–9980.
Talbot, D.N. and Yphantis, D.Y. (1971) Anal. Biochem. *44*, 246–256.
Tanabe, Y., Omi, T. and Ota, K. (1978) Biochem. Genet. *9*, 79–83.
Tate, M.E. (1981) Biochem. J. *195*, 419–429.
Tate, S.S. and Ross, E.M. (1977) J. Biol. Chem. *252*, 6042–6045.
Taylor, J., Anderson, N.L. and Anderson, N.G. (1981) in: Electrophoresis '81 (Allen, R.C. and Arnaud, P., eds.) de Gruyter, Berlin, pp. 383–400.
Taylor, J., Anderson, N.L., Scandora Jr., A.E., Willard, K.E. and Anderson, N.G. (1982) Clin. Chem. *28*, 861–866.
Teng, Y.S. and Tan, S.G. (1982) Hum. Hered. *32*, 362–366.
Thomas, W.C., Morgan, H.G., Connor, T.B., Haddock, L., Bills, C.E. and Hovord, J.E. (1959) J. Clin. Invest. *38*, 1078–1082.
Thymann, M. (1978) Hum. Genet. *43*, 225–229.
Thymann, M. and Eiberg, M. (1986) Advances in Forensic Haemogenetics (Brinkmann, B. and Henningsen, K., edt.) Springer, Berlin, Vol. 1, pp. 162–166.
Tiselius, A. (1937) Trans. Faraday Soc. *33*, 524–540.
Tollaksen, S.L., Edwards, J.J. and Anderson, N.G. (1981) Electrophoresis *2*, 155–160.
Towbin, H., Staehelin, T. and Gordon, J. (1979) Proc. Natl. Acad. Sci. USA *76*, 4350–4355.
Towbin, H. and Gordon, J. (1984) J. Immunol. Methods *138*, 1–5.
Tracy, R.P., Currie, R.M. and Young, D.S. (1982a) Clin. Chem. *28*, 890–899.
Tracy, R.P., Wold, L.E., Currie, R.M. and Young, D.S. (1982b) Clin. Chem. *28*, 915–919.
Tracy, R.P. and Young, D.S. (1984) in: Two-Dimensional Gel Electrophoresis of

Proteins (Celis, J.E. and Bravo, R., eds.) Academic Press, New York, pp. 193–240.
Tsugita, A., Sasada, S., Van den Broek, R. and Scheffler, J.J. (1982) Eur. J. Biochem. *124*, 171–176.
Tunon, P. and Johansson, K.E. (1984) J. Biochem. Biophys. Methods *9*, 171–179.
Tuszyncki, G.P., Buck, C.A. and Warren, L. (1979) Anal. Biochem. *85*, 224–229.
Tyson, J.J. and Haralick, R.H. (1986) Electrophoresis *7*, 107–113.
Utermann, G., Jaeschke, M. and Menzel, J. (1975) FEBS Lett. *56*, 352–355.
Utermann, G., Feussner, G., Franceschini, G., Haas, J. and Steinmetz, A. (1982) J. Biol. Chem. *247*, 501–507.
Vaith, P., Assmann, G. and Uhlenbruck, G. (1978) Biochim. Biophys. Acta *541*, 234–240.
Vandekerckhove, J.F., Bauw, G., Puype, M. Van Damme, J., and Van Montagu, M. (1986) Eur. J. Biochem. *152*, 9–19.
Vandekerckhove, J.F., Bauw, G., Van Damme, J., Puype, M. and Van Montagu, M. (1987) in: Methods in Protein Sequence Analysis (Walsh, K., ed.) Humana Press, Clifton, pp. 261–276.
Van Eijk, H.G., Van Noort, W.L., de Jong, G. and Koster, J.F. (1987) Clin. Chim. Acta *165*, 141–145.
Van Keuren, M.L., Goldman, D. and Merril, C. (1982) Ann. N.Y. Acad. Sci. *396*, 55–67.
Van Oss, C.J., Good, R.J. and Chaudhury, M.K. (1987) J. Chromatogr. *391*, 53–65.
Vesterberg, O. (1969) Acta Chem. Scand. *23*, 2653–2666.
Vesterberg, O. and Svensson, H. (1966) Acta Chem. Scand. *20*, 820–834.
Vesterberg, O. (1972) Biochim. Biophys. Acta *257*, 11–19.
Vesterberg, O. (1975) in: Isoelectric Focusing (Arbuthnott, J.P. and Beeley, J.A., eds.) Butterworths, London, pp. 78–96.
Vincens, P., Paris, N., Pujol, J.L., Gaboriaud, C., Tabilloud, T., Pennetier, J.L., Matherat, P. and Tarroux, P. (1986) Electrophoresis *7*, 347–356.
Vincens, P. (1986) Electrophoresis *7*, 357–367.
Vincens, P. and Tarroux, P. (1987a) Electrophoresis *8*, 100–107.
Vincens, P. and Tarroux, P. (1987b) Electrophoresis *8*, 173–186.
Vincens, P. and Tarroux, P. (1988) Int. J. Biochem. *20*, 499–509.
Vincent, R.K., Hartman, J., Barret, A.S. and Sammons, D.W. (1981) in: Electrophoresis '81 (Allen, R.C. and Arnaud, P., eds.) De Gruyter, Berlin, pp. 371–382.
Visvikis, S., Dumon, M.F., Steinmetz, J., Galteau, M.M., Clerc, M., Siest, G. (1986) in: Electrophoresis '86 (Dunn, M.J., ed.), VCH, Weinheim, pp. 638–641.
Vo, K.M., Miller, M.J., Geiduschek, E.P., Nielsen, C., Olson, A. and Xuong, N.H. (1981) Anal. Biochem. *112*, 258–271.
Wagner, H. and Kessler, R. (1983) in: Electrophoresis '82 (Stathakos, D., ed.) de Gruyter, Berlin, pp. 303–310.
Wagner, H., Mang, V., Kessler, R., Heydt, A. and Manzoni, R. (1984) in Electrophoresis '83 (Hirai, H., ed.) de Gruyter, Berlin, pp. 283–290.
Wajcman, H., Bianchi-Bosisio, A. and Righetti, P.G. (1989) J. Biochem. Biophys. Methods *18*, 65–76.
Warburg, O. and Christian, W. (1941) Biochem. Z. *310*, 384–421.
Warnke, R. and Levy, R. (1980) J. Histochem. Cytochem. *28*, 771–779.
Weast, R.C. (ed.) (1987) CRC Handbook of Chemistry and Physics (CRC Press, Baton Rouge, FL.) 67th Ed., p. D-161.
Weidekamm, E., Wallach, D.H.F. and Fluckiger, R. (1973) Anal. Biochem. *54*, 102–114.

Weidinger, S., Cleve, H., Schwarzfischer, F., Postel, W., Weser, J. and Görg, A. (1984) Hum. Genet. *66*, 356–360.
Weidinger, S. and Cleve, H. (1984) Electrophoresis *5*, 223–226.
Weidinger, S., Jahn, W., Cujnik, F. and Schwartzfischer, F. (1985) Hum. Genet. *71*, 27–29.
Weidinger, S. and Cleve, H. (1986) Prot. Biol. Fluids *34*, 863–866.
Weisgraber, K.H., Rall, S.C., Jr. and Mahley, R.W. (1981) J. Biol. Chem. *256*, 9077–9083.
Weisgraber, K.H., Newhouse, Y.M., Seymour, J.L., Rall, S.C., Jr. and Mahley, R.W. (1985) Anal. Biochem. *151*, 455–461.
Wenger, P., de Zuanni, M., Javet, P., Gelfi, C. and Righetti, P.G. (1987) J. Biochem. Biophys. Methods *14*, 29–43.
Westermeier, R., Postel, W. and Görg, A. (1981) in: Electrophoresis '81 (Allen, R.C. and Arnaud, P., eds.) de Gruyter, Berlin, pp. 281–287.
Westermeier, R., Postel, W., Weser, J. and Görg, A. (1983) J. Biochem. Biophys. Methods *8*, 321–330.
Westwood, S.A. and Sutton, J.G. (1984) Electrophoresis *5*, 162–164.
Westwood, S.A. (1985) Electrophoresis *6*, 498–503.
Whitehead, A.S., Solomon, E., Chambers, S., Povey, S. and Badmer, W.F. (1982) Proc. Natl. Acad. Sci. USA *79*, 5021–5025.
Whitney III, J.B., Cobb, R,.R., Popp, R.A. and O'Rourke, T.W. (1985) Proc. Natl. Acad. Sci USA *82*, 7646–7650.
Wiederkehr, F., Ogilivie, A. and Vonderschimmt, D.J. (1985) Clin. Chem. *31*, 1537–1542.
Wieme, R.J. and Demeulenaere, L. (1967) Nature *214*, 1042–1043.
Wilchek, M. and Bayer, E.A. (1984) Immunol. Today *5*, 39–48.
Willard, K.E., Giometti, C.S., Anderson, N.L., O'Connor, T.E. and Anderson, N.G. (1979) Anal. Biochem. *100*, 289–298.
Willers, I., Singh, S., Goedde, H.W. and Klose, J. (1981) Clin. Genet. *20*, 217–221.
Williams, K.W. and Söderberg, L. (1979) Int. Lab. Jan./Febr., 45–53.
Wrightstone, R.N. (1986) in: The Hemoglobinopathies (Huisman, T.H.J., ed.) Churchill Livingstone, Edinburgh, pp. 160–193.
Yang, F., Lum, J.B., McGill, J.R., Moore, M.C., Naylor, S.L., Van Bragt, P.H., Baldwin, W.D. and Bowman, B.H. (1984) Proc. Natl. Acad. Sci. USA *81*, 2752–2756.
Yuasa, I. and Okada, K. (1985) Hum. Genet. *70*, 333–336.
Yuasa, I., Suenaga, K., Umetsu, K., Inagaki, O., Ikebuchi, J., Ito, K. and Okada, K. (1988) Electrophoresis 9,151–153.
Young, D.A. (1984) Clin. Chem. *30*, 2104–2108.
Yuen, S., Hunkapillar, M.W., Wilson, K.J. and Yuen, P.M. (1986) Applied Biosystems Users Bulletin No. *25*, Foster City, CA.
Zannis, V.T. and Breslow, J.L. (1981) Biochemistry *20*, 1033–1041.
Zeman, I. (1988) J. Chromatogr. *426*, 452–453.
Zimmer, H.G., Kronberg, H. and Neuhoff, V. (1980) Electrophoresis *1*, 27–32.
Ziola, B.R. and Scraba, D.G. (1976) Anal. Biochem. *72*, 366–371.

Subject index